Comprehensive and Clinical Anatomy of the Middle Ear

Salah Mansour
Jacques Magnan
Hassan Haidar Ahmad
Karen Nicolas
Stéphane Louryan

Second Edition

Springer

Comprehensive and Clinical Anatomy of the Middle Ear

Salah Mansour • Jacques Magnan
Hassan Haidar Ahmad • Karen Nicolas
Stéphane Louryan

Comprehensive and Clinical Anatomy of the Middle Ear

Second Edition

Springer

Salah Mansour
Amoudi Center
Mazraa Blvd
Beirut
Lebanon

Hassan Haidar Ahmad
Hamad Medical Corporation
Weill Cornell Medicine
Doha
Qatar

Stéphane Louryan
Université Libre de Bruxelles
Faculté de Médecine
Laboratoire d'Anatomie
Biomécanique et Organogenèse
Brussels
Belgium

Jacques Magnan
Clinique CAUSSE
Colombiers
France

Karen Nicolas
Bsalim Hospital
Middle East Institute of Health
Mount Lebanon
Lebanon

ISBN 978-3-030-15362-5 ISBN 978-3-030-15363-2 (eBook)
https://doi.org/10.1007/978-3-030-15363-2

This Springer imprint is published by the registered company Springer Nature Switzerland AG.
The registered company address is: Gewerbestrasse 11, 6330 Cham, Switzerland

To my wife, Ruth, for her constant love and support; for my three sons, grandchildren, and all the Mansour family.

Salah Mansour

Preface

Following the great success of the first edition of *Comprehensive and Clinical Anatomy of the Middle Ear*, our publisher invited the team of authors to produce a second edition. We worked diligently to present new anatomical facts and concepts, which build upon continuing surgical experience and advanced correlated endoscopic and imaging acquisitions.

Although human anatomy is a stable basic knowledge, when it concerns the ear, it remains a dynamic discipline where nothing is set in stone. This second edition reports the latest observations to enable better otology training and enhance surgical approaches.

Most of the anatomy described in the first edition is still valid and pertinent. However, additional anatomical details and their functional importance are reported in this second edition. These additions and other refinements provide improved diagnostic orientations and suggest more precise surgical procedures in the middle ear.

In every chapter of this second edition, subchapters and subdivisions report and illustrate updated elements of embryology and anatomy, as well as relevant modern endoscopic and imaging illustrations to better perform otological surgery. Additional knowledge concerning the mechanics of middle ear anatomical content is introduced to assist in the understanding of its clinical significance and its importance to the surgical setting.

We have also added a new chapter to explain the fragile structure of the middle ear as an organ and its comparative evolution during phylogenesis, aiming to offer a holistic vision for handling the middle ear.

Most illustrations, anatomical plate dissections, endoscopic and microscopic pictures, and imaging demonstrations were revisited for the purposes of this second edition. This allows us to better highlight normal middle ear anatomical details, congenital abnormalities, and conflictual pathological presentations. We wish to offer students and teachers a complete and up-to-date reference book concerning the functional anatomy of the middle ear. To do so, we not only draw from our knowledge and experience as practitioners but also discuss current modern otology research. This second edition reviews the recent literature relative to the discipline and references many new and interesting sources.

This second edition is the result of close collaboration among good friends and colleagues. It is a tribute to their dedication to medical teaching and their desire to expand the knowledge of practitioners everywhere.

Beirut, Lebanon Salah Mansour

Preface

A second edition gives the opportunity to revisit our knowledge, expand upon our experiences, and offers an updated presentation. I also think of it as confirmation that the Comprehensive and Clinical Anatomy of the Middle Ear met the expectations of our fellow specialists. So, again under the guidance of Prof. Salah Mansour, it was a great pleasure to work with the same enthusiastic team. New anatomical pictures have been added. This edition reconfirms the notion that temporal bone dissection is an indispensable step for the theoretical teaching of surgery.

Colombiers, France

Jacques Magnan

Preface

The great success of the first edition of this book motivates us to go further in depth digging for a complete and most interesting knowledge concerning middle ear anatomy and its complex functional architecture. Our aim was to update advances recently found following correlated disciplines, especially ear endoscopy, in order to make available a complete reference book for learners and teachers.

I am thankful for the active collaboration between all members of the team of authors; their central collaboration and conjugate efforts render the present work most enjoyable and informative.

Doha, Qatar
Hassan Haidar

Preface

Computed tomography is the most precise radiologic modality available for the study of the anatomy of the middle ear. The otologist's practice and teaching during clinical, preoperative, and postoperative work are supported by the knowledge of the usual CT aspects of the walls, contents, and compartments neighboring the noble anatomic structures of the temporal bone. Such knowledge should be a baseline for any otology candidate.

This second edition showcases new CT images to illustrate the detailed anatomy of middle ear structures. Anatomical variants and pathological aspects have been added to enlarge the imaging spectrum in several sections.

I want to thank Professor Mansour and my coauthors for their constructive and active collaboration: their contribution was essential to the orientation of imaging studies to the needs of the otologist.

I hope this book will encourage continued dialogue among radiologists and surgeons in their daily practice. I firmly believe such collaboration is key to advancing both disciplines.

Mount Lebanon, Lebanon — Karen Nicolas

Preface

This second edition adds data concerning the developmental genetics and comparative anatomy of the middle ear structures.

Embryology progressively gives place to developmental biology, which offers ways to understand congenital malformations. Some of these abnormalities can be understood in the light of evolution and comparative anatomy. The close relationships of middle ear ossicles with the temporo-mandibular joint are also discussed and can explain some pathological signs, such as tinnitus.

The precise embryological origin of middle ear ossicles is still debated, and this second edition takes account of such controversy.

The human embryo histological sections come from collections of the Louis Deroubaix anatomy and embryology Museum, Université libre de Bruxelles.

Brussels, Belgium — Stéphane Louryan

Contents

1 Temporal Bone

Contents

The temporal bone is situated at the inferior and lateral part of the skull and lateral to the temporal cortex. It is the center of anatomy knowledge to the otologist because it contains the hearing organ and equilibrium with various cavities and recesses associated with the ear.

The temporal bone is the most complex bone in the human body and further complicated by the small size and three-dimensional orientation of associated structures.

Temporal bone has multiple embryological origins and shows adverse developmental aspects. It houses several important structures such as the outer ear, the *middle ear* and internal ear apparatus, the facial nerve (VII), the vestibulocochlear nerve (VIII), the internal carotid artery, and the jugular vein, which contract major impacts on the ME surgical anatomy.

This chapter will be mostly oriented, not to study the temporal bone as such but to address it in a specific and restricted scope aiming to describe precisely the developmental and anatomical environment in which the middle ear achieves its final architecture.

S. Mansour et al., *Comprehensive and Clinical Anatomy of the Middle Ear*,
https://doi.org/10.1007/978-3-030-15363-2_1

Our target will be to demonstrate the relationship of critical structures around and inside the middle ear. Knowledge about the anatomical details of the temporal bone surfaces is a milestone for any surgical approach, which will be briefly illustrated when the corresponding anatomic area is described.

1.1 Embryology of the Temporal Bone

Temporal bone formation results from the fusion and growth of four bones: the squamous, the petrous, the tympanic, and the styloid bone. These bones interact to build up the final temporal bone.

Being a part of the skull, the temporal bone development is an integral part in the process of skull development. The human skull is developed from three components:

1. *The cartilaginous neurocranium or chondrocranium* is the part of the skull formed by endochondral ossification; it constitutes the majority of the skull base (ethmoid bone and portions of the occipital, temporal, and sphenoid bones). Endochondral ossification takes place in a cartilaginous anlage; chondroblasts become hypertrophied and progressively change into osteoblasts, which elaborate the bony matrix. The corresponding area is the "ossification center."
2. *The membranous neurocranium or neuroskull* is the part of the skull formed by intramembranous ossification; it constitutes the vault of the skull (frontal, parietal portions of the temporal, occipital, and sphenoid bone). Intramembranous ossification happens when a cluster of mesenchymal cells in a membranous structure gives rise to osteoblasts, in the absence of any cartilaginous matrix.
3. *The viscerocranium or visceroskull* is the part of the skull derived from the visceral (branchial) arches and is suspended to the rest of the cranium [1]. It includes the facial bones.

These three components of the skull contribute actively in the formation of the temporal bone in the following way:

The deep part of the petrous bone is derived from the cartilaginous neurocranium, but the more superficial parts are derived from the membranous neurocranium. The squamous bone is derived from the membranous neurocranium, and the tympanic bone is a part of the visceral skull [2].

1.1.1 Cartilaginous Neurocranium

The majority of the skull base develops from the cartilaginous neurocranium. The formation of the human skull base is a complex process that begins during the fourth week of fetal development. Neural crest cells and paraxial mesoderm derived from occipital somites migrate to sit between the emerging brain and foregut. These cells migrate around and in front of the notochord to form condensations accumulating within the emerging cranial base. The chondrocranium begins to form when these cells condense into cartilage early in the seventh week; these cells are named parachordal cartilages and contribute to the creation of the basal plate. These parachordal cartilages give rise to the body, greater and lesser wings of the sphenoid bones as well as the perpendicular plate of the ethmoid and the crista galli. These embryonic cartilages fuse around the existing cranial nerves and blood vessels to create the primordia of neural foramina.

1.1.1.1 The Cartilaginous Otic Capsule

Between the eighth and ninth week of gestation, the cartilaginous otic capsule appears as budge in the base of the cartilaginous cranium. It develops from the mesenchymal tissue that surrounds the otic vesicle. Later, the otic capsule becomes surrounded by membranous layers (internal and external periosteal layers); these layers will become the extracapsular part of the petrous bone [3] (Fig. 1.1).

Shortly after this process, the lateral and superior boundaries of the otic capsule begin to appear with the earliest development of the mastoid

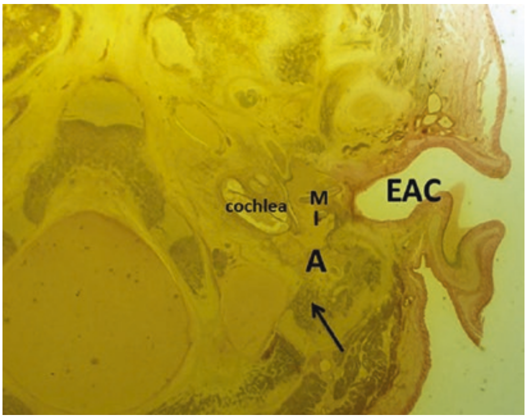

Fig. 1.1 The left temporal bone in a 6-month, 250 mm, human fetus. The mastoid area contains external periosteal layer bone (arrow) and will transform into the mastoid bone. Notice that the mastoid antrum (A) and the cochlea are already developed. *M* malleus, *I* incus, *EAC* external auditory canal

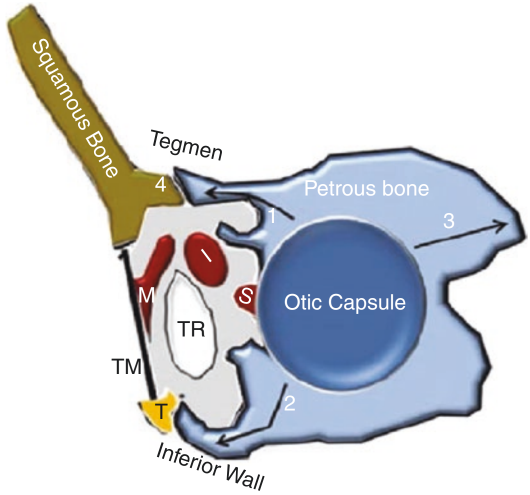

Fig. 1.2 Schematic drawing, frontal plane (34-week-old fetus). Schema showing the cartilaginous flanges running out from the otic capsule: (1) Lateral and superior flange or the tegmental plate growing from the otic capsule superior to the tubotympanic recess (TR) to form part of the tegmen tympani and the walls of the Eustachian tube. (2) Lateral and inferior cartilage flange, growing from the otic capsule to form the jugular plate and the floor of the tympanic cavity. (3) Anteromedial flange growing from the otic capsule anteromedially to form the petrous apex. The inferior wall of the middle ear is built up by the inferior plate of the petrous bone (2) which runs laterally to join the tympanic bone (T); the plane of fusion constitutes the hypotympanic fissure(*). The tympanic bone (T) and the tympanic membrane (TM) form the lateral wall of the middle ear cavity. The tegmen tympani is formed by fusion of the tegmental process of the petrous bone (2) and the transverse plate of the squamous bone (4). *M* malleus, *I* incus, and *S* stapes

process and tegmen tympani [4]. A cartilaginous flange grows from the lateral and superior part of the otic capsule and goes downward and outward superior to the tubotympanic recess and above the Meckel's cartilage to form the tegmen tympani and the lateral wall of the Eustachian tube (ET) (Fig. 1.2) (see Sect. 2.5.1). Thus, *the tympanic cavity and the bony part of the ET originate from the petrous bone.* Furthermore, from the lateral and inferior part of the cartilaginous otic capsule, another flange grows below the tubotympanic recess to form the jugular plate and the floor of the tympanic cavity. Anteromedially, another periosteal layer grows to form the petrous apex (Fig. 1.2).

By the 16th week, the labyrinth reaches its adult size. Only at this time, the first part of the petrous bone starts to ossify by the endochondral ossification process. There are 14 different ossification centers in the otic capsule, which progressively fuse during the fetal period [4].

The ossification proceeds and continues in the remaining part of the petrous bone to gain its final aspect by about midterm. By the 23rd week of gestation, the rest of the ossification process of the extracapsular parts of the temporal bone continues by extension of the surrounding periosteum forming the mastoid process, the tegmen tympani, the middle ear floor, and the walls of the Eustachian tube (Figs. 1.2 and 1.3). The floor of the middle ear ossifies between the 24th and 29thweek from an extension of the jugular plate ossification center [5]. Ossification of the otic capsule is completed only shortly before birth [5]. A delay or a focal lack of the ossification process may explain the dehiscence of the superior semicircular canal [6, 7].

1.1.2 Membranous Neurocranium and the Squamous Bone

The squamous part of the temporal bone develops from intramembranous ossification; it is formed from one ossification center that appears

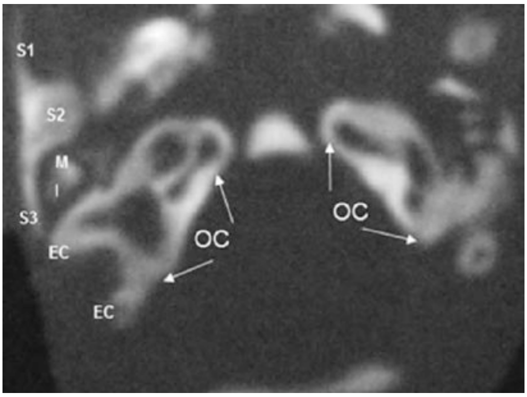

Fig. 1.3 Transversal CT scan of a 22-week-old 220 mm fetus, showing ossification of the otic capsule (OC) and beginning of the ossification process in the extracapsular parts of the petrous bone (EC) extending to form the mastoid process. The inferior part of the squamous bone with its three parts: S1 anterior part forming the zygomatic process, S2 middle part forming the roof of the EAC and part of the tegmen, and S3 the posterior part forming the anterior part of the mastoid process. Notice that the petrous bone and the squamous bone are not yet fused. *M* malleus, *I* incus

during the eighth week of gestation [8]. The development of the upper and lower halves of the bone primordium differs:

- The upper part is flat and thin; it becomes the vertical portion.
- The lower part, due to the presence of the tympanic bone by the 16th week, bulges and grows rapidly into three directions (Fig. 1.2):
  1. *The anterior part* extends anteriorly around the tympanic ring toward the zygomatic bone primordium. It is fixed to the anterior-superior part of the tympanic bone. It forms the zygomatic process of the squamous bone and is involved in the formation of the roof of the temporomandibular joint.
  2. *The middle part* sinks medially above the tympanic ring to form the superior wall of the external auditory canal, the attic outer wall, and the lateral part of the tegmen tympani [9].
  3. *The posterior part* extends posteriorly behind the tympanic ring to cover a major part of the base of the petrous bone. It forms the anterior portion of the mastoid process.

1.1.3 The Viscerocranium

1.1.3.1 The Styloid Process

The styloid process derives directly from the Reichert's cartilage of the second visceral arch. It develops from two parts:

1. The proximal part or the base, also named *the tympanohyale*, is situated close to the tympanic bone. Its ossification center appears before birth and continues to grow until the age of 4 years. It fuses with the petromastoid component during the first year of life [10].
2. The distal part, *the stylohyale*, starts its ossification only after birth. It fuses with the proximal part only after puberty.
3. The stylohyoid ligament can ossify, which causes dysphagia (Eagle's syndrome) (Fig. 1.9).

1.1.3.2 The Tympanic Bone

The tympanic ring is a C-shaped bone that provides physical support to the tympanic membrane. It is formed by intramembranous ossification (Fig. 1.4).

At the eighth week of gestation, the tympanic ring appears as a condensation in the cephalic part of the mandibular part of the first branchial arch, which is situated ventral to the first pharyngeal cleft and lateral to Meckel's cartilage.

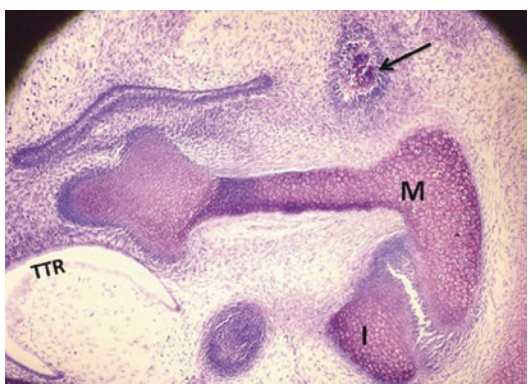

Fig. 1.4 An intramembranous area of ossification (arrow) corresponding to the tympanic bone in an E17 mouse embryo (sagittal section, toluidine blue). The cartilaginous primordial of the malleus (M) and incus (I) are also visible. Tubotympanic recess (TTR). Toluidine blue staining at pH4

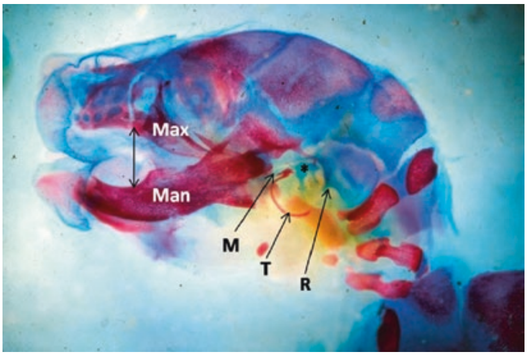

Fig. 1.5 Skeletal staining of a mouse E 16 embryo. In blue, the Meckel's (M) and Reichert's (R) cartilages appear in close relationship with the ossicles rudiment (*). In red, we can see maxillary (Max) and mandibular (Man) bones around the oral cavity (double arrow). The tympanic ring (T) is also red and ossifies following intramembranous process

This condensation will extend in a circumferential fashion around the first pharyngeal cleft resulting in the C-shaped structure [11]. Within 2 weeks, the ossification is first detected in the part of the condensation adjacent to Meckel's cartilage, and then, it progresses through the rest of the condensation to form a fully developed tympanic ring that is well recognized by the 11th week of gestation (Fig. 1.5).

At 12th week, growth of the tympanic ring proceeds rapidly with a consequent increase in its overall size. The tympanic ring is never closed superiorly, giving rise to the incisura tympanica (*notch of Rivinus*) where the pars flaccida of the tympanic membrane will insert.

Fusion of the tympanic ring with the other components of the temporal bone starts first at 31st week in the posterior part. The anteromedial segment of the tympanic bone does not join the temporal bone until 37th week. Its fixation to the temporal bone is complete at birth.

The tympanic bone is 9 mm in diameter at birth, almost its definitive size. At this time, it is ring shaped and is open superiorly [12–16].

The formation of the external auditory meatus and the formation of the manubrium are in close association with the tympanic ring formation [11]. The tympanic ring plays an instructive role for the external auditory canal development. Very likely, aural atresia results from the failure of the tympanic ring to develop [17]. In addition, the formation of the tympanic ring is essential for the insertion of the manubrium of the malleus into the tympanic membrane [18]. Several experimental conditions leading to a lack of external auditory meatus formation also result in a severe underdevelopment of the manubrium with a normal aspect of the rest of the malleus. This fact is confirmed in cases of major aural atresia, showing an absence of the manubrium with otherwise normal looking of the rest of the malleus [18, 19].

1.2 Perinatal Changes of the Temporal Bone

At the time of the perinatal period, the squamous and tympanic bones have already fused together; but the resultant segment is still separated from the petrous segment [20]. Early in the perinatal period, these two segments begin to fuse simultaneously at several locations, beginning with the medial surface of the squamous part to the lateral edge of the tegmental process of the petrous bone. This zone of fusion becomes the internal petrosquamous suture [7]. The fusion continues posteriorly between the petrous and squamous parts of the mastoid process; failure of complete fusion of the two parts leads to formation of a bony septum inside the mastoid process, called *Koerner's septum* [21] (see Sect. 5.1). The external petrosquamous suture present on the outer surface of the mastoid process marks the plane of fusion between these two parts.

Finally, the inferior portion of the tympanic ring fuses medially to the inferior process of the petrous bone, thus forming the inferior wall of the tympanic cavity.

1.3 Postnatal Changes of the Temporal Bone

Expansion pressures and antagonist forces exerted by the cephalic neuroskull and the muscular visceroskull, in addition to the pneumatization

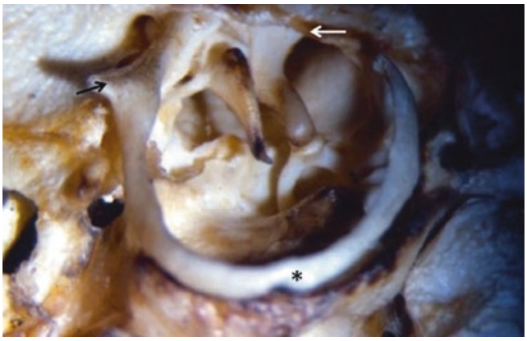

Fig. 1.6 Neonate skull with tympanic annulus bone (*) with its anterior tubercle (white arrow) and posterior tubercle (black arrow). The external auditory meatus is short and ossicles are completely visible

process, are the main factors for the remodeling process and postnatal changes of the temporal bone.

Bone growth around the tympanic ring following its fusion to the petrous bone proceeds laterally around its circumference. This results in the development of the bony external auditory canal [22]. This lateral extension of the tympanic ring results from the growth of two tympanic tubercles, one from the anterior aspect of the ring and the second from the posterior aspect (Fig. 1.6). These projections grow laterally and then toward each other inferiorly to form the inferior wall of the external auditory canal. By doing so, these projections delimit two openings: the first is in the upper part, *the notch of Rivinus*, and the second is inferior, *the foramen of Huschke* [23].

Clinical Pearl

Usually the foramen of Huschke closes by the age of 5 years by additional bone growth. This foramen remains patent in about 7% of adults; in such cases, the skin of the external auditory canal may invaginate into the residual foramen and migrate under the inferior wall of the external bony canal, leading to the formation of a canal cholesteatoma (Fig. 1.7).

Enclosure of the base of the styloid process occurs simultaneously with the lateral extension of the tympanic bone as well. In addition, the tympanic ring changes its orientation relative to the rest of the cranium.

At birth, the tympanic ring lies beneath the skull in an almost horizontal plane. By the third month, because of the upward and lateral rotation of the petrous bone caused by a rapid enlargement of the forebrain, the tympanic ring appears on the inferolateral aspect of the skull; few months later, it attains its final near vertical orientation [21].

The mastoid process is flat at birth. The stylomastoid foramen is superficial with the facial nerve lying on the lateral surface behind the tympanic bone. Due to pneumatization process in the mastoid process, its lateral portion grows downward and forward so that the stylomastoid foramen is pushed medially onto the undersurface of the temporal bone (see Sect. 5.2).

The styloid process does not make its appearance until after birth. It becomes attached to the tympanic bone during its lateral extension. The progression by which the styloid process grows and ossifies is variable, explaining the variable size and shape of the styloid process in adult skulls [24].

The squamous part of the temporal bone grows rapidly along with the cranial vault during the first 4 years of life and continues at a much slower pace until adulthood [7, 20].

Clinical Pearl

Parallel to the orientation changes of the tympanic bone, changes also occur in tympanic membrane orientation. At birth, the tympanic membrane is in almost horizontal plane; this explains the difficulty of exposure of the tympanic membrane in newborns during otoscopy for paracentesis. Associated to the tympanic ring changes of orientation, the inferior tympanic sulcus lateralizes accordingly so the tympanic membrane becomes more vertical and more accessible for examination.

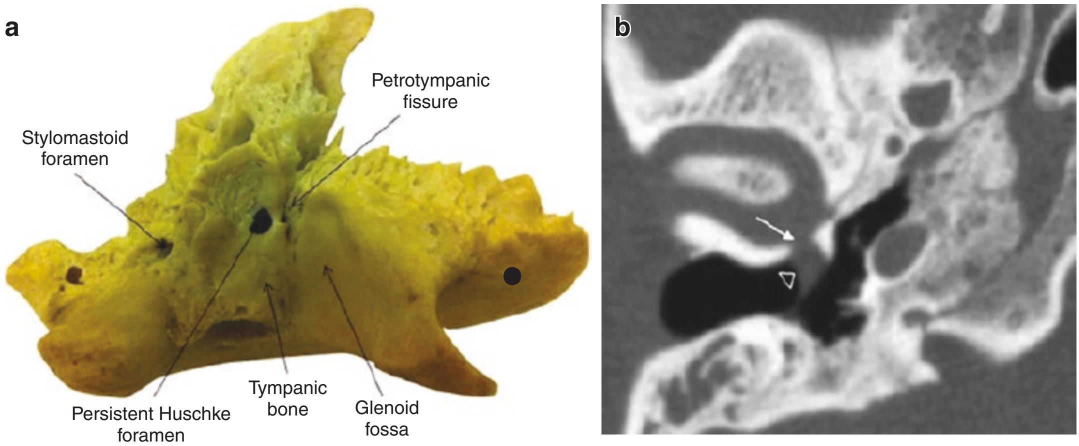

Fig. 1.7 Persistent foramen of Huschke. (**a**) Cadaveric temporal bone, inferior surface, showing a persistent foramen of Huschke. (**b**) Transversal computed tomography of the external auditory canal of a right ear, showing a persistent foramen of Huschke (white arrow) with a secondary cholesteatoma (arrowhead)

1.4 Anatomy of the Temporal Bone

The temporal bone, a paired and symmetrical bone, participates in the formation of the base and the calvarium of the skull. It is formed from the fusion of four different embryological bones: **the petrous bone, the squamous bone, the tympanic bone, and the styloid bone**.

The auditory system is disposed on two axes: the yellow text is original from the introduction.

1. *Anteroposterior air axis* consisting of the Eustachian tube, middle ear, and mastoid antrum.
2. *Latero-medial sensorial axis* consisting of the external and internal auditory canals.

These two axes intersect at the level of the middle ear cavity (Fig. 1.8).

The temporal bone connects with four bones: the occipital bone posteriorly and laterally, the parietal bone superiorly, the sphenoid bone anteriorly and the zygomatic bone laterally.

1.4.1 The Petrous Bone

Petrous comes from the Latin word “petra” meaning rock; it is the hardest bone of the human skull. It houses the inner ear, the internal carotid artery, the Fallopian canal, and the major part of

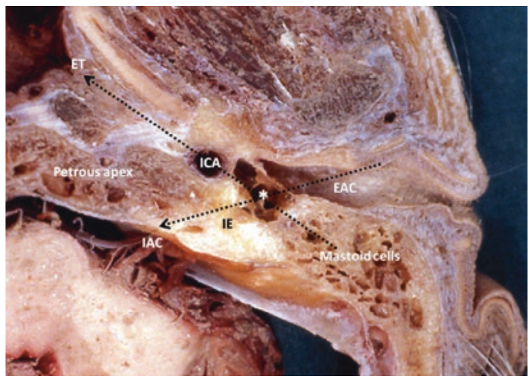

Fig. 1.8 Transverse cut through a left (view from below) temporal bone showing the middle ear cavity (*) hollowed out in the center of the temporal bone between the external auditory canal (EAC) and the inner ear (IE). The middle ear lies at the intersection of two axes (black dotted arrows), external - internal auditory canal (EAC-IAC) axis and mastoid - Eustachian tube (Mastoid cells - ET) axis. *ICA* internal carotid artery

the middle ear. It results from the ossification of the otic capsule and its flanges.

The petrous bone is shaped like a pyramid that project anteromedially forming a 45° angle with the transverse axis. This pyramid has a posterolateral base (the mastoid) and an anteromedial summit (the petrous apex). It is wedged between the basioccipital and the greater wing of the sphenoid. Its anterosuperior surface is endocranial and participates in the formation of middle cranial fossa floor. Its posterosuperior surface is also endocranial and forms the anterolateral wall of the posterior cranial fossa. Its inferior surface is exocranial and corresponds to the posteromedial part of the mastoid process.

1.4.2 The Squamous Bone

The squamous bone constitutes the major part of the lateral surface of the temporal bone. The squamous bone presents two parts:

1. *The vertical part* is a flat and a thin plate of bone that extends upward to form part of the lateral wall of the middle cranial fossa.
2. *The horizontal part* is prolonged anteriorly as the zygomatic process, which originates from two roots: a sagittal posteroexternal root that overhangs the external auditory canal forming its superior part and a transversal anterointernal root that forms the condyle of the temporomandibular joint.

1.4.3 The Tympanic Bone

The tympanic portion of the temporal bone is a gutter-shaped plate of the bone. It is situated below the squamous bone between the glenoid fossa anteriorly and the mastoid process posteriorly. The inferior surface of the tympanic bone presents a plate of bone called the vaginal process, which surrounds the styloid process and merges with the petrous bone near the carotid canal.

The tympanic bone forms the anterior, inferior, and posterior walls of the bony external auditory canal. Its attachment to the mastoid and the squamous delineates two suture lines: the tympanosquamous suture anterosuperiorly and the tympanomastoid suture posteroinferiorly. Medially, the tympanic bone articulates with the petrous bone to form the *petrotympanic fissure*.

The junction between the tympanic bone and the squamous bone superiorly corresponds to *the notch of Rivinus.*

Medially, the tympanic bone presents a narrow furrow: the *tympanic sulcus* to which the tympanic membrane annulus is inserted.

1.4.4 The Styloid Bone

The styloid process is a long, slender, and pointed bone of variable length averaging from 20 to 25 mm. It lies anteromedial to the stylomastoid foramen.

The tip of the styloid bone is located between the external and internal carotid arteries, lateral to the pharyngeal wall, and immediately behind the tonsillar fossa.

Three muscles and two ligaments are attached to the styloid process: the stylopharyngeus muscle, the stylohyoid muscle, and the styloglossus muscle. The stylohyoid ligament extends from the tip of the styloid process to the lesser horn of the hyoid bone and the stylomandibular ligament, which starts under the attachment of the styloglossus muscle and ends on the mandibular angle [10, 22, 25–27].

Clinical Pearl

The ossification process of the styloid ligament may involve the whole length of the ligament, giving rise to a bony prolongation between the skull and the hyoid bone; this may manifest clinically by odynophagia, Eagle's syndrome (Fig. 1.9).

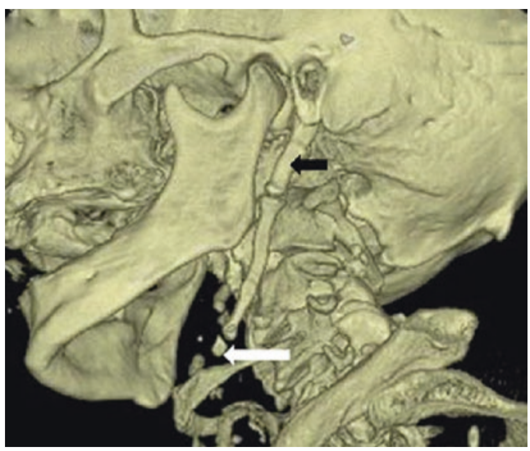

Fig. 1.9 Computed tomography with 3D reformation showing complete ossification of the stylohyoid ligament from the styloid process (upper arrow) to its insertion on the hyoid bone (lower arrow)

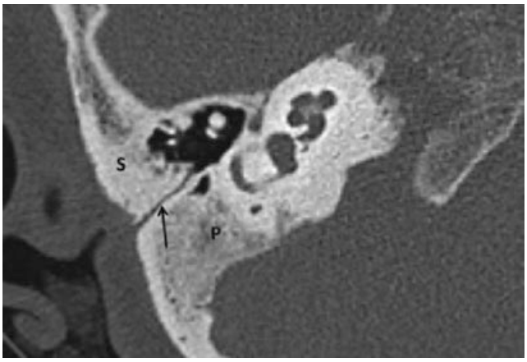

Fig. 1.10 Transversal computed tomography of the right temporal bone of a child with hereditary cleidocranial dysostosis: prominent petrosquamous suture (black arrow) that could be misinterpreted as a temporal bone fracture. *S* squamous bone, *P* petrous bone

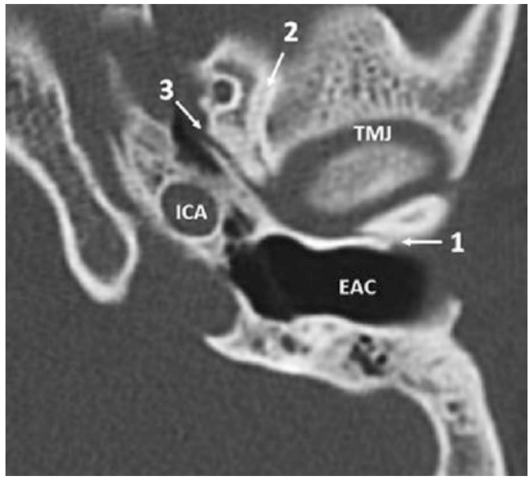

Fig. 1.11 Transversal computed tomography of a left ear, showing the three different sutures appearing with a Y shape. They form together the Glaserian fissure, (1) the tympanosquamous fissure, (2) the anterior petrosquamous fissure, and (3) the posterior petrotympanic fissure. *ICA* internal carotid artery, *EAC* external auditory canal, *TMJ* temporomandibular joint

1.4.5 Temporal Bone Fissures

Four intrinsic fissures form at the fusion lines of the four bones forming the temporal bone.

1.4.5.1 The Petrosquamous Fissure

The petrosquamous fissure or suture connects the petrous bone and the squamous bone and opens directly into the mastoid antrum. It is a narrow fissure and continuous with the petrotympanic fissure.

The external petrosquamous fissure, which links the squamous and the petrous parts of the mastoid process, is sometimes visible on the outer surface of the mastoid process (Fig. 1.10). The internal petrosquamous fissure is located in the tegmen tympani and joins its squamous and petrous portions.

1.4.5.2 Tympanomastoid Fissure

The tympanomastoid fissure or suture anchors the tympanic bone to the mastoid process. This suture is situated in the posteroinferior part of the external auditory canal (see Fig. 1.12).

The auricular branch of the vagus nerve, Arnold's nerve, emerges through the tympanomastoid suture to innervate part of the external auditory canal skin.

1.4.5.3 Tympanosquamous Fissure

The tympanosquamous fissure connects the tympanic bone to the squamous bone. The tympanosquamous fissure is seen in the anterosuperior part of the external auditory canal and continues medially into the petrotympanic and petrosquamous fissures (see Figs. 1.11 and 1.12).

1.4.5.4 The Petrotympanic Fissure

The petrotympanic fissure or Glaserian fissure is situated between the medial aspect of the tympanic bone and the mandibular fossa. It transmits the chorda tympani, the anterior tympanic artery, and the anterior malleal ligament (Fig. 1.11).

Clinical Pearl

In the context of trauma, these normal fissures, especially if evident, may be misinterpreted as temporal bone fractures (Figs. 1.10 and 1.11).

The petrosquamous fissure may remain open until the age of 20 years, providing a route for a spread of infection from the middle ear to the intracranial cavity.

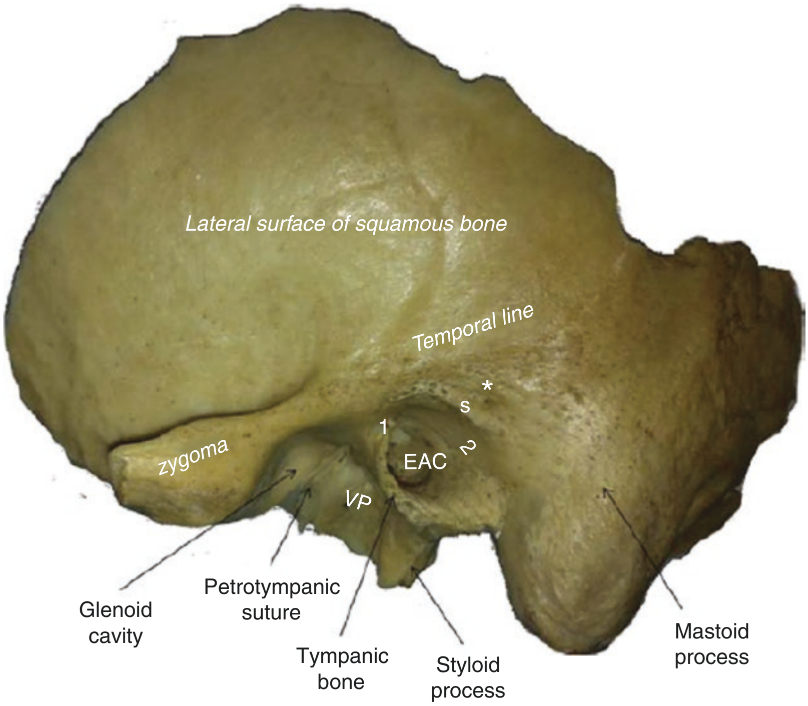

Fig. 1.12 Lateral surface of a left temporal bone. *1* tympanosquamous fissure, *2* tympanomastoid fissure, *EAC* external auditory canal, *S* Henle's spine, * suprameatal triangle, *VP* vaginal process

1.4.6 Temporal Bone Surfaces

The temporal bone exhibits four surfaces: the lateral, posterior, superior, and inferior surface.

1.4.6.1 The Lateral Surface (Fig. 1.12)

The squama constitutes the major part of the lateral surface of the temporal bone and extends upward as a flat bone to cover part of the temporal lobe of the cerebrum.

The lateral surface of the squama shows a vertical groove for the middle temporal artery and serves as an area of attachment for the temporalis muscle. The medial surface of squama is grooved for the branches of the middle meningeal artery. Inferior to the squama, the external auditory canal is located. The tympanic bone forms the anterior, inferior, and posterior walls of the bony external auditory canal. The hiatus between the tympanic bone and the squamous bone corresponds to *the notch of Rivinus.* Anterior to the external auditory canal is the temporomandibular joint; a thin bony shell separates them from each other.

Several important landmarks characterize the lateral surface of the temporal bone:

- *The mastoid process* refers to the bony process located on the posteroinferior border of the lateral surface of the temporal bone. Two distinct bones contribute to the formation of the mastoid process: the anterosuperior portion is formed by squamous bone, and the petrous bone forms the posteroinferior portion. These processes serve laterally for the attachment of the sternocleidomastoid muscle and medially to the posterior belly of the digastric muscle (see Sect. 5.2).
- *The zygomatic process* originates above the external auditory canal. It leaves the squama and projects anteriorly to unite the zygomatic bone. On the inferior surface of the zygomatic process is the mandibular or glenoid fossa, which accommodates the condyle of the mandible. The anterior limit of the glenoid fossa is demarcated by the articular eminence; the postglenoid process demarcates its posterior limit. The glenoid fossa communicates with the middle ear through the petrotympanic fissure.
- *The temporal line or supramastoid crest*: posterior to the external auditory canal, the zygomatic process prolongs as a faint line or the supramastoid crest. This crest serves for the attachment of the temporal muscle. It is an

important landmark for the level of middle cranial fossa dura.

- *Suprameatal Mac Ewen's triangle*: located between the posterosuperior wall of the external auditory canal and the temporal line. This triangle corresponds medially to the antrum.
- *Henle's spine*: it is a bony spine implanted on the posterosuperior edge of the external auditory canal; it corresponds to the aditus ad antrum medially.
- *The scutum* is a sharp bony spur formed at the junction of the lateral wall of the middle ear cavity and the superior wall of the external auditory canal, part of the squamous bone.

1.4.6.2 Posterior Surface

The posterior surface of the temporal bone is formed exclusively by the petrous part. It represents the anterolateral wall of the posterior cranial fossa. This surface is limited superiorly by the sulcus for the superior petrosal venous sinus, which separates the superior and the posterior surfaces of the petrous bone. Laterally it presents the sigmoid sinus sulcus and the internal orifice of the emissary vein canal.

The most important feature of the posterior surface is the internal auditory meatus, which lies in the center of this surface midway between the apex and the anterior border of the sigmoid sinus sulcus. An important structure situated at the lateral part of this surface is the endolymphatic sac; this sac lies medial to the level of the posterior semicircular canal (Fig. 1.13).

The average dimensions of the internal auditory canal are 1 cm horizontally and 0.5 cm vertically. The mean distance from the highest border of the jugular bulb to the inferior border of the internal auditory canal is about 0.5 cm [28] (Fig. 1.14). The mean distance from the lateral border of the internal auditory canal to the endolymphatic sac is about 1 cm [29].

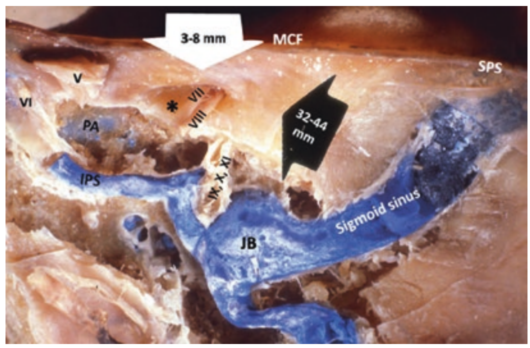

Fig. 1.14 Posterior surface of a right temporal bone showing the relation of the internal auditory canal (*) with the sigmoid sinus (black arrow), the middle cranial fossa (MCF) (white arrow), and the jugular bulb (JB). *SPS* superior petrosal sinus, *IPS* inferior petrosal sinus, *PA* petrous apex, *V* fifth CN, *VI* sixth cranial nerve in Dorello's canal, *IX, X, XI* ninth, tenth, and eleventh CN

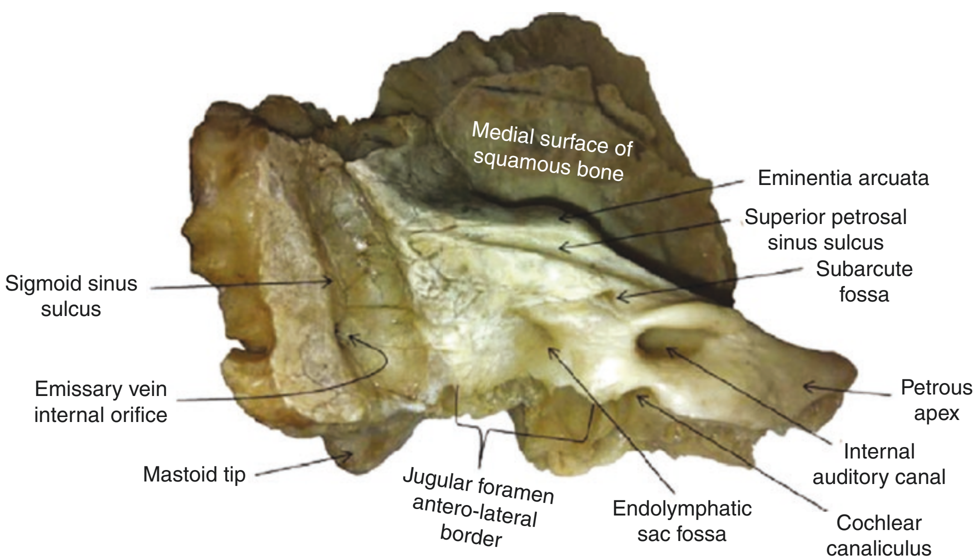

Fig. 1.13 Posterior surface of a left temporal bone

Based on these measurements mentioned above, 0.5 cm of bone can be safely drilled away from the posterior lip of the canal without injuring any structure.

1.4.6.2.1 Retrosigmoid Approach (Fig. 1.15)

The retrosigmoid approach is versatile for the treatment of different pathologies of the posterior surface of temporal bone and cerebellopontine angle. The narrow corridor created by this approach provides adequate exposure of the contents of the cerebellopontine angle and IAC. It is the most common approach for exposing the IAC with a trajectory parallel to the petrous surface. It allows resection of tumors of different sizes with the possibility of preserving facial and cochlear function.

Surgical Implications

During retrosigmoid approach for hearing preservation surgery in vestibular schwannoma, drilling of the posterior lip of the internal auditory canal may be necessary in order to remove the intrameatal portion of the tumor. This step carries a risk of injuring the posterior semicircular canal or a high-riding jugular bulb.

1.4.6.3 Superior Surface (Fig. 1.16)

The superior surface of the temporal bone forms part of the middle cranial fossa floor; it is limited posteromedially by the superior petrosal sinus sulcus.

The superior surface presents from lateral to medial several structures that serve as important surgical landmarks during middle cranial fossa approach.

- *Tegmen Tympani*
  The most lateral part of this surface contains the tegmen tympani, which separates the middle cranial fossa from the middle ear. It is formed partly from the caudal portion of the squamous bone, which extends medially to join the petrous bone. The petrous bone forms the major part of the tegmen. The fusion line of the two bones forms the petrosquamous fissure.
- *Eminentia Arcuata*
  The eminentia arcuata is an important surgical landmark. It lies on the posterior part of the superior surface, near the superior petrosal sinus, about 20–25 mm from the inner tablet of the cranium [30, 31]. It corresponds to the wall of the superior semicircular canal. Usually the posterior aspect of the eminentia arcuata is rotated lateral to the posterior crus

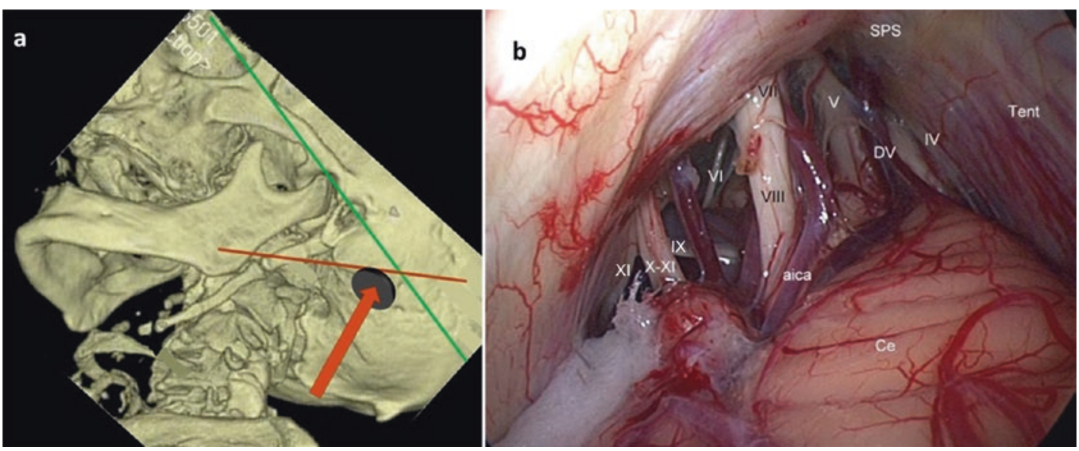

Fig. 1.15 Retrosigmoid approach. (**a**) Craniotomy site (black hole) is just behind the sigmoid sinus (red line) and below the lateral sinus (green line), it allows full exposure of the posterior surface of the temporal bone and cerebellopontine angle. (**b**) Left cerebellopontine angle: *tent* tentorium, *IV* trochlear nerve, *SPS* superior petrosal sinus, *DV* Dandy vein, *V* trigeminal nerve, *VII* facial nerve, *VIII* cochleovestibular nerve, *AICA* anterior inferior cerebellar artery, *VI* abducens nerve, *XII* hypoglossal nerve, *IX* glossopharyngeal nerve, *X* vagus nerve, *XI* accessory nerve, *Ce* cerebellum

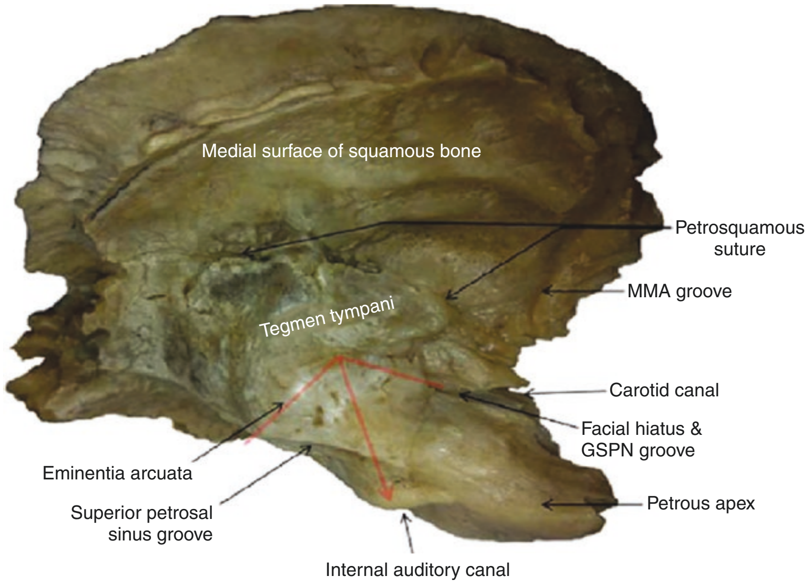

Fig. 1.16 Superior view of a left temporal bone. The red lines represent the relation of the internal auditory canal with respect to the eminencia arcuata and the greater superficial petrosal nerve (GSPN), middle meningeal artery (MMA)

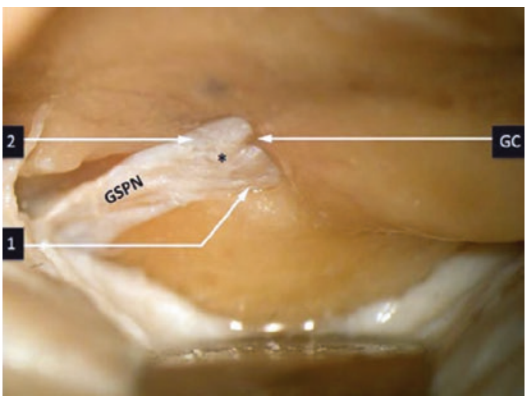

Fig. 1.17 Middle cranial fossa view of a right-side facial nerve. View after drilling off the bone covering the geniculate ganglion (*). *G.C.* geniculate crest; (1) labyrinthine segment of facial nerve; (2) tympanic segment of facial nerve (Courtesy of Dr Tardivet [33])

of the superior semicircular canal, but the anterior aspect of the eminentia arcuata is located over the anterior crus of this canal [30, 32].

- *Greater Superficial Petrosal Nerve and Geniculate Ganglion* (Fig. 1.17)
  The superior surface of the temporal bone is marked also by the geniculate ganglion and the greater superficial petrosal nerve, which runs from the geniculate ganglion to the middle cranial fossa. The distance from the geniculate ganglion and the inner tablet of the cranium is of 2.7 mm. Embryologically, two bony plates form the bony roof of the geniculate ganglion and the proximal part of the greater superficial petrosal nerve bony canal: a medial plate, which is a periosteal derivative of the petrous bone, and a lateral plate, which is a membranous derivative from the squamous bone.

Surgical Implication

The geniculate ganglion could be dehiscent in 15–20% of cases. In these cases, the risk of injuring the facial nerve during middle cranial fossa approach is very high while elevating the dura mater from the superior surface of the temporal bone [30, 34, 35]. (Fig. 1.18).

In middle cranial fossa approach, the internal auditory meatus is within 3–8 mm distant from the superior border of the petrous bone. The bisection of the angle formed by the greater superior petrosal nerve and the eminence arcuate marks the position of the internal auditory meatus (Fig. 1.16).

- *The Petrous Apex*
  The petrous apex is situated in the angular interval between the posterior border of the sphenoid and the basilar part of the occipital bone. The main portion of the apex lies anterior to the cochlea. Through the apex, the internal carotid artery exits the petrous bone through the foramen lacerum, which is found between the apex and the sphenoid bone (Fig. 1.19).

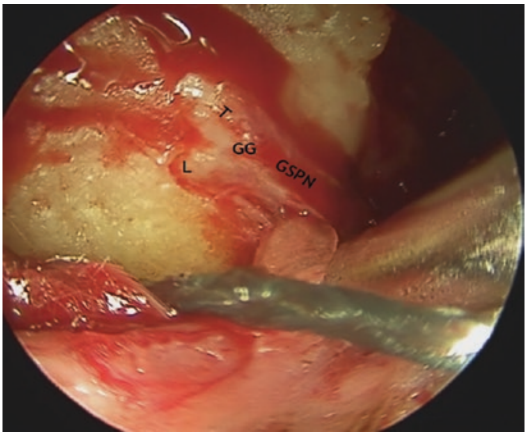

Fig. 1.18 Left middle cranial fossa approach showing geniculate ganglion (GG) dehiscence. *T* tympanic segment, *L* labyrinthine segment, *GSPN* greater superficial petrosal nerve

1.4.6.3.1 Middle Cranial Fossa Approach

The middle cranial fossa approach is an extradural access route to approach the superior surface of temporal bone and IAC. The access through this approach is via a small temporal craniotomy, and visualization can be difficult owing to the limited extradural space available and desire not to apply too much retraction on the temporal lobe (Fig. 1.20).

Common neurotologic indications for middle cranial fossa approach are facial nerve decompression, superior semicircular canal dehiscence repair (Fig. 1.20), repair of large tegmen defects and meningoencephalocele, and removal of small intracanalicular acoustic neuroma.

Fig. 1.19 Anteromedial view of a left petrous bone showing the petrous apex and the exit orifice of the carotid canal (CA) from the temporal bone anterolateral to the petrous apex. Notice the position of the ET isthmus and the tensor tympani muscle (TTM) semicanal lateral to the carotid canal

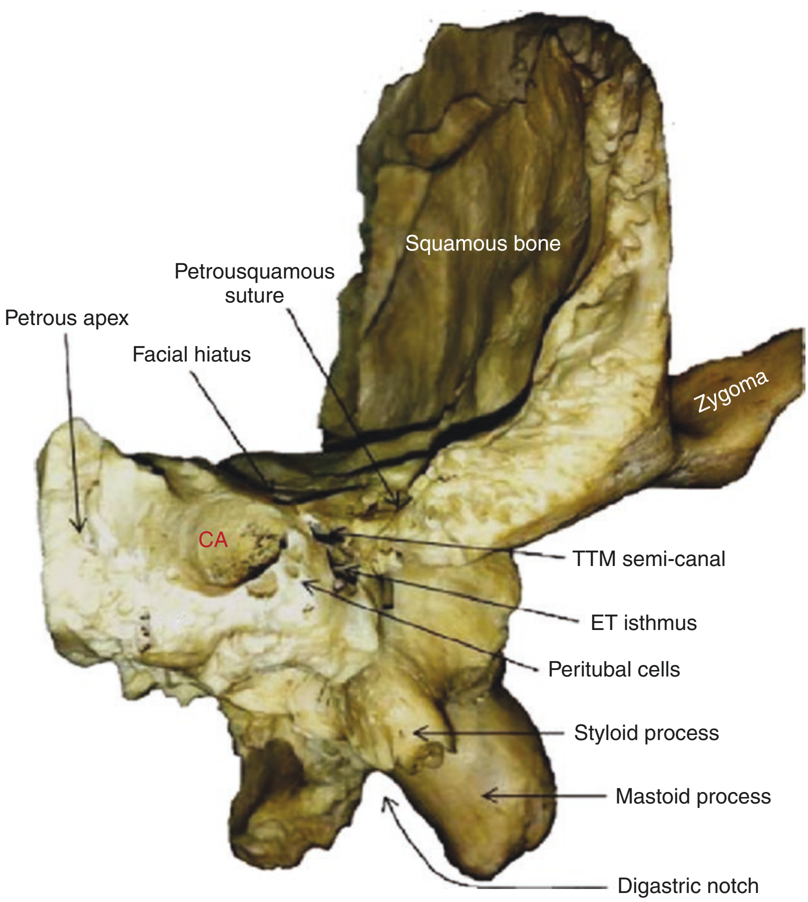

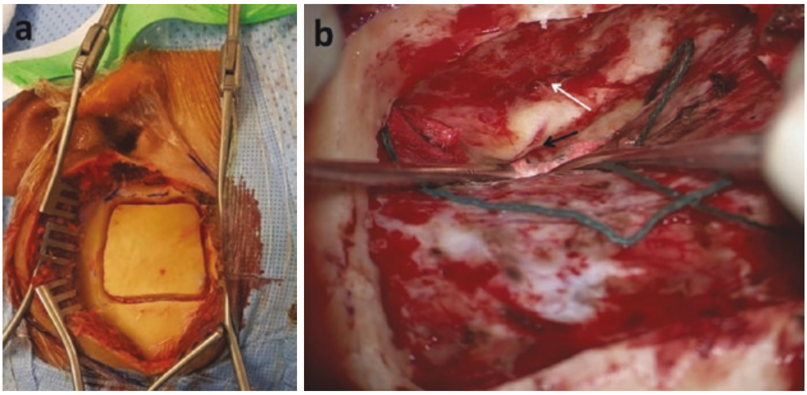

Fig. 1.20 Middle cranial fossa approach for left super semicircular dehiscence plugging, (**a**) Incision and elevation of skin flaps: from tragus up 4–5 cm above helical root and curve slightly to forehead; skin incision to level of TP fascia. Elevate skin flap in plane of TP fascia. Muscle flap elevation. Elevate the temporalis off the calvarium using periosteal elevator. Temporal craniotomy/bone flap of 4 × 5 cm centered over zygoma (zygoma estimates level of floor of middle fossa). Remove the bone flap and set aside for later. (**b**) Retraction of temporal lobe (bipolar cautery can be used judiciously to contract the dura and decrease the need for mechanical retraction). Carefully dissect the dura off of the middle fossa floor in a posterior to anterior direction (prevents avulsion of the GSPN). Dissect dura off the GSPN taking care to leave the nerve down while elevating the dura up with the temporal lobe. Arcuate eminence and SSCC dehiscence identified clearly (black arrow). Notice the associated tegmental defect (white arrow)

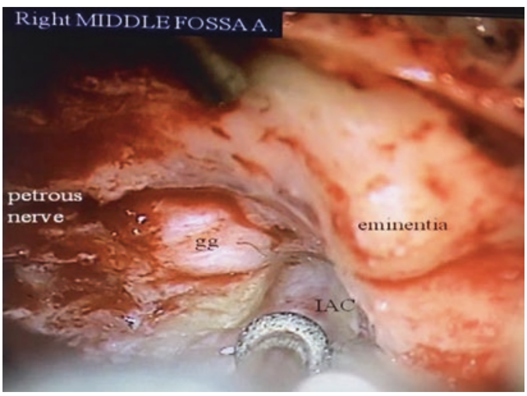

Fig. 1.21 Middle cranial fossa approach to the right internal auditory canal using retrograde technique. After identification of petrosal nerve, retrograde drilling is carried on until the geniculate ganglion is identified, and then the labyrinthine segment of facial nerve is identified and tracked medially until the internal auditory canal dura is exposed

The lack of definitive landmarks on the superior surface of the temporal bone makes this approach technically difficult. Two important landmarks are the GSPN and the eminentia arcuata (see above). Using the middle cranial fossa approach to access the IAC requires in-depth knowledge of the anatomy of temporal bone to avoid injury to vital structures such as the cochlea, labyrinth, and facial nerve (Fig. 1.21).

1.4.6.4 Inferior Surface (Fig. 1.22)

The inferior surface of the temporal bone represents posterolaterally the inferior part of the mastoid and the digastric notch. Anterior to the digastric notch and posterior to the styloid process is the stylomastoid foramen, from which the facial nerve leaves the temporal bone. Medial to the digastric notch is a shallow groove for the occipital artery.

More anteriorly lies the inferior surface of the tympanic bone, which forms the posterior boundary of the mandibular fossa and expands inferiorly to form the vaginal process.

Anteromedial to the stylomastoid foramen and styloid process is the jugular foramen; it is formed by the petrous bone anterolaterally and the occipital bone posteromedially.

The jugular foramen is separated by the jugular spine and a fibrous band into two fibro-osseous compartments:

1. *Pars vascularis*: posterolateral vascular compartment, which is larger and receives the internal jugular vein, the vagus nerve (CN X) with Arnold's branch, the spinal nerve (CN XI), and the posterior meningeal artery
2. *Pars nervosa:* anteromedial nervous compartment, which is smaller and receives the

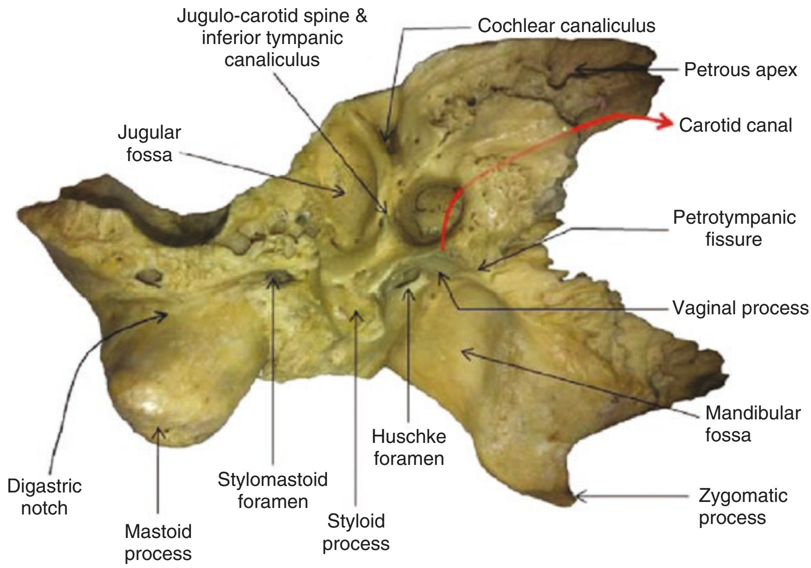

Fig. 1.22 Inferior view of a left temporal bone. The red arrow passes through the carotid canal.

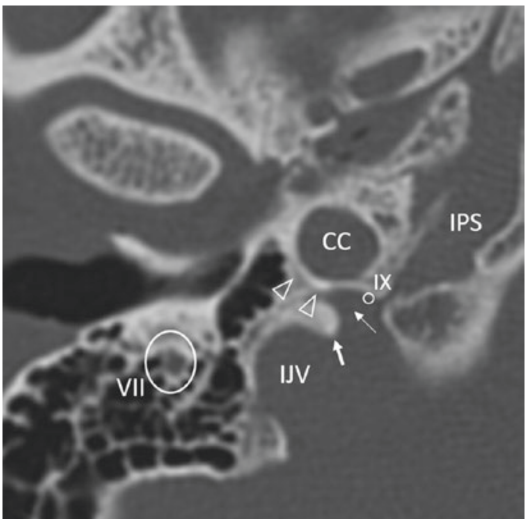

Fig. 1.23 Axial CT-scan of the skull base, intrapetrous carotid (CC), inferior petrous sinus (IPS), pars nervosa (thin arrow), topography of the nerve IX ganglion (circle), jugular spine (thick arrow), pars vascularis with internal jugular vein (IJV), inferior tympanic canaliculus (arrowheads)

glossopharyngeal nerve (CN IX), the Jacobson's branch, and the inferior petrosal sinus [36]

- Posterior to the jugular fossa lies the small canal of Arnold's nerve.
- Medial to the jugular fossa, there is the groove of the inferior petrosal sinus and the opening of the cochlear aqueduct.

The foramen of the internal carotid artery lies anterior to the jugular foramen and is separated from its anterior border by the jugulo-carotid spine through which we find a canal for the passage of Jacobson's nerve (IX) to the tympanic cavity (Fig. 1.23).

Medially, near the petrous apex, the inferior surface presents the site of insertion of the levator veli palatini and the cartilaginous portion of the Eustachian tube.

1.4.6.4.1 Fish Infratemporal Fossa (ITF) Approach

Management of tumors of the inferior surface of temporal bone and of base of skull is one of the most challenging surgeries. The intimate association of these tumors with the carotid artery, jugular vein, and the V through XII cranial nerves has, in the past, rendered many patients inoperable.

The development of the infratemporal fossa approaches, as pioneered by Fisch, has allowed the excision of lateral skull-based lesions which were previously deemed unresectable.

These approaches are classified as Fisch type A, B, and C.

- **Type A Approach** (Fig. 1.24)
  This approach is used for removal of tumors of the jugular foramen involving the vertical segment of petrous internal carotid artery, primarily class C and D glomus tumors. Surgical

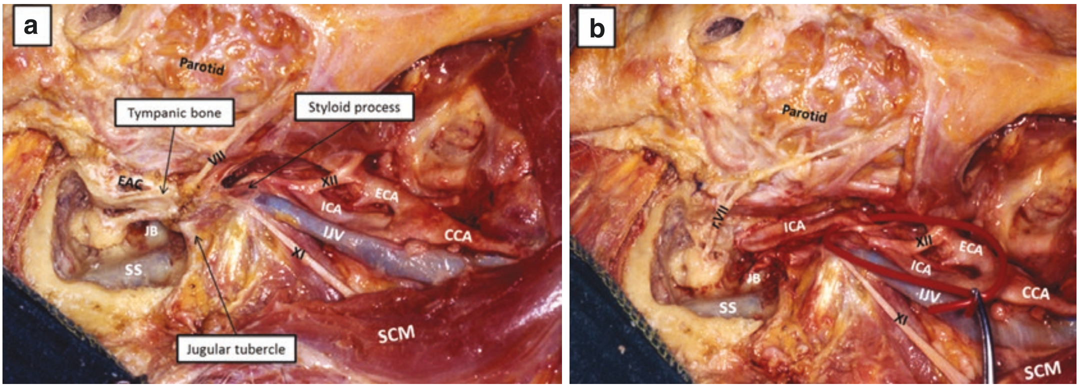

Fig. 1.24 Right side ITF type A. (**a**) A standard, curvilinear postauricular incision extended into the upper neck. The anterior flap is elevated superficial to periosteum over the mastoid and deep to platysma in the neck. The external canal (EAC) is transected at the bony cartilaginous junction, the flap continued forward over the parotid for 2–3 cm. The facial nerve (VII) is dissected from the parotid. The upper neck is next dissected and great vessels (*IJV* internal jugular vein, *CCA* common carotid artery, *ECA* external carotid artery, *ICA* internal carotid artery) and cranial nerves exposed in the neck. The vagus and accessory nerves (XI) are identified as they exit the jugular foramen, and the hypoglossal (XII) is noted as it crosses the carotid bifurcation. The sternocleidomastoid muscle (SCM) is dissected from the lateral and medial mastoid tip and mobilized with the postauricular flap. A well-beveled canal wall down mastoidectomy is next performed, and the sigmoid sinus (SS) and jugular bulb (JB) are completely skeletonized. The entire tympanic and mastoid course of the facial nerve is identified and decompressed to 270° of its circumference, from the geniculate ganglion to the stylomastoid foramen. (**b**) The bony EAC and the tympanic bone are removed, the facial nerve is anteriorly transposed, and the styloid process removed to allow complete exposure of internal carotid artery *ICA*

steps are resumed in (Fig. 1.24).The key point of this approach is the anterior transposition of the facial nerve, which provides optimal control of the infralabyrinthine and jugular foramen regions, as well as the vertical portion of the internal carotid artery.

- **Type B Approach**
  This approach provides access to the clivus and petrous apex and is applicable to glomus tumors involving the horizontal petrous carotid artery, clival chordoma, and congenital cholesteatoma of the petrous apex. In this approach, the skin incision is extended anteriorly, the zygomatic arch is divided, and the petrous carotid artery is skeletonized. The temporomandibular joint is then disarticulated, the Eustachian tube detached anteriorly with associated soft tissue, and the middle meningeal artery and mandibular nerve divided as needed.
- **Type C Approach**
  This approach is an anterior extension of type B and allows for exposure of the parasellar region, nasopharynx, pterygomaxillary fossa, and Eustachian tube. It has been used primarily for extensive juvenile nasopharyngeal angiofibroma and post-radiation failure squamous cell carcinoma.

1.5 Conclusion

The vital neurovascular structures, the intricate three-dimensional relationships involved, and the manner the ear is encased in the temporal bone pose major learning challenges to trainees and surgeons. Structured sessions of cadaver's dissections are mandatory to enable good progress in the understanding of the normal and surgical anatomy of the temporal bone.

Success in ear surgery depends on the hands-on, mastered knowledge of temporal bone anatomical landmarks: only methodological learning provides skills.

References

1. Leland Albright A, David Adelson P, Pollack F. Principles and practice of pediatric neurosurgery, vol. 2. New York: Thieme Publishers; 2007. p. 668–9.

2. Le Douarin NM, Kalcheim C. The neural crest. 2nd ed. Cambridge: Cambridge University Press; 1999.
3. Doden E, Halves R. On the functional morphology of the human petrous bone. Am J Anat. 1984;169(4):451–62.
4. Bast TH. Ossification of the optic capsule in human fetuses. Washington, DC: Carnegie Institution of Washington; 1930.
5. Dahm MC, Shepherd RK, Clark GM. The postnatal growth of the temporal bone and its implications for cochlear implantation in children. Acta Otolaryngol Suppl. 1993;505:1–39.
6. Zhou G, Ohlms I, Ohlms I, Amin M. Superior semicircular canal dehiscence in a young child; implication of development defect. Int J Pediatr Otorhinolaryngol. 2007;71(12):1925–8.
7. Jacquot S, Bertholon P, Chaudron S, Prade J-M, Martin C. Déhiscence du canal semi-circulaire supérieur. Fr ORL. 2006;91:249–25610.
8. Tortori-Donati P, Rossi A, editors. Pediatric neuroradiology: brain, head, neck, and spine. New York: Springer; 2005. p. 1255–65.
9. Schuknecht H. Pathology of the ear. Cambridge: Harvard University Press; 1974. p. 503.
10. Monsour PA, Young WG. Variability of the styloid process and stylohyoid ligament in panoramic radiographs. Oral Med Oral Pathol. 1986;61:522–6.
11. Mallo M, Gridley T. Development of the mammalian ear: coordinate regulation of formation of the tympanic ring and the external acoustic meatus. Development. 1996;122:173–9.
12. Ars B, Decraemer W, Marquet J, Ars-Piret N. Sulcus tympanicus. In: Comptes-rendus du Congrès de la Société Française d'ORL. Paris: Arnette; 1980. p. 401–68.
13. Ars B, Ars-Piret N. Mouvements embryogéniques de l'anneau tympanique. In: Martin H, editor. Comptes rendus du Congrès de la Société Française d'ORL. Paris: Arnette; 1981. p. 117–9.
14. Ars B. Pars Tympanica Ossis Temporalis. Academicalthesis, thèse d'agrégation de l'Enseignement supérieur, University of Antwerp; 1982.
15. Ars B. La partie tympanale de l'os temporal. Cahiers ORL. 1983;18:435–523.
16. Anson BJ, Bast TH, Richamy SF. The fetal and early postnatal development of the tympanic ring and related structures in man. Ann Otol Rhinol Laryngol. 1955;64:802–22.
17. Michaels L, Soucek S. Development of the stratified squamous epithelium of the human tympanic membrane and external canal: the origin of auditory epithelial migration. Am J Anat. 1989;184:334–44.
18. Mallo M, Schrewe H, Martin JF, Olson EN, Ohnemus S. Assembling a functional tympanic membrane: signals from the external acoustic meatus coordinate development of the malleal manubrium. Development. 2000;127(19):4127–36.
19. Yamada G, Mansouri A, Torres M, Stuart ET, Blum M, Schultz M, De Robertis EM, Gruss P. Targeted mutation of the murine goosecoid gene results in craniofacial defects and neonatal death. Development. 1995;121(9):2917–22.
20. Eby TL, Nadol JB. Postnatal growth of the human temporal bone. Implications for cochlear implants in children. Ann Otol Rhinol Laryngol. 1986;95:356–64.
21. Wright A. Chapter 1: Anatomy and ultrastructure of the human ear. In: Kerr GA, editor. Scott Brown's otolaryngology, vol. 1. 6th ed. London: Butterworth Heinemann; 1997. p. 1–50.
22. Gulya AJ. Developmental anatomy of the temporal bone and skull base. In: Glasscock ME, Gulya AJ, editors. Glasscock-Shambaugh surgery of the ear. 5th ed. Hamilton: BC Decker Inc.; 2003. p. 4–7.
23. Ars B. Foramen of Huschke. Valsalva. 1984;60(3):205–11.
24. Simms DL, Neely JG. Growth of the lateral surface of the temporal bone in children. Laryngoscope. 1989;99(8 Pt 1):795–9.
25. Moffat DA, Ramsden RT, Shaw HJ. The styloid process syndrome: aetiological factors and surgical management. J Laryngol Otol. 1977;91(4):279–94.
26. Jung T, Tschernitschek H, Hippen H, Schneider B, Borchers L. Elongated styloid process: when is it really elongated? Dentomaxillofac Radiol. 2004;33(2):119–24.
27. Gözil R, Yener N, Calgüner E, Araç M, Tunç E, Bahcelioğlu M. Morphological characteristics of styloid process evaluated by computerized axial tomography. Ann Anat. 2001;183(6):527–35.
28. Kolagi S, Herur A, Ugale M, Manjula R, Mutalik A. Suboccipital retrosigmoid surgical approach for internal auditory canal—a morphometric anatomical study on dry human temporal bones. Indian J Otolaryngol Head Neck Surg. 2010;62(4):372–5.
29. Koval J, Molcan M, Bowdler AD, Sterkers JM. Retrosigmoid transmeatal approach: an anatomic study of an approach used for preservation of hearing in acoustic neuroma surgery and vestibular neurotomy. Skull Base Surg. 1993;3(1):16–21.
30. Chopra R, Fergie N, Mehta D, Liew L. The middle cranial fossa approach: an anatomical study. Surg Radiol Anat. 2003;24(6):348–51; discussion 352–3.
31. Clerc P, Batisse R. [Approach to the intrapetrosal organs by the endocranial route; graft of the facial nerve]. Ann Otolaryngol. 1954;71(1):20–38.
32. Kartush JM, Kemink JL, Graham MD. The arcuate eminence. Topographic orientation in middle cranial fossa surgery. Ann Otol Rhinol Laryngol. 1985;94(1 Pt 1):25–8.
33. Tardivet L. Anatomie Chirurgicale du nerf facial intrapetreux, Thèse Med, Aix Marseille University; 2003.
34. Dobozi M. Surgical anatomy of the Geniculate ganglion. Acta Otolaryngol. 1975;80(1–2):116–9.
35. Rhoton AL Jr, Pulec JL, Hall GM, Boyd AS Jr. Absence of bone over the geniculate ganglion. J Neurosurg. 1968;28(1):48–53.
36. Roche PH, Mercier P, Sameshima T, Fournier HD. Surgical anatomy of the jugular foramen. Adv Tech Stand Neurosurg. 2008;33:233–63.

2 Middle Ear Cavity

Contents

S. Mansour et al., *Comprehensive and Clinical Anatomy of the Middle Ear*,
https://doi.org/10.1007/978-3-030-15363-2_2

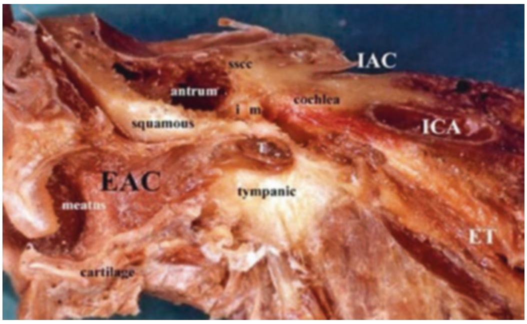

Fig. 2.1 Oblique cut of a right temporal bone. The middle ear cavity lies in the center of the temporal bone between the outer ear (EAC) and the inner ear. *T* the tympanic membrane, *i* incus, *m* malleus, *sscc* superior semicircular canal, *ET* Eustachian tube, *IAC* internal auditory canal, *ICA* internal carotid artery

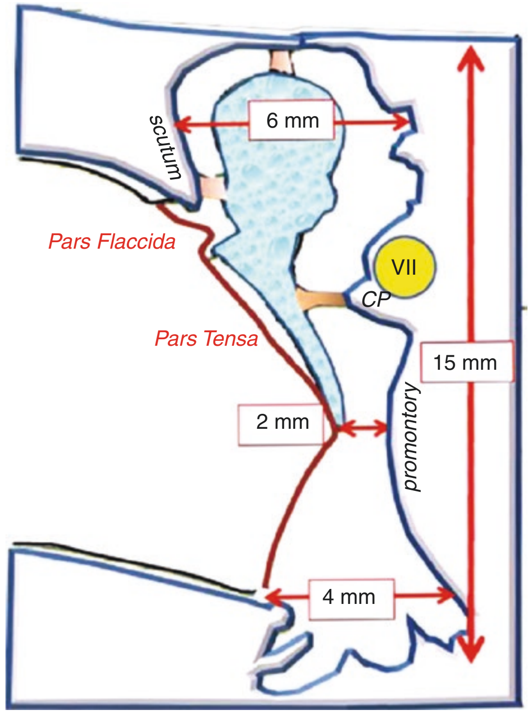

Fig. 2.2 Schematic drawing of the middle ear cavity showing its different dimensions. *VII* facial nerve, *CP* cochleariform process

The middle ear cavity is an irregular air-filled space hollowed out in the center of the temporal bone between the external auditory meatus laterally and the inner ear medially (Fig. 2.1). It lies at the intersection between two important axes: one latero-medial between the external and the internal auditory canal and the other one posteroanterior between the mastoid antrum and the Eustachian tube (see Fig. 1.8).

For descriptive purposes, the tympanic cavity may be considered as a box with four walls, a roof, and a floor. Because of the convexity of the medial wall and the concavity of the lateral wall, the middle ear cavity is constricted at its center. The width of the middle ear cavity is 2 mm at the center, 6 mm superiorly in the attic, and 4 mm inferiorly in the hypotympanum. In the sagittal plane, the middle ear cleft measures about 15 mm both in the vertical and horizontal directions (Fig. 2.2).

The middle ear cavity is in contact with the outside world by the lateral wall and is delimited inferiorly by its floor or the jugular wall, posteriorly by the mastoid wall, superiorly by the roof or tegmen, anteriorly by the carotid wall, and finally medially by the cochlear wall.

2.1 The Lateral Wall

The lateral wall of the middle ear is formed by the tympanic membrane, the bony tympanic ring, and the attic outer wall (Fig. 2.2). It is the only wall accessible to clinical examination, and it is the site of most middle ear pathologies. In addition, the lateral wall represents the classic entrance way to the middle ear during ear surgery.

2.1.1 Embryology of the Lateral Wall

The development of the tympanic bone and membrane starts as early as the fourth week of intrauterine life [1]. All the embryological events take place in an area smaller than 1 mm wide. A funnel-shaped ectodermal groove invaginates inward from the first pharyngeal (branchial) cleft until it reaches an endodermal pouch that evaginates laterally from the first pharyngeal pouch, known as the *tubotympanic recess*. The contact between the ectodermal and the endodermal pouches is short-living.

By the fifth week of the embryological life and due to the growth of the cephalic extremity with its flexion and secondary extension positions, the region of the future neck creates two types of forces: an expansive force and a depressive force. Under the expansive cephalic flexion, the mesenchyme interposes between the ectodermal and the endodermal pouches. *At the seventh week, this mesenchyme contributes to the formation of the fibrous stratum of the tympanic membrane and the handle of the malleus* (Fig. 2.3).

At the eighth week, the epithelial cells at the bottom of the ectodermal pouch proliferate and form a compact epithelial plate reaching the endoderm. Later, this ectodermal plate gives rise to the bony external auditory canal with the tympanic membrane at its end. When the tympanic membrane appears, it consists already of three layers and has an elliptical form with a horizontal diameter of approximately 2 mm.

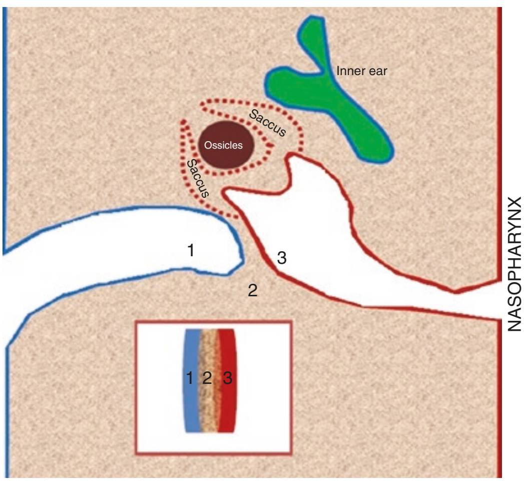

Fig. 2.3 Tympanic membrane formation. The tympanic membrane is formed from the three germ layers: ectoderm (1), mesoderm (2), and endoderm (3)

At birth, the tympanic membrane is almost lying in an horizontal plane (Fig. 2.4a). As the tympanic ring changes its orientation, the caudal tympanic sulcus is pushed laterally, and the tympanic membrane becomes more vertical (Fig. 2.4b) (also see Sect. 1.3). This explains the difficulty of a good exposure of the tympanic membrane in newborns during otoscopic examination or paracentesis.

Clinical Pearl

Congenital Cholesteatoma

Congenital cholesteatomas consist of residual squamous inclusion cysts that arise from epithelial rests in the middle ear. These epithelial rests are normally seen during fetal development and usually disappear by the third trimester. The failed involution of these epithelial rests leads to a congenital cholesteatoma [2, 3].

2.1.2 Lateral Wall Anatomy

The lateral wall of the tympanic cavity is partly bony and partly membranous. The central portion of the lateral wall is formed by the tympanic membrane and the incomplete tympanic ring to which the membrane is attached. Above the tympanic membrane, there is a bony wall forming the attic outer wall.

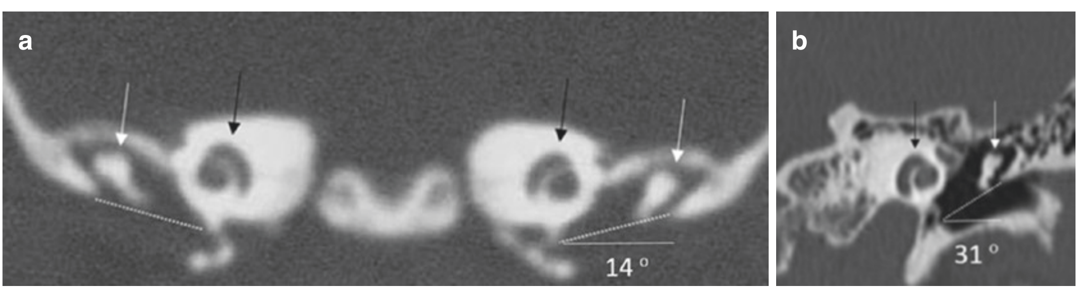

Fig. 2.4 (**a**) Coronal CT reconstruction of a fetal temporal bone, anterior third, showing horizontalization of the tympanic membrane (measured at 14° on the left side) in comparison to (**b**) coronal CT reconstruction of an adult left ear (inclination of the tympanic membrane measured at 31°); incudomalleolar chain (white arrow), cochlea (black arrow)

2.1.2.1 The Attic Outer Wall

The attic outer wall, part of the squamous bone, is the bony lateral wall of the attic. It is a wedge-shaped plate of bone that separates the attic from the zygomatic mastoid cells laterally (Fig. 2.5).

The portion of the attic outer wall lying below the plane tracing the roof of the external auditory canal is called the *scutum* (means shield in Latin).

The scutum is a thin sharp bony spur formed by the junction of the attic outer wall and the superior wall of the external auditory canal. The scutum forms part of the superior deep portion of the external meatus and gives attachment to the pars flaccida of the tympanic membrane, which is the lateral wall of the *Prussak's space* (Fig. 2.5).

Clinical Impact
The scutum is the first bony structure to be eroded by an attical cholesteatoma secondary to a pars flaccida retraction pocket (Fig. 2.5b).

2.1.2.2 The Tympanic Ring

The tympanic ring is the most medial portion of the tympanic bone; it is C shaped and represents the frame in which inserts most of the tympanic membrane's periphery. In the inner aspect of the tympanic ring, there is a gutter, *the tympanic sulcus*, which houses the annulus of the tympanic membrane.

The tympanic ring is deficient superiorly forming the *notch of Rivinus*. The pars flaccida inserts directly on this notch; due to the absence of a sulcus and the lack of the tympanic ring at this site, the pars flaccida is lax and more predisposed to retraction along with invagination of the skin canal (Fig. 2.6).

2.1.2.2.1 The Tympanic Sulcus

Situated at the inner end of the external meatus, the tympanic sulcus houses the annulus of the tympanic membrane. The lateral edge of the tympanic sulcus is higher than the medial edge. The average depth of the sulcus is about 1 mm; however this depth is not constant; it is maximal at 6 o'clock and decreases gradually as it goes up toward the tympanic spines where it disappears superiorly completely at the notch of Rivinus. The posterosuperior part of the sulcus is shallow.

2.1.2.2.2 Tympanic Spines

At the junction of the tympanic ring and the attic outer wall, we can identify two spines—the anterior and the posterior tympanic spines (Fig. 2.6):

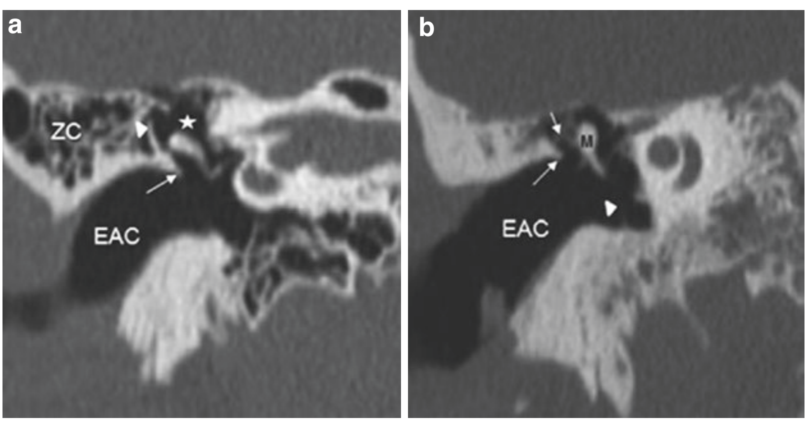

Fig. 2.5 (**a**) Coronal CT reconstruction of a right ear, showing the scutum as a sharp bony spur (arrow) and the attic outer wall (white arrowhead) that separates the attic (*) from the zygomatic cells (ZC). (**b**) Coronal CT reconstruction of a right ear: erosion of the scutum (long arrow), due to a retraction pocket in the Prussak's space with keratin debris (short arrow). Tympanic membrane (arrowhead); *M* malleus, *EAC* external auditory canal

1. Anterior tympanic spine: present at the anterosuperior end of the tympanic ring and represents the anterior limit of the notch of Rivinus
2. Posterior tympanic spine: present at the posterosuperior end of the tympanic ring and represents the posterior limit of the notch of Rivinus

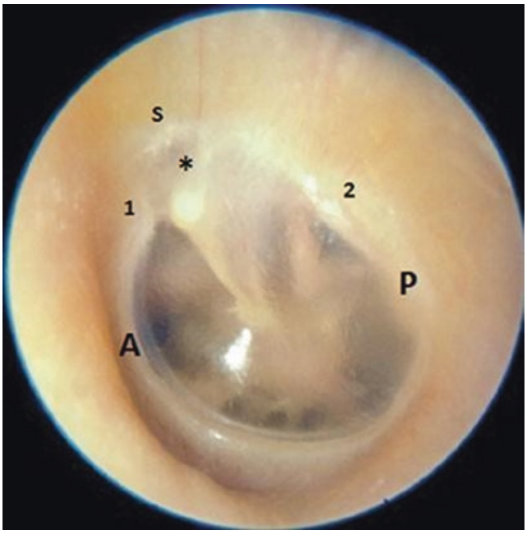

Fig. 2.6 Left tympanic membrane showing the notch of Rivinus (*) limited by the anterior (1) and posterior (2) tympanic spines. Notice the direct insertion of the tympanic membrane on the scutum (S) and the absence of annulus in this zone. Also notice the difference in size between the anterior part (A) and the posterior part (P) of the annulus

2.1.2.2.3 Tympanic Canaliculi

The medial surface of the tympanic ring, near the tympanic spines, presents three openings (Fig. 2.7):

1. *The Petrotympanic Fissure (Glaserian Fissure)*
   The petrotympanic Glaserian fissure opens anteriorly just above the attachment of the tympanic membrane. It is a slit about 2 mm long, which receives the anterior malleal ligament and transmits the anterior tympanic artery, a branch of the internal maxillary artery to the tympanic cavity (see Fig. 1.11).
2. *The Iter Chordæ Anterius (Canal of Huguier)*
   The canal of Huguier is a separate canaliculus placed in the medial end of the petrotympanic fissure; through this canal of Huguier, the chorda tympani nerve leaves the tympanic cavity toward the infratemporal fossa.
3. *The Iter Chordæ Posterius*
   The iter chordæ posterius is situated medial to the posterior tympanic spine. It leads into a minute canal through which the chorda tympani nerve exits to enter the tympanic cavity. It lies immediately medial to the tympanic membrane at the level of the upper limit of the malleus handle.

Fig. 2.7 Schematic drawing of the medial surface of a right tympanic membrane showing the Glaserian fissure containing the anterior malleal ligament (AML), the more medial canal of Huguier giving exit for the chorda tympani to the infratemporal fossa. The chorda tympani enters the middle ear through the iter chordæ posterius

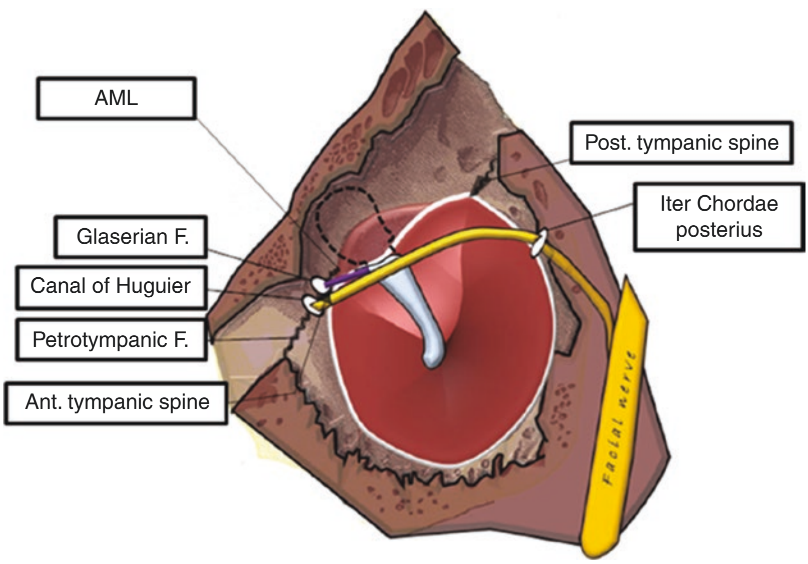

Clinical Implications
The changes in the depth of the tympanic sulcus reflect the stability of the annulus insertion; in the posterosuperior quadrant, the annulus is not totally inserted into the sulcus and is merely supported (Fig. 2.8). This weak insertion of the posterosuperior quadrant of the tympanic membrane in the tympanic ring makes it lax and predisposed to retraction and skin canal migration [4].

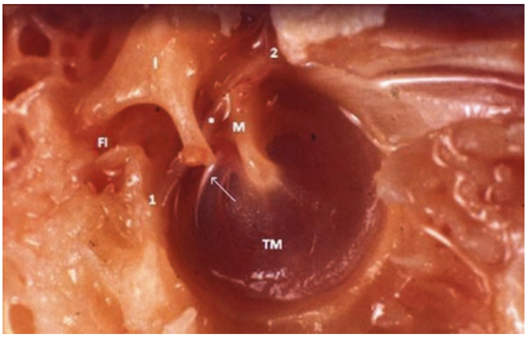

Fig. 2.8 A medial view of the lateral wall of a left middle ear showing the incomplete insertion of the posterosuperior part of the annulus (white arrow) in the tympanic sulcus. *1* Iter chordæ posterius, *2* iter chordæ anterius, *FI* fossa incudis, *TM* tympanic membrane, *M* malleus, *I* incus, * chorda tympani

2.1.2.3 The Tympanic Membrane

The tympanic membrane (TM) separates the external auditory meatus from the middle ear. It is a thin semitransparent membrane that is nearly circular in form and is approximately 8 mm wide, 9–10 mm high, with a mean total area of 85 mm^2 and a thickness of 0.1 mm.

The tympanic membrane, situated at the end of the outer ear canal, shows a particular oblique orientation which allows to the eardrum a larger surface than the ear canal section itself. The inferior part of the tympanic membrane lies more medially than its superior part with an inclination of about 40° relative to the inferior wall of the external auditory meatus (Figs. 2.1 and 2.9). A typical angle between the TM and the superior and posterior wall of the ear canal is 140°, while between the TM and the inferior and anterior wall, it is 30°.

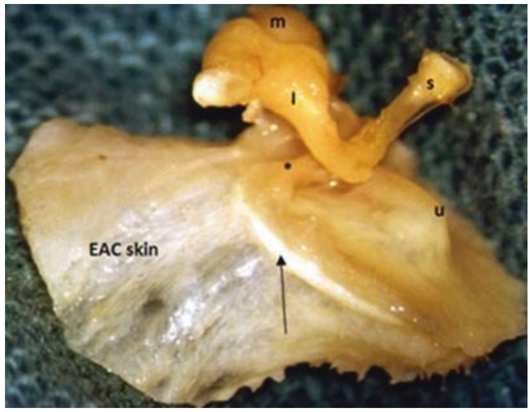

Fig. 2.9 Left ear tympanic membrane allograft showing the annulus (black arrow) and the posterior tympanomalleal fold (*). *I* incus, *m* malleus, *u* umbo, *s* stapes

The TM is almost conical in cross section, its apex points medially toward the middle ear. In physiological conditions, its curved conical shape has a cone angle of 132–137° [5] with a cone depth included in the range 1.42–2 mm [6, 7].

The handle of the malleus is firmly attached to the central part of the inner surface of the TM and draws it centrally; this particular zone of the TM is called *the umbo* (Fig. 2.21).

The periphery of the TM is firmly anchored to the lateral wall of the tympanic cavity by the *tympanic annulus*.

The anterior and posterior malleal ligaments divide the TM into two parts, an upper small part called *pars flaccida* and a lower bigger part called *pars tensa*. The pars tensa, the largest part of the TM, is taut, thickened peripherally into the annulus inserted into the tympanic sulcus. The pars flaccida, or Shrapnell's membrane, is lax; it occupies the notch of Rivinus and is directly attached to the scutum [8].

2.1.2.3.1 The Tympanic Annulus

The tympanic annulus, or Gerlach's ligament, is a horseshoe-like fibrocartilaginous structure that maintains the insertion of the tympanic membrane in the tympanic sulcus (Fig. 2.9). The annulus is absent superiorly at the level of the notch of Rivinus.

In cross section, the annulus shows a triangular form with a summit pointing toward the pars tensa and a base inserted on the tympanic sulcus [9].

At the level of the tympanic spines, the tympanic annulus extends centrally toward the lateral process of the malleus constituting two strands: the anterior and the posterior tympano-malleal strands. These two strands divide the tympanic membrane into the pars flaccida superiorly and the pars tensa inferiorly. Medially, these two strands rise up two slight ridges of mucous membrane on the inner aspect of the tympanic membrane called the anterior and posterior tympano-malleolar folds (Fig. 2.9).

The diameter of the annulus is not uniform. The mean caliber of the annulus is at 6 o'clock level; from this point, the annulus gradually thins out in both directions until it reaches about 15% of its maximal caliber at the anterior and posterior tympanic spines [4, 10] (Fig. 2.6).

Surgical Application

During middle ear surgery, the annulus allows an operative delivery of the tympanic membrane out of the sulcus without tearing it. The most difficult part of the annulus to dislodge is the anterior part because of its firm attachment to the sulcus.

2.1.2.3.2 Microscopic Structure of the Tympanic Membrane

The pars tensa and pars flaccida differ in structure despite the fact that they are both made of three layers: a lateral epidermal layer, a medial mucosal layer, and an intermediate fibrous layer (middle connective lamina propria of mesenchymal origin) (Fig. 2.10).

1. **The Epidermal Layer**

   The thin epidermal layer is continuous with the epidermis of the external canal, and it is a typical keratinizing epithelium composed of four strata, made of different cell types. The epidermis of the TM and the bony part of the external ear canal is a specialized type of skin: it does not contain any glands or hair follicles, and it has a potential of lateral migration not encountered in any epidermis elsewhere. Epithelial cells migrate centrifugally outward from the center of the drum desquamating only when they reach the cartilaginous portion of the ear canal. This process accounts for the self-cleaning ability of the ear canal [11].

2. **The Mucosal Layer**

   The mucosal layer of the eardrum is a continuation of the mucosal lining of the middle ear cavity. It is a very thin monocellular layer of cells.

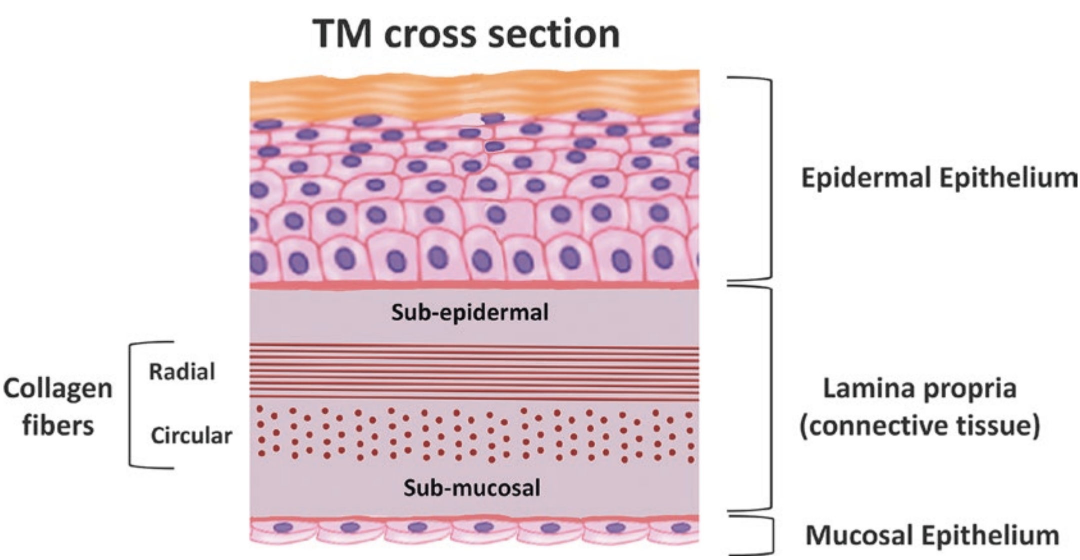

Fig. 2.10 Schematic drawing of tympanic membrane microscopy showing the three layers of the tympanic membrane

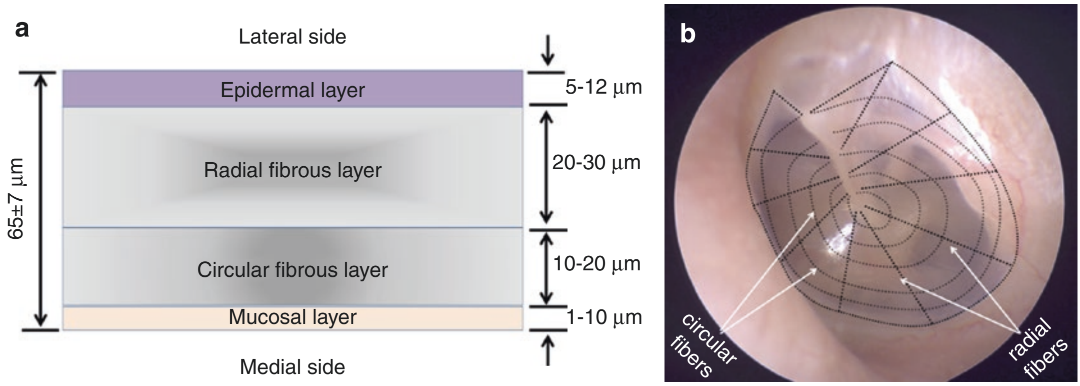

Fig. 2.11 (**a**) A schematic diagram of a typical TM cross section through the pars tensa showing the arrangement and thickness of different layers, (**b**) schematic fiber orientation in human TM

3. **Lamina Propria**

   This is the intermediate layer. It consists of fibrous tissue. The amount and organization of this fibrous tissue represents the main difference between the pars tensa and the pars flaccida of the TM.

Pars Tensa

The lamina propria of the pars tensa is attached to the malleus handle and to the tympanic bone and consists of two layers of densely packed collagenous fibers; one is oriented radially and another one oriented circularly [12, 13]: (Fig. 2.11).

1. *The radial fibrous layer* (stratum radiatum) is attached to the manubrium and radiates outward to the annulus.
2. *The circular fibrous layer* (stratum circulare) lies medial to the radial layer and has its fibers arranged concentrically to insert on the manubrium. The circular fibers reinforce the radiating fibers peripherally to become thickened at the margin of the drum, forming the annulus tympanicus.

The radial fibers become more packed as they converge on the manubrium, while the circular fiber layer grows thicker toward the periphery. These collagen fibers exhibit a viscoelastic and orthotropic behavior with membrane (or in-plane) properties different from through-thickness (or out-of-plane) properties [5] (Fig. 2.11).

It is to emphasize that the overall membrane thickness is not uniform but tapered from the periphery to the umbo.

Pars Flaccida

The lamina propria of the pars flaccida is composed of small amounts of elastic and collagenous fibers with no special arrangement and gradually passes into the dermis of the meatal skin [14].

2.1.2.3.3 Blood Supply of the Tympanic Membrane

1. *Inner surface of the tympanic membrane*: supplied by a vascular circle formed by anastomosis of the *anterior tympanic artery* (branch from the internal maxillary artery) and a branch from the stylomastoid (branch of the posterior auricular artery) (Fig. 2.12)
2. *Outer surface of the tympanic membrane*: supplied by the arteria manubrio having origin from the deep auricular branch of the internal maxillary artery.

2.1.2.3.4 Nerves of the Tympanic Membrane

The tympanic membrane receives its innervation from the auriculotemporal branch of the mandibular nerve (CN **V3**), the tympanic branch of the glossopharyngeal nerve (CN **IX**), and the auricular branch of the vagus (CN **X**).

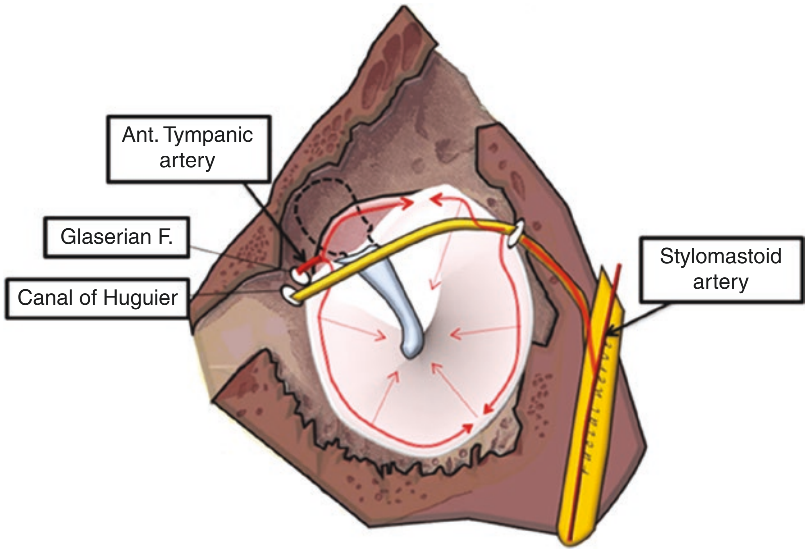

Fig. 2.12 Medial view of a left tympanic membrane showing tympanic membrane vascularization

1. *Outer surface*:

   Similar to the external ear skin canal, the outer surface of the tympanic membrane is innervated by several nerve branches (Fig. 2.13).

   (a) The auriculotemporal branch of the mandibular nerve V3 *supplies the anterior and aspects of the external tympanic membrane*.

   (b) The auricular branch of facial nerve (CN VII) innervates *the posterosuperior portion of the tympanic membrane*.

   (c) The auricular branch of *vagus nerve* (CN X) *innervates the posteroinferior portion of the tympanic membrane* (*Arnold's nerve*).

2. *Inner surface*:

   The medial surface of the tympanic membrane and middle ear are similarly innervated primarily by the tympanic plexus of the glossopharyngeal nerve IX.

Clinical Application

Tympanic Membrane Retraction Pockets

Pars flaccida retraction pockets

The pars flaccida is the most common area of TM retraction pockets because it is the weakest part of the TM. Two reasons stand behind this weakness:

– Sparse amount of unorganized fibers in its lamina propria
– Direct insertion of the skin of the pars flaccida on the scutum in the absence of the combination annulus-sulcus, which acts like a ligament stabilizing the insertion of the TM to the surrounding bone [15]

Pars tensa retraction pockets

Pars tensa retraction pockets are more common in its posterosuperior part. Three reasons stand behind this fact:

– This part of the TM is more vascularized and thus more vulnerable to inflammation, which leads to secretion of collagenase and destruction of collagen fibers. This renders this part of the TM atrophic and prone to retraction in case of middle ear negative pressure.
– The middle fibrous layer of the posterosuperior part lacks a well-developed circular fibrous layer.
– The weak annulus insertion on the tympanic ring because of a shallow sulcus at this level [4].

In contrary, the anterosuperior quadrant of the TM is less prone to retraction because of its strong insertion into the sulcus, the better arrangement of its circular fibers and the presence of the anterior malleal ligament acting as a support [4].

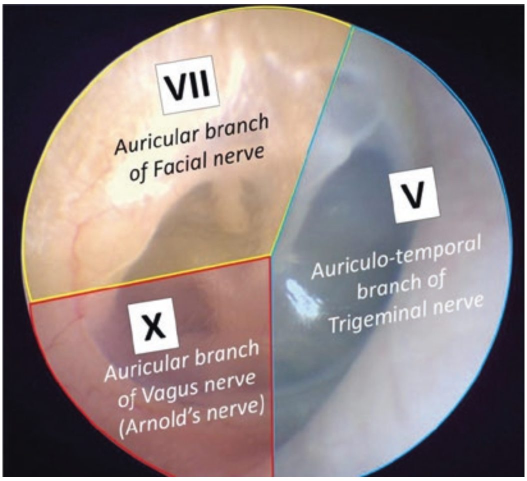

Fig. 2.13 Pattern of neural innervations of the outer surface of the tympanic membrane. Notice its similarity to the vascular topography of the external aspect of the tympanic membrane

2.1.3 Mechanics of the Tympanic Membrane

During evolution steps, human middle ear had to play two major roles: **impedance matching system** and **amplifier**. As part of the middle ear, the tympanic membrane acts essential role in both middle ear functions.

The unique anatomical shape and material properties of the TM contribute to its motion. Thus the function of the TM relies on its specific motion and how that motion transduces sound to the middle ear ossicles. Certain portions of the tympanic membrane move differently depending on the frequency of sounds:

- At low frequencies, the entire tympanic membrane moves in one phase (the entire tympanic membrane and malleus vibrate as a single unit).
- At higher frequencies, the tympanic membrane divides into smaller vibrating portions that vibrate at different phases [16].

2.1.3.1 Role in the Middle Ear Impedance Matching System

Sounds impinging on the external ear are airborne; however, the environment within the inner ear, where the sound-induced vibrations are converted to neural impulses, is aqueous. There is an impedance mismatch between the outer (air) and inner ear (fluid), and the major function of the middle ear is to match relatively low-impedance airborne sounds to the higher-impedance fluid of the inner ear. For instance, in the absence of functioning middle ear structures, 99.9% of sound is reflected at the oval window due to high impedance of fluid in the cochlea (only 0.1% of the sound is transmitted = **−30 dB sound loss from air-fluid impedance mismatch,** Fig. 2.14).

The tympanic membrane is designed to absorb acoustic energy from the external ear canal, transform it into a mechanical vibration, and transmit it to the ossicular chain (*mechanical transformer*), which in turn transmits the vibrations to the inner ear fluid.

2.1.3.2 Role in the Middle Ear Amplifier System

The middle ear amplifies the sound before reaching the inner ear, and this amplification is frequency dependent; it is 20 dB at 250–500 Hz, maximal of 28 dB at 1000 Hz, and decreases at high frequencies about 6 dB for each additional 1 kHz above 1000Hz [17].

Three mechanisms for sound amplification exist:

1. *Hydraulic Lever*
2. *Catenary lever*
3. *Lever action of the ossicles* (1.3:1)

The tympanic membrane plays a major role in the hydraulic and catenary lever system:

– **Hydraulic lever**: The hydraulic lever acts because of the size difference between the tympanic membrane and the stapes footplate. Sound pressure collected over the large area of the tympanic membrane and transmitted to the area of the smaller footplate results in an increase in force proportional to the ratio of the areas. The average ratio has been calculated to be 21:1, and gain (**+26 dB SPL**) is boosted by this area ratio between eardrum and stapes footplate (Fig. 2.15).

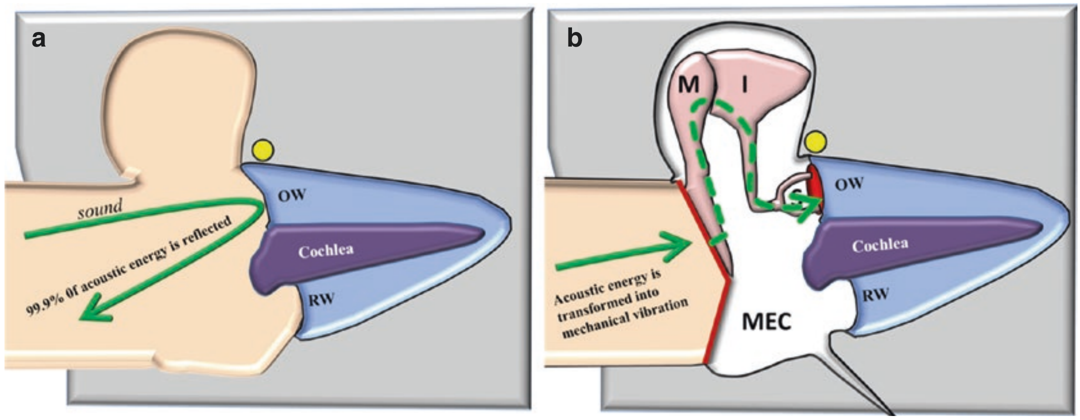

Fig. 2.14 Schematic drawing to show the role of middle ear as impedance matching system. (**a**) in absence of middle ear, 99.9% of acoustic energy will be reflected at the oval window (OW) due to the high impedance of cochlear fluid. (**b**) The middle ear acts as impedance matching system, the tympanic membrane which is surrounded by air on both sides absorbs the acoustic energy and transforms it into mechanical vibrations which will be transmitted by ossicles into inner ear fluid. *M* malleus, *I* incus, *S* stapes, *OW* oval window, *RW* round window, *MEC* middle ear cavity

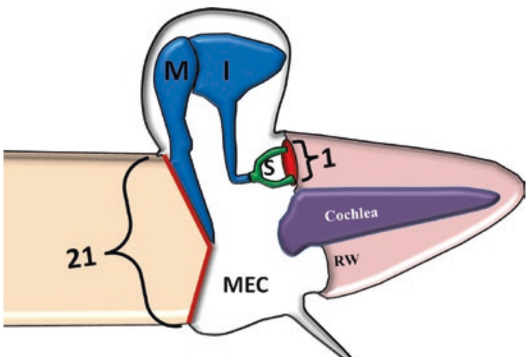

Fig. 2.15 Schematic drawing to show the hydraulic lever of middle ear. The average ratio between the ear drum 21 times larger than the oval window, this means that sound pressure collected at the large ear drum will be transmitted in an amplified manner to the small oval window. *M* malleus, *I* incus, *S* stapes, *MEC* middle ear cavity, *RW* round window

Clinical Applications

TM Perforations and Their Impact on Hearing Loss

The dominant mechanism of tympanic membrane perforation on hearing loss is a reduction in the pressure difference across both sides of the tympanic membrane.

– Hearing loss is largest at the lowest frequency and decreases with increasing frequency.
– Hearing loss increases as perforation size increases.
– Hearing loss does not depend on the location of the perforation.

– **Catenary lever: buckling of the eardrum**

The power of sound in the ear canal is matched to the outer rim of the TM, because the annular ligament surrounding the tympanic membrane is immobile and sound energy is directed away from the edges of the drum and toward the center of the drum via waves that travel on the TM surface. The attachment of the tympanic membrane at the annulus amplifies the energy at the malleus because of the elastic properties of the stretched drumhead fibers and thus works as a **catenary lever** (ratio of force acting on tympanic membrane to that acting on the malleus) where large displacements near the annular ring (the outer edge) produce small displacements of the malleus, so the ear drum itself can increase force when it moves. **This buckling effect increases pressure by a factor of 2 = 6 dB** (Fig. 2.16).

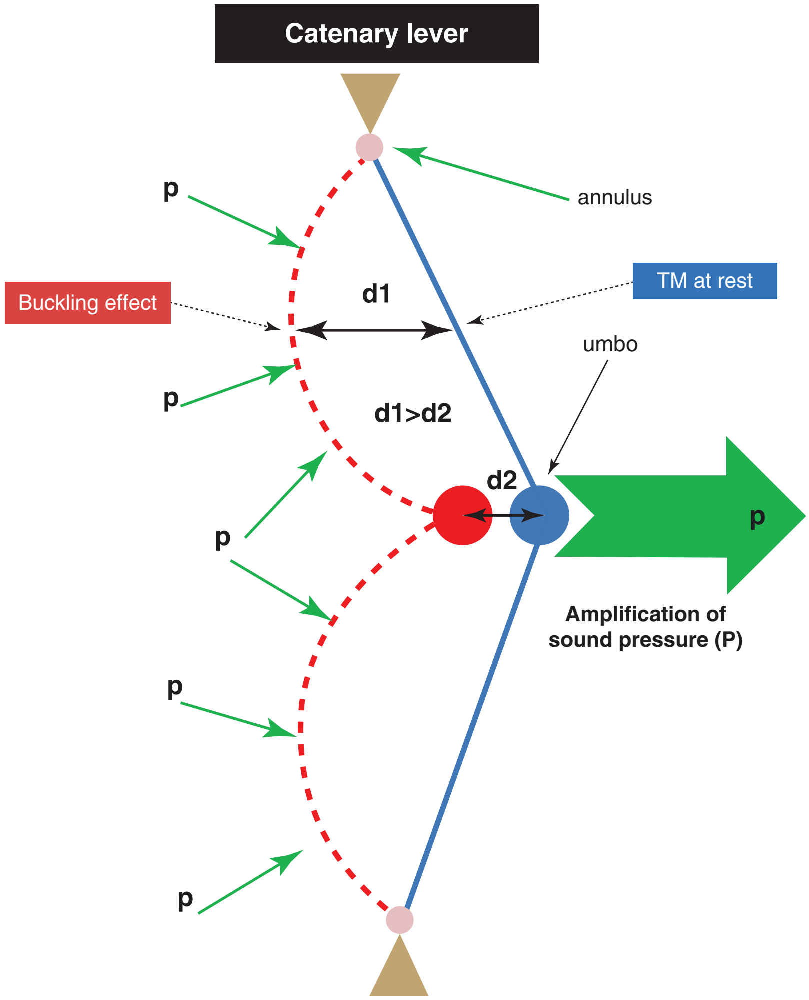

Fig. 2.16 Schematic drawing to show the catenary lever of the tympanic membrane. The attachment of the tympanic membrane (TM) at the annulus amplifies the energy at the malleus where large displacements near the periphery (d1) produce small displacements of the malleus (d2)

2.2 The Inferior Wall (Jugular Wall)

2.2.1 Embryology of the Inferior Wall

The inferior wall of the middle ear develops between the 21st and the 31st gestational week, from the fusion of the tympanic bone and the petrosal bone. The fusion of these two bones, at 24th gestational week, closes the hypotympanum incompletely and leaves a persistent hypotympanic fissure, which houses the inferior tympanic canaliculus. The inferior tympanic canaliculus transmits the Jacobson's branch of the glossopharyngeal nerve (located anterior to the jugular fossa) and the inferior tympanic artery (branch of the ascending pharyngeal artery) [18] to the middle ear (see Fig. 1.2) (see Sect. 1.1.1)

2.2.2 Development of the Jugular Bulb After Birth

The jugular bulb, absent at birth, is a dynamic structure which develops after the age of 2 years and reaches its definite size in adulthood. *Children younger than 2 years old do not demonstrate the typical bulbous enlargement of the jugular bulb.*

The "jugular sinus," present at the junction of transverse sinus and internal jugular vein during fetal life until the age of 2 years (from which the jugular bulb will originate), is surrounded by cartilaginous and bony structures that do not permit expansion during fetal life. This needs the pounding effects of ascending negative pulse waves originating from the right atrium, traversing upward to strike the "jugular sinus." The ham-

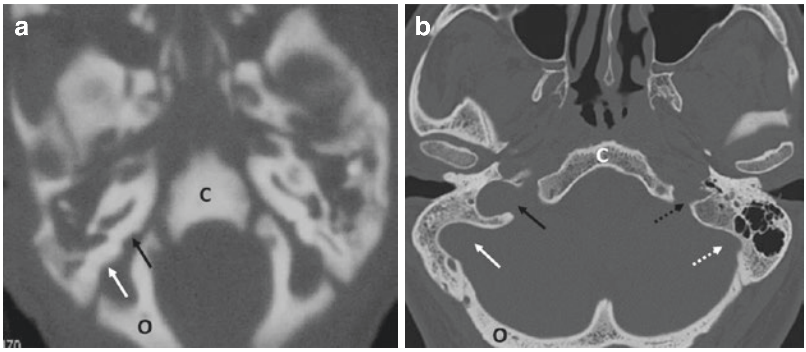

Fig. 2.17 Axial CT of the skull base of a fetus in the last trimester (**a**) in comparison with an adult (**b**): (**a**) Slight impressions visible on the posterior surface of the temporal bone, corresponding to the sigmoid sinus (white arrow) and the jugular bulb (black arrow). The level of the occipital bone (O) is very close to the posterior edge of the temporal bone. (**b**) axial CT-scan of an adult skull base: the sigmoid sinus (white arrow) and the jugular bulb (black arrow) are predominantly developed on the right side, already with a great distance to the occipital bone (O). The left sigmoid sinus (white dashed arrow) and the left jugular bulb (black dashed arrow) are hypoplastic. *C* clivus

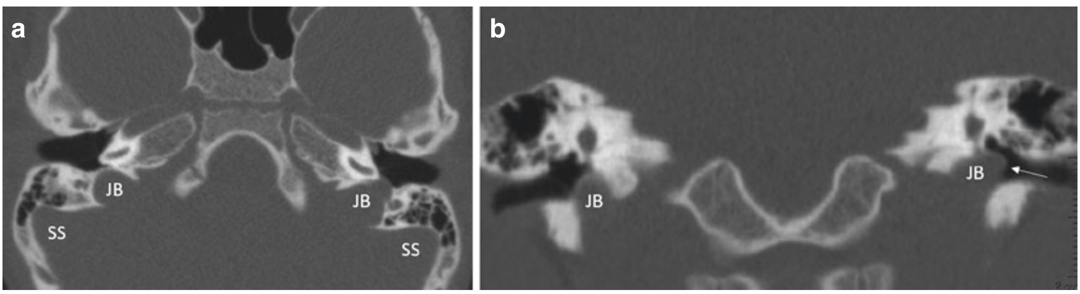

Fig. 2.18 Axial (**a**) and coronal (**b**) CT images of a 7-year-old child at the base of the skull: normal development of sigmoid sinus on both sides (SS) but prominent jugular bulb, (JB) moderatly on the right, very prominent on the left, where it is coming in close contact with the tympanic membrane (arrow)

mering effect (upward forces) of the negative pulse waves, hitting the roof of the "jugular sinus" at near right angle at the base of the skull (jugular foramen), takes place only after the infants assume erect posture (as opposed to the "fetal" or lying down position maintained in utero). These forces create the jugular bulb and enlarge the surrounding bony structures, to form the bony jugular fossa [19–21]. According to Hirakoh [20], the volume of each jugular bulb in adults far exceeds the total combined blood volume of the sigmoid and the inferior petrosal sinuses. (see Figs. 2.17 and 2.18).

As the left brachiocephalic (innominate) vein is relatively longer and more curved than the right one, it may dissipate the energy of the venous pulsations generated from the heart and consequently could explain the development of larger jugular bulb more frequently seen on the right side (see Fig. 2.19). Another possible explanation is that the jugular vein is frequently larger on the right side because its direct alignment with the superior vena cava, allowing a higher flow than at the left side.

There are also theories that the mastoid pneumatization partly determines the location of the jugular bulb; the distance from the external auditory canal to the sigmoid sinus appears to be relatively short in ears with high jugular bulb (Fig. 2.18) [22].

The dynamics of venous blood flow and mastoid pneumatization will ultimately determine the variations in final size and position of the jugular bulb [23].

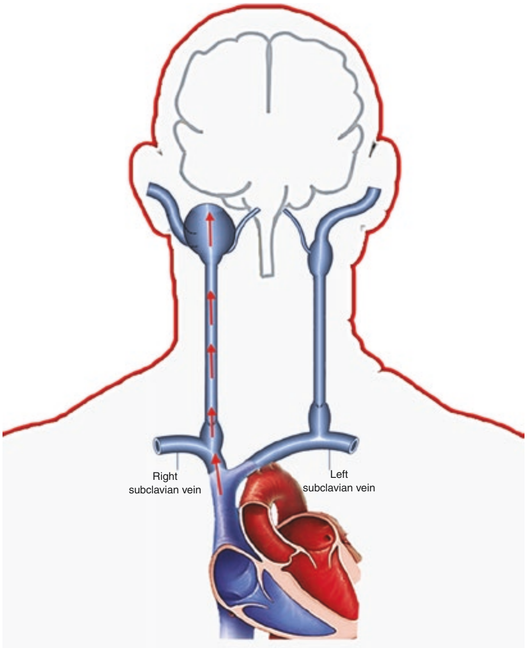

Fig. 2.19 Because the left brachiocephalic vein is longer and more curved than the right one, it may dissipate the energy of the venous pulsation generated from the heart and consequently could explain the development of larger jugular bulb more frequently seen on the right side. Another possible explanation is that the jugular vein is frequently larger on the right side because its direct alignment with the superior vena cava, allowing a higher flow than at the left side.

2.2.3 The Inferior Wall Anatomy

The floor of the middle ear cavity is narrow and consists of a thin plate of bone that separates the middle ear from the jugular bulb posteriorly and the internal carotid artery anteriorly.

In the bone between the carotid artery canal and the jugular bulb fossa, near the medial wall, opens a small canal, the *inferior tympanic canaliculus*, localized near the fossula petrosa which houses the inferior ganglion of the glossopharyngeal nerve (CN IX). It is often a faintly marked depression on the inferior surface of the petrous portion of the temporal bone (Fig. 2.20).

The inferior tympanic canaliculus transmits up to the tympanic cavity *the Jacobson's nerve* (Fig. 2.20), branch of the glossopharyngeal nerve (CN IX), and the inferior tympanic artery (branch of the ascending pharyngeal artery) (Fig. 2.21).

The surface of this wall may show irregularities due to the overlying pneumatized cells. In the posterior part of the floor is the root of the styloid process which gives rise to a bony eminence, the styloid eminence.

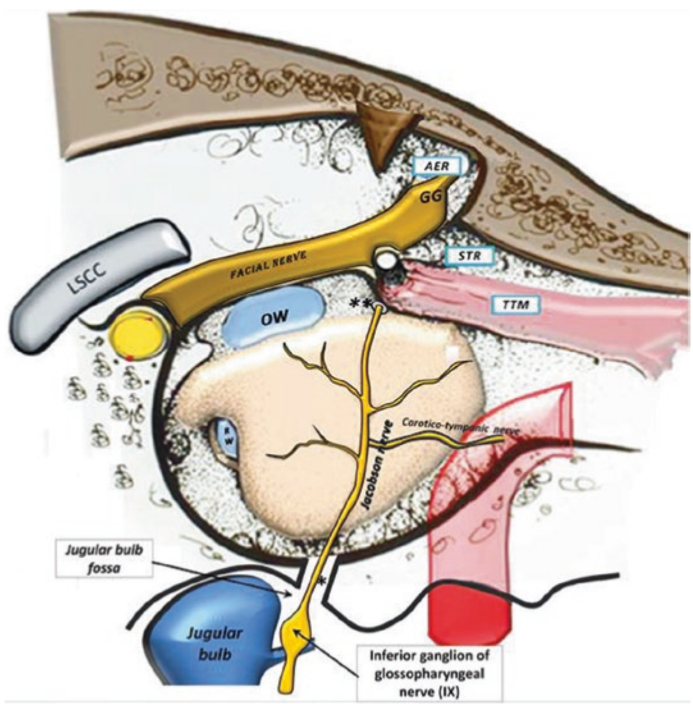

Fig. 2.20 The floor of the middle ear cavity is narrow and consists of a thin plate of bone that separates the middle ear from the jugular bulb posteriorly and the internal carotid artery anteriorly. The *inferior tympanic canaliculus (*) in the inferior wall* gives passage for the Jacobson's nerve originating from the inferior ganglion of IX which is located in the jugular fossa bulb

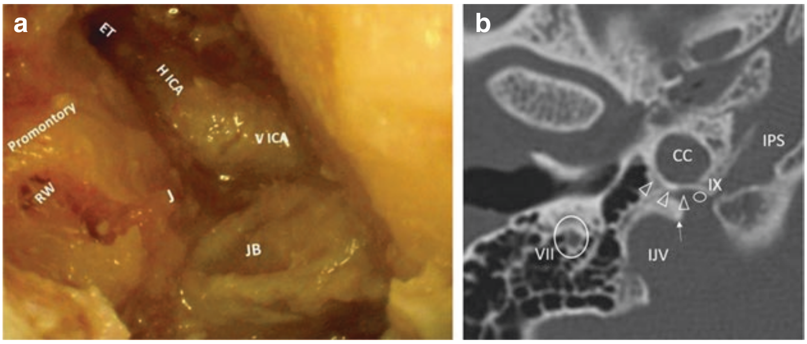

Fig. 2.21 (**a**) Right ear after transcanal hypotympanotomy and dissection of the vertical portion of internal carotid artery (VICA) and the jugular bulb (JB). Notice the emergence of the Jacobson's nerve (J) between the VICA and the JB and its relation to the round window (RW); also notice the relation of the horizontal portion of the internal carotid artery (HICA) and the Eustachian tube (ET); the HICA lies in the medial wall of the Eustachian tube. (**b**) Axial CT-images through the inferior part of the tympanic cavity: intrapetrous carotid (CC), internal jugular vein (IJV), inferior petrous sinus (IPS). Jugular spine (arrow), topography of glossopharyngeal nerve IX (small circle), trajectory of the Jacobson`s nerve indicated by the arrowheads. Facial nerve (VII)

2.2.3.1 Jugular Bulb Anatomy

The jugular bulb connects the sigmoid sinus to the internal jugular vein. It is located in the jugular fossa; posterolaterally within the pars vascularis of the jugular foramen. The jugular bulb inhabits the posterior and largest compartment of the jugular foramen. The cranial nerves IX, X, and XI pass the skull base juxtaposing this venous system. The jugular bulb communicates with the cavernous sinus through the inferior petrosal sinus. The jugular bulb dome lies at the floor of the middle ear cavity below the labyrinth and medial to the mastoid segment of the facial nerve (Fig. 2.22).

Fig. 2.22 Left temporal bone dissection showing the relation of jugular bulb to temporal bone structures. The jugular bulb dome lies at the floor of the middle ear cavity below the labyrinth and medial to the mastoid segment of the facial nerve. *Anteriorly* the jugular bulb is limited by the internal carotid artery, *the posterior limits* of the jugular bulb include the sigmoid sinus, *the superior limits* of the jugular bulb include the hypotympanum and otic capsule. *tt* tensor tympani, *IAC* internal auditory canal, *dig* digastric crest, *gg* geniculate ganglion

- *Anteriorly* the jugular bulb is limited by the internal carotid artery, cochlear aqueduct, inferior petrosal sinus, meningeal branch of the ascending pharyngeal artery, lower cranial nerves, and posterior meningeal artery.
- *The posterior limits* of the jugular bulb include the sigmoid sinus, occipital bone, and facial nerve.
- *The superior limits* of the jugular bulb include the external auditory canal, hypotympanum, posterior semicircular canal (PSCC), vestibule, and the internal auditory canal. The upper limit of the jugular bulb is commonly found under the hypotympanum and an atypical presentation of the jugular bulb may be visualized as an upward extension of the bulb that invades into the hypotympanum [24].

Anatomical Relations of the JB

- Superiorly: external auditory canal, middle ear, posterior semicircular canal, vestibule, internal auditory canal
- Anteriorly: internal carotid artery, cochlear aqueduct, inferior petrosal sinus, meningeal branch of the ascending pharyngeal artery, lower cranial nerves, posterior meningeal artery
- Posteriorly: sigmoid sinus, occipital bone, facial nerve

Right-sided JB dominance is a common finding and is present in 70–80% of cases [23]. It is variably positioned in relation to the hypotympanum, and its distance from the facial nerve laterally and the labyrinth superiorly is variable (Fig. 2.23). The distance from the jugular bulb to the posterior semicircular canal superiorly ranges from 0 to 10 mm (mean 4 mm). The distance from the jugular bulb to the facial nerve laterally ranges from 0 to 12 mm (mean 7 mm) [25]. A high-riding JB may obliterate the round window recess in 9% of temporal bones (Fig. 2.24a–c). A high-riding jugular bulb may be visualized otoscopically as a blue mass behind the tympanic membrane (Fig. 2.24d) [24].

A Valsalva maneuver or ipsilateral jugular compression can cause distension of the jugular bulb and facilitates its diagnosis during micro-otoscopy. When the jugular bulb plate is absent, the bulb may protrude into the middle ear cavity, which is classified as a dehiscent jugular bulb (Fig. 2.15a) [26, 27].

Surgical Application:
Retrofacial Approach to the Middle Ear

The retrofacial approach to the middle ear is done by drilling the area between the facial nerve laterally, the jugular bulb inferiorly and medially, and the ampulla of the posterior semicircular canal superiorly. This approach can provide a good access to the hypotympanum and the related structures without transposing the facial nerve or taking down the posterior external auditory canal wall. In cases with a high and lateral jugular bulb, this approach could not be easily done [25] (Fig. 2.25).

HRCT is the imaging modality of choice for evaluating the jugular bulb [28].

2.3 The Posterior Wall

2.3.1 Embryology of the Posterior Wall

The posterior wall develops from the Reichert's cartilage. The facial nerve develops in a groove on the otic capsule. By the 20th week, the facial canal becomes better defined by fibrous tissue lateral to the otic capsule that ossifies medially. Reichert's cartilage persists as a cartilage bar interposed between the otic capsule and the facial nerve medially and the tympanic annulus laterally [29]. Ossification starts in this cartilage

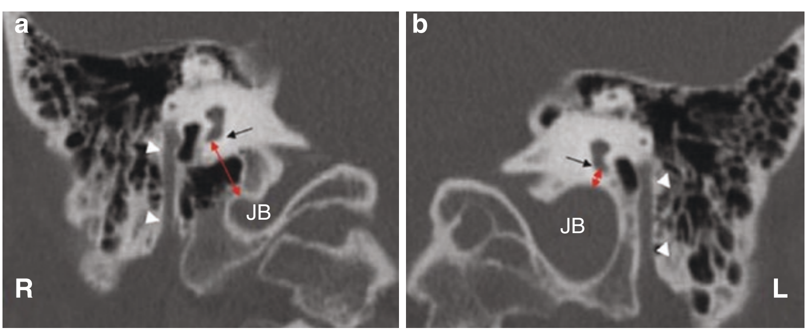

Fig. 2.23 Coronal CT reconstruction on the mastoid segment of the facial nerve (arrowheads) on both ears and the relation to the jugular bulb (JB) and the posterior semicircular canal (PSCC) (black arrow): (**a**) on the right side (R), small jugular bulb (JB) with a large distance (red arrow) to the PSCC. (**b**) On the left side (L), huge JB with a short distance (red arrow) to the PSCC

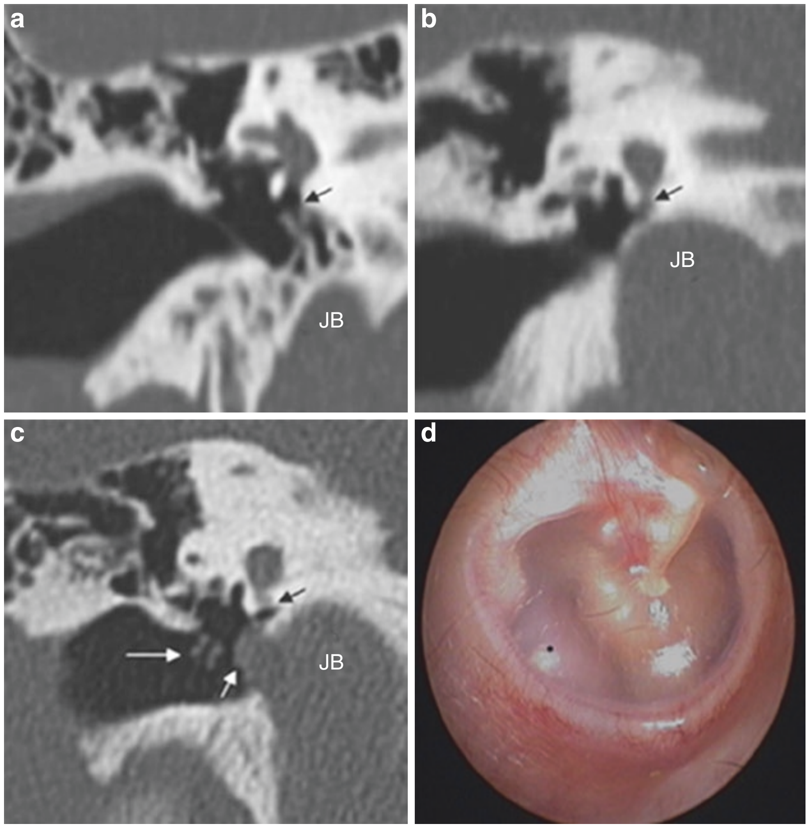

Fig. 2.24 (**a**) Coronal computed tomographic view on a right ear with a normal jugular bulb (JB), round window recess (black arrow). (**b**) High-riding JB obliterating the round window recess (black arrow). (**c**) Protruding JB (small white arrow), reaching the round window recess (black arrow). Notice the transtympanic ventilation tube in place (long white arrow), (**d**) otoscopic view of a jugular bulb bulging in the hypotympanum (*)

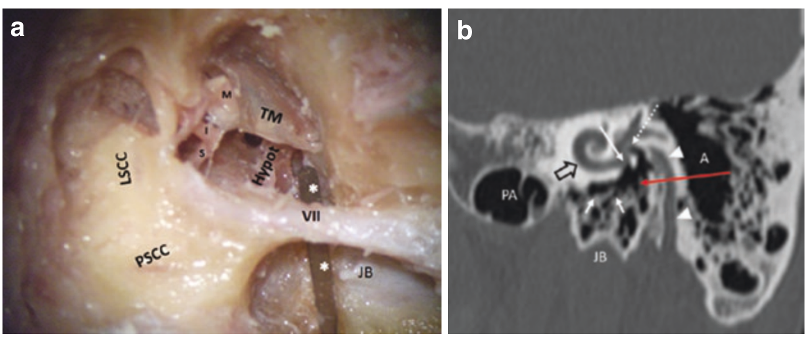

Fig. 2.25 (**a**) Retrofacial approach in a left ear hypotympanum. (*) surgical instrument, *VII* mastoid segment of the facial nerve, *JB* jugular bulb, *TM* tympanic membrane, *M* malleus, *I* incus, *S* stapes, *LSCC* lateral semicircular canal, *PSCC* posterior semicircular canal; (**b**) Sagittal oblique reconstruction of a computed tomography showing the retrofacial hypotympanotomy approach (red arrow). Mastoid segment of the VII nerve (arrowheads), hypotympanic air cells (short white arrows), round window (long white arrow), oval window (dashed arrow), basal turn of the cochlea (empty arrow). *A* antrum, *JB* jugular bulb, *PA* petrous apex cells

bar and continues in the mesenchyme both medial and lateral to this cartilage bar, forming the facial canal and the posterior wall of the middle ear cavity. The cartilage remnant of Reichert's bar frequently persists to the time of birth, ossifying separately from the surrounding mesenchyme. The first cartilaginous wall of the facial canal is the laterohyale connected primitively with the interhyale, rudiment of the stapedial tendon (Fig. 2.26).

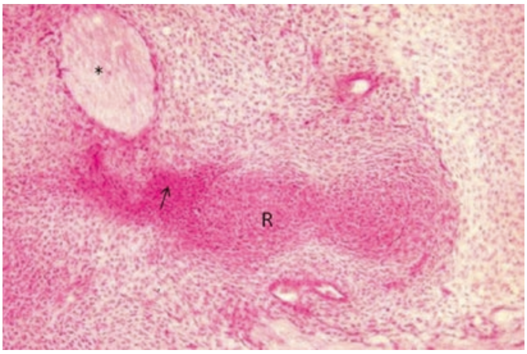

Fig. 2.26 Five weeks 15.5 mm embryo coronal section showing the laterohyale (arrow) covering facial nerve rudiment (*), in connection with the Reichert's cartilage (R). Hematoxylin-eosin staining

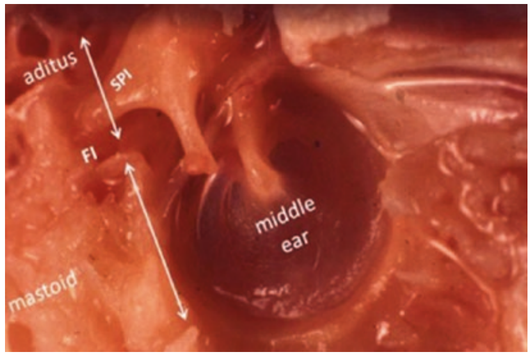

Fig. 2.27 A medial view of a left middle ear showing the posterior wall composed of an inferior closed part separating the middle ear from the mastoid and a superior open part, the aditus ad antrum, which connects the middle ear to the mastoid. Notice that the floor of the aditus houses the fossa incudis (FI), which lodges the short process of the incus (SPI)

2.3.2 Posterior Wall Anatomy

The posterior wall is the highest wall of the middle ear and measures about 14 mm. It is formed essentially by the petrous bone. The posterior wall separates the middle ear from the mastoid air cells, except at the area of the aditus ad antrum, where bone is deficient and permits communication between the attic and the mastoid antrum.

The posterior wall can be divided into two distinct parts: the upper third which corresponds to the aditus ad antrum and represents the posterior limit of the epitympanum and the lower two-thirds which correspond to the posterior wall of the retrotympanum.

The two parts are separated by the **incudal buttress** which is a compact bone that runs from the tympanic ring laterally to the lateral semicircular canal medially. It houses the **incudal fossa** in its superior surface to lodge the short process of the incus (Fig. 2.27).

2.3.2.1 The Upper Part: The Aditus Ad Antrum

The aditus ad antrum connects the epitympanum of the middle ear to the mastoid antrum posteriorly. The aditus is of a triangular shape with dimensions of **4 × 4 × 4 mm** (see Sect. 5.4.3 and Figs. 5.21 and 5.22).

2.3.2.2 The Lower Part: The Posterior Wall of the Tympanum

The posterior wall of the tympanum is a complete bony wall; it extends from the bony annulus of the tympanicus to the bony labyrinth. It is the extension of the styloid eminence upward to the pyramidal eminence and to the level of the fossa incudis. It houses the vertical segment of the facial nerve.

This wall is wider above than below and presents three eminences directed anteriorly, seven bony ridges, and four sinuses and spaces delimiting the retrotympanum compartment (Fig. 2.28).

2.3.2.2.1 Posterior Wall Eminences

The posterior wall presents three bony eminences: the pyramidal, chordal, and styloid eminences.

1. **The Pyramidal Eminence**

   The pyramidal eminence is situated at the center of the posterior wall immediately behind the oval window; it is about 2 mm in height. Its base is fused with the canal of the facial nerve. It lodges the body of the stapedial muscle, and its apex gives passage to the stapedial tendon. The pyramidal eminence communicates with the facial bony canal by a minute aperture which transmits the stapedial branch of the facial nerve (Fig. 2.29a). Cases

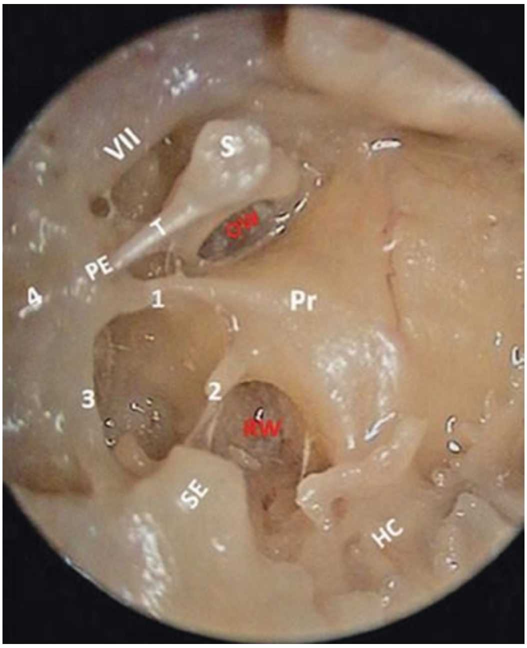

Fig. 2.28 Endoscopic view of a right middle ear showing the different ridges of the posterior wall. *1* ponticulus, *2* subiculum, *3* pyramidal ridge, *4* chordal ridge, *PE* pyramidal eminence, *SE* styloid eminence, OW oval window, *RW* round window, *S* stapes, *T* stapedial tendon, *Pr* promontory, *HC* hypotympanic cells, *VII* facial nerve

of very prominent eminences are reported, as shown in the figure 2.29b.

2. **The Chordal Eminence**

   The chordal eminence is situated lateral to the pyramidal eminence and 1 mm medial to the tympanic membrane. The chordal eminence shows a foramen: the iter chordæ posterius, where the chorda tympani passes through.

3. **The Styloid Eminences or Styloid Complex**

   The styloid complex is a derivative of the superior portion of the second branchial arch and composed of the:

   - *Styloid eminence*.
   - *Styloid peg* which is the tympanic part of the styloid process.
   - *Styloid button* which is a round button medial to styloid eminence. This button is not constant; when found, it indicates the presence of a retrofacial cellular tract.

2.3.2.2.2 Posterior Wall Ridges

We can identify in the posterior wall seven bony ridges which connect the eminences with each other and with the promontory Fig. 2.27).

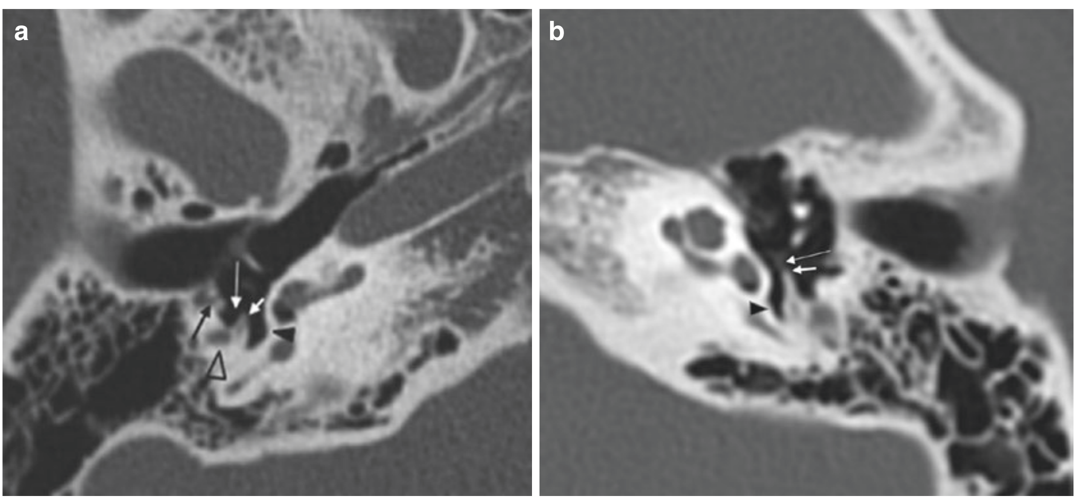

Fig. 2.29 (**a**) Transversal CT of the posterior wall of the cavity. From lateral to medial: chordal eminence (black arrow), facial recess (long white arrow), facial nerve (empty arrowhead), pyramidal eminence (short white arrow), sinus tympani (black arrowhead). (**b**) transversal CT showing a very prominent pyramidal eminence (short arrow) and a very short stapedial tendon (long arrow) inserting on the head of the stapes, sinus tympani (arrowhead)

Surgical Application

- During transcanal hypotympanotomy, the styloid eminence represents a very important landmark for the facial nerve; the styloid eminence is always anterior to the facial nerve and represents the posterior limit of safe drilling in the posterior part of the hypotympanum.
- During endoscopic endomeatal surgery, one should be thoroughly familiar with the styloid complex area. In microscopic surgery this specific area is not well visualized. Identification of the styloid complex facilitates the faster and safer exposure of the VII. In intact Fallopian bridge technique for glomus jugulare surgery, identification of VII and drilling of the styloid complex are most important.
- The styloid button indicates the presence of a retrofacial cell tract, site of possible cholesteatoma invasion.
- The styloid peg is the tympanic portion of the styloid process and is a good landmark.
- Above the styloid complex, the middle retrotympanum is a hosting chamber for cholesteatomas.

1. **The Chordal Ridge of Proctor**

   The chordal ridge runs laterally and transversely from the pyramidal eminence to fuse with the chordal eminence.
2. **The Pyramidal Ridge**

   The pyramidal ridge is very prominent. It runs inferiorly from the base of the pyramidal eminence to the styloid eminence. It could be absent.
3. **The Styloid Ridge**

   The styloid ridge connects the styloid eminence to the chordal eminence.
4. **The Ponticulus**

   The ponticulus is a central structure in the retrotympanum. It is a bony ridge extending from the pyramidal process to the promontory. There are two different variants of the ponticulus:
   - Complete ponticulus: when the ponticulus is completely formed and extends from the pyramidal process to the promontory area. In this case, the ponticulus represents the superior frontier of the sinus tympani and separates the latter from the posterior sinus.
   - Incomplete ponticulus: in this case the ponticulus does not connect with the pyramidal process making the sinus tympani and the posterior sinus one confluent sinus.
5. **The Subiculum**

   The subiculum is a smooth bony projection that is situated posterior to the promontory and extends inferiorly from the posterior lip of the round window niche toward the styloid eminence. Therefore, it intervenes between the sinus tympani superiorly and the RW niche inferiorly.
6. **The Fustis**

   The fustis is a thick solid bone projection linking the basal turn of the cochlea with the styloid eminence. *The fustis gives a strong support to the RWM; unnecessary drilling of fustis in cholesteatoma surgery has to be avoided because of the risk of sensorineural hearing loss.*
7. **The Finiculus** is a bony ridge arising from the anterior pillar of the RW and running toward the floor of the hypotympanum separating the inferior retrotympanum from the hypotympanum, where the jugular bulb is located (Fig. 2.30).

Due to its eminences and ridges, the posterior bony wall lodges five different spaces that are completely separated from the mastoid cavity (see Sect. 4.4).

2.4 The Superior Wall (The Tegmen)

The superior wall of the middle ear cavity, the tegmen, is a plate of bone that separates the middle ear cavity from the overlying middle cranial fossa dura and temporal lobe of cerebrum. The integrity of the tegmen is essential to avoid spread of infection from the middle ear to the intracranial cavity, as well as to prevent herniation of the brain into the middle ear.

2.4.1 Superior Wall Development

The superior wall forms from the fusion of two horizontal plates, a small lateral plate (horizontal process) derived from the squamous bone and a large medial plate (tegmental process) derived from the otic capsule of the petrous bone. The lateral plate shows membranous ossification, whereas the medial one shows endochondral ossification (see Fig. 1.2) (see Sect. 1.1.1).

At the line of fusion of both plates, a bony log is formed and is called the *tignum transversum* that is the major supporting element of the tegmen. The tignum transversum extends anteriorly to the Glaserian fissure and then beaks medially to form the so-called ***cog*** [30].

At 19 weeks of gestation, the endosteal ossification center of the superior semicircular canal is not yet completely developed. At 23 weeks, however, the center is complete. Scattered intrachondral and endochondral ossification forms the middle layer, and outer periosteal bone completes the trilaminar structure.

After birth and up to 10 months of age, only a thin inner layer of bone covers the superior canal in the middle fossa. Thus bone is added over the superior canal for almost three postnatal years; hence only after the age of 3 years can the bone overlying the superior semicircular canal be reliably detected on a CT scan [31, 32].

Delayed or incomplete ossification of the tegmen may lead to tegmen defects observed in childhood or early adulthood (Fig. 2.31), with possible meningocele or spontaneous CSF fistula (Fig. 2.32).

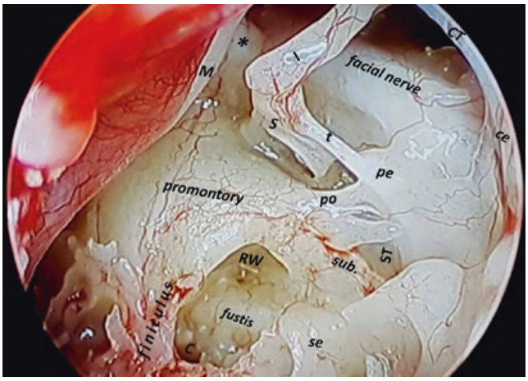

Fig. 2.30 Endoscopic picture of left ear posterior wall showing the three eminences: chordal eminence (ce) from where the chorda tympani (CT) is emerging to middle ear, pyramidal eminence (pe) giving rise to stapedial tendon (t), and the styloid eminence (se). The sinus tympani ST is located between ponticulus (Po.) superiorly and subiculum (sub.) inferiorly. The fustis is a thick solid bone projection linking the basal turn of the cochlea with the styloid eminence. The fustis gives a strong support to the round window membrane RW; the finiculus is a bony ridge arising from the anterior pillar of the RW and running toward the floor of the hypotympanum separating the inferior retrotympanum from the hypotympanum. The subcochlear canaliculus (C) is a deep tunnel between the fustis and finiculus; it may reach the petrous apex cells. *S* stapes; *I* incus; *M* malleus; * cochleariform process

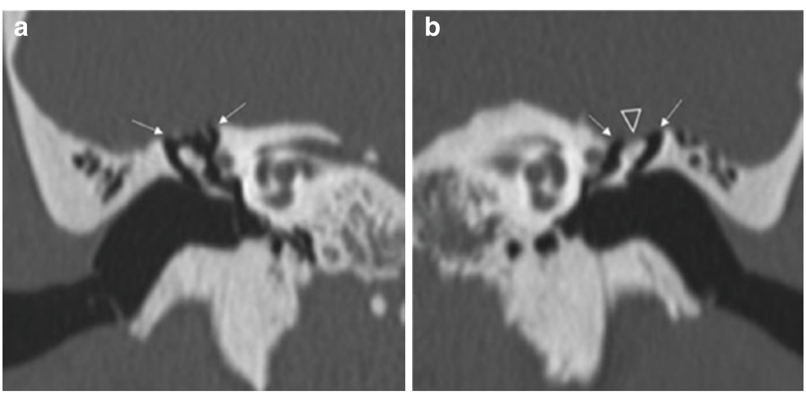

Fig. 2.31 Coronal reconstruction of two ears with congenital dehiscence of the tegmen (between arrows). (**a**) Right ear, no contact between the middle cranial fossa structures and the ossicles. (**b**) Left ear, herniation of endocranial tissue (arrowhead) of the middle cranial fossa through the congenital dehiscence of the tegmen reaching the incudomalleolar chain

Clinical Implications

Middle Ear Meningoencephalocele

Middle ear meningoencephalocele is a herniation of brain tissue through a bony defect into the middle ear. Middle cranial fossa meningoencephaloceles are the most common, and this is related to tegmen tympani dehiscence under the weight of the temporal brain lobe and CSF pulsations effect [33, 34]. The most frequent bony defect in the tegmen tympani is in the region next to the geniculate ganglion [35] (see Fig. 2.31).

Posterior cranial fossa meningoencephalocele into the middle ear is rare.

2.4.2 Superior Wall Anatomy

The tegmen is a thin bony plate that forms the roof of the middle ear cavity and separates it from the overlying temporal lobe. The part of the tegmen overlying the Eustachian tube is called tegmen tubari, the part overlying the tympanic cavity is called the tegmen tympani, and that overlying the mastoid antrum is called the tegmen antri (Fig. 2.33).

The superior surface of the tegmen forms part of the middle cranial fossa floor and is covered by the dura; the inferior surface of the tegmen is lined by middle ear mucosa. The tegmen separates the cerebrospinal fluid superiorly from the air space of the middle ear inferiorly [36].

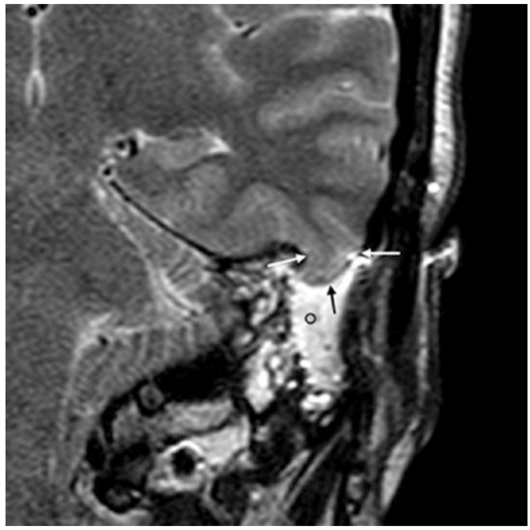

Fig. 2.32 Coronal T2-weighted MR image showing encephalocele (black arrow) herniating through a tegmen defect (between the white arrows) into the tympanic cavity that is filled with hyperintense fluid (o)

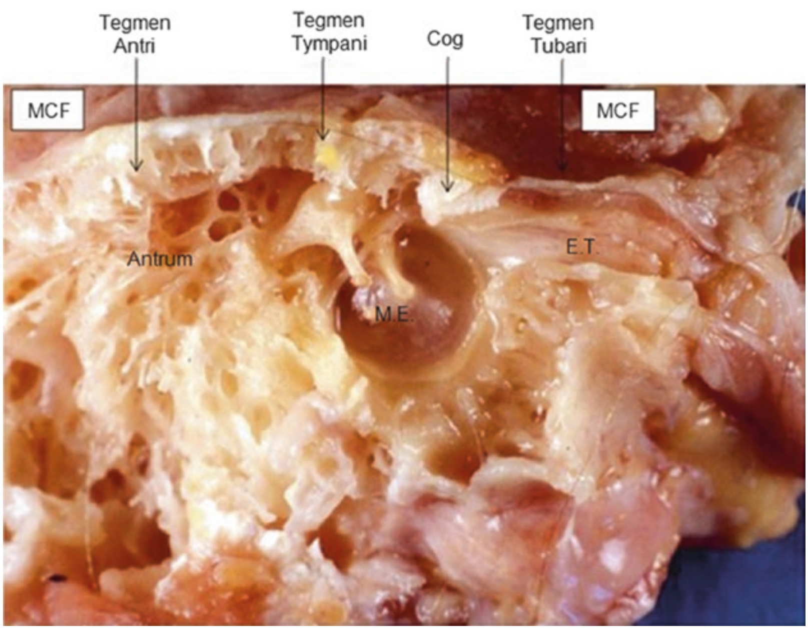

Fig. 2.33 A sagittal cut of the temporal bone, showing the superior wall of a left middle ear (ME). *MCF* middle cranial fossa, *ET* Eustachian tube

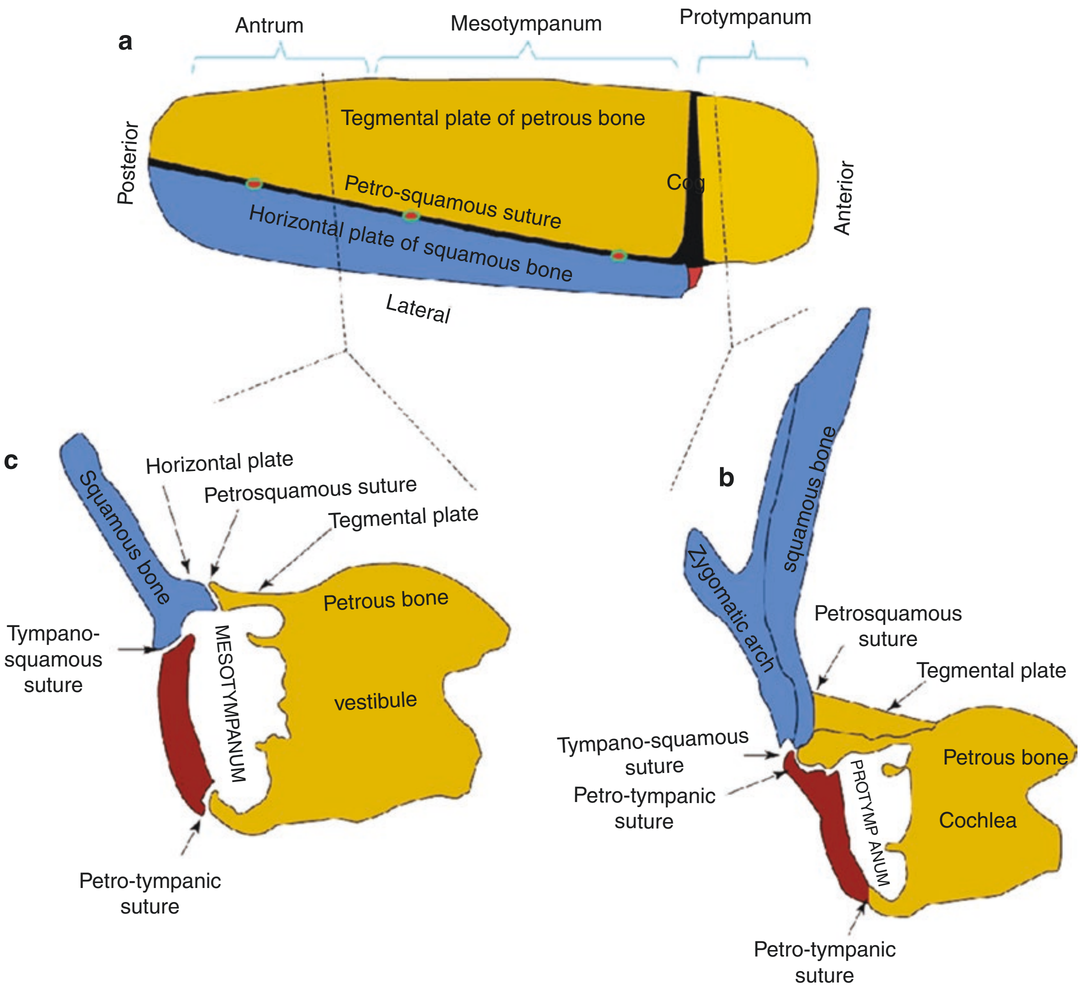

Fig. 2.34 (**a**) Superior view of the tegmen from the middle cranial fossa demonstrates the setup of the tegmen tympani formed by two distinct bony plates of the temporal bone, with the horizontal process of the squamous part laterally and the tegmental process of the petrous part medially. Both plates meet at the petrosquamous fissure. (**b**) Section made through the protympanum shows that the roof of the protympanum is built up only by the tegmental process. (**c**) Section made through the mesotympanum showing that the squamous part contributes to the formation of the tegmen tympani in this area

The tegmen tympani is formed from two unequal bony plates. The largest medial portion develops from the tegmental plate of the petrous bone, and the smaller lateral portion develops from the horizontal plate of the squamous bone (Fig. 2.34).

The suture line between these two plates is known as the internal petrosquamous suture. In newborns, this suture is not ossified and is filled with connective tissue; it does not close until adulthood [37]. In adults, the dura of the middle cranial fossa is tightly adherent to this suture; sharp dissection may be required for elevation of the dura at this level during middle cranial fossa approach.

In the middle ear, the surface of the petrosquamous fissure serves as a point of attachment to the superior malleal and superior incudal ligaments.

In the anterior attic, the tegmen is formed completely by the tegmental plate of the petrous bone. In the posterior attic and in the antrum, the horizontal plate of the squamous bone contributes to the formation of the tegmen tympani [35].

At the level of fusion between the tegmental plate and anterior limit of the horizontal plate, the **cog** appears (Fig. 2.34a). The cog is a 0.5-mm-long transversal hard and dense bony crest situated 1–2 mm anterior to the malleus head and heading vertically toward the cochleariform process. Its medial part may eventually prolong to reach the cochleariform process [38, 39].

2.4.2.1 Supportive Mechanisms of the Tegmen

As described above, the *tignum transversum* is the major supporting element of the tegmen. In addition to the tignum transversum, the carrying capacity of the tegmen depends on the lateral and medial processes of the tignum as well. The tignum transversum and the medial and lateral processes establish a structure similar to the nervation of a leaf. This aspect of a nervation insures an evenly distributed mechanical support for the thin and eventually perforated plate of the tegmen. Thus, the resistivity of a thin tegmen against the weight of the temporal lobe and cerebrospinal pulsations is determined more by the complete structure of the described network of the bone rather than by the thickness of the plate [30] (Fig. 2.35).

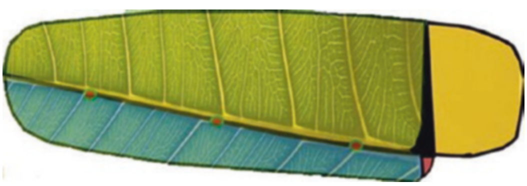

Fig. 2.35 The carrying capacity of the tegmen depends on the tignum transversum (black line) and its associated lateral and medial processes establishing a structure similar to the nervation of a leaf

2.4.3 Surgical Anatomy of the Tegmen

Mastoid surgery and atticotomy require complete conservation of the tegmental plate. Since the tegmen shows a variable shape and inclination and because the dura and the arachnoid are closely adherent to the bone in the middle fossa region, iatrogenic injuries by drilling could lead to cerebrospinal fluid leak, pneumocephalus, brain herniation, or cerebral abscess. Thus, a thorough knowledge of the tegmen slopes as well as its relationship with the external auditory canal is essential for a safe and successful atticomastoid surgery. The tegmen is not a simple horizontal plane, but it is an irregular plate of bone with undulating slopes.

There are two distinct slopes in the configuration of the tegmen: one is oriented from lateral to medial and the second one in the posterior to anterior direction.

2.4.3.1 Lateral-to-Medial Slope

In the lateral-to-medial direction, the tegmen presents an inferiorly directed hang before heading up to its highest point above the superior semicircular canal (Fig. 2.36). This shape of hanging down laterally and rising up medially concerns the whole course of the tegmen throughout its anterior to posterior extension [40].

Above the external auditory canal (Fig. 2.37), the majority of the population has a narrower bony thickness laterally than medially [40].

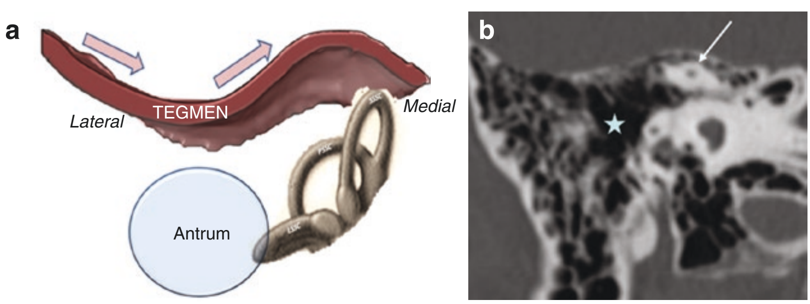

Fig. 2.36 (**a**) 3D image of the tegmen in the coronal plane. The tegmen slopes down above the antrum and then goes up to cover the superior semicircular canal *SSCC*, *PSCC* posterior semicircular canal, *LSCC* lateral semicircular canal. (**b**) Computed tomography of a right ear showing the shape variations of the tegmen relatively to the antrum (*) and the superior arch of the SCCC (white arrow)

2.4.3.2 Posterior-to-Anterior Slope

In the sagittal plane, the tegmen shows also a descending slope in the posterior to anterior direction and becomes close to the superior part of the external auditory canal [40]. The tegmen is higher posteriorly by about 1–10 mm than anteriorly (Figs. 2.38 and 2.39).

Surgical Application

During mastoid dissection anteriorly, it is recommended to start first inferiorly and then progress back around superiorly. Therefore, while approaching the superior wall of the external auditory canal and knowing that the dura hangs down laterally, the surgeon, while drilling, must work from medial to lateral to avoid lowering or injuring the canal wall or hitting the dura. The tegmen can be easily damaged laterally where the dura is low lying. Also this lateral overhang can obscure the disease tissues hidden medially.

In addition, if the medial level of the dura is wrongly expected to be at the same lower lateral level, the drilling may wrongly progress much lower medially and could traumatize the lateral semicircular canal or facial canal [40].

The sagittal plane is especially relevant when extending the drilling from the antrum to the attic region anteriorly: the tegmen slopes inferiorly as the drilling progresses anteriorly. One should expect a much lower dura anteriorly at the level of root of the zygoma; this is of most concern during anterior epitympanic recess approach (Figs. 2.38 and 2.39).

The space available to work between the EAC wall and the dural plate in canal wall-up atticomastoidectomy is smaller than posteriorly. Basically this finding confirms that the root of zygoma is a surgically challenging area, especially when approaching the anterior attic with conservation of the ossicular chain in place. In this procedure care must be taken not to penetrate the external canal wall nor to injure the dura in a canal wall-up technique.

2.4.4 The Tegmen Dehiscence and Association to SSCC Dehiscence

The tegmen tympani and the superior semicircular canal originate from the same structure: the otic capsule; therefore they have the same type of endochondral ossification. Minor was the first author who demonstrated dehiscent defects of the tegmen concurrent with dehiscence of the superior semicircular canal [41] (Fig. 2.40).

Superior canal dehiscence is a pathologic condition of the otic capsule responsible of an aberrant third window of the inner ear and cochleovestibular syndrome.

The lack of bone coverage in the tegmen tympani seems to take place before the dehiscence of the superior semicircular canal [42, 43]. It was shown that patients diagnosed with superior semicircular canal dehiscence presented about 10 times greater probability of presenting tegmen dehiscence than patients with a normal SSCC bone coverage [44]. Also several other associated abnormalities are encountered which include tegmen defects, geniculate ganglion dehiscences, temporal lobe encephalocele, and cerebrospinal fluid fistula.

Cases of SSCC dehiscence caused by an enlarged superior petrosal sinus receiving drainage from a large cerebellar developmental venous abnormality are reported [45]. In fact, this type of dehiscence is not rare and also encountered as an anatomical variant in patients without developmental venous abnormalities [46].

Different theories are described about the etiology of these dehiscences, and the most accepted one is the developmental abnormalities.

2.5 The Anterior Wall (Carotid Wall)

The anterior wall separates the middle ear cavity from the petrous carotid artery canal. It houses the tympanic orifice of the Eustachian tube.

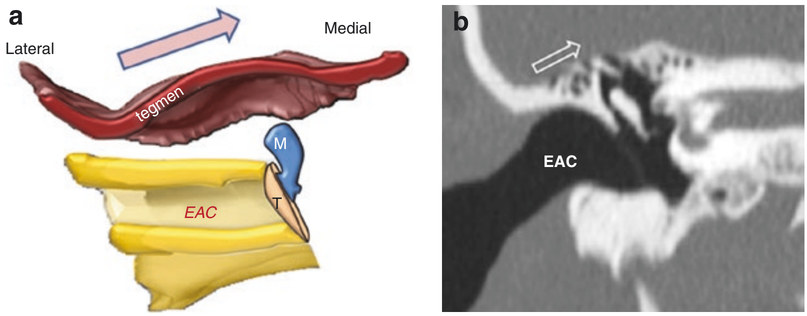

Fig. 2.37 (**a**) 3D image in the coronal plane showing the relationship between the tegmen and the bony external ear canal. Notice that the tegmen rises up as we move medially (arrow). *EAC* external auditory canal, *T* tympanic membrane, *M* malleus. (**b**) Coronal computed tomography of a right ear showing the slope of the tegmen (arrow) upward in relation to the superior wall of the external auditory canal (EAC) in lateral-to-medial direction

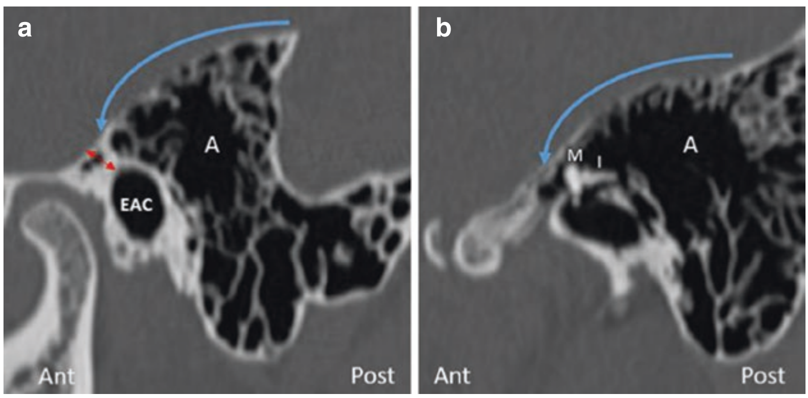

Fig. 2.38 (**a**) Sagittal CT reconstruction along the lateral part of the temporal bone, showing the descending slope (blue arrow) and its close relation (red double headed arrow) to the superior wall of the EAC (external auditory canal). *A* antrum. (**b**): Sagittal CT reconstruction passing by the center of the middle ear cavity showing *M* malleus, *I* incus and *A* antrum

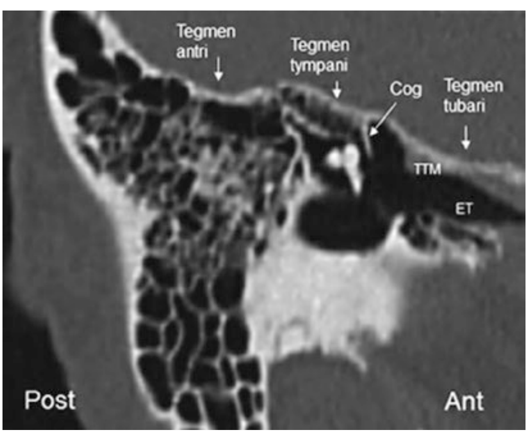

Fig. 2.39 Sagittal oblique CT reconstruction through the tympanic cavity showing the different parts of the tegmen and the cog. Note that the tegmen slopes downward from posterior (Post) to anterior (Ant). *TTM* tensor tympani muscle, *ET* Eustachian tube

2.5.1 Anterior Wall Development

The development of the anterior wall and the protympanum is in close relationship to that of the carotid canal and the Eustachian tube. The anterior wall arises completely from the petrous bone.

After the development of the otic capsule at the 16th week of gestation, multiple plates extend laterally from the otic capsule around the developing tubotympanic recess and ICA to build up almost the entire protympanum (Fig. 2.41). The tympanic bone, which forms the posterior border of the lateral wall of the protympanum [47], appears in the 18th week.

The developmental junction between the petrous and the tympanic bone is marked by the petrotympanic fissure, or Glaserian fissure, which continues laterally into the tympanosquamous fissure.

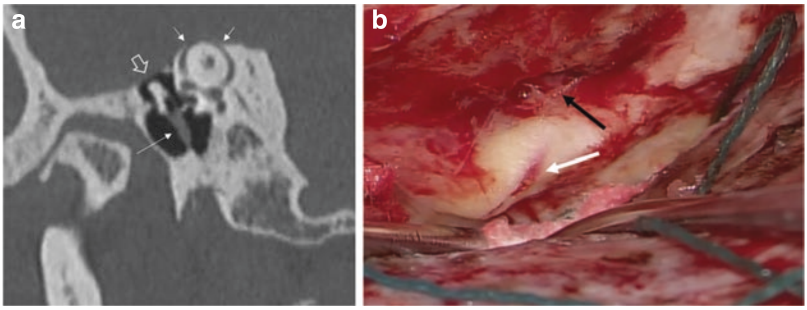

Fig. 2.40 (**a**) Coronal CT reconstruction of a right ear after tympanoplasty for CHL, but no post-op closure of the AB gap. CT shows a large dehiscence of the SSCC (between short arrows) associated to a dehiscent tegmen (empty arrow). (**b**) Per-operative findings: dehiscence of the SSCC (white arrow) and the tegmen (black arrow)

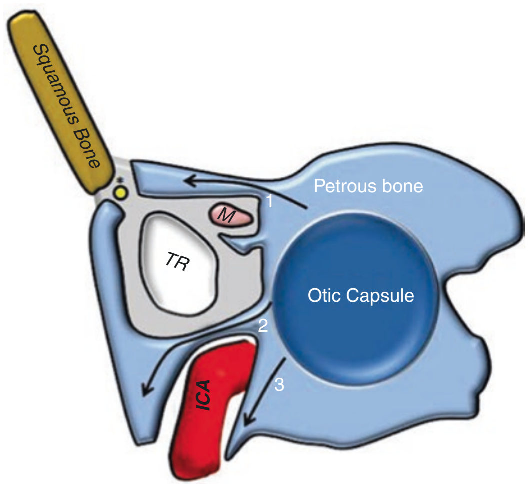

Fig. 2.41 Schematic drawing of the developing protympanum and its surroundings in the frontal plane (34-week-old fetus). The walls of the protympanum are built up by several processes of the petrous bone: the tegmental plate (1) forming the roof, the superior lamina of the carotid canal (2), and the inferior lamina of carotid canal (3) forming the inferomedial wall. The medial wall of the protympanum is created by the promontory itself. *M* tensor tympani muscle, *TR* tubotympanic recess, *ICA* internal carotid artery, * chorda tympani

2.5.1.1 Development of the Carotid Canal

The development of the carotid canal has a close relationship with the internal carotid artery (ICA) development. In the early embryonic period, the ICA lies on the anterior part of the cartilaginous otic capsule; ossification of the otic capsule that starts in the 18th week produces two plates around the ICA, the superior and the inferior plate. At birth, the plates of the carotid canal have enclosed the ICA in a bony channel in the medial wall of the protympanum [47] (Fig. 2.41).

If the ICA is not directly located beside the otic capsule, the bony canal of the ICA will not be formed [26]. Consequently ICA dehiscence encountered in children is the result of incomplete fusion of the superior and inferior bony plates of the carotid canal. Furthermore, agenesis of the internal carotid artery is associated to an absence of the carotid canal [48] (see Sect. 3.5.1).

2.5.2 Anterior Wall Anatomy

The anterior wall of the tympanic cavity is very narrow because the medial and lateral walls of the middle ear cavity converge anteriorly in an acute angle. The anterior wall is formed entirely from the petrous bone and can be divided into three portions: the lower, the middle, and the upper portion (Fig. 2.42).

2.5.2.1 The Lower Portion

The lower portion of the anterior wall is the largest portion and represents the anterior wall of the hypotympanum. It is a thin plate of bone that separates the middle ear cavity from the vertical segment of the petrous carotid artery. This bony plate has two tiny openings for the caroticotympanic nerves: the upper opening transmits the superior caroticotympanic nerve and the inferior opening transmits the inferior caroticotympanic nerve. These nerves originate from the pericarotid sympathetic chain; they transmit sympathetic fibers coming from the superior cervical ganglia to the tympanic plexus of the middle ear.

2.5.2.2 The Middle Portion

The middle portion of the anterior wall corresponds to the protympanum. The middle portion has two tunnels placed one below the other: the upper tunnel transmits the tensor tympani muscle, and the lower tunnel corresponds to the bony portion of the Eustachian tube. A thin horizontal plate of bone, the *septum canalis musculotubarius*, separates these two tunnels from each other.

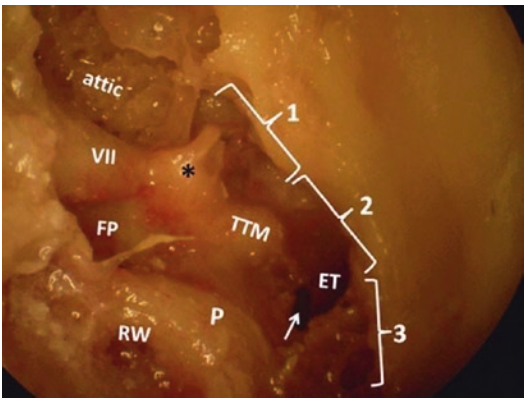

Fig. 2.42 Anterior wall of a right middle ear. (1) Upper third, (2) middle third, (3) inferior third; notice the internal carotid artery dehiscence (white arrow) in the medial wall of the Eustachian tube (ET); *TTM* tensor tympani muscle canal, * cochleariform process, *VII* tympanic portion of the facial nerve, *FP* footplate, *RW* round window, *P* promontory

- The semicanal for the tensor tympani (semicanalis tensor tympani) is cylindrical and lies beneath the tegmen tympani. It extends to join the cochleariform process.
- The septum canalis musculotubarius passes posteriorly below the tensor tympani semicanal; it expands above the anterior end of the oval window and terminates by curving laterally forming a pulley, *the cochleariform process*, over which the tendon of the tensor tympani muscle passes [49].
- The bony portion of the Eustachian tube is situated below the septum canalis (see Sect. 7.3.1).

2.5.2.3 The Upper Portion

The upper portion of the anterior wall corresponds to the root of the zygoma which represents the anterior wall of the epitympanum.

2.5.2.4 The Carotid Artery and the Anterior Wall

The carotid artery enters the temporal bone through the carotid foramen. It ascends vertically in the anterior wall of the hypotympanum and in the medial wall of the bony Eustachian tube at the area just beneath the cochlea (the vertical segment); then it turns anteromedially at almost a right angle toward the petrous apex, forming the horizontal segment anteroinferiorly to the cochlea (Figs. 2.21 and 2.43).

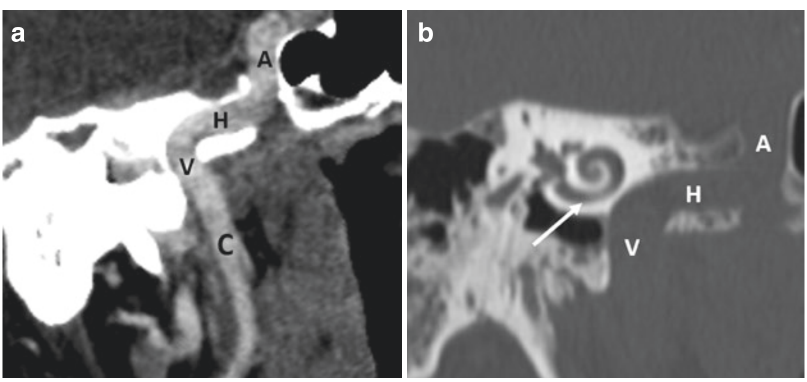

Fig. 2.43 (a) CT angio-scan of the supra-aortic right vessels, with a sagittal oblique reconstruction, showing the trajectory of the internal carotid artery with its cervical (C), vertical (V) horizontal (H) and ascending (A) cavernous segment. (b) another sagital oblique reconstruction displayed in the bone window showing the proximity of the basal turn of the cochlea (white arrow) with the intrapetrous cartoid artery, vertical (V) and horizontal (H) portion of the carotid artery

2.5.2.4.1 The Vertical Segment of the Petrous Carotid Canal

The vertical segment of the petrous carotid canal is 5.0–12.5 mm in height and 4.0–7.5 mm in diameter. The vertical segment is separated from the middle ear cavity by a thin plate of bone of about 0.25 mm. There is no difference in thickness between pediatric and adult subjects. A dehiscence of carotid canal is observed in about 5% of temporal bones, usually located at the medial wall of the bony portion of Eustachian tube (Fig. 2.42).

The intrapetrous carotid artery may also present in a more posterolateral position regarding the cochlea that is usually completely posterior to the posterior genu between the horizontal and the vertical portion of the artery. This anatomical variant (lateralized IC) may lead to a partial to total obliteration of the entry to the Eustachian tube and may come in a relatively close contact to the tympanic membrane (Fig. 2.44) [50].

Another congenital anomaly of an aberrant internal carotid artery is rarely encountered (see Fig. 3.52), when the vertical segment of the IC passes through an enlarged inferior canaliculus tympanicum possibly associated to a persistent stapedial artery [50].

The tympanic bone is anterolateral to the vertical segment [51]. The distance from the anterior margin of the tympanic annulus to the nearest point of carotid canal is about 5 mm [27].

The average distance between the carotid canal and the cochlea is about 1 mm near the basal turn, 2 mm near the middle turn, and 6 mm near the apical turn (Fig. 2.45) [52].

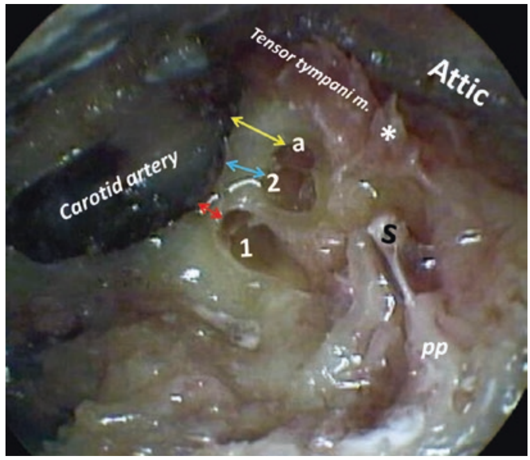

Fig. 2.45 Left ear with drilling of the medial wall to show the relationships between the carotid artery and turns of the cochlea: the vertical segment approximates the basal turn of cochlea (1) by about 1 mm (red arrow) and the middle turn (2) by about 2 mm and the apical turn by about 6 mm (a). *S* stapes, *pp* pyramidal process, * cochleariform process

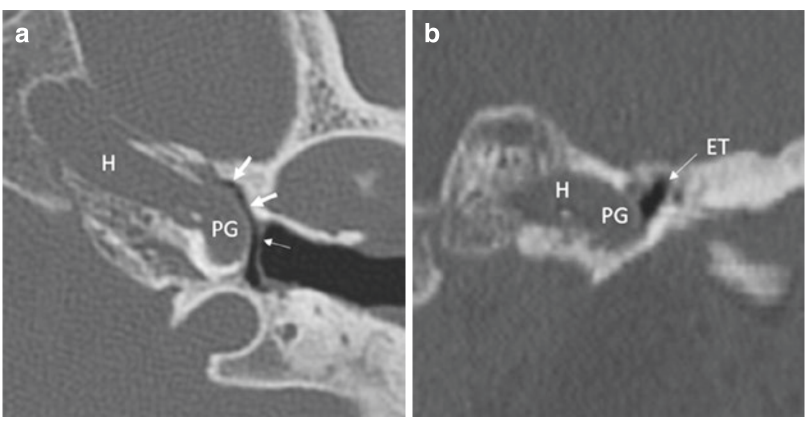

Fig. 2.44 (**a**) Axial CT image showing the horizontal part (H) of the intrapetrous carotid artery that becomes prominent at the level of the posterior genu (PG), protruding in the protympanum and almost completely obliterating the bony part of the Eustachian tube (thick arrows). It is also very close to the anteroinferior tympanic membrane (thin arrow). (**b**) Coronal reconstruction, showing the obstruction of the inferior part of the ET by the protruding posterior genu of the carotid artery (PG)

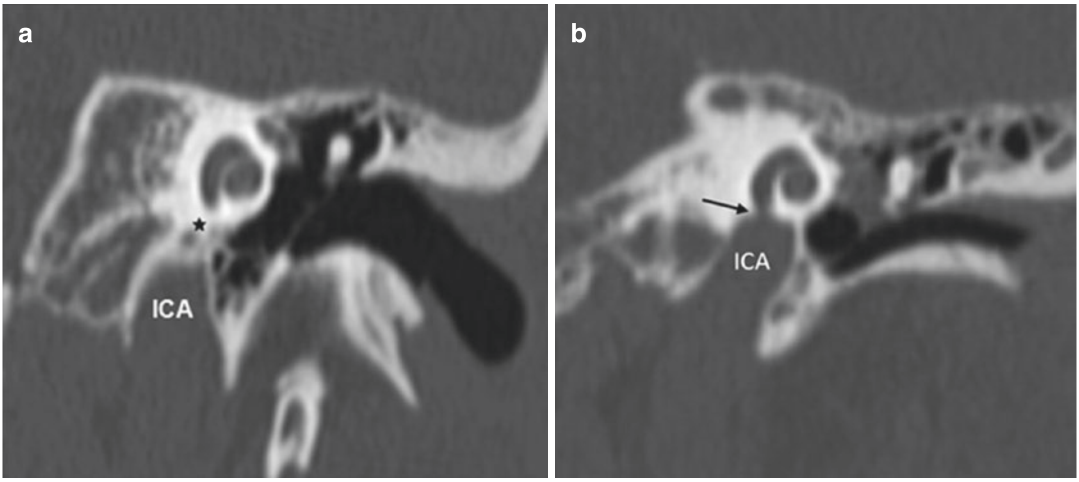

Fig. 2.46 Coronal reconstruction of a computed tomography of a left ear with (**a**) normal bony separation (*) between the cochlea and the internal carotid artery (ICA); (**b**) a dehiscent internal carotid artery (arrow) into the basal turn of the cochlea

2.5.2.4.2 The Horizontal Segment of the Petrous Carotid Canal

The horizontal segment of the petrous carotid canal is directed anteromedially by a path of 14.5–24 mm long and 4.5–7.0 mm in diameter [51].

> **Surgical Implication**
> Rarely, there is partial absence of septation between the cochlea and the carotid canal. In these cases, preoperative imaging of the temporal bone shows the anatomical relationship between the cochlea and petrous carotid canal and may help to prevent inadvertent penetration of the carotid canal during cochlear implant surgery (Fig. 2.46).

2.6 The Medial Wall (Cochlear Wall)

The medial wall is formed mainly by the cochlear promontory in addition to several important structures: the tympanic segment of the facial nerve, the oval and the round windows, the tensor tympani canal, the cochleariform process, and the lateral semicircular canal.

2.6.1 Embryology of the Medial Wall Structures

2.6.1.1 Facial Nerve: Tympanic Segment (See Chap. 6)

The horizontal segment of the facial nerve is recognized by the sixth week of gestation when it passes between the developing membranous labyrinth and the primitive stapes [53]. By the eighth week, soon after the stapes blastema reaches the otic capsule, a sulcus forms within the lateral margin of the cartilaginous otic capsule, initiating the formation of the horizontal facial nerve canal; this groove forms by the tenth week. If this canal is deep and well formed, the facial nerve will be "locked in" to its normal anatomic position against the otic capsule [53]. The facial nerve groove will begin to enclose the facial nerve in the fourth gestational month. Ossification of the canal is completed during or shortly after the first year of life [54].

2.6.1.2 Oval Window

The oval window is derived from the lateral surface of the otic capsule. Its development is related directly to the development of second branchial arch structures and most importantly the stapes and the facial nerve. As early as the fifth week, the blastemal mass of the stapes becomes

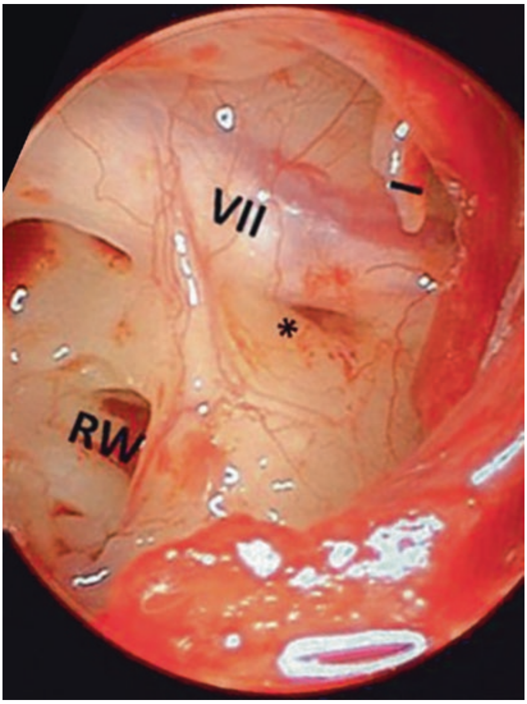

Fig. 2.47 Right ear with oval window aplasia. Peroperative view showing the congenital absence of the oval window (*) and abnormal trajectory of the facial nerve (VII), rudimentary incus (I)

recognizable as a ring-shaped structure around the stapedial artery. This rudimentary stapes grows medially and then contacts and indents the developing otic capsule at the future oval window during the seventh week. The mesenchyme in this depression fuses with the stapedial ring to form the stapes footplate [55, 56]. Once the base of the stapes has fully developed, dedifferentiation of the oval window cartilage occurs, and a rim of fibrous tissue forms to produce the annular ligament [54].

Clinical Implications

Oval Window Atresia

When the primitive stapes fails to fuse with the primitive vestibule, the oval window cannot develop, resulting in its congenital absence (Fig. 2.47). One widely accepted explanation for the congenital absence of the oval window proposes that during the fifth and sixth weeks of gestation, the developing facial nerve becomes anteriorly displaced and interposed between the otic capsule and the stapes blastema. As a result, the contact between the stapes and the otic capsule is prevented; thus, the development of the oval window is not initiated [53, 57, 58]. An abnormal appearance of the stapes is often associated with congenital absence of the oval window.

In addition, a congenital absence of the oval window could be associated with different anomalies of the tympanic segment of the facial nerve canal such as a low-lying facial nerve relative to the oval window or a canal situated within or below the expected location of the oval window or a dehiscent large facial nerve [59] (Figs. 2.48 and 2.49).

Failure of development of the annular ligament results in a congenital fixation of the stapes footplate.

2.6.1.3 Fissula Ante Fenestram

The fissula ante fenestram is part of the perilymphatic labyrinth, and it is unique to humans. The fissula is first apparent in the ninth week (embryo of 34 mm) [60], as a strip of precartilage in the lateral wall of the cartilaginous otic capsule immediately anterior to the oval window. During the next 3 weeks, this extension of periotic tissue stretches as a connective tissue ribbon from the vestibule to the middle ear. The fissula continues to grow until mid-fetal life about 21st week, at which time the ossification of the otic capsule is almost completed (Fig. 2.50). The cartilage border, that separates the connective tissue of the fissula from the bony border of the otic capsule, is gradually replaced by endochondral bone.

Because of the metamorphosis of the lining cartilage rests, the fissula is thought to be the area of histological instability. Later in life the new bone-forming process may be enhanced and expand to become an active focus of otosclerosis [61].

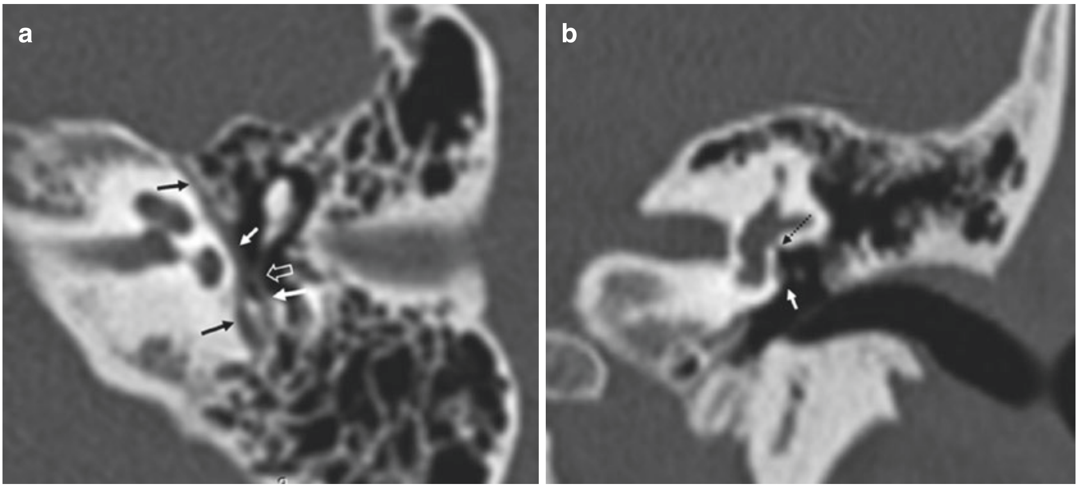

Fig. 2.48 (**a**) Axial CT image showing the abnormal low-lying tympanic segment of the facial nerve (between the black arrows) on the promontory (thin white arrow). Anomalies of the stapes (empty arrow) seen in continuity with the thickened stapes muscle tendon (thick white arrow). (**b**) The coronal view shows the almost complete atretic plaque of the oval window, just a rudimentary opening is visible (dashed black arrow). Notice the low-lying facial nerve running on the promontory (white arrow)

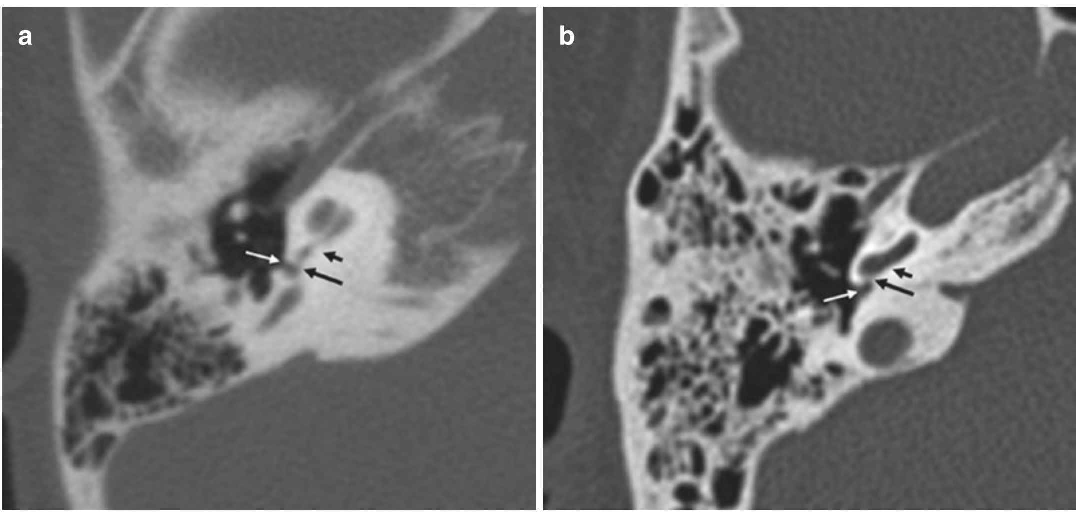

Fig. 2.49 (**a**) Axial CT image of a right ear showing an important hypoplasia of the round window recess (white arrow) and a very small round window (long black arrow). Important hypoplasia of the scala tympani of the basal turn of the cochlea (small black arrow). (**b**) Axial CT image of a right ear showing an important hypoplasia of the round window recess (long black arrow). Normal size and aspect of the basal turn of the cochlea (short black arrow)

2.6.1.4 Round Window

The round window area appears during the 11th week. By this time, ossification has started in the otic capsule. During the ossification of the otic capsule, the round window niche is surrounded by a thickened ring of cartilage which isolates the round window mesenchyme from the ossifying otic capsule and prevents the ossification of the round window opening. Further differentiation of the cartilage ring forms the round window niche, and the round window membrane appears inside the niche with an epithelial layer of mucous membrane. Mesenchymal tissue left unabsorbed in the round window niche may form a separate outer membrane, closing off the actual niche.

Fig. 2.50 Transverse cut of a left temporal bone of a 28-week-old embryo showing the fissula ante fenestram (*) in front of the footplate (FP) and the fossula postfenestram posterior to the footplate (white arrow). *VII* facial nerve, *I* incus, *M* malleus

The ossification of the walls of the round window niche starts at the 16th week and is established by both membranous and endochondral ossification. However, related to the different degrees of this double ossification types, there will be a great variability in the phenotypes of the round window niche. Depending on the state of development of the upper and anterior walls of the niche, the plane of the opening of the round window niche can be horizontal, dorsal, or lateral. Anterior, superior, and posterior walls are the first to appear, while the inferior wall is completely absent at this time. One week later, a bony process grows into the niche forming its inferior wall, but this process will only reach the anterior wall by the 18th week [8].

A process of the otic capsule, called the cartilage bar, forms the inferior wall of the round window niche. The anterior and superior walls of the niche form by intramembranous ossification, whereas the posterior and inferior walls predominantly form by endochondral ossification. The uneven growth of different walls of the round window niche can alter the shape of the entrance, which results in eight different types of niches: extremely narrow, descending tegmen, anterior septum, bony membrane, open fundus, exostosis, jugular dome, and trabeculae [62].

In the 23-week-old fetus, the bony structure forming the inferior wall appears, the so-called fustis. This structure runs in the middle of the inferior wall and points to the crest of the round window. After the 20th exponential prenatal week, an intensive growth can be observed in the anterior wall where the inferior tympanic artery and the tympanic nerve run [8]. During this week some form a complete bony canal around the tympanic nerve and the inferior tympanic artery; this bony structure arises from the anterior pillar and runs inferiorly to the hypotympanic cells, forming the so-called finiculus [8].

> When the cartilage ring does not develop, osseous obliteration will occur and lead to congenital round window atresia [63].

2.6.2 Medial Wall Anatomy

The medial wall of the tympanic cavity separates the middle ear cleft from the adjacent inner ear. The canal of the tensor tympani muscle anteriorly and the tympanic Fallopian canal posteriorly are two landmarks that divide the medial wall into upper third part and lower two third part. The upper third forms the medial wall of the epitympanum and is demarcated posteriorly by the lateral semicircular canal (LSCC). The lower two-thirds form the medial wall of the mesotympanum and include the cochlear promontory on the center, the oval window posterosuperiorly, and the round window posteroinferiorly (Figs. 2.51, 2.52, and 2.53).

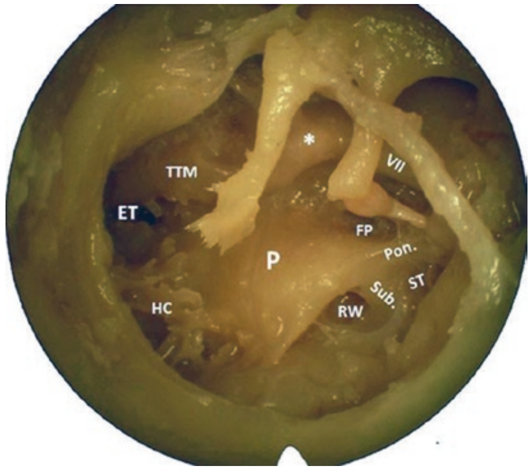

Fig. 2.51 Endoscopic view of a left middle ear. VII tympanic facial nerve, * cochleariform process, *TTM* tensor tympani muscle, *RW* round window, *ET* Eustachian tube, *FP* footplate, *P* promontory, *HC* hypotympanic cells, *ST* sinus tympani, *Pon* ponticulus, *Sub* subiculum

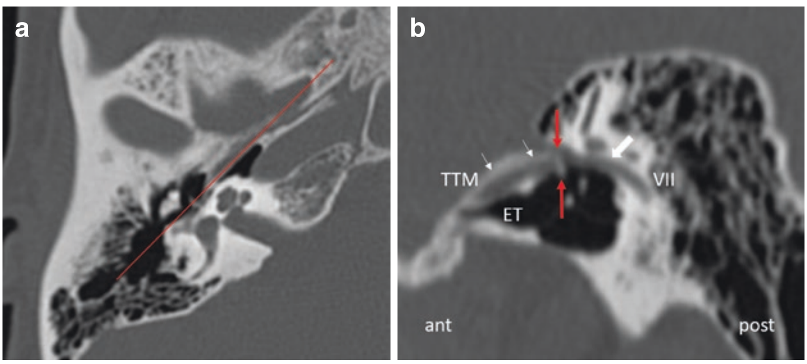

Fig. 2.52 (**a**) Reference line for a sagittal oblique reconstruction on an axial CT image, along the axis of the TTM and the VII nerve. (**b**) The sagittal oblique reconstruction along the reference line shows two landmark structures, anteriorly the TTM (small arrows), posteriorly the VII nerve (plain arrows). These two structures overlap at the cochleariform process (situated between the two red arrows). *ant* anterior, *post* posterior

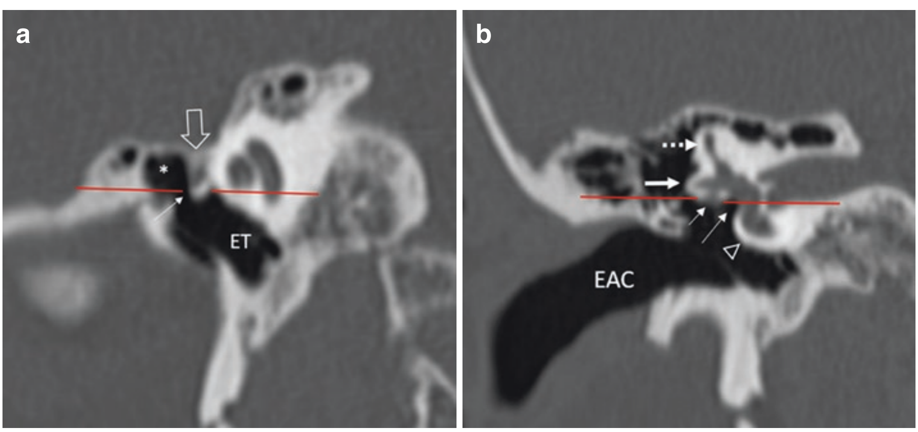

Fig. 2.53 Coronal CT reconstruction of a right ear showing the anatomical structures of the medial wall: (**a**) passing through the anterior third of the cavity: TTM (empty arrow), cochleariform process (between the red lines), AER (*); (**b**) passing through the mid-third of the cavity, SSCC (dashed arrow), LSCC (thick plain arrow), VII nerve (small arrow), oval window niche (long arrow), promontory (arrowhead), *EAC* external auditory canal

2.6.2.1 Tensor Tympani Muscle Bony Canal and the Cochleariform Process (Fig. 2.54)

The semicanal of the tensor tympani muscle (semicanalis m. tensor tympani) is cylindrical and extends from the protympanum on to the labyrinthine wall of the tympanic cavity and ends immediately in front of the oval window niche.

The medial wall of the tympanic cavity is marked by a slightly curved bone protruding laterally called the cochleariform process which is situated anterosuperior to the oval window and just inferior to the tympanic segment of the facial nerve. It represents the posterior end of the bony canal of the TTM. This curved projection of bone is concave anteriorly, and it houses the tendon of the tensor tympani muscle. This tendon turns laterally and attaches at the medial aspect of the malleus handle.

The apex of the cochleariform process, at which the TTM turns sharply laterally, is the landmark for the position of the turn between the anterolateral and the posteriorly directed horizontal portion of the facial nerve.

*The cochleariform process is the termination of the **bony septum** separating the Eustachian tube and the canal of the tensor tympani muscle.*

Surgical Application

- The cochleariform process is the most resistant bony part to cholesteatoma.
- The facial nerve is superior and posterior to the cochleariform process.
- The Jacobson's nerve passes perpendicular to the cochleariform process at the hypotympanic level, so the cochleariform process is a useful anatomic landmark to Jacobson neurectomy.
- Medial to the cochleariform process, the basal turn of the cochlea ends and the second turn starts.
- The cog is situated anterior and superior to the cochleariform process.

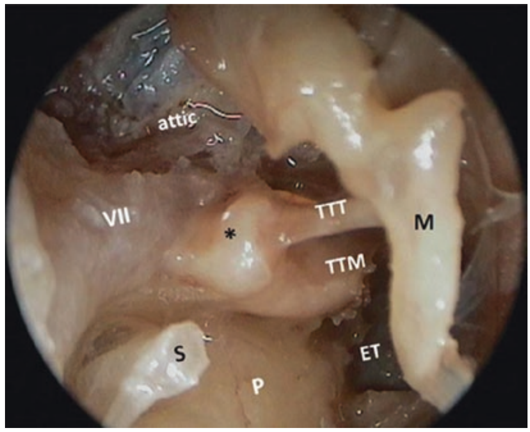

Fig. 2.54 Endoscopic view of a right middle ear through a posterior tympanotomy showing the tympanic segment of the facial nerve (VII) and its relationship with the cochleariform process (*) and stapes (S). *TTM* tensor tympani muscle, *TTT* tensor tympani tendon, *P* promontory, *ET* Eustachian tube, *M* malleus

Surgical Pearl

The cochleariform process is a highly important anatomical and surgical landmark to identify the facial nerve and the oval window in invasive pathologies (Fig. 2.54).

2.6.2.2 Facial Nerve Canal

The prominence of facial nerve canal is an important anatomical structure present in the upper part of the medial wall of the mesotympanum. This nerve canal runs obliquely above the promontory and above the oval window in an anteroposterior direction from above the cochleariform process anteriorly down below and medial to the dome of the lateral semicircular canal. It presents its second genu at the turning point between the horizontal tympanic portion and the vertically descending mastoid portion in the posterior wall of the tympanic cavity.

In the medial wall, the bony canal of VII could be dehiscent to leave the VII only covered with a submucosa or even prolapsing lying over the oval window (see Chap. 6). This situation is highly at risk during middle ear surgery. Even infections of

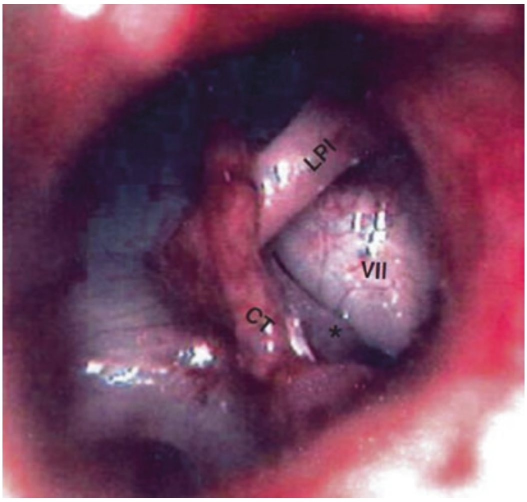

Fig. 2.55 Left middle ear exploration showing dehiscent facial nerve (VII) and prolapse on stapes (*). *LPI* long process of incus, *CT* chorda tympani

the middle ear mucosa can cause facial nerve palsy in patients with an exposed facial nerve (Figs. 2.52, 2.53, 2.54, and 2.55).

> **Surgical Application**
> Occasionally, the facial nerve is not covered with bone in its canal, most often in its tympanic segment right above the oval window niche. In these cases, the nerve may prolapse over the niche, tilting the stapes toward the promontory and partially covering the stapes footplate. Any surgical manipulation in the OW niche must take into account this vulnerability of an uncovered nerve: any soft structure in this region has to be addressed potentially as being the nerve, until proven otherwise!

2.6.2.3 Lateral Semicircular Canal

The region above the level of the facial nerve canal forms the medial wall of the attic. The dome of the lateral semicircular canal extends a little lateral to the facial canal and is the most prominent structure of the posterior portion of the epitympanum (Figs. 2.52, 2.53, and 2.56).

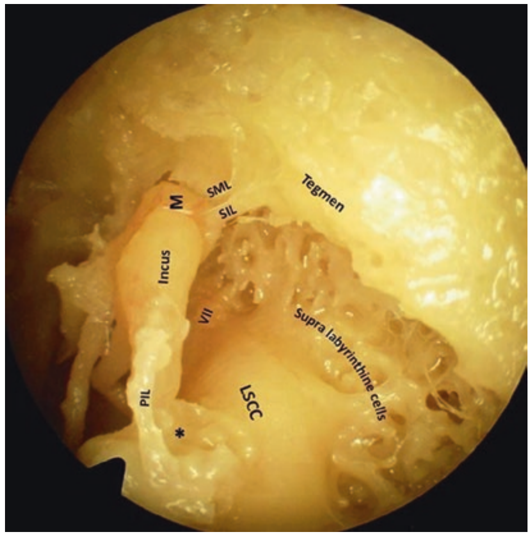

Fig. 2.56 Medial wall of the attic. *LSCC* lateral semicircular canal, *VII* facial nerve, *M* malleus, *PIL* posterior incudal ligament, *SIL* superior incudal ligament, *SML* superior malleal ligament, * incudal fossa

2.6.2.4 The Cochlear Promontory

The promontory is a prominent eminence occupying most of the central portion of the medial wall of the middle ear and lodges between the oval and round windows. The promontory represents the underlying basal turn of the cochlea (Figs. 2.57 and 2.58).

The promontory surface is grooved to accommodate the branches of the tympanic plexus (Jacobson's nerve), which enters the temporal bone through the tympanic canaliculus, just anterior to the jugular foramen.

> **Surgical Pearl**
> The basal turn of the human cochlea is a bony canal. The least covered portion is located behind the apex of the promontory. The lower half of the basal turn of the cochlea can be approached from the facial recess or external auditory canal during cochlear implantation. The second and third turn of the cochlea are also approachable from the tympanic cavity; nevertheless, to be able to reveal the second and third turns fully, the tensor tympani muscle and the semicanal must be completely removed (Fig. 2.59).

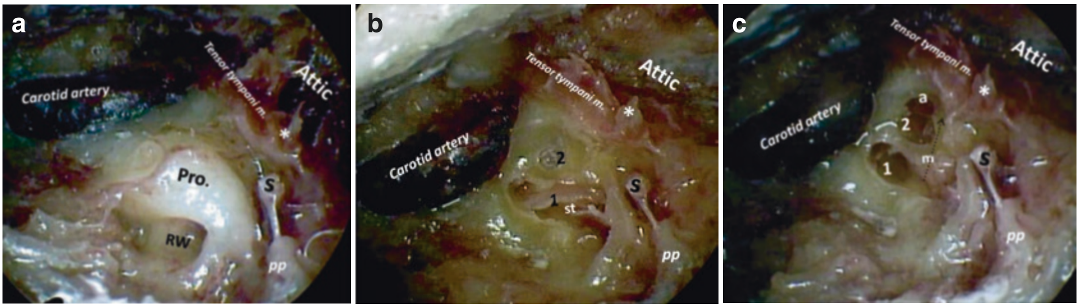

Fig. 2.57 Relationship of medial wall to cochlear turn. (**a**) Before drilling of the medial wall, showing the promontory (Pro.), the round window (RW), the stapes (s), the pyramidal process, the tensor tympani superiorly, and the carotid artery anteriorly. (**b**) After drilling the apex of the promontory, the basal turn of cochlea (1) is exposed, further drilling anterosuperiorly exposed the second turn (2), *st* scala tympani (2). (**c**) Deeper and superior drilling exposed the second (2) and apical turn (a) of the cochlea, to be able to fully expose the apical, the tensor tympani muscle and the semicanal must be removed. Notice the modiolus (m) and its axis (black arrow). *St* scala tympani, * cochleariform process, *pp* pyramidal process

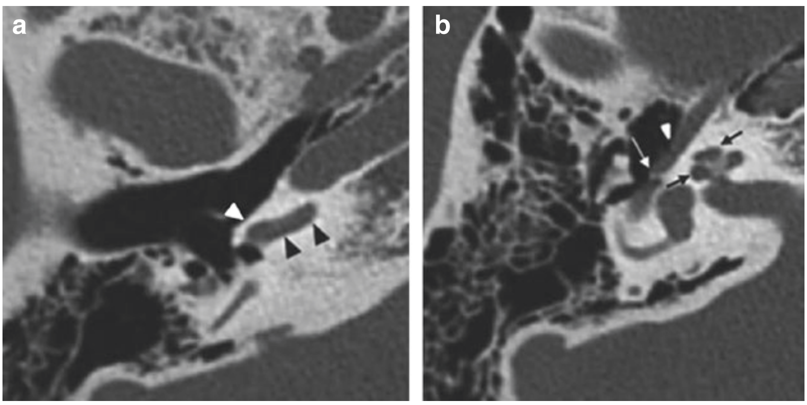

Fig. 2.58 Transversal computed tomography of a right ear. The medial wall of the middle ear in relation to (**a**) the basal turn of the cochlea (arrowheads), the promontory (white arrowhead). (**b**) The second turn of the cochlea (black arrows) is hidden by the tensor tympani muscle (white arrowhead), extended until the cochleariform process (white arrow)

2.6.2.5 The Oval Window Niche

The oval window niche (fenestra vestibuli) is located in the medial wall of the posterior part of the mesotympanum behind and above the promontory inferior to the facial nerve canal.

The oval window niche is limited anteriorly and superiorly by the cochleariform process and posteriorly by the ponticulus and pyramidal eminence. It is situated in a depression called the fossula vestibuli where its depth depends on the facial nerve position and the variable prominence of the promontory (Fig. 2.59).

The oval window leads to the inner ear vestibule (scala vestibuli). The long diameter of the oval window is horizontal, and its convex border is directed upward. It is closed by the stapes footplate which is surrounded by the annular ligament. The dimensions of the oval window are in average 3.25 mm long and 1.75 mm wide.

The fossula vestibuli is surrounded by four walls [64]:

- The upper wall is formed by the facial canal.
- The lower wall is formed by the promontory.
- The anterior wall is formed by the bony lamella of the medial wall and part of the cochleariform process.
- The posterior wall is formed by the bony lamella of the medial wall of the tympanic cavity.

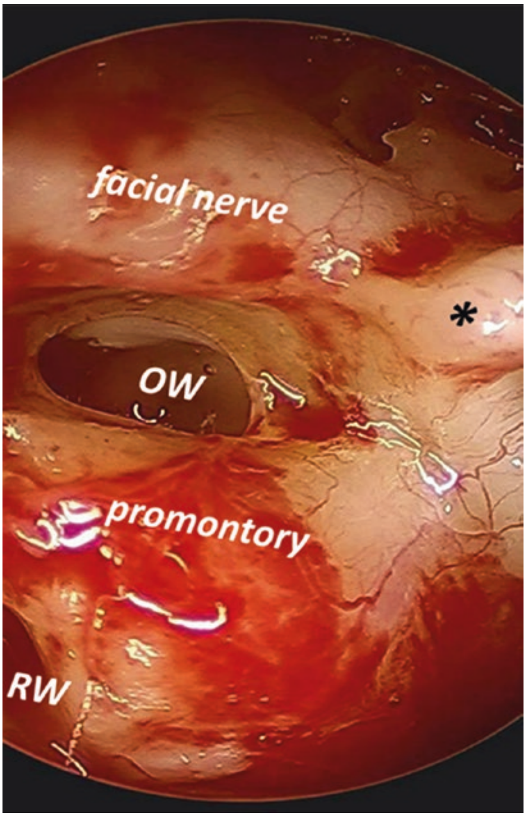

Fig. 2.59 Right ear showing oval window (OW) after removal of footplate. OW upper wall is formed by the facial canal, the lower wall is formed by the promontory, the anterior wall is formed by the bony lamella of the medial wall and part of the cochleariform process (*)

Measurements of the OWN height on CT scan provide an accurate and relevant evaluation of this region before surgery: a height below **1.4 mm** should be considered at risk for technical difficulties during stapes surgery. A height of the oval window niche below 1.1 mm is considered in favor of a narrow OW niche [65].

In such conditions, also surgical removal of a cholesteatoma from the niche may be challenging (Fig. 2.60).

2.6.2.5.1 Fissula Ante Fenestram

The fissula ante fenestram is a cleft, special to human, seen less often with advancing age mainly due to bone remodeling of the otic capsule. It is considered as an appendage of the perilymphatic labyrinth; it is a strip of periotic connective tissue extending from the vestibule just anterior to the oval window through an irregular still-like space in the bony otic capsule to join the mucoperiosteum of the tympanic cavity below the pulley of the tensor tympani muscle. Usually it is obliterated by fibrous tissue and immature cartilage (Fig. 2.61). The cartilage border that separates the connective tissue of the fissula ante fenestram from the bone of the otic capsule becomes gradually replaced by an endochondral bone [66].

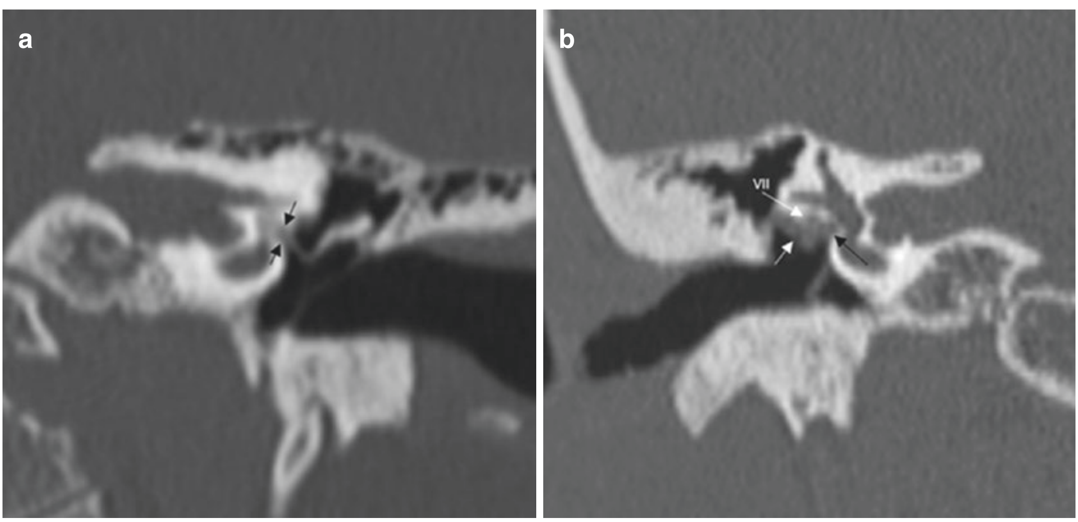

Fig. 2.60 Different pathologies of the oval window niche: (**a**) Reduced height of the oval window niche (between arrows). (**b**) Mesotympanic cholesteatoma (short white arrow) invading the oval window niche (black arrow) with invisible stapes superstructure. The facial nerve (long white arrow) shows lysis of its bony canal, (the VII is indistinguishable from the condensation images of the cholesteatoma)

Clinical Application

In cases of otosclerosis, the oval window can be the site of different degrees of invasion, ranging from a typical focal anteroinferior thickening to a complete obliteration (Fig. 2.62).

Perilymph leakage through the fissula ante fenestram was reported as a potential cause of sudden hearing loss [67].

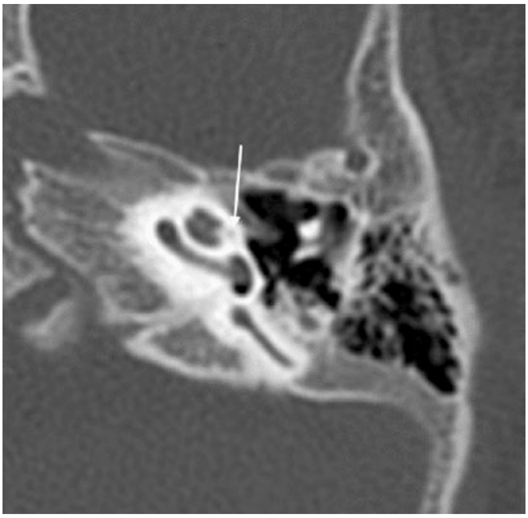

Fig. 2.61 Transversal computed tomography of a 2 yr old child, showing the normal appearance of the cochlear cleft (arrow) at the site of the fissula ante fenestram - its a physiologic aspect

2.6.2.5.2 Fissula Postfenestram

This is an evagination of the periotic tissue into the otic capsule just posterior to the oval window at a point about one-third of the way between the window and the non-ampullary end of the lateral semicircular canal.

2.6.2.6 The Round Window

The round window region is rich of anatomical details which imply important surgical concerns. We will describe the following: the round window niche, the round window skeleton, and the round window membrane.

2.6.2.6.1 The Round Window Niche

The round window niche is located in the posteroinferior aspect of the promontory in the medial wall of the tympanic cavity. The round window niche is defined as an anatomical bony entrance to the cochlear membrane. Its bony structures are confluent posteriorly and laterally toward the inferior retrotympanum which lies between the subiculum (posteriorly, laterally, and slightly superiorly) and the finiculus (anteriorly, laterally, and inferiorly).

The round window niche is of an average of 2 mm from the inferior margin of the oval window and is separated from the promontory by the subiculum. The mean width of the RW niche is around 2 mm. Its height varies up to 1 mm.

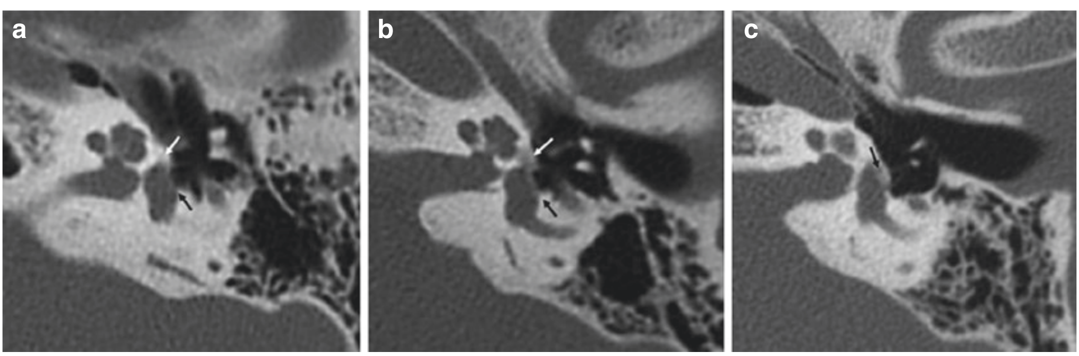

Fig. 2.62 Transversal computed tomography of the left ear: (**a**) normal thin aspect of the footplate (black arrow), very small prevestibular otospongiosis focus (white arrow); (**b**) moderate otosclerotic footplate thickening (black arrow) with a large prevestibular focus (white arrow); (**c**) obliterative footplate otosclerosis (black arrow)

2.6.2.6.2 Ridges of the RW Niche (Fig. 2.63)

– The **fustis** is a thick smooth bone ridge linking the basal turn of the cochlea with the styloid eminence. The fustis gives a strong support to the RWM; unnecessary drilling of the fustis in cholesteatoma has to be avoided because of a possible secondary SNHL.
– The **finiculus** is a bony ridge arising from the anterior pillar and running toward the floor of the hypotympanum where the jugular bulb is located; it divides the inferior retrotympanum from the hypotympanum cells anteroinferiorly.

2.6.2.6.3 Spaces of the RW Niche

The funiculus and the fustis divide the round window niche in three spaces situated below the subiculum and in continuity with the inferior retrotympanum:

- The **sinus subtympanicus** is the space between the subiculum superiorly and the finiculus inferiorly forming a deep space into the inferior retrotympanum below the sinus tympani (Figs. 2.63 and 2.64).
- The **area concamerata** of **Proctor**: is an anatomical area composed by bony cells developed around the fustis bone.
- **The subcochlear canaliculus** (Fig. 2.64) is a deep tunnel between the fustis and finiculus; it may reach the petrous apex cells. The subcochlear canaliculus was found in 81% with a pneumatisation directly extended to the petrous apex in 48%.

Clinical Application (Residual Cholesteatoma)
Conformation and limits of the round window niche may influence the surgical view of the round window membrane. Hence endoscopic approach enables a comprehensive exploration of the round window region; accurate knowledge of the anatomical relationships of this region has important advantages during middle ear surgery [68].

2.6.2.6.4 The Round Window Chamber

The round window chamber is defined as the three dimensional space lying between the round window niche and the round window membrane (Fig. 2.63).

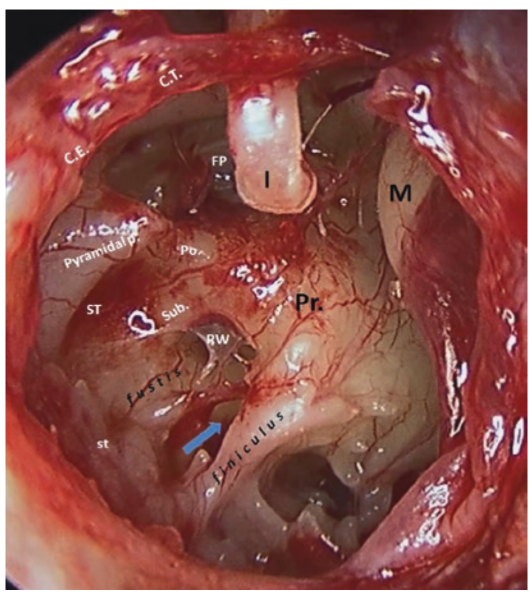

Fig. 2.63 Endoscopic picture of right ear posterior wall showing the three eminences: chordal eminence (CE) from where the chorda tympani (CT) is emerging to middle ear, pyramidal process, and styloid process (ST). The sinus tympani ST is located between ponticulus (Po.) superiorly and subiculum (sub.) inferiorly. The fustis is a thick solid bone projection linking the basal turn of the cochlea with the styloid eminence. The fustis gives a strong support to the round window membrane RW; the finiculus is a bony ridge arising from the anterior pillar of the RW and running toward the floor of the hypotympanum separating the inferior retrotympanum from the hypotympanum. The subcochlear canaliculus (blue arrow) is a deep tunnel between the fustis and finiculus; it may reach the petrous apex cells. *FP* footplate, *I* incus, *M* malleus, *Pr* promontory

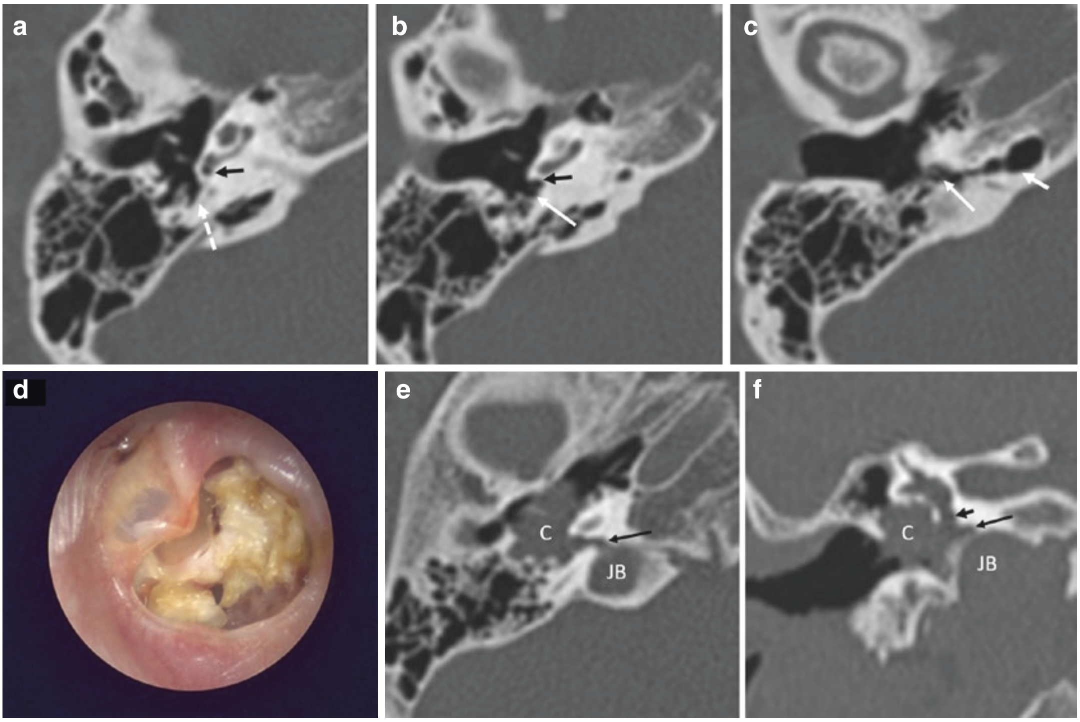

Fig. 2.64 Axial CT-images displayed in cranio-caudal sequence from the round window level down to the hypotympanum: (**a**) round window chamber (arrow), sinus tympani (dashed arrow) (**b**) round window niche (black arrow), entry of the subcochlear canaliculus (white arrow), (**c**) subcochlear canaliculus (long arrow) in continuity with the aerated cells of the petrous apex (short arrow). (**d**) otoscopic view of a cholesteatoma invading the retrotympanum and the RW niche (**e**) axial and (**f**) coronal CT view of a large meso et retrotympanic cholesteatoma in an 11 year old child, insinuating into the subcochlear canaliculus (long black arrow), inferior to the round window chamber (short arrow). The jugular bulb (JB) is moderately prominent and reaches the subcochlear canaliculus. No further aerated subcochlear cells are visible in this case

2.6.2.6.5 The Round Window Skeleton (Fig. 2.66)

The round window is the second opening of the labyrinth into the middle ear. The round window is not always round but could show different forms. Adult dimensions are reached early during fetal development. The average height of the RW was found to be 1.91 ± 0.78 mm, and the average width was 1.37 ± 0.43 mm [69].

The RW shows the following bony structures:

- **The tegmen of the RW**: is defined as the oblique dorsolateral edge of the promontory forming a convex edge over the entrance of the RW. *The configuration of the tegmen of the round window may influence the surgical view of the round window membrane.*
- **The posterior pillar**: is a pillar located near the bony edge of the round window niche entrance. In its posterior and superior aspect, it forms an acute angle with the tegmen.
- **The anterior pillar**: is a pillar located in the anterior and superior aspect of the round window niche, fusing with the anterior portion of the tegmen.

  The posterosuperior and posteroinferior walls of the RW meet posteriorly, leading to the sinus tympani (Fig. 2.66).

The anterior and posteroinferior margins of the round window overlie a crest, the *crista fenestrae*. It forms the anteroinferior sharp bony margin of the round window, with a variable shape, covering about 36–50% of the round window [70]. The membrane of the round window arises from the free edge of the crista.

The crista fenestra projects at a mean distance of 0.2 mm from the border of the RW; due to its location in the inferior and anterior border of the window, it represents the most important barrier to the scala tympani. The crista fenestra can be defined as a "doorstep" at the entrance of the basal turn of the cochlea [71]. During cochlear implantation, it could push the electrodes toward the modiolusleading to increased insertion resistance and possible electrode tip kincking.

The superior border of the niche (the tegmen) and the posterior pillar are important anatomical obstacles to proper visualization of the round window membrane through the posterior tympanostomy. A good view along the basal turn of the cochlea is achieved when the anteroinferior overhang and the crista fenestrae are removed to facilitate a tangentially cochlear implant insertion [72]. Narrower bony niches tend to house small crests. In this situation, removal of the crista fenestra could not provide enough additional room in the circumference of the niche (Fig. 2.65).

2.6.2.6.6 Topographic Anatomy of the Round Window

Preoperative awareness of possible anatomical variations of the RW and its relationships to the carotid canal (CC), jugular bulb (JB), facial nerve (FN), and oval window (OW) can help reduce complications in CI surgery (see Fig. 2.67).

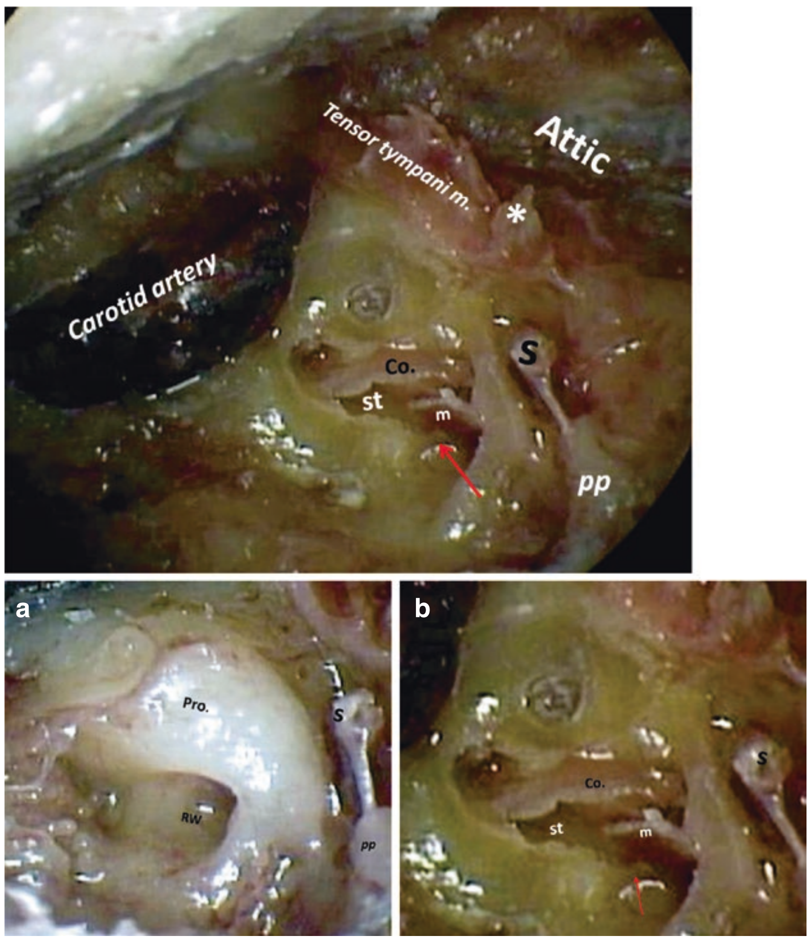

Fig. 2.65 Anatomy of round window and basal turn of cochlea. (**a**) Before drilling. (**b**) After drilling of round window niche and promontory to expose the round window membrane (m) and basal turn of cochlea (Co.). The round window leads to scala tympani (st). Red arrow is the crista fenestrae

- Distance between RW and carotid canal (RW-CC): average 2–4 mm
- Distance between RW and roof of jugular fossa (RW-JF): average of 2–4 mm
- Distance from RW to the horizontal facial canal (RW-HFC): average 2–3 mm and between RW and vertical facial canal (RW-VFC): average range of 2–4 mm
- Distance between RW and oval window (RW-OW): average of 2–4 mm
- Distance between pyramidal eminence and anterior round window (PE-RW): average 2.5 mm
- Maximum height of RW is 1 mm and maximum width is 2 mm

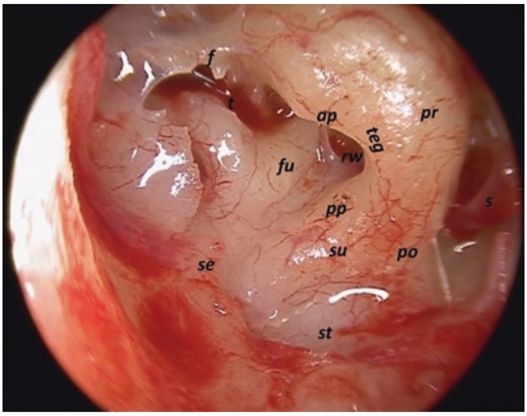

Fig. 2.66 *pp* posterior pillar, *ap* anterior pillar, *teg* tegmen, *fu* fustis, *f* finiculus, *su* subiculum, *rw* round window, *pr* promontory, *t* tunnel of subcochlear canaliculus, *st* sinus tympani, *po* ponticulus, *s* stapes

2.6.2.6.7 The Round Window Membrane (Fig. 2.68)

The RW membrane has a saddle point shape. The visible central portion is concave toward the cavity, but its edges are convex. The internal aspect of the RW membrane faces the scala tympani of the basal turn of the cochlea.

The thickness of the RW membrane is of 70 µm which does not change with advancing age [73]. Its length is 1.70 mm and its width is 1.35 mm. Like the tympanic membrane, the RW membrane is composed of three layers: an outer epithelium of low cuboidal cells lining the middle ear, an inner

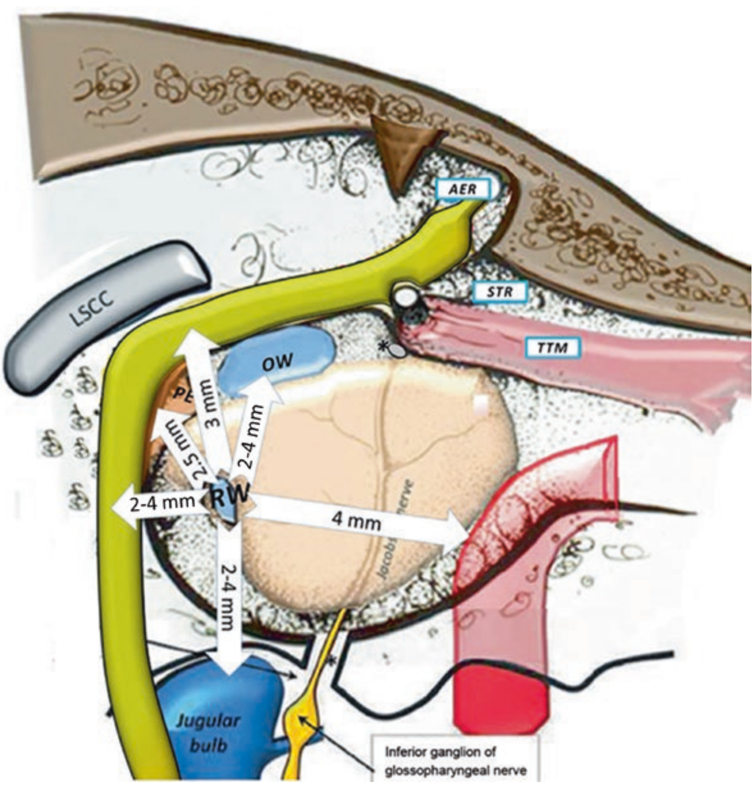

Fig. 2.67 A schema illustration of the topographic anatomy of the Round Window (RW) in relation to middle ear structures. *PE* pyramidal eminence, *OW* oval window, *LSCC* lateral semicircular canal, *AER* anterior epitympanic recess, *TTM* tensor tympani muscle, *STR* supratubal recess

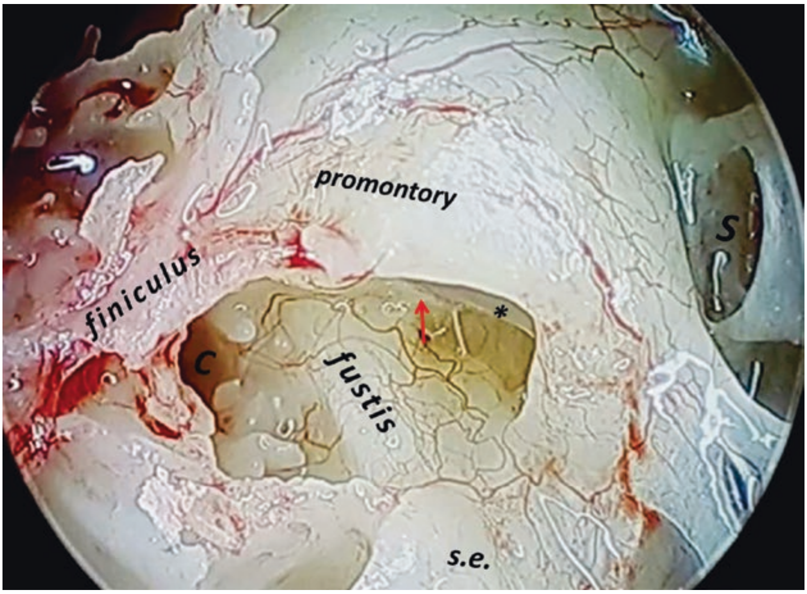

Fig. 2.68 Endoscopic picture of left ear round window niche showing the round window membrane (*). Notice that the round window membrane (RWM) is perpendicular to stapes footplate (s) plane. The RWM inserts inferiorly to a crest of bone, crista fenestra (red arrow). The fustis is a thick solid bone projection linking the basal turn of the cochlea with the styloid eminence (s.e.). The fustis gives a strong support to the RWM; the finiculus is a bony ridge arising from the anterior pillar of the RW and running toward the floor of the hypotympanum separating the inferior retrotympanum from the hypotympanum. The subcochlear canaliculus (C) is a deep tunnel between the fustis and finiculus; it may reach the petrous apex cells

epithelium of squamous cells bordering the inner ear, and a layer of connective tissue between the epithelial layers. The connective tissue layer consists of fibroblasts, collagen, and elastic fibers. The distance between the hinge of the RW niche and the center of the RW membrane ranges from 1.39 to 2.12 mm [74].

In the posterior part, the membrane lies very close to the lamina spiralis ossea with a distance of around 0.1 mm. In the center, this distance is around 1 mm [75]. The membrane does not lie at the end of the scala tympani but forms part of its floor. The hook region of the scala tympani is slightly posterior and superior to the RW membrane (see Fig. 2.65). The superior margin of the RWM has a close relation to the basilar membrane.

Only the anterior half of the RWM is visible through the surgical facial recess approach. The posterosuperior overhang is much smaller than the anteroinferior overhang. After removal of the posterosuperior overhang *via* a posterior tympanotomy, the posterior portion of the round window membrane is still difficult to see as it lies in the plane of vision. RWM is not directly posterior to the scala tympani; the scala is present just anterosuperior to the RWM.

The RW membrane transports macromolecules to the inner ear either by diffusion or pinocytosis. Micromolecules of 1 mue easily pass

Pearl

- *Drilling the niche overhang increases the visible surface area of the RW membrane by a factor of 1.5–3 times and provides an unrestricted access of the electrode to the scala tympani* [76].
- *The inferior part of RWM neighbors the cochlear aqueduct and vein and must be protected from surgical damage* (Fig. 2.69).

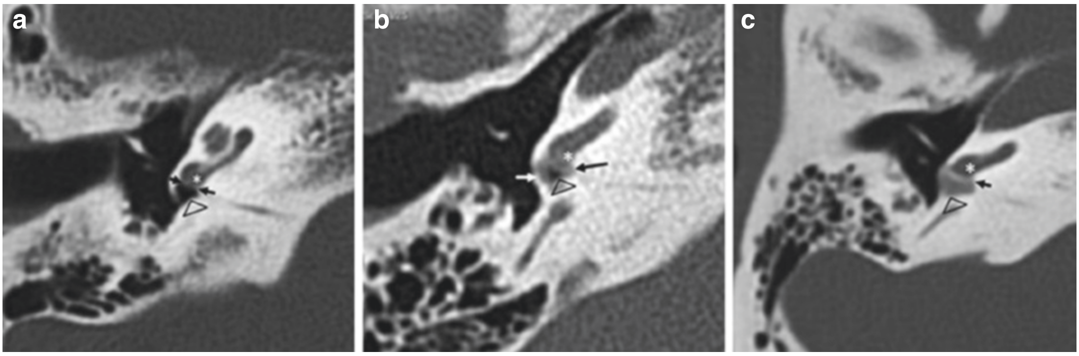

Fig. 2.69 Computed tomography in the transversal plan of the right ear showing (**a**) normal round window membrane (between the small black arrows), very thin limit between the air-filled round window recess (arrowhead) and the endolymph in the scala tympani of the basal turn of the cochlea (*); (**b**) otosclerotic foci on the promontory (white arrow) and of the round window (black arrow), presence of air in round window recess (arrowhead), but separated from the scala tympani (*) by the otosclerotic focus, RW3; and (**c**) condensation of the round window membrane (black arrow), scala tympani (*), complete obliteration of the round window recess (arrowhead), RW4

Surgical Applications

Large hypotympanic cells in the hypotympanum border inferiorly the round window niche. These prominent cells must not to be mistaken for the round window niche, especially during cochlear implant surgery.

The round window membrane is obscured to a variable degree by a bony overhang, which extends over the membrane anteriorly and superiorly for a distance of up to 1 mm. The round window membrane is oriented at a right angle to the plane of the footplate.

The more the distance between the oval window and the round window niche increases (>4 mm), more the visibility of the entry of the round window becomes difficult through the facial recess.

Surgical Application

The ampulla of the posterior semicircular canal is the closest vestibular structure to the round window. The *singular nerve*, supplying this ampulla, lies close to the round window niche. The round window represents a landmark for the position of the singular nerve. The singular canal, which contains the nerve, lies immediately inferior to the posterior attachment of the round window membrane.

Clinical Applications

– The RW membrane releases mechanical energy to the labyrinthine fluids, permitting movement of the inner ear fluids consecutive to the movements of the stapedial footplate; thus, patency of the niche is essential for efficient acoustic transmission; it can serve as an alternative route for sound energy to enter the cochlea.
– Infectious pathologies increase the thickness of RWM possibly to double, due to its collagen constituents; this offers a protective effect to the inner ear against infection or toxics. Nevertheless, the most common route of spread of middle ear enzymes and inflammatory interleukins (exotoxins or endotoxins) into the inner ear occurs through the round window membrane, (awareness about high frequency SNHL in chronic otitis media!)
Post-inflammatory increased thickness and hardening of the round window membrane and shrinkage of the membrane area reduce the maximum displacement of the membrane gradually, leading to a decrease in its sound transmission [69].
– Permeability of the RWM can be affected by factors such as molecular size, configuration, concentration, liposolubility, electrical charge level, and membrane

thickness. Regarding size, in vivo experiments have revealed that 1 μm microspheres can traverse chinchilla RWMs, whereas 3 μm spheres cannot [77].

Clinical Implication

The round window is the second most common site of otosclerosis. Round window involvement varies from mild involvement of the edge to a complete obliteration of the niche. Round window involvement could be diagnosed and staged by HRCT scan with thin cuts and classified from RW1 to RW5 [78] (Fig. 2.69).

Clinical Application

The promontory covers completely the round window membrane which is oriented inferiorly and posteriorly. Therefore, in a transcanal approach, it is difficult to see the membrane per se directly even through endoscope. The correct assessment of a diseased round window membrane such as in otosclerosis with its different stages or an invasive tympanosclerosis is only possible with thin cut computed tomography [78]. In addition, a good access to the membrane requires surgical removal of the superior overhang of the niche. Moreover, some strands draped over the RW niche, remnants of embryonic connective tissue, render the RW membrane difficult to be seen (Fig. 2.70).

through the RWM, but micromolecules more than 3 mue cannot pass through the membrane (this has to be considered during injection of intratympanic gentamicin, not to add sodium bicarbonate in gentamicin solution)

Clinical Application

Passage through the membrane is possible for small molecules by passive diffusion and for larger molecules probably by endocytosis [79, 80]. The round window membrane acts as the main gateway for local therapy of inner ear diseases. Drugs (such as dexamethasone and gentamicin) or bacterial exotoxins (in case of acute and chronic otitis media) present in the middle ear may pass through the round window membrane to reach the inner ear [81].

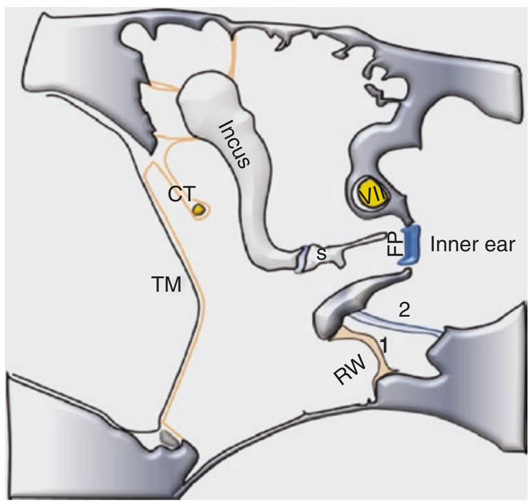

Fig. 2.70 Schematic drawing showing the round window (RW) with its false membrane (1) and true membrane (2). *S* stapes, *TM* tympanic membrane, *FP* footplate, *CT* chorda tympani

Surgical Implications of Anatomical Variations of the OW and RW Niche

- In addition to surgical concerns in stapedoplasty and cochlear implant, the variable anatomic dimensions and shape of the RW and OW have an impact on vibroplasty technique applications: the main concern is to achieve good stabilization of the device [82].

- Stimulation of the RW membrane with an active middle ear implant (AMEI) without drilling the niche is sufficient for successful hearing outputs. However, the resection of the bony rim of the RW niche improved significantly the RW stimulation at medium and higher frequencies. Drilling the niche enhances the exposure of the RW membrane and facilitates positioning of the implant tip [83].

2.6.2.7 Cochlear Aqueduct

Neighboring the round window, close to its posterior border, medial to the opening for the carotid canal in front of the jugular fossa, superior to the tympanic canaliculus, just anterior to the crista semilunaris, there is a triangular opening in the petrous bone that continues laterally a small only faintly visible canaliculus until the medial side of the basal turn of the cochlea: *the cochlear aqueduct*. The cochlear aqueduct lodges a tubular prolongation of the dura mater, establishing a communication between the perilymphatic space and the subarachnoid space (CSF); it transmits a vein from the cochlea (cochlear vein) to join the internal jugular vein; generally, the cochlear aqueduct is located 7 mm below the internal acoustic meatus and at the upper edge of the jugular foramen [84, 85] (Fig. 2.71).

The cochlear aqueduct contains the perilymphatic duct and is filled with a loose mesh of connective tissue that, although permeable to fluid, limits the patency of the CA. Therefore, unlike the vestibular aqueduct, the cochlear aqueduct does not contain a true epithelium-lined duct [86].

The CA provides a conduit between the posterior fossa and the inner ear, thereby permitting transmission of perilymphatic fluid, which originates partly from cerebrospinal fluid, into the inner ear [87, 88].

The narrow diameter of the CA is thought to buffer the inner ear from the wide pressure variations present within the posterior fossa subarachnoid spaces; CA is supposed to filter out cardiac and respiration-induced pulses of CSF not to affect cochlear function [89].

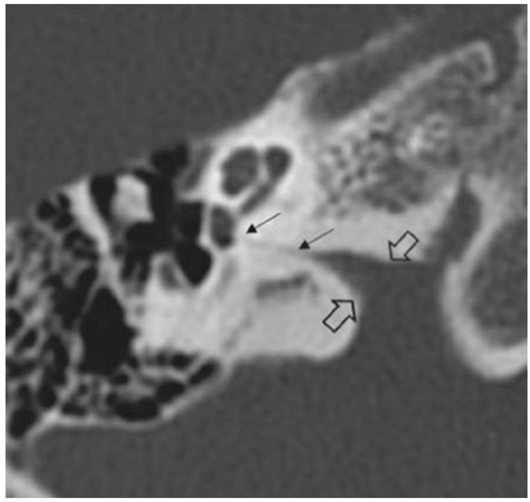

Fig. 2.71 Axial CT image showing the proximal part of the cochlear aqueduct (between empty arrows) with its characteristic triangular shape and its thin distal part (black arrows)

CA enlargement was defined as a diameter of more than 1 mm in the whole otic capsule; some authors support the thesis that the enlargement of the cochlear aqueduct can cause a gusher [89].

However, in a recent study, there was no evidence of CA enlargement found, not even in patients with inner ear malformations [90].

2.6.2.8 Singular Nerve

The singular canal conveys vestibular nerve fibers from the ampulla of the posterior semicircular canal to the posteroinferior border of the internal auditory meatus; it originates from the internal auditory canal, passes below and behind the inferior vestibular nerve, the porus acusticus, to the vestibule and posterior canal ampulla. The shortest distance between the singular nerve and round window membrane was 0.7 mm in average; the nerve could be found at a depth of 1.3 mm [91].

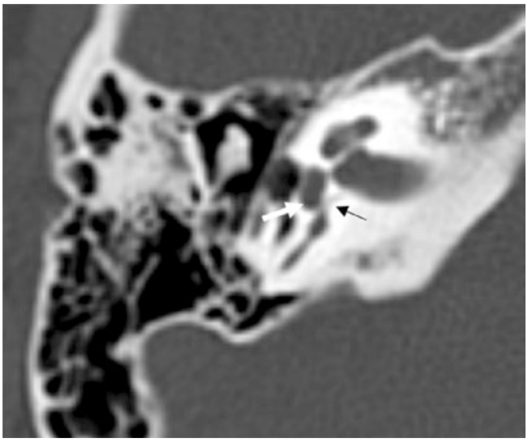

Fig. 2.72 Axial CT image of the right ear: round window recess (white arrow), singular nerve canal (black arrow)

The singular canal is approximately 4.5 mm long and 1 mm wide; the singular nerve lies very close to the round window membrane, which can be located 1–2 mm deep to its posteroinferior margin [92] (Fig. 2.72).

Clinical Correlations

Because of the close anatomic relationship of the singular nerve and the round window membrane, singular neurectomy for VBPP has declined due to the high risk of profound SNHL.

References

1. Langman J. Embryologie Médicale. Paris: Masson; 1965. p. 34.
2. Michaels L. An epidermoid formation in the developing middle ear: possible source of cholesteatoma. J Otolaryngol. 1986;15(3):169–74.
3. Michaels L. Origin of congenital cholesteatoma from a normally occurring epidermoid rest in the developing middle ear. Int J Pediatr Otorhinolaryngol. 1988;15(1):51–65.
4. Paço J, Branco C, Estibeiro H, Oliveira E, Carmo D. The posterosuperior quadrant of the tympanic membrane. Otolaryngol Head Neck Surg. 2009;140(6):884–8.
5. Daphalapurkar NP, Dai C, Gan RZ, Lu H. Characterization of the linearly viscoelastic behavior of human tympanic membrane by nanoindentation. J Mech Behav Biomed Mater. 2009;2(1):82–92.
6. Gan RZ, Feng B, Sun Q. Three-dimensional finite element modeling of human ear for sound transmission. Ann Biomed Eng. 2004;32:847–59.
7. Zhao F, Koike T, Wang J, Sienz H, Meredith R. Finite element analysis of the middle ear transfer functions and related pathologies. Med Eng Phys. 2009;31:907–16.
8. Shrapnell HJ. On the form and structure of the membrane timpani. Lond Med Gazette. 1832;10:120–4.
9. Henson OW Jr, Henson MM. The tympanic membrane: highly developed smooth muscle arrays in the annulus fibrosus of mustached bats. J Assoc Res Otolaryngol. 2000;1:25–32.
10. Adad B, Ragson BM, Ackerson L. Relationship of the facial nerve to the tympanic annulus: a direct anatomic examination. Laryngoscope. 1999;109:1189–92.
11. Makino K, Amatsu M. Epithelial migration on the tympanic membrane and external canal. Arch Otorhinolaryngol. 1986;243(1):39–42.
12. Lim DJ. Tympanic membrane: electron microscopic observations, part I: pars tensa. Acta Otolaryngol. 1968;66:181–98.
13. Lim DJ. Structure and function of the tympanic membrane: a review. Acta Otorhinolaryngol Belg. 1995;49:101–15.
14. Lim DJ. Tympanic membrane: electron microscopic observations, part II: pars fláccida. Acta Otolaryngol. 1968;66:515–32.
15. Sadé J. Retraction pockets and attic cholesteatomas. Acta Otorhinolaryngol Belg. 1980;34:62–84.
16. Merchant S, Rosowski J, Ravicz M. Middle-ear mechanics of type IV and type V tympanoplasty. II. Clinical analysis and surgical implications. Am J Otol. 1995;16:565–75.
17. Kurokawa H, Goode RL. Sound pressure gain produced by the human middle ear. Otolaryngol Head Neck Surg. 1995;113(4):349–55.
18. Spector GJ, Ge XX. Development of the hypotympanum in the human fetus and neonate. Ann Otol Rhinol Laryngol Suppl. 1981;90(6 Pt 2):1–20. https://doi.org/10.1097/MAO.0b013e31822e5b8d.
19. Noda R. Development of the cerebral vessels of the human fetus [in Japanese]. Fukuoka Acta Med. 1958:1057–72.
20. Hirakoh G. On the fossa jugularis and outflow cranial venous blood through it [in Japanese]. J Kurume Med Assoc. 1962;25:965–71.
21. Okudera T, et al. Development of posterior fossa dural sinuses, emissary veins, and jugular bulb: morphological and radiologic study. AJNR Am J Neuroradiol. 1994;15:1871–83.
22. Park JH, Son SB, Hong HP, Lee HS. A case of jugular bulb diverticulum invading the internal auditory canal. Korean J Audiol. 2012;16:39–42.
23. Friedmann DR, Eubig J, McGill M, Babb JS, Pramanik BK, Lalwani AK. Development of the jugular bulb: a radiologic study. Otol Neurotol. 2011;32(8):1389–95.
24. Semaan M, et al. Jugular bulb and skull base pathologies: proposal for a novel classification system for

jugular bulb positions and microsurgical implications. Neurosurg Focus. 2018;45(1):E5.
25. Roland JT Jr, Hoffman RA, Miller PJ, Cohen NL. Retrofacial approach to the hypotympanum. Arch Otolaryngol Head Neck Surg. 1995;121(2):233–6.
26. Potter GD, Graham MD. The carotid canal. Radiol Clin North Am. 1974;12:483–9.
27. Hasebe S, Sando I, Orita Y. Proximity of carotid canal wall to tympanic membrane: a human temporal bone study. Laryngoscope. 2003;113(5):802–7.
28. Brook CD. The prevalence of high-riding jugular bulb in patients with suspected endolymphatic hydrops. J Neurol Surg B Skull Base. 2015;76(6):471–4.
29. Eby TL. Development of the facial recess: implications for cochlear implantation. Laryngoscope. 1996;106(5 Pt 2 Suppl 80):1–7.
30. Tóth M. Pre- and postnatal changes in the human tympanic cavity, Semmelweis University School of Doctoral Studies for Developmental Biology Ph.D. Thesis, Budapest; 2007.
31. Carey JP, Minor LB, Nager GT. Dehiscence or thinning of bone overlying the superior semicircular canal in a temporal bone survey. Arch Otolaryngol Head Neck Surg. 2000;126(2):137.
32. Bast TH. Ossification of the otic capsule in human fetuses. Contrib Embryol. 1930;121:53–82.
33. Sanna M, Fois P, Paolo F, Russo A, Falcioni M. Management of meningoencephalic herniation of the temporal bone: personal experience and literature review. Laryngoscope. 2009;119:1579–85.
34. De Carpentier J, Axon PR, Hargreaves SP, Gillespie JE, Ramsden RT. Imaging of temporal bone brain hernias: atypical appearances on magnetic resonance imaging. Clin Otolaryngol. 1999;24:328–34.
35. Toth M, Helling K, Baksa G, Mann W. Localization of congenital tegmen tympani defects. Otol Neurotol. 2007;28:1120–3.
36. Weber PC. Iatrogenic complications from chronic ear surgery. Otolaryngol Clin North Am. 2005;38:711–22.
37. Lang J. Skull base and related structures: atlas of clinical anatomy. 2nd ed. Stuttgart: Schattauer; 2001.
38. Horn KL, Brackman DE, Luxford WM, Shea JJ III. The supratubal recess in cholesteatoma surgery. Ann Otol Rhinol Laryngol. 1986;95:12–5.
39. Schuknecht HF, Gulya AJ. Anatomy of the temporal bone with surgical implications. Philadelphia: Lea & Febiger; 1986. p. 89–90.
40. Makki FM, Amoodi HA, van Wijhe RG, Bance M. Anatomic analysis of the mastoid tegmen: slopes and tegmen shape variances. Otol Neurotol. 2011;32(4):581–8.
41. Minor LB. Superior canal dehiscence syndrome. Am J Otol. 2000;21:9–19.
42. Ahren C, et al. Lethal intracranial complications following inflation in the external auditory canal in treatment of serous otitis media and due to defects in petrous bone. Acta Otolaryngol (Stockh). 1965;60:407–21.
43. Lang DV. Macroscopic bony deficiency of the tegmen tympani in adult temporal bones. J Laryngol Otol. 1983;97:685–8.
44. Nadaraja GS, Gurgel RK, Fischbein NJ, Anglemyer A, Monfared A, Jackler RK. Radiographic evaluation of the tegmen in patients with superior semicircular canal dehiscence. Otol Neurotol. 2012;33:1245–50.
45. Puwanarajah P, Pretorius P, Bottrill I. Superior semicircular canal dehiscence syndrome: a new aetiology. J Laryngol Otol. 2008;122(7):741–4.
46. Dubrulle F, Kohler R, Vincent C, Casselman J. Deux cas particuliers de déhiscence du canal semicirculaire supérieur par déhiscence du sinus pétreux supérieur. J Neuroradiol. 2009;36:240–3. https://doi.org/10.1016/j.neurad.2009.02.002.
47. Tóth M, Medvegy T, Moser G, Patonay L. Development of the protympanum. Ann Anat. 2006;188(3):267–73.
48. Grand CM, Louryan S, Bank WO, Balériaux D, Brotchi J, Raybaud C. Agenesis of the internal carotid artery and cavernous sinus hypoplasia with contralateral cavernous sinus meningioma. Neuroradiology. 1993;35(8):588–90.
49. Savic D, Djeric D. Anatomical variations and relations in the medial wall of the bony portion of the eustachian tube. Acta Otolaryngol. 1985;99(5–6):551–6. https://doi.org/10.3109/00016488509182260.
50. Glastonbury CM, Harnsberger HR, Hudgins PA, Salzman KL. Lateralized petrous internal carotid artery: imaging features and distinction from the aberrant internal carotid artery. Neuroradiology. 2012;54(9):1007–13. https://doi.org/10.1007/s00234-012-1034-8.
51. PenidoNde O, Borin A, Fukuda Y, Lion CN. Microscopic anatomy of the carotid canal and its relations with cochlea and middle ear. Braz J Otorhinolaryngol. 2005;71(4):410–4.
52. Young RJ, Shatzkes DR, Babb JS, Lalwani AK. The cochlear-carotid interval: anatomic variation and potential clinical implications. AJNR Am J Neuroradiol. 2006;27(7):1486–90.
53. Jahrsdoerfer RA. Embryology of the facial nerve. Am J Otol. 1988;9:423–6.
54. Nager GT, Proctor B. Anatomical variations and anomalies involving the facial canal. Otolaryngol Clin North Am. 1991;24:531–53.
55. Jahrsdoerfer RA. Congenital absence of the oval window. ORL J Otorhinolaryngol Relat Spec. 1977;84:904–14.
56. Harada T, Black FO, Sand OI, Singleton GT. Temporal bone histopathologic findings in congenital anomalies of the oval window. Otolaryngol Head Neck Surg. 1980;88:275–87.
57. Gerhardt HJ, Otto HD. The intratemporal course of the facial nerve and its influence on the development of the ossicular chain. Acta Otolaryngol. 1981;91:567–73.
58. Lambert PR. Congenital absence of the oval window. Laryngoscope. 1990;100:37–40.
59. Zeifer B, Sabini P, Sonne J. Congenital absence of the oval window: radiologic diagnosis and associated anomalies. AJNR Am J Neuroradiol. 2000;21(2):322–7.
60. Cauldwell EW, Anson BJ. Stapes, fissula ante fenestram and associated structures in man. II. From embryos 6.7 to 50 mm in length. Arch Otolaryngol. 1942;36:891–925.

61. Anson BJ, Cauldwell EW, Bast TH. The fissula ante fenestram of the human otic capsule. II. Aberrant form and contents. Ann Otol Rhinol Laryngol. 1948;57:103–28.
62. Tóth M, et al. Development and surgical anatomy of the round window niche. Annals of Anatomy - Anatomischer Anzeiger. 2006;188(2):93–101. https://doi.org/10.1016/j.aanat.2005.09.006.
63. Linder TE, Ma F, Huber A. Round window atresia and its effect on sound transmission. Otol Neurotol. 2003;24(2):259–63.
64. Djerić D, Savić D. Anatomical characteristics of the fossula fenestrae vestibule. J Laryngol Otol. 1987;101(5):426–31.
65. Ukkola-Pons E, Ayache D, Pons Y, Ratajczak M, Nioche C, Williams M. Oval window niche height: quantitative evaluation with CT before stapes surgery for otosclerosis. Am J Neuroradiol. 2013;34(5):1082–5.
66. Anson B, et al. The fissula ante fenestram of the human otic capsule; developmental and normal adult structure. Ann Otol Rhinol Laryngol. 1947;56:957–85.
67. Toth M, et al. The role of Fissula ante fenestram in unilateral sudden hearing loss. Laryngoscope. 2016;126:2823–6.
68. Marchioni D, Soloperto D, Colleselli E, Tatti MF, Patel N, Jufas N. Round window chamber and fustis: endoscopic anatomy and surgical implications. Surg Radiol Anat. 2016;38(9):1013–9. Epub 2016 Mar 14.
69. Chen Y, Yao W. Mechanical model of round window membrane under reverse excitation. Appl Math Mech. 2016;37(10):1341–8. 8p.
70. Angeli RD, Lavinsky J, Setogutti ET, Lavinsky L. The crista fenestra and its impact on the surgical approach to the scala tympani during cochlear implantation. Audiol Neurotol. 2017;22:50–5.
71. Atturo F, Barbara M, Rask-Andersen H. On the anatomy of the 'hook' region of the human cochlea and how it relates to cochlear implantation. Audiol Neurootol. 2014;19(6):378–85.
72. Li PM, Wang H, Northrop C, Merchant SN, Nadol JB Jr. Anatomy of the round window and hook region of the cochlea with implications for cochlear implantation and other endocochlear surgical procedures. Otol Neurotol. 2007;28(5):641–8.
73. Carpenter A-M, Muchow D, Goycoolea MV. Ultrastructural studies of the human round window membrane. Arch Otolaryngol Head Neck Surg. 1989;115(5):585–90. https://doi.org/10.1001/archotol.1989.01860290043012.
74. Fugita, et al. Otol Neurotol xx:xx (c) 2016.
75. Rask-Andersen H, Liu W, Erixon E, Kinnefors A, Pfaller K, Schrott-Fischer A, Glueckert R. Human cochlea: anatomical characteristics and their relevance for cochlear implantation. Anat Rec. 2012;295:1791–811.
76. Kim M, Yang WS, Jeon JH, Choi JY. Electrode misdirection into the superior semicircular canal: complication of cochlear implantation by round window approach. Int Adv Otol. 2014;10(3):246–50.
77. Goycoolea MV, Muchow DD, Sirvio LM, Winandy RM, Canafax DM, Hueb M. Extended middle ear drug delivery. Acta Otolaryngol Suppl. 1992;493:119–26.
78. Mansour S, Nicolas K, Ahmad HH. Round window otosclerosis: radiologic classification and clinical correlations. Otol Neurotol. 2011;32(3):384–92.
79. Goycoolea MV, Muchow D, Schachern P. Experimental studies on round window structure: function and permeability. Laryngoscope. 1988;98(6 Pt 2 Suppl 44):1–20.
80. Kim CS, Cho TK, Jinn TH. Permeability of the round window membrane to horseradish peroxidase in experimental otitis media. Otolaryngol Head Neck Surg. 1990;103:918–25.
81. Penha R, Escada P. Round-window anatomical considerations in intratympanic drug therapy for inner-ear diseases. Int Tinnitus J. 2005;11(1):31–3.
82. Mancheño M, Aristegui M, Sañudo JR. Round and oval window anatomic variability: its implications. Otol Neurotol. 2017;38(5):e50–7.
83. Tringali S, Koka K, Deveze A, Holland NJ, Jenkins HA, Tollin DJ. Round window membrane implantation with an active middle ear implant: a study of the effects on the performance of round window exposure and transducer tip diameter in human cadaveric temporal bones. Audiol Neurootol. 2010;15(5):291–302.
84. Gopen Q, Rosowski JJ, Merchant SN. Anatomy of the normal human cochlear aqueduct with functional implications. Hear Res. 1997;107(1–2):9–22.
85. Ghiz AF, et al. Quantitative anatomy of the round window and cochlear aqueduct in guinea pigs. Hear Res. 2002;162(1–2):105–12. https://doi.org/10.1016/S0378-5955(01)00375-6. Source: PubMed.
86. Anson BJ, Donaldson JA, Warpeha RL, Winch TR. The vestibular and cochlear aqueducts: their variational anatomy in the adult human ear. Laryngoscope. 1965;75(8):1203–23.
87. Park TS, Hoffman HJ, Humphreys RP, Chuang SH. Spontaneous cerebrospinal fluid otorrhea in association with a congenital defect of the cochlear aqueduct and Mondini dysplasia. Neurosurgery. 1982;11(3):356–62.
88. Carlborg BIR, Farmer JC Jr. Transmission of cerebrospinal fluid pressure via the cochlear aqueduct and endolymphatic sac. Am J Otolaryngol Head Neck Med Surg. 1983;4(4):273–82.
89. Bianchin G, et al. Cerebrospinal fluid leak in cochlear implantation: enlarged cochlear versus enlarged vestibular aqueduct (common cavity excluded). Int J Otolaryngol. 2016;2016:6591684. https://doi.org/10.1155/2016/6591684. 9 pages.
90. Stimmer H. Enlargement of the cochlear aqueduct: does it exist? Eur Arch Otorhinolaryngol. 2011;268(11):1655–61.
91. Leuwer RM, Westhofen M. Surgical anatomy of the singular nerve. Acta Otolaryngol. 1996;116(4):576–80.
92. Leveque M, Labrousse M, Seidermann L, Chays A. Surgical therapy in intractable benign paroxysmal positional vertigo. Otolaryngol Head Neck Surg. 2007;136:693–8. Review.

Middle Ear Contents

3

Contents

Traditionally, the ossicular chain is considered as the essential content of the middle ear. It is suspended inside the cavity by ligaments and muscles, which will be addressed in their embryological development and their anatomical details in this chapter. Also development and functional anatomy of middle ear articulations, muscles, vessels, nerves, and folds will be studied in a comprehensive methodology.

S. Mansour et al., *Comprehensive and Clinical Anatomy of the Middle Ear*,
https://doi.org/10.1007/978-3-030-15363-2_3

Nowadays, it is admitted through middle ear mechanic studies that in addition to the ossicular chain, the most important content of the middle ear to assure a normal sound transmission is air. The tympanic cavity contains an average of 1–2 cm^3 of air. The minimal volume of air necessary for a normal function of the middle ear is at least 0.5 cm^3. Air transmits the sound wave from outside to the tympanic membrane (as a *vehicle*) and serves inside the middle ear air as an *isolator* (impedance matching system). The air content's exchange and pathways of ventilation will be discussed in Chap. 4.

3.1 The Auditory Ossicles

The auditory ossicles, the malleus, incus, and stapes, are named after the objects they resemble to (hammer, anvil, and stirrup). The ossicles are suspended in the middle ear cavity by numerous suspensory ligaments, and they are covered by the mucous membrane of the middle ear cavity. The auditory ossicles are responsible for transmission of sound-induced vibrations from the tympanic membrane to the oval window. This system, along with the aeration, is the cornerstone of middle ear mechanics.

3.1.1 Embryology of the Auditory Ossicles

The ossicles, muscles, and tendons of the middle ear are formed from the mesenchyme of the middle ear and are covered by the epithelial lining of the first pharyngeal pouch [1].

The mesenchyme forming the ossicles is derived from neural crest cells present in the first and second visceral (branchial) arches. These cells migrate to the branchial arch from the dorsal part of the developing neural tube during the fourth week of gestation [2].

There is a controversy about the specific contribution of each arch to the ossicular formation; there are two main theories regarding this issue:

- **The classical theory** postulates that the incus and the malleus are derived from Meckel's cartilage of the first branchial arch; the stapes is derived from Reichert's cartilage of the second branchial arch [3–7].
- **The alternative theory** proposes that the head of the malleus and the body of the incus originate from the first arch, while the handle of the malleus, the long process of the incus, and most of the stapes originate from the second arch (Fig. 3.1) [8–13].

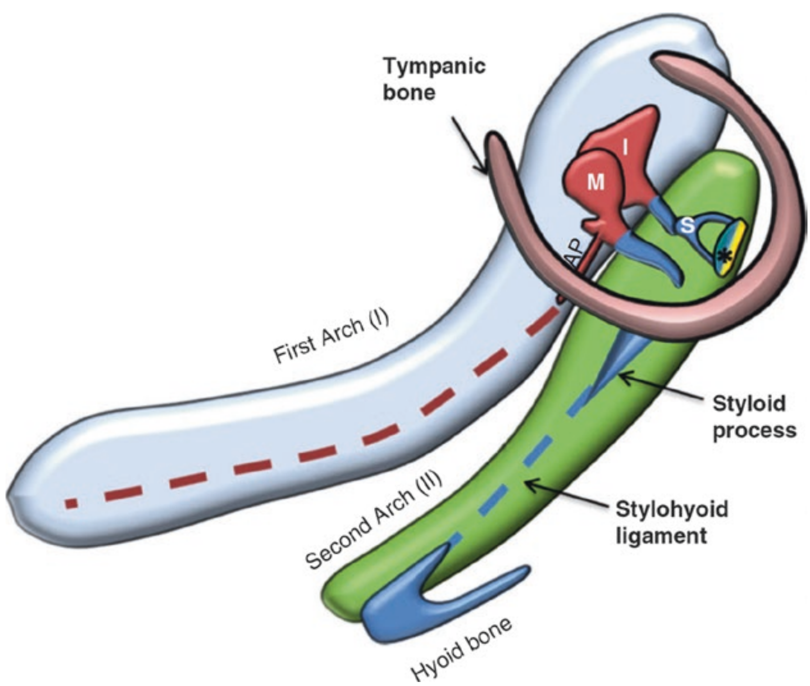

Fig. 3.1 Destination of the first and the second branchial arches. *M* malleus, *I* incus, *S* stapes, *AP* anterior malleal process, (*) double origin of the footplate

In both theories, the labyrinthine aspect of the footplate was considered to originate from the mesenchyme of the otic capsule. However, some normal and teratologic observations in the literature support the idea that the stapes could entirely derive from the Reichert's cartilage without any contribution of the otic capsule [14–16].

Recent morphological observations in the human embryo could suggest that malleus and incus derived from the first arch only, with eventual exception for the short process of the malleus [17]. However, molecular data support a new theory, suggesting that both pharyngeal arches could contribute to malleus and incus rudiments [18]. This makes obsolete the opposite anterior theories.

Ossicular development in the human embryo starts at the fourth week of gestation as an interbranchial mesenchymal bridge connecting the mesenchyme of the upper part of the first branchial arch and the central part of the second branchial arch. This condensed mesenchyme gives rise to the primordial malleus and incus [12, 19, 20]. This mesenchymal mass is crossed by the chorda tympani that divide it in two parts: the malleal primordium laterally and the incudal primordium medially (Fig. 3.2). This common rudiment keeps connection with the Reichert's cartilage, supporting the "alternative" theory that all of the stapes blastema derives from the second arch mesenchyme.

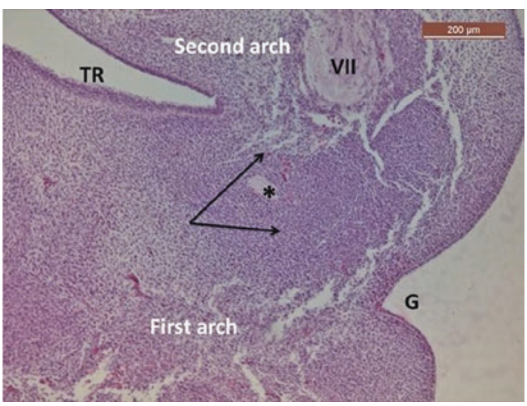

Fig. 3.2 Five weeks 13-mm human embryo. The common blastema of the handle of the malleus and the long crus of the incus (the two arrows) crossed by the chorda tympani (*). TR tubotympanic recess of the first branchial pouch, (G) the first ectodermal groove, VII facial nerve in the second branchial arch. Hematoxylin-eosin staining

During the sixth week, a precartilage forms the future ossicles. A rapid transformation into true cartilage occurs during the seventh week. By the end of the eighth week, the cartilaginous malleus resembles the adult aspect. Thereafter, progressive and extensive ossicular growth occurs, and, by the 20^{th} week, the ossicles reach adult size and have begun to ossify.

Ossification of the incus takes place slightly earlier than that of the malleus. In the 25^{th} to 26^{th} week, both the incus and malleus are fully ossified (see Chap. 1, Fig. 1.3) with the exception of the distal extremity of the malleus handle. Meanwhile, the pneumatization process of the tympanic cavity extends into the epitympanum and antrum, making the ossicles free, only tethered to the tympanic cavity in a mesentery-like fashion.

3.1.1.1 Developmental Genetics of the Middle Ear and Its Contents

The craniofacial development is largely controlled by Homeobox (Hox) genes. These genes are segmentally expressed in the rhombomeres and in the branchial arches, except the first one.

Knockout of Hoxa-2 gene in the mouse gives rise to a "duplication" of the first arch derivatives inside the second arch, with a double "mirror-shaped" malleus and incus complex, without any stapes [21]. Hox genes expression can be modified by retinoic acid because of the presence of a specific sequence called "rare" (for *retinoic acid response elements*). Administration of retinoic acid to pregnant mice extends the expression of Hoxb1 and Hoxb2 in the mandibular arch [22] and gives rise to severe ossicular malformations (Fig. 3.3), with increase of the apoptotic process in the first arch [23].

Some middle ear malformations can be allowed by the loss of function of genes Hoxa-2, Prx1 and 2, and Goosecoid (responsible for tympanic ring development) [24, 25].

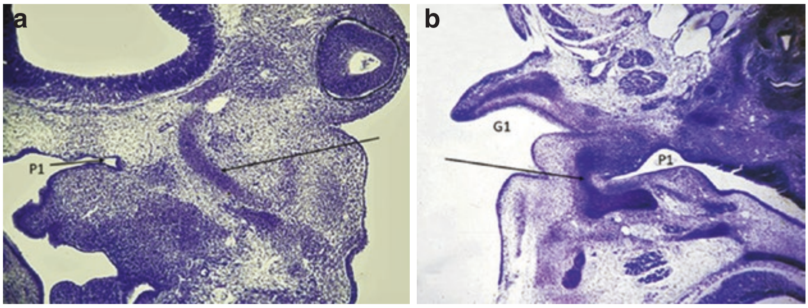

Fig. 3.3 Mouse embryos whose mothers were exposed to 4 mg/kg of 13-cis retinoic acid at embryonic day 9 (E9). (**a**) E13 embryo showing a curved Meckel's cartilage medially displaced (arrow). (**b**) E17 embryo. A "mirror" structure crosses the tympanic area and joins both first and second branchial arches and suggests a duplicated handle of the malleus (arrow). *G1* first branchial groove, *P1* first pharyngeal pouch. Toluidine blue staining

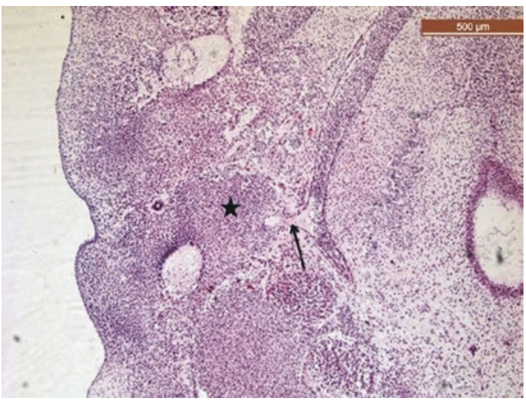

Fig. 3.4 13-mm human embryo section showing the stapedial rudiment (*) passed by the stapedial artery (arrow). Hematoxylin-eosin staining

3.1.1.2 Stapes Development

The stapes, the first ossicle to appear, develops from an independent anlage derived from the cranial end of the cartilage of the second branchial arch (Fig. 3.1). The stapedial anlage connects to the remaining Reichert's cartilage by a formation called the interhyale; the internal part of the interhyale gives rise to the tendon of the stapedial muscle. The stapedial anlage will be crossed by the stapedial artery during embryonic period, giving the stapes its characteristic ring shape (Fig. 3.4).

3.1.1.2.1 Footplate Development

There are two theories regarding the origin of stapedial footplate. Despite the fact that there are several differences between both theories, there is a consensus that footplate development is characterized by a progressive replacement of undifferentiated mesenchyme by chondroblasts and differentiation of the peripheral mesenchyme into the annular ligament around the presumptive footplate, as demonstrated by Jaskoll in the chick embryo [26] (Fig. 3.5).

Classical Theory of Footplate Origin

The classical theory presumes that the footplate has two origins: the tympanic side derived from the stapedial ring and the vestibular side derived from the *lamina stapedialis* of the otic capsule [16]. The medial border of the stapedial ring comes in contact with a facing depression in the lateral wall of the otic capsule. This depression, called the *lamina stapedialis*, is the future oval window. The medial border of the stapedial ring fuses with the *lamina stapedialis* to form the stapedial footplate (Fig. 3.6).

Alternative Theory of Footplate Origin

According to this theory, the otic capsule is not involved in the formation of the base of the stapes, and the entire stapes derives from the stapedial anlage of the Reichert's cartilage [14, 15, 26, 27] (Fig. 3.7).

3.1.1.2.2 Annular Ligament

At the beginning, the footplate is attached to the otic capsule by a band of mesenchyme that later transforms into the annular ligament, once the footplate reaches adult size [26, 27]. The stape-

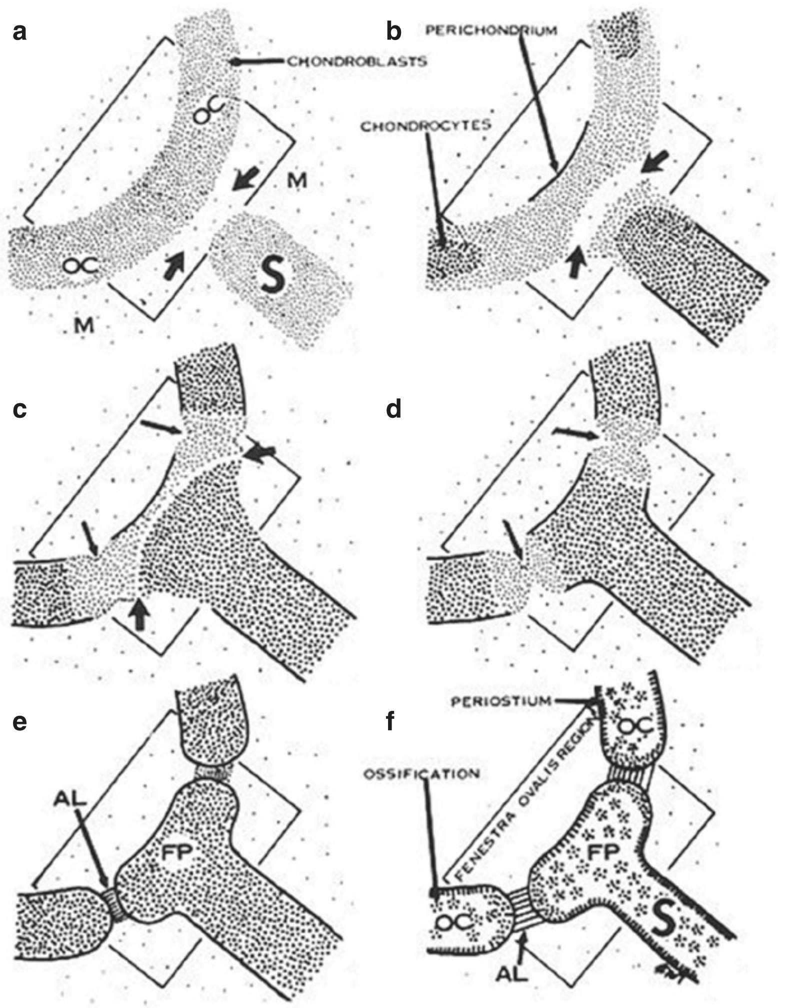

Fig. 3.5 Footplate development in the bird (According to Jaskoll 1980 [26]. (**a**–**f**): Successive stages of development of the footplate and related structures. This material is reproduced with permission of John Wiley & Sons, Inc.). Chondroblasts of the otic capsule and stapes are initially separated by undifferentiated mesenchyme. This mesenchyme progressively disappears and becomes present in the "isthmus" (arrows) in which will develop the annular ligament. *FP* footplate, *AL* annular ligament, *OC* otic capsule

diovestibular joint—stapes and the inner ear being decoupled—shows its definitive characteristics at 12th week (Figs. 3.4 and 3.5).

3.1.1.2.3 Stapes Ossification

Stapes endochondral ossification starts at the end of the fourth month from a single ossification center present at the center of the footplate. The ossification extends to the two branches and then to the head of the stapes [28].

> **Clinical Application**
> Congenital stapes anomalies are sometimes related to an aberrant facial nerve development. During the crucial time period of sixth week, anterior displacement of the second genu region of the VII hinders the normal fusion of the stapedial ring with the lamina stapedialis, resulting in a malformed stapes associated to abnormal facial nerve trajectory (cf examples below).

3.1.1.3 Incus Development

The incus is the second ossicle to appear but the first to be ossified. The body of the incus derives from the cranial part of the Meckel's cartilage. The origin of the incus was attributed to Reichert's cartilage (Figs. 3.1 and 3.8). However, a recent work in 2016 [17], based

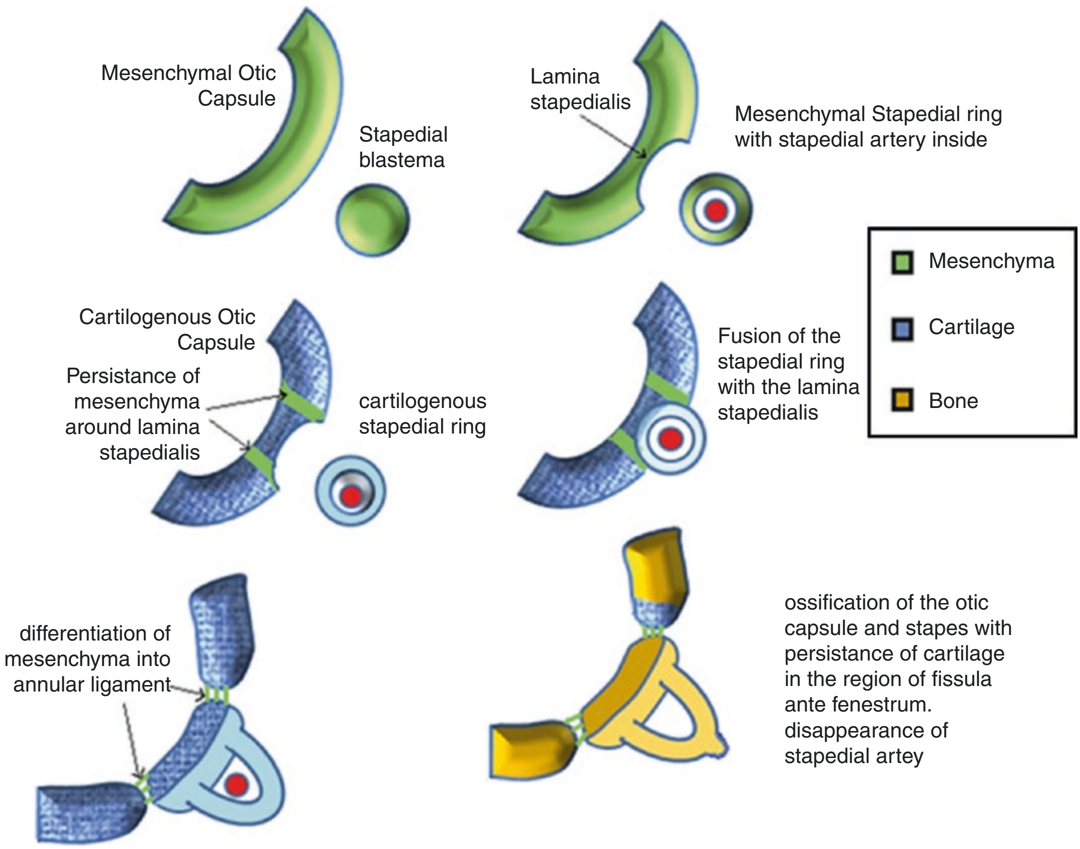

Fig. 3.6 Stapes development according to the classical theory

Fig. 3.7 E16 mouse embryo whose mother received a teratogen molecule (methyl triazene) disturbing ossicle formation. A complete stapes develops independently from the otic capsule (arrow). In front of the stapes, we observe a narrowing of the otic capsule cartilage. Toluidine blue staining at pH2

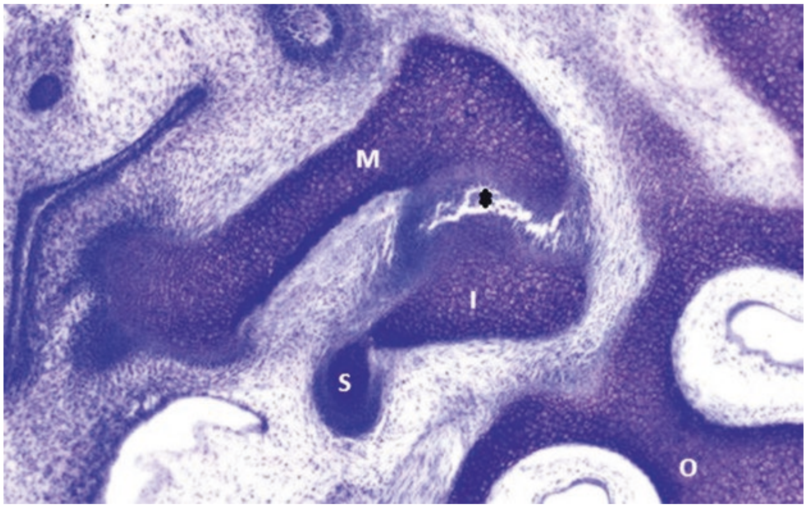

Fig. 3.8 Sagittal section of E17 mouse embryo displaying the cartilaginous malleus (M), incus (I), and stapes (S) in close relationship with the otic capsule (O). The incudomalleolar joint is just forming (*). Toluidine blue staining at pH4

upon morphological observations, stated that the early anlagen of the malleus handle and the long process of the incus are very difficult to identify on very young embryos. Thus, the authors conclude that their evidences support the "classical" theory that the entire malleus and incus derive from the first arch. Meanwhile, this opinion neglects the *in vitro* and teratologic evidences, favorable to the alternate hypothesis previously described [20, 29].

Burford and Mason [17] suggested to explore the Hoxa2 gene (specific of second arch) expression in developing ossicles. Preliminary results [18] demonstrate that the ossicle's development is less schematic than supposed: the entire malleus and incus rudiments seem to include cells arising from both first branchial arches.

Endochondral ossification starts at the beginning of the 16th gestational week from the anterior face of the long process and ends at the 24th week reaching adult size.

3.1.1.4 Malleus Development

The head of the malleus (Figs. 3.1, 3.8, and 3.9) appears as a mass connected to the cranial extremity of the Meckel's cartilage. This connection disappears later to be replaced by the anterior process of the malleus and anterior malleal ligament. The anterior process, which can be up to 10 mm in neonates, remains in the adult malleus only as a small prominence. A lack of bony

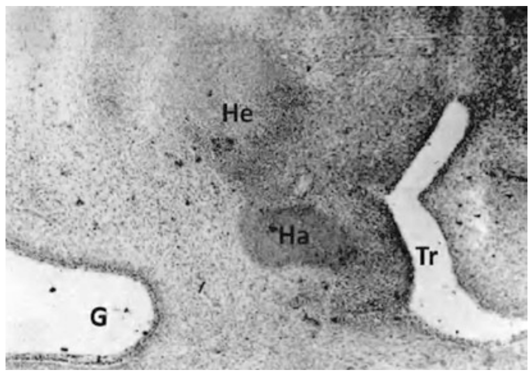

Fig. 3.9 Coronal section of a 6-week 19 mm human embryo revealing the coalescence of the handle of malleus (Ha) and the head of malleus (He). The handle projects between the first ectodermal groove (G) and the first endodermal pouch (TR). At this stage, the ossicles are cartilaginous. Hematoxylin-eosin staining

involution can keep the malleus fixed at the petrotympanic fissure [30].

The handle of the malleus has close relationships with the long process of the incus in a blastema originally connected to the Reichert's cartilage. Failure of resorption of this connection with Reichert's cartilage leads to the formation of a *malleus handle bony bar*. Later, the handle of malleus becomes inserted in the tympanic membrane rudiment.

This different origin of the head and of the handle and lateral process of the malleus explains why in aural atresia the handle is missing whereas the head of the malleus is present. Malleus ossification ends by the sixth month of fetal life [31].

The development of the temporomandibular joint and the malleus is reciprocal. Several anatomical and embryological researches have shown that the intermediate lamina of the TMJ disk continues via the petrotympanic fissure to the malleus [32], forming the disco-malleolar ligament (Fig. 3.10) [33]. Furthermore, the sphenomandibular ligament connects with the TMJ disk and with the malleus [34].

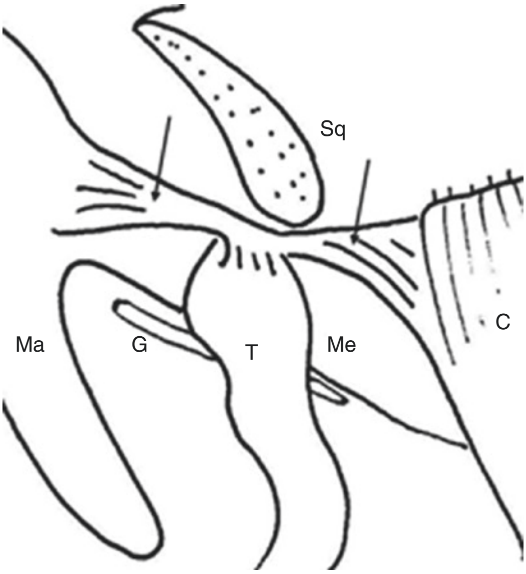

Fig. 3.10 Reconstruction of the middle ear primordium of a 87 mm fetus, showing the disco-mandibular ligament (arrows) (modified after Smeele [32]). *C* condyle, *G* goniale bone (anterior process of the malleus), *Ma* malleus, *Me* Meckel's cartilage, *Sq* squamous part of the temporal bone

These connections and relationships could explain several clinical associations between TMJ disorders and ear complaints.

3.1.1.5 Congenital Ossicular Malformations

Congenital ossicular malformations could be associated with aural atresia and microtia (Figs. 3.11 and 3.12) or could be isolated without external ear anomaly as in minor ear atresia. Ossicular anomalies in minor atresia are subdivided into incudomalleal fixation, stapes fixation, and incudostapedial disconnection [35]. Incudomalleal fixations are the least common, where the malleus head and incus body are usually fused or fixed to the epitympanic walls [36]. Triple ossicular malformations are rare and could be associated with inner ear anomalies [37].

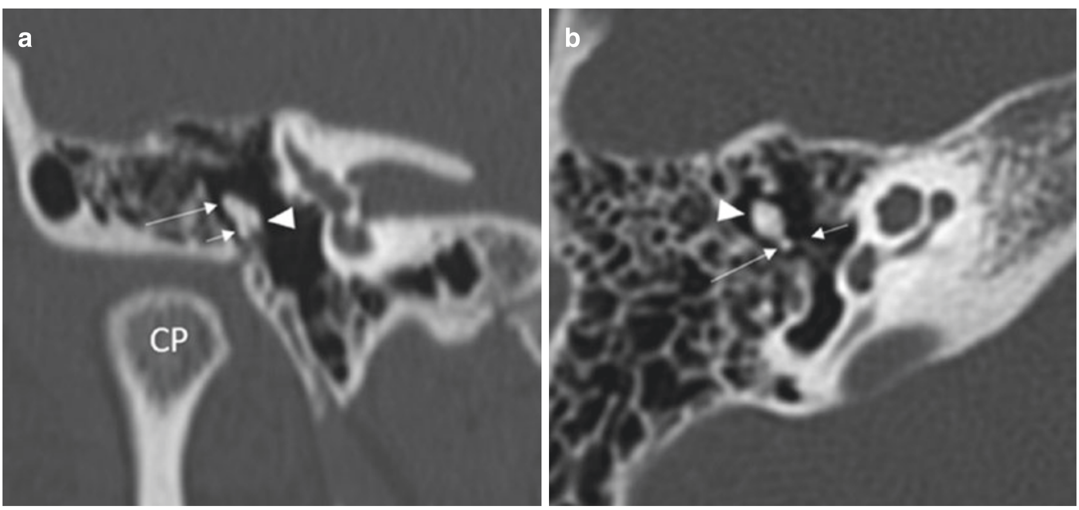

Fig. 3.11 Ossicular malformations in atresia of the external auditory canal (EAC): (**a**) Coronal CT image of a right ear showing the head of the malleus (long arrow). The neck of the malleus (short arrow) inserting on the outer attic wall. Absence of EAC, the tympanic membrane and the malleus handle. Condylar process (CP). Incus (arrowhead). (**b**) Axial CT image of the same ear, showing a rounded aspect of the incus (arrowhead) because of rotation and a shortened hypoplastic long process of the incus (long arrow), in discontinuity with the head of the stapes (short arrow)

Malleus Congenital Anomalies

The incidence of malleus anomalies is lower than anomalies of the incus or stapes. Hypoplasia or aplasia of the malleus results from a failure of embryogenesis between 7th and 25th week. Given the common pharyngeal arch origin, hypoplasia of the malleus is often associated with hypoplasia of the incus (Fig. 3.13) [38].

Epitympanic fixation of the head of malleus is by far the most congenital anomaly of the malleus (Fig. 3.14). This anomaly is related to an incomplete pneumatization of the epitympanum during malleus head ossification. Temporal bone exploration in these patients reveals bony bridges between the head of the malleus and the lateral epitympanum in the majority of cases [30, 36].

Malleus bar is a persistent bony bridge that connects the malleus handle to the posterior tympanic wall [39, 40].

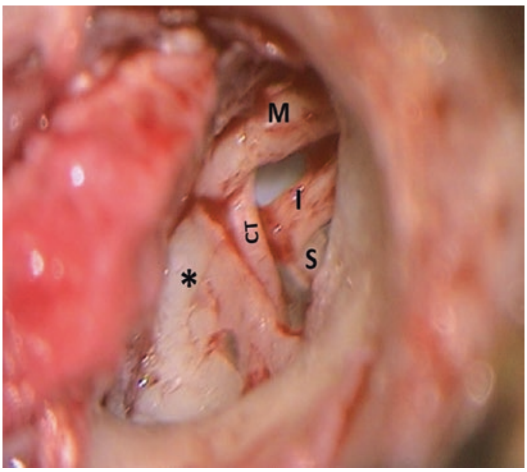

Fig. 3.12 Left ear with atresia plate (*) replacing the tympanic membrane, absence of the malleus handle, chorda tympani (CT) below the bony atresia plate overlying incus (I) and below the malleus neck (M); *S* stapes

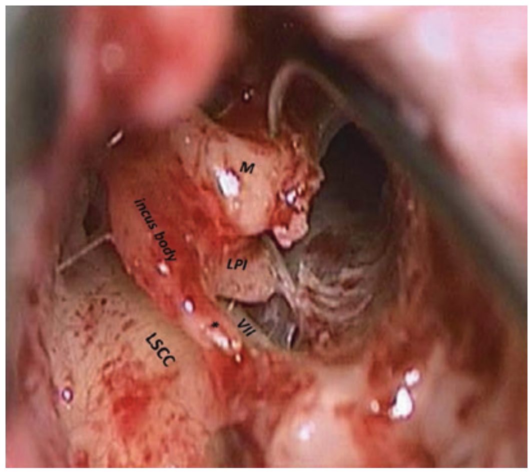

Fig. 3.14 Left ear transmastoid atticotomy view showing aplasia of the malleus handle (M) and lenticular process of the incus. Stapes is present. *M* malleus head, * short process of incus, *VII* facial nerve, *LSCC* lateral semicircular canal

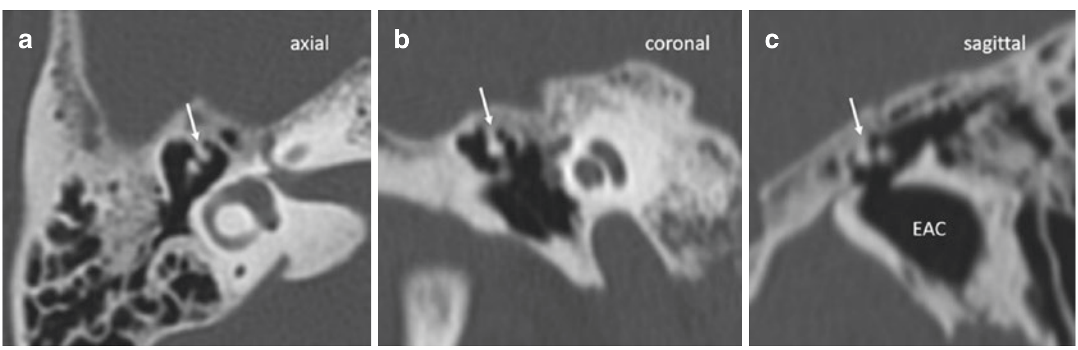

Fig. 3.13 Epitympanic fixation of the malleus head (arrow) on axial (**a**), coronal (**b**), and sagittal (**c**) CT images

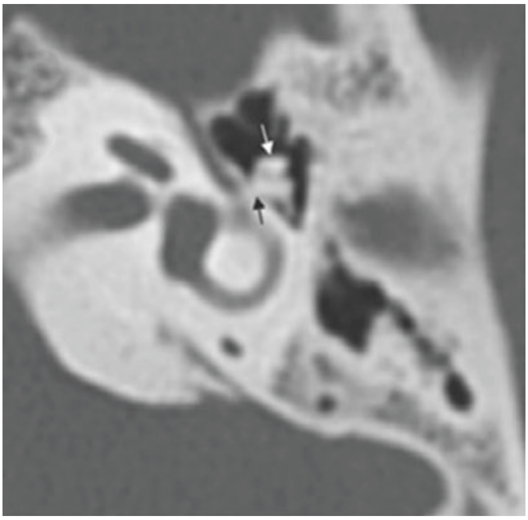

Fig. 3.15 Transversal CT image of a left ear with fixation of the incus on the Fallopian canal (black arrow), malleus head (white arrow)

Incus Congenital Anomalies
Hypoplasia or aplasia of the incus typically occurs in conjunction with hypoplasia of the malleus but may occur in isolation. The incus is also susceptible to fixation to the epitympanum (Fig. 3.15). Congenital absence of the long process of the incus might be associated with aplasia of the stapes and of the handle of malleus, supporting the hypothesis of their common origin [38, 41] (Fig. 3.16).

Congenital absence of the long process of the incus results in a near-maximal conductive hearing loss [38, 41].

Stapes Congenital Anomalies
Congenital stapes footplate fixation is the most common isolated ossicular anomaly, approximately 40% of all congenital ossicular malformations. It is thought to result from ossification of the peripheral mesenchyme of the footplate instead of differentiating into the annular ligament [42]. Although aplasia of the stapes is rare, multiple forms of hypoplasia that include small or absent crura and blob-like stapes have been described. In contrast, isolated hyperplasia of the stapes is often an incidental finding that does not require therapy; this anomaly is thought to result from a failure of the resorption and remodeling that occurs during the final stages of stapes development. Several crural anomalies have been described, including thin, absent, fused, and angled crura (Figs. 3.17 and 3.18). The crura may also be replaced with a columella-like structure. Congenital stapes disorders are often related to aberrant facial nerve development [10, 38, 43].

3.1.2 Anatomy of the Auditory Ossicles

3.1.2.1 The Malleus

The malleus is shaped like a hammer and is the largest of the three middle ear ossicles. It is 8–9 mm in length and weighs about 20–25 mg. It consists of a head, neck, handle, and two processes arising below the neck (Fig. 3.19).

3.1.2.1.1 The Malleus Head

The malleus head lies in the attic region of the middle ear and is 2.5 by 2 mm in size. On its posteromedial surface, there is an elongated saddle-shaped facet to articulate with the incus. This facet is covered by an articular cartilage.

Malleus Head Fixation
Malleus head fixation is not an uncommon pathology. It may be a congenital anomaly (as shown above in Fig. 3.15) or acquired as in tympanosclerosis (Figs. 3.20 and 3.21). Clinically it manifests as a 15–25 dB conductive hearing loss [44].

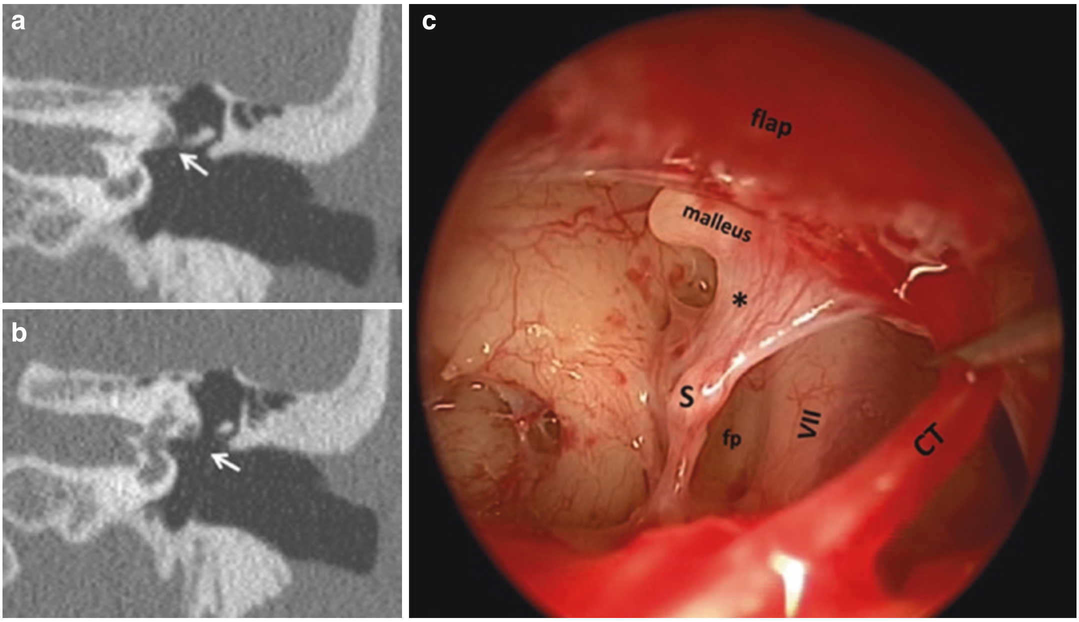

Fig. 3.16 A case of left CHL with normal tympanic membrane. (**a**, **b**) Coronal CT scan showing the absence of the long process of incus (arrow). (**c**) Intraoperative view showing the complete absence of the incus which is replaced by a fibrotic band (*) connecting the head of stapes (S) to the malleus; notice that the chorda tympani (CT) is unusually large: Second arch anomaly. *VII* facial nerve, *fp* footplate

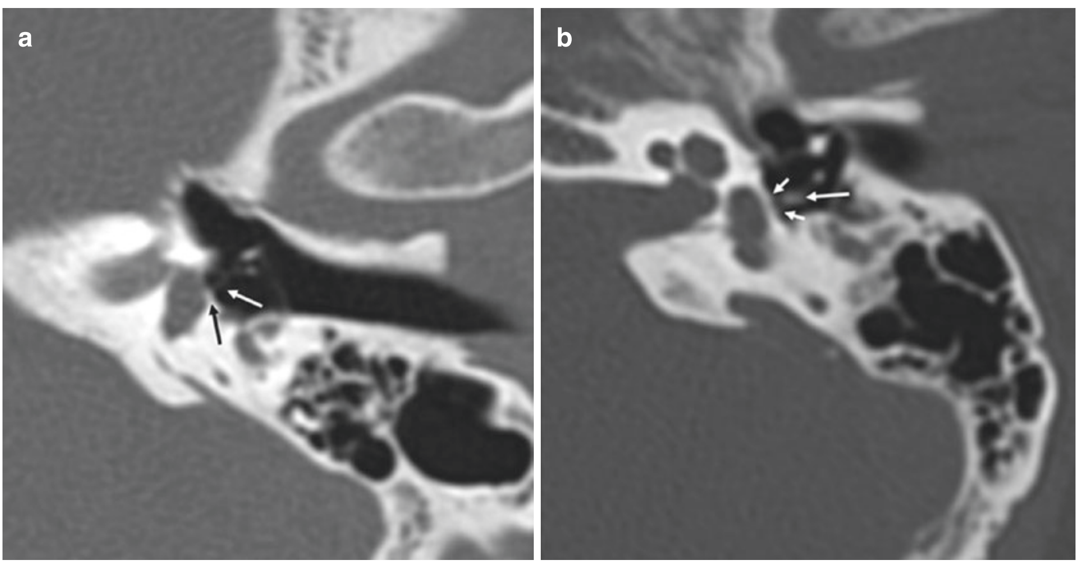

Fig. 3.17 Axial CT images of left ears: (**a**) Hypoplasia of the stapes (white arrow), the posterior part of the oval window is dense and thick (black arrow). (**b**) Fusion of the proximal parts of the crura (long arrow) and two very small distal parts of the crura (small arrows) inserting on the footplate

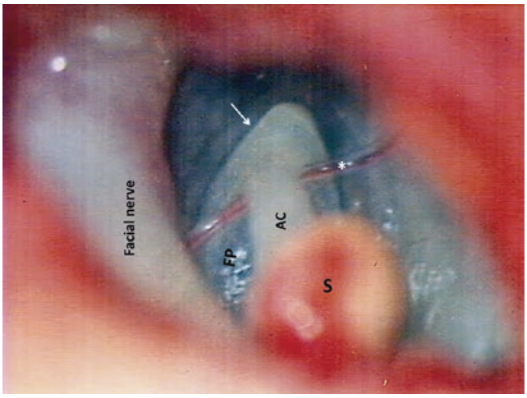

Fig. 3.18 Left ear with posteriorly displaced stapes (white arrow), persistent tiny stapedial artery (*) passing between the posterior crura and anterior crura (AC) above the footplate (FP)

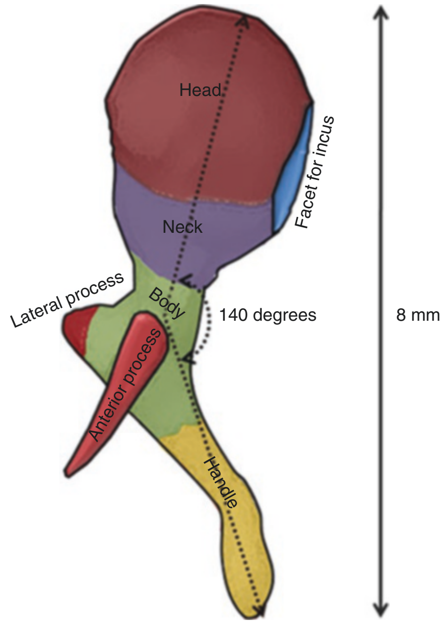

Fig. 3.19 Schematic drawing of the malleus

Fig. 3.20 Attical tympanosclerosis of a left ear, (**b**) coronal CT reconstruction showing tympanosclerotic calcifications (arrows) surrounding and fixing the malleus to the tegmen, and (**c**) surgical aspect of TS (*) fixing the malleus head. *M* malleus, *I* incus

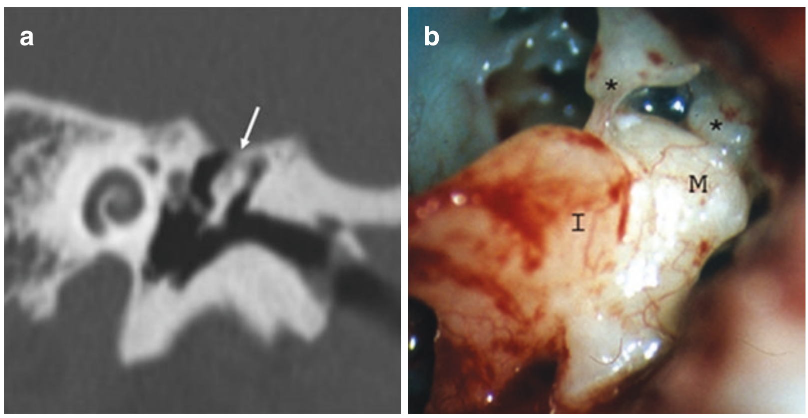

Fig. 3.21 Left ear atticotomy showing attical tympanosclerosis involving the head of malleus and body of incus intraoperative endoscopy after raising the drum (T) and endaural atticotomy showing incudomalleal complex fixation by epitympanic tympanosclerosis (*) fixing the malleus (M) and the incus (I); the stapes (S) is free

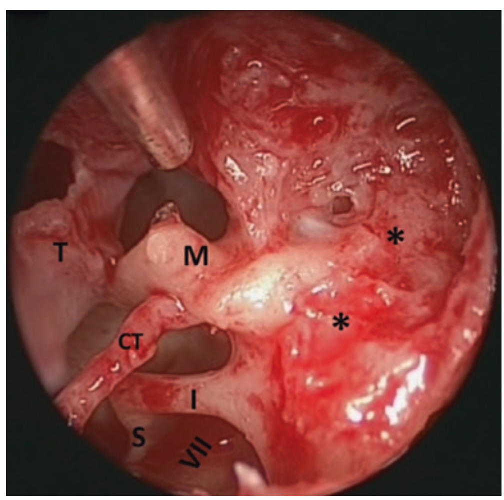

3.1.2.1.2 The Neck

The neck is a narrow and flattened portion. The tendon of the tensor tympani muscle inserts on its medial surface, and the chorda tympani crosses its medial surface above the insertion of this tendon. Its lateral surface forms the medial wall of the Prussak's space.

3.1.2.1.3 The Manubrium (The Handle)

The handle forms with the malleus head a superoposteriorly open angle of 135–140°. It runs downward, medially, and slightly backward between the mucous and fibrous layers of the tympanic membrane. The inferior end of the handle is flattened and firmly attached to the tympanic membrane as the pars propria splits to envelop it forming the umbo.

In surgical procedures, the tympanic membrane can be readily separated from the malleus except at the umbo where the periosteum of the handle continues directly with the fibrous layer. Midway between the lateral process and the umbo, the handle has a gentle medial curvature. At this level the handle is not embedded in the tympanic membrane, rather it is linked to the tympanic membrane by a mucosal fold, *the plica mallearis*. A prosthesis clamped to the manubrium in this area may have little or no contact with the pars propria of the normal tympanic membrane and therefore carries a very low risk of extrusion (Fig. 3.22).

Clinical Application

Usually the malleus handle lies midway between the anterior and posterior borders of the tympanic membrane but may occupy a more anterior position. Surgical procedures on the tympanic membrane are especially difficult when an anteriorly located malleus is associated with bulging of the anterior canal wall. Rarely, the malleus handle is fixed to the tympanic bone posteriorly by a bony bar, a *malleus bar* [39, 40, 43].

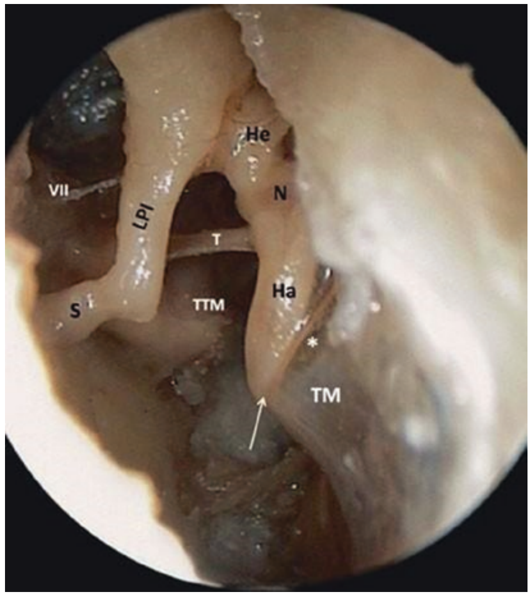

Fig. 3.22 Posterior view of a right middle ear cavity. The inferior end of the handle (Ha) is firmly attached to the tympanic membrane (TM) forming the umbo (white arrow). Relation of the middle part of the handle and the lamina propria of the tympanic membrane, plica mallearis (*). *LPI* long process of the incus, *S* stapes, *N* neck of the malleus, *He* head of the malleus, *VII* facial nerve, *TTM* tensor tympani muscle, *T* tensor tympani tendon

3.1.2.1.4 Malleus Processes

The malleus has two processes located at the union of the neck and the malleus handle.

- *The lateral process*: The lateral process is a small conical eminence of 1 mm. It protrudes laterally to the side of the tympanic membrane and gives attachment to the anterior and posterior tympano-malleal ligaments.
- *The anterior process* (processus gracilis): The anterior process is a 3–5-mm long thin bony spine which extends from the neck of the malleus into the petrotympanic Glaserian fissure. On its medial aspect runs the chorda tympani nerve to enter anteriorly the petrotympanic fissure. It gives origin to the anterior malleal ligament, which also traverses the petrotympanic fissure to reach the angular spine of the sphenoid bone.

3.1.2.1.5 Malleus Ligaments (Figs. 3.23 and 3.24)

The malleus is stabilized in place by five ligaments, one articulation, one tendon, and the tympanic membrane. Three of the five ligaments are outside the axis of rotation: they offer only a suspensory function. They are:

- The anterior suspensory ligament (ASL) lies superior to the anterior malleal ligament and attaches the head of the malleus to the anterior wall of the epitympanum.
- The lateral suspensory ligament (LSL) attaches the neck of the malleus to the bony margins of the tympanic notch (the notch of

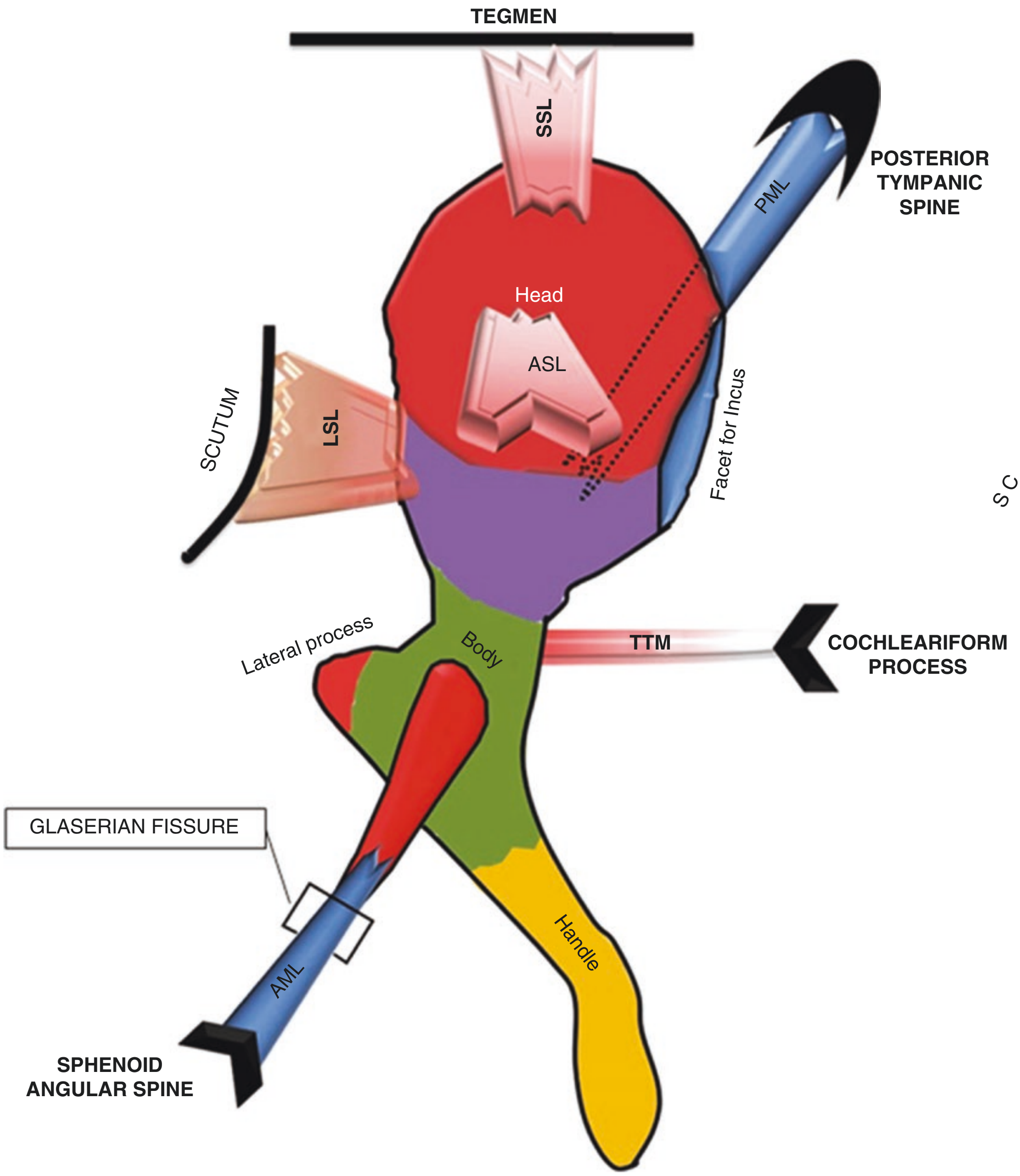

Fig. 3.23 Schema showing malleal ligaments and tensor tympani muscle tendon (TTM). *SSL* superior suspensory ligament, *ASL* anterior suspensory ligament, *LSL* lateral suspensory ligament, *AML* anterior malleal ligament, *PML* posterior malleal ligament. The AML and PML in blue color represent the rotation axis of the malleus

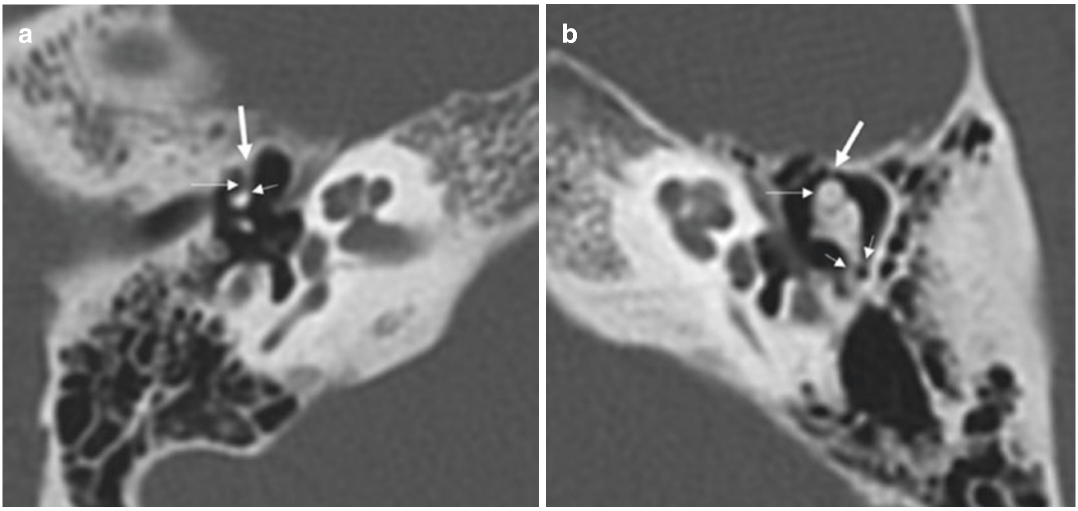

Fig. 3.24 Right transversal CT image: (**a**) Thickened and calcified anterior malleal ligament (long slim arrow), angular spine (thick arrow) of the sphenoid bone, and anterior process of the malleus body (short arrow). (**b**) Anterior suspensory ligament with insertion on the attic wall (thick arrow), malleus head (thin long arrow), and posterior incudal ligaments (small arrows)

Rivinus) and forms the superior wall of the Prussak's space.

- The superior suspensory ligament (SSL) bridges the gap between the head of the malleus and the tegmen of the epitympanum and carries the superior tympanic artery branch of the middle meningeal artery.

  These three ligaments apparently do not interfere with sound transmission because of the small movements of the ossicles at their points of attachment. The suspensory ligaments do not play a role in middle ear mechanics.
- The anterior malleal ligament (AML) together with the posterior incudal ligament serves to establish the axis of rotation of the ossicles. The anterior malleal ligament must not be confused with the anterior suspensory ligament of the malleus. The anterior malleal ligament extends from the angular spine of the sphenoid bone, passes through the petrotympanic fissure, accompanied by the anterior tympanic artery, and *inserts on the neck* of the malleus at the base of the anterior process of the malleus.
- The posterior malleal ligament (PML) extends from the neck of the malleus to the posterior tympanic spine.
- The superior malleal ligament attaches the malleus head to the tegmen and separates the posterior attic from the anterior attic.

Clinical Application: Anterior Malleal Ligament Fixation

Undetected concurrent malleus fixation may account for 0.8–4.0% of stapedotomy revision, with anterior malleus ligament fixation being the most common origin [45]. Fixation of the malleus head can be caused by tympanosclerosis (Fig. 3.25) or new bone formation due to chronic otitis media or as a result of a congenital anomaly. The malleus can also be "fixed" by increased stiffness of the anterior malleal ligament. Stiffening of the anterior malleal ligament by hyalinization or calcification results in decreased transduction of sound to the cochlea (Fisch et al. 2001; [46]). However, stiffening of the anterior malleal ligament resulted in only insignificant decrease (about 5 dB) of stapes velocity (Nakajima et al. 2005b; Dai et al. 2007). The little impact on hearing of such stiffening of the anterior malleal ligament is due to the fact that the anterior malleal ligament is along the ossicular axis of rotation for low-frequency stimuli, the stiffening torque at the axis itself would be expected to be small, and this torque is proportional to the distance between the stiffening element and the axis of rotation.

Surgical Implications

1. The malleus is a very important bone in ossiculoplasty: it contributes to restore the function of catenary lever, ossicular lever, and prosthesis stabilizer.
2. In contrary to the head of the malleus, the manubrium plays an important role in sound transmission.
3. The handle moves more than other ossicles: 4.5 nm at 80 dB.
4. The vibrations of the manubrium are bigger outward than inward
5. For each sneeze, the malleus handles move 1 mm laterally.
6. The handle is oval in shape with 0.9 mm of diameter.
7. At lower frequencies, the malleus neck does not vibrate; above 4 kHz it vibrates a little; this is why piston prosthesis, in malleo-stapedial reconstruction, must be fixed not at the center of the neck but on the manubrium.

3.1.2.2 The Incus (Fig. 3.26)

The incus measures about 5 by 7 mm and weighs about 30 mg. It has a trapezoidal body, a short and a long process, and a rounded lenticular process.

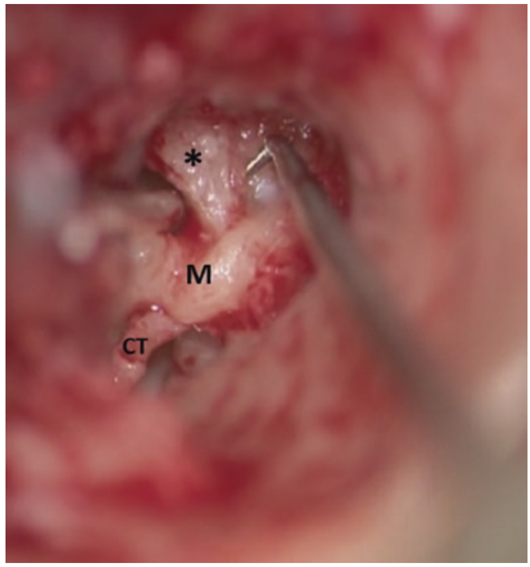

Fig. 3.25 Left ear endoscopy showing tympanosclerosis of the anterior malleal ligament (*). *M* malleus head, *CT* chorda tympani

Fig. 3.26 Schematic drawing of the incus. *Pe* lenticular process pedicle, *Pl* lenticular process plate

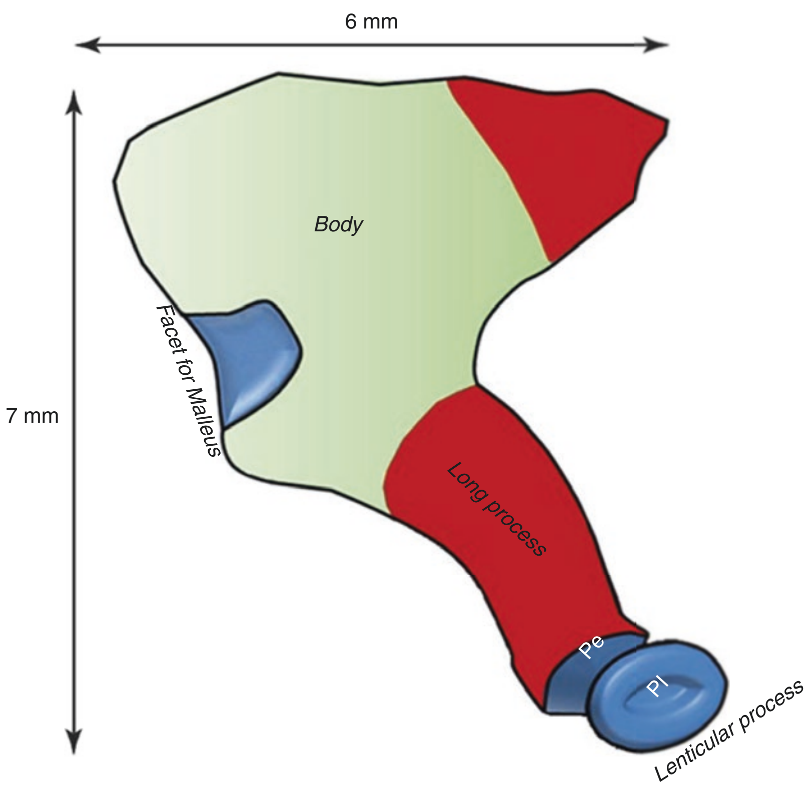

3.1.2.2.1 Body of the Incus

The body of the incus is flat. Its anterior surface houses an elliptical articular surface to receive the head of the malleus. Both body of the incus and head of the malleus are situated in the attic. Two spines arise from the lower posterior part of the body, the long and short processes. These two processes diverge from each other in a right angle:

3.1.2.2.2 Short Process of the Incus

The short process of the incus extends posteriorly from the body as a thick and triangular process; its major axis is horizontal. Its dorsal end lies on the incudal fossa situated in the floor of the aditus ad antrum.

3.1.2.2.3 Long Process of the Incus

The long process or vertical process of the incus follows a direction similar to the handle of the malleus but in a more posterior and medial plane. Its caudal end forms a hook at a right angle to end up with the lenticular process. The horizontal, cross-sectional configuration of the long process of the incus is circular, in contrary to the ovoid shape of the manubrium of the malleus. The mean diameter of the distal extremity of the long process is 0.63 mm [47]. Because of its terminal and poor vascularization, the long process of the incus is highly susceptible to osteitic resorption secondary to several conditions such retraction pocket, adhesive otitis media, or extremely tightened stapes prosthesis.

3.1.2.2.4 Lenticular Process

The lenticular process connects the long process of the incus to the head of the stapes. The lenticular process consists of a narrow *bony pedicle* and a flattened *distal plate*.

The *bony pedicle* is surrounded by a joint capsule of thick fibers. The mean diameter of the bony pedicle (0.26 mm) is less than half of the mean diameter of the distal long process (0.63 mm) and less than half of the mean diameter of the distal plate (0.71 mm) [47]. The bony pedicle is flexible and plays a role in the piston-like transmission of the incus movement to the stapes, lateral to medial, by the rotation movement of the incus. All other movements are reduced by the bending of this pedicle before reaching the stapes [48].

The lenticular process of the incus shows a second facet for the stapes *distal plate* which is perpendicularly located to the axis of the long apophysis of the incus which, in turn, is located parallel and medial to the malleus handle and the tympanic membrane.

Clinical Application

Chronic otitis media (COM) is the most common cause of ossicular chain necrosis and concerns most frequently the long process of the incus (Fig. 3.27a). It is the most vulnerable part of the ossicles because of its poor blood supply [49–51]. The malleus and the footplate are more resistant to necrosis [50, 51]. The blood supply of the long process of the incus is provided by end vessels, which descend down along the long process of the incus. Persistent or repeated infection in some cases of COM, or pressure from a retracted eardrum (Fig. 3.27b), or over-crimped stapes prosthesis, combined with the lack of collateral blood supply, is thought to be the cause of aseptic necrosis [49].

Occasionally, dissolution is complete with total incudostapedial separation, but more frequently slow dissolution leads to replacement of the bone by a fibrous tissue [50, 51].

3.1.2.2.5 Ligaments of the Incus (Fig. 3.28)

The incus has the smallest number of ligaments and is therefore more susceptible to traumatic dislocation compared to other ossicles. Two ligaments stabilize the incus in place:

- The posterior incudal ligament (PIL) secures the short process in the incudal fossa (Fig. 3.24b). It is in the axis of rotation of the ossicular chain.
- The superior incudal ligament (SIL) descends from the tegmen to the incus body. It could be reduced to a single mucosal fold only. It separates the upper lateral attic from the upper medial attic.

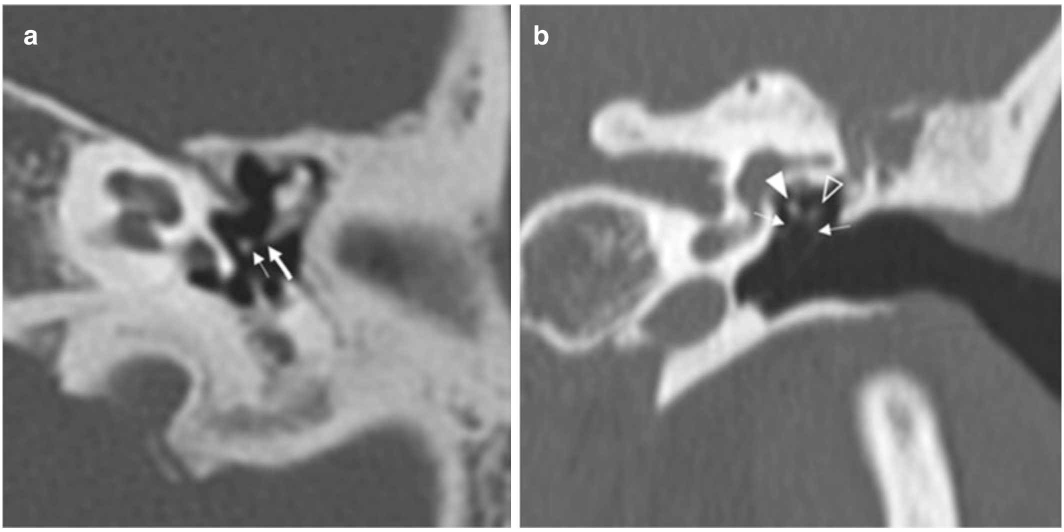

Fig. 3.27 Incus erosion: (**a**) Axial CT image: discontinuity of the incudostapedial articulation, between the stapes head (short arrow) and the shortened end of the long process of the incus (long arrow). (**b**) Coronal reconstruction: part of the tympanic membrane is retracted (small arrows) on the stapes head (plain arrowhead) and the long process of the incus (empty arrowhead)—myringostapediopexy and lysis of the long process

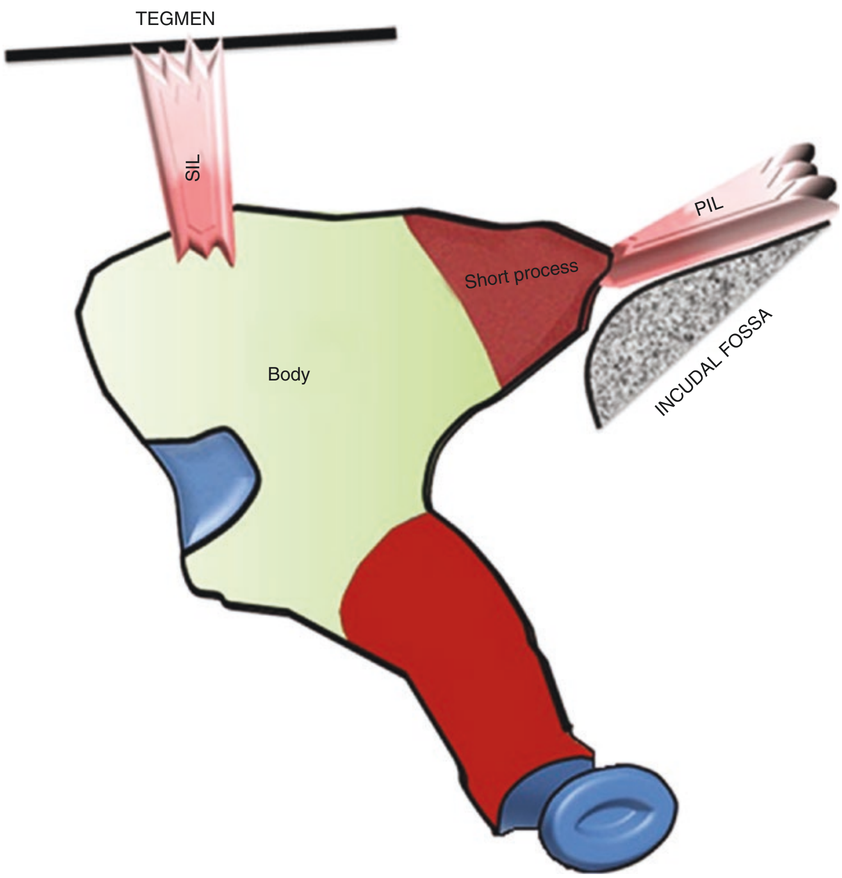

Fig. 3.28 Schematic drawing of incudal ligaments. *SIL* superior incudal ligament, *PIL* posterior incudal ligament

3.1.2.3 The Stapes

The stapes (Fig. 3.29) is the smallest bone of the human body; it is 3.25 mm high and 1.4 mm wide with a weight of 3–4 mg [52]. It is situated in an almost horizontal plane between the lenticular process and the oval window and below the facial nerve canal. The stapes consists of a round head, a short neck, anterior and posterior crura, and an oval footplate.

3.1.2.3.1 The Head

The head is the most lateral part of the stapes. It is cylindrical or discoid in shape and bears laterally a glenoid cavity, *the fovea*, which corresponds to the articular surface of the lenticular process. Its medial end is constricted, forming the neck. Its anterior edge is smooth. Its posterior edge presents a small rough surface for the insertion of the stapedial muscle tendon.

> **Surgical Implication**
> Partial ossicular replacement requires implants (PORP) which fit onto the head of the stapes alone, thus necessitating the knowledge of the dimensions of the stapedial head. The width of the stapes head is about 1–1.5 mm (Fig. 3.30) [52].

3.1.2.3.2 The Crura

The stapes presents two crura of unequal size: the posterior and the anterior crura. The posterior crus is longer, thicker, and more curved than the anterior one. The relative thickness, the curvature, and the excavation of the crura vary

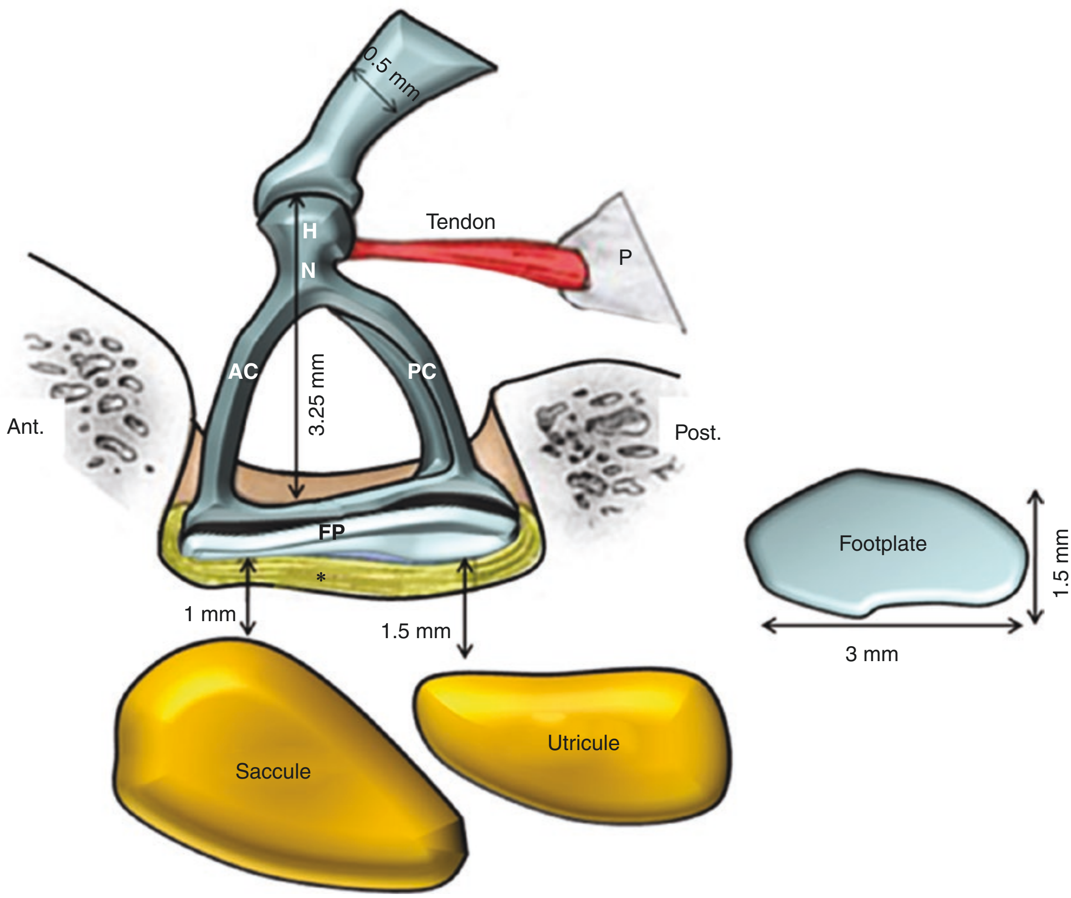

Fig. 3.29 Schematic drawing of the stapes in the oval window niche and its relationship with the underlying saccule and utricle. Stapedial tendon in red. (*) annular ligament, *P* pyramidal eminence, *H* head, *N* neck, *AC* anterior crus, *PC* posterior crus, *FP* footplate

among individuals. The area delimited by the concave arches of the crura is the obturator foramen, sometimes bridged by a veil of mucous membrane. The two crura could be very close to the walls of the niche of the oval window.

> **Surgical Implication**
> During stapedectomy, it is safer to cut the posterior crus of the stapes rather than to fracture it because of a risk of footplate luxation. This is not the case of the anterior crus which is thinner and can be safely fractured.

3.1.2.3.3 The Footplate

The footplate is a thin and oval lamella of bone. Its length is about 3 mm; its width is about 1.5 mm; its thickness is about 0.25 mm [53].

The lateral or tympanic surface of the footplate is covered by mucoperiosteum of the middle ear; it is slightly twisted around its polar axis so that the anterior half looks to the floor of the vestibule and the posterior part looks up to the tegmen. The distance from the long process of the incus to the tympanic surface of the footplate is about 4 mm. The medial or vestibular surface of the footplate is flat; it is lined by the endosteum of the otic capsule and is in close relation with the saccule and utricle. The saccule is 1 mm deep from the anterior part of the vestibular surface of the footplate, and the utricle is at 1.5 mm deep from its posterior part (Fig. 3.29).

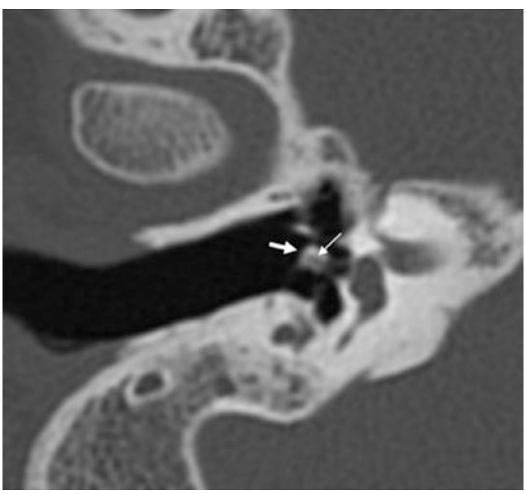

Fig. 3.30 Axial CT image showing a PORP (thick arrow), connecting the tympanic membrane laterally with the stapes medially, the head of the stapes (thin arrow) is entirely surrounded by the prosthesis

> **Surgical Implication**
> During reconstructive ear surgery, total ossicular replacement prosthesis (TORP) may be used to bridge the gap between the tympanic membrane or the malleus and the stapes footplate. It corresponds to columellar effect which comes from the bird columella ossicle. The positioning of the TORP shaft on the footplate has a significant impact on the eventual hearing outcome of the surgery. Putting the prosthesis on the anterior part of the footplate is preferable because the annular ligament is thinner and wider and thus the footplate is more mobile [54].

3.1.2.3.4 The Annular Ligament

The annular ligament of the stapes is a ring of elastic fibers that attaches the cartilaginous margin of the footplate to the border of the oval window. The annular ligament is a typical viscoelastic material with hysteresis, nonlinear shear stress-shear strain relationship and stress relaxation function.

The fibers of the annular ligament fuse with the periosteum and endosteum all around the oval window borders. The ligament is thinner anteriorly than posteriorly, thus more mobile anteriorly [54]. *Because of the differential thickness between its anterior and posterior aspects, the annular ligament works as a hinge-like attachment of the stapes into the oval window.*

This type of attachment allows a *rocking oscillation* of the footplate in the oval window, which is the essential movement for the transmission of high-frequency sounds. Low-frequency sound transmission depends on *piston-like* movements of the stapes that necessitate the elasticity of the whole annular ligament.

The piston-like and rotational forms of stapes motion induce shear deformation of the annular ligament where its mechanical properties affect directly the mechanical-acoustic transmission from the middle ear to the cochlea [55].

Clinical Application
In otosclerosis, the otosclerotic changes induce increased stiffness of the stapedial annular ligament, which can range from 10 to 100 times of its normal value [46, 56].

Otosclerotic involvement of the anterior aspect of the annular ligament hinders the piston-like movement of the stapes rather than the rocking movement. This explains why in early stages of otosclerosis, there is only a low-frequency conductive hearing loss. In addition, the posterior part of the annular ligament conserves its insulator capacity; this explains the on/off stapedial reflex phenomena found in early stages of otosclerosis.

3.2 Ossicular Articulations

3.2.1 Embryology of Ossicular Articulations

3.2.1.1 The Incudostapedial Joint

At the seventh to eighth week of gestation, the outlines of the lenticular process and of the stapes head are separated by a condensed mesenchyme interzone. After the 12th week of gestation, cavitation phenomena begin in this interzone. The different cavitations consolidate then to form the incudostapedial joint at the 16th week of gestation.

The primordium of the capsular ligament develops from the surface of the interzone by a condensation of the surrounding mesenchyme which forms a layer that is continued with the perichondrium of the ossicles [57].

3.2.1.2 The Incudomalleal Joint

The incus and malleus, previously one collection of mesenchyme, separate with formation of the incudomalleal joint at eighth to ninth week by the same mechanism as the incudostapedial joint (Fig. 3.8). Failure of this step results in a fused malleus-incus mass that is commonly found in patients with aural atresia.

3.2.2 Anatomy of the Ossicular Articulations

The articulating surfaces between the ossicles are lined by cartilage, and there may or may not be an intra-articular disc. Each articulation has a true capsule composed of ligamentous fibers originating from the periosteum of the linked bones and lined by a synovial membrane.

3.2.2.1 The Incudomalleal Articulation

The incudomalleal articulation is situated in the epitympanum and is classified as a synovial joint. The head of the malleus articulates with the body of the incus (Fig. 3.31).

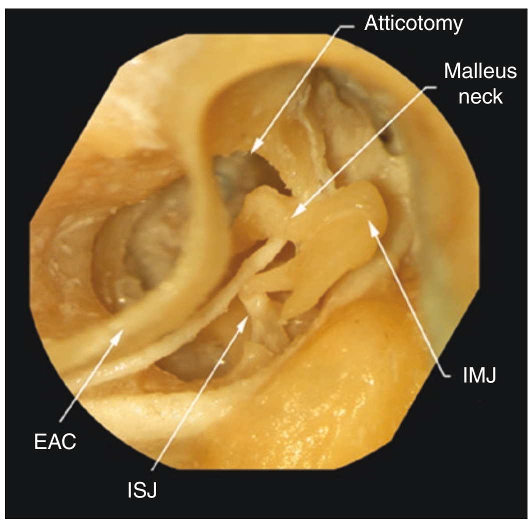

Fig. 3.31 Left middle ear after large mastoidectomy and anterior and posterior tympanotomy, showing both incudomalleal joint (IMJ) and incudostapedial joint (ISJ). *EAC* external auditory canal

The joint contains a synovial cavity lined by a synovial membrane and articular cartilage. It is made up of curved reciprocal concave-convex surfaces ("saddle-shaped surfaced"), separated on average by 150 µm. The joint cavity is incompletely divided into two compartments by a wedge-shaped articular disk or meniscus.

An elastic tissue capsule surrounds the articular margin and holds the articular surfaces in intimate contact. The capsule is trilaminar with (1) the synovial membrane lining the cavity, (2) the mucous membrane of the middle ear, and (3) an intervening fibrous layer.

Partial subluxation of the incudomalleal joint, happening during middle ear surgery, usually heals without sequelae. Complete luxation will not heal, and ossicular reconstruction is recommended.

3.2.2.1.1 Mechanics of the Malleus-Incus Complex (MIC)

Due to its particular shape, the mobility is restricted to a rotatory movement on an anteroposterior axis which passes through the short process of the incus and the anterior process of the malleus:

- *Complete ossicular disarticulation, in the presence of an intact tympanic membrane, leads to a reduction of middle ear transmission of 40–60 dB depending on frequency (Merchant et al. 1997, Nakajima et al. 2012, Peake et al. 1992). It has been showed that such a loss of ossicular coupling is consistent with the situation when the cochlea is responding only to the pressure difference at its oval and round windows (i.e., acoustic coupling).*
- *Partial ossicular disarticulation (fibrous connection) generally results in less conductive hearing loss at low frequencies as compared to high frequencies (Nakajima et al. 2012).*

3.2.2.2 The Incudostapedial Articulation (Figs. 3.31 and 3.32)

The incudostapedial articulation is a synovial diarthrodial articulation; it joins the convex lenticular process of the incus and the concave surface of the head of the stapes, thus forming a ball and socket joint which are held bound by a tissue capsule. The concave articular surface of the stapes head is covered with cartilage and synovium overlying the cartilage. An intra-articular cartilage is not usually present. The outer surface of the joint is covered by a fibrous capsule. The joint capsule is attached to the full length of the lenticular process and extends medially to the rim of the stapes head [47].

At the inferior aspect of the articulation, the posterior capsular fibers merge sometimes with those of the tendon of the stapedius muscle, with a result that contraction of the stapedius muscle, in addition to pulling the head of the stapes posteriorly, also draws the long process of the incus posteriorly [58].

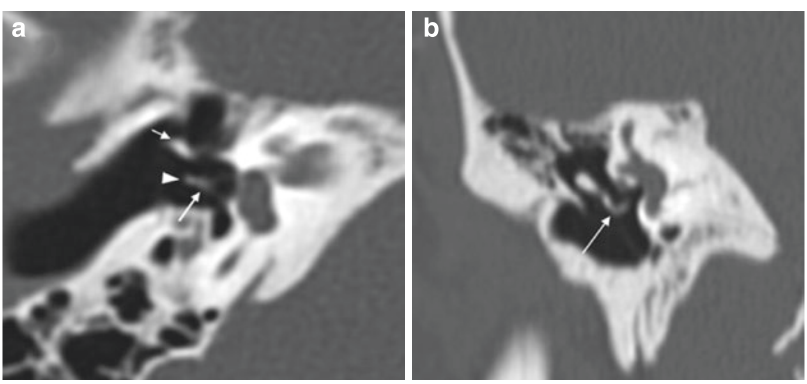

Fig. 3.32 Computed tomography of the normal aspect of the incudomalleal joint. (**a**) In the transversal view: continuity between the long process of the incus (arrowhead) and the head of the stapes (long arrow). Malleus handle (short arrow). (**b**) Coronal reconstruction: "ossicular V" (long arrow) = continuity between the long process of the incus and the head of the stapes

This joint is fragile. Delicate movements of the incus with an instrument create a line where the joint capsule bends. During incudostapedial joint separation, there is a risk of damaging the lenticular process especially in cases where its pedicle is very thin.

The ossicular chain is especially fragile at its articulations. The most often encountered fractures along the ossicular chain are at the incudostapedial joint and the incudomalleal joint (Figs. 3.33 and 3.34), whereas the malleus is the most resistant ossicle with the less common post-traumatic injuries.

Causes of nontraumatic disjunction of the incudostapedial joint are retraction pocket, chronic otitis media, mesotympanic cholesteatoma, traumatic or iatrogenic injuries, and congenital malformations.

3.2.2.2.1 Mechanics of the Incudostapedial Joint (ISJ)

- *In negative middle ear pressure, the malleus is moving medially, but the incus moves inferiorly causing stapes rotation along its long axis* [59].
- *Temporary surgical ISJ separation without distanced joint surfaces may not result in an appreciable conductive hearing loss and does not need reconstruction; however a secondary healing process can potentially lead to ankylosis which would result in moderate conductive hearing loss* [22].

3.2.2.3 The Stapediovestibular Joint (SVJ)

The SVJ is the junction between the stapes footplate and the oval window. It is a half-joint (syndesmosis). The annular ligament holds the

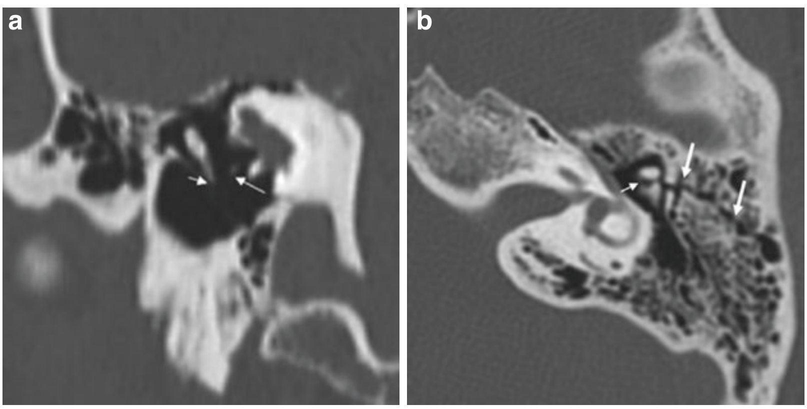

Fig. 3.33 Traumatic lesions of the ossicular chain. (**a**) Complete disconnection and luxation laterally of the long process of the incus (long arrow) far away from the stapes suprastructure (short arrow) secondary to traumatic incudostapedial luxation. (**b**) Horizontal temporal bone fracture (long arrows) with incudomalleal joint interruption (short arrow) and luxation of malleus head anteriorly

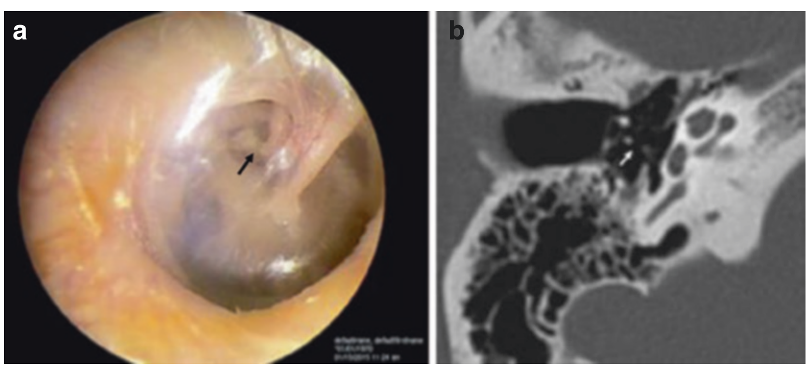

Fig. 3.34 (**a**) Right ear otoscopy showing discontinuity of the incudostapedial joint (arrow) (**b**) axial CT image: large diastasis of the incudostapedial joint (arrow)

footplate attached to the oval window borders. Peripherally, the connective fibers of the annular ligament fuse with the periosteum and endosteum of oval window niche.

3.2.2.3.1 Mechanics of the Stapes and Stapediovestibular Joint

The stapes has two types of movement:

– *Piston like movement* for low-frequency sounds.
– *Rocking like movement* for high frequency sounds.

In early stages of otosclerosis, fixation of the anterior pole of footplate affects the piston like movement only and thus leads to low frequency conductive hearing loss. In more advanced involvement, both movements will be restricted and hearing loss will affect both low and high frequency sounds.

The rigidity of the annular ligament represents 90% of the total impedance of the human middle ear at lower frequencies and thus dominates the sound transmission for speech frequencies through the normal middle ear. The sound pressure at the entrance of the cochlea is directly proportional to the volume velocity of the stapes. This corresponds to the volume of the liquid that is displaced by the movement of the footplate. This volume velocity is defined by the product of footplate area and stapes amplitude of movement. Otosclerotic changes in stiffness of the annular ligament increase significantly its rigidity and hinder sound transmission to inner ear fluids; these changes affect first the transmission of low-frequncy sounds, however, when the involvement is more advanced, all frequencies are affected. Replacement of an otosclerotic stapes by a piston prosthesis eliminates the annular ligament as the dominating factor of the impedance of the middle ear. A piston prosthesis move with a much larger amplitude at equivalent sound pressures. This increased linear velocity of the smaller piston compensates for the decrease in the surface area (Fig. 3.35).

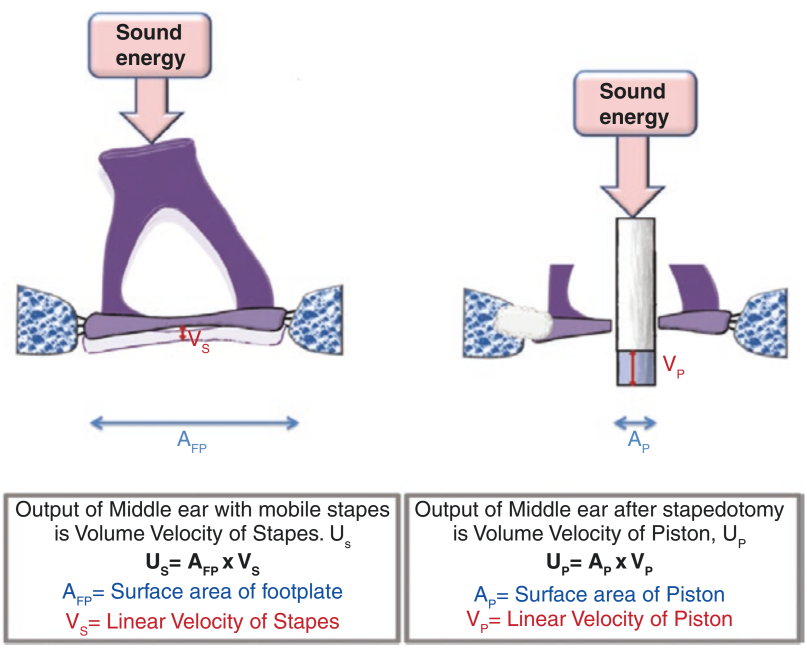

Fig. 3.35 Biomechanics of stapedotomy: The stapes footplate has an area of approximately 3.2 mm^2. This exerts vibrations with amplitudes of only a few nanometers for displacement of a large amount of fluid to transmit sound pressure into the cochlea at physiologic sound pressures. Following stapedotomy, the annular ligament effect is canceled, and the piston will have increased linear velocity. At the same time, the effective vibrating area is reduced to the area where the prosthesis has been inserted. A stapes prosthesis, with its smaller contact area (3.2 mm^2 area of footplate vs. 0.28 mm^2 area of fenestra in a 0.6 mm stapes prosthesis), can vibrate with much larger amplitude at equivalent sound pressures. Compensation takes place because the increased linear velocity of the smaller piston compensates for the decrease in the surface area

3.2.2.3.2 Ossicular Coupling (Fig. 3.36)

Ossicular coupling refers to the true sound pressure gain that occurs through the actions of the tympanic membrane and the ossicular chain:

- *The hydraulic lever acts because of the size difference between the tympanic membrane and the stapes footplate. Sound pressure collected over the area of the tympanic membrane and transmitted to the area of the smaller footplate results in an increase in force proportional to the ratio of the areas. The average ratio has been calculated to be 21:1. Taking the three levers together, the middle ear offers a theoretical gain of approximately 34 dB. But the true gain of the middle ear is less than the theorized 34 dB.*
- *The pressure gain provided by the normal middle ear with ossicular coupling is frequency dependent. The actual mean middle ear gain is 20 dB at 250–500 Hz, reaching a maximum of 25 dB at 1 kHz and then decreasing about 6 dB per octave at frequencies above 1 kHz.*
- *Patients with ossicular disruption behind an intact tympanic membrane suffer of a maximal conductive hearing loss of 60 dB. The intact eardrum reflects sound energy back into the external auditory canal, causing an additional conductive loss of 17 dB above what was expected from removal of the hydraulic and catenary-ossicular lever action.*

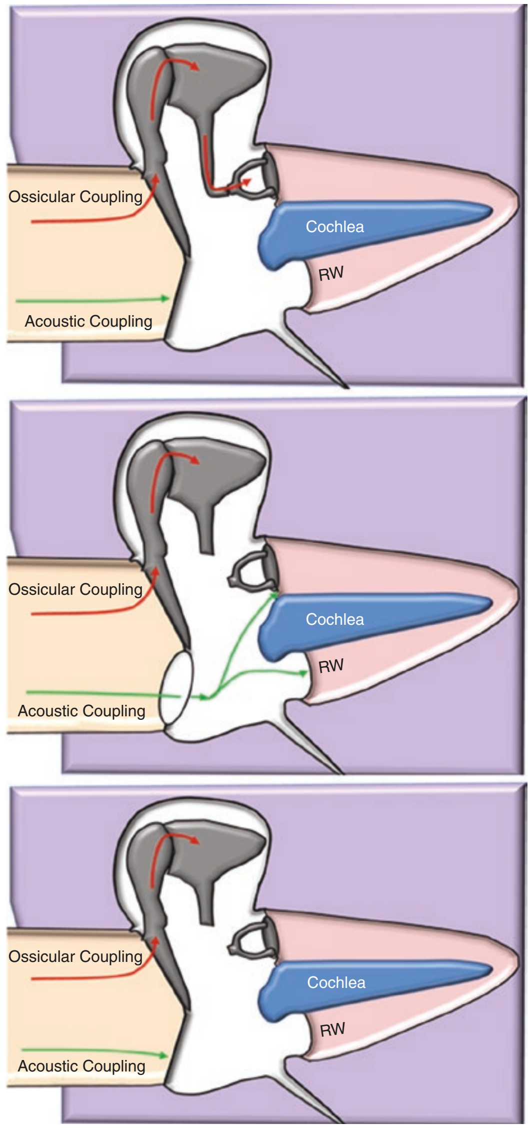

Fig. 3.36 (**a**) Middle ear mechanics in normal ear. (**b**) Middle ear mechanics in the ear with tympanic membrane perforation and ossicular chain discontinuity. Acoustic coupling with sound pressure difference on oval window and round window is the main mechanism for transmitting sound energy into the cochlea. Sound energy through ossicular coupling will not reach the cochlea. (**c**) Middle ear mechanics in the ear with intact tympanic membrane perforation and ossicular chain discontinuity. Sound energy will not reach the cochlea neither through ossicular coupling nor through acoustic coupling which will result in a maximal conductive hearing loss

3.3 Middle Ear Muscles

3.3.1 Embryology of Middle Ear Muscles

The embryological origin of middle ear muscles follows the same patterns as the other muscles in the craniofacial area [60]. They develop from the paraxial mesoderm (mesenchyme) that migrates into the branchial arches.

3.3.1.1 Tensor Tympani Muscle

The tensor tympani muscle develops from the mesoderm of the first branchial arch. It is innervated by a branch from the trigeminal nerve, the nerve of the first branchial arch.

3.3.1.2 Stapedial Muscle

The stapedial muscle starts to develop, at the ninth week, as a condensation of blastema cells in the mesenchyme of the interhyale (which connects the stapedial anlage to the second branchial arch) close to the facial nerve. The internal segment of the interhyale gives rise to the tendon of the stapedial muscle. Moreover, the interhyale contributes to the development of the facial nerve canal, as well as the pyramidal eminence [61] (see Fig. 2.23). The bone of the pyramidal eminence housing the muscle derives from the precartilaginous cells of the second branchial arch [62].

3.3.2 Anatomy of the Middle Ear Muscles

3.3.2.1 The Tensor Tympani Muscle (TTM)

The TTM is fusiform in shape and is around 20 mm in length. The intratympanic portion of this muscle is 2.5 mm long. It arises from the cartilage of the Eustachian tube, from the walls of its enveloping bony semicanal, and from the adjacent portion of the greater wing of the sphenoid bone (Fig. 3.37). The fibers converge to form a central fibrous core which, proceeding posteriorly, forms the tendon of the muscle. The most medial fibers of the tendon attach to the cochleariform process, at which point the main body of the tendon turns laterally into the cavity to attach to the medial surface of the junction of the neck and the manubrium of the malleus (Figs. 3.37 and 3.38). It is innervated by the trigeminal nerve, via the nerve to the medial pterygoid muscle.

Although the distal tensor tympani tendon inserts on the malleus in the middle ear, the muscle location and major functions of the tensor tympani predominantly characterize a peritubal muscle. Repetitive contraction of the tensor tympani assists the tensor veli palatini and other peritubal muscles with opening and closing the tube during a variety of speech and swallowing activities.

Within the middle ear, contraction of tensor tympani pulls on the malleus to dampen TM

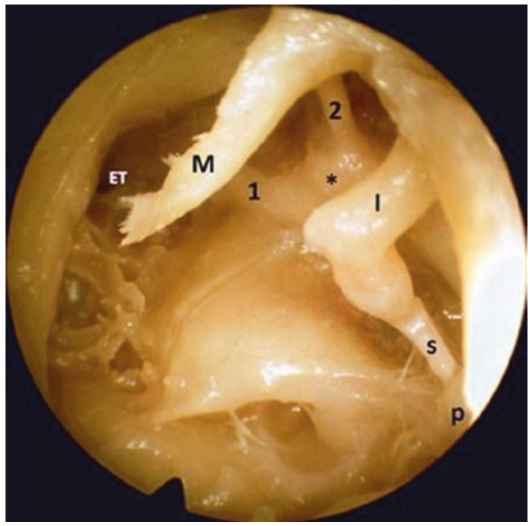

Fig. 3.38 Endoscopic view of a left middle ear showing the stapedial tendon(s) rising from the pyramidal process (p), the tensor tympani muscle (1) turning around the cochleariform process (*) to give the tensor tympani tendon (2) that inserts on the neck of malleus (M); *I* incus, *ET* Eustachian tube

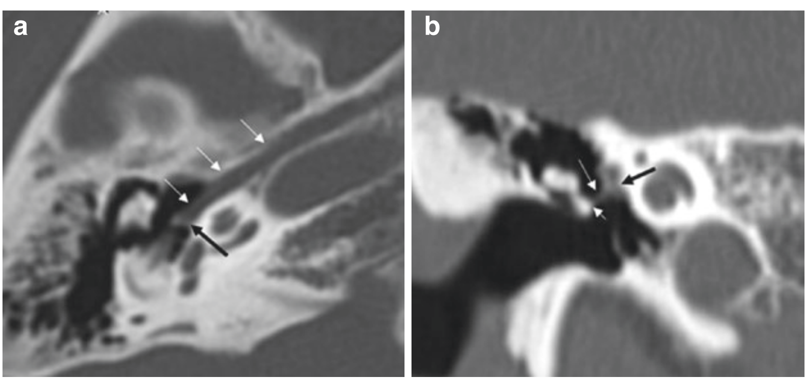

Fig. 3.37 (**a**) Axial CT image of a right ear: TTM (white arrows), along the Eustachian tube to the cochleariform process (black arrow); (**b**) coronal reconstruction of the right ear—at the cochleariform process (black arrow), the TTM tendon (long white arrow) turns laterally to insert on the malleus neck (small white arrow)

vibrations and damping the movements of the ossicular chain [63, 64]. This action is primarily described in the context of preventing autophony associated with the palatal actions of chewing and swallowing and is considered less important during vocalization.

Tensor tympani muscle spindles have also been described as having barometric properties, reflexively contracting in response to pressure changes [65].

Cadaveric human samples indicated that tensor tympani muscle hypercontraction should result in a low-frequency HL, with a decrease in ME compliance [66].

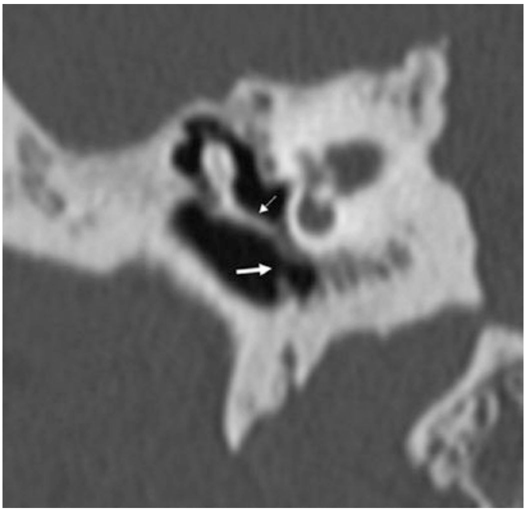

Fig. 3.39 Coronal CT image showing medialization of the malleus handle (small arrow) due to tympanic perforation (thick arrow)

In normal conditions, the pull of the TTM is opposed by the elasticity of the pars tensa of the tympanic membrane. In a long-standing large perforation of the tympanic membrane, the unopposed pull of the TTM causes a medial displacement of the inferior end of the manubrium (so called malleus handle medialization) (Fig. 3.39).

3.3.2.2 Stapedial Muscle

The stapedial muscle is the smallest skeletal muscle in the body measuring only 1 mm. It lies in a bony cavity in the posterior wall of the tympanic cavity to emerge from the pyramidal eminence. The fibers of this muscle converge into a tendon which variably attaches to the head and/or posterior crus of the stapes (Fig. 3.40) [63, 64].

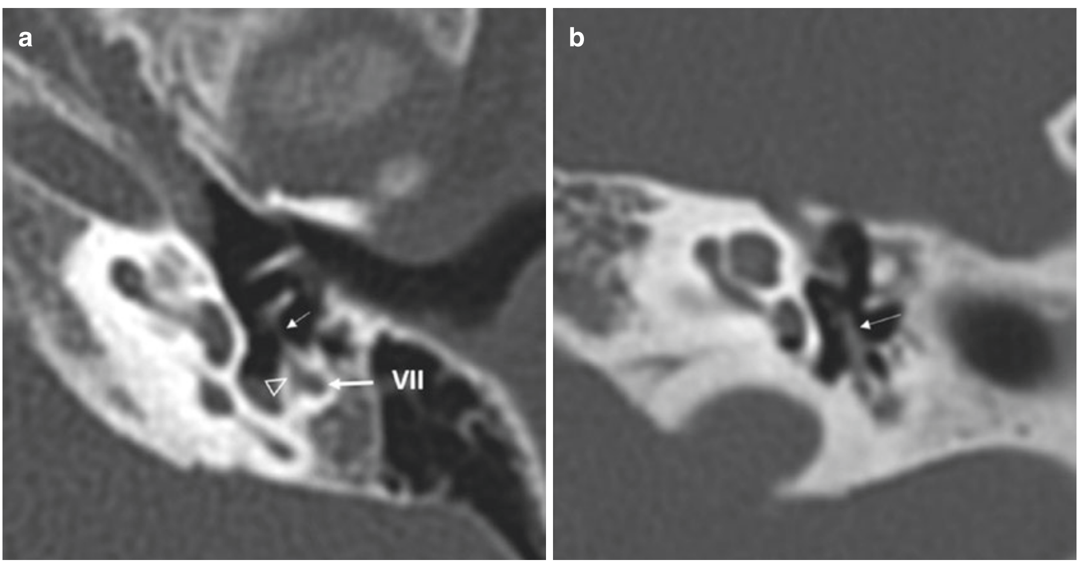

Fig. 3.40 Axial CT scan on left ears: (**a**) Visibility of the thin stapedial tendon (small arrow) emerging from the pyramidal eminence and inserting on the stapes head. Stapes muscle (empty arrowhead). *VII* facial nerve. (**b**) Thickened and calcified stapedial tendon in tympanosclerosis (arrow)

The stapedial muscle is innervated by the stapedial branch of the facial nerve. Its contraction provokes a tilting of the stapes by moving the anterior border of the footplate laterally and the posterior border medially. This tilting of the stapes stretches the annular ligament, thus fixing the footplate and damping its movements. It protects the inner ear from damage caused by loud noise. Lack of action of this muscle from nerve section or facial nerve palsy induces hyperacusis [63, 64].

The brain stem-mediated acoustic reflex between the vestibulocochlear nerve, the superior olive, and the facial nerve is routinely evoked to measure indirectly the stapedius function via tympanometry.

Surgical Application

During microsurgical dissection around the stapes, for instance, a removal of the cholesteatoma matrix from the stapes, it is advisable to work parallel to the plane of the stapedial tendon, from posterior to anterior, so that the tendon prevents luxation of the stapes.

Clinical Application

Middle ear myoclonus tinnitus is commonly characterized as *clicking* (suggested to be due to the tensor tympani movement) or *buzzing* (suggested to be due to stapedius movement): objective tinnitus.

3.4 Middle Ear Nerves

The middle ear receives and transmits branches from the facial nerve VII, the glossopharyngeal nerve IX, and the sympathetic carotid plexus. The branches of the glossopharyngeal nerve and sympathetic carotid plexus contribute to the formation of an important middle ear neural plexus, *the tympanic plexus.*

3.4.1 Facial Nerve Branches

One branch of the facial nerve, t**he chorda tympani,** passes through the middle ear cavity on its route to the infratemporal fossa. This is a sensory and secretory-motor branch of the facial nerve. It enters the middle ear cavity through the *iter chordae posterior*. It runs across the medial surface of the tympanic membrane lateral to the long process of the incus and passes medial to the upper portion of the handle of the malleus above the tendon of the TTM. It leaves the middle ear through the *canal of Huguier* within the petrotympanic fissure. It joins the lingual branch of the mandibular nerve in the infratemporal fossa (see Sect. 6.2.3.6).

3.4.2 Tympanic Plexus (Fig. 3.41)

The tympanic plexus consists of a network of nerves lodged in small grooves on the cochlear promontory of the medial wall of the middle ear. It is formed by the tympanic nerve and two or three filaments from the carotid plexus.

- *The tympanic (Jacobson's) nerve*, carrying parasympathetic fiber, arises from the inferior ganglion of the glossopharyngeal nerve when it exits the jugular foramen and enters *the inferior tympanic canaliculus* accompanied by the inferior tympanic artery. The inferior tympanic canaliculus, with a mean length of 9.5 mm, is located in the medial hypotympanic fissure medial to the styloid process and the stylomastoid foramen between the internal carotid foramen medially and the internal jugular foramen laterally [67] (see Figs. 2.18 and 3.42). After entering the tympanic cavity, the tympanic nerve traverses superiorly on the promontory anterior to the inferior half of the round window, and then it branches repeatedly within shallow bony channels overlying the promontory to form the tympanic plexus. Two or three filaments, the caroticotympanic nerves, coming from the carotid

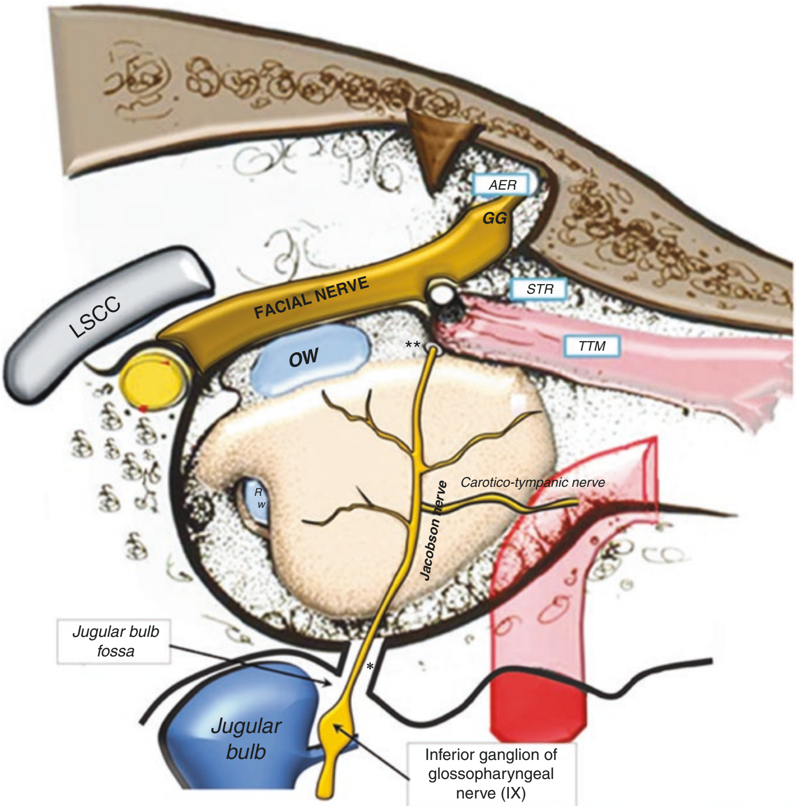

Fig. 3.41 *The tympanic (Jacobson's) nerve*, carrying parasympathetic fiber, arises from the inferior ganglion of the glossopharyngeal nerve when it exits the jugular foramen and enters *the inferior tympanic canaliculus (*)*. After entering the tympanic cavity, the tympanic nerve traverses superiorly on the promontory. Two or three filaments, the caroticotympanic nerves, coming from the carotid plexus and carrying sympathetic fibers join the tympanic plexus on the promontory (this figure) to exit the middle ear through its own canal (**) underneath the cochleariform process to give the lesser superficial petrosal nerve. *TTM* tensor tympani muscle, *STR* supratubal recess, *AER* anterior epitympanic recess

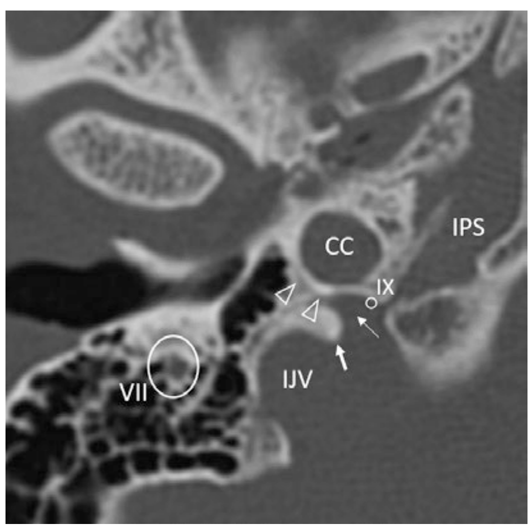

Fig. 3.42 Axial CT image through the inferior part of the tympanic cavity: intrapetrous carotid (CC), internal jugular vein (IJV), inferior petrous sinus (IPS). Jugular spine (thick arrow), pars nervosa (thin arrow), topography of glossopharyngeal nerve IX (small circle), trajectory of the Jacobson's nerve indicated by the arrowheads. Facial nerve VII (large circle)

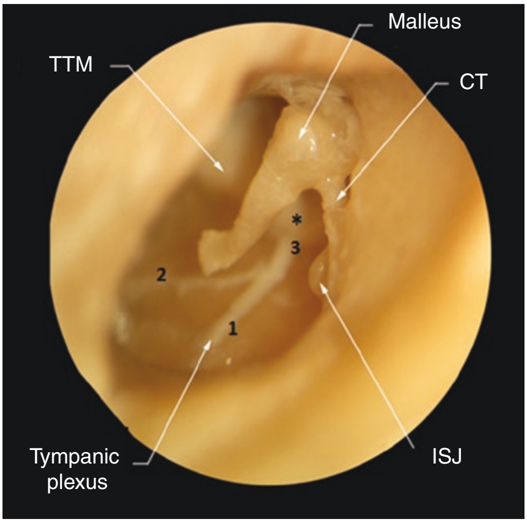

Fig. 3.43 Endoscopic view of a left middle ear showing the Jacobson's nerve (1), the caroticotympanic nerve (2), and the lesser petrosal superficial nerve (3) passing outside the middle ear below the cochleariform process (*). *ISJ* incudostapedial joint, *CT* chorda tympani, *TTM* tensor tympani muscle

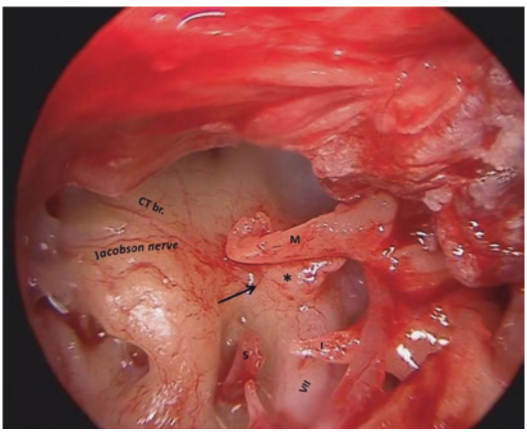

Fig. 3.44 Endoscopic view of a left middle ear showing the Jacobson's nerve, the caroticotympanic branches (CT br.), and the lesser petrosal superficial nerve passing outside the middle ear below the cochleariform process (*). *M* malleus, *I* eroded incus, *s* stapes, *VII* facial nerve

plexus and carrying sympathetic fibers, join the tympanic plexus on the promontory (Figs. 3.43 and 3.44) to exit the middle ear through its own canal underneath the cochleariform process to give the lesser superficial petrosal nerve (Fig. 3.44) [68, 69]

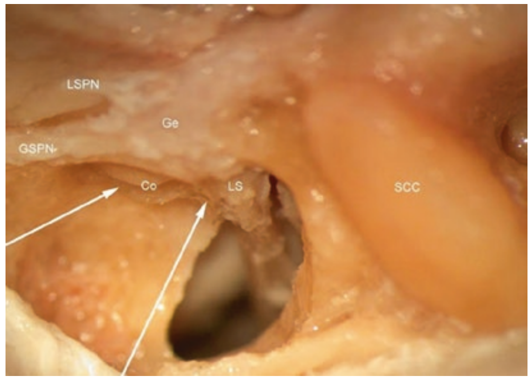

Fig. 3.45 Middle cranial fossa view of a right side showing the lesser superficial petrosal nerve (LSPN) which emerges on the floor of the middle cranial fossa lateral to the greater superficial petrosal nerve (GSPN). *Ge* geniculate ganglion, *Co* cochlea, *LS* labyrinthine segment of facial nerve, *SCC* superior semicircular canal

The tympanic plexus gives off:

– **The lesser superficial petrosal nerve**: parasympathetic fibers to the parotid. The mean length of the LPN is 15 mm. It originates from the tympanic plexus at the level of the cochleariform process and leaves the middle ear through a small canal below the tensor tympani muscle (Fig. 3.44). It passes through the temporal bone to emerge on the floor of the middle cranial fossa lateral to the greater superficial petrosal nerve (Fig. 3.45). It exits the middle cranial fossa through the foramen ovale together with the mandibular nerve to join the otic ganglion in the infratemporal fossa. From there, the postganglionic fibers travel with the auriculotemporal nerve, a sensory branch of the mandibular division of the trigeminal nerve to provide the parasympathetic innervation of the parotid gland. The lesser petrosal nerve carries preganglionic parasympathetic fibers of the glossopharyngeal nerve (IX) to the parotid gland via the otic ganglion. After synapsing in the otic ganglion, postganglionic fibers supply secretory fibers to the parotid gland by the way of the auriculotemporal nerve [70].
– Branches **to the tympanic cavity mucosa**: somatic fibers to the tympanic cavity

involved in the aeration pressure regulation of the middle ear cleft, taking part in a neural pathway between the glomus bodies of the tympanic nerve, the tympanic plexus, the pons, and the Eustachian tube function (see paragraph of aeration regulation of the middle ear).

Clinical Applications

- *Anatomic topography and cochlear implant surgery*: The tympanic nerve has a close anatomical relationship with the cochlea and represents a useful marker in identifying the anterior and posterior parts of the basal segment of the scala tympani being of particular relevance in cochlear implantation [71].
- *Tympanic nerve section*: For post-parotidectomy Frey syndrome (facial transpiration during eating) and crocodile syndrome (paradoxical gustatory lacrimal reflex). In some anatomic situations, when the nerve is covered by bone, a hypotympanic drilling could be indicated to be able to do a total resection of the tympanic nerve.
- *Middle ear surgery* and the importance of its preservation with its supposed role in aeration control and tympanoplasty success.

Clinical Application

Tympanic paragangliomas are mostly small-sized tumors originating from the tympanic plexus of the middle ear.

Clinically, these tumors are symptomatic as pulsatile tinnitus and conductive hearing loss. Tympanic paragangliomas are diagnosed by careful otoscopic examination; they appear as a reddish retrotympanic mass behind a translucent tympanic membrane.

Frequently, the glomus tumor is extended to the jugular plexus and the jugular bulb. To determine the extensions of the entire tumor, computed tomography (Fig. 3.46) or magnetic resonance imaging is imperative, to decide of the need of a preoperative embolization.

3.5 Middle Ear Vessels

3.5.1 Embryology of Middle Ear Vessels (Fig. 3.47)

During the fourth week of gestation, the first and second aortic arches begin to involute, and they leave behind the mandibular and hyoid arteries, respectively. At the same time, the third arch artery becomes the internal carotid artery.

During the fourth to fifth week of gestation, the ventral pharyngeal artery arises from the aortic sac. This artery supplies the bulk of the first two branchial bars and is subsequently involved in the formation of the stapedial and external carotid arteries.

During the sixth week, the stapedial artery arises as a small offshoot of the hyoid artery near its origin from the internal carotid artery. It extends cranially and passes through the stapes blastema to enter the mandibular bar (Fig. 3.3). The stapedial artery divides into two arteries: the maxillomandibular artery and the supraorbital artery (which supplies the primitive orbit). The maxillomandibular division of the stapedial artery joins the distal part of the ventral pharyngeal artery, the future external carotid artery [72].

Over the seventh week, the two major divisions of the stapedial artery are annexed by the internal maxillary artery (from the external carotid artery) and the ophthalmic artery, respectively. The trunk of the maxillomandibular division becomes the stem of the middle meningeal artery. As the stapedial artery withers proximal to the stapes, its more distal stem becomes the superior tympanic branch of the adult middle meningeal artery. The hyoid artery, which gave rise to the stapedial artery, involutes to become a caroticotympanic branch of the internal carotid artery [72].

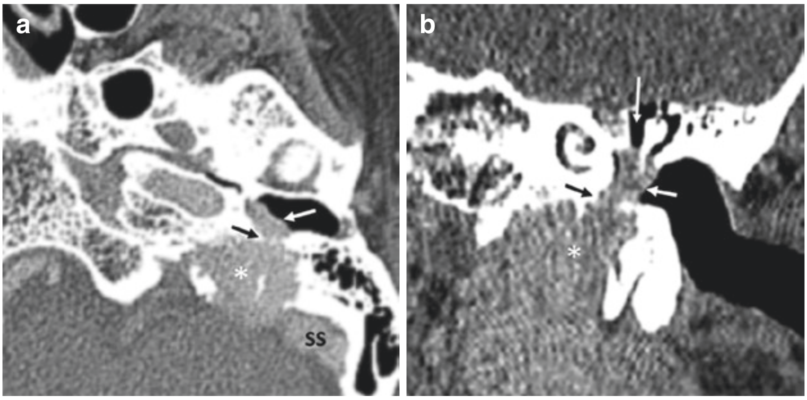

Fig. 3.46 (**a**) Transversal CT image of a left ear with IV contrast: large contrast uptake around the jugular vein (*) with erosion of the adjacent hypotympanic osseous structures (black arrow) and continuity with a process of the same density in the hypotympanum (white arrow). (**b**) Coronal CT reconstruction of the same ear: the process is extended along the entire tympanic membrane (short white arrow), encasing the mesotympanic ossicular chain. The attic is spared (long white arrow) and still aerated

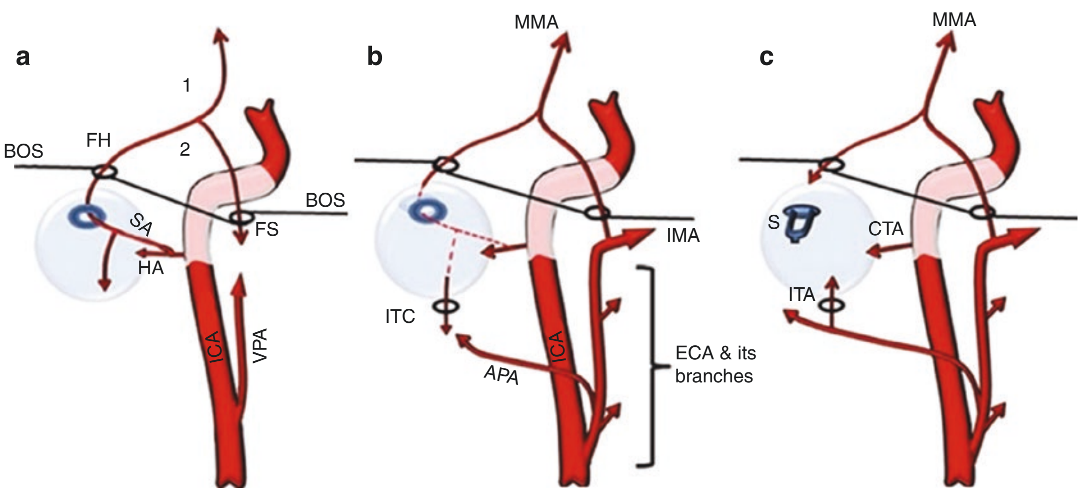

Fig. 3.47 Schema illustrating normal development of middle ear vessels. (**a**) Approximately 6 weeks. (**b**) Approximately 8 weeks. (**c**) Adult configuration. *BOS* base of skull, *FH* facial hiatus, *SA* stapedial artery, blue disk, otic capsule, *HA* hyoid artery, *ICA* internal carotid artery, *FS* foramen spinosum, *VPA* ventral pharyngeal artery, *1* supraorbital artery, *2* maxillomandibular artery, *APA* ascending pharyngeal artery, *ITC* inferior tympanic canaliculus, *MMA* middle meningeal artery, *IMA* internal maxillary artery, *ECA* external carotid artery, *ITA* inferior tympanic artery, *CTA* caroticotympanic artery, *STA* superior tympanic artery, *S* stapes

Persistent Stapedial Artery

Persistent stapedial artery is a rare vascular anomaly of the middle ear. The reported prevalence is of 0.5% in cadaveric studies [73] and less than the 0.02–0.05% in surgical series [74, 75]. Usually asymptomatic, it may cause pulsatile tinnitus and hearing loss [76].

Normally, the stapedial artery atrophies by 3 months of fetal development; however, in very rare cases, it may persist as a 1.5–2.0 mm branch of the petrous internal carotid artery [76].

A persistent stapedial artery arises from the petrous part of the internal carotid artery, enters the hypotympanum through the medial hypotympanic fissure, crosses the cochlear promontory, and passes through the obturator foramen of the stapes. It enters the Fallopian canal behind the cochleariform process and travels anteriorly with the greater superficial petrosal nerve to enter the middle cranial fossa through the facial hiatus where it ends up as the middle meningeal artery (Fig. 3.48).

On CT studies, in case of a persistent stapedial artery, the foramen spinosum will be absent [77] (Fig. 3.49).

If it occurs in cases of otosclerosis, it may render the acces to the footplate difficult, or even unfeasable (Fig. 3.50).

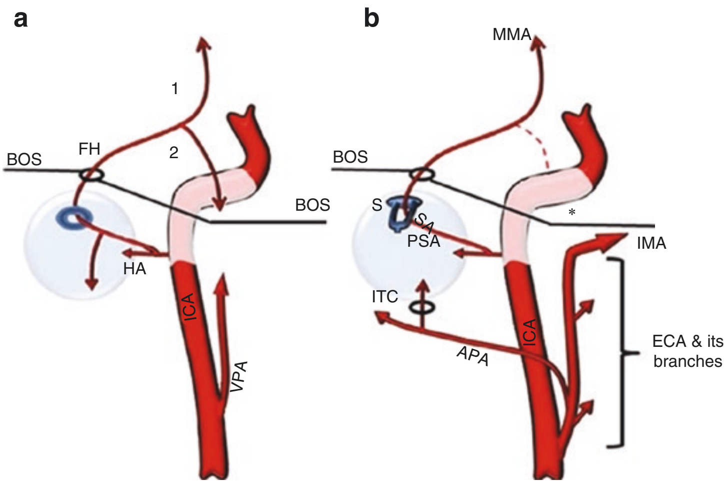

Fig. 3.48 Schema illustrating the development of persistent stapedial artery (PSA). (**a**) Embryonic phase: failure of development of foramen spinosum (*) and communication between maxillomandibular branch (2) of stapedial artery (SA) and ventral pharyngeal artery (VPA). (**b**) Adult configuration of persistent stapedial artery. *BOS* base of skull, *FH* facial hiatus, *SA* stapedial artery, *HA* hyoid artery, *ICA* internal carotid artery, *APA* ascending pharyngeal artery, *ITC* inferior tympanic canaliculus, *MMA* middle meningeal artery, *IMA* internal maxillary artery, *ECA* external carotid artery, *S* stapes

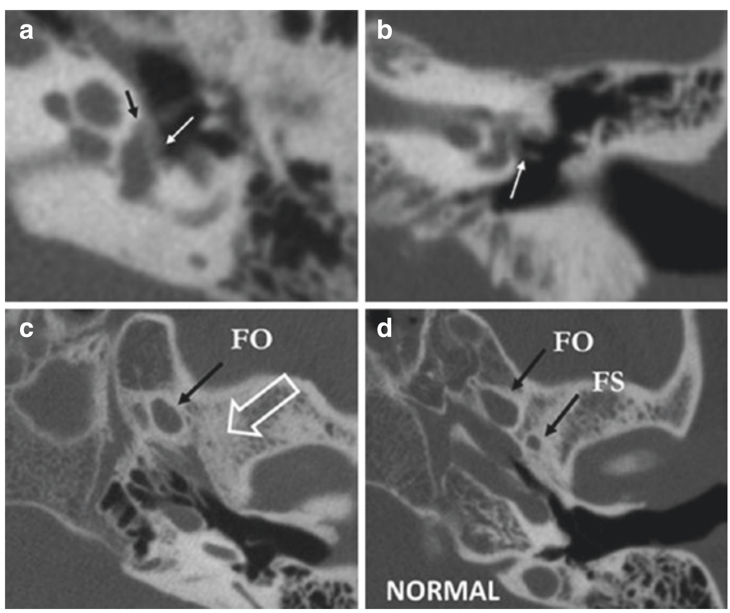

Fig. 3.49 (**a**) Axial CT image left ear: typical otosclerosis in the fissula ante fenestram (black arrow), a rounded isodense structure in close contact with the footplate (white arrow), is not specific but raises the suspicion of a persistent stapedial artery; (**b**) coronal CT image of the same ear: atypical round soft tissue formation along the oval window niche (arrow); (**c**) absent foramen spinosum at the skull base (empty arrow) (**d**) compared with a normal image of the skull base: *FO* foramen ovale, *FS* foramen spinosum

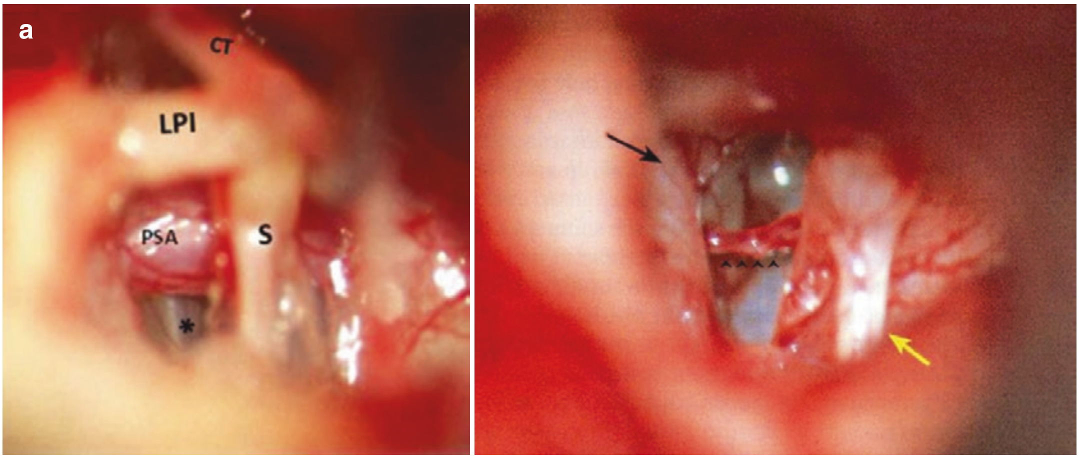

Fig. 3.50 (**a**) Right ear otosclerosis with persistent stapedial artery (PSA). (**a**) The posterior half of the footplate is visible (*) and could be accessible for fenestration. (**b**) Left middle ear exploration showing persistent stapedial artery (black arrowheads) passing above the footplate; *F* facial nerve, *st* stapedial tendon

Aberrant Internal Carotid Artery

An aberrant internal carotid artery (ICA) is a variant of the ICA that passes through the middle ear. Clinical signs and symptoms include pulsatile tinnitus, otalgia, aural fullness, vertigo and hearing loss [77, 78]. The most accepted theory of the etiology of an aberrant internal carotid artery is the agenesis of the vertical internal carotid artery with compensatory vascular communication branches of the developing external carotid artery system. The ascending pharyngeal artery gives rise to the inferior tympanic artery, which is the aberrant internal carotid artery; then it enters the middle ear through the inferior tympanic canaliculus, passing through the middle ear, it joins the horizontal petrous carotid artery anteriorly (Fig. 3.51). It appears as a red mass in the anteroinferior quadrant of the middle ear (Fig. 3.52). Otologists should be aware of the possibility of an aberrant ICA when the patient presents with a tympanic mass. If mistaken for a tumor and biopsied, the results can be disastrous. Imaging is required to make the differential diagnosis (Fig. 3.53).

A temporal bone CT scan in patients with carotid agenesis shows the complete absence of carotid bony canal (see Sect. 2.6.1.1).

3.5.2 Anatomy of the Middle Ear Vessels (Fig. 3.54)

The blood supply of the middle ear and mastoid cavity originates from the internal and external carotid arteries. We recognize the following important feeding arteries of the middle ear:

3.5.2.1 The Anterior Tympanic Artery

The anterior tympanic artery is a terminal branch of the internal maxillary artery. It gives rise to an important branch, the ossicular branch, which provides the main blood supply for the malleus

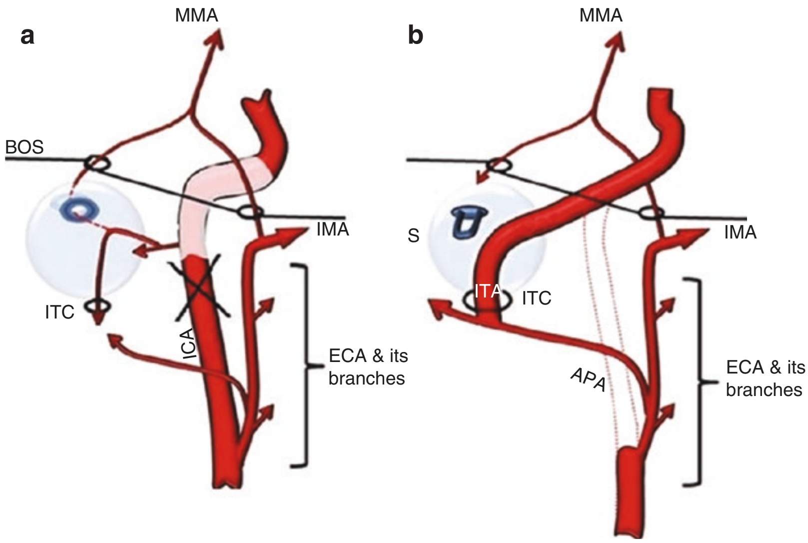

Fig. 3.51 Schema illustrating the development of aberrant internal carotid artery. (**a**) Embryonic phase, failure of development of vertical part of internal carotid artery (ICA). (**b**) Adult configuration of aberrant carotid artery. Notice the absence of development of the carotid canal. *BOS* base of skull, *ICA* internal carotid artery, *APA* ascending pharyngeal artery, *ITC* inferior tympanic canaliculus, *MMA* middle meningeal artery, *IMA* internal maxillary artery, *ECA* external carotid artery, *ITA* inferior tympanic artery

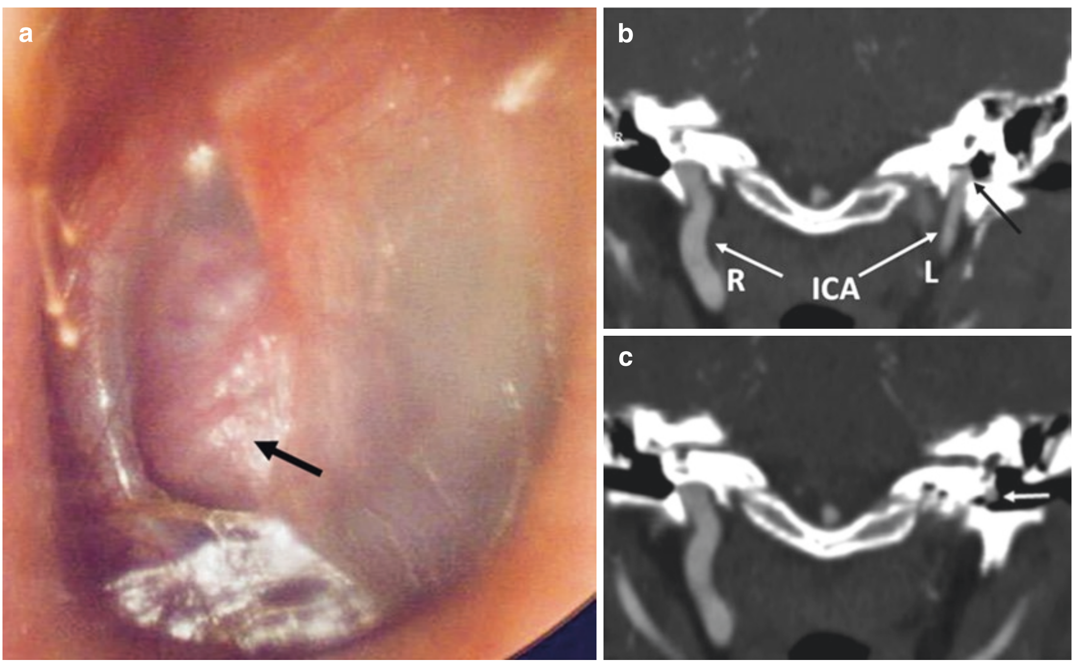

Fig. 3.52 Case of left ear aberrant carotid artery. (**a**) Otoscopic view showing the carotid artery (black arrow) passing in the middle ear and in touch with the malleus. (**b**, **c**) Coronal CT reconstruction after iv contrast, (**b**) is slightly more posterior than (**c**): Comparison between the trajectory of the right and left ICA. Black arrow in (**a**) and white arrow in (**b**) show the intracavitary trajectory of the aberrant internal carotid artery on the left

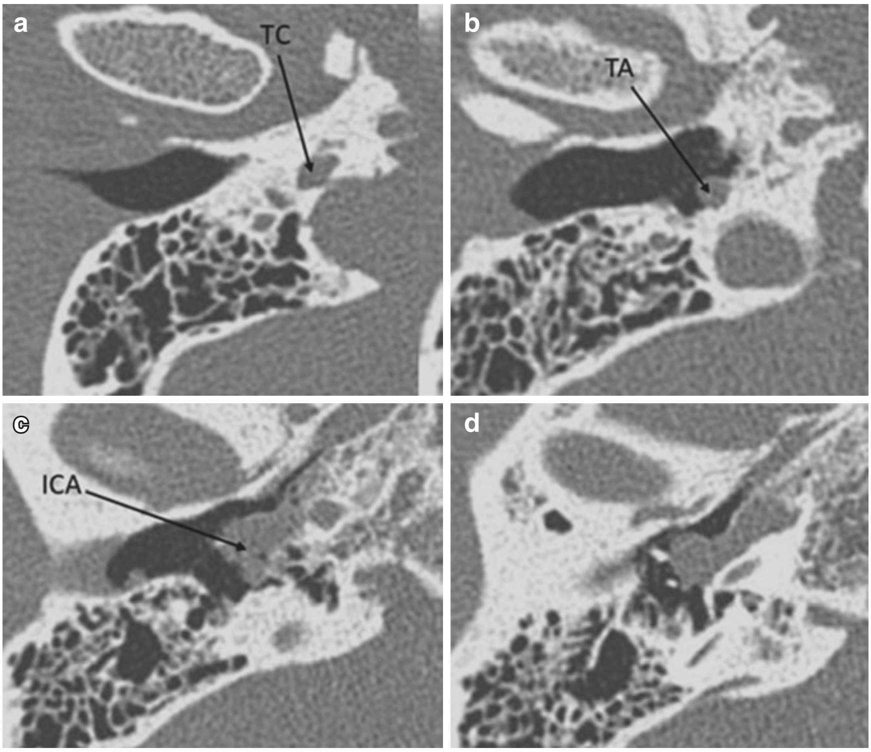

Fig. 3.53 Transverse CT imaging of an aberrant internal carotid artery: (**a**) Dilatation of the tympanic canal (TC) = Jacobson's canal, (**b**) by the inferior tympanic artery (TA), (**c**) that becomes the intratympanic carotid artery (ICA) in case of agenesis of the tympanic segment of the "true" internal carotid artery. (**d**) Mass effect of the intracavitary component on the ossicles

3.5.2.2 The Posterior Auricular Artery

The posterior auricular artery is another branch of the internal maxillary artery which provides two branches to the vascular ring of the tympanic membrane. A posterior branch supplies most of the tympanic membrane, whereas the anterior branch supplies a lesser portion of the anterior and inferior region.

3.5.2.3 Branches of the Middle Meningeal Artery

3.5.2.3.1 The Superior Petrosal Artery

The superior petrosal artery enters the middle ear through the facial hiatus; it enters the Fallopian canal and provides blood supply to the geniculate ganglion and the tympanomastoid segment of the facial nerve. Also it provides vascularization of the incudostapedial joint and posterior part of stapes by giving rise to the superior and inferior arteries of the stapedial tendon and posterior crural artery.

3.5.2.3.2 The Superior Tympanic Artery

The superior tympanic artery enters the middle ear adjacent to the lesser petrosal nerve. The artery supplies the tensor tympani and a portion of the epitympanic space. It also forms an anastomotic plexus with the inferior tympanic artery, giving rise to the anterior stapedial artery and the anterior crural artery.

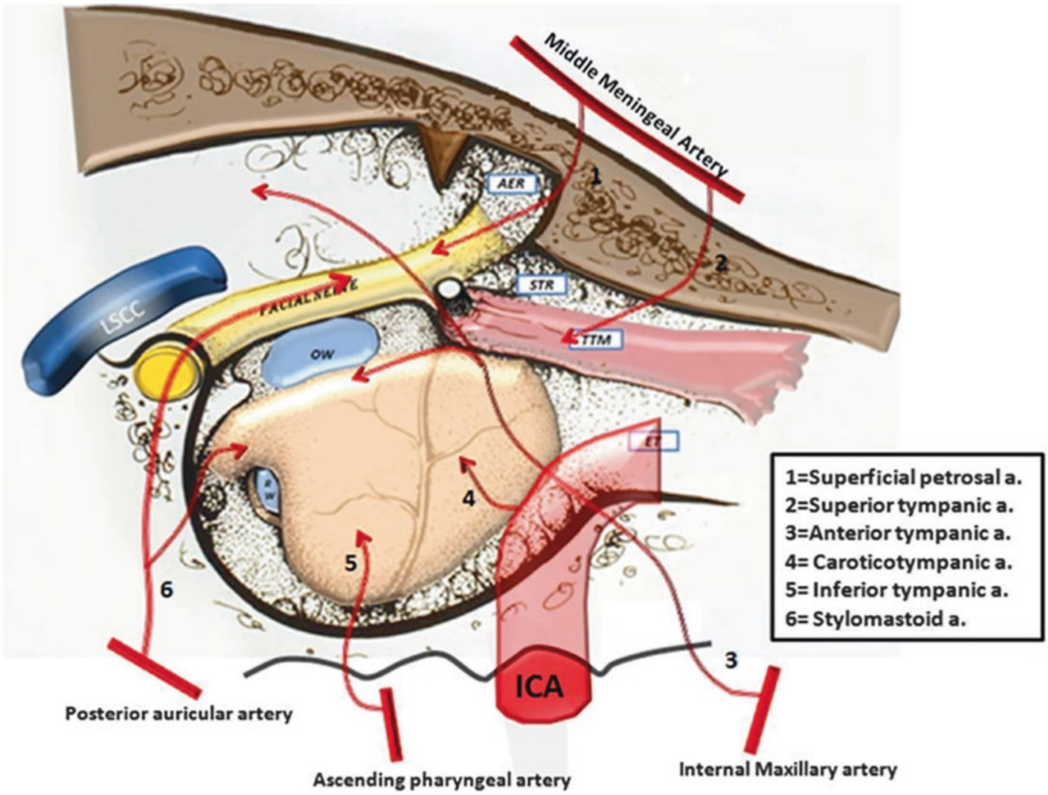

Fig. 3.54 Middle ear vessels. *ICA* internal carotid artery, *LSCC* lateral semicircular canal, *OW* oval window, *RW* round window, *AER* anterior epitympanic recess, *STR* supratubal recess, *TTM* tensor tympani muscle, *ET* Eustachian tube and incus. The anterior tympanic artery also gives rise to branches that supply the bone and mucosa of the superior and lateral walls of the epitympanic cavity

3.5.2.4 The Caroticotympanic Arteries

The caroticotympanic arteries are branches of the internal carotid artery that pass through the bony wall of the carotid canal to enter the middle ear cleft and eventually anastomose with branches of the inferior tympanic artery.

3.5.2.5 The Inferior Tympanic Artery

The inferior tympanic artery is a branch of the ascending pharyngeal artery; it enters the middle ear cleft with the tympanic (Jacobson's) nerve. This artery, along with the caroticotympanic arteries, provides the major blood supply to the mucosa of the promontory and the lower tympanic cavity (hypotympanum).

3.6 Middle Ear Mucosal Folds

In this section, a detailed description of the mucosal folds of the middle ear will be presented in order to clarify their anatomical organization. A good understanding of the anatomy of these folds and their relationships inside the middle ear cavity is fundamental in the learning process of functional middle ear surgery. These folds delimit different compartments, spaces, and recesses, which will be described in detail in Chap. 4.

3.6.1 Mucosal Fold Development

Between the third and seventh fetal month, the mesenchymal tissue of the middle ear cleft is gradually absorbed. At the same time, the primitive tympanic cavity develops by a growth of an endothelium-lined fluid pouch extending from the Eustachian tube into the middle ear. Four primary sacci bud out to define the different middle ear spaces. They are the *saccus anticus*, the *saccus medius*, the *saccus superior*, and the *saccus posticus* [79] (see Chap. 4). These sacci or pouches start to enlarge in the middle ear cleft to replace the preexisting mesenchyme. The walls of the pouches become the mucosal lining of middle ear cavity. At the plane of contact between two neighboring pouches, mucosal folds are formed. Between the mucosal layers of the folds, there are remnants of the mesenchyme that will transform into ligaments and blood vessels supplying the "viscera" of the tympanic cavity.

3.6.2 Mucosal Fold Anatomy

Middle ear mucosal folds pass from the walls of the middle ear to its contents and carry ligaments and blood vessels to the ossicles. Bruce Proctor is the first to describe the development of the middle ear spaces [80]. However, his description and figures have been difficult to understand and to teach. The clinical relevance of these folds lies in their role in chronic inflammatory otitis and their impact on selective dysventilation syndrome and the pattern of cholesteatoma spread.

Despite the fact that these folds may orient the progress of middle ear pathologies, they are not true barriers against their extension. Hence the clear anatomic description is crucial to understand the topographic architecture of middle ear compartments (Figs. 3.55, 3.56, 3.57 and 3.58).

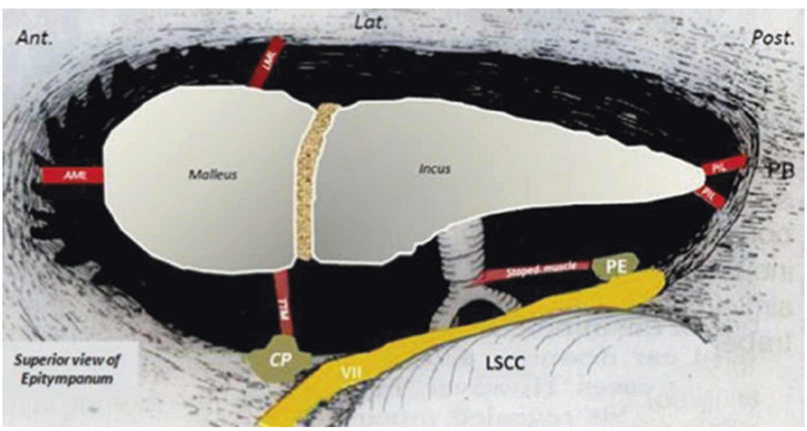

Fig. 3.55 Superior view of a right middle ear, showing middle ear ossicles and their ligaments after removal of all mucosal folds. *AML* anterior malleal ligament, *LML* lateral malleal ligament, *PIL* posterior incudal ligament, *TTM* tensor tympani muscle tendon, *CP* cochleariform process, *PE* pyramidal eminence, *LSCC* lateral semicircular canal, *PB* petrous bone. (Reproduced from Tos [81], (Fig. 83) with permission from Thieme publishers)

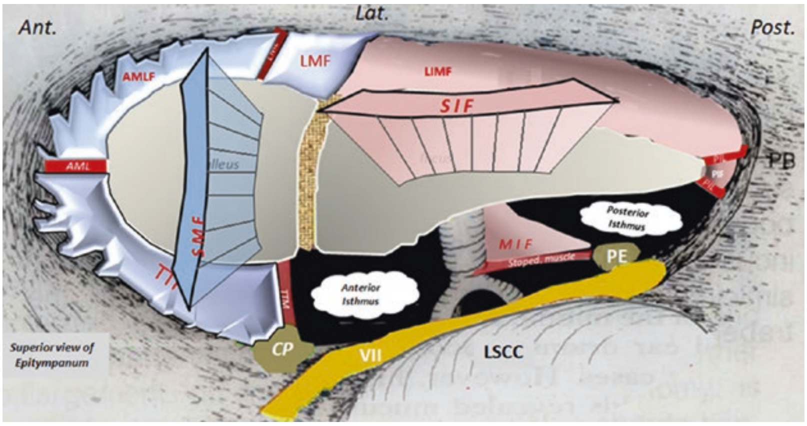

Fig. 3.56 Superior view of a right middle ear showing middle ear ossicles, ligaments, and mucosal folds. *AML* anterior malleal ligament, *LML* lateral malleal ligament, *PIL* posterior incudal ligament, *TTM* tensor tympani muscle tendon, *CP* cochleariform process, *PE* pyramidal eminence, *LSCC* lateral semicircular canal, *TTF* tensor tympani fold, *AMLF* anterior malleal ligament fold, *LMF* lateral malleal fold, *SMF* superior malleal fold, *MIF* medial incudal fold, *LIMF* lateral incudomalleal fold, *SIF* superior incudal fold, *PIF* posterior incudal fold

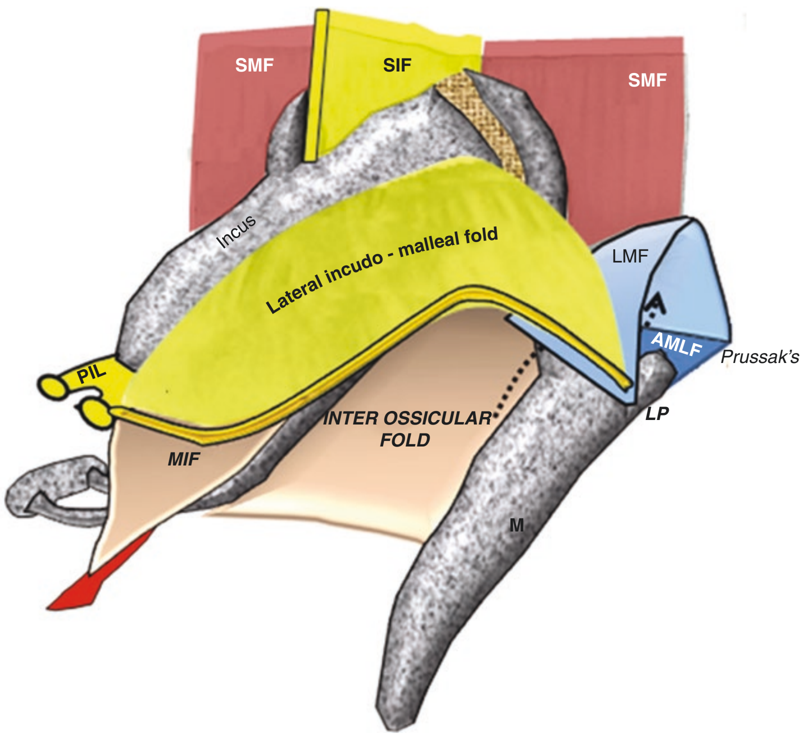

Fig. 3.57 Posterolateral view of a right middle ear showing middle ear ossicles and mucosal folds. *SMF* superior malleal fold, *SIF* superior incudal fold, *LMF* lateral malleal fold, *AMLF* anterior malleal ligamental fold, *MIF* medial incudal fold, *PIL* posterior incudal ligament, *M* malleus, *LP* lateral process of the malleus. The dotted arrow represents the ventilation tract of the Prussak's space

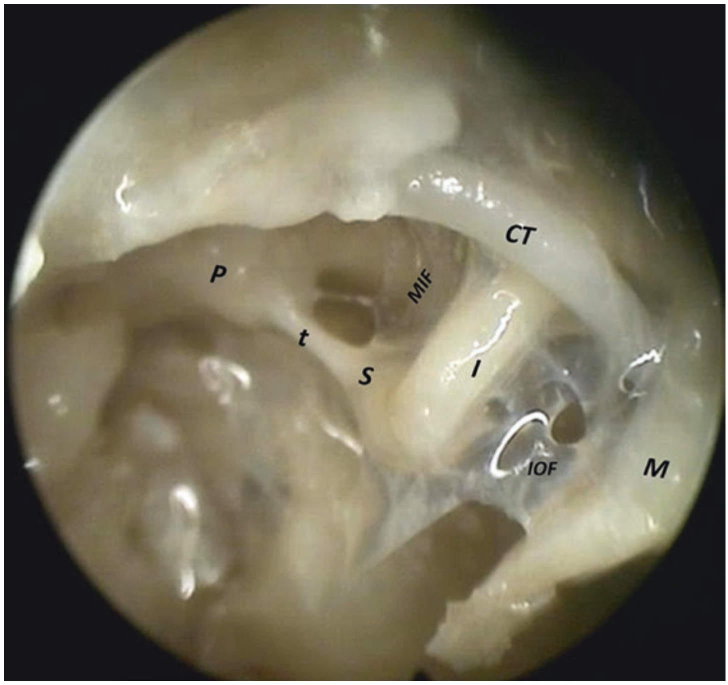

Fig. 3.58 Right ear showing interossicular fold (IOF) extending between malleus handle (M) and long process of incus (I) and medial incudal fold extending between incus and stapes (S). *P* pyramidal process, *t* tendon, *CT* chorda tympani

There are two different types of mucosal folds: composite folds and duplicate folds.

- *The composite folds*, like the anterior malleal ligament fold, the lateral malleal ligament fold, and the posterior incudal fold, have an essential common feature: a combination of a ligament and lining mucosa, with a varying degree of mucosal extension over the ligamental limits and ending with free edges. They are formed when the expanding air sacs meet the preexisting ligament and cover it with mucosal membrane.
- *The duplicate folds*, like the tensor tympani fold (TTF) and lateral incudomalleal fold (LIMF), are thin mucosal structures arising from the fusion of two expanding air sac walls in the absence of any interposing structure. Their position changes because the extent of the expansion of each air sac varies in different individuals [82, 83].

3.6.2.1 The Posterior Tympano-Malleal Fold

The posterior tympano-malleal fold, a ligamental fold, inserts on the posterior portion of the neck of the malleus. It involves the upper portion of the handle of the malleus and merges superiorly with the downturn of the anterior portion of the lateral incudomalleal fold. It inserts posteriorly on the posterior tympanic spine and represents the medial wall of the posterior pouch of von Tröltsch. Its medial edge envelops the posterior portion of the chorda tympani [84] (Fig. 3.59).

3.6.2.2 The Anterior Tympano-Malleal Fold

The anterior tympano-malleal fold arises from the anterior portion of the neck of the malleus and inserts anteriorly on the anterior tympanic spine. It forms the medial wall of the anterior pouch of von Tröltsch [84] (Figs. 3.59 and 3.60).

3.6.2.3 The Anterior Malleal Ligament Fold (AMF)

The anterior malleal ligament fold was described by von Tröltsch in 1856. It is part of the tympanic diaphragm. It originates from the neck of the malleus and extends to the anterior attic bony wall. It is reflected from the lateral wall of the middle ear over the anterior process and ligament

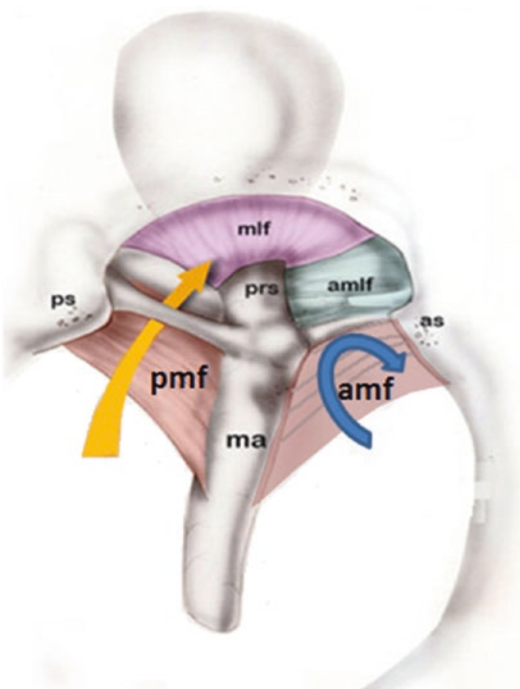

Fig. 3.59 Lateral view of a right middle ear after removal of the tympanic membrane, showing the anterior (amf) and the posterior (pmf) malleal folds. *as* anterior tympanic spine, *ps* posterior tympanic spine. The yellow arrow represents the route of ventilation of the Prussak's space (prs). Blue arrow represents the complete closure of the Prussak's space floor anteriorly, *mlf* lateral malleal fold, *amlf* anterior malleal ligamental fold, *ma* manubrium. (Reproduced with modification from Marchioni [85], (figure 1). With kind permission from Springer Science and Business Media, Springer and the original publisher)

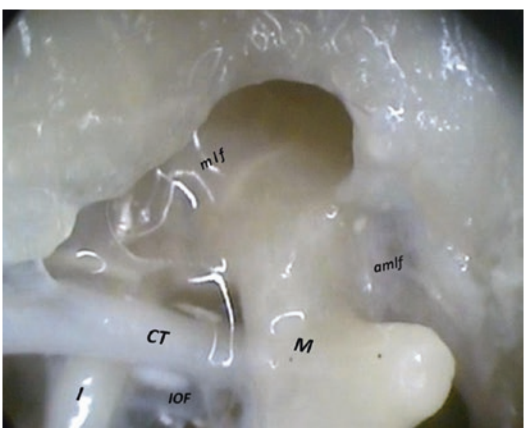

Fig. 3.60 Right ear after removal of pars flaccida to expose the Prussak's space showing the lateral malleal fold (mlf) and the anterior malleal ligamental fold (amlf). *IOF* interossicular fold, *M* malleus, *I* incus, *CT* chorda tympani

of the malleus and the anterior part of the chorda tympani. Its low posterior part is broad and represents the anterior limit of Prussak's space [84] (Fig. 3.61).

3.6.2.4 The Lateral Malleal Ligament Fold (LMF)

The lateral malleal ligament fold is a thick fold; it is first described by Helmholtz in 1868 [86]. This fold starts from the middle portion of the neck of the malleus to develop a fanlike spread before attaching to the attic outer wall; posteriorly, it is confluent with the anterior descending portion of the lateral incudomalleal fold (Fig. 3.62).

This fold is usually complete; it represents the roof of the Prussak's space and the floor of the lateral malleal space. It is considered to be strong to prevent progression of pars flaccida retraction pockets [87].

Defects in this fold, usually in its thin posterior membranous part, are observed in 7%. In such cases, the defect provides a direct small communication between the upper and lower epitympanic units [82, 83] (see Sect. 4.5).

3.6.2.5 The Superior Malleal Fold (SMF)

The superior malleal fold extends between the superior surface of the malleus head and the tegmen in a transversal plane. It contains the superior malleal ligament and divides the attic into anterior and posterior parts (Figs. 3.56 and 3.57).

3.6.2.6 The Lateral Incudomalleal Fold (LIMF)

The lateral incudomalleal fold is a part of the tympanic diaphragm. It lies superiorly in relation to the lateral malleal ligament fold and separates the upper lateral attic space from the lower lateral attic space. The level of this fold is about 1 mm higher than the roof of the Prussak's space [86]. This fold presents a defect in its anterior portion in about 20% of cases [83].

The lateral incudomalleal fold has a posterior and a lateral extension: posteriorly, it presents a horizontal extension to insert medially onto the body of the incus and the incudomalleal joint. Laterally, it inserts onto the medial surface of the bony wall of the scutum.

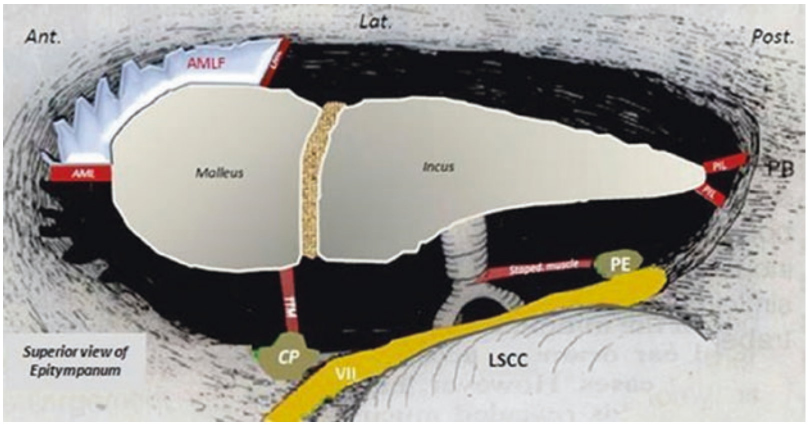

Fig. 3.61 Superior view of a right middle ear showing the anterior malleal ligamental fold (AMLF). *AML* anterior malleal ligament, *LML* lateral malleal ligament, *PIL* posterior incudal ligament, *TTM* tensor tympani muscle tendon, *CP* cochleariform process, *PE* pyramidal eminence, *LSCC* lateral semicircular canal, *PB* petrous bone

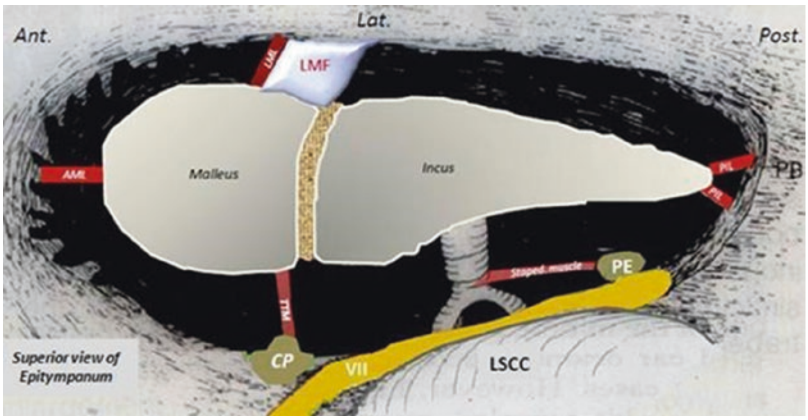

Fig. 3.62 Superior view of a right middle ear showing the lateral malleal fold (LMF). *AML* anterior malleal ligament, *LML* lateral malleal ligament, *PIL* posterior incudal ligament, *TTM* tensor tympani muscle tendon, *CP* cochleariform process, *PE* pyramidal eminence, *LSCC* lateral semicircular canal, *PB* petrous bone

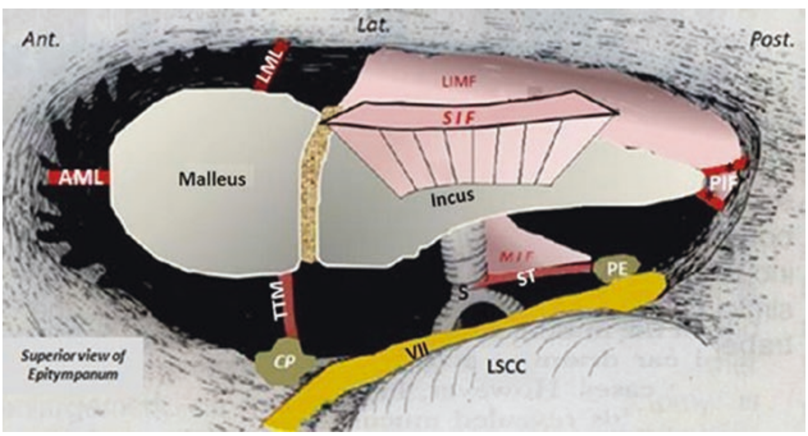

Fig. 3.63 Superior view of the right middle ear, showing the superior incudal fold (SIF), the medial incudal fold (MIF), the lateral incudomalleal fold (LIMF), and the posterior incudal fold (PIF). *TTM* tensor tympani muscle, *ST* stapedial tendon, *AML* anterior malleal ligament, *LML* lateral malleal ligament, *CP* cochleariform process, *VII* facial nerve, * posterior incudal ligament, *S* stapes, *PE* pyramidal eminence, *LSCC* lateral semicircular canal

The anterior portion of this fold bends inferiorly toward the neck of the malleus and merges with the posterior portion of the lateral malleal ligament fold, representing the posterior limit of the lateral malleal space (Figs. 3.57, 3.63 and 3.64).

3.6.2.7 The Medial Incudal Fold (MIF)

The medial incudal fold is located between the long process of the incus and the tendon of the stapedial muscle as far as the pyramidal eminence (Fig. 3.63).

3.6.2.8 The Superior Incudal Fold (SIF)

The superior incudal fold extends like the superior incudal ligament from the superior surface of the incudal body to the tegmen (Fig. 3.63). It separates the lateral posterior attic from the medial posterior attic (Fig. 3.63).

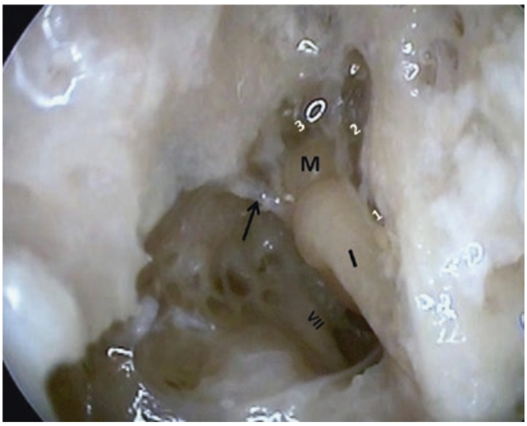

Fig. 3.64 Transattic superior view of the right middle ear showing the inter-attico-tympanic diaphragm with the lateral incudal fold (1), lateral malleolar fold (2), anterior malleolar fold (3), and the superior malleolar fold (black arrow). *M* malleus, *I* incus

3.6.2.9 Posterior Incudal Fold (PIF)

The posterior incudal fold is the fold that runs between the fibers of the posterior incudal ligament (Fig. 3.63). It is a part of the tympanic diaphragm (Fig. 3.63).

3.6.2.10 The Tensor Tympani Fold (TTF)

The TTF is a major part of the tympanic diaphragm (Figs. 3.65 and 3.66). It arises posteriorly from the tensor tympani tendon, about 1.5 mm lower than the roof of Prussak's space [88]. It runs anteriorly toward the anterior wall of the attic inserting into a transverse crest: the supratubal ridge. Medially it inserts on the bony canal of the TTM, and laterally it inserts on the anterior malleal ligament. The lateral part of the tensor fold keeps a close relationship with the most anterior portion of chorda tympani. It separates the anterior epitympanic recess superiorly from the supratubal recess inferiorly.

Embryologically, the TTF results from the fusion of the saccus anticus and the anterior saccule of the saccus medius. The inclination angle of the TTF varies between 80° and 120° depend-

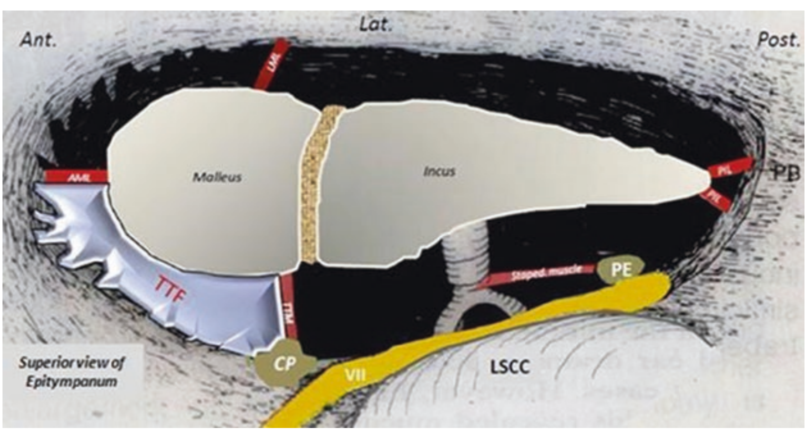

Fig. 3.65 Superior view of a right middle ear showing the tensor tympani fold (TTF) that inserts posteriorly on the tensor tympani muscle tendon (TTM), laterally on the anterior malleal ligament (AML), and anteriorly on the anterior attic wall. *LML* lateral malleal ligament, *PIL* posterior incudal ligament, *CP* cochleariform process, *PE* pyramidal eminence, *LSCC* lateral semicircular canal, *PB* petrous bone

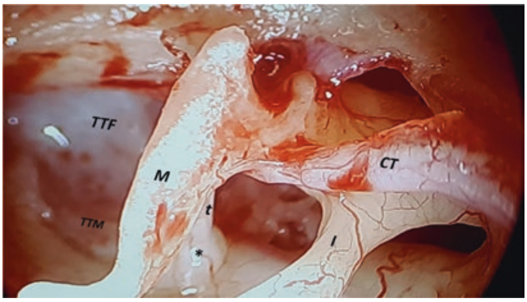

Fig. 3.66 Left ear showing the tensor tympani fold (TTF) extending between the tensor tympani muscle canal (TTM) to the lateral wall of middle ear and from the tensor tympani tendon (t) to the anterior wall. *M* malleus, *I* incus, *CT* chorda tympani, * cochleariform process. Courtesy Dr Murthy Sreeram

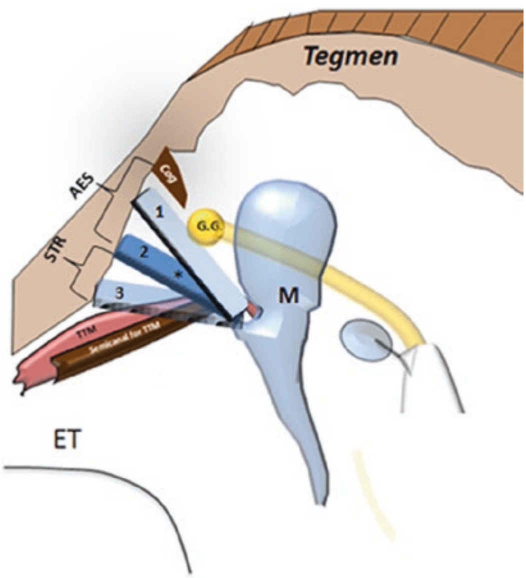

Fig. 3.67 Lateral view of a left ear showing the tensor tympani fold (*) with its variable anterior insertion (*1* high insertion, *2* intermediate insertion, *3* low insertion). The variable insertion of the TTF determines the volume of the anterior epitympanic recess (AER) which lies above the TTF and the supratubal recess (STR) which lies below the TTF. *TTM* tensor tympani muscle, *M* malleus, *GG* geniculate ganglion

ing on the variable growth of each saccus [89, 90]. The size of the supratubal recess and the anterior epitympanic recess is dependent on the vertical orientation of the TTF. The more vertical the TTF is, the wider is the supratubal recess [88] (Figs. 3.67 and 3.69). A horizontal TTF results in

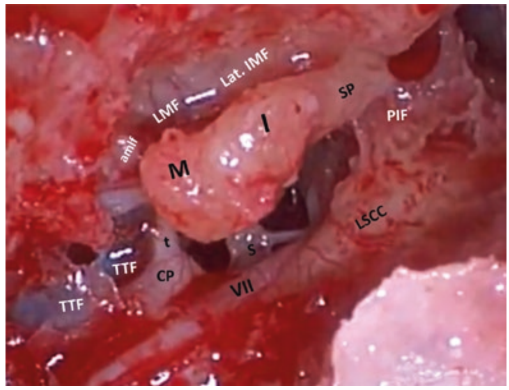

Fig. 3.68 Superior view of a right middle ear showing the tympanic diaphragm. Amlf anterior malleal ligament fold, *TTF* tensor tympani fold, *LMF* lateral malleal fold, *Lat. IMF* lateral incudomalleal fold, *PIF* posterior incudal fold, *t* tensor tympani muscle tendon, *CP* cochleariform process, *S* stapes, *I* incus, *M* malleus, *VII* facial nerve, *LSCC* lateral semicircular canal, *SP* short process of incus

a very small or *even* inexistent supratubal recess [89]. A direct aeration of the epitympanum, from the supratubal recess through an incomplete TTF, prevents the development of attic dysventilation [90].

The peripheral portion of the TTF is thick, while the central portion is thin and transparent. Palva and colleagues stated that the TTF is incomplete in only 25% of ears; this allows a direct communication from the Eustachian tube and supratubal recess to the anterior epitympanic recess and then to the posterior attic (anterior route of attic aeration) (Figs. 3.70 and 3.71). In ears with a complete TTF, the anterior epitympanum and protympanum are totally separated. These ears lack the anterior route of aeration and become more susceptible of selective dysventilation syndrome (see 4.8.1.1).

3.6.3 The Tympanic Diaphragm

Chatellier and Lemoine introduced the concept of the “epitympanic diaphragm” in 1946 [91] that raised the modern theories of tympanic ventilation. The authors described how the diaphragm was made up of various fold structures and membranous ligament that form together with the malleus and the incus the floor of the epitympanic compartment.

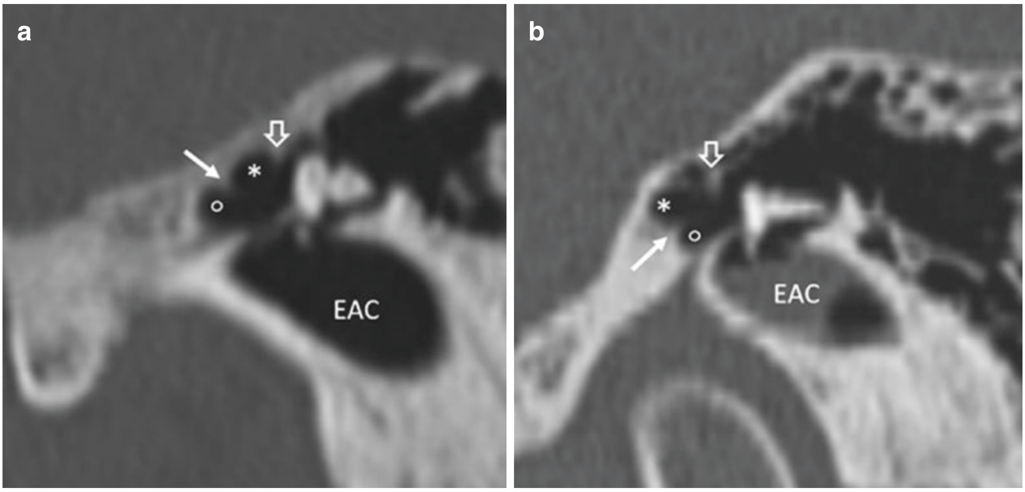

Fig. 3.69 Sagittal reconstructions showing different degrees of inclination of the TTF (white arrow) between the STR (o) and the AER (*), resulting in different sizes of both compartments. Cog (empty arrow), *EAC* external auditory canal

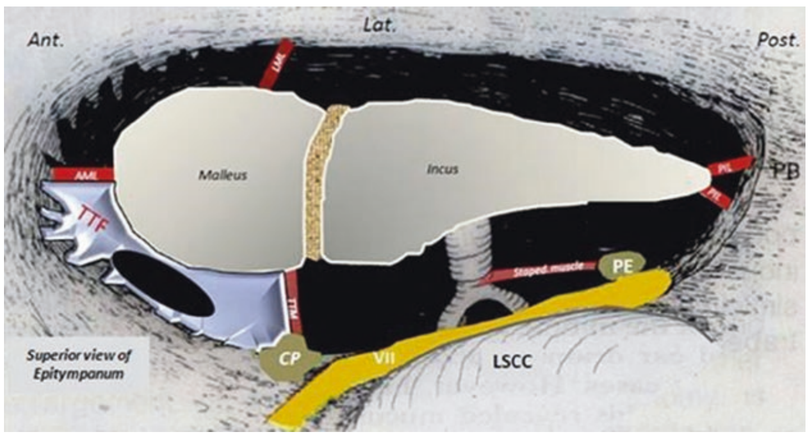

Fig. 3.70 Superior view of a right middle ear showing incomplete tensor tympani fold (TTF). *AML* anterior malleal ligament, *LML* lateral malleal ligament, *PIL* posterior incudal ligament, *TTM* tensor tympani muscle tendon, *CP* cochleariform process, *PE* pyramidal eminence, *LSCC* lateral semicircular canal, *PB* petrous bone

Palva et al. revised Chatellier's concept of the epitympanic diaphragm and added two other important folds: the TTF and the lateral incudomalleal fold [92, 93]. According to them, the complete tympanic diaphragm is made up of the three malleal ligament folds (anterior, lateral, and posterior), the posterior incudal fold, the TTF, the lateral incudomalleal fold, and the incus and the malleus [88, 94] (Figs. 3.68 and 3.72).

The tympanic diaphragm is not fully horizontal because its components are on different levels. It separates the upper unit of the attic superiorly from the mesotympanum and the lower unit of the attic, the Prussak's space, inferiorly. The lateral malleal fold separates Prussak's space from the upper unit of the epitympanum; this is why we call the Prussak's space the lower unit of the attic [88] (see Sect. 4.5).

The lateral incudomalleal fold separates the epitympanum and mesotympanum in the posterior part of the tympanic cavity, and the tensor fold separates the epitympanum from the protympanum in the anterior part of the tympanic cavity. All the compartments delimited by the epitympanic diaphragm receive air through the only ventilation way that is always present, the tympanic isthmus route, located between the medial aspect of the posterior incudal ligament and the tensor fold. Post-inflammatory pathological and irreversible changes may involve the tympanic diaphragm ventilation routes to promote chronic middle ear diseases.

3.6.4 The Tympanic Isthmus

The mesotympanum is connected with the Eustachian tube. However, the attic and the mastoid are isolated from the mesotympanum by the tympanic diaphragm. Attic aeration occurs through a 2.5 mm opening in the tympanic diaphragm called the tympanic isthmus (Fig. 3.73).

The entire attic is ventilated through the tympanic isthmus. The Prussak's space is ventilated through the posterior pouch of von Tröltsch [92, 94].

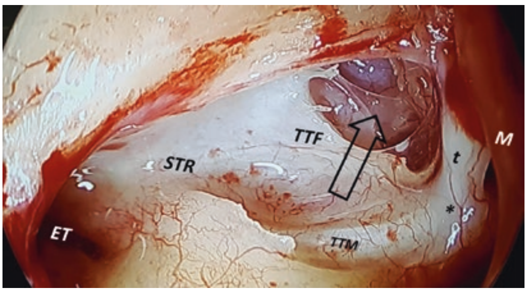

Fig. 3.71 Left ear endoscopic exploration where the endoscope is placed anterior to the malleus handle (M) to show the tensor tympani fold (TTF) which is incomplete (black arrow). *ET* Eustachian tube, *STR* supratubal recess, *TTM* tensor tympani muscle, *t* tensor tympani tendon, * cochleariform process

The tympanic isthmus extends from the tensor tympani muscle anteriorly to the posterior incudal ligament posterosuperiorly and the pyramidal eminence posteroinferiorly. The distance from the TTM to the anterior edge of the posterior incudal ligament is around 6 mm [88]. The tympanic isthmus is limited medially by the attic bone and laterally by the body and short process of the incus and the head of the malleus.

The tympanic isthmus is divided by the medial incudal fold into two portions (Fig. 3.73):

3.6.4.1 The Anterior Tympanic Isthmus

The anterior tympanic isthmus, most important, is situated between the TTM anteriorly and the stapes posteroinferiorly. The diameter of this pathway is from 1 to 3 mm (Fig. 3.73).

3.6.4.2 The Posterior Tympanic Isthmus

The posterior tympanic isthmus, less important, is situated between the short process of the incus and the stapedial muscle [80, 92]. The posterior tympanic isthmus is inconstant and often closed by the posterior tympanic fold; when it is open, it can have a role in the aeration of the upper retrotympanum, epitympanum, and the mastoid through the incudal fossa (Figs. 3.73, 3.74 and 3.75).

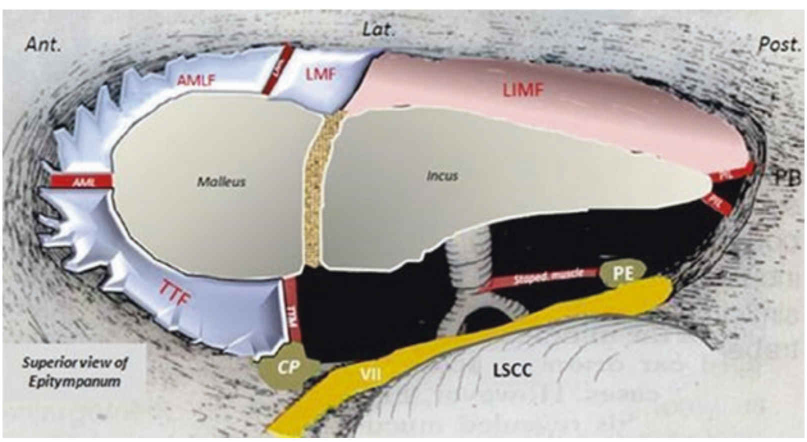

Fig. 3.72 Superior view of a right middle ear showing the tympanic diaphragm. *AMLF* anterior malleal ligament fold, *TTF* tensor tympani fold, *LMF* lateral malleal fold, *LIMF* lateral incudomalleal fold, *AML* anterior malleal ligament, *LML* lateral malleal ligament, *PIL* posterior incudal ligament, *TTM* tensor tympani muscle tendon, *CP* cochleariform process, *PE* pyramidal eminence, *LSCC* lateral semicircular canal, *PB* petrous bone

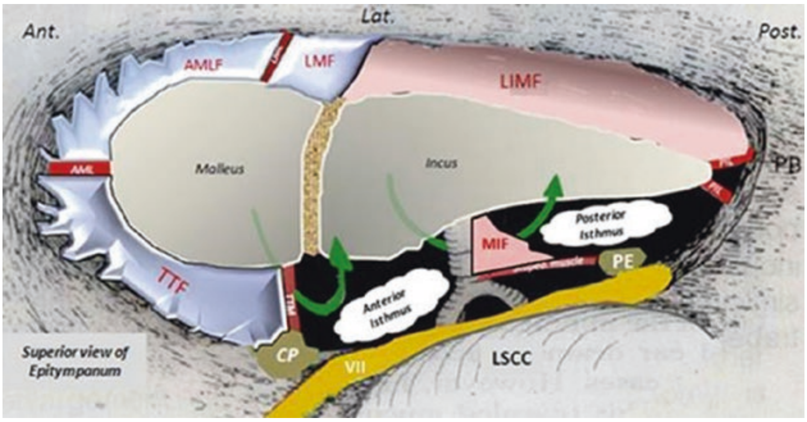

Fig. 3.73 Superior view of a right middle ear showing the tympanic diaphragm and the tympanic isthmus. The tympanic isthmus is divided into anterior and posterior isthmus by the medial incudal fold (MIF). The green arrows represent the normal route of attic aeration from the mesotympanum. *AMLF* anterior malleal ligament fold, *TTF* tensor tympani fold, *LMF* lateral malleal fold, *LIMF* lateral incudomalleal fold, *AML* anterior malleal ligament, *LML* lateral malleal ligament, *PIL* posterior incudal ligament, *TTM* tensor tympani muscle tendon, *CP* cochleariform process, *PE* pyramidal eminence, *LSCC* lateral semicircular canal, *PB* petrous bone

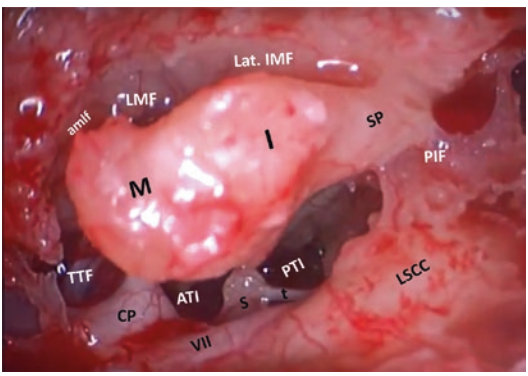

Fig. 3.74 Superior view of a right middle ear tympanic diaphragm through middle cranial fossa approach after drilling the tegmen showing the anterior tympanic isthmus (ATI) and posterior tympanic isthmus (PTI) communicating the epitympanum to the mesotympanum. *M* malleus head, *I* incus body, *SP* short process of incus, *TTF* tensor tympani fold, *AMLF* anterior malleal ligamental fold, *LMF* lateral malleal fold, *LIMF* lateral incudomalleal fold, *PIF* posterior incudal fold, *LSCC* lateral semicircular canal, *CP* cochleariform process; *PE* pyramidal eminence, *LSCC* lateral semicircular canal, *PB* petrous bone

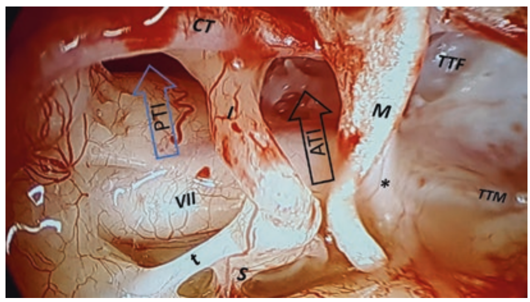

Fig. 3.75 Endoscopic examination of right ear showing anterior tympanic isthmus (ATI) in black arrow and posterior tympanic isthmus (PTI) in blue arrow. *t* stapedial tendon, *M* malleus, *I* incus, *S* stapes, *CT* chorda tympani, *TTF* tensor tympani fold, *TTM* tensor tympani fold, * cochleariform process. Courtesy Dr Murthy Sreeram

References

1. Moore KL, Persaud TVN. The developing human: clinically oriented embryology. 5th ed. Philadelphia: W. B. Saunders Company; 1993.
2. le Douarin N, Kalcheim C. The neural crest. Cambridge: Cambridge University Press; 1999.
3. Keith A. Human embryology and morphology. London: Edward Arnold; 1948.
4. Baxter JS. Frazer's manual of embryology. 3rd ed. London: Baillière, Tindall & Cox; 1953. p. 202–5, 235–43.
5. Bast TH, Anson BJ, Richany SF. The development of the second branchial arch (Reichert's cartilage), facial canal and associated structures in man. Q Bull Northwest Univ Med Sch. 1956;30:235–49.
6. Anson BJ, Hanson JR, Richany SF. Early embryology of the auditory ossicles and associated structures in relation to certain anomalies observed clinically. Ann Otol. 1960;69:427–47.
7. Bastian D, Tran Ba Huy P. Organogenèse de l'oreille moyenne. Encycl Med Chir Paris: ORL. 1996;20-005-A-30:4–12.

8. Nager GT. Aural atresia: anatomy and surgery. Postgrad Med. 1961;29:529–41.
9. Hough JV. Congenital malformations of the middle ear. Arch Otolaryngol. 1963;78:127–35.
10. Nomura Y, Nagao Y, Fukaya T. Anomalies of the middle ear. Laryngoscope. 1988;98:390–3.
11. Rahbar R, Neault MW, Kenna MA. Congenital absence of the incus bilaterally without other otologic anomalies: a new case report. Ear Nose Throat J. 2002;81:274–8.
12. Hanson JR, Anson BJ, Strickland EM. Branchial sources of the auditory ossicles in man: part II observation of embryonic stages from 7 mm to 28 mm (CR length). Arch Otolaryngol. 1962;76:200–15.
13. Louryan S. Développement des osselets de l'ouïe chez l'embryon humain: corrélation avec les données recueillies chez la souris. Bull Assoc Anat. 1993;77:29–32.
14. Louryan S, Glineur R. The mouse stapes develops mainly from the Reichert's cartilage independently of the otic capsule. Eur Arch Biol. 1993;103:211–2.
15. Louryan S, Heymans O, Goffard J-C. Ear malformations in the mouse embryo after maternal administration of triazène, with clinical implications. Surg Radiol Anat. 1995;17:59–64.
16. Louryan S, Vanmuylder N, Resimont S. Ectopic stapes: a case report with embryologic correlations. Surg Radiol Anat. 2003;25:342–4.
17. Burford CM, Mason MJ. Early development of the malleus and incus in humans. J Anat. 2016;229(6):857–70.
18. Louryan S, Lejong M, Choa-Duterre M, Vanmuylder N. Hox-A2 protein expression in mouse middle ear ossicles. Morphologie. 2018;102(339):243–9. https://doi.org/10.1016/j.morpho.2018.09.002.
19. Louryan S. Morphogénèse des osselets de l'oreille moyenne chez l'embryon des souris: I. Aspects morphologiques. Arch Biol. 1986;97:317–37.
20. Louryan S. In vitro development of mouse middle ear ossicles: a preliminary report. Eur Arch Biol. 1991;102:55–8.
21. Mark M. Les gènes du développement. In: Saloba E, Hamamah S, Gold F, Benhamed M, editors. Médecine et biologie du développement. Paris: Masson; 2001.
22. Szymanski M. The influence of incudostapedial joint separation on the middle ear transfer function. Clin Exp Otorhinolaryngol. 2014;7(4):250–3.
23. Louryan S, Glineur R, Tainmont S, Van Dam P. Tératogénicité de l'acide 13-cis rétinoïque sur les ébauches mandibulo-otiques de l'embryon de souris: approche histologique et histochimique. Bull Group Int Rech Stomatol Et Odontol. 1990;33:147–53.
24. Mallo M. Formation of the middle ear: recent progress on the developmental and molecular mechanisms. Dev Biol. 2001;231:410–9.
25. Louryan S. Embryologie fondamentale. In: Veillon F, editor. Imagerie de l'os temporal, tome 5: pédiatrie. Paris: Lavoisier; 2014.
26. Jaskoll F. Morphogenesis and teratogenesis of the middle ear in animals. Birth Defects Orig Artic Ser. 1980;XVI(7):9–28.
27. Jaskoll TF, Maderson PFA. A histological study of the development of the avian middle ear and tympanum. Anat Rec. 1978;190:177–99. https://doi.org/10.1002/ar.1091900203.
28. Anson BJ, Caulowell EW. The developmental anatomy of the human stapes. Ann Otol Rhinol Laryngol. 1942;51:891–904.
29. Louryan S, Glineur R, Dourov N. Induced and genetic mouse middle ear ossicles malformations: a model for human malformative ossicular diseases and a tool for clarifying their normal ontogenesis. Surg Radiol Anat. 1992;14:227–32.
30. Davies DG. Malleus fixation. J Laryngol Otol. 1968;82:331–51.
31. Martin JF, Bradley A, Olson EN. The paired-like homeobox gene MHox is required for early events of skeletogenesis in multiple lineages. Genes Dev. 1995;9:1237–49.
32. Smeele LE. Ontogeny of relationship of the human middle ear ant temporomandibular (squamosomandibular) joint. I. Morphology and ontogeny in man. Acta Anat. 1988;131:338–41.
33. Rodriguez-Vazquez JF, Merida-Velasco JR, Merida-Velasco JA, Jimenez-Collado J. Anatomical considerations on the disco-malleolar ligament. J Anat. 1994;192:617–21.
34. Rodriguez-Vazquez JF, Merida-Velasco JR, Jimenez-Collado J. Development of the sphenomandibular ligament. Anat Rec. 1993;233:453–60.
35. Funasaka S. Congenital ossicular anomalies without malformations of the external ear. Arch Otorhinolaryngol. 1979;224:231–40.
36. Tabb HG. Symposium: congenital anomalies of the middle ear. I. Epitympanic fixation of incus and malleus. Laryngoscope. 1976;86(2):243–6.
37. Mansour S, Nicolas K, Sbeity S. Triple ossicular fixation and semicircular canal malformations. J Otolaryngol. 2007;36(3):E31–4.
38. Rodriguez K, Shah RK, Kenna M. Anomalies of the middle and inner ear. Otolaryngol Clin North Am. 2007;40(1):81–96, vi. Review. PubMed PMID: 17346562.
39. Kurosaki Y, Tanaka YO, Itai Y. Malleus bar as a rare cause of congenital malleus fixation: CT demonstration. AJNR Am J Neuroradiol. 1998;19:1229–30.
40. Carfrae MJ, Jahrsdoerfer RA, Kesser BW. Malleus bar: an unusual ossicular abnormality in the setting of congenital aural atresia. Otol Neurotol. 2010;31(3):415–8.
41. Louryan S. Pure second branchial arch syndrome. Ann Otol Rhinol Laryngol. 1993;102:904–5.
42. Nandapalan V, Tos M. Isolated congenital stapes ankylosis: an embryologic survey and literature review. Am J Otol. 2000;21(1):71–80.
43. Herman HK, Kimmelman CP. Congenital anomalies limited to the middle ear. Otolaryngol Head Neck Surg. 1992;106:285–7.

44. Swartz JD, Wolfson RJ, Marlowe FI, Popky GL. Postinflammatory ossicular fixation: CT analysis with surgical correlation. Radiology. 1985;154:697–700.
45. Vaisbuch Y, Hosseini DK, Oghalai JS. Otosclerosis with concomitant anterior malleolar ligament fixation. Otol Neurotol. 2018;39(1):e58–9.
46. Huber A, Koike T, Wada H, Nandapalan V, Fisch U. Fixation of the anterior mallear ligament: diagnosis and consequences for hearing results in stapes surgery. Ann Otol Rhinol Laryngol. 2003;112(4):348–55.
47. Chien W, Northrop C, Levine S, Pilch BZ, Peake WT, Rosowski JJ, et al. Anatomy of the distal incus in humans. J Assoc Res Otolaryngol. 2009;10(4):485–96.
48. Funnell W, Robert J, Heng Siah T, McKee Marc D, et al. On the coupling between the incus and the stapes in the cat. J Assoc Res Otolaryngol. 2005;6:9–18.
49. Watson C. Necrosis of the incus by the chorda tympani nerve. J Laryngol Otol. 1992;106:252–3.
50. Lannigan FJ, O'Higgins P, McPhie P. The vascular supply of the lenticular and long processes of the incus. Clin Otolaryngol Allied Sci. 1993;18:387–9.
51. Alberti PW. The blood supply of the long process of the incus and the head and neck of stapes. J Laryngol Otol. 1965;79:966–70.
52. aWengen DF, Nishihara S, Kurokawa H, Goode RL. Measurements of stapes superstructure. Ann Otol Rhinol Laryngol. 1995;104:311–6.
53. House JW. Otosclerosis. In: Hughes GB, Pensak ML, editors. Clinical otology. 2nd ed. New York: Thieme; 1997. p. 241–9.
54. Bruner H. Attachment of the stapes to the oval window in man. Arch Otolaryngol. 1954;50:18–29.
55. Gan RZ, et al. Mechanical properties of stapedial annular ligament. Med Eng Phys. 2011;33(3):330–9. https://doi.org/10.1016/j.medengphy.2010.10.022. Author manuscript; available in PMC 2012 Apr 1. Published online 2010 Nov 26.
56. Feng B, Gan RZ. Lumped parametric model of the human ear for sound transmission. Biomechanics and Modeling in Mechanobiology. 2004;3(1):33–47.
57. Whyte Orozco JR, Cisneros Gimeno AI, Yus Gotor C, Obón Nogues JA, Pérez Sanz R, Gañet Solé JF, et al. Ontogenic development of the incudostapedial joint. Acta Otorrinolaringol Esp. 2008;59(8):384–9.
58. Gulya AJ, Schuknecht's anatomy of the temporal bone with surgical implications (3rd ed). New York Informa Healthcare, 2007.
59. Mills R, Szymanski M, Abel E. Movements of the intact and reconstructed ossicular chain during changes in static pressure. Acta Otolaryngol. 2004;124(1):26–9.
60. Noden DM. The embryonic origins of the avian cephalic and cervical muscles and associated connective tissues. Am J Anat. 1983;168:257–76.
61. Kurosaki Y, Kuramoto K, Matsumoto K, Itai Y, Hara A, Kusukari J. Congenital ossification of the stapedius tendon: diagnosis with CT. Radiology. 1995;195:711–4.
62. Hough JV. Congenital malformation of the middle ear. Arch Otolaryngol. 1963;78:335–43.
63. Williams PL, Bannister LH, Berry MM, Collins P, Dyson M, Dussek JE, et al., editors. Gray's anatomy. 38th ed. New York: Churchill Livingstone Publishers; 1995. p. 263–84.
64. Wynsberghe DV, Noback CR, Carola R. The senses. In: Wynsberghe DV, Noback CR, Carola R, editors. Human anatomy and physiology. 3rd ed. New York: McGraw-Hill Inc.; 1995. p. 512.
65. Malkin DP. The role of TMJ dysfunction in the etiology of middle ear disease. Int J Orthod. 1987;25:20–1.
66. Bance M, Makki FM, Garland P, Alian WA, Van Wijhe RG, Savage J. Effects of tensor tympani muscle contraction on the middle ear and markers of a contracted muscle. Laryngoscope. 2013;123:1021–7.
67. Kanzara T, et al. Clinical anatomy of the tympanic nerve: a review. World J Otorhinolaryngol. 2014;4(4):17–22.
68. Schuknecht HF. Pathology of the ear. 2nd ed. Philadelphia: Lea and Febiger; 1993. p. 40–1.
69. Goravalingappa R. Cochlear implant electrode insertion: Jacobson's nerve, a useful anatomical landmark. Indian J Otolaryngol Head Neck Surg. 2002;54:70–3.
70. Mavridis IN, Pyrgelis E. Clinical Anatomy of the Lesser Petrosal Nerve. Arch Neurosci. 2016; 3(2):e34168.
71. Todd NW. Jacobson's nerve clues to the round window niche. Cochlear Implants Int. 2009;10:63–9.
72. Glasscock ME, Gulya AJ. Developmental anatomy of the temporal bone and skull base. In: Gulya AJ, editor. Glasscock-Shambaugh surgery of the ear. 5th ed. Hamilton: BC Decker Inc.; 2003. p. 19–25.
73. Moreano EH, Paparella MM, Zeltman D, Goycoolea MV. Prevalence of facial canal dehiscence and of persistent stapedial artery in the human middle ear: a report of 1000 temporal bones. Laryngoscope. 1994;104:309–20.
74. Steffen TN. Vascular anomalies of the middle ear. Laryngoscope. 1968;78:171–97.
75. David GD. Persistent stapedial artery: a temporal bone report. J Laryngol Otol. 1967;81:649–60.
76. Silbergleit R, Quint DJ, Mehta BA, et al. The persistent stapedial artery. Am J Neuroradiol. 2000;21:572. (Case series and review of persistent stapedial artery, with a detailed discussion of embryology and developmental anatomy). [PMID: 10730654].
77. Lasjaunias P, Moret J, Maelfe C. Arterial anomalies of the base of the skull. Neuroradiology. 1997;13:267–72.
78. Moret J. La vascularisation de l'appareil auditif. J Neuroradiol. 1982;9:209–60.

79. Hammar JA. Studien ueber die Entwicklung des Vorderdarms und einiger angrenzender Organe. Arch Mikroskop Anat. 1902;59:471–628.
80. Proctor B. The development of the middle ear spaces and their surgical significance. J Laryngol Otol. 1964;78:631–48.
81. Tos M. Manual of middle ear surgery and reconstructive procedures, vol. 2. New York: Thieme Publishers; 1995.
82. Palva T, Ramsay H, Böhling T. Prussak's space revisited. Am J Otol. 1996;17(4):512–20.
83. Palva T, Ramsay H. Aeration of Prussak's space is independent of the supradiaphragmatic epitympanic compartments. Otol Neurotol. 2007;28(2):264–8.
84. Von Tröltsch A. Lehrbuch der Ohrenheilkunde mit Einschluss der anatomie des Ohres. 7th ed. Leipzig: FCW Vogel; 1881.
85. Marchioni D. Lateral endoscopic approach to epitympanic diaphragm and Prussak's space: a dissection study. Surg Radiol Anat. 2010;32(9):843–52.
86. Helmholtz H. Eine kürzlich in der Zeitschrift ftir rationelle Medicin. In: Archiv für die gesamte Physiologie des Menschen und der Tiere 1868. Vol. 1, Issue 1. Heidelberg: Springer; 1868. p. 1–60.
87. Prussak A. Zur Anatomie des menschlichen Trommelfells. Arch Ohrenheilkd. 1867;3:255–78.
88. Palva T, Johnsson LG. Epitympanic compartment surgical considerations: reevaluation. Am J Otol. 1995;16(4):505–13.
89. Onal K, Haastert RM, Grote JJ. Structural variations of supratubal recess: the anterior epitympanic space. Am J Otol. 1997;18:317–21.
90. Palva T, Ramsay H, Bohlurg J. Lateral and anterior view to tensor fold and supratubal recess. Am J Otol. 1998;19:405–14.
91. Chatellier HP, Lemoine J. Le diaphragme interattico-tympanique du nouveau-né. Description de sa morphologie; considérations sur son rôle pathogénique dans les oto-mastoïdites cloisonnées du nourrisson. Ann Otolaryngol Chir Cervicofac (Paris). 1946;13:534–66.
92. Palva T, Ramsay H. Incudal folds and epitympanic aeration. Am J Otol. 1996;17:700–8.
93. Palva T, Ramsay H, Böhling T. Tensor fold and anterior epitympanum. Am J Otol. 1997;18:307–16.
94. Chateliere HP, Lemoine J. Le diaphragme interattico- tympanique du nouveau-né´. Ann Otolaryngol Chir Cervicofac. 1946;13:534–66.

4 Middle Ear Compartments

Contents

S. Mansour et al., *Comprehensive and Clinical Anatomy of the Middle Ear*,
https://doi.org/10.1007/978-3-030-15363-2_4

The middle ear cavity is anatomically and functionally not only a sole chamber, but a complex of interconnected compartments. The objective of this chapter is to present a detailed and exhaustive description of these compartments, their frontiers, their relationship, and their communication pathways in order to better understand the pathogenesis of inflammatory middle ear diseases and cholesteatoma.

The middle ear cavity used to be divided into five compartments: the mesotympanum in the center, the epitympanum superiorly, the protympanum anteriorly, the hypotympanum inferiorly, and the retrotympanum posteriorly (Fig. 4.1).

However, based on the descriptive anatomy of the middle ear folds (see Chap. 3), this chapter will illustrate several anatomo-functional units inside the middle ear beyond the traditional division of its compartments, due to the implications of the tympanic diaphragm. A new comprehensive knowledge of such a functional anatomy remains the key of success of any middle ear reconstructive surgery.

4.1 Embryology of Middle Ear Compartments

The tympanomastoid system appears in the third week of life from an outpouching of the first pharyngeal pouch called the tubotympanic recess. The endodermal tissue of the dorsal end of this pouch becomes the Eustachian tube and the tympanic cavity [1].

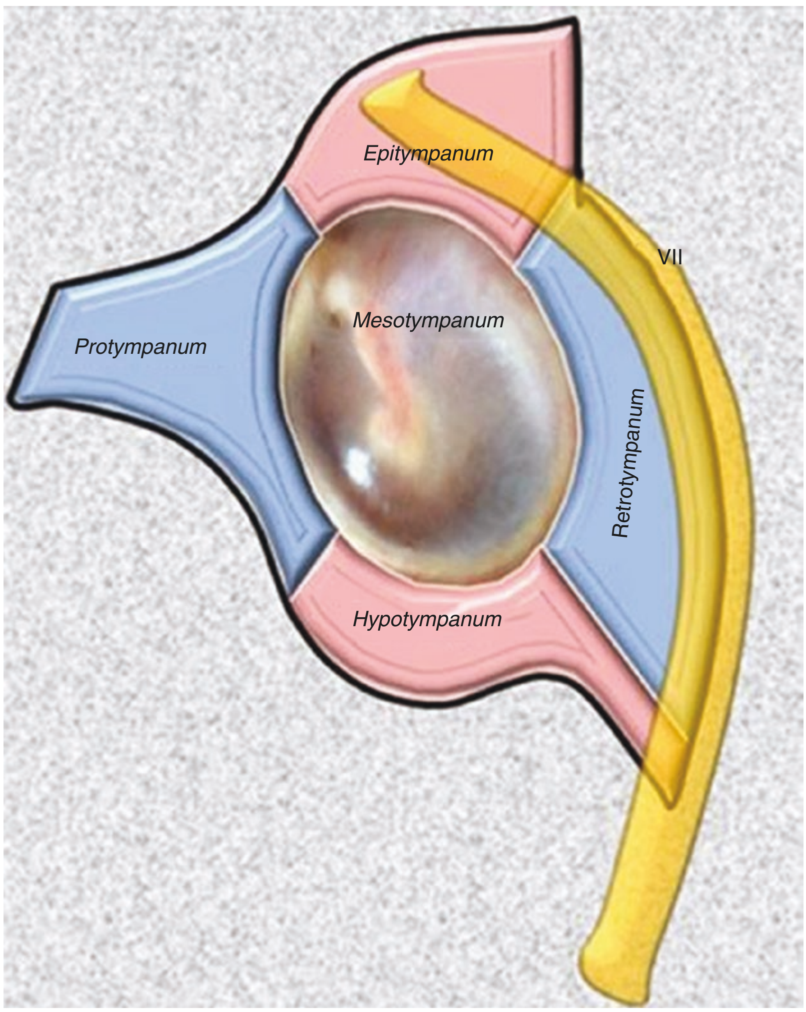

Fig. 4.1 Middle ear compartments; *VII* facial nerve

By the seventh week, a concomitant growth of the second pharyngeal arch constricts the mid-portion of the tubotympanic recess, placing the primary tympanic cavity lateral to this constriction and the primordial Eustachian tube medial to this constriction [1]. The future development of the Eustachian tube is marked by a lengthening, a narrowing, and a mesodermal chondrification to establish the fibrocartilaginous Eustachian tube (see Sect. 7.1).

The terminal end of the tubotympanic recess buds into four sacci: the saccus anticus, the saccus medius, the saccus superior, and the saccus posticus [1–3]. These sacci expand progressively to replace middle ear and mastoid mesenchyme (Fig. 4.2). As described in the previous chapter, the walls of the expanding sacci envelop the ossicular chain and line the walls of middle ear cavity; the interface between two sacci gives rise to several mesentery-like mucosal folds, transmitting blood vessels and ligaments to middle ear contents.

4.1.1 The Saccus Anticus

The saccus anticus is the smallest saccus. It extends upward anterior to the tensor tympani tendon to form the anterior epitympanic recess and the anterior pouch of von Tröltsch. At the level of the tensor tympani muscle canal, it fuses with the anterior saccule of the saccus medius to form the important mucosal fold, the *tensor tympani fold*. The tensor tympani fold separates the anterior epitympanic recess superiorly from the supratubal recess inferiorly [2] (Figs. 4.2 and 4.3).

4.1.2 The Saccus Medius

The saccus medius forms the attic. It extends upward and divides into three saccules:

1. Anterior saccule: It develops upward to form the anterior compartment of the *attic*.

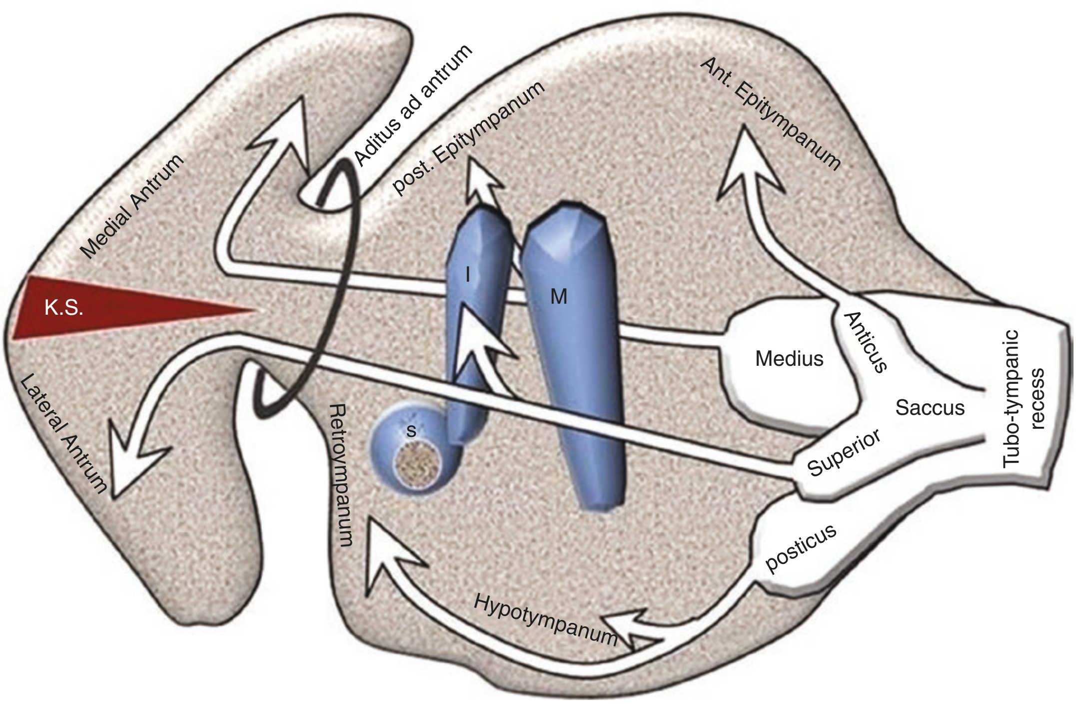

Fig. 4.2 Embryology of middle ear spaces. *I* incus, *M* malleus, *S* stapes, *KS* Korner's septum

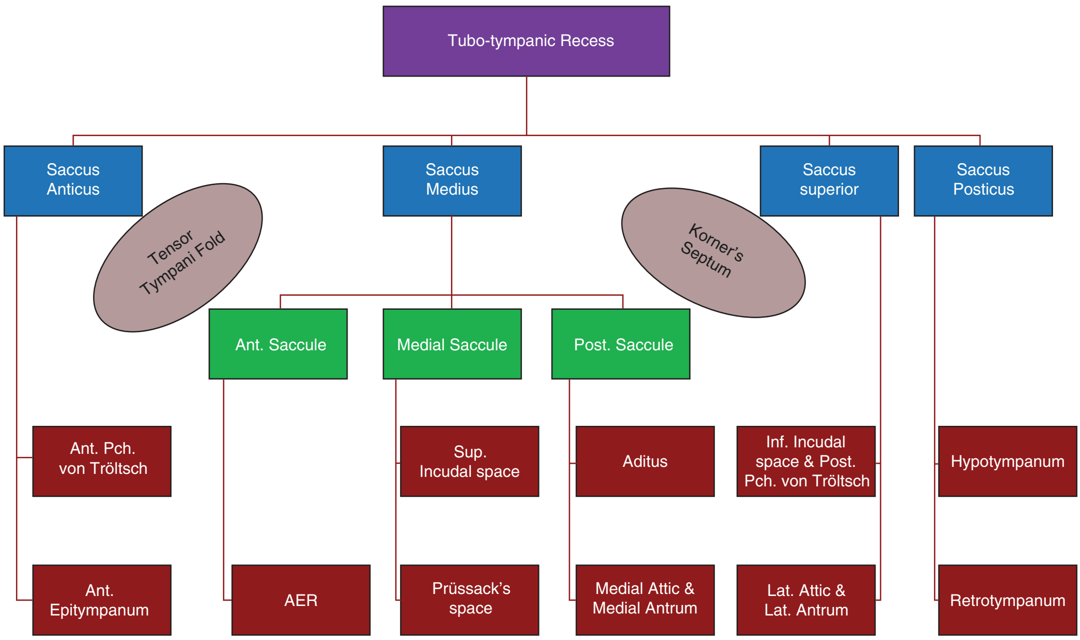

Fig. 4.3 Origin of the different spaces, recesses, and pouches of the middle ear

2. Medial saccule: It forms the *superior incudal space* by its growth over the incudomalleal bodies and the posterior incudal ligament. The medial saccule sends an offshoot forward to form *Prussak's space*.
3. Posterior saccule: It extends posteriorly between the long process of the incus and the stapes to form the *medial portion of the mastoid antrum* which is derived from the petrous part of the temporal bone [2] (Figs. 4.2 and 4.3).

4.1.3 The Saccus Superior

The saccus superior extends posteriorly and laterally between the handle of the malleus and the long process of the incus to form the *posterior pouch of von Tröltsch*, the *inferior incudal space*, and the *lateral part of the antrum* which derives from the squamous part of the temporal bone.

The plane of fusion between the posterior saccule of the saccus medius (which forms the medial part of mastoid air cell system) and the saccus superior (which forms the lateral part of mastoid air cell system) usually breaks down. If the breakdown fails, a bony septum persists between the two parts, called *Koerner's septum* [2] (Figs. 4.2 and 4.3).

4.1.4 The Saccus Posticus

The saccus posticus extends along the *hypotympanum* and rises up posteriorly to form *the round window niche*, *the oval window niche*, *the facial recess*, and *the sinus tympani*. The sinus tympani has a variable size and depth posteriorly; this variation is dependent on the degree of extension of the saccus posticus under the stapedial tendon during fetal development [2] (Figs. 4.2 and 4.3).

4.2 The Protympanum

4.2.1 Development of the Protympanum

True ossification of the protympanum walls starts only at the 18th fetal week since it depends of the bone growth of the otic capsule.

Fig. 4.4 *A schematic drawing illustarting the development of the protympanum from several processes of the petrous bone: 1* tegmental plate, *2* superior lamella, *3* inferior lamella, *M* tensor tympani muscle, *TR* tubotympanic recess

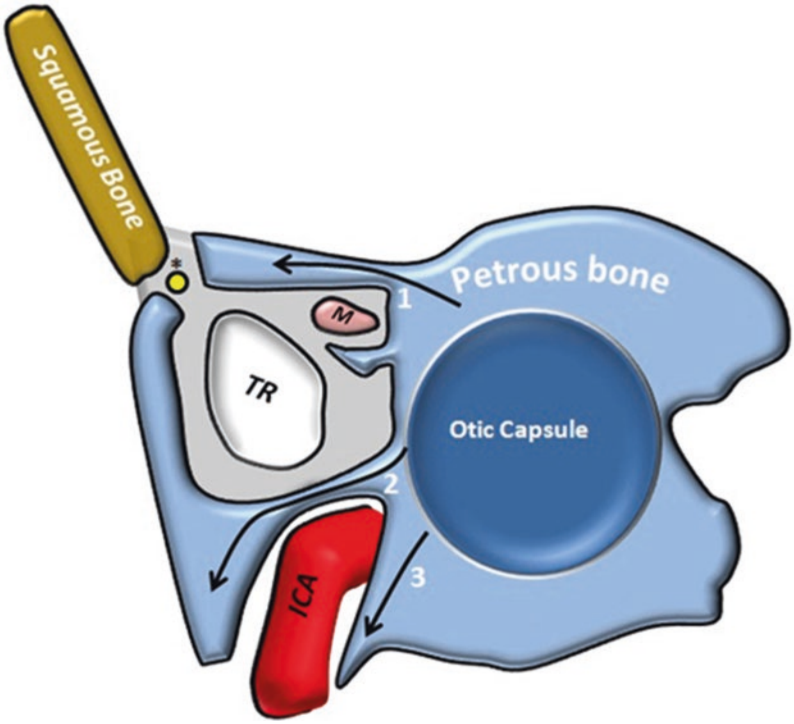

Starting the 21st fetal week, the walls of the protympanum are built up by several processes of the petrous bone (Fig. 4.4):

1. The tegmental plate forming the roof of the protympanum
2. The superior lamina forming the lateral side of the carotid canal
3. The inferior lamina of carotid canal forming the inferomedial wall

The medial wall of the protympanum is created by the promontory itself.

Similarly, from the 23rd fetal week on, the canal of the tensor tympani muscle forms from the superior and inferior laminae. In addition, the tegmen tympani and promontory help to complete the formation of the superior and medial walls of the protympanum, respectively.

4.2.2 Anatomy of the Protympanum

The protympanum is the middle ear compartment that lies anterior to a frontal plane drawn through the anterior margin of the tympanic annulus (Fig. 4.1). This space is widely open posteriorly into the mesotympanum and leads anteriorly into the Eustachian tube. We include into the protympanum the whole bony portion of the Eustachian tube which is 1 cm long in adults.

The protympanum starts superior to a bony ridge called *protiniculum*, extending from the promontory on the medial wall to the lateral wall. The protiniculum extends from the funiculus posteriorly to the Eustachian tube orifice anteriorly. The protiniculum marks the end of the most anterior hypotympanic air cells (Fig. 4.5).

4.2.2.1 Walls of the Protympanum

The protympanum is situated between its lateral bony wall, the *lateral lamina*, a thin plate of the tympanic bone (which separates the protympanum from the mandibular fossa), and its medial wall, with the cochlea posteriorly and the carotid canal anteriorly. Its roof is composed of the bony semicanal for the tensor tympani muscle and the tensor tympani fold. The TTF separates the protympanum from the anterior epitympanic recess (Fig. 4.6).

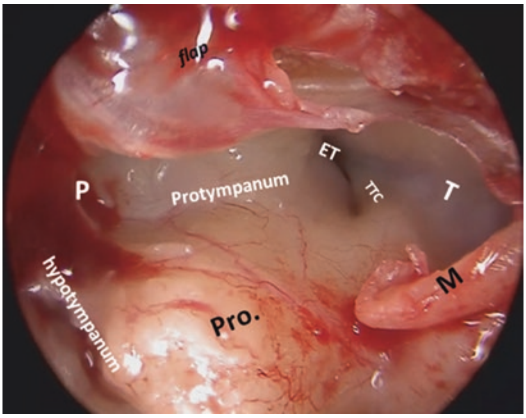

Fig. 4.5 The protympanum starts superior to a bony ridge called protiniculum (P), extending from the promontory (Pro.) on the medial wall to the lateral wall. The protiniculum marks the end of the hypotympanum. *T* tegmen, *TTC* tensor tympani muscle canal, *M* malleus

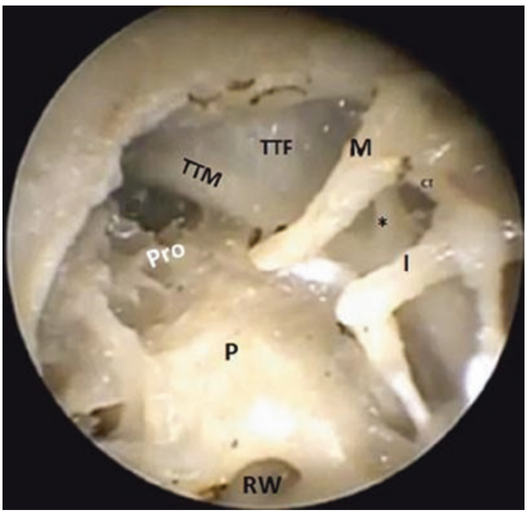

Fig. 4.6 Endoscopic view of a left cadaveric middle ear showing the protympanum (Pro) which is limited superiorly by the canal of the tensor tympani muscle (TTM) and the tensor tympani fold (TTF). (*) cochleariform process, *M* malleus, *I* incus, *P* promontory, *RW* round window, *CT* chorda tympani

Surgical Boundaries of the Protympanum

- **Superior**: the tegmen tympani and entire tensor tympani canal, merging posteriorly and including the supratubal recess delimited here by the tensor fold.
- **Inferior**: from the protiniculum (an oblique bony ridge demarcating the transition between protympanum and hypotympanum).
- **Anterior**: confluent with the junctional and cartilaginous portion of the ET.
- **Posterior**: confluent with the mesotympanum.
- **Medial**: the cochlea posteriorly and the lateral wall of the carotid canal anteriorly, extending from the caroticocochlear recess, with caroticotympanic vessels and nerves including anterior branches from Jacobson's nerve (IX).
- **Lateral**: *called the lateral lamina* separating this space from the mandibular fossa and extending to the anterior annulus, from the level of the protiniculum inferiorly to the anterior limit of the notch of Rivinus at the anterior tympanic spine. It is more commonly convex toward the lumen, but may also be concave. A convex conformation appears to result in a narrower lumen and may obstruct the view of the anterior boundary.

  In conditions when the tensor tympani bony canal is prominent and raised superiorly, an area of pneumatization is developed in the protympanum, mostly recognized with endoscopy, inferomedial to the tensor tympani canal, and it is called the *subtensor recess (SbTR)* (Fig. 4.7).

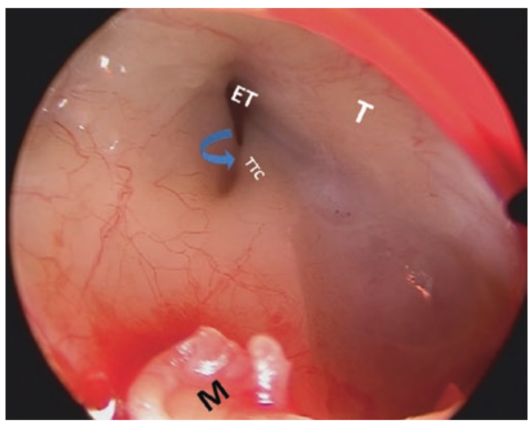

Fig. 4.7 Endoscopic picture of a left ear showing the subtensor recess (blue arrow). *T* tegmen, *TTC* tensor tympani muscle canal, *M* malleus

Anatomic Variants: Carotid Canal Dehiscence
Carotid canal dehiscence on the medial wall of the protympanum has been identified in up to 7.7% of temporal bones and was more common in patients younger than 2 years and older

than 40 years [4]. *The dehiscence generally arises from a failure of the laminae to fuse congenitally. The mean thickness of the thinnest bone overlying the carotid artery was 1.5 mm (range 0–3 mm), and bulging of the carotid artery into the protympanum was barely mentioned in 31%, moderately noticeable in 56%, and markedly noticeable in only 13%* [5] (See also Sect. 3.5.1.).

4.2.2.2 The Supratubal Recess (STR)

The supratubal recess is the superior extension of the protympanum. It corresponds to the space lying between the superior border of the tympanic orifice of the Eustachian tube and the tensor tympani fold. It lies below the anterior attic from which it is separated by the tensor tympani fold (TTF).

The size of the supratubal recess depends on the anatomy of the TTF (see Sect. 3.6.2.10). The TTF forms the roof of the protympanum and has variable orientations depending on the level of its anterior insertion. For instance, a more horizontal TTF results in a small or even absent supratubal recess, and a more vertical TTF gives place to a large supratubal recess [6–8] (see Fig. 3.68).

4.3 The Hypotympanum

The hypotympanum is a crescent-shaped space located at the bottom of the middle ear. It extends from the funiculus posteriorly to the protiniculum inferiorly and the Eustachian tube orifice anteriorly.

The craniocaudal dimension of the hypotympanum is variable from 1 to 6 mm, the anteroposterior distance is 10 mm, and the mediolateral diameter is 4 mm.

4.3.1 Walls of the Hypotympanum

- **The anterior wall** is formed by the carotid canal medially.
- **The posterior wall** is formed by the funiculus and the inferior part of the styloid complex. The funiculus separates the subtympanic sinus from the hypotympanum. Frequently, the posterior wall of the hypotympanum is pneumatized by air cells (retrofacial air cells) which extend from the mastoid antrum to the hypotympanum medial to the facial nerve. The posterior wall of the hypotympanum corresponds to a vertical plane from the posterior semicircular canal to the junction of the sigmoid sinus with the jugular bulb.
- **The lateral wall** is formed by the tympanic bone.
- **The medial wall** is formed by the lower part of the promontory and a part of the petrous bone which extends under the promontory. This wall is usually pneumatized; its air cell system may extend beneath the cochlea to reach the petrous apex air cells (Fig. 4.8).
- **The inferior wall** or the floor is dome shaped and corresponds to a thin bony plate separating the hypotympanum from the jugular bulb (Fig. 4.8). In cases of a high jugular bulb, the hypotympanum is significantly reduced in size.

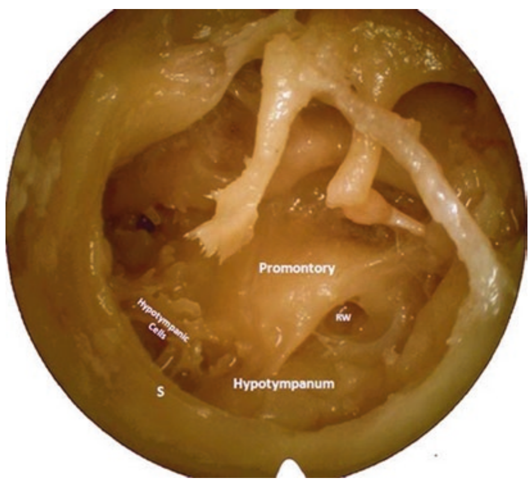

Fig. 4.8 Endoscopic view of a left ear showing the hypotympanum and some hypotympanic cells. Notice that the hypotympanum lies below the level of the tympanic sulcus (S). In this case, the inferior wall of the hypotympanum is smooth and consists of a thin plate of bone separating the middle ear from the jugular bulb. *RW* round window

Normally, the hypotympanum is occupied by trabeculae of variable heights usually about 7–9 mm, and the anterior long ones are called *trabeculae longae*, whereas the posterior long ones are called *trabeculae profundae*. When the trabeculae are absent, the jugular wall raises up to the cochlear capsule. After opening the hypotympanum, surgery is safe when the trabeculae are present, because the jugular dome is 6 mm deeper and the sigmoid sinus is posterior.

Anatomical Variants
In 16% of cases, the bony jugular wall is dehiscent; the surgeon should be very careful during cholesteatoma surgery while elevating the matrix or removing the disease. A high jugular bulb may be associated with an anteriorly placed sigmoid sinus, in such case translabyrinthine and intact Fallopian bridge techniques are challenging (Fig. 4.9).

4.3.2 Air Cells in the Hypotympanum

The air cells of the hypotympanum are divided into the following.

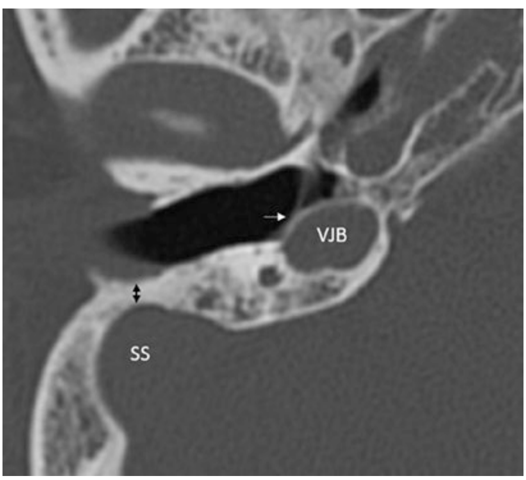

Fig. 4.9 Axial CT image passing by a very prominent jugular bulb (VJB) that is in contact with the tympanic membrane (white arrow), associated with an anteriorly advanced sigmoid sinus (SS), leading to a significant decrease of the thickness of the retro metal tympanic bone (double headed arrow)

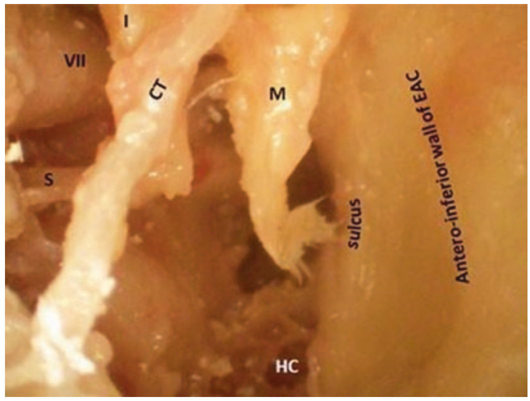

Fig. 4.10 Endoscopic view of a right ear showing hypotympanic cells in the inferior and medial wall of the hypotympanum. *M* malleus, *I* incus, *S* stapes, *CT* chorda tympani, *VII* tympanic segment of the facial nerve

4.3.2.1 Hypotympanic Air Cells

The hypotympanic air cells, present in the medial and inferior wall of the hypotympanum, may extend below the labyrinth to reach the petrous apex cells (infralabyrinthine tract) (Fig. 4.10 and see Fig. 2.21b).

Surgical Applications: **Infracochlear Approach**
Through a transcanal hypotympanotomy, removal of the bone and the cells of the medial wall of the hypotympanum, between the carotid artery anteriorly and the jugular bulb posteriorly, offers a direct surgical approach for the drainage of the petrous apex [9–11].

4.3.2.2 Retrofacial Cells

The retrofacial cells extend from the mastoid tract posterior and medial to the facial nerve and drain into the hypotympanic cells.

By dissecting these cells, one is able to identify the facial nerve, the endolymphatic sac, and the lateral portion of the jugular bulb. Once the Fallopian canal is identified, removal of the *retrofacial air cells* between the facial nerve and the jugular bulb determines the feasibility of a retrofacial approach toward the sinus tympani or the petrous apex aiming the eradication of otherwise hidden disease.

The boundaries of the retrofacial approach include the facial nerve and stapedius muscle laterally, the lateral semicircular canal superiorly, the posterior semicircular canal posteromedially, the vestibule anteromedially, and the jugular bulb inferiorly. When the sinus tympani is well developed, saucerization within these boundaries gives wide access into the sinus tympani and round window niche [12].

> *Surgical Application:* **Retrofacial Hypotympanotomy**
> Dissecting the retrofacial cells medial to the vertical segment of the facial nerve between the jugular bulb inferiorly and the posterior semicircular canal superiorly provides a good access to the hypotympanum and the related structures without transposing the facial nerve or taking down the posterior external auditory canal wall (retrofacial hypotympanotomy) [13]. A high-riding jugular bulb obstructs this approach (see Fig. 2.20).

4.4 The Retrotympanum

The retrotympanum is the most complex compartment of the middle ear. It includes several separate spaces lying in the posterior aspect of the tympanic cavity, medial and posterior to the tympanic annulus (Fig. 4.1). The retrotympanum is the site of the highest incidence of middle ear pathologies especially retraction pockets and cholesteatoma (Fig. 4.11).

From an anatomical point of view, the retrotympanum consists of lateral and medial spaces relative to the facial nerve and pyramidal eminence:

- Two lateral spaces lying lateral to the VII and the pyramidal eminence
- Two medial spaces lying medial to the vertical segment of the VII and the pyramidal eminence

These spaces are separated from each other by the posterior wall *bridges* and *eminences* of the middle ear cavity. The pyramidal eminence is the fulcrum of the retrotympanum (Fig. 4.12) (see Sect. 2.4.2).

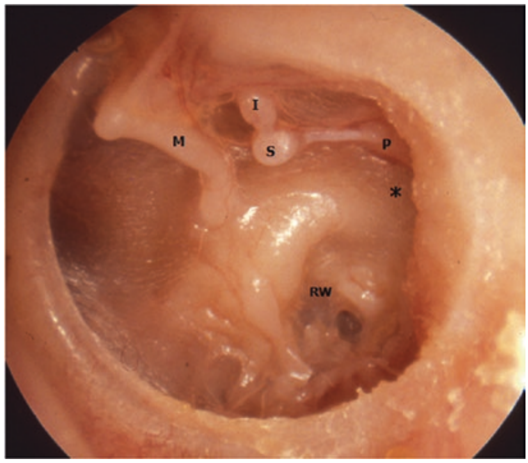

Fig. 4.11 Otoscopic view of a left ear showing adhesive otitis media and a posterior pars tensa retraction pocket into the retrotympanum (*). *I* incus with lysis of its long process, *M* malleus, *S* stapes, *P* pyramidal eminence, *RW* round window

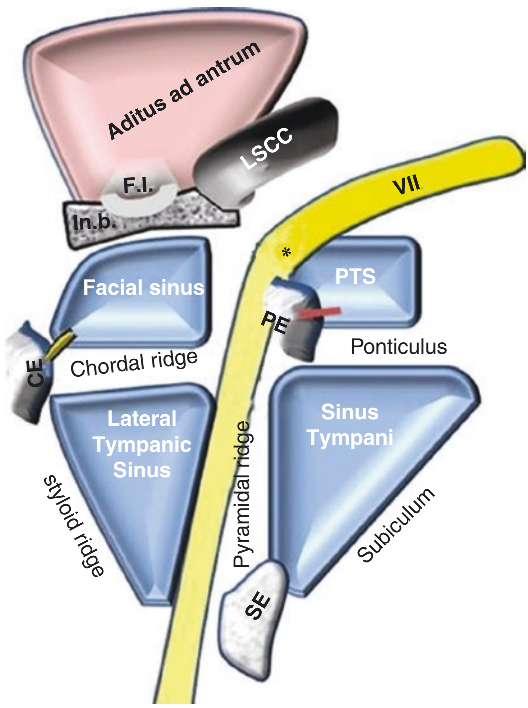

Fig. 4.12 Schematic drawing of the retrotympanum as viewed from the mesotympanum. *PE* pyramidal eminence, *CE* chordal eminence, *SE* styloid eminence, *VII* tympanic segment of facial nerve, * second genu of facial nerve, *FI* fossa incudis, *In.b.* incudal buttress, *PTS* posterior tympanic sinus, *LSCC* lateral semicircular canal

4.4.1 Lateral Spaces

The lateral spaces of the retrotympanum form the facial recess. The facial recess is bordered medially by the facial nerve canal and the pyramidal eminence and laterally by the chorda tympani.

- Superiorly, the facial recess is bounded by the *incudal buttress*, bony boundary of the incudal fossa, which lodges the short process of the incus. The incudal buttress separates the facial recess from the aditus ad antrum.
- Inferiorly, the facial recess is limited by the chordo-facial angle which varies from 18 to 30°.

The distance between the origin of the chorda tympani and the short process of the incus ranges from 5 to 10 mm [14].

The size of the facial recess is variable among individuals; however, it does not differ between age groups ranging from newborns to adults, indicating that it is near adult size at birth [15–17]. It measures about 2 mm latero-medial at the level of the round window and 3 mm at the level of the oval window [18, 19].

The chordal ridge, which runs between the pyramidal eminence and the chordal eminence, divides the facial recess into the *facial sinus* superiorly and the *lateral tympanic sinus* inferiorly.

4.4.1.1 Facial Sinus

The facial sinus is the superior part of the facial recess. It is a small pouch that is situated between the incudal buttress superiorly, the chordal ridge inferiorly, and the second genu of the facial nerve medially. There is no connection of the facial sinus with the air cells of the aditus, the attic or mastoid process.

4.4.1.2 Lateral Tympanic Sinus

The lateral tympanic sinus is the inferior part of the facial recess and is the most lateral and narrowest sinus of the retrotympanum. It occupies the space between the three eminences: pyramidal eminence, styloid eminence, and chordal eminence. It lies medial to the chordal eminence, inferior and lateral to the pyramidal eminence, and superior to the styloid eminence. The craniocaudal dimensions of the lateral tympanic sinus vary from 1.5 to 2.5 mm [20, 21]; it does not have connection with the attic or the antrum.

Surgical Application: Transmastoid Posterior Tympanotomy or Facial Recess Approach
The facial recess serves as a posterior window to reach the middle ear from the mastoid cavity, enabling the visualization of the oval window and ponticulus superiorly and the round window and subiculum inferiorly. This important surgical approach is called transmastoid posterior tympanotomy; it is done by a transmastoid drilling of the posterior wall of the facial recess, between the chorda tympani laterally and the facial nerve medially (Fig. 4.13).

In cases of a narrow facial recess or incomplete exposure of the targeted middle ear structure, an extended facial recess approach could be done. In this technique, the chorda tympani nerve is sacrificed, and the space between tympanic annulus and the VII nerve is drilled out.

4.4.2 Medial Spaces

The medial spaces of the retrotympanum are divided in two areas: the superior retrotympanum and the inferior retrotympanum.

4.4.2.1 The Superior Retrotympanum

Also called the *tympanic sinus*, it includes the depressions in the posterior wall of the middle ear that lies between the facial nerve and pyramidal eminence laterally and the labyrinth medially (Figs. 4.12, 4.14, and 4.15). The ponticulus, which runs from the promontory to the pyramidal eminence, divides the tympanic sinus in two spaces: the *posterior tympanic sinus* superiorly and the *sinus tympani* inferiorly.

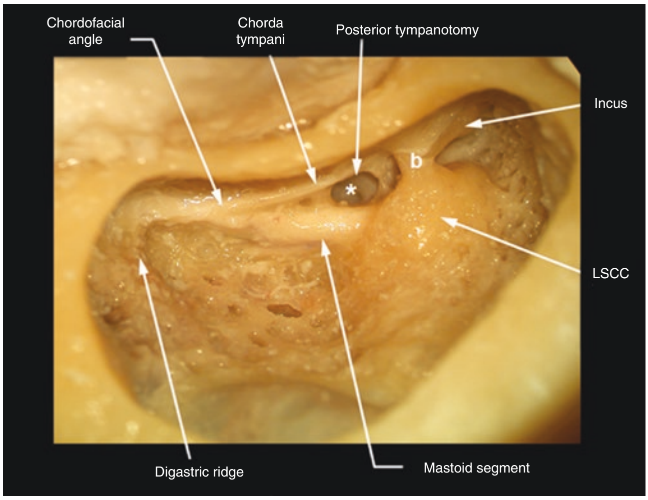

Fig. 4.13 Left ear, transmastoid posterior tympanotomy (*). *b* incudal buttress, *LSCC* lateral semicircular canal

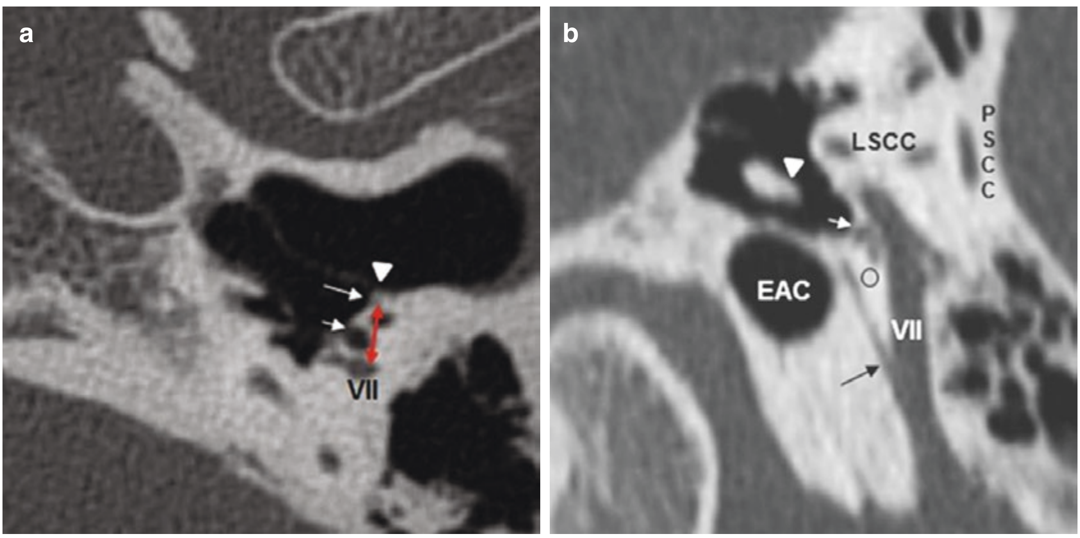

Fig. 4.14 (**a**) A transversal computed tomography showing the distance (red double arrow) between the chorda tympani (long white arrow) and the mastoid segment of the facial nerve (VII); facial recess (short arrow), annulus tympani (arrowhead). (**b**) Sagittal reconstruction of a computed tomography showing the emergence of the chorda (black arrow) from the facial nerve (VII), the chordo-facial angle, and the bony wall (circle) between the chorda and the VII (facial recess approach). Facial recess (white arrow), short process of the incus (arrow head) *LSCC* lateral semicircular canal, *PSCC* posterior semicircular canal, *EAC* external auditory canal

4.4.2.1.1 Posterior Tympanic Sinus

The posterior tympanic sinus is present in most middle ears [22]; it lies superior to the ponticulus and medial to the pyramidal eminence and facial nerve. It is about 1 mm deep and about 1.5 mm long [23]. In ears where the ponticulus does not reach the posterior wall of the middle ear, the posterior tympanic sinus merges with the sinus tympani to form one confluent sinus (in 10% of the population) [23].

Surgical Application
During middle ear surgery, section of the stapedial tendon and drilling of the pyramidal process may be required to reach the posterior tympani sinus.

4.4.2.1.2 The Sinus Tympani

The sinus tympani is the largest sinus of the retrotympanum. It lies medial to the mastoid portion of the facial nerve and lateral to the posterior semicircular canal. It is limited superiorly by the ponticulus and the pyramidal eminence and inferiorly by the subiculum and the styloid eminence.

The sinus tympani has a great variability in size and shape and depth. Its posterior extension varies between 0.2 and 10 mm with an average of 2 mm [24–26] (Fig. 4.16).

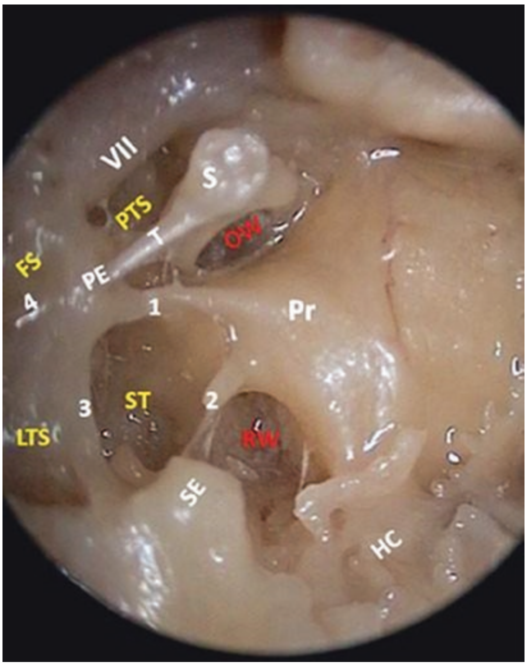

Fig. 4.15 Endoscopic view of a right middle ear showing the different sinuses and recesses of the retrotympanum. *PTS* posterior tympanic sinus, *ST* sinus tympani, *LTS* lateral tympanic sinus, *FS* facial sinus, *PE* pyramidal eminence, *SE* styloid eminence, *1* ponticulus, *2* subiculum, *3* pyramidal ridge, *4* chordal ridge, *OW* oval window, *RW* round window, *S* stapes, *T* stapedial tendon, *Pr* promontory, *HC* hypotympanic cells, *VII* facial nerve

Sinus Tympani Types and Surgical Approaches

Based on its depth, the sinus tympani is classified into three types with an equal frequency in the general population [27, 28] (Fig. 4.16).

- Type A is a shallow sinus tympani; it is small and does not reach the level of the vertical portion of the facial nerve posteriorly. In such cases, surgical transcanal access to the sinus tympani is feasible.
- Type B sinus tympani is of intermediate depth; it lies medial to the vertical portion of the facial nerve but does not extend posteriorly deeper than the level of the facial nerve. A total and clear visualization of such sinus tympani could not be achieved without the use of an endoscope. Any blind dissection in the sinus tympani without endoscopic visualization carries a risk of residual disease or a possible injury to a dehiscent facial nerve or a high jugular bulb [29].
- Type C sinus tympani is very deep; it extends posteriorly more deeply than the vertical portion of the facial nerve. This type is frequently encountered in a well-pneumatized mastoid. Despite the use of an otoendoscope, the pathology of such deep sinus could not be explored entirely from the middle ear; therefore, access should be obtained through a transmastoid retrofacial approach. This approach requires enough distance of more than 2 mm between the facial nerve and the posterior semicircular canal (see example Fig. 2.20); otherwise, these structures could be easily injured. To access the ST posterior from the mastoid, it is necessary to dissect the compact bone at the area located in a triangle formed by the FN, LSCC, and PSCC. The dimensions of this triangle are almost constant. This triangle seems to be isosceles with edges of 5 mm. This allows the surgeon a sufficient area for bony dissection. Nevertheless, the surgical access to the ST mainly depends on the posterior extension of the sinus. The more the sinus extends posterior, the less will the bone be dissected. The distances from the posterior wall of the ST to the LSCC dome, PSCC dome, and FN are, on average, 4.3, 4.8, and 3.4 mm, respectively [30].

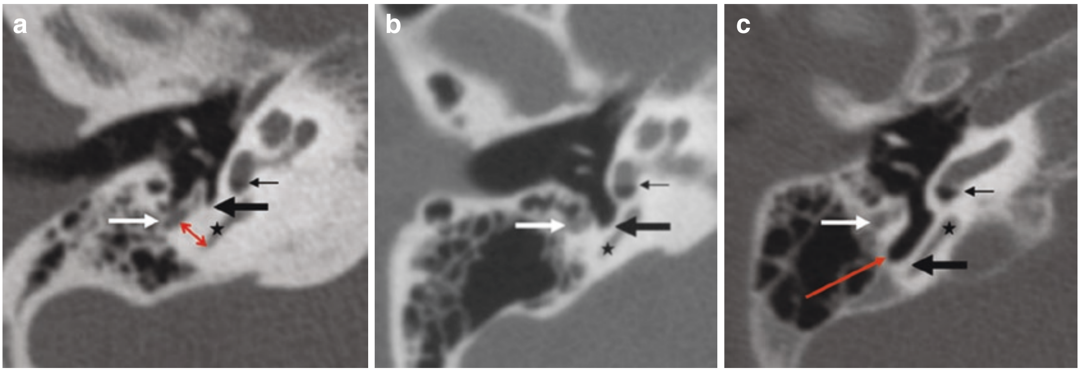

Fig. 4.16 Transversal computed tomographic view of right ears with different depths of the sinus tympani. (**a**) Type A, (**b**) Type B, (**c**) Type C. Deepest point of the sinus tympani (thick black arrow), facial nerve (white arrow), round window membrane (thin black arrow), posterior semicircular canal PSCC (*). The red double arrow in (**a**) represents the distance between the facial nerve and the PSCC. The red arrow in (**c**) represents the retrofacial approach to the sinus tympani

4.4.2.2 The Inferior Retrotympanum

It includes the space situated between the *subiculum* superiorly and the *finiculus* inferiorly.

- The subiculum (from latin, ‘‘support’’) extends from the posterior pillar towards the styloid proeminence, limiting the sinus tympani inferiorly.
- The finiculus (from latin, ‘‘borderline’’) extends from the anterior pillar toward the jugular dome, separating the retrotympanum from the hypotympanum.

The inferior retrotympanum includes the following:

4.4.2.2.1 The Sinus Sub-tympanicus

Defined as an anatomical space between the subiculum superiorly and the finiculus inferiorly, developing medially and posteriorly with respect to the styloid eminence, forming a deep space into the retrotympanum. It lies inferiorly with respect to the subiculum and becomes confluent medially with the round window niche.

The sinus sub-tympanicus lies inferiorly to the sinus tympani, forming a well delineated space (Fig. 4.17) between:

- The subiculum superiorly and posteriorly
- The finiculus inferiorly and anteriorly
- The styloid prominence posteriorly and inferiorly

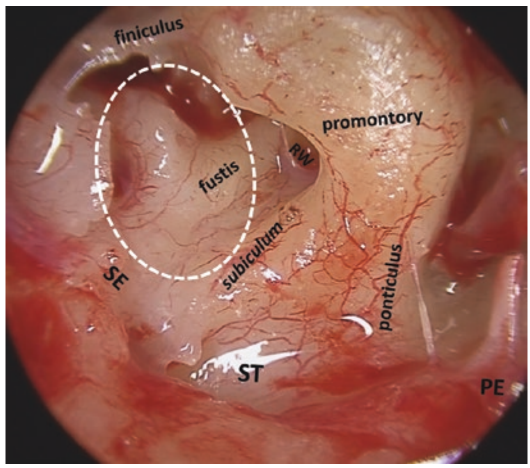

Fig. 4.17 The sinus sub-tympanicus (white circle) lies inferiorly to the sinus tympani (ST), forming a well-delineated space between the subiculum superiorly and posteriorly and the funiculus inferiorly and anteriorly, the styloid eminence (SE) posteriorly and inferiorly. *RW* round window, *PE* pyramidal eminence

4.4.2.2.2 The “Subcochlear Canaliculus” Confound with the “Proctor’s Area Concamerata”

The fustis (from latin, ‘‘club’’) is a smooth bony structure, which forms the floor of the round window chamber and seems to indicate the entrance to the round window niche. The structure links the styloid proeminence with the basal turn of the cochlea (Fig. 4.17). Between the fustis and the finiculus, often a subcochlear canaliculus is seen (Figs. 4.18, 4.19 and 4.20), which is a tunnel that

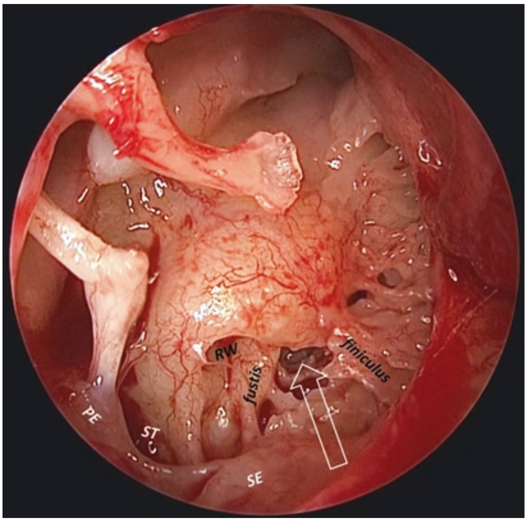

Fig. 4.18 Left middle ear endoscopy showing the subcochlear canaliculus (white arrow) extending below the round window between the finiculus anteriorly and the fustis posteriolry. *SE* styloid eminence, *ST* sinus tympani, *PE* pyramidal eminence

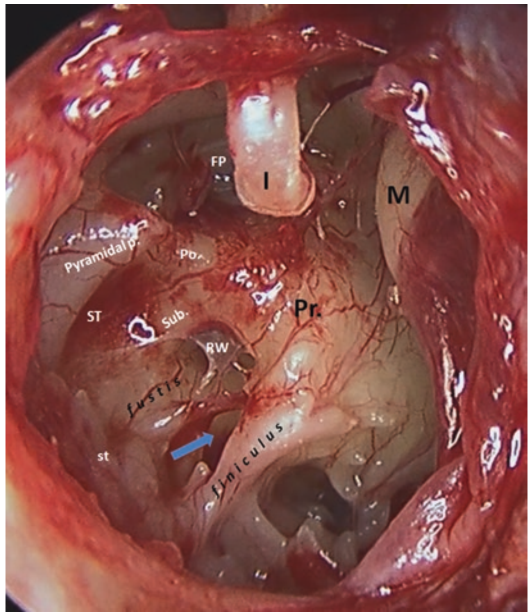

Fig. 4.19 The subcochlear tunnel (blue arrow)

onnects the inferior retrotympanum with the petrous apex via a series of pneumatized cells.

It is very likely that the formation of the subcochlear canaliculus could arise from the nonfusion between the fustis area and the finiculus during fetal development.

The subcochlear tunnel presents a pathway for the extension of cholesteatoma inferior to the otic capsule through this tunnel (Fig. 5.25). *Using microscope, this tunnel is hardly visible but the use of endoscope permits the cholesteatoma surgery to be performed safely following this tunnel. In case of a high jugular bulb in contact with the cochlea, an infracochlear approach to the petrous apex is impossible to achieve. In contrary, a wide infracochlear space permits to drill and perform an infracochlear drainage of the petrous apex. Note that the subcochlear tunnel is in relation to the vertical internal carotid; therefore, the surgeon should be careful while drilling in this delicate site for cholesteatoma removal.*

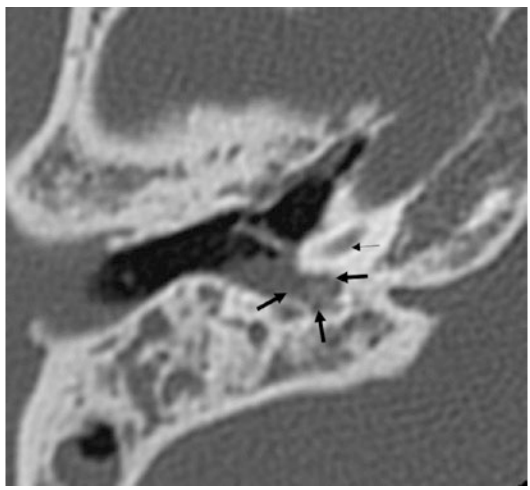

Fig. 4.20 Axial CT image showing the subcochlear canaliculus with some subcochlear air cells completely filled with condensation images (thick arrows). The most inferior part of the basal turn of the cochlea (thin arrow)

4.5 The Epitympanum or the Attic

The attic is the part of the tympanum situated above an imaginary plane passing through the short process of the malleus. The attic occupies approximately one-third of the vertical dimension of the entire tympanic cavity and lodges the head and neck of the malleus, the body, and the short process of the incus (Fig. 4.21).

The attic is bounded by the following walls:

- **The lateral wall** of the attic is formed inferiorly by Shrapnell's membrane and superiorly

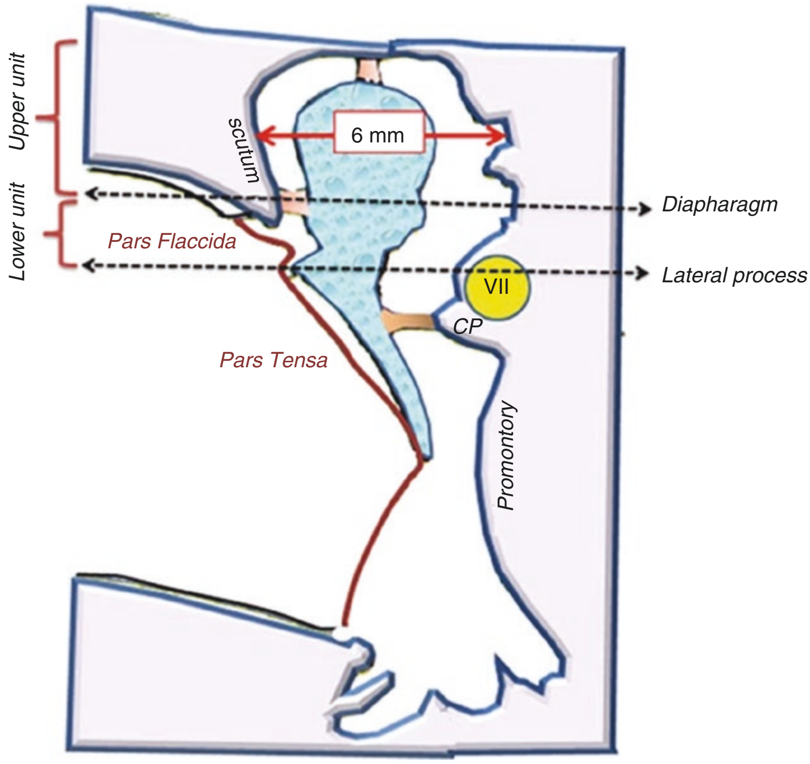

Fig. 4.21 Schema showing the upper unit and the lower unit of the attic. *VII* facial nerve, *CP* cochleariform process

by a bony wall, called the outer attic wall, *le mur de la logette des osselets.*

- **The medial wall** of the attic is situated above the tympanic segment of the facial nerve and tensor tympani muscle. It contains the lateral semicircular canal. This wall may be pneumatized by the supralabyrinthine cell tract (see Sect. 2.7.2 and Fig. 2.53).
- **The posterior wall** is occupied almost entirely by the aditus ad antrum. It is 5–6 mm high and is usually larger superiorly than inferiorly. The aditus provides a communication between the antrum and the rest of the tympanic cavity.
- **Inferiorly**, the tympanic diaphragm divides the attic into an *upper unit* situated above the tympanic diaphragm and a *lower unit* of the attic (*Prussak's space*), situated below the tympanic diaphragm. Medially, the tympanic diaphragm separates the upper unit of the attic from the underlying upper mesotympanum. For ventilation purposes, the upper unit of the attic communicates with the mesotympanum through a window in the diaphragm called the *tympanic isthmus* [31, 32] (Fig. 4.22) (see Sect. 3.6.3).
- **The anterior wall** is delimited by the zygoma.

4.5.1 The Upper Unit of the Attic

The upper unit of the attic lies above the tympanic diaphragm (see Chap. 3, Mucosal Folds).

- Medially, the tympanic diaphragm separates completely the upper unit of the attic from the underlying upper mesotympanum; its aeration is insured by the *tympanic isthmus* (see Fig. 3.55). The tympanic isthmus is situated between the tensor tympani muscle anteriorly and the posterior incudal ligament posteriorly (see Sect. 3.6.4).
- Laterally, the tympanic diaphragm separates the upper unit of the attic from the lower unit of the attic, Prussak's space.
- Posteriorly, the upper unit of the attic communicates with the mastoid cavity through the aditus ad antrum.
- Anteriorly the zygoma.

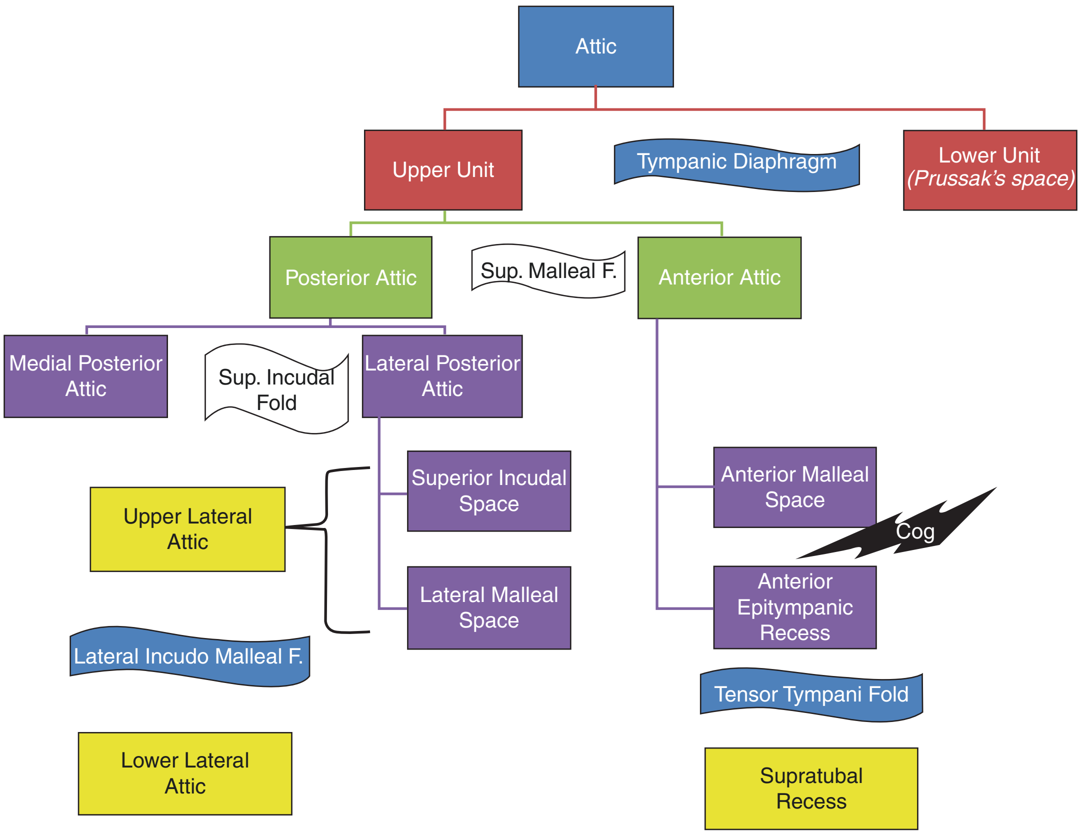

Fig. 4.22 Organization of the different compartments of the attic, flags with a clear blue background are representative for the tympanic diaphragm

In addition to this separation by the tympanic diaphragm in the horizontal plane, several folds and ligaments in the perpendicular planes lead to further divisions and spaces of the upper unit of the attic. They include:

- *The superior malleal fold* with a *coronal* orientation divides the upper unit of the attic into two different spaces: a posterior (the larger one), the posterior attic, and an anterior (smaller one), the anterior attic (Figs. 4.22 and 4.23).

4.5.1.1 Posterior Attic or Posterior Epitympanum

The posterior attic, posterior to the superior malleal fold, is largely occupied by the posterior part of the head of the malleus, the body, and short process of the incus. In adult, the distance from the tip of the incus to the attic roof is about 6 mm [33].

- *The superior incudal fold*, oriented in a *sagittal* plane, divides the posterior attic into the medial posterior attic and the lateral posterior attic (Figs. 4.22 and 4.24).

4.5.1.1.1 The Medial Posterior Attic

The medial posterior attic (or *the medial incudal space*) is the larger compartment of the posterior attic; it is bounded by the lateral semicircular canal and the Fallopian canal medially and the ossicles and the superior incudal fold laterally. The distance between the lateral semicircular canal and the incus body is 1.7 mm [31]. The medial posterior attic contains essentially the tympanic isthmus that is divided by the medial incudal fold into an anterior and a posterior tympanic isthmus. These openings represent the main route of aeration of the whole epitympanum (Figs. 4.22 and 4.24).

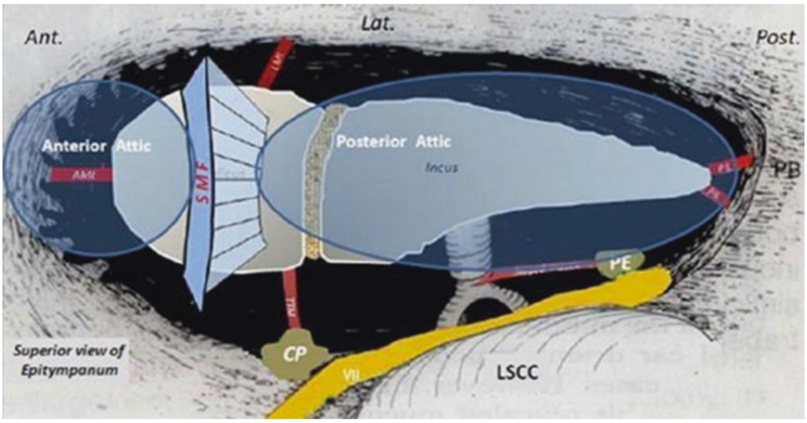

Fig. 4.23 Superior view of a right middle ear, showing the attic divided by the superior malleal fold (SMF) into a smaller anterior attic and a larger posterior attic. *AML* anterior malleal ligament, *LML* lateral malleal ligament, *TTM* tensor tympani muscle tendon, *PB* petrous bone, *PIL* posterior incudal ligament, *PE* pyramidal eminence, *CP* cochleariform process, *VII* facial nerve, *LSCC* lateral semicircular canal

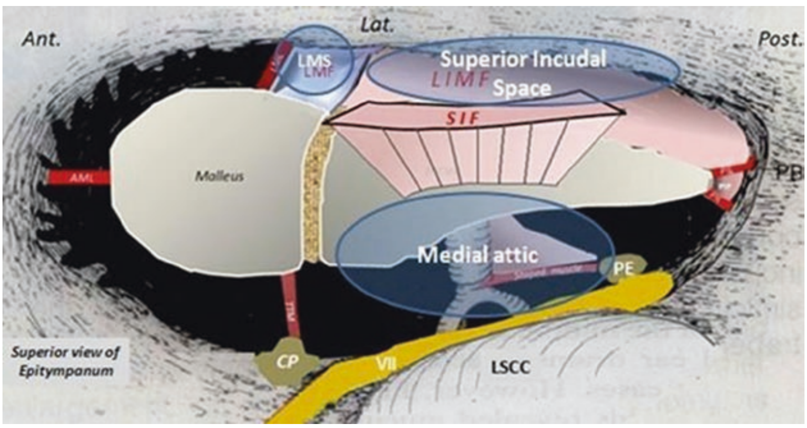

Fig. 4.24 Superior view of the right middle ear, showing the different compartments of the posterior attic. The medial attic lies medial to the superior incudal fold (SIF), the superior incudal space lies above the lateral incudomalleal fold (LIMF) and superior to SIF, and the lateral malleal space (LMS) lies above the lateral malleal fold (LMF). *MIF* medial incudal fold, *AML* anterior malleal ligament, *LML* lateral malleal ligament, *TTM* tensor tympani muscle, *PB* petrous bone, *PIL* posterior incudal ligament, *PE* pyramidal eminence, *CP* cochleariform process, *VII* facial nerve, *LSCC* lateral semicircular canal

4.5.1.1.2 The Lateral Posterior Attic

The lateral posterior attic is narrower, located between the outer attic wall laterally and the malleus head, incus body, and superior incudal fold medially.

The lateral posterior attic is further divided into three spaces (Figs. 4.22 and 4.24):

- The *superior incudal space*
- The *lateral malleal space* forming together the *upper lateral attic*
- The *inferior incudal space*, called the *lower lateral attic*

The Upper Lateral Attic

The upper lateral attic is formed of two spaces, largely opened to each other, but at different levels, posteriorly the superior incudal space, lying above the lateral incudomalleal fold and more anteriorly the lateral malleal space, lying above the lateral malleal fold (Figs. 4.22, 4.24, and 4.25)

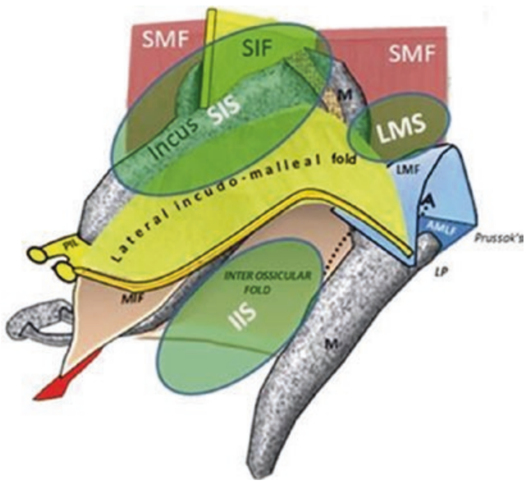

Fig. 4.25 Lateral view of a right middle ear after removal of the tympanic membrane and the outer attic wall, showing the different compartments of the lateral attic: the superior incudal space (SIS) above the lateral incudomalleal fold (LIMF), the inferior incudal space below the LIMF, and the lateral malleal space (LMS) above the lateral malleal fold (LMF) on a more inferior level than the SIS, but usually in open communication with each other. The posterior boundary of the LMS is represented by the descending portion of the LIMF. *SMF* superior malleal fold, *SIF* superior incudal fold, *PIL* posterior incudal ligament, *MIF* medial incudal fold, *M* malleus, *LP* lateral process of malleus, *AMLF* anterior malleal ligament fold

- ***Superior incudal space (SIS)***: The superior incudal space lies in a more superior position in relation to the lateral malleal space. It is limited inferiorly by the incudomalleolar fold which separates it from the inferior incudal space.
- ***Lateral malleal space (LMS)***: The lateral malleal space is a distinct anatomic area, part of the lateral attic; it lies above the lateral malleal fold. It is limited:
  - Medially by the malleus head and neck
  - Laterally by the outer attic wall
  - Anteriorly by the anterior malleal fold
  - Posteriorly by the downward turning end of the incudomalleal fold [34]

The lateral malleal space is regularly opened superiorly; thus, it is in free communication with the superior incudal space (Figs. 4.22, 4.24, and 4.25).

Infrequently, the lateral malleal fold is incomplete, and a direct communication exists between Prussak's space and the lateral malleal space [31, 32, 35–37].

In rare cases, the incudomalleal fold may extend over the entire lateral malleal space; that means that the lateral incudomalleal fold slopes down and joins the posterior malleal fold. In such cases, the lateral malleal space is isolated, separated from the superior incudal space, but it gets in direct communication with the inferior incudal space [34].

The Lower Lateral Attic or the Inferior Incudal Space (IIS)

The inferior incudal space lies below the lateral incudomalleal fold, therefore inferior to the tympanic diaphragm. It is located between the more dependent portion of the short process and the body of the incus medially and the scutum laterally (Figs. 4.22 and 4.25).

A particular region of the mesotympanum guarantees the ventilation of this space. This region of ventilation for the inferior incudal space is limited medially by the medial incudal fold and anteriorly by the interossicular fold which lies between the long process of the incus and the upper 2/3 of the malleus handle [33].

4.5.1.2 Anterior Attic or Anterior Epitympanum

The anterior attic or anterior epitympanum is a separate compartment of varying shape. It is situated anterior to the head of malleus and the superior malleal fold.

The anterior epitympanum is divided into two spaces by the cog [36]: *the anterior malleal space* and *the anterior epitympanic recess* (Figs. 4.22, 4.23, and 4.26). The cog is a bony crest that extends inferiorly from the tegmen toward the cochleariform process and anterosuperior to the malleus head.

- **The Anterior Malleal Space (AMS)**
  The anterior malleal space is of variable size and situated between the head of the malleus posteriorly and the cog anteriorly (Figs. 4.21 and 4.25).

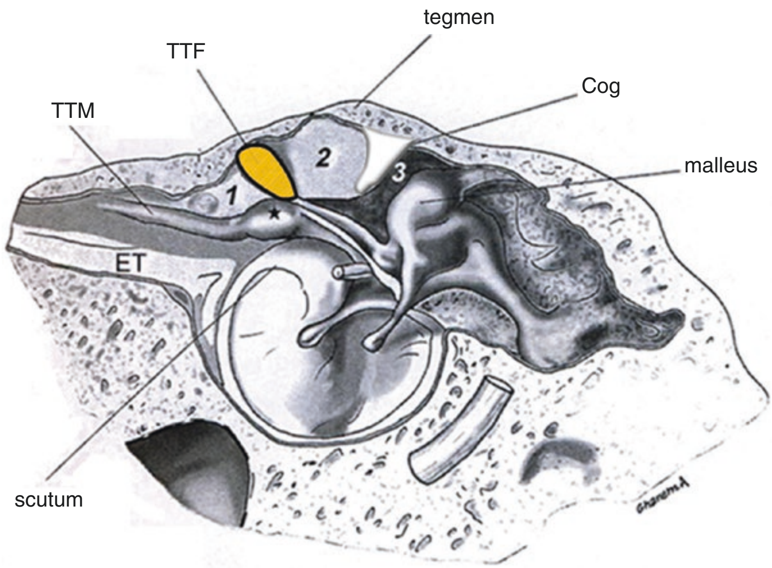

Fig. 4.26 Schema of a medial view of a right middle ear showing the different spaces of the anterior attic: *1* supratubal recess, *TTF* tensor tympani fold, *2* anterior epitympanic recess, *3* anterior malleal space, *TTM* tensor tympani muscle (Reproduced with permission from the Journal of Otolaryngology-Head And Neck Surgery, Decker Publishing Publisher [37])

- **The Anterior Epitympanic Recess (AER)**
  The anterior epitympanic recess has been given different names such as anterior epitympanic sinus, anterior epitympanic space, epitympanic sinus, and even confused with the supratubal recess. However, additional anatomic studies identified the supratubal recess (STR) and the anterior epitympanic recess (AER) as two distinct spaces separated by the tensor tympani fold (TTF) [8, 33, 37]. Therefore, the term anterior epitympanum should be reserved for the whole anatomic entity composed of the anterior malleal space and the AER. The supratubal recess is considered as a part of the protympanum (see Sect. 4.2.2).

The AER presents the following boundaries [37–39]:

- **Superiorly**: the anterior part of the tegmen tympani
- **Anteriorly**: the zygomatic root
- **Posteriorly**: the cog
- **Laterally**: the scutum
- **Medially**: the anterior portion of the tympanic segment of the VII and the geniculate ganglion
- **The floor**: represented by the cochleariform process and the **TTF** (Fig. 4.26)

The AER is situated above the STR. Depending on the inclination of the TTF, the floor of the AER may appear on axial CT images more laterally than the STR, and the TTF may become visible even on axial cuts due to its obliquity (see Fig. 4.29b). It may be easily found on coronal images (Fig 4.30b). Note that the AER is always situated at the same level as the VII nerve and the STR at the same level as the TTM (also see Fig. 4.31).

The tensor tympani fold is an integral part of the tympanic diaphragm (see Sect. 3.6.3). When the TTF is complete, the anterior tympanic recess and the supratubal recess form two separate spaces. When there is a congenital defect in the TTF (in 25–40%), the AER is in direct communication with the supratubal recess serving as an accessory route of aeration to the attic called the anterior route of ventilation and the posterior route being represented by the anterior and posterior tympanic isthmus [35, 36, 38]. The orientation of the tensor fold is the determining structure that dictates the conformation, limits, and size of the anterior epitympanic space (see Fig. 3.66).

The size of the AER is variable between individuals. CT scan permits the size measurement of the recess; its mean size is about 4 × 4 mm. Surgical transmastoid indirect approach to the

AER with conservation of the ossicular chain requires minimum dimensions of 3 × 3 mm [37] (Figs. 4.27, 4.28, and 4.29).

In a study done by the authors, it was found that the AER has considerably smaller size in patients with chronically affected inflammatory ears than in the non-affected ones [37, 40].

In some instances, the AER could be difficult to visualize by the microscope when bony structures are standing in front the lateral wall

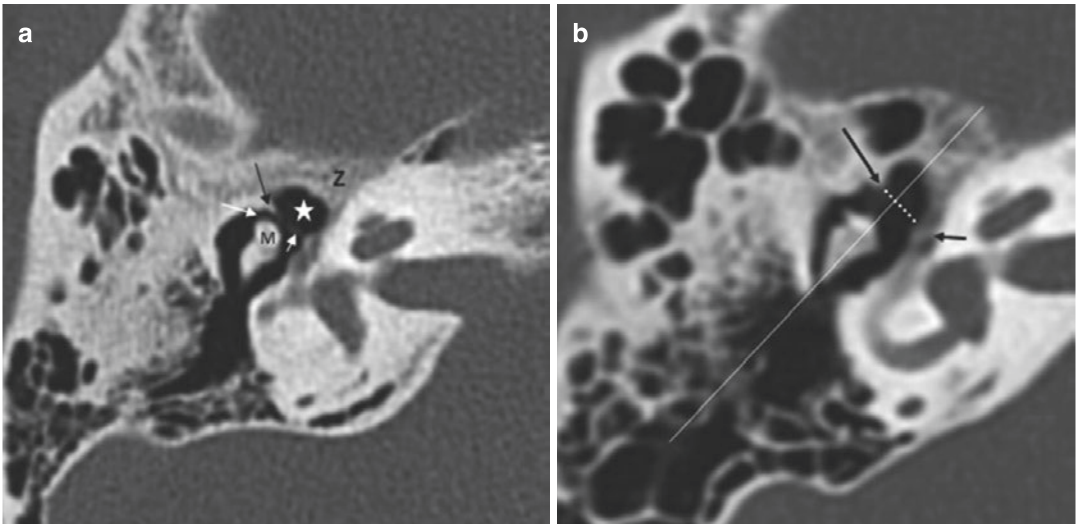

Fig. 4.27 Axial computed tomographic views of the anterior epitympanum. (**a**) The cog with its largest lateral part (black arrow) and its continuity toward the medial attic wall (small white arrow); anterior malleal space (white long arrow); anterior epitympanic recess AER (*); *M* malleus head, *Z* zygoma. (**b**) Mensuration of the relevant transversal diameter of the AER (punctated line), perpendicular to the incudomalleal axis (long white line) between the lateral limit of the cog (long black arrow) and the cochleariform process (short black arrow)

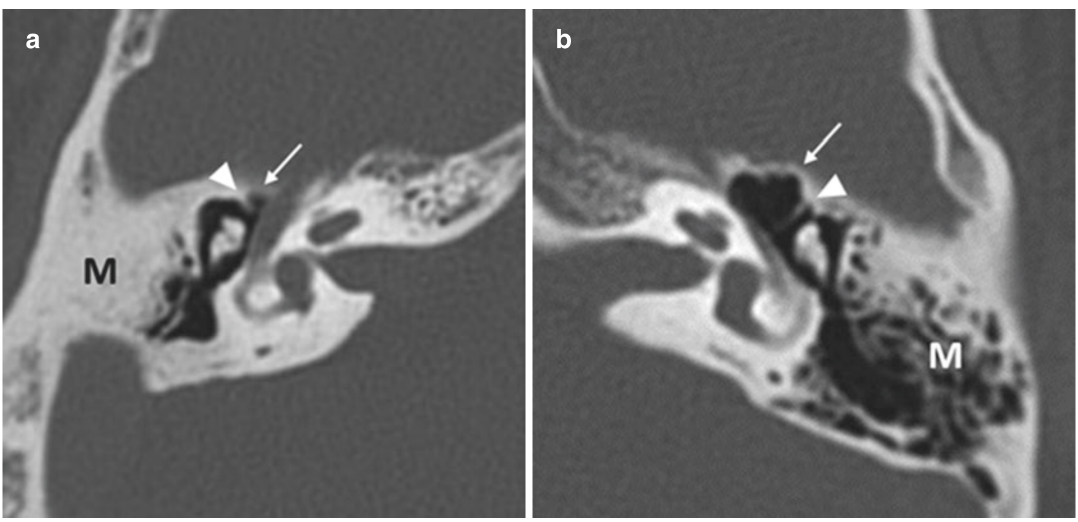

Fig. 4.28 Variable sizes of the AER: (**a**) axial CT image of a right ear, very small AER (arrow), cog (arrowhead); the mastoid (M) is sclerotic. (**b**) Axial CT image of a left ear: large AER (arrow); cog (arrowhead), well-pneumatized mastoid (M)

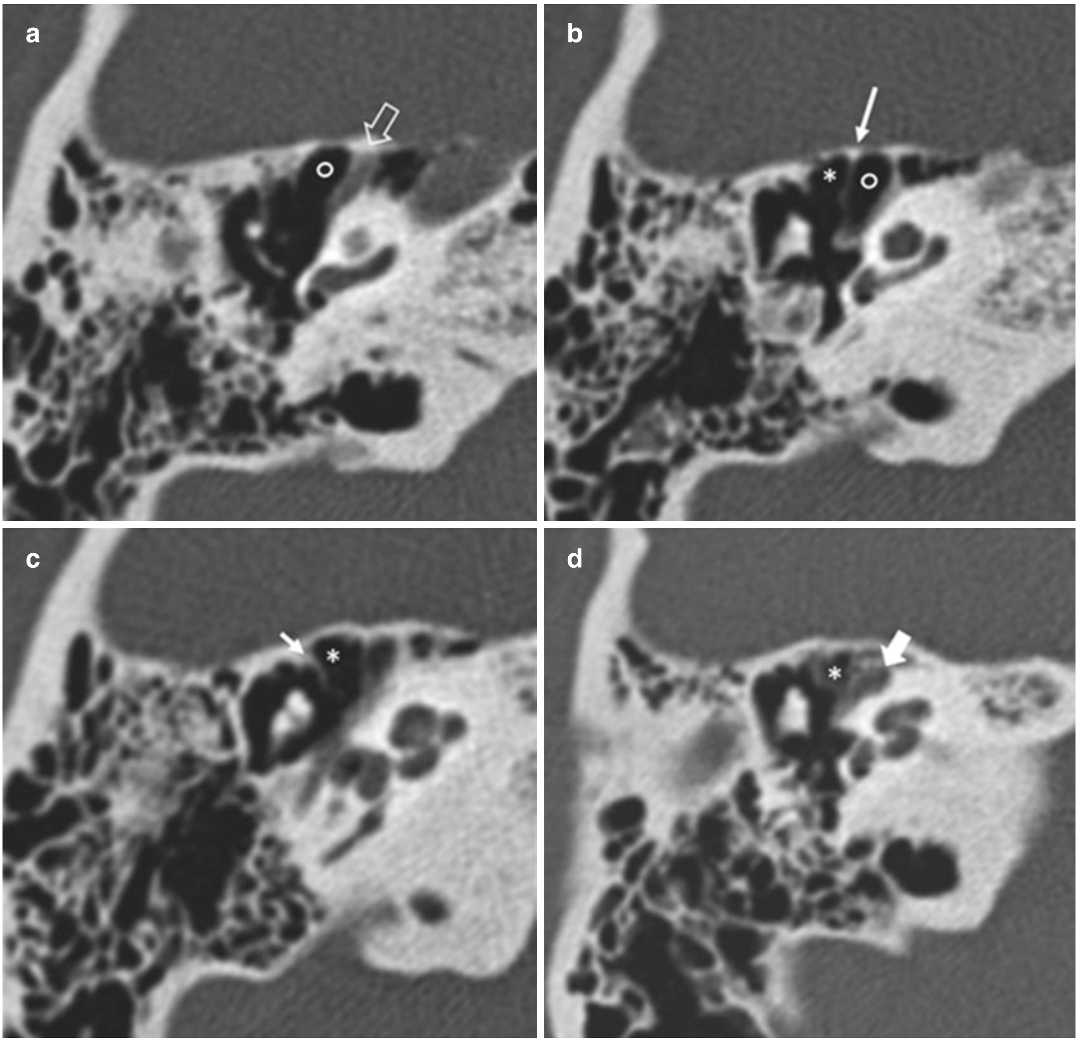

Fig. 4.29 Consecutive axial CT images of a right ear in caudocranial direction: (**a**) STR (o), tensor tympani muscle TTM (empty arrow), (**b**) the AER (*) lateral and *superior* to the STR (o), separated by the tensor tympani fold TTF (white arrow), (**c**) the AER (*) anterior to the cog (arrow), (**d**) AER (*) lateral to the facial nerve and geniculate ganglion (plain arrow)

of the attic (the external auditory canal and the ossicules). The use of the 30° endoscope through posterior tympanotomy may provide access to the TTF in most cases. Using this approach, the TTF could be somehow opened; however, in chronic inflammatory otitis, the complete excision of the TTF along with the cog is required in order to create and maintain a wide and permanent anterior route of aeration to the attic.

4.5.2 The Lower Unit of the Attic (Prussak's Space) (Figs. 4.21, 4.22, and 4.32)

In 1867, Prussak described a superior pouch of the tympanic membrane located between Shrapnell's membrane and the neck of malleus and distinct from the anterior and posterior pouches of von Tröltsch. Later, this superior pouch was renamed Prussak's space [41].

Clinical Applications: **The AER in Chronic Otitis Media** (Figs. 4.30 and 4.31)

The AER is highly important to consider in cases of recurrent otorrhea with central or anterior perforation not responding to conventional medical therapy or in front of a mucoid middle ear effusion that persists or recurs despite repetitive myringotomies with tube insertion. In addition, the AER must be investigated in the presence of a retraction pocket especially when it is anterosuperiorly oriented. In these cases, the TTF is complete and blocks the aeration of the anterior epitympanum from the anterosuperior mesotympanum creating a dysventilation syndrome. This situation will not respond to posterior atticotomy alone.

When performing middle ear surgery for dysventilation pathology with isthmus blockage, an imaging study of the AER with CT scan is mandatory not only to assess its involvement but also to obtain its dimensions in order to select the surgical approach. Resection of the cog and the TTF is fundamental to create an anterior route of ventilation between the protympanum, the supratubal recess, the AER, and the posterior attic [35, 37].

Prussak's space is formed from the posterior pouch of von Tröltsch as a prolongation of either a low or a high portion of the superior saccus, replacing the mesenchymal tissue between the neck of the malleus and Shrapnell's membrane [2]. The aeration pathway remains the same as the route of origin which is the posterior pouch of von Tröltsch.

Prussak's space is situated inferior to the tympanic diaphragm and represents the lower unit of the attic. Laterally, Prussak's space extends superior to the roof of the external auditory canal by 0.4 mm and attains its largest cross section of 2.6 mm at the level of the roof of the external ear canal [6]. It extends from the scutum to the umbo. It presents the following frontiers:

- **The roof or vault** is the lateral ligament malleal fold (LMF) which is at a low portion of the tympanic diaphragm. This LMF is also the floor of the lateral malleal space. *The lateral malleal fold separates Prussak's space from the upper unit of the attic*.

Space		Structure
AER	⟺	VII nerve
STR	⟺	TTM

Fig. 4.31 Landmarks for CT reading of anterior spaces

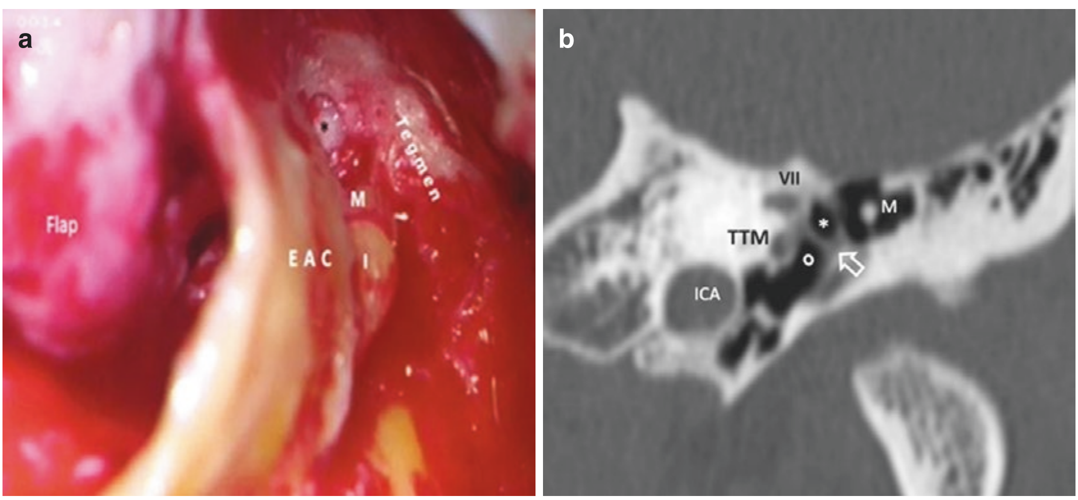

Fig. 4.30 (**a**) Left ear after transmastoid anterior atticotomy showing a complete tensor tympani fold (*) after removal of the cog. *I* incus, *M* malleus head, *EAC* external auditory canal. Notice that the tensor tympani fold is thick and inflammatory secondary to chronic otitis media. (**b**) Coronal CT image passing by the protympanum: *ICA* intrapetrous carotid artery, *TTM* tensor tympani muscle, *VII* facial nerve, M malleus head. The thickened TTF (empty arrow) separating the AER (*) above from the STR (o) beyond

- **The floor** is formed by the neck of the malleus.
- **The anterior limit** is the anterior malleal fold (AMF).
- **The lateral wall** is formed by the pars flaccida and the lower edge of the outer attic wall, the scutum.
- **The posterior wall** is opened to the posterior pouch of von Tröltsch and then to the mesotympanum.

The ventilation route of Prussak's space is independent of the upper unit of the attic. Prussak's space is ventilated through the posterior pouch of von Tröltsch which is particularly rough and narrow, as compared to the tympanic isthmus, that is wider and provides large ventilation of the upper unit of the attic [34] (Fig. 4.32). The posterior pouch of von Tröltsch is bounded laterally by the pars tensa of the tympanic membrane and medially by the posterior malleolar ligament fold (PMF), which originates from the posterior portion of the malleus neck and the upper third of the malleus handle and inserts posteriorly in the posterior tympanic spine. This posterior pouch develops in a posteroinferior direction and opens at the most cranial portion of mesotympanum; for these reasons, closing of the posterior pouch by viscous secretions is a plausible cause of a chronic selective dysventilation associated with a retraction of Shrapnell's membrane and its adhesion to the malleus neck.

Although Prussak's space is anatomically inseparable from the epitympanum, in terms of ventilation and drainage, it represents an independent unit. This space could be diseased alone with obliteration without any involvement of the compartments above the epitympanic diaphragm, like the anterior and posterior epitympanum, the aditus, and mastoid cells.

Surgical Application

This physiological concept in the functional anatomy of the middle ear is of extreme importance in transcanal endoscopic middle ear surgery: restoration of ventilation pathways with reunification of the upper and the lower unit of the attic through the creation of a large tympanic isthmus is crucial to avoid tympanic membrane retraction or recurrence of retraction after repair.

Clinical Applications: **Prussak's Space Dysventilation and Attical Cholesteatoma**

The possibility of closure of the posterior pouch of von Tröltsch by thick mucus secretions during chronic inflammatory otitis is high. This event may cause a selective dysventilation of Prussak's space and development of a pars flaccida retraction pocket with adhesion to the malleus neck (Fig. 4.33). This event may take place without any involvement of the other compartments of the upper unit that are situated superior to the tympanic diaphragm [43].

Initially, the sac of the retraction pocket remains small and superficial to the ossicles. However, continued retraction and keratin accumulation lead to an enlargement of the sac and its expansion via pathways of least resistance.

The growth pathways of attical cholesteatoma can be one of the following (Fig. 4.34):

- *Pathway 1*: The cholesteatoma progresses through the posterior pouch of von Tröltsch. The posterior tympanomalleolar fold orients this expansion toward the inferior incudal space. From there, cholesteatoma may extend medial to the long process of the incus and then through the tympanic isthmus, into the medial attic (Fig. 4.35).
- *Pathway 2*: The cholesteatoma progresses through a thin part of the lateral malleal fold directly to the upper unit of the attic and from there to the posterior attic, aditus, and then to the antrum (Fig. 4.36).

- *Pathway 3*: The cholesteatoma progresses from the lateral malleal space to the anterior attic and anterior epitympanic recess, and then it extends downward to invade the supratubal recess and the protympanum (Fig. 4.37).

It should be emphasized that the folds of the attic may direct the spread of cholesteatoma, but they do not constitute effective barriers to retain its expansion [6].

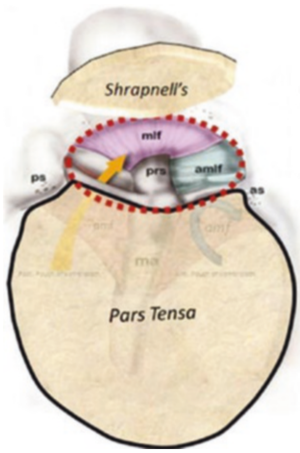

Fig. 4.32 Lateral view of Prussak's space (prs) after reflection of Shrapnell's membrane. *mlf* lateral malleal fold, *amlf* anterior malleal ligamental fold, *ps* posterior tympanic spine, *as* anterior tympanic spine. Yellow arrow, aeration of Prussak's space through the posterior pouch of von Tröltsch. Reproduced with modification from Marchioni [42, Fig. 1] (With kind permission from Springer Science and Business Media, Springer and the original publisher)

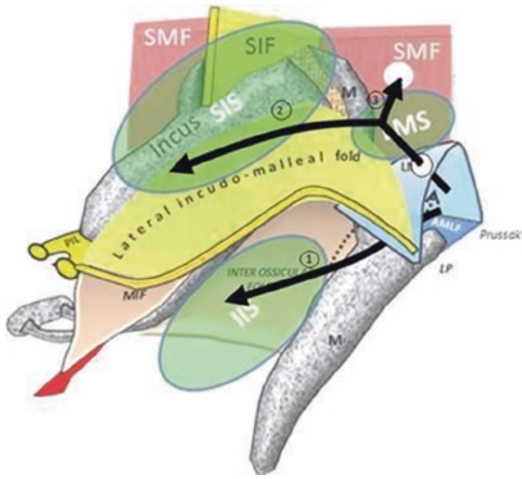

Fig. 4.34 Attical cholesteatoma growth pattern. From Prussak's space, cholesteatoma can extend through one of the following three tracts: (1) through the posterior pouch of von Tröltsch to the lower lateral attic (inferior incudal space, IIS), (2) through a defect in the lateral malleal fold (LMF) to the lateral malleal space (LMS) and then to the superior incudal space (SIS), or (3) from the lateral malleal space through the superior malleal fold defect (SMF) to the anterior attic. *SIF* superior incudal fold, *PIL* posterior incudal ligament, *MIF* medial incudal fold, *M* malleus, *LP* lateral process of malleus, *AMLF* anterior malleal ligamental fold

Fig. 4.33 (**a**) Attical cholesteatoma. (**b**) Coronal CT reconstruction of a right ear, showing a retraction pocket of the pars flaccida (empty arrow) with scutum amputation (long thin arrow), cholesteatoma (*), ossicular lyses (thick arrow). *EAC* external auditory canal

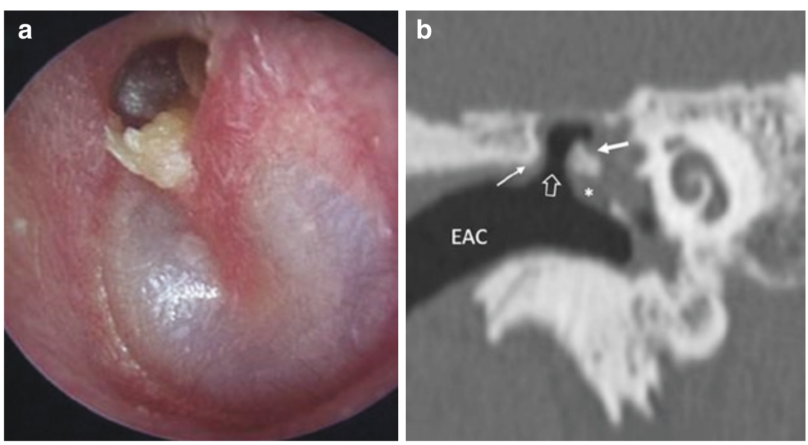

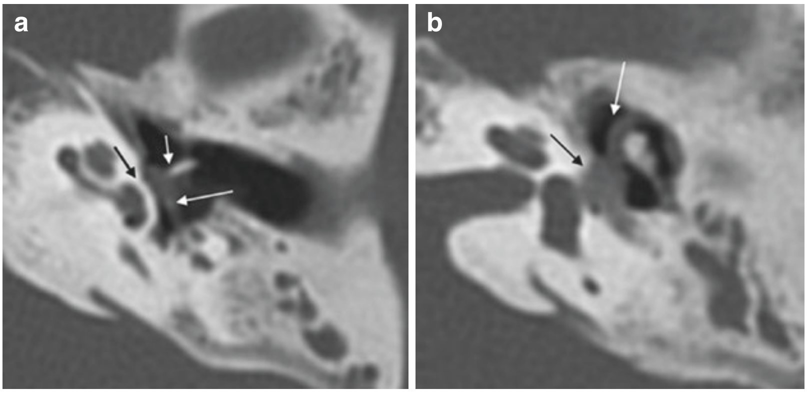

Fig. 4.35 Cholesteatoma growing according to the first pathway (illustrated in Fig. 4.34) from the posterior pouch of von Tröltsch to the inferior incudal space between the malleus handle and the long process of the incus, on transverse CT images of a left ear: (**a**) Obliteration of the interossicular space between the malleus handle (short white arrow) and the long process of the incus (long white arrow) reaching the promontory (black arrow). (**b**) Large extension medially with obliteration of the oval window niche (black arrow) and further above around the malleal head in the anterior malleal space (white arrow)

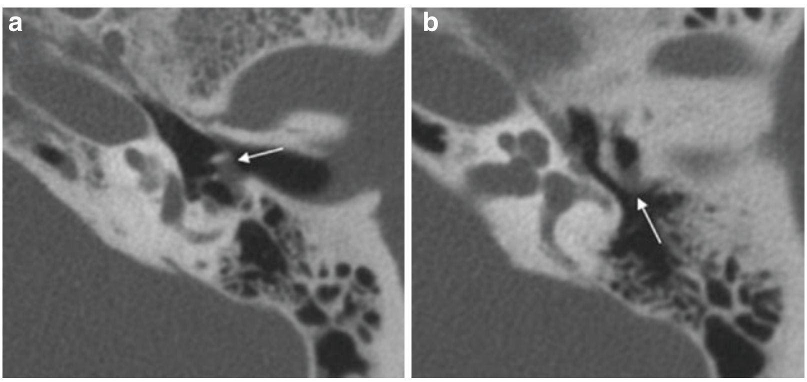

Fig. 4.36 Cholesteatoma growing according to the second pathway (as illustrated in Fig. 4.34) from the posterior pouch of von Tröltsch into the superior incudal space along the incudomalleal fold: (**a**) axial CT image with obliteration of the posterior pouch von Tröltsch (arrow) on the incudomalleal fold until the posterior attic; (**b**) axial CT image showing the limit of the lateral incudomalleal space as a rounded limit posteriorly (arrow)

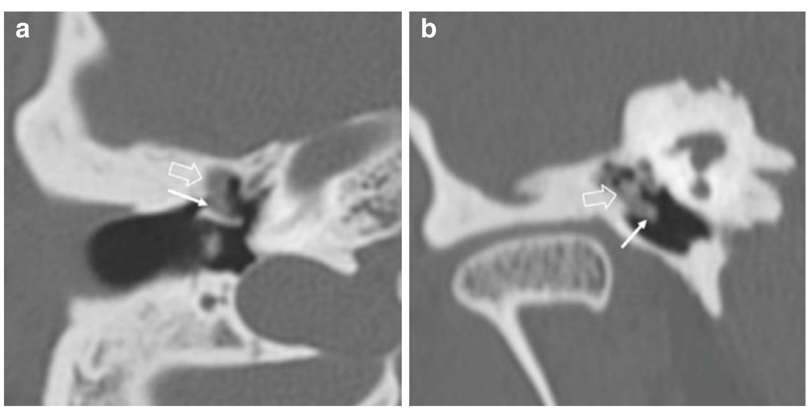

Fig. 4.37 Cholesteatoma growing according to the third pathway (illustrated in Fig. 4.34) from the anterior pouch de von Tröltsch (long arrow) directly into the anterior epitympanum (empty arrow): (**a**) axial CT view, (**b**) coronal oblique CT view

4.6 The Mesotympanum

The mesotympanum is the central and the largest compartment of the middle ear cavity. However, it is the narrowest one; its depth (the latero-medial diameter) is about 2 mm only. It is limited medially by the promontory and laterally by the pars tensa of the tympanic membrane. It is widely open anteriorly, inferiorly, and posteriorly to the protympanum, hypotympanum, and retrotympanum, retrospectively. Superiorly, it is separated from the attic by the tympanic diaphragm.

The mesotympanum acts like a tunnel, allowing air coming from the Eustachian tube to pass through the tympanic isthmus upward to provide aeration of the whole attic.

The lateral wall of the mesotympanum houses two important compartments:

4.6.1 Tympanic Membrane Compartments or Pouches (Fig. 4.38)

- ***Anterior Pouch of von Tröltsch***
  This pouch is situated between the anterior malleal fold and the pars tensa of the eardrum; it communicates with the supratubal recess and the protympanum [44].
- ***Posterior Pouch of von Tröltsch***
  This pouch is situated between the posterior malleal fold and the pars tensa of the eardrum. The posterior pouch of von Tröltsch develops posteroinferiorly, and it opens in the most cranial portion of the mesotympanum [44]. It is the main route of ventilation of Prussak's space.

4.7 Middle Ear Ventilation Pathways

The Eustachian tube ventilates the protympanum and the mesotympanum. The tympanic diaphragm separates the mesotympanum from the epitympanum. Understanding of the tympanic aeration pathways as an anatomical entity is essential in the management of middle ear and attic disease. The contribution of Proctor and Aimi in 1970 to explore the aeration pathways of different middle ear compartments had an important surgical impact [21, 45, 46].

One of the authors demonstrated, in a clinical series, the efficiency of a surgical removal of the TTF and cog excision to insure the aeration of the AER, freeing the anterior route of attic ventilation, in order to control chronic inflammatory otitis media and disease recurrence [37].

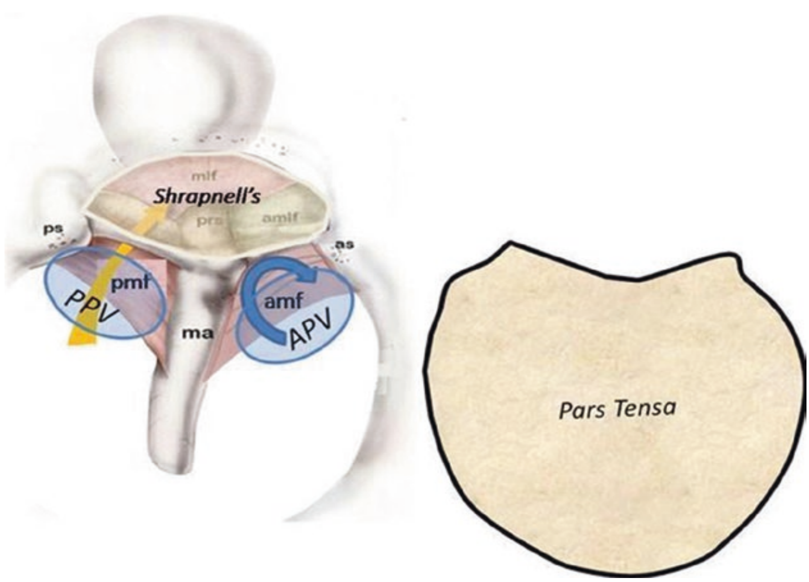

Fig. 4.38 Schema of a right middle ear lateral wall compartments after removal of the pars tensa, showing the anterior pouch of von Tröltsch (APV) that is isolated from Prussak's space (blue arrow) and the posterior pouch of von Tröltsch (PPV) that is in communication with Prussak's space (yellow arrow). *as* anterior tympanic spine, *ps* posterior tympanic spine, *amf* anterior malleal fold, *pmf* posterior malleal fold, *ma* malleus handle

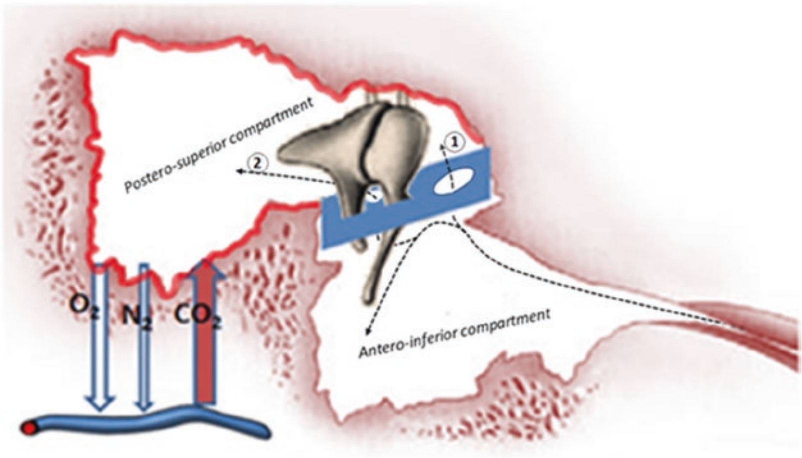

Fig. 4.39 The Eustachian tube ventilates the protympanum and the mesotympanum. The tympanic diaphragm separates the mesotympanum from the epitympanum. Two main ventilatory routes to the epitympanum are described the anterior route (1) and the posterior route (2) of ventilation. Furthermore, middle ear pressure is related not only to a functioning Eustachian tube but also to transmucosal gas exchange through mastoid mucosa

More recently, Marchioni illustrated the endoscopic anatomy of the aeration pathways and discussed the extent of selective dysventilation phenomena as a principal factor in influencing middle ear pressure homeostasis [47].

Two main ventilatory routes to the upper unit of attic are described: the anterior route and the posterior route of ventilation.

1. ***The Anterior Route***: from the protympanum to the STR, through an incomplete TTF into the AER and anterior attic. This pathway is functional only in 25–40% of ears when the TTF is incomplete. When the TTF is complete (60–75% of ears), the anterior attic ventilation relies only on the posterior route (through the anterior tympanic isthmus).
2. ***The Posterior Route***: the main route of ventilation of the epitympanum extends through the anterior tympanic isthmus and occasionally the posterior tympanic isthmus (ventilation to the upper unit of the attic and posterior attic).

In addition to the above-described routes of aeration, *the posterior pouch of von Tröltsch* ventilates the *lower unit of the attic* (Prussak's space). The posterior pouch of *von Tröltsch* is narrow and susceptible of blockage that may lead to *pars flaccida retraction pocket formation*.

In cases with a tympanic isthmus blockage associated with a complete tensor tympani fold, posterior attic and the AER become completely excluded from ventilation.

Furthermore, middle ear pressure is related not only to a functioning Eustachian tube but also to transmucosal gas exchange through the upper unit and mastoid mucosa, depending on the extent of mastoid pneumatization (Fig. 4.39).

4.8 "*Anatomo-physiological Addendum*": Middle Ear Aeration Pressure Regulation

4.8.1 The Middle Ear Mucosa

The middle ear is lined by cuboidal to columnar mucosal epithelium with scattered **goblet cells**. The auditory tube is lined by pseudostratified, ciliated columnar epithelium. The goblet cells are more prominent proximal to the ET contributing to the surfactant nature of the secretions containing **lecithin**, lipids, and **mucopolysaccharides** that decrease surface tension and keep the tube patent. The density of **cilia** increases as the tube runs dorsolaterally to open into the nasopharynx behind the soft palate, facilitating movement and drainage of mucus and other materials.

The ME mucosa is a modified respiratory mucosa; non-ciliated cells are the principal secretory cells; the latter have the cytologic characteristics of goblet cells.

The mucociliary cell system functions principally in the hypotympanum, protympanum, and ET. This mucous floats on an aqueous layer that is critical for ciliary function; if this aqueous layer is too thick, the cilia will not reach the mucous; if it is too thin, the ciliary movement is impeded by mucous viscosity.

4.8.1.1 The Middle Ear Cleft: A "Miniature Nose and Lung System"

The normal middle ear, being a very sensitive pressure receptor, responds to atmospheric air pressure changes: the direction of gas exchange is determined by the difference in partial pressure of gases in the middle ear cleft and blood.

The middle ear cleft is affected by Eustachian tube obstruction. Also obstruction of the tympanic isthmus induces dysventilation and affects air flow within the pneumatized temporal bone. Thus, the tympanic diaphragm plays a major role in partial or complete isolation and hypoxia of the middle ear spaces. The tympanic diaphragm divides the middle ear cleft into two separate compartments: an anteroinferior one, principally devoted to the mucociliary clearance function, and a posterosuperior one, more devoted to the gas exchange function.

- ***The anteroinferior compartment*** of the middle ear cleft, situated below the diaphragm, includes the protympanum, mesotympanum, and hypotympanum and is covered by secretory ciliated cells that enable mucociliary clearance (Figs. 4.40 and 4.41). It communicates with the posterosuperior compartment by both the anterior and posterior tympanic isthmi. An inflammatory process involving the mucosa of the anteroinferior middle ear cleft compartment (ET dysfunction with secondary global dysventilation) leads to a dysregulation of the mucociliary clearance with mucus accumulation and effusion.
- ***The posterosuperior compartment*** of the middle ear cleft, which is situated above the

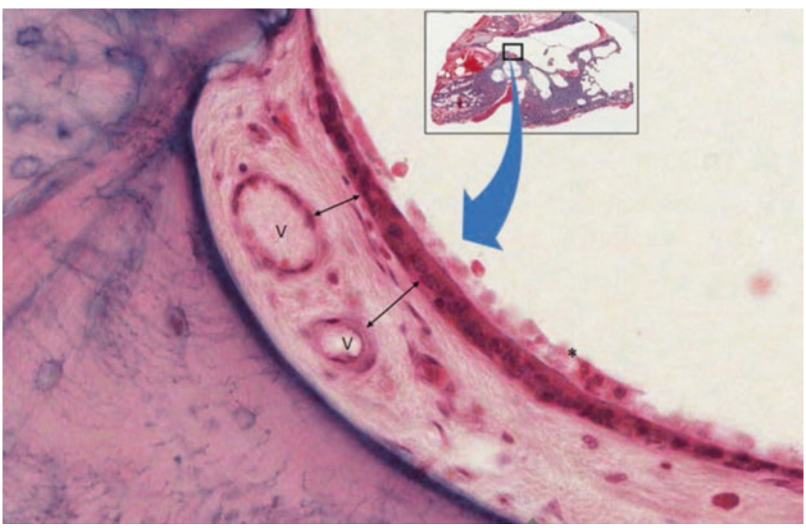

Fig. 4.40 Microphotography of ME mucosa (HE staining; 40×) showing the pseudostratified epithelium with ciliated cells and superficial mucus layer (*). Vessels (*V*) can be seen in the submucosal connective tissue. The average distance between the blood vessels and the epithelium (double head arrows) is 70 μm (From Massachusetts Eye and Ear Infirmary, Temporal Bone Consortium, Boston—http://temporalboneconsortium.org/educational-resources/atlas/image-library/)

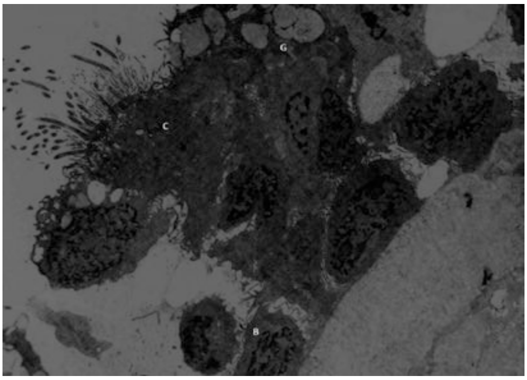

Fig. 4.41 Electronic microscopy slide of middle ear mucosa showing a clear view of different types of mucosa cells: ciliated cells (*C*), goblet cells with their mucus containing vacuoles (*G*), and *small undifferentiated cells near the basilar membrane* (B)

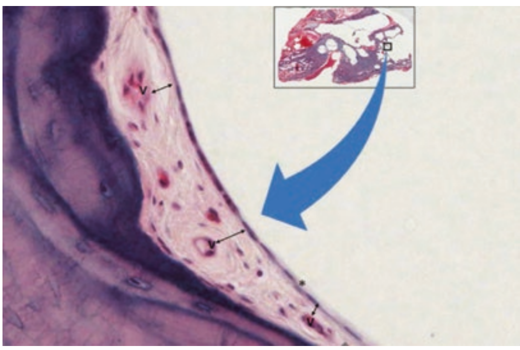

Fig. 4.42 Microphotography of mastoid mucosa (HE staining; 40×). Flat monolayer epithelium (*) with underlying subepithelial loose connective tissue and abundant vessels (*V*). The average distance between the blood vessels and the epithelium (*double head arrows*) is 40 μm (From Massachusetts Eye and Ear Infirmary, Temporal Bone Consortium, Boston—at http://temporalboneconsortium.org/educational-resources/atlas/image-library/)

diaphragm, includes the epitympanum and retrotympanum, aditus ad antrum, antrum, and mastoid gas cell system (*can be compared to the lung*). It is covered by a richly vascularized cuboidal epithelium that is devoted primarily to gas exchange (Figs. 4.42 and 4.43).

The net result of mucosal gas exchange is a status of gas deficit which is compensated by intermittent ET openings and ventilation (Fig. 4.44). Inflammation of the mucosa of the posterosuperior middle ear cleft compartment impairs the gas exchange and leads to the

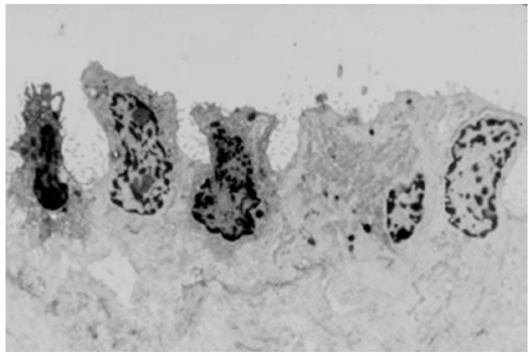

Fig. 4.43 Electronic microscopy slide of mastoid mucosa showing the epithelial mucosal cells forming a unicellular layer. Notice the absence of ciliated and goblet cells

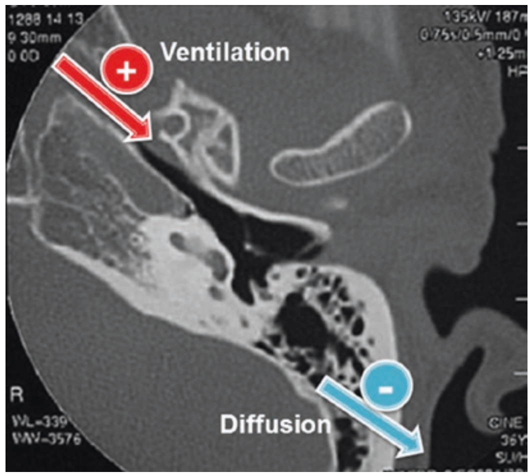

Fig. 4.44 Balance between transmastoid gas diffusion (blue arrow) and ventilation (red arrow)

development of an "excessive gas deficit status." If it couldn't be compensated by the ET, it will result in negative middle ear pressure.

4.8.2 Combined Mucosal Cell and ET Pressure Regulation

According to Magnuson, the ME pressure-regulation system depends on three components:

- Intermittent bidirectional gas passage by the ET.
- Bidirectional continuous diffusion of gas through the mucosal cells [48].

- The tensor veli palatini, with its dilator fibers, moves air to the ME by the pumping movement of the TM, maintaining air pressure at the level of ambient atmospheric pressure.

The ME "air" is in fact not air but rather a relatively hypercapnic, hypoxic, hypernitrous gaseous mixture (CO2+, O−, N+) fully saturated with water vapor. It is the result of a bidirectional diffusion between the mucosal blood vessels of the ME cleft (partial pressure of gases in the middle ear cleft and blood) together with periodic air pressure regulations via the ET during deglutition and yawning; all are done under gas pressure regulation phenomena.

The normal ear is a very sensitive pressure receptor; the sensation is probably registered by stretch receptors in the tympanic membrane [49].

Small fluctuations in pressure gradients of the ME can be buffered by the limited mobility of TM. However, displacement of the TM can compensate only volume changes of 0.2–0.3 mL [50].

The human mastoid and the Eustachian tube were capable of active counter-regulation of the middle ear pressure (mastoid and ET function in a complementary way). The mastoid provides continuous regulation of smaller pressures, whereas the ET is involved in intermittent regulation of higher pressures [51].

4.8.3 Neural Control of Middle Ear Pressure Regulation

4.8.3.1 Peripheral Neural Receptors

Studies support the hypothesis of neural connections between the middle ear baroreceptors and chemoreceptors, Eustachian tube, and brain centers to the neural circuits that monitor and regulate aeration in the middle ear [52].

Tympanic glomus cells seem to act as middle ear *chemosensory organs* and are involved in the regulation of middle ear aeration. Disruption of these neural elements has a negative impact on middle ear functions and may result in atelectasis[53]. This tissue is a sensory component essential for neural feedback circuits, which control the ET function [54].

The pars flaccida with its unique structure plays a key role as a baroreceptor in middle ear ventilation [49, 55].

It remains that the precise anatomical site of these receptors is unknown, being located in the tympanic membrane (pars flaccida), the middle ear, and the mastoid. These receptors take part in the middle ear pressure control and are governed by a neural feedback system possibly similar to the neural respiratory and cardiovascular feedback control [56].

4.8.3.2 Central Regulatory Mechanism for Middle Ear Aeration

A neural loop, between the baroreceptors of the ME cleft and the baroreceptors in the nasopharyngeal area connecting the solitary nucleus of the Pons, regulates the neural control of the ET opening and the ME gas exchanges. For instance, a decrease in middle ear pressure as compared to nasopharyngeal pressure will be detected by the solitary nucleus of the Pons which will initiate orders for tubal muscles to contract and open the ET (increase gaz ventilation) and for mastoid mucosal vessels to constrict (decrease mucosal gaz diffusion). Both mechanisms will increase middle ear pressure (Fig. 4.45). Neural connectivity from the tympanic plexus **(IX)** to the subnucleus of the *solitary tract in the brain stem* represents sensory inputs from chemoreceptors and baroreceptors in the ME to regulate the aeration. Myelination process of these nerve connections (axonal conduction efficiency) is age dependent. Delayed maturation of these neural connections might be an important factor in the pathophysiology of otitis media with effusion in children [57].

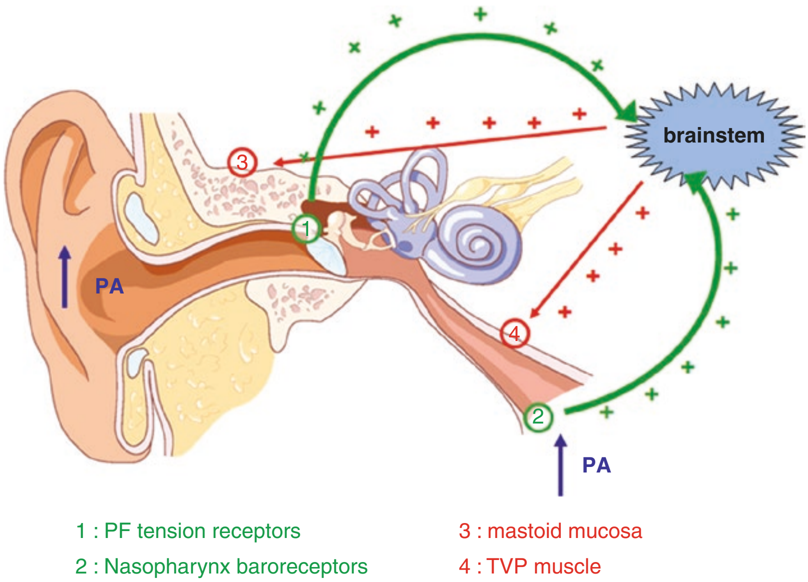

Fig. 4.45 A neural loop, between the baroreceptors of the ME cleft (1) and the baroreceptor in the nasopharyngeal pre-tubal area (2) connecting (green arrows) the solitary nucleus of the brain stem, regulates (red arrows) the neural control of the ET opening (4) and the mastoid mucosa gas exchanges (3)

Clinical Implications

Until now, most invasive procedures on the ET in order to improve ME ventilation are based on purely mechanical and not dynamic concepts of tubal dysfunction; this is why ET procedures failed to change substantially the control of chronic otitis media. On the other hand, surgeries directed only to sequela repair of chronic otitis media remain insufficient and fail to control the underlying cause of the diseases which is a vicious circle between dysventilation / hypoxia / inflammation.

References

1. Proctor B. Embryology and anatomy of the Eustachian tube. Arch Otolaryngol. 1967;86:503–14.
2. Hammar JA. Studien ueber die Entwicklung des Vorderdarms und einiger angrenzender Organe. Arch Mikrosk Anat. 1902;59:471–628.
3. Proctor B. The development of the middle ear spaces and their surgical significance. J Laryngol Otol. 1964;78:631–48.
4. Moreano EH, Paparella MM, Zelterman D, et al. Prevalence of carotid canal dehiscence in the human middle ear: a report of 1000 temporal bones. Laryngoscope. 1994;104(5 Pt 1):612–8.
5. Savic D, Djeric D. Anatomical variations and relations in the medial wall of the bony portion of the eustachian tube. Acta Otolaryngol. 1985;99(5–6):551–6.
6. Palva T, Johnsson LG. Epitympanic compartment surgical considerations: reevaluation. Am J Otol. 1995;16(4):505–13. Review. PubMed PMID: 8588652.
7. Onal K, Haastert RM, Grote JJ. Structural variations of supratubal recess: the anterior epitympanic space. Am J Otol. 1997;18:317–21. [PubMed].
8. Palva T, Ramsay H, Bohlurg J. Lateral and anterior view to tensor fold and supratubal recess. Am J Otol. 1998;19:405–14.
9. Giddings NA, Brackmann DE, Kwartler JA. Transcanal infracochlear approach to the petrous apex. Otolaryngol Head Neck Surg. 1991;104(1):29–36.
10. Mosnier I, Wu H, Chelly H, Cyna-Gorse F, Sterkers O. Infralabyrinthine approach for cholesterol granuloma of the petrous apex. Ann Otolaryngol Chir Cervicofac. 2000;117(3):174–82.
11. Ghorayeb BY, Jahrsdoerfer RA. Subcochlear approach for cholesterol granulomas of the inferior petrous apex. Otolaryngol Head Neck Surg. 1990;103(1):60–5.
12. Pickett BP, Cail WS, Lambert PR. Sinus tympani: anatomic considerations, computed tomography, and a discussion of the retrofacial approach for removal of disease. Am J Otol. 1995 Nov;16(6):741–50.
13. Roland JT Jr, Hoffman RA, Miller PJ, Cohen NL. Retrofacial approach to the hypotympanum. Arch Otolaryngol Head Neck Surg. 1995;121(2):233–6.

14. Calli C, Pinar E, Oncel S, Tatar B, Tuncbilek MA. Measurements of the facial recess anatomy: implications for sparing the facial nerve and chorda tympani during posterior tympanotomy. Ear Nose Throat J. 2010;89:490–4.
15. Dahm MC, Shepherd RK, Clark GM. The postnatal growth of the temporal bone and its implications for cochlear implantation in children. Acta Otolaryngol Suppl. 1993;505:4–27.
16. Eby TL, Nadol JB. Postnatal growth of the human temporal bone: implications for cochlear implants in children. Ann Otol Rhinol Laryngol. 1986;95:356–64.
17. Eby TL. Development of the facial recess: implications for cochlear implantation. Laryngoscope. 1996;106:1–7.
18. Bielamowicz SA, Coker NJ, Jenkins HA, Igarashi M. Surgical dimensions of the facial recess in adults and children. Arch Otolaryngol Head Neck Surg. 1988;114(5):534–7.
19. Dahm M, Seldon HL, Pyman BC, Clark GM. 3D reconstruction of the temporal bone in cochlear implant surgery. In: Yanagihara N, Suziki J, editors. Transplants and implants in otology II. Amsterdam: Kugler; 1992. p. 271–5.
20. Parlier-Cuau C, Champsaur P, Perrin E, Rabischong P, Lassau JP. High-resolution computed tomographic study of the retrotympanum. Anatomic correlations. Surg Radiol Anat. 1998;20(3):215–20.
21. Proctor B. Surgical anatomy of the posterior tympanum. Ann Otol Rhinol Laryngol. 1969;78(5):1026–40.
22. Marchioni D, Molteni G, Presutti L. Endoscopic anatomy of the middle ear. Indian J Otolaryngol Head Neck Surg. 2011;63(2):101–13.
23. Holt JJ. Posterior sinus of the middle ear. Ann Otol Rhinol Laryngol. 2007;116(6):457–61.
24. Ozturan O, Bauer C, Miller C, et al. Dimensions of the sinus tympani and its surgical access via retrofacial approach. Ann Otol Rhinol Laryngol. 1996;105:776–83.
25. Nitek S, Wysocki J, Niemczyk K, Ungier E. The anatomy of the tympanic sinus. Folia Morphol (Warsz). 2006;65(3):195–9.
26. Amjad AH, Starke JJ, Scheer AA. Tympanofacial recess in the human ear. Arch Otolaryngol. 1968;88(2):131–7.
27. Donaldson JA, Anson BJ, Warpeha RL, et al. The surgical anatomy of the sinus tympani. Arch Otolaryngol. 1970;91:219–27.
28. Thomassin JM, Danvin BJ, Collin M. Endoscopic anatomy of the posterior tympanum. Rev Laryngol Otol Rhinol (Bord). 2008;129(4–5):239–43.
29. Thomassin JM, Korchia D, Doris JM. Endoscopic-guided otosurgery in the prevention of residual cholesteatomas. Laryngoscope. 1993;103:939–43.
30. Aslan A, Guclu G, Tekdemir I, Elhan A. Anatomic limitations of posterior exposure of the sinus tympani. Otolaryngol Head Neck Surg. 2004;131(4):457–60.
31. Savic D, Djeric D. Anatomical variations and relations of the medial and lateral portions of the attic and their surgical significance. J Laryngol Otol. 1987;101(11):1109–17.
32. Palva T, Johnsson LG, Ramsay H. Attic aeration in temporal bones from children with recurrent otitis media: tympanostomy tubes did not cure disease in Prussak's space. Am J Otol. 2000;21:485–93.
33. Palva T, Ramsay H, Northrop C. Color atlas of the anatomy and pathology of the epitympanum. Basel: Karger; 2001.
34. Palva T, Ramsay H, Böhling T. Prussak's space revisited. Am J Otol. 1996;17(4):512–20.
35. Palva T, Ramsay H. Chronic inflammatory ear disease and cholesteatoma: creation of auxiliary attic aeration pathways by microdissection. Am J Otol. 1999;20:145–51.
36. Horn KL, Brackmann DE, Luxford WM, et al. The supratubal recess in cholesteatoma surgery. Ann Otol Rhinol Laryngol. 1986;95:12–5.
37. Mansour S, Nicolas K, Naim A, et al. Inflammatory chronic otitis media and the anterior epitympanic recess. J Otolaryngol. 2005;34:149–58.
38. Hoshino T. Surgical anatomy of the anterior epitympanic space. Arch Otolaryngol Head Neck Surg. 1988;114:1143–5.
39. Todd NW, Heindel NH, PerLee JH. Bony anatomy of the anterior epitympanic space. J Otorhinolaryngol Relat Spec. 1994;56:146–53.
40. Marchioni D, Mattioli F, Cobelli M, et al. CT morphological evaluation of anterior epitympanic recess in patients with attic cholesteatoma. Eur Arch Otorhinolaryngol. 2009;266:1183–9. https://doi.org/10.1007/s00405-008-0871-x.
41. Prussak A. Zur Anatomie des menschlichen Trommelfells. Arch Ohrenheilkd. 1867;3:255–78.
42. Marchioni D. Lateral endoscopic approach to epitympanic diaphragm and Prussak's space: a dissection study. Surg Radiol Anat. 2010;32(9):843–52.
43. Palva T, Ramsey H. Aeration of Prussak's space is independent of the supradiaphragmatic epitympanic compartment. Otol Neurotol. 2007;28:264–8.
44. Von Tröltsch A. Lehrbuch der Ohrenheilkunde mit Einschluss der anatomie des Ohres. 7th ed. Leipzig: FCW Vogel; 1881.
45. Proctor B. Attic-aditus block and the tympanic diaphragm. Ann Otol Rhinol Laryngol. 1971;l80:371–5.
46. Aimi K. The clinical significance of epitympanic mucosal folds. Arch. Otolaryng. 1971;94:499–505.
47. Marchioni D, Mattioli F, Alicandri-Ciufelli M, et al. Endoscopic evaluation of middle ear ventilation route blockage. American Journal of Otolaryngology. 2010;31(6):453–66.
48. Magnuson B. Functions of the mastoid cell system: auto-regulation of temperature and gas pressure. J Laryngol Otol. 2003;117(2):99–103.
49. Rockley TJ, Hawke WM. The middle ear as a baroreceptor. Acta Otolaryngol. 1992;112(5):816–23.
50. Lima MAR, et al. Update on middle ear barotrauma after hyperbaric oxygen therapy—insights on pathophysiology. Int Arch Otorhinolaryngol. 2014;18:204–9.

51. Gaihede M, Dirckx JJ, Jacobsen H, Aernouts J, Søvsø M, Tveterås K. Middle ear pressure regulation—complementary active actions of the mastoid and the Eustachian tube. Otol Neurotol. 2010;31(4):603–11. https://doi.org/10.1097/MAO.0b013e3181dd13e2.
52. Eden AR. Neural control of middle ear aeration. New York, NY: Mount Sinai School of Medicine; 1987.
53. Ceylan A, et al. Impact of Jacobson's (tympanic) nerve sectioning on middle ear functions. Otol Neurotol. 2007;28(3):341–4.
54. Eden AR, Gannon PJ. Neural control of middle ear aeration. Arch Otolaryngol Head Neck Surg. 1987;113(2):133–7.
55. Swarts JD, Alper CM, Luntz M, et al. Panel 2: Eustachian tube, middle ear, and mastoid—anatomy, physiology, pathophysiology, and pathogenesis. Otolaryngol Head Neck Surg. 2013;148(4 Suppl):E26–36.
56. Gaihede M, et al. Chronic otitis media: pathogenesis-oriented therapeutic management edited by Bernard Ars. Amsterdam, The Netherlands: Kugler Publications.
57. Eden AR, Laitman JT, Gannon PJ. Mechanisms of ME aeration: anatomic and physiologic evidence in primates. Laryngoscope. 1990;100(1):67–75.

5 The Mastoid

Contents

The term "mastoid" is derived from the Greek word mastós, meaning breast, in reference to the shape of this bone. The mastoid process projects from the base of the skull and is situated behind the external auditory meatus at the inferior part of the outer surface of the temporal bone.

The mastoid process houses several important structures such as the facial nerve, the sigmoid sinus, and the labyrinth; it neighbors the middle and the posterior cranial fossa. Therefore, a good knowledge of the mastoid process anatomy is essential to perform adequate surgical approaches and to avoid complications or pitfalls.

In addition, the mastoid process is the site of numerous air-filled cavities known as mastoid air cells which play an important role in middle ear aeration and functions.

S. Mansour et al., *Comprehensive and Clinical Anatomy of the Middle Ear*,
https://doi.org/10.1007/978-3-030-15363-2_5

5.1 Embryology of the Antrum and Mastoid

The antrum, which is the biggest of all mastoid air cells, starts its development between the 22nd and the 24th week of fetal life. It reaches its adult size on the 35th week of gestation [1–3]. At birth, the antrum has a mean surface of 1 cm^2 [4].

The antrum develops at the center of the mastoid process on both sides of the petrosquamous fissure. The medial part of the antrum, the petrous part, develops from the saccus medius, while the lateral part, the squamous part, develops from the saccus superior (Figs. 4.2 and 4.3) (see Chap. 4). The fusion plane between the petrous part and the squamous part of the antrum corresponds to the petrosquamous fissure. Failure of complete fusion between the two sacci leads to a residual septation of the mastoid antrum by a bony partition called *Korner's septum* [5] (Fig. 5.1).

The mastoid process appears at the 29th week of gestation as a result of the fusion of the petrous layers of the otic capsule and the tympanic process of the squamous bone (see Figs. 1.1 and 1.3).

The size of the antrum does not change after birth; however, it undergoes medial and inferior displacement due to the growth of the mastoid process. In contrary, the mastoid process continues to grow until puberty and even beyond.

5.2 Postnatal Mastoid Pneumatization

At birth, the mastoid process presents only the antrum. The mastoid air cells develop as an outgrowth of the antrum; epithelial air tracts bud from the antrum and extend to the adjacent areas of the temporal bone to form the mastoid air cells (Fig. 5.2). This air cell extension, called mastoid pneumatization, is facilitated by the differentiation of bone marrow into loose mesenchyme.

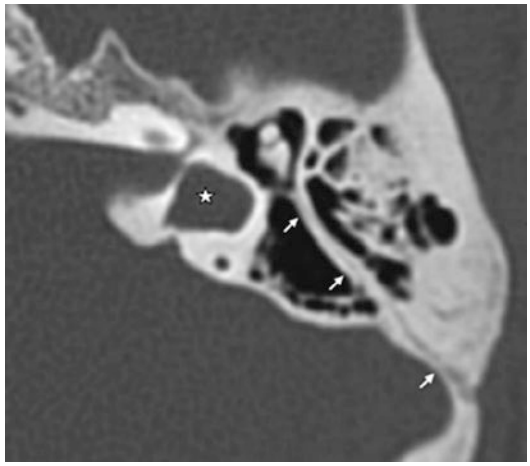

Fig. 5.1 Transversal CT view of a left ear. The fusion line between the squamous and petrosal part of the mastoid, resulting in a bi-lamellar Korner's septum (white arrows). Developmental arrest of the vestibule (*)

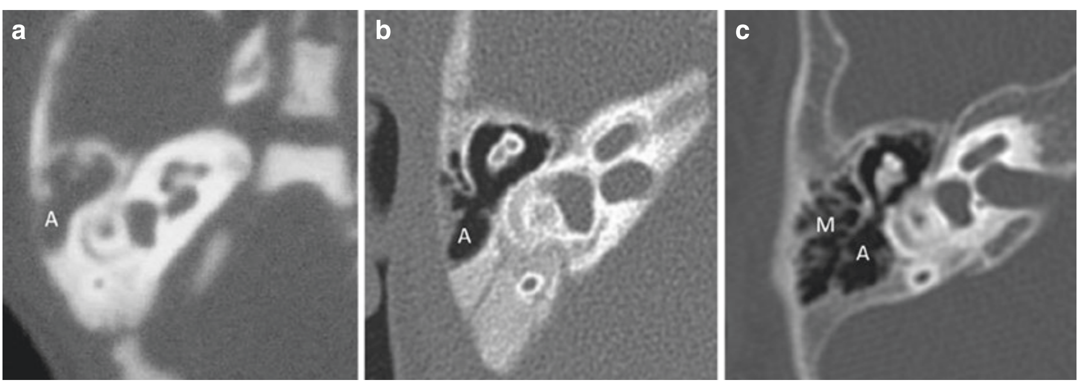

Fig. 5.2 Transversal computed tomography of right ears from the fetal period third trimester to the age of 1 year. (**a**) Fetal temporal bone CT showing the antrum (**A**) lateralized as the only mastoid cell at this age; (**b**) at birth still the antrum is the only aerated mastoid cell; (**c**) in a 1-year-old child, advanced mastoid pneumatization (M) laterally to the antrum (A) that became medialized in comparison to the previous images

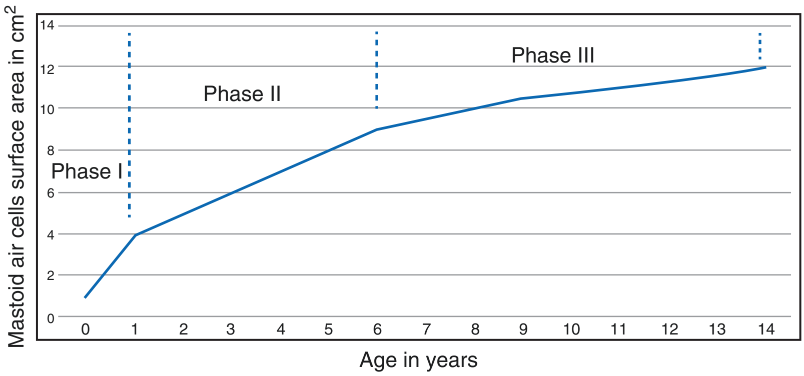

Fig. 5.3 Graph showing the three phases of mastoid pneumatization from birth to puberty

Thereafter, the mastoid becomes the site of an air-containing cavity called the mastoid air cells. The residual dense bone, which did not pneumatized, forms the septations between the mastoid air cells (the mastoid intercellular bony septa) [1, 6–16].

From birth until puberty, three phases of mastoid pneumatization take place (Fig. 5.3):

- *Phase I (0–1 year)*: The antrum is found at birth with a mean surface of 1 cm^2 (Fig. 5.2). During the first year of life, there is a rapid development of mastoid air cells, adding 3 cm^2 to reach a total surface of 4 cm^2 at the age of 1 year. During that time, the mastoid process increases 1 cm in length and width and 0.5 cm in depth.
- *Phase II (1–6 years)*: the mastoid pneumatization follows a linear pattern adding about 1 cm^2 per year. Due to this pneumatization progress, at the age of 2 years, the mastoid tip covers the emergence of the facial nerve at the stylomastoid foramen; the mastoid process growth increases then by about 0.5 cm per year in length and width and 0.25 cm per year in depth (Fig. 5.2).
- *Phase III (6 years–puberty)*: at this period, the pneumatization process becomes very slow. It continues until puberty when the aerated mastoid process reaches its adult size. *The mean adult surface of the mastoid air cell system is about 12 cm^2* [4, 6]. The last air cells to develop are the cells of the petrous apex. These air cells are present in about 35–40% of adult temporal bones [6, 17, 18].

Postnatal mastoid pneumatization displays considerable variations, and this is related to several factors including heredity, environment, infections, and Eustachian tube function. A controversy still exists concerning the various degrees of mastoid pneumatization encountered. There are two theories:

1. *Environmental theory*: according to this theory, middle ear infectious diseases occurring early in childhood are the main cause responsible of the failure of the pneumatization process in infants and children [8–11, 19–21].
2. *Genetic theory*: this theory relates the extent of pneumatization to genetic factors, suggesting that an inherited reduced pneumatization predisposes the children to otitis media [6, 12–14].

5.3 The Tracts of Pneumatization

The mastoid air cells represent an extension of the air tracts into the mastoid process from the first pharyngeal pouch. Pneumatization in the mastoid extends from the middle ear cleft through the aditus ad antrum to the central air cell tract from which further extension in several directions may occur.

Mastoid pneumatization proceeds through several well-established tracts. These tracts of pneumatization vary considerably. The two main tracts of mastoid pneumatization are:

1. **The anterolateral tract** which pneumatizes the squamous portion of the temporal bone.

2. **The posteromedial tract** which pneumatizes the petrous portion of the temporal bone. This tract branches into several tracts as the following:
   - ***The posterosuperior cell tract***

     The posterosuperior tract extends medially from the antrum at the junction of the posterior and middle fossa dural plates and above the superior semicircular canal and the internal auditory canal. It insures the pneumatization of the medial pyramid of the temporal bone.
   - ***The posteromedial cell tract (superior retrolabyrinthine)***

     The posteromedial tract extends medially through the antrum, parallel and inferior to the posterosuperior tract, to perform the pneumatization of the medial pyramid.
   - ***The subarcuate cell tract (translabyrinthine)***

     The subarcuate tract is situated more medially. It arises from the mastoid antrum and extends anteromedially passing below the superior semicircular canal to insure the pneumatization of the petrous apex.
   - ***The perilabyrinthine cell tract***

     The perilabyrinthine cell tract arises from the antrum and pneumatized the labyrinthine area. It is divided into the supralabyrinthine and the infralabyrinthine tracts. It can extend to the petrous apex.
   - ***The peritubal tract***

     This tract arises from the mastoid antrum and pneumatized the tubal and peritubal area passing inferior to the labyrinth.

Pneumatization of the *petrous apex* is the last to develop. The petrous apex cells develop from the posterosuperior and posteromedial cell tracts. The subarcuate cell tract, the perilabyrinthine cell tract, and the peritubal cell tract can also participate in the pneumatization of the petrous apex to variable degrees [22, 23].

Some authors suggest that pneumatization of the petrous apex may be an independent process from those of the middle ear and mastoid air cells and may not be influenced by major anatomical structures nearby (carotid canal and labyrinth). Also it is reported that the well-aerated anterior epitympanic recess (AER) is associated with a well-pneumatized petrous apex; hence, the anterior saccule of the saccus medius might be a major influencing factor in the pneumatization of the petrous apex [24].

Temporal bone pneumatization is symmetrical in both sides in 75% of normal individuals. Any asymmetric pneumatization found in individual cases could indicate a history of previous middle ear disease during the period of pneumatization.

Clinical Implications

The mastoid process is underdeveloped at birth. This situation leaves the facial nerve relatively superficial and unprotected where it emerges from the stylomastoid foramen. During difficult delivery, the use of forceps may damage the facial nerve by compression at this level.

At the age of 2 years, as the air cells develop, the lateral part of the mastoid process grows downward and forward to form the mastoid tip. In addition, growth of the neck, with hyperextension, allow the sternocleidomastoid muscle to pull the mastoid tip downwards and slightly outwards to cover the stylomastoid foramen and offers progressively a better protection to the facial nerve.

5.4 Mastoid Process Anatomy

The adult mastoid process has a cone shape and is slightly oblique forward and downward. Its anterior border is rounded and vertical. Its posterior border is inclined about 45° downward and forward. Behind the superior part of the mastoid process, the mastoid foramen is situated where the mastoid emissary vein passes.

The squamous bone forms the anterosuperior portion of the mastoid process. The petrous bone forms its posteroinferior part. The junction of the

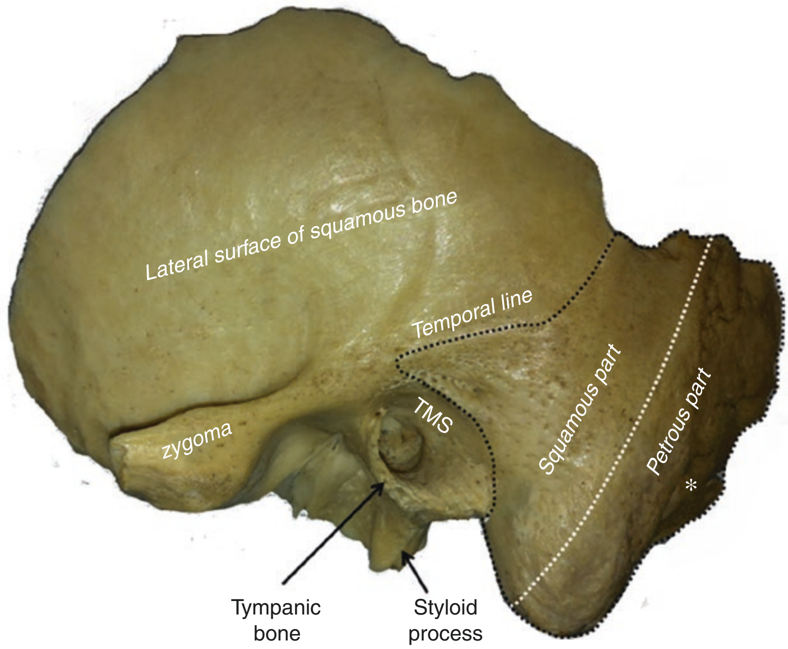

Fig. 5.4 Lateral surface of a left temporal bone, showing the mastoid process (black dotted line), that formed from a squamous part and a petrous part, joined by the petrosquamous suture (white dotted line). The mastoid process is attached to the tympanic bone by the tympanomastoid suture (TMS); * digastric notch

two parts forms the petrosquamous suture. The petrosquamous suture runs vertically from the superior border of the mastoid process to join its anteroinferior border just above the mastoid tip (Fig. 5.4).

The mastoid process serves as a point of attachment for several muscles like the splenius capitis, the longissimus capitis, the digastric, and the sternocleidomastoid muscles. The mastoid process is larger in men because they require larger points of attachment for their bigger muscles. The sternocleidomastoid muscle inserts to the outer surface of the mastoid tip. The posterior belly of digastric muscle inserts on the digastric groove situated on the medial surface of the mastoid tip. The digastric groove is an infallible guide to point the facial nerve emergence from the stylomastoid foramen at the anterior end of the groove.

5.4.1 Surface Landmarks of the Mastoid Process

Along the lateral surface of the mastoid process, we distinguish several important surgical landmarks:

5.4.1.1 The Temporal Line

The temporal line is a horizontal ridge situated at the upper limit of the mastoid process. It extends behind the posterior root of the zygomatic process and marks the inferior margins of the insertion of the temporal muscle (Fig. 5.4). The temporal line may be a prominent sharp edge or a broad prominence or it may be absent as well [25].

Surgical Pearl: Temporal Line

It is widely accepted that the temporal line is indicative of the inferior level of the middle fossa dura. Hence, during mastoidectomy, it is always recommended to drill along, not above, the temporal line in order to avoid inadvertent injury to the dura [26].

Cadaveric studies found that the temporal line is located about 5 mm inferior to the middle fossa dura [27]. This may suggest that the drilling could start even at 5 mm above the temporal line without danger to the dura in order to increase the surgical exposure of the mastoid antrum.

The distance between the temporal line and the middle fossa dura tends to be bigger in temporal bones with an absent Henle's spine [27, 28]. In cases where the temporal line is absent, the Henle's spine could be used as an anatomic landmark to presume the level of the middle fossa dura.

5.4.1.2 Henle's Spine

Henle's spine is a prominent bony spine on the outer surface of the mastoid process (see also Fig. 5.17b). It is situated behind and above the posterosuperior quadrant of the external auditory meatus and below the origin of the temporal line [28]. This lamella is incurved nearly concentrically to the circumference of the meatus, and its upper extremity is more anterior than its inferior one (Fig. 5.5). Henle's spine could be small and smooth or sharp and long. It is absent in about 6% of temporal bones [29, 30]. It serves as a point of attachment to the ligaments fixing the cartilaginous parts of the external acoustic meatus.

5.4.1.3 Mac-Ewen's Triangle

The suprameatal triangle or "Mac-Ewen's triangle" is a depression on the lateral surface of the mastoid process. It is located just between the anterior end of the temporal line, Henle's spine, and the posterosuperior quadrant of the external acoustic meatus (Fig. 5.5).

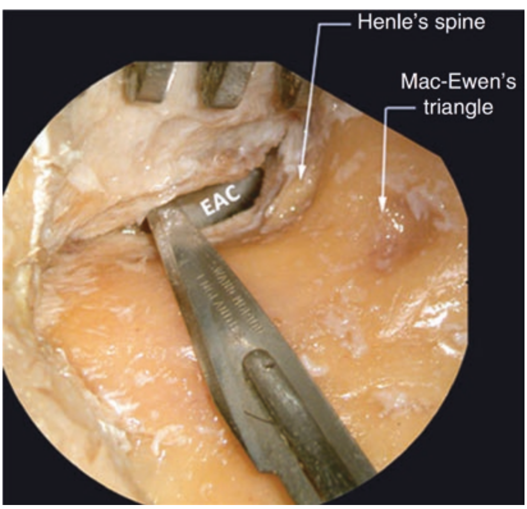

Fig. 5.5 Left cadaveric mastoid surface showing Henle's spine and Mac-Ewen's triangle. *EAC* external auditory canal

Surgical Pearl: Henle's Spine
Henle's spine is an excellent landmark during mastoidectomy because it indicates the location of the deeply seated aditus ad antrum. In addition, it may serve as a landmark for middle fossa dura when the temporal line is absent; the dura is situated about 1 cm superior to Henle's spine [27].

Surgical Pearl: Mac-Ewen's Triangle
Mac-Ewen's triangle is a useful anatomic landmark for the surgical access to the antrum; the mastoid antrum lies about 12–15 mm deeper to this triangle. This triangle is absent in 10% of the population [31–34].

5.4.2 Surgical Anatomy of the Mastoid Antrum

The mastoid antrum (tympanic antrum, antrum mastoideum, Valsalva's antrum) is the biggest mastoid air cell, communicating posteriorly with the mastoid cells and anteriorly with the epitympanic recess of the middle ear via the aditus to mastoid antrum (*entrance to the mastoid antrum*).

1. The mastoid antrum is of 1 cm × 1 cm × 1 cm in average. It is located posterior to the external auditory canal and middle ear, inferior to the middle fossa dural plate, and anterior to the sigmoid sinus and the posterior fossa dural plate. The mastoid antrum communicates anteriorly with the attic through the *aditus ad antrum* (Figs. 5.6 and 5.7). The antrum is the key landmark in mastoid surgery: high degree of pneumatization eases antrum localization.

Surgical identification of the tegmen and thinning of the posterior canal wall are very important surgical steps to reach the antrum. Posteriorly, the sigmoid sinus must be looked for: it could be situated rather anterior in poorly pneumatized mastoid. Failure to identify the tegmen could cause a dissection that is too much inferiorly, exposing the lateral semicircular canal or the facial nerve to risk of injury.

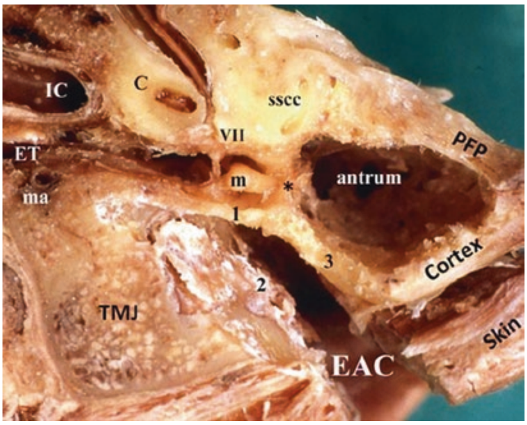

Fig. 5.6 Sagittal oblique cut of a left cadaveric temporal bone showing the antrum at the level of the aditus ad antrum (*). *PFP* posterior fossa plate, *EAC* external auditory canal, *1* attic outer wall, *2* anterior wall of the EAC, *3* posterior wall of the EAC, *C* cochlea, *sscc* superior semicircular canal, *m* malleus, *VII* facial nerve, *IC* internal carotid artery, *ET* Eustachian tube, *ma* middle meningeal artery, *TMJ* temporomandibular joint

5.4.2.1 Position of the Antrum in Relation to Surface Landmarks

The depth of the mastoid antrum is a cardinal point in mastoid surgery. Despite the fact that the antrum reaches its adult size at birth, its medial displacement secondary to the pneumatization process renders its depth dependent of the age of the subject. Its depth varies also from person to person at the same age. In infants less than 1 year of age, the distance between the cortical bone and the antrum is only 2–4 mm (Fig. 5.2a). At 3 years of age, the antrum is at 10 mm from the cortical bone, and in adults, the antrum is at about 25 mm from the mastoid cortical bone [35].

In young children, the antrum is easily reached by curetting the cortical bone. In adults, the antrum is situated below the supramastoid ridge, above and in front of the petrosquamous suture. *Mac-Ewen's triangle is an important indicator of the antrum area* (compare Figs. 5.5 and 5.8).

The relation of the antrum and Henle's spine is also age-dependent. At about 10 years, it is on the horizontal track designed by Henle's spine; after this age, the antrum sets about 1 cm behind Henle's spine.

5.4.2.2 Deep Relationships of the Antrum

Several important structures must be considered while operating on the mastoid antrum; the most

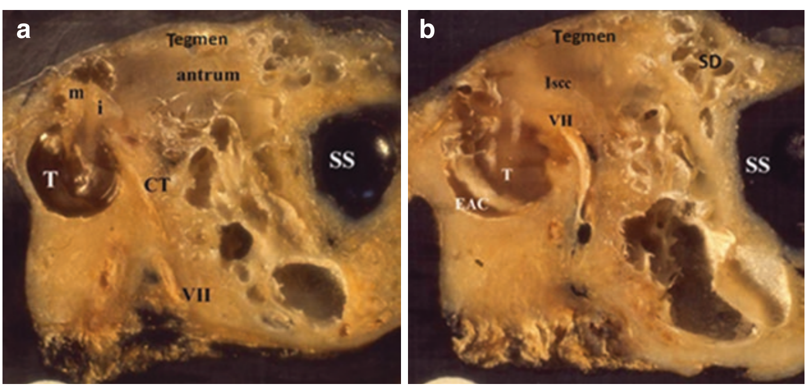

Fig. 5.7 Sagittal cuts through the temporal bone, showing in (**a**) the medial wall of the antrum containing the labyrinth and in (**b**) the lateral wall of the antrum. Notice that the antrum is posterosuperior to the tympanic cavity (*T*). The tegmen antri slopes down as it goes anteriorly. Sinodural angle cells (*SD*) are located posterior to the antrum between the sigmoid sinus (*SS*) and the tegmen. The facial nerve VII is anteroinferior to the antrum. *EAC* external auditory canal, *m* malleus, *i* incus, *lscc lat*eral semicircular canal, *CT* chorda tympani

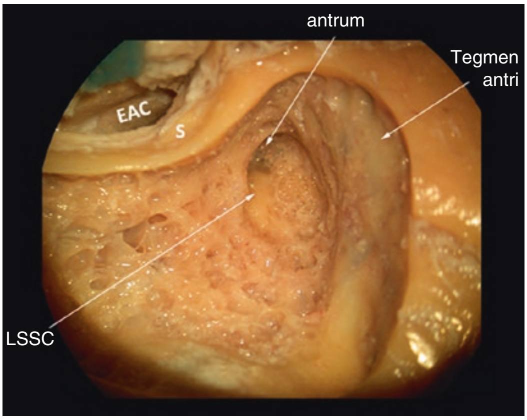

Fig. 5.8 A left mastoidectomy showing the antrum, with the lateral semicircular canal (LSSC) in its medial wall. Notice the relation between Henle's spine (S) and the antrum: the antrum is always superior and posterior to the spine (S) and the external auditory canal (EAC)

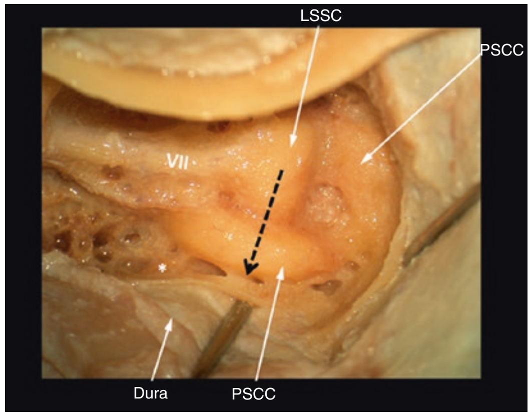

Fig. 5.9 Cadaveric left mastoidectomy showing lateral semicircular canal (LSCC), the superior semicircular canal (SSCC), and the posterior semicircular canal (PSCC). Notice the relationship between the PSCC and the facial nerve (VII). Notice Donaldson's line (the black dotted line) and the endolymphatic sac (*)

important are the lateral semicircular canal, the facial nerve, the sigmoid sinus, the posterior fossa dural plate, and the tegmen antri. Good knowledge of the anatomy of the antrum and its close relationship with these structures is essential for a safe mastoid surgery.

5.4.2.2.1 The Lateral Semicircular Canal and the *Solid Triangle*

Medially, the antrum is limited by the *solid triangle* of the mastoid, which is the compact bony triangle formed by the three semicircular canals:

- The lateral semicircular canal (LSCC) is situated just behind the inner wall of the antrum. The canal is surrounded by a solid compact bony shell, which by itself offers a strong resistance to instruments. The distance from the tegmen antri to the lateral semicircular canal is about 6 mm [27].
- The superior semicircular canal (LSCC) runs perpendicular to the LSCC. It is about 2 mm more medially situated. Its anterior crus runs superiorly toward the tegmen tympani and then curves posteriorly to join the posterior semicircular canal forming the common crus.
- The posterior canal also runs perpendicular to the LSCC. The superior half of the posterior canal is located superior to a line bisecting the lateral canal (Donaldson's line). The inferior half of the posterior canal runs inferiorly to Donaldson's line and emerges deep to the vertical portion of the facial nerve to enter the vestibule (Fig. 5.9).

Surgical Application: **Donaldson's Line**

Donaldson's line is a straight line that runs in the axis of the lateral semicircular canal and bisects the posterior semicircular canal. It is an important landmark for searching the endolymphatic sac (Figs. 5.9 and 5.10). The endolymphatic sac lies on the posterior fossa dura inferior to Donaldson's line and medial to the labyrinth. Surgical exposure of the endolymphatic sac is carried out through the retrofacial air cells tract in the area and bounded anteriorly by the mastoid segment of the facial nerve, posteriorly by the posterior fossa plate, superiorly by the posterior semicircular canal, and inferiorly by the jugular bulb.

As the endolymphatic sac extends toward and emerges from under the operculum, the distance between the sac and the posterior canal increases to about 2 mm of dense bone. The sac would be identifiable within the dura immediately inferior and lateral to the operculum. However, the position of the extraosseous component of the sac varies considerably, and it may not be present [36].

Poor pneumatization of the mastoid and a prominent sigmoid sinus may close the way to the sac.

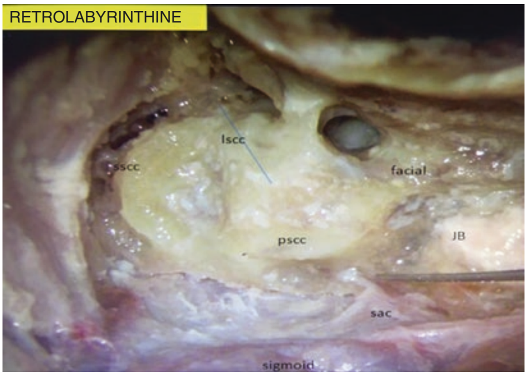

Fig. 5.10 Retrolabyrinthine approach of right ear after dissection of the three semicircular canals to show the endolymphatic sac. The blue line represents Donaldson's line. *lscc* lateral semicircular canal, *pscc* posterior semicircular canal, *sscc* superior semicircular canal

5.4.2.2.2 The Petromastoid Canal

The petromastoid canal runs from the posterior cranial fossa to the mastoid antrum; it is usually a closed vestige. It starts at the subarcuate fossa, situated on the posterior surface of the temporal bone superiorly and posteriorly in relation to the internal auditory canal. It traverses the temporal bone laterally underneath the superior semicircular canal and above the lateral semicircular canal to reach the mastoid antrum (Figs. 5.11 and 5.12). It

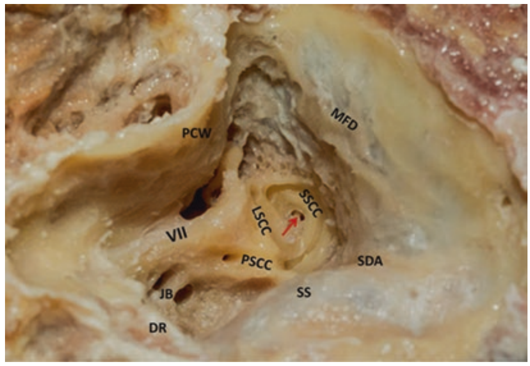

Fig. 5.11 Left temporal bone mastoidectomy with dissection and opening of the three semicircular canals showing the mastoid opening of the petromastoid canal (red arrow). *lscc* lateral semicircular canal, *pscc* posterior semicircular canal, *sscc* superior semicircular canal, *SDA* sinodural angle, *DR* digastric ridge, *SS* sigmoid sinus, *MFD* middle fossa dura, *PCW* posterior canal wall, *VII* mastoid segment of facial nerve, *JB* jugular bulb

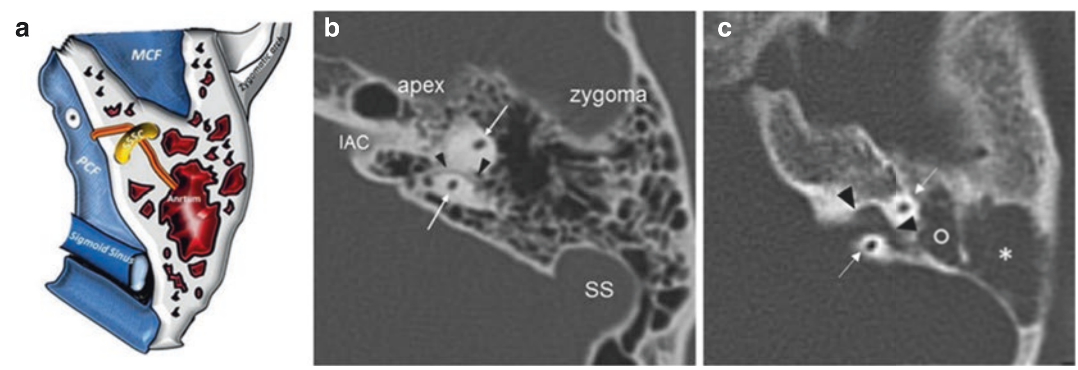

Fig. 5.12 (**a**) Schema showing a right petromastoid canal taking origin from the posterior cranial fossa (*PCF*) anterosuperior to the internal auditory canal (*) and passing below the superior semicircular canal SSCC to the antrum. *MCF* middle cranial fossa. (**b**) Transversal CT image of a left ear with a very thin aspect of the petromastoid canal (*arrowheads*) passing in between the two arms of the superior semicircular canal (*arrows*). *SS* sigmoid sinus, *IAC* internal auditory canal. (**c**) Transversal CT image of a left ear of a young child with a hypoplastic oval window and associated stapes malformation; showing also a patent large petromastoid canal (*arrowheads*), antrum (○) and mastoid condensations (*); the two arms of the SSCC (*arrows*)

establishes a potential communication between the mastoid cavity and the endocranium. If it is patent, it may be a cause of recurrent meningitis secondary to otomastoiditis (Fig. 5.12c).

5.4.2.2.3 The Mastoid Segment of the Facial Nerve

The vertical part of the Fallopian canal drops down in the anterior wall of the mastoid cavity in a plane almost parallel to the posterior wall of the external auditory canal. It passes through a compact lamina of bone known under the name of the arclied pre-mastoid lamina.

In adults, the inferior part of the antrum neighbors the second genu of the facial nerve. The facial nerve must be recognized as it emerges from the tympanic cavity between the horizontal semicircular canal medial and the short process of the incus. The incudal process is always more than 2 mm lateral to the facial nerve, and it is an important landmark to localize the facial nerve.

In children, the antrum is highly situated in relation to the facial nerve; therefore, the surgical approach to the antrum has a low risk for an eventual VII injury.

The distance from the vertical segment of the facial nerve to the posterior fossa dura ranges from 5 to 10 mm [7]. The distance between the mastoid segment of the facial nerve canal and the sigmoid sinus is highly variable; it is around 4 mm [37]. The distance between the facial nerve and the tympanic membrane annulus is about 2–3 mm (Fig. 5.13). The lower one-third of the mastoid segment of the facial nerve is in close proximity to the digastric ridge where the nerve is always medial and anterior to this structure. The digastric ridge represents a landmark for the facial nerve identification. At this level, the sigmoid sinus passes medially to the facial nerve (Fig. 5.14). In a poorly pneumatized temporal bone, the digastric ridge may be difficult to identify.

The facial nerve exits the Fallopian canal via the stylomastoid foramen. The mean depth of the facial nerve from the mastoid cortex at the stylomastoid foramen is 13 mm.

Fig. 5.13 Right mastoidectomy with posterior tympanotomy (PT) showing the relation of the facial nerve (VII) with the sigmoid sinus and jugular bulb (JB). *M* malleus; *I* incus

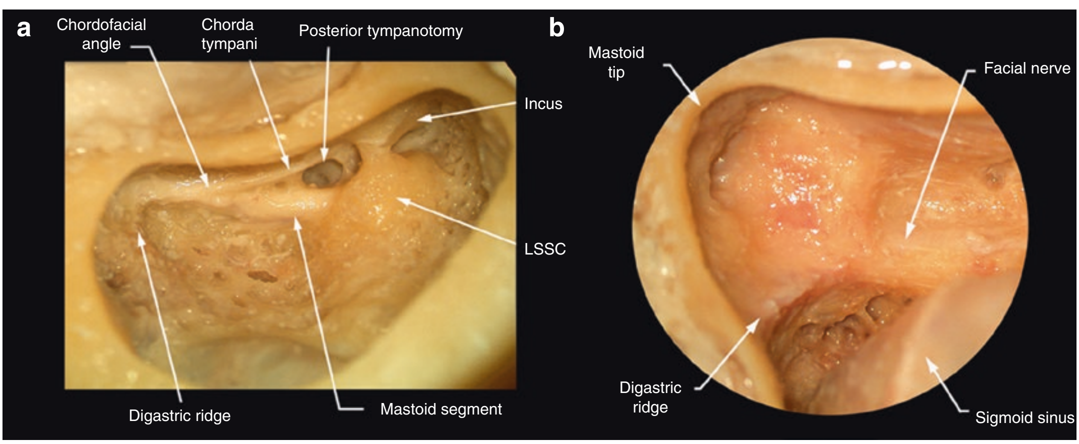

Fig. 5.14 (**a**) Microscopic view of posterior tympanotomy and the relationship between the second genu, the incus, and the lateral semicircular canal (*LSCC*). (**b**) View of the mastoid tip showing the relationship between the digastric ridge and the facial nerve

5.4.2.2.4 The Sigmoid Sinus

The sigmoid sinus is a continuation of the transverse sinus. It passes through the mastoid process in an anteroinferior direction to join the jugular bulb, forming a curvature with an anterior angle. The posterosuperior part of the sigmoid sinus is the most superficial part; then the sinus lays gradually deeper in the mastoid process. Inferiorly, at the level of the mastoid tip, it passes medial to the digastric ridge and the facial nerve to join the jugular bulb (Fig. 5.15).

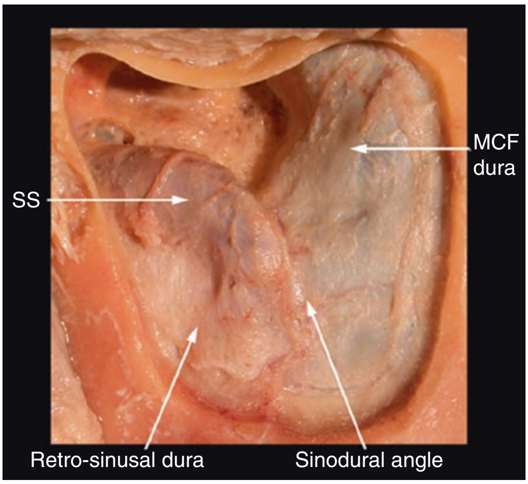

Fig. 5.15 Left enlarged mastoidectomy for skull base approaches with exposure of sigmoid sinus (*SS*). *MCF* middle cranial fossa

At the junction with the jugular bulb, the sigmoid sinus receives the inferior petrosal sinus, which courses along the inferior portion of the posterior surface of the petrous pyramid. The superior petrosal sinus enters the sigmoid sinus at its junction with the transverse sinus. Both the superior and the inferior petrosal sinuses are connected to the cavernous sinus. The inferior petrosal sinus is also connected to the basilar plexus (Fig. 5.16).

The position of the sigmoid sinus with respect to the external auditory canal is variable. The distance from the sigmoid sinus to the posterior external auditory canal ranges from 10 to 20 mm [37]. This distance is dependent on the degree of the mastoid pneumatization. The sigmoid sinus could be very anterior in poorly pneumatized bones (Fig. 5.17). In a well-pneumatized mastoid process, the lateral aspect of the sigmoid sinus could be covered by mastoid air cells (Fig. 5.27).

- **The superior petrosal venous sinus (SPS)** is located at the junction between the middle and posterior cranial fossae. It originates in the cavernous sinus and passes dorsolaterally to drain into the transverse-sigmoid junction. It runs in the superior petrosal sulcus that begins from the posterolateral base of the petrous ridge and travels at an anteromedial angle toward its apex. It receives drainage from the

Fig. 5.16 Schema showing a right sigmoid sinus and its connection with the cavernous sinus through the superior and inferior petrosal sinuses. *JB* jugular bulb

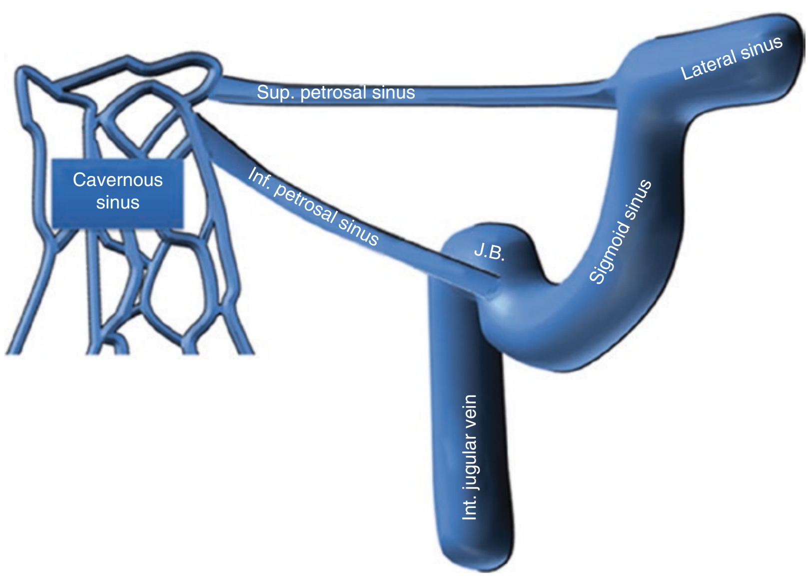

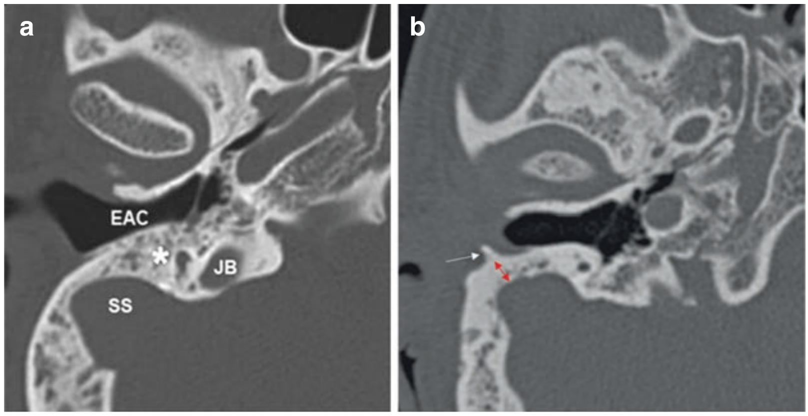

Fig. 5.17 Transversal computed tomographic view of a sclerotic mastoid (*) of a right ear; (**a**) advanced and lateralized sigmoid sinus (SS). *JB* jugular bulb, *EAC* external auditory canal. (**b**) The thin retromeatal cortical bone (red double arrow) is measured immediately behind Henle's spine (white arrow)

cerebellum, the inferior cerebellar vein, and the veins of the tympanic cavity. The SPS runs above the trigeminal ganglion and below the oculomotor and trochlear nerves.

- **The inferior petrosal sinus** is situated in the inferior petrosal sulcus, formed by the junction of the **petrous** part of the temporal bone with the basilar part of the occipital bone. It begins in the posteroinferior part of the cavernous sinus and, passing through the anterior part of the jugular foramen, terminates in the superior bulb of the internal jugular vein. It receives the internal auditory veins, veins of the medulla oblongata, the pons, and the undersurface of the cerebellum.

Surgical Implication: Sigmoid Sinus Variations

The most common anatomic variant of the sigmoid sinus is its anterior displacement. This situation can obscure the view of the mastoid structures and pathology and eventually require a decompression to improve access to the needed structures (Figs. 5.17 and 5.18). Decompression is accomplished by removing bone around the sinus itself leaving a bony island plate that can be pressed down on the sinus without significant risk of tearing the sinus.

Also bipolar cauterization of the sinus wall makes the sinus shrink and secondarily increase the space for a comfortable surgical approach.

5.4.2.2.5 The Posterior Fossa Dural Plate

The posterior fossa dural plate is a thin plate of bone that separates the mastoid antrum and mastoid air cells from the posterior cranial fossa. It is demarcated by the superior petrosal sinus superiorly, by the sigmoid sinus latero-inferiorly, and by the posterior semicircular canal medially (Fig. 5.19).

5.4.2.2.6 The Tegmen Antri

The tegmen antri is the part of the tegmen lying above the mastoid antrum. It separates the antrum from the overlying middle fossa dura and the temporal lobe (see Sect. 2.5.2., Figs. 2.30 and 2.36).

5.4.2.2.7 Trautman's Triangle

Trautman's triangle is an imaginary triangle bounded by the tegmen, the superior petrosal sinus, the sigmoid sinus, and the bony labyrinth (Fig. 5.19). Most of the posterior fossa dura is included in Trautman's triangle. In well-pneumatized temporal bones, the distance between the sigmoid sinus and the labyrinth may measure up to 10 mm. This distance may be much smaller. Exposure of Trautman's triangle is essential for the most neurosurgical approaches through the temporal bone. The access from the mastoid cavity to the posterior cranial fossa is gained by traversing this triangle.

5.4.2.2.8 The Sinodural Angle (The Citelli Angle)

The Citelli angle is the angle between the middle fossa and the posterior fossa dural plates

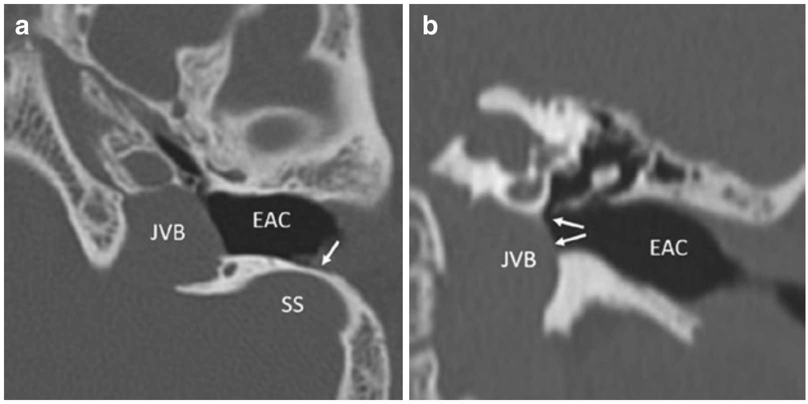

Fig. 5.18 Extremely advanced sigmoid sinus (SS) and very huge jugular vein bulb (JVB). EAC; external auditory canal. (**a**) Axial CT image, the posterior tympanic bone is of 1 mm thickness (arrow); (**b**) coronal CT image showing the retracted tympanic membrane (arrows) on the jugular bulb

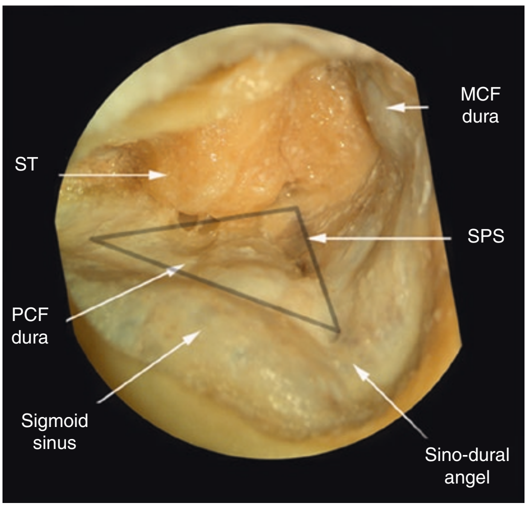

Fig. 5.19 Cadaveric large mastoidectomy showing the middle cranial fossa (*MCF*) and posterior cranial fossa (*PCF*) dura, the sinodural angle, and the imaginary Trautman's triangle (*black lined triangle*). *ST* solid triangle, *SPS* superior petrosal sinus

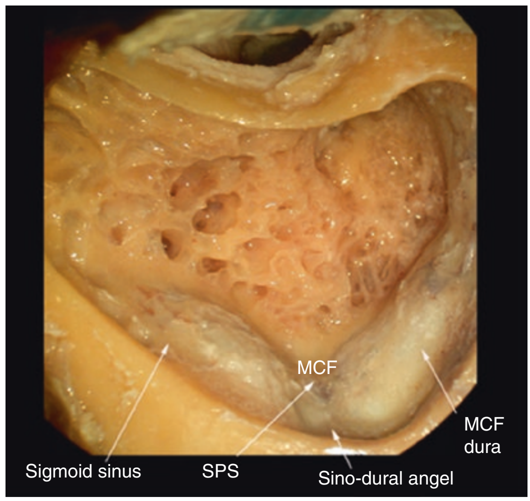

Fig. 5.20 Left mastoidectomy, showing the sinodural angle. *SPS* superior petrosal sinus, *MCF* middle cranial fossa

(Figs. 5.19 and 5.20). In a well-pneumatized mastoid, this angle is occupied by many small air cells, called Citelli cells. These cells must be completely exenterated during mastoidectomy for chronic suppurative otitis media; otherwise, persistent disease, infection, or residual cholesteatoma in these cells may lead to recurrence of the pathology. In certain cases, drilling deep enough down into the angle to expose the superior petrosal sinus is mandatory in order to dissect all these cells.

5.4.2.2.9 Koerner's Septum

Koerner's septum is a dense bony plate of the bone in the plane of fusion of the two primordia sacci of the mastoid antrum: the saccus medius and the saccus superior (see Sect. 4.1). This septum divides the mastoid process into a superficial squamous portion and a deep petrous portion. Koerner's septum extends from the posterior wall of the external auditory canal; it disperses in the air cells close to the middle fossa plate, the sinodural angle, and the sigmoid sinus plate; it then runs inferiorly lateral to the facial canal as it proceeds to the mastoid tip.

Surgical Implication: Koerner's Septum
During mastoid surgery, a well-developed Korner's septum may be mistaken for the medial wall of the antrum. If it is not recognized, the deep part of the antrum would not be exposed. A preoperative high-resolution CT scan of the temporal bone may demonstrate the presence of this septum (Fig. 5.1).

5.4.3 The Aditus Ad Antrum

The mastoid antrum communicates anteriorly with the middle ear attic through a narrow pathway called the *aditus ad antrum*.

The aditus ad antrum is a short and restricted bony canal situated at the posterior prolongation of the attic. It has a triangular shape with dimensions of 4 × 4 × 4 mm. In adults, the aditus is present in the upper part of the anterior wall of the mastoid antrum. However, in newborns and infants, it is present in the middle part of this wall. This is because of the postnatal migration of the mastoid antrum downward.

The aditus ad antrum is bounded:

- *Superiorly* by the tegmen
- *Medially* and *inferiorly* by the lateral semicircular canal; the second genu of the facial nerve being there inferior and medial to the LSCC
- *Laterally* by the scutum

At the level of the aditus, the lateral semicircular canal, the short process of the incus, and the second genu of the facial nerve are all closely related. The lateral semicircular canal is seen as a solid whitish bony prominence positioned from anterosuperior to posteroinferior at approximately 30° angle from the aditus. *The second genu of the facial nerve lies just inferior and medial to the lateral semicircular canal* (Figs. 5.21 and 5.22).

5.4.4 The Mastoid Air Cells

The mastoid air cell system is categorized according to the various regions of the temporal bone. These air cells include:

5.4.4.1 Squamo-mastoid Cells

These air cells are limited to the mastoid process itself and are subdivided into:

- *The antrum.*
- *The central mastoid tract*, which is the direct extension of the antrum inferiorly.
- *The peripheral mastoid area* arising from the antrum; the peripheral tract is further subdivided into:
  - *Tegmental cells* above the external auditory canal
  - Posterosuperior cells (*sinodural angle*)
  - *Sinusal cells* posteroinferior (around the sigmoid sinus)
  - *Facial cells* (around the mastoid portion of the facial nerve)
  - *Mastoid tip cells*, which are divided into medial and lateral groups by the digastric ridge

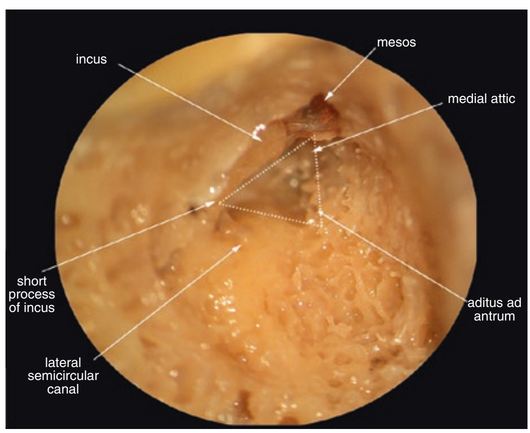

Fig. 5.21 Left mastoidectomy showing the aditus ad antrum (imaginary triangle)

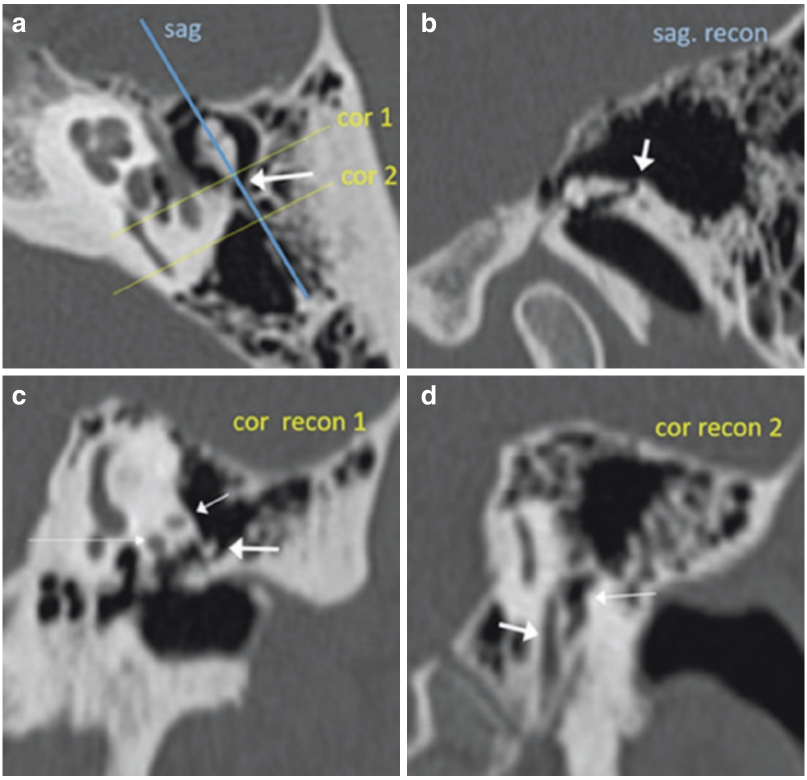

Fig. 5.22 (**a**) Transverse CT image passing by the aditus ad antrum (arrow) of a left ear. Reference lines for the three following reconstructions are drawn inside the figure. (**b**) Sagittal reconstruction along the incudomalleolar axis showing the position of the short process of the incus facing the aditus (arrow). (**c**) Coronal reconstruction (1) passing by the aditus, showing the short incus process (thick arrow), the LSCC (short thin arrow), the facial nerve at the second genu (long arrow). (**d**) Coronal reconstruction (2) more posteriorly than (1): showing the vertical third portion of the facial nerve (short arrow) and the facial recess (long arrow)

Depending on their extension in regard to the sigmoid sinus, the mastoid cells are classified into presinusoidal, sinusoidal, and postsinusoidal mastoid cells.

5.4.4.2 Petrous Cells

The petrous cells are subdivided into perilabyrinthine cells and apical cells (Figs. 5.23 and 5.24).

5.4.4.2.1 Perilabyrinthine Cells

These are the air cells surrounding the labyrinth; they include:

1. The supralabyrinthine cells, subdivided into posterosuperior, posteromedial, and subarcuate cells [1, 38]:
   - *The posterosuperior cells*, arising from the antrum, are located around the superior semicircular canal and along the posterior surface of the petrous bone above the internal auditory canal.
   - *The posteromedial cells* extend along the posterior surface of the petrous bone beneath the posterosuperior cells toward the posterior wall of the internal auditory canal [39].
   - *The subarcuate cells* extend through the arch of the superior semicircular canal into the subarcuate fossa [1, 38].
2. The infralabyrinthine cells extend inferior to the labyrinth. Air cells may be found extending from the mastoid, middle ear, and follow-

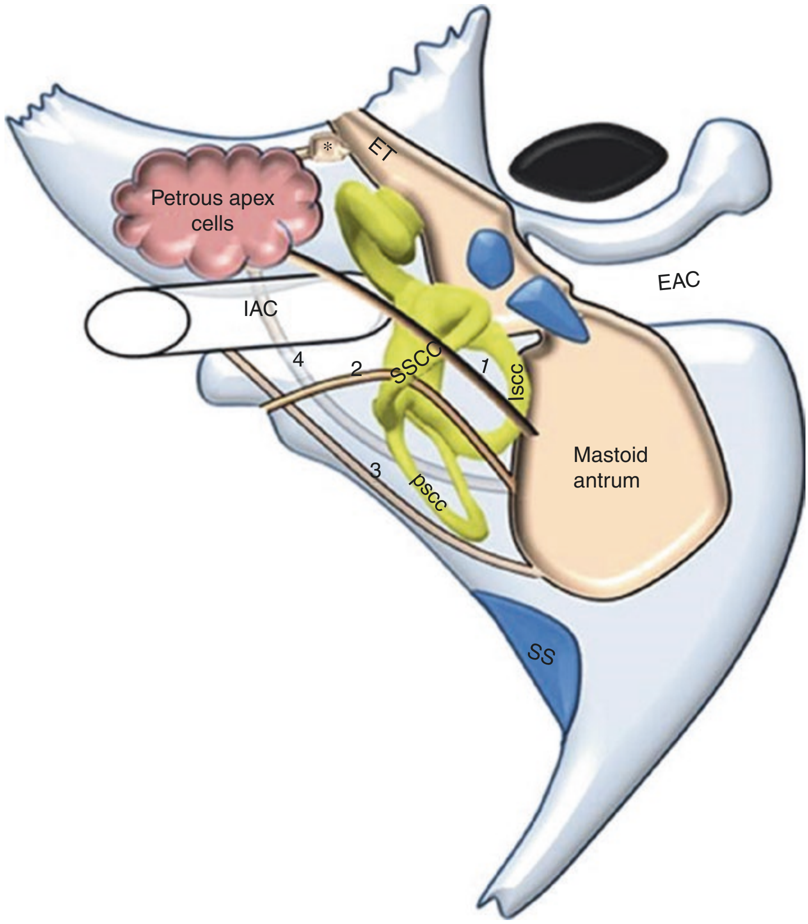

Fig. 5.23 Schematic drawing showing perilabyrinthine cells: *1* supralabyrinthine cells, *2* subarcuate cells, *3* posteromedial cells, *4* infralabyrinthine cells, (*) peritubal cells, *SS* sigmoid sinus, *IAC* internal auditory canal, *EAC* external auditory canal, *ET* Eustachian tube, *lscc* lateral semicircular canal, *pscc* posterior semicircular canal, *sscc* superior semicircular canal

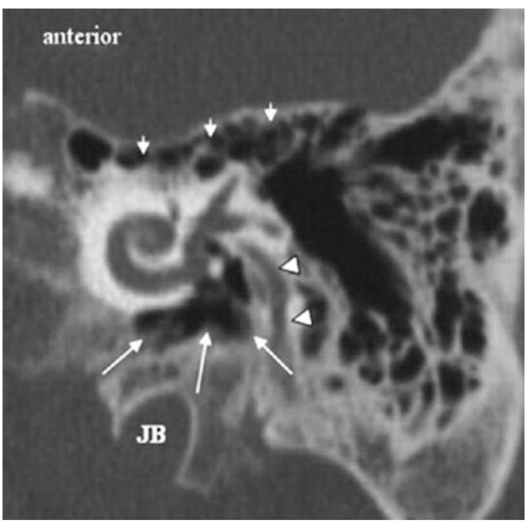

Fig. 5.24 Sagittal oblique computed tomographic reconstruction showing the supralabyrinthine air cells (*small arrows*) and the infralabyrinthine air cells (*long arrows*). Mastoid segment of the facial nerve (*arrow heads*). Jugular bulb (*JB*)

ing tracts above and below the cochlea and into the petrous apex.

Careful inspection of the hypotympanum in primary surgery for chronic ear disease and exenteration of the hypotympanic and proximal infralabyrinthine cell tract are advocated when these regions contain cholesteatoma (Fig. 5.25) or extensive granulomatous disease [40].

5.4.4.2.2 Apical Cells

The apical cells are located medial to the internal auditory canal (IAC) and posteromedial to the carotid canal.

The degree of pneumatization of the petrous apex is variable, and it is correlated with the extent of the mastoid cells [1, 38, 39]. The petrous apex is usually occupied by a soft bone marrow and contains no air cells, so defined as diploic petrous apex. However, 30% of patients have a petrous apex which contains air cells (pneumatized petrous apex) (Fig. 5.26) [17, 39]. The apical cells communicate with the perilabyrinthine cells laterally and with the peritubal cells anteriorly.

5.4.4.2.3 Accessory Air Cells

These cells include zygomatic, occipital, squamous, and styloid air cells (Fig. 5.26).

5.5 CT Evaluation

CT scan evaluation of the temporal bone is considered to be the best modality to assess the mastoid air cell system and the type of pneumatization (Fig. 5.28).

The pneumatization of the mastoid air cell system can be divided into three types:

1. Sclerotic mastoid—pneumatization is absent.
2. Diploic mastoid—pneumatization is sparse.
3. Pneumatic mastoid—normal or very extensive pneumatization.

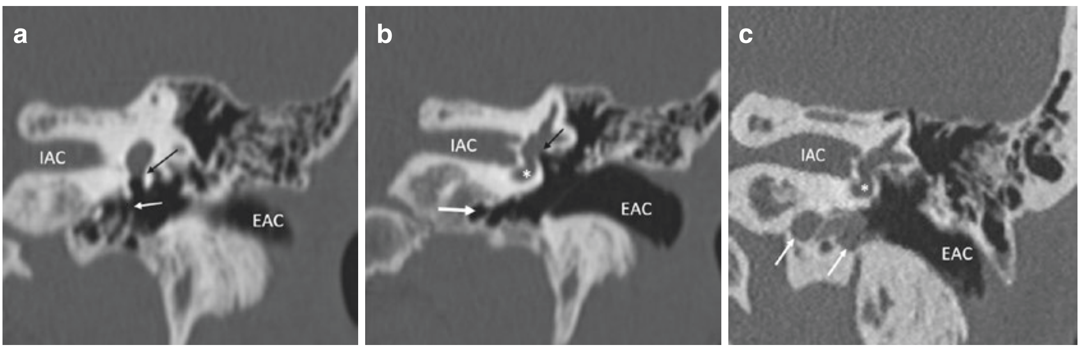

Fig. 5.25 Coronal CT-images of left ears: **(a)** CT-slice passing at the level of the round window (black arrow), with entry of the subcochlear canaliculus (white arrow). **(b)** CT-slice passing slightly more anterior through the level of the oval window (black arrow). Infracochlear cells are well aerated (white arrow). **(c)** same slice level as in **(b)** in another patient with intratympanic cholesteatoma: the infracochlear cells are obliterated (white arrows) by the pathology. (*) basal turn of the cochlea. *IAC* internal auditory canal, *EAC* external auditory canal

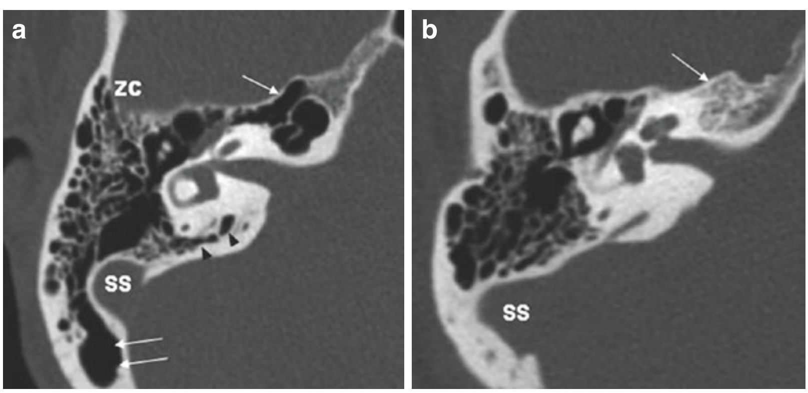

Fig. 5.26 Computed tomography of right ears. (**a**) Well-pneumatized petrous apex (*arrow*) with well-pneumatized postsinusoidal cells (*double arrows*), posteromedial retrolabyrinthine cells (*arrowheads*), and zygomatic cells (*ZC*). (**b**) Diploic petrous apex (*arrow*); *SS* sigmoid sinus

Clinical Implication

A communication between the mastoid antrum and the petrous apex exists through the perilabyrinthine cells (Figs. 5.23, 5.26). The spread of an ear infection can involve the air cells around the petrous apex leading to osteomyelitis of the petrous apex, "petrous apicitis." Inflammation of this region may involve the sixth cranial nerve at the Dorello's canal and the fifth cranial nerve in the Meckel's cave giving symptoms of Gradenigo syndrome with the triad of a discharging ear, retro-orbital pain due to the involvement of trigeminal ganglion, and diplopia (see Fig. 5.27).

5.6 *Addendum:* Role of the Mastoid Air Cell System Volume

5.6.1 Gas Exchange

The mastoid air cells please very important roles in the physiology and mechanics of middle ear:

The mastoid air cell system is covered with a vascularized cuboidal epithelium that lacks cilia and goblet cells. The distance between the submucosal blood vessels and the mucosal surface of this epithelium is rather close resembling that of the alveoli where extensive *gas exchange* takes place. The surface of this epithelium is greatly increased by air cell's bony septa by which the volume is subdivided into multiple small cavities. The mastoid gas cell system constitutes the most important volume of the middle ear cleft and therefore represents the major part of the middle ear cleft mucosal area available for vascular gas exchange [41]. The total area of mucosal surface affects the gas exchange rate; thus *increased mastoid pneumatization enhances the ability of regulating middle ear pressure* [42].

5.6.2 Buffer System

The mastoid air cell system serves as a reservoir of air and a *buffer system* to replace air in the middle ear cavity temporarily in case of Eustachian tube dysfunction.

The tympanic cavity has a volume ranging from 0.5 to 1 ml; the mastoid air cell system volume is reported to be of 1–21 ml. The mastoid air volume "dilutes" pressure changes relatively to its size: the volume change required to alter a given pressure in an average (6 ml) mastoid is six-fold that which is needed in a small (1 mL) mastoid.

The cell system can be seen as a passive container, an extra volume serving to buffer pressure changes for example, when a small volume of gas is absorbed from the mastoid air cells by diffusion, and the Eustachian tube is closed, the resulting pressure change will be less in the presence

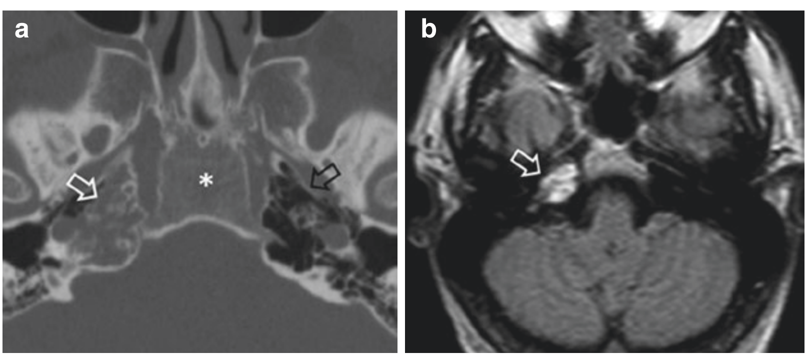

Fig. 5.27 Gradenigo syndrome on the right side: (**a**) axial CT image with condensation images of the whole right petrous apex (empty white arrow) and focal thinning of the trabeculations. Normal widely pneumatized petrous apex on the contralateral side (empty black arrow); clivus (*). (**b**) Axial flair MRI showing a hyperintense petrous apex on the right side

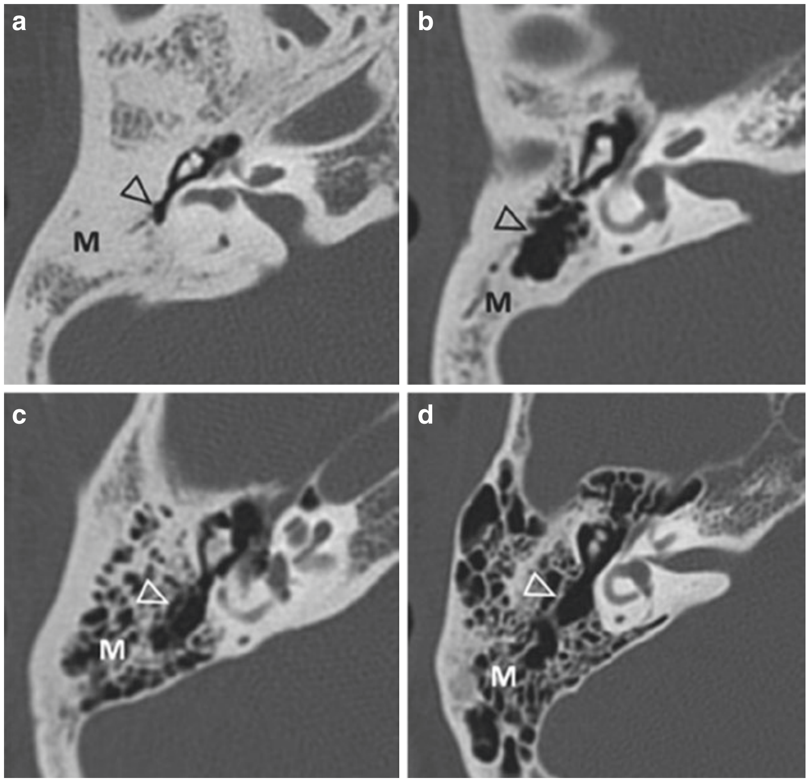

Fig. 5.28 Transversal computed tomographic views on right ears with different pneumatization status. Antrum (arrowhead), mastoid (M): (**a**) totally sclerotic mastoid with tiny antrum, (**b**) poorly pneumatized/diploic mastoid, (**c**) normal pneumatization of mastoid and antrum, (**d**) very well-pneumatized mastoid

of a well-pneumatized mastoid in comparison to a sclerotic mastoid. At the same time, the extra volume of the cell system implies negative consequences. Once a certain pressure level is induced, as, for example, a negative intratympanic pressure induced by sharp sniffing or when landing in an aeroplane, the amount of gas that must ultimately be passed through the Eustachian tube to eliminate this pressure change will be larger in the presence of a well-pneumatized mastoid, as compared with a sclerotic one.

5.6.3 Middle Ear Mechanics

The greater the volume of middle ear cleft air cells, the more compliant is the system.

The middle-ear air space in normal ears may play a role in some of the variability observed in ear-canal based acoustical measurements on normal populations. For instance, variations in volume of the middle-ear air space result in variations in the middle-ear air space impedance which can affect the middle-ear impedance at the tympanic membrane by as much as 10 dB at frequencies greater than 1000 Hz. This effect can contribute to intersubject variations in both impedance measurements and otoacoustic emissions measured at the tympanic membrane [43].

The volume of human middle-ear air has important acoustical effects and is known to be important in determining middle-ear sound transmission in several pathological middle-ear conditions. The volume of the middle-ear air space plays a major role in middle-ear function in ears with tympanic membrane perforations or tubes at frequencies below about 1000 Hz. In some pathological ears, the air volume of the middle-ear air space can influence the sound produced by hearing aids [44–47]. The mastoid air cell system plays a role in middle ear pressure regulation able to modify sound transmission. Well-pneumatized mastoids had larger volumes which add to the resonance of hearing in contrary to sclerotic mastoids that offer less resonance. Therefore, in case of tympanic membrane perforation, hearing loss varies inversely to the volume of middle ear and mastoid (pneumatization status of the mastoid): other factors, as size and location of the perforation, being the same, the air bone gap varies up to 35 dB depending of the air volume in the ME and mastoid. This is an important knowledge with regard to the effect of transmission of sound in hearing. *While treating patients with tympanic membrane perforations, the clinician should consider not only the size of the perforation but also the mastoid air space volume while evaluating hearing loss and chance of success of postoperative hearing recovery.*

5.6.4 As Protector

The mastoid air cell system plays a role in the absorption and dispersion of kinetic energy during direct lateral temporal bone trauma, thus protecting the vital structures in the temporal bone [43].

References

1. Allam AF. Pneumatization of the temporal bone. Ann Otol Rhinol Laryngol. 1969;78:48–64.
2. Bast TH, Forester HB. Origin and distribution of air cells in the temporal bone. Arch Otolaryngol. 1939;30:183–205.
3. Bast TH, Anson BJ. The temporal bone and the ear. Springfield: Charles C Thomas; 1949. p. 162–291.
4. Cinamon U. The growth rate and size of the mastoid air cell system and mastoid bone: a review and reference. Eur Arch Otorhinolaryngol. 2009;266(6):781–6.
5. Virapongse C, Kirschner JC, Sasaki C, et al. Computed tomography of Koerner's septum and the petrosquamosal suture. Arch Otolaryngol Head Neck Surg. 1986;112:81–7.
6. Diamant M. Otitis and pneumatization of the mastoid bone. Acta Otolaryngol (Suppl) (Stockh). 1940;41:1–149.
7. Wittmaack K. Über die normale und Pathologische Pneumatisation des Schläfenbeins einschließlich ihrer Beziehungen zu der Mittelohrerkrankungen. Jena: Fischer; 1918. p. 1–64.
8. Gans H, Wlodyka J. Mastoid pneumatization in chronic otitis media. Acta Otolaryngol. 1966;33:343–6.
9. Palva T, Palva A. Size of the human mastoid air cell system. Acta Otolaryngol. 1966;62:237–51.
10. Hug JE, Pfaltz CR. Temporal bone pneumatization. A planimetric study. Arch Otorhinolaryngol. 1981;233:145–56.
11. Tos M. Mastoid pneumatization. A critical analysis of the hereditary theory. Acta Otolaryngol. 1982;94:73–80.
12. Ueda T, Eguchi S. Distribution of pneumatization of the temporal bone in chronic otitis media seen during the age of antibiotic therapy. J Otol Rhinol Laryngol (Japan). 1962;64:1539–42.
13. Schulter-Ellis F. Population differences in cellularity of the mastoid process. Acta Otolaryngol. 1979;87:461.
14. Sade J, Hadas E. Prognostic evaluation of secretory otitis media as a function of mastoidal pneumatization. Arch Otorhinolaryngol. 1979;225:39–44.
15. Holmquist J. Aeration in chronic otitis media. Clin Otolaryngol. 1978;3:278–84.
16. Sade J. The correlation of middle ear aeration with mastoid pneumatization. Eur Arch Otorhinolaryngol. 1992;249:301–4.
17. Virapongse C, Sarwar M, Bhimani S, Sasaki C, Shapiro R. Computed tomography of temporal bone pneumatization: 1 normal pattern and morphology. AJR Am J Roentgenol. 1985;145:473–81.
18. Hentona H, Ohkubo J, Tsutsumi T, Tanaka H, Komatsuzaki A. Pneumatization of the petrous apex. Nippon Jibiinkoka Gakkai Kaiho. 1994;97:450–6.
19. Tumarkin A. On the nature and significance of hypocellularity of mastoid. J Laryngol Otol. 1959;73:34–44.
20. Tumarkin A. On the nature and vicissitudes of the accessory air spaces of the middle ear. J Laryngol Otol. 1957;71:210–48.
21. Kolihova E, Abraham J, Blahova O. Rezidivierende Mittelohrentzündung im frühen Kindesalter und ihr Einfluss auf die Zellsystementwicklung des Schläfenbeins. Radiologie. 1966;12:62–5.
22. Snow JB Jr, Wackym PA, editors. Ballenger's otorhinolaryngology head and neck surgery. 17th ed. Hamilton, ON: BC Decker; 2008.
23. Tos M. Manual of middle ear surgery. New York: Thieme; 1997.
24. Lee D-H, Kim M-J, Lee S, Hana C. Anatomical Factors Influencing Pneumatization of the Petrous Apex. Clin Exp Otorhinolaryngol. 2015;8(4):339–44. https://doi.org/10.3342/ceo.2015.8.4.339.
25. Tos M. Manual of middle ear surgery, Mastoid surgery and reconstructive procedures, vol. 2. Stuttgart: Thieme; 1995.
26. Sanna M, Saleh E, Taibah A, Russo A. Atlas of temporal bone. 1st ed. Stuttgart: Thieme; 1995.
27. Aslan A, Mutlu C, Celik O, Govsa F, Ozgur T, Egrilmez M. Surgical implications of anatomical landmarks on the lateral surface of the mastoid bone. Surg Radiol Anat. 2004;26(4):263–7. Epub 2004 Jun 17.
28. Williams PL, Bannister LH, Berry MM, Collins P, Dyson M, Dussek JE, et al., editors. Gray's anatomy:

the anatomical basis of medicine and surgery. 38th ed. London: Churchill Livingstone; 1995. p. 56.
29. Anson B, Donaldson JA. Surgical anatomy of the temporal bone. 4th ed. New York: Raven; 1992.
30. Peker TV, Pelin C, Turgut HB, Anil A, Sevim A. Various types of suprameatal spines and depressions in the human temporal bone. Eur Arch Otorhinolaryngol. 1998;255:391–5.
31. Williams PL, Warwick R, Dyson M, Bannister LH. Gray's anatomy. 37th ed. Edinburg: ELBS with Churchill Livingstone; 1993.
32. Berkovitz BKB, Moxham BJ. A textbook of head and neck anatomy. London: Wolfe Medical; 1988.
33. Akabori E. Crania nipponica recentia. Analytical inquiries into the non-metric variations in the Japanese skull. Jpn J Med Sci I Anat. 1933;4:61–318, 11.
34. Romanes GJ. Cunningham's manual of practical anatomy, Head and neck and brain, vol. III. London: Oxford University Press; 1992.
35. Schwartze A. Handbuch der Ohrenheilkunde. Leipzig: Vogel; 1893.
36. Richard R Locke. Anatomy of the transmastoid endolymphatic sac decompression in the management of Ménière's disease. PhD thesis, Faculty of Biomedical and Life Sciences, The University of Glasgow; 2008.
37. Măru N, Cheiţă AC, Mogoantă CA, Prejoianu B. Intratemporal course of the facial nerve: morphological, topographic and morphometric features. Romanian J Morphol Embryol. 2010;51(2):243–8.
38. Pellet W, Cannoni M, Pech A. Basic anatomy. In: Otoneurosurgery. Berlin: Springer; 1990. p. 5–72.
39. Yamakami I, Uchino Y, Kobayashi E, Yamaura A. Computed tomography evaluation of air cells in the petrous bone—relationship with postoperative cerebrospinal fluid rhinorrhea. Neurol Med Chir (Tokyo). 2003;43(7):334–8.
40. Nadol JB Jr, Krouse JH. The hypotympanum and infralabyrinthine cells in chronic otitis media. Laryngoscope. 1991;101(2):137–41.
41. Doyle J. The mastoid as a functional rate-limiter of middle ear pressure change. Int J Pediatr Otorhinolaryngol. 2007;71:393–402.
42. Manjuran DJ, Bahuleyan B. Effect of middle ear and mastoid air space volume on acoustic transmission of sound in tympanic membrane perforation. Int J Res Med Sci. 2016;4:2611–4.
43. Stepp CE, Voss SE. Acoustics of the human middle-ear air space. J Acoust Soc Am. 2005;118(2):861–71.
44. Voss SE. Effects of tympanic-membrane perforations on middleear sound transmission: measurements, mechanisms, and models. PhD thesis, Massachusetts Institute of Technology; 1998.
45. Voss SE, Rosowski JJ, Merchant SN, Peake WT. How do tympanic-membrane perforations affect human middle-ear sound transmission? Acta Otolaryngol. 2001a;121:169–73.
46. Voss SE, Rosowski JJ, Merchant SN, Peake WT. Middle-ear function with tympanic-membrane perforations. I. Measurements and mechanisms. J Acoust Soc Am. 2001b;110:1432–44.
47. Voss SE, Rosowski JJ, Merchant SN, Peake WT. Middle-ear function with tympanic-membrane perforations. II. A simple model. J Acoust Soc Am. 2001c;110:1445–52.
48. Ilea A, Butnaru A, Sfrangeu SA, et al. Role of mastoid pneumatization in temporal bone fractures. AJNR Am J Neuroradiol. 2014;35:1398–404.

Facial Nerve

6

Contents

The facial nerve, or cranial nerve (CN) VII, is the nerve of facial expression. Due to various developmental events, the trajectory of the facial nerve is tortuous and complex from its origin in the brain stem to the muscles of the face. The ingenious pathway of the facial nerve through the middle ear and mastoid adds to the complexity and refinement of middle ear microsurgery. Thus, a thorough knowledge of the facial nerve anatomy along with its multiple landmarks is essential for an accurate, safe, and effective surgical intervention in the middle ear.

A basic understanding of the developmental anatomy of the facial nerve is necessary to anticipate the various anatomical situations that can be encountered during ear surgery.

6.1 Facial Nerve Development

The facial nerve primordium (nerve of the second branchial arch or hyoid arch) is first recognized at the fourth week of gestation as a collection of cells at the vicinity of the auditory placode, which will generate the otocyst (Fig. 6.1). These cells are derived from neural crest cells and epibranchial microplacodes of the second branchial arch. Then, the facial nerve primordium extends to the primitive geniculate ganglion region as a narrow band; meanwhile, the acoustic nerve has reached the otic vesicle [1].

The fibers of the facial nerve arise from the fourth and fifth rhombomeres of the brain stem. Congenital hypoplasia of the nerve in the mouse can result from hypoplasia of the fourth rhombomere, secondary to misexpression of Hoxa1 and Hoxb1 homeobox genes, in close association with abnormalities of second arch derivatives in the middle ear. This kind of pattern can be observed in clinical practice (Fig. 6.6) [2].

The intermediate part of the nerve (in fact, the sensory and several autonomic fibers) exits the brain stem between the vestibulocochlear nerve

S. Mansour et al., *Comprehensive and Clinical Anatomy of the Middle Ear*,
https://doi.org/10.1007/978-3-030-15363-2_6

Fig. 6.1 Frontal (asymmetric) section of a head of a E9 mouse embryo. At the right side, we observe facial nerve fibers (arrow) in contact with the rhombencephalon (Rh). At the left side, rudiment of the geniculate ganglion is visible (large arrow) at the vicinity of the otic vesicle (O) and the anterior cardinal vein (V). *I* and *II* first and second branchial arches

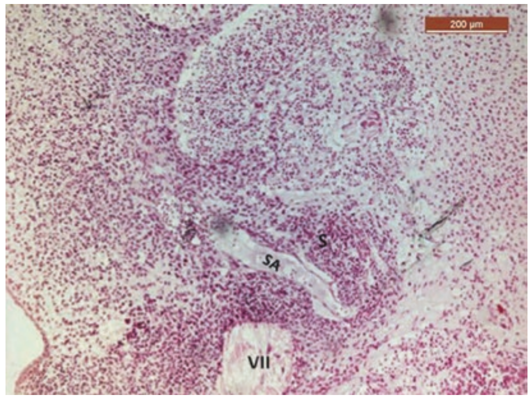

Fig. 6.2 Transverse section of a 5 week 13 mm human embryo, showing the close relationship of the facial nerve rudiment (VII) with the stapes (S) anlage, passed by the stapedial artery (SA). Hematoxylin-eosin staining

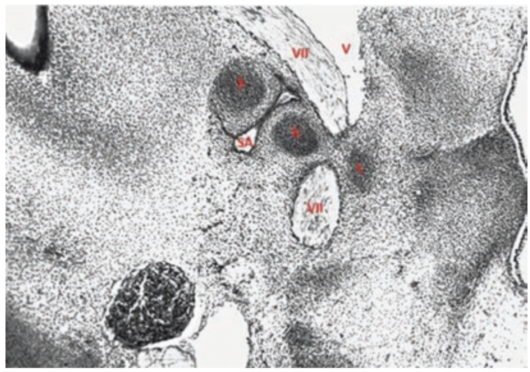

Fig. 6.3 Frontal section in a 5–6-week 15.5 mm human embryo. The facial nerve rudiment (VII) is partially covered by the laterohyale (L), derived from Reichert's cartilage, and crosses the stapes (S), itself passed by the stapedial artery (SA). The anterior cardinal vein (V) is lateral to the nerve. Hematoxylin-eosin staining

and the efferent part of the facial nerve. Because of the lesser amount of fibers, this component of the facial nerve is thinner than the motor part. The corresponding neurons lie in the geniculate ganglion [3].

In the fifth week, the facial motor nucleus can be identified in the developing brain stem. Nerve fibers leave the nucleus and pass caudal to the region of the geniculate ganglion. These fibers bend dorsally to give the horizontal segment of the nerve which passes between the developing labyrinth and the upper end of Reichert's cartilage. The upper end of Reichert's cartilage will become the blastema of the stapes (Fig. 6.2). Finally the facial nerve bends vertically before passing into the substance of the second branchial arch, recovered laterally by the *laterohyale* [1] (Fig. 6.3). During the fifth week, the chorda tympani constitutes the first branch of the facial nerve to appear. At this time, the chorda tympani nerve and the facial nerve trunk are of approximately equal size; this state could be encountered clinically in adult ears with major atresia [4]. The chorda tympani nerve (Fig. 6.3) divides into the mandibular arch to terminate in the same region as the lingual nerve ends and where the submandibular ganglion develops. The chorda tympani nerve primordium divides the mandibular ossicular blastema into malleus laterally and incus medially. By the seventh week, however, the chorda tympani nerve is smaller than the facial nerve and remains so into adulthood [4] (see Fig. 3.2).

At the phylogenetic point of view, the chorda tympani is a "pretrematic nerve" joining the second arch nerve (the facial nerve) to the first arch one (the trigeminal nerve and its lingual part), similar to the connections between branchial nerves in the first gnathostomes.

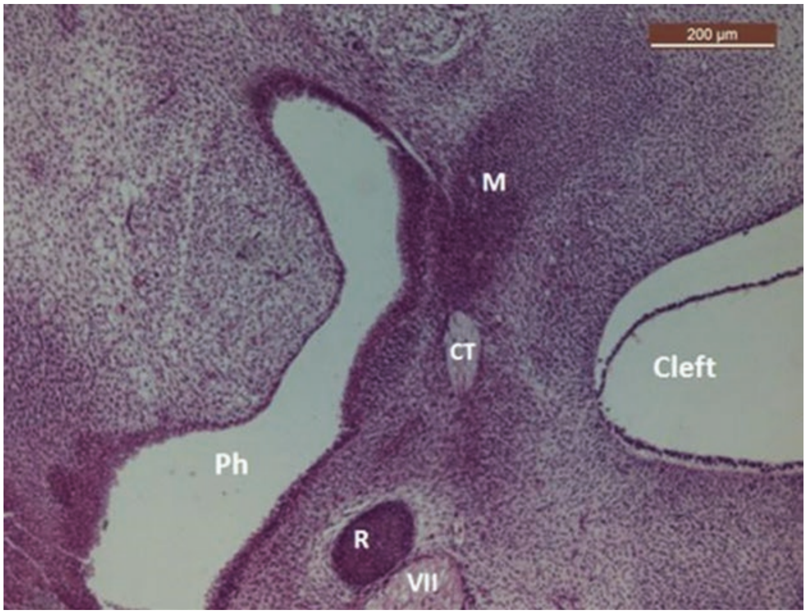

Fig. 6.4 A 5–6 week 15.5 mm human embryo, transverse section. Facial nerve is visible in close relationship with Reichert's cartilage (R). Chorda tympani (CT) is more anterior, between first and second arches, in relationship with the malleus (M). Ph first pharyngeal pouch, cleft first branchial cleft. Hematoxylin-eosin staining

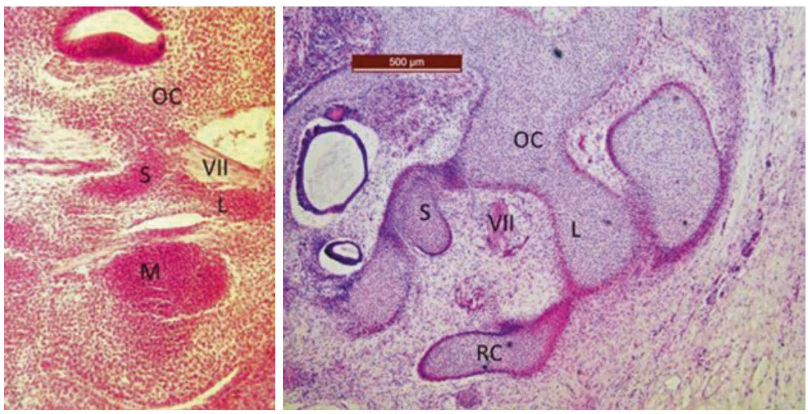

Fig. 6.5 Development of the laterohyale (L), derived from Reichert's cartilage (RC), in a sagittal section of a 14-day mouse embryo (A) and in a frontal section of a 27.5 mm human embryo. The laterohyale covers earlier the facial nerve (VII) and then fuses with the otic capsule (OC). *M* handle of malleus, *S* stapes

The mesenchyme around the facial nerve develops later into the facial nerve canal. The first cartilaginous anlage of the facial canal derives from the laterohyale (Figs. 6.3 and 6.4). The complex development of the contiguous structures, such as the stapes, the labyrinthine capsule, the mastoid bone, and the tympanic bone, will determine the ultimate trajectory of the facial nerve canal.

Originally, the facial nerve passes through a sulcus in the cartilaginous otic capsule; later this sulcus ossifies and becomes the bony canal of the facial nerve, where the lateral wall derives from the laterohyale (Fig. 6.5), called the periotic process [5].

The process of ossification of facial nerve canal has two centers:

- An anterior center: it develops at the apical cochlear ossification center by the end of the 20th week gestation.
- A posterior center: it arises at the pyramidal eminence by the 25th gestation week [3].

Each ossification center emits two bony projections that ideally encircle progressively the entire length of the facial nerve. A contribution of intramembranous bone from the periosteal layer of the otic capsule is also involved in the covering of the facial canal [2].

At term, about 80% of the tympanic segment of the Fallopian canal is ossified; the ossification is almost completed around 3 months after birth. Facial nerve dehiscence (which occurs in 25% of cases) could be related to failure of complete fusion of these two ossification centers [6] and/or to loss of intramembranous ossification of the periosteal layer of the otic capsule at the vicinity of the vestibule [2]. Some authors have proposed that the failure of ossification could be related to the persistent aperture of the stapedial artery [5, 7].

Due to the embryonic association of facial nerve with other second arch derivatives, a dehiscence of the facial canal can be associated with some middle ear or inner ear malformations (Fig. 6.6), in clinical situations as well as in experimental conditions [8].

At the end of the embryonic period, the definitive path of the facial nerve is completed, and the growth in length of the facial nerve is closely associated with the enlargement of the fetal head [7].

6.1.1 Facial Nerve Connections

At the seventh week, a ventral offshoot from the geniculate ganglion reaches the glossopharyngeal ganglion. This will form the lesser superficial petrosal nerve (LSPN). At approximately the same time, the nerve branch of the stapedial muscle appears [9]. Between the 12th and 13th weeks, two twigs from the dorsomedial surface of the facial nerve between the stapedial muscle and the chorda tympani nerve fuse together and reach the superior ganglia of the vagus (CN X) and glossopharyngeal (CN IX) nerves to give Arnold's nerve, that is the auricular branch of the vagus nerve. Arnold's nerve traverses the primitive tympanomastoid fissure and innervates the subcutaneous tissue of the posterior aspect of the external auditory canal (Ramsay Hunt area) [9]. By the 17th week, the definitive communications of the facial nerve, including those with the second and third cervical nerves (C2 and C3), the trigeminal nerve, the vagus nerve, and the glossopharyngeal nerve, are established.

Clinical Applications: **Facial Nerve in Aural Atresia**

Facial nerve abnormal trajectory is common in major aural ear atresia. This is due to the abnormal development of the tympanic bone, which normally pushes the mastoid segment of the facial nerve posteriorly. The facial nerve may be placed in the middle ear cavity, mostly between the oval and the round windows (Figs. 6.7 and 6.8) [10].

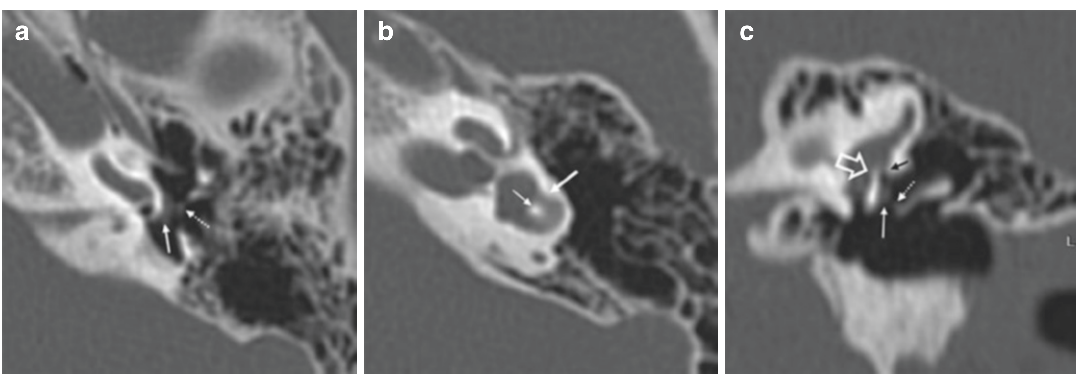

Fig. 6.6 Associated malformations of the middle and inner ear with second arch structures in a 9-year-old boy: (**a**) transverse CT image showing a low-lying facial nerve (VII, white arrow) running on the promontory. Rudimentary head of the stapes (dashed arrow) in contact with the stapedial tendon. (**b**) Associated malformation of the LSCC that harbors a very small central island (thin arrow) and shows a concave impression on the lateral arm (long white arrow). (**c**) Coronal view showing a very small rudimentary opening (black arrow) on the floor of the vestibule, in the absence of any oval window opening (empty arrow). Aberrant facial nerve trajectory (white arrow) covering the promontory. Rudimentary stapes head (dashed arrow). This abnormality is similar to experimental features obtained by knock-out of both Hoxa-1 and Hoxb-1 genes

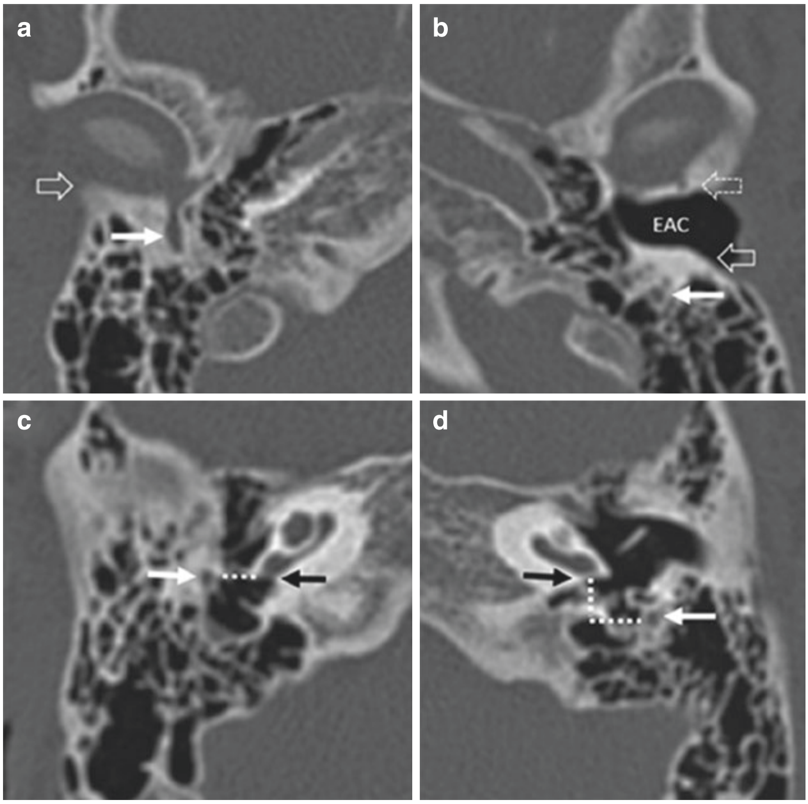

Fig. 6.7 A transversal computed tomographic view of (**a**) Right ear with complete aplasia of the tympanic bone. The anterior wall of the mastoid (empty arrow) represents the posterior wall of TM Joint. VII nerve in anterior position (plain arrow). (**b**) Normal contralateral side with anterior tympanic bone (dashed empty arrow), posterior tympanic bone (empty arrow). VII nerve (plain arrow). (**c**) Cut above (**a**), showing the anteriorly displaced VII nerve (white arrow) at the same level (dashed line) as the round window (black arrow). (**d**) Normal contralateral side showing the normal situation of the VII nerve (white arrow) clearly behind the level (dashed lines) of the round window (black arrow)

6.2 Facial Nerve Anatomy

The facial nerve is the nerve of the second branchial arch. It contains motor and somatosensory components. The somatosensory fibers of the facial nerve are carried by the nervus intermedius, or pars intermedia of Wrisberg.

The facial nerve is composed of approximately 10,000 neurons:

- 7000 myelinated neurons form the motor part of the facial nerve that innervates the muscles of the face expression and the stapedial muscle.
- 3000 neurons form the nervus intermedius with secretory and somatosensory components. They include:
  – The afferent taste fibers from the *chorda tympani* nerve, coming from the anterior two-thirds of the tongue
  – The afferent taste fibers from the soft palate via the *palatine* and *greater petrosal* nerves
  – The *parasympathetic secretory* innervations to the submandibular, sublingual, and lacrimal glands
  – The *cutaneous sensory* component from afferent fibers originating from the skin of the auricle and postauricular area and concha or Ramsay Hunt area [11]

The facial nerve exits the brain stem at the pontomedullary junction; it traverses the cerebellopontine angle (CPA) and enters the internal auditory canal (IAC), where it runs in the antero-

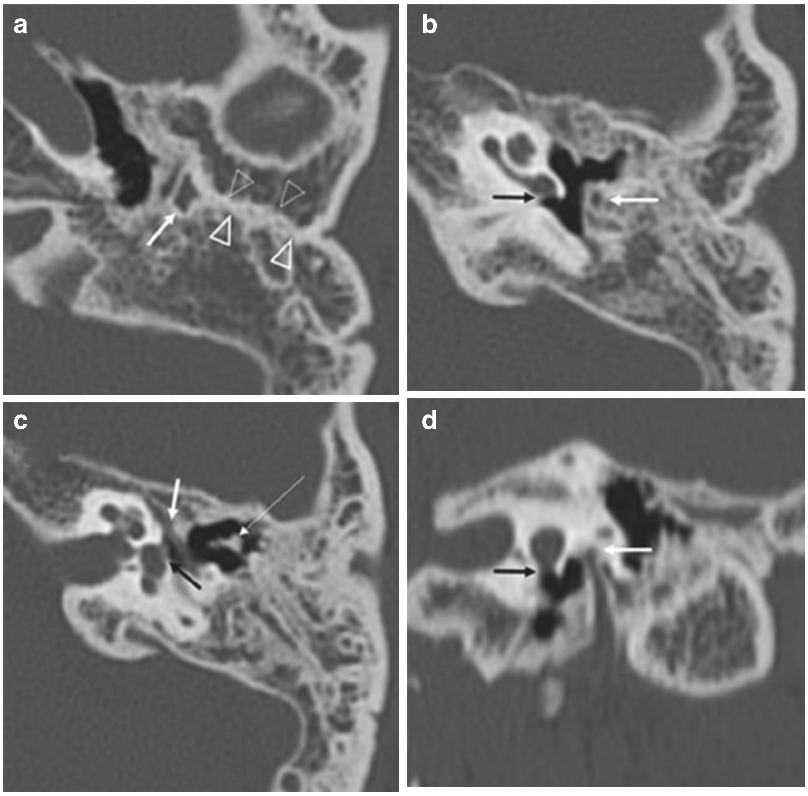

Fig. 6.8 Axial CT images passing in caudal to cranial direction through the middle ear. (**a**) Complete atresia of the tympanic bone, visibility of a petrosquamous suture at its place (empty arrowheads). Foramen styloideum (plain arrow) for the VII nerve. (**b**) Some mm above (**a**), the advanced VII (white arrow) is seen at the same level as the round window (black arrow). (**c**) Trajectory of the facial nerve (white arrow) in front of the oval window (black arrow): (VII protrusion). Rudimentary ossicular chain (long thin arrow). (**d**) Coronal CT reconstruction showing a high riding second genu of the facial nerve largely above the level of the round window

superior part of the canal. It traverses the temporal bone in a bony canal, the Fallopian canal, until it reaches the stylomastoid foramen where it exits the temporal bone anterior and medial to the digastric ridge and enters the parotid gland [12, 13] to divide into its terminal branches.

6.2.1 The Cerebellopontine Angle (CPA) Segment

The facial nerve (CN VII) leaves the brain stem at the pontomedullary junction almost 1.5 mm anterior to the vestibulocochlear nerve (VIII) [14]. The facial nerve then follows a rostro-lateral course through the cerebellopontine angle for a distance of 15–17 mm, to enter finally the porus of the internal auditory canal (IAC) in the temporal bone (Fig. 6.9).

The CPA segment of the facial nerve is 1.8 mm in diameter and is smaller than the cochleovestibular nerve (CN VIII) which is of around 3 mm [14]. A third smaller nerve, the nervus intermedius, emerges between CN VII and CN VIII.

Clinical Application

The root exit zone of the facial nerve (REZ) corresponds to a transitional area between central and peripheral myelin. At this level the facial nerve is covered by a thin layer of nerve sheath and is sensitive to compression by a vascular loop (Fig. 6.9). This neurovascular compression is responsible for almost all cases of hemifacial spasm [15–18].

6.2.2 The Internal Auditory Canal Segment (IAC)

The IAC segment of the facial nerve occupies the anterosuperior quadrant of the IAC and measures 8–10 mm; it lies superior to the cochlear nerve, and it passes above the crista falciformis [19] (Fig. 6.10). The nervus intermedius passes between the motor root of the facial nerve and the cochlear nerve (Fig. 6.11).

A crest of bone, “Bill’s bar,” hangs in the vertical plane of the fundus of the IAC between the superior vestibular nerve and the facial nerve, the latter being anterior to the vestibular nerve (Fig. 6.12). At the fundus of the IAC, the facial nerve enters the Fallopian canal. The transit zone between the IAC and the Fallopian canal is called the *meatal segment* and is the narrowest zone of the bony facial canal; it is around 0.65 mm in diameter [19]. At this zone, the nerve is only envelopped by pia mater and an arachnoid membrane because the dural investment terminates at the fundus of the IAC. The meatal segment is the most common site of facial nerve entrapment during inflammatory disorders of the facial nerve, such as Bell’s palsy and Ramsay Hunt syndrome.

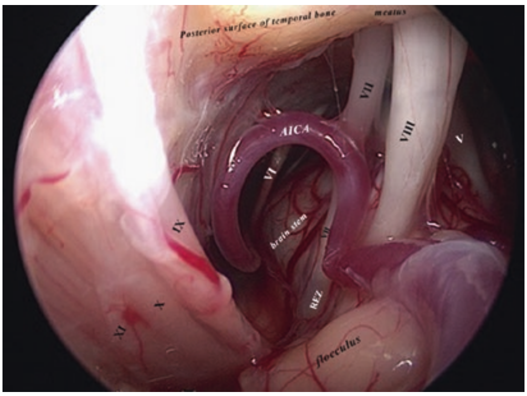

Fig. 6.9 Left cerebellopontine angle during endoscopic exploration through a retrosigmoid approach showing the facial nerve (VII) that exits from the brain stem at the REZ zone just medial to the flocculus and extends medial to the cochleovestibular nerve (VIII); they enter together the meatus of the internal auditory canal; *V* trigeminal nerve, *VI* abducens nerve, *IX* glossopharyngeal nerve, *X* vagus nerve, *XI* accessory nerve

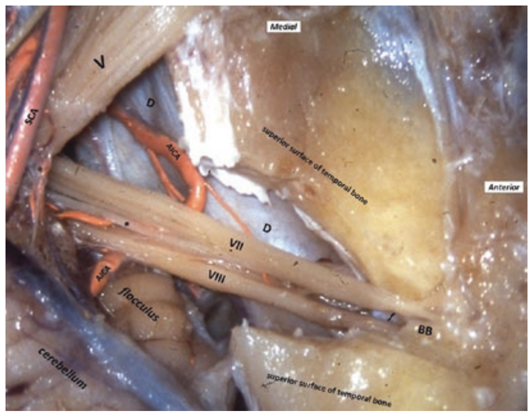

Fig. 6.11 Superior view of the right CerebelloPontine Angle showing the nervus intermedius (*) passing between the facial nerve (VII) and the cochleovestibular nerve (VIII) facial nerve (VII). At the fundus of internal auditory canal, Bill’s bar (BB) seperates VII from VIII posteriorly. *D* dura of posterior fossa extending to internal auditory canal, *AICA* anterior inferior cerebellar artery, *f* crista falciformis

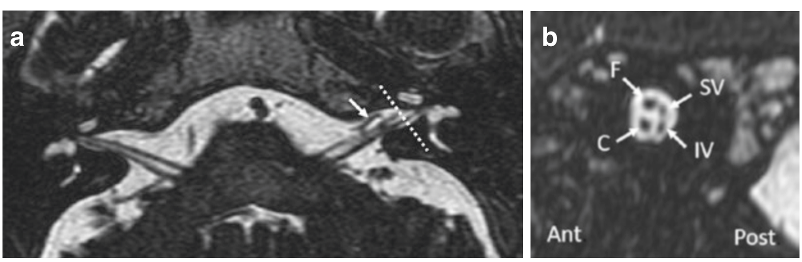

Fig. 6.10 (**a**) Axial MRI T2 3D drive (0.8 mm) with high resolution on the internal auditory canal (IAC), vascular loop (arrow) in close contact to the cranial nerves inside the canal. Dashed line: reference line for the reconstruction perpendicular to the auditory canal done in (**b**) F (facial nerve) and C (cochlear nerve) are lying superposed in the anterior part (Ant) of the IAC, and SV (superior vestibular nerve) and IV (inferior vestibular nerve) are lying superposed in the posterior part (Post) of the IAC

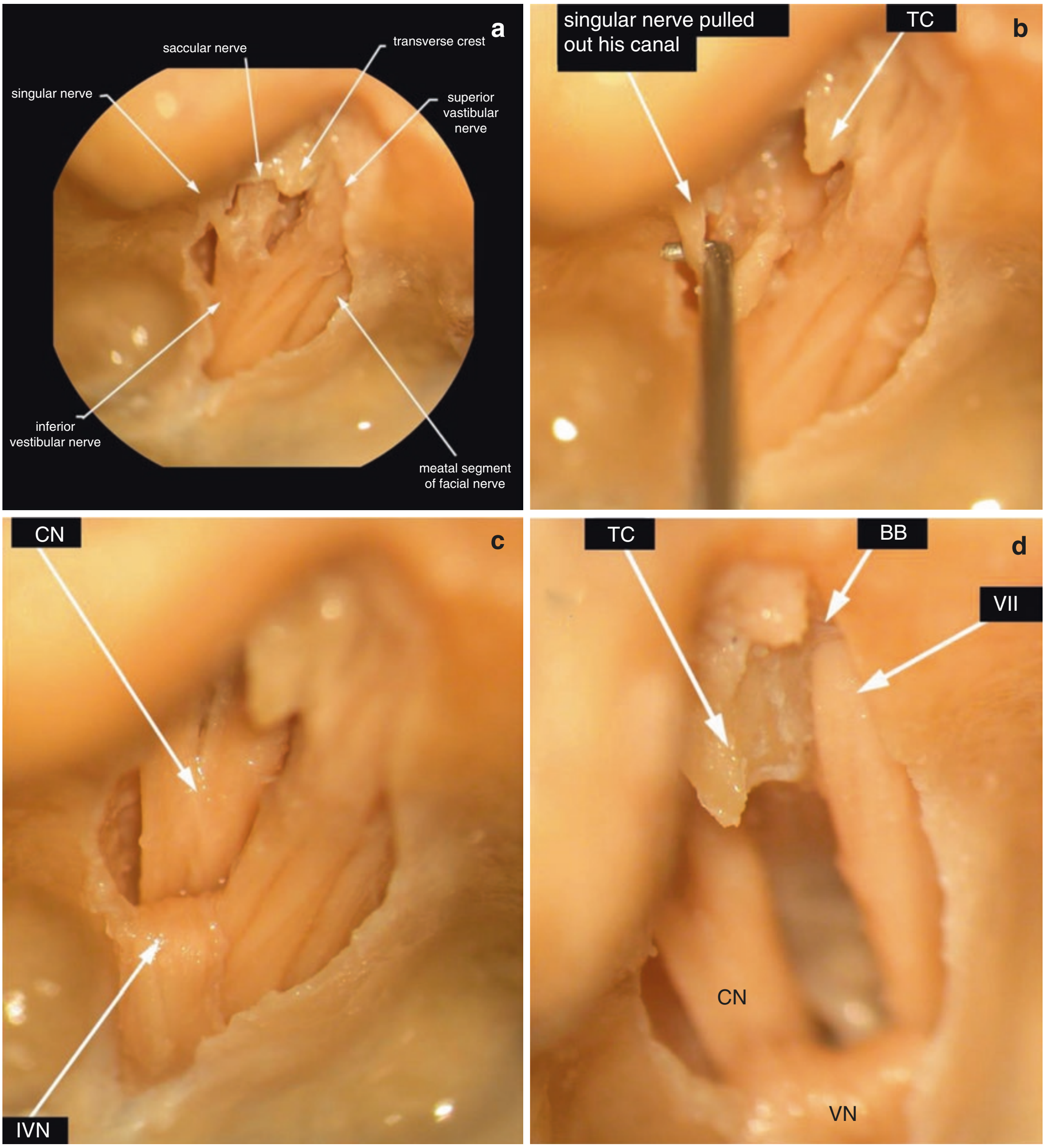

Fig. 6.12 Left ear translabyrinthine approach to the internal auditory canal (**a**) dura is opened to show the superior and inferior vestibular nerves; (**b**) the singular branch of inferior vestibular nerve is pulled out of its canal, notice the transverse crest separating the superior and inferior vestibular nerves; (**c**) after cut and reflection of inferior vestibular nerve (IVN), showing the cochlear nerve (CN); (**d**) after cut of superior vestibular nerve and reflection of the whole vestibular nerve (IVN), showing the facial nerve (VII) lying superiorly and the cochlear nerve (CN) inferiorly (the VII is anterior to the vestibular nerve). Bill's bar (BB) is present in the fundus of the internal auditory canal and separates the facial nerve from the superior vestibular nerve. *TC* transverse crest (Courtesy of Tardivet [20])

6.2.3 The Facial Canal (Fallopian Canal)

At the fundus of IAC, the facial nerve enters through the metal foramen in a bony canal called the Fallopian canal (after Gabriel Fallopius): It is 25–30 mm long [12]. No other nerve in the body travels such a long distance through a bony canal. The Fallopian canal is divided into three distinct anatomic segments defined by two genus (Fig. 6.13):

6.2.3.1 The Labyrinthine Segment (First Segment)

The labyrinthine segment of the facial nerve is 3–5 mm long; it is the shortest and the narrowest segment of the Fallopian canal. It lies beneath the middle cranial fossa and extends from the meatal foramen to the geniculate ganglion [21]. The narrowest part is at its entrance, the meatal segment. The labyrinthine segment travels anteriorly, superiorly, and laterally, forming an anteromedial angle of 120° with the IAC portion. It lies immediately above the anterior part of the vestibule.

The basal turn of the cochlea is anteroinferior to the labyrinthine segment.

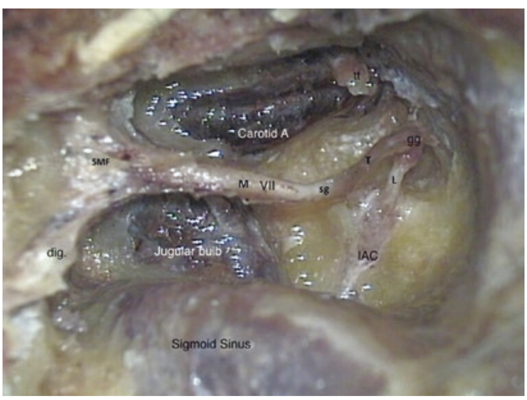

Fig. 6.13 Left transmastoid-translabyrinthine-transotic approach. The Fallopian canal dissected from the IAC to the stylomastoid foramen (SMF). It consists of three segments: labyrinthine segment (L), tympanic segment (T), and mastoid segment (M). The three segments are connected by two genus: first genu, the geniculate ganglion (gg), between labyrinthine and tympanic segment, and second genu (sg) between tympanic and mastoid segment. *dig* digastric ridge, *tt* tensor tympani muscle

When the nerve reaches a point just lateral and superior to the cochlea, it angles sharply forward, nearly at a right angle to the long axis of the petrous bone until the geniculate ganglion (Fig. 6.14).

Before reaching the geniculate ganglion, both the facial nerve and the nervus intermedius remain distinct entities, and they join each other just before reaching the geniculate ganglion.

Clinical Application

In case of an inflammatory swelling of the facial nerve, Bell's palsy, for example, the bony shell around the nerve may lead to a facial nerve compression. A severe facial nerve compression for a long time may result in a nerve ischemia with a worse prognosis for facial paralysis recovery. Facial nerve decompression consists of opening the facial bony canal in the areas of facial nerve inflammation and swelling. The inflammatory segment could be identified with MRI by its strong enhancement after injection of Gadolinium.

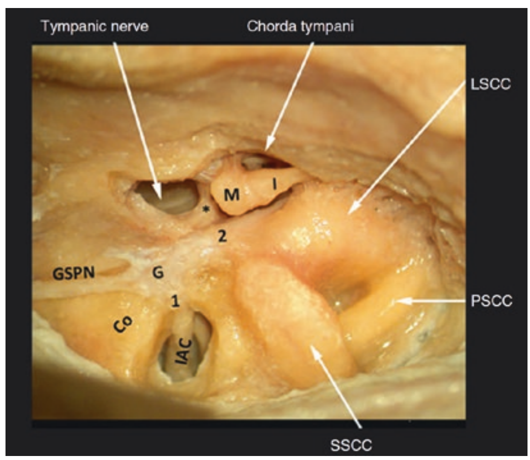

Fig. 6.14 Middle cranial fossa view of a right-side facial nerve after drilling the bone covering the labyrinth, the facial nerve, and the tegmen tympani. *IAC* internal auditory canal segment of the facial nerve, *1* labyrinthine segment, *G* geniculate ganglion, *GSPN* greater superficial petrosal nerve, *2* tympanic segment, *Co* cochlear area, *M* malleus, *I* incus, * cochleariform process, *LSCC* lateral semicircular canal, *PSCC* posterior semicircular canal, *SSCC* superior semicircular canal (Courtesy of Tardivet [20])

6.2.3.2 The Geniculate Ganglion

The geniculate ganglion is situated at the lateral end of the labyrinthine segment. The pain fibers of the auricular branch and the taste fibers of the chorda tympani synapse with the second sensory neuron at the level of the geniculate ganglion; the secretomotor fibers to the lacrimal gland pass through the geniculate ganglion and form the greater petrosal superficial nerve (GSPN).

At the level of the geniculate ganglion, the facial nerve takes an abrupt posterior direction, forming an acute angle 48–86° between the first and the second segments of the facial nerve; this is the "first genu" of the facial nerve [22] (Figs. 6.13, 6.14, and 6.15). The geniculate ganglion is dehiscent in 15% of temporal bones, a condition which makes the facial nerve vulnerable to injury during anterior epitympanic recess surgery or middle cranial fossa surgery (Fig. 6.16).

6.2.3.3 The Greater Superficial Petrosal Nerve

The greater superficial petrosal nerve (GPSN) is a secretomotor branch of the facial nerve. It emerges from the anterior upper portion of the geniculate ganglion; it carries secretory fibers to the lacrimal glands. This nerve exits the petrous temporal bone in an anterointernal direction through the *facial hiatus* to enter the middle cranial fossa (Figs. 6.14, 6.16, and 6.17).

In the middle cranial fossa, the GSPN passes deep to the Gasserian ganglion to reach the foramen lacerum where it enters the pterygoid canal. In the pterygoid canal, the GSPN joins the deep petrosal nerve to become the nerve of the pterygoid canal or *Vidian nerve*. This nerve traverses the pterygoid canal to reach the sphenopalatine ganglion in the pterygopalatine fossa, where the sensory fibers have their cell bodies. These sensory fibers are distributed to the soft palate and the tongue. Preganglionic secretory fibers from the cell bodies in the superior salivary nucleus also end in the sphenopalatine ganglion. Their corresponding postganglionic fibers innervate the lacrimal gland and the nasal cavity.

The greater superficial petrosal canal also contains the superficial petrosal artery that supplies the geniculate ganglion region (see Sect. 6.2.4.1).

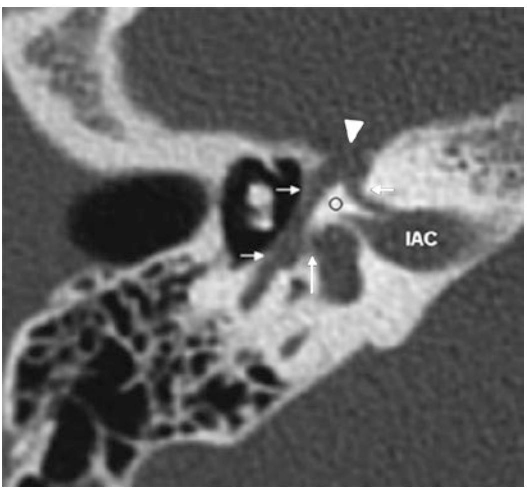

Fig. 6.15 Transversal CT view on a right ear. Labyrinthine segment (*short black arrow*), geniculate ganglion (*white arrowhead*), tympanic segment of the facial nerve (*white arrows*), oval window niche (*long black arrow*). Notice the acute angle between the first and second segment of the facial nerve (*circle*). *IAC* internal auditory canal

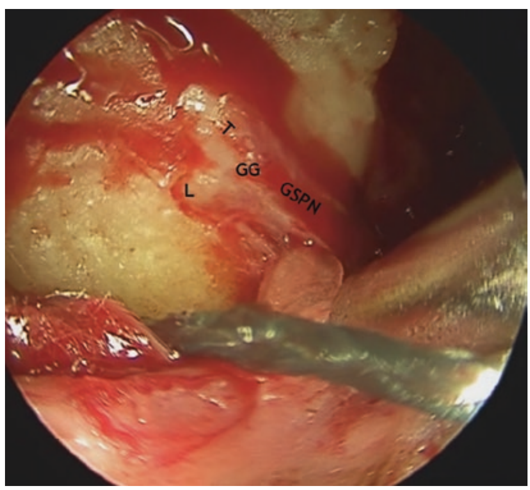

Fig. 6.16 Left middle cranial fossa approach showing geniculate ganglion (*GG)* dehiscence during MCF surgery, *T* tympanic segment, *L* labyrinthine segment, *GSPN* greater superficial petrosal nerve

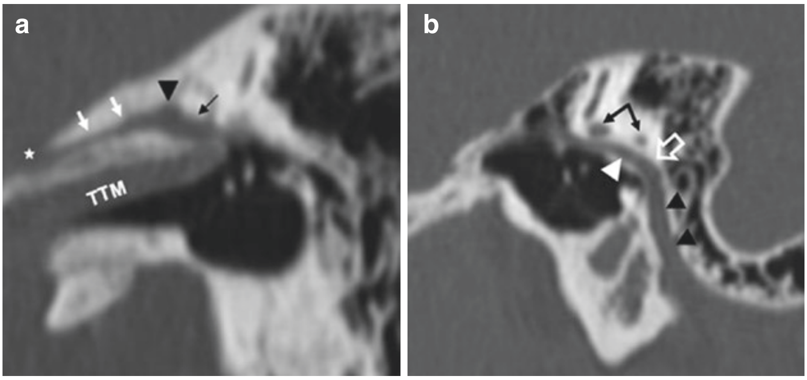

Fig. 6.17 CT reconstructions in the sagittal plane of a left ear along the different portions of the facial nerve: (**a**) Facial nerve (*black arrow*), leaving posteriorly the geniculate ganglion (*black arrowhead*). Greater superior petrosal nerve (*white arrows*) leaving anteriorly the geniculate ganglion. Hiatus of the facial canal (*), *TTM* tensor tympani muscle. (**b**) Tympanic portion of the facial nerve (white arrowhead) inferior to the LSCC (black arrows), second genu of the facial nerve (empty arrow), mastoid segment of the facial nerve (black arrowheads)

Clinical Implications

The greater superficial petrosal nerve GSPN represents an important landmark for facial nerve identification during middle cranial fossa approach.

The section of the GSPN or the section of Vidian nerve has been proposed in the past to treat intractable vasomotor rhinitis; this surgery was abandoned because of the troublesome side effects of such reduction of the lacrimal secretions (dry eyes).

Combined damage to the GSPN and lesser petrosal nerve could be associated with paradoxical phenomena including: face hyperemia, abundant salivation, lacrimation, and mucus secretion from the nose during eating. These phenomena are explained by the development of a "false" relationship between the damaged nerves [23].

6.2.3.4 The Tympanic Segment (Second Segment)

The tympanic segment of the facial nerve extends from the geniculate ganglion anteriorly to the second genu of the facial nerve posteriorly. The tympanic segment inclines inferiorly and posteriorly to descend obliquely along the medial wall of the tympanic cavity, above the cochleariform process and the oval window and below the bulge of the lateral semicircular canal. The second genu of the facial nerve is situated posterior to the oval window (Figs. 6.14 and 6.18).

The length of the tympanic segment of the facial nerve varies between 9 and 12 mm. The width of the tympanic segment varies between 1.2 and 1.6 mm [22].

The anterior part of the tympanic segment of the facial nerve lies slightly above and medial to the cochleariform process [18]. The relationship between the facial nerve and the cochleariform process is stable and constant. The cochleariform process is resistant to necrosis even in the presence of aggressive otitis media or cholesteatoma; therefore, it remains a persistent landmark helping to localize the facial nerve during middle ear surgery. The mean distance between the tympanic segment and the cochleariform process is around 2 mm (Fig. 6.19). The mean distance between the second genu of the facial nerve and the oval window is of 3–4 mm [22] (Fig. 6.19). The tympanic segment of the facial nerve courses posteriorly below and medial to the bulging of the lateral semicircular canal [24, 25].

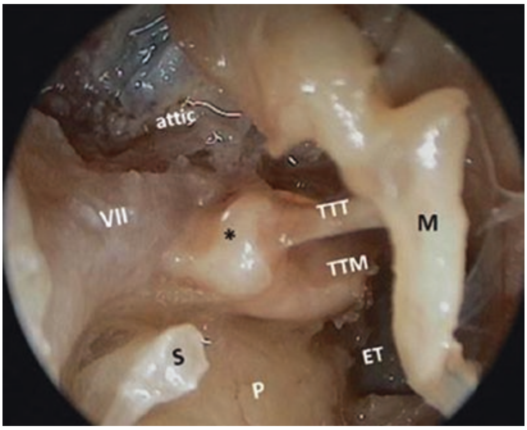

Fig. 6.18 Endoscopic view of a right middle ear through a posterior tympanotomy showing the tympanic segment of the facial nerve (VII) and its relationship with the cochleariform process (*) and stapes (S) and oval window. *TTM* tensor tympani muscle, *TTT* tensor tympani tendon, *P* promontory, *ET* Eustachian tube, *M* malleus

The bony wall of the tympanic segment canal can be very thin or even dehiscent, and the middle ear mucosa may lay in direct contact with the facial nerve sheath [26, 27].

Within the Fallopian canal, bundles of nerve fibers lie in a definite order: the oral branch lies next to the oval window, the frontal branches farthest from it, and the ocular branches in between [28, 29].

The lateral bony wall of the nerve is well visualized by CT scan. Dehiscence of the inferior wall may be difficult to assess correctly on the coronal views, but these views are demonstrative for the different degrees of prolapse of the facial nerve in front of the oval window niche or even in close contact to the stapes (Figs. 6.20 and 6.21).

Fig. 6.19 Tympanomastoid segments of the facial nerve and their relationship to the middle ear structures. *GSPN* greater superficial petrosal nerve, *GG* geniculate ganglion, *CP* cochleariform process, *RW* round window, *LSCC* lateral semicircular canal, *SMF* stylomastoid foramen

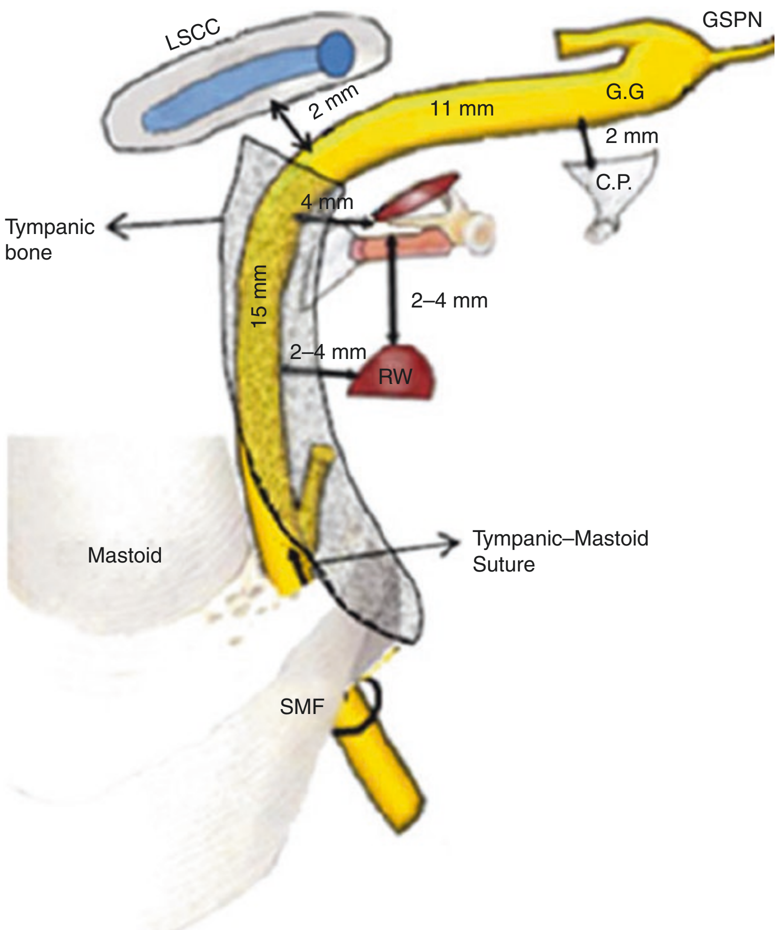

Surgical Implications

In Gusher syndrome, an X-linked congenital mixed deafness, the IAC is abnormally wide. This creates a communication between the high-pressure cerebrospinal fluid in the IAC and the perilymph of the inner ear, leading to a heavy leakage, "stapes gusher," during stapes surgery. The pathological widening concerns also the Fallopian canal. The enlarged IAC may be seen on CT scan, with a globulous aspect, but this aspect is not specific. The widened angle between the first and the second segment of the facial nerve is highly suggestive of the Gusher syndrome, enabling the preoperative diagnosis of this pathology [30, 31] (Fig. 6.22).

The perigeniculate area is the weakest zone of the Fallopian canal; it is the most common localization of traumatic facial nerve injury in temporal bone fracture [24] (Fig. 6.23). It is of interest to note that compression of the nerve due to the bony spicules occurs much more frequently than nerve transaction: this is why adequate urgent surgery is mandatory.

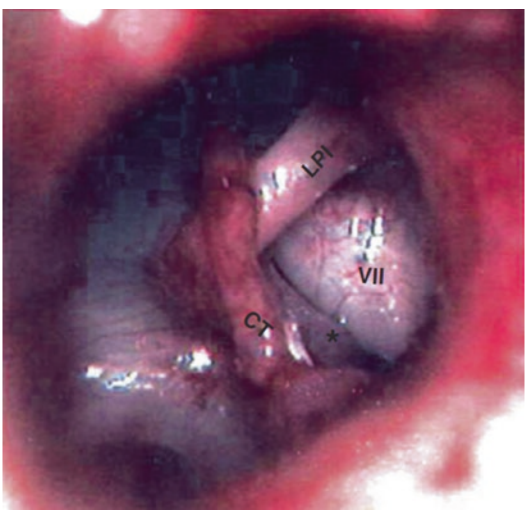

Fig. 6.20 Left ear during stapes surgery showing dehiscent tympanic segment of facial nerve (VII) and prolapsing on the stapes (*). *CT* chorda tympani, *LPI* long process of incus

6.2.3.5 Second Genu

The second genu is at the junction between the tympanic and the mastoid segments of the facial nerve. Just lateral and posterior to the pyramidal eminence, the facial nerve changes its direction and courses inferiorly about 2–3 mm to form an angulation of about 90–125° called the second genu. The second genu lies inferior and medial to the lateral semicircular canal and medial to the short process of the incus. The mean distance between the short process of the incus and the second genu is relatively constant and measures about 2 mm (Figs. 6.24, 6.25, and 6.26).

Surgical Impacts

The second genu of the facial nerve is the most susceptible portion of the nerve to suffer from a iatrogenic injury during ear surgery because it is not visible before identifying the nerve itself, especially in cases of invasive cholesteatoma and granulation tissues.

Knowing that the second genu is located inferior and medial to the aditus, the nerve could be at risk of injury while drilling toward the aditus during mastoid surgery. A sclerotic mastoid or the presence of extended chronic ear pathologies may hinder the proper identification of the anatomical structures bordering the aditus and expose the facial nerve to a risk of injury [24].

6.2.3.6 The Mastoid Segment (Third Segment)

The mastoid segment of the facial nerve is the longest part of the intra-temporal part of the facial nerve. This segment is vertical and its length is about 15 mm [25]. The mastoid Fallopian canal is relatively the largest part of the Fallopian canal; the nerve fills only 25–50% of the Fallopian canal lumen at this level. Inflammatory entrapment of the facial nerve is rare in the mastoid segment [32, 33]. The mastoid segment descends downward in the posterior wall of the tympanic cavity from the second genu superiorly to the stylomastoid foramen

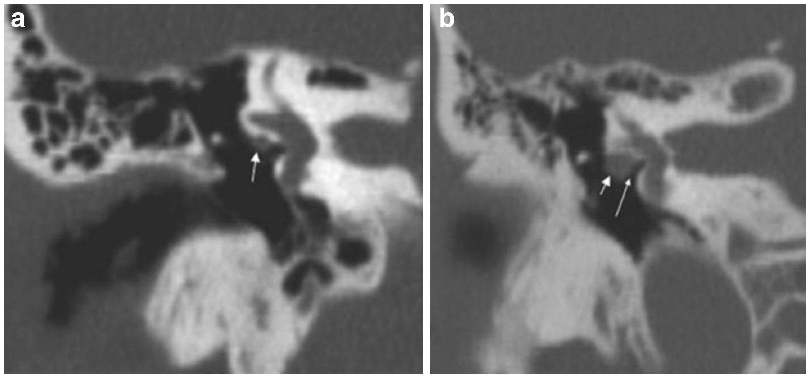

Fig. 6.21 Transversal computed tomographic views of the right ear showing (**a**) moderate prolapse of the tympanic segment of the facial nerve (arrow). (**b**) A bulging tympanic segment of the facial nerve (short arrow), obstructing almost completely the oval window niche (long arrow)

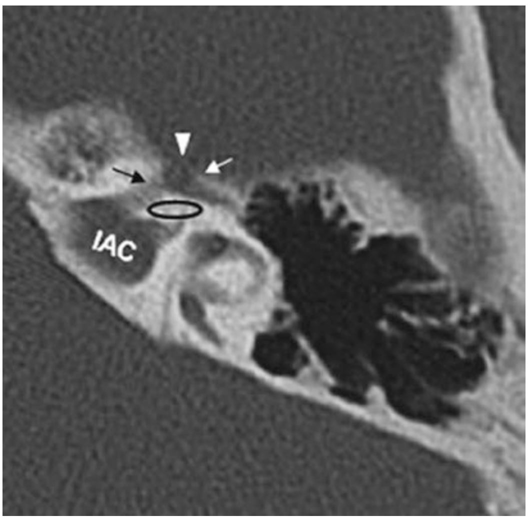

Fig. 6.22 Transversal CT image of a left ear showing a widened angle between the labyrinthine (*black arrow*) and tympanic segment (*white arrow*) of the facial nerve, suggesting a Gusher syndrome. Geniculate ganglion (*white arrowhead*). Note the bulbous aspect of the IAC

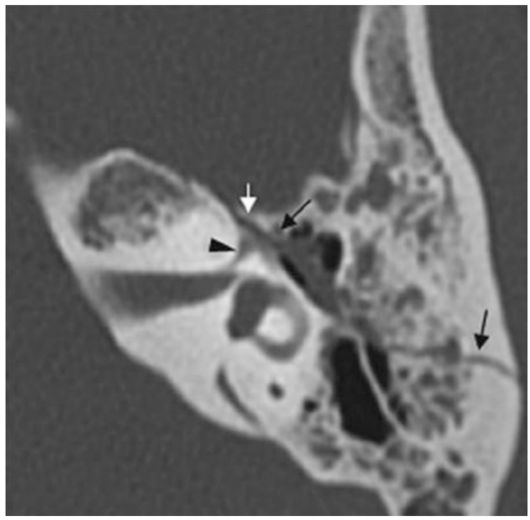

Fig. 6.23 Transversal CT view of a left ear with a longitudinal temporal bone fracture (*black arrows*), transgressing the geniculate ganglion (*white arrow*). Labyrinthine segment of the facial nerve (*arrowhead*)

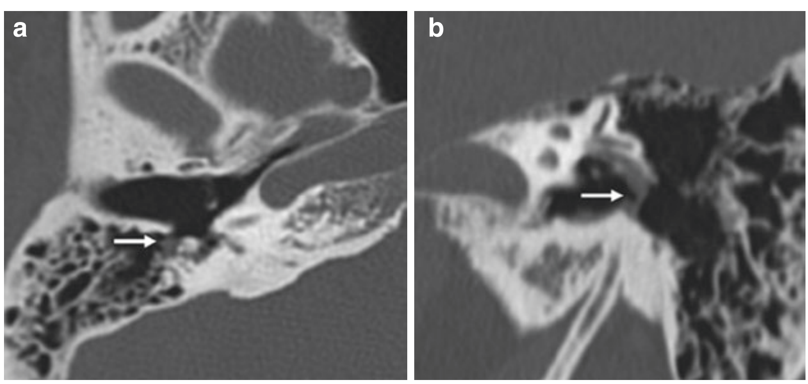

Fig. 6.24 (**a**) Axial CT image showing a denuded facial nerve (arrow) at the level of the second genu. (**b**) Sagittal oblique reconstruction along the tympanic segment of the facial nerve trajectory showing an irregular shape of the nerve (arrow) at the second genu

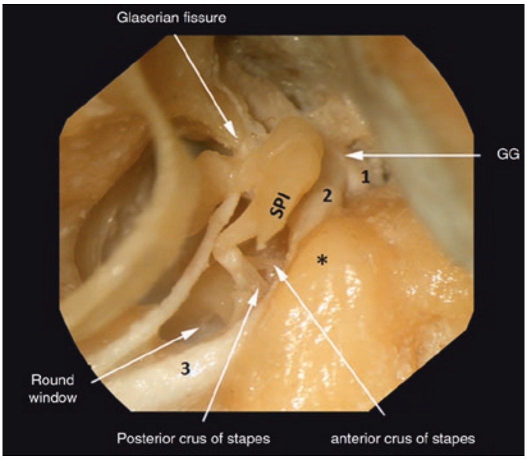

Fig. 6.25 Transmastoid view of a left ear after posterior and anterior tympanotomy with supralabyrinthine approach, showing the relationship between the lateral semicircular canal (*) and the second genu of the facial nerve between the tympanic segment (2) and the mastoid segments (3) of facial nerve. *GG* geniculate ganglion, (1) labyrinthine segment of the facial nerve, *SPI* short process of the incus (Courtesy of Tardivet [20])

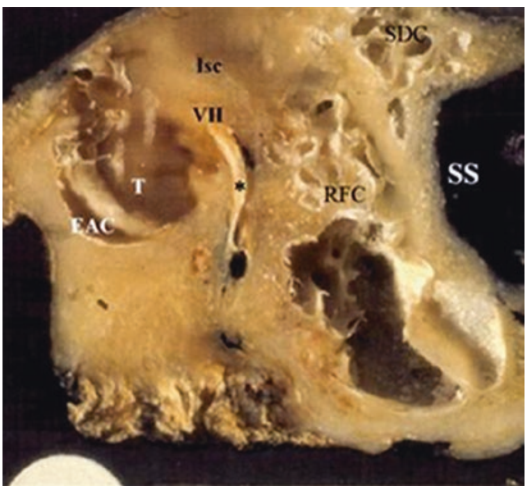

Fig. 6.26 A sagittal cut of a left middle ear in the plane of mastoid segment of facial nerve (*); notice the relationship between the second genu (VII) and the lateral semicircular canal (lsc); retrofacial cells (RFC) separate the sigmoid sinus (SS) from the facial nerve. *SDC* sinodural angle cells, *T* tympanic cavity, *EAC* external auditory canal

inferiorly. As the nerve descends inferiorly toward the mastoid tip, it becomes more lateral. In many cases, the inferior portion of the mastoid segment may course lateral to the plane of the posteroinferior quadrant of the annulus [34] (Fig. 6.27).

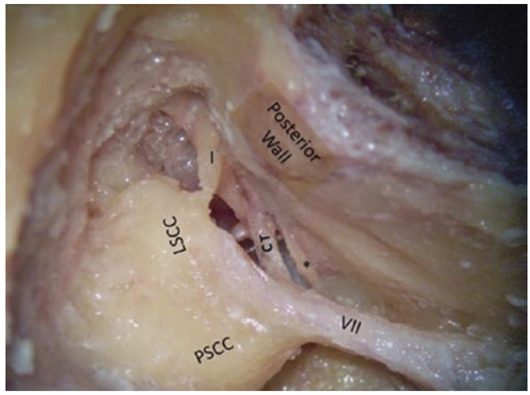

Fig. 6.27 Right ear after dissection of the mastoid segment of the facial nerve (VII), showing its relation with tympanic annulus (*); notice that the inferior portion of the mastoid facial nerve is lateral to the annulus. *CT* chorda tympani, *LSCC* lateral semicircular canal, *PSCC* posterior semicircular canal, *I* incus short process

Clinical Impact
During canaloplasty, the annulus should not be considered as a secure landmark for facial nerve; the facial nerve may pass lateral to the annulus [34]. In such cases, drilling in the posteroinferior quadrant of the external auditory canal, even lateral to the annulus, may lead to a facial nerve injury.

6.2.3.6.1 Relationship Between the Mastoid Segment of the Facial Nerve and the Tympanum

The mastoid segment of the facial nerve lies in the posterior wall of the tympanum in a position lateral to the pyramidal process, stapedial muscle, and the sinus tympani. The mean distance between the mastoid segment of the facial nerve and the posterior border of the oval window is 4 mm. Also the distance between the facial nerve and the round window is 4 mm (Fig. 6.21). In addition, the minimal distance from the annulus tympanicus to the facial nerve is about 1 mm at 9 o'clock position [22]. This fact permits to increase surgically the dimensions of the posterior tympanotomy by sacrificing the chorda tympani nerve (see Chap. 4).

6.2.3.6.2 Relationship Between the Mastoid Segment of the Facial Nerve and the Mastoid Structures

In the mastoid cavity, the mastoid segment runs straight downward from below the most overlapping part of the lateral semicircular canal to the stylomastoid foramen. The nerve is surrounded by the compacta of the bony wall of the ear canal and by mastoid cells. Occasionally, there is a bony defect in the Fallopian canal, and the nerve is dehiscent into the mastoid air cells.

The lower one-third of the mastoid segment of the facial nerve is always medial and anterior to the digastric ridge which represents an important landmark for the facial nerve exposure in a lateral skull base approaches (Fig. 6.28). However the digastric ridge may be difficult to identify when the mastoid is poorly pneumatized.

The sigmoid sinus passes always posterior and medial to the facial nerve. The distance between the mastoid segment of the VII and the sigmoid sinus is highly variable (4 mm average). The distance from the facial nerve to the jugular bulb ranges from 0 to 12 mm [22].

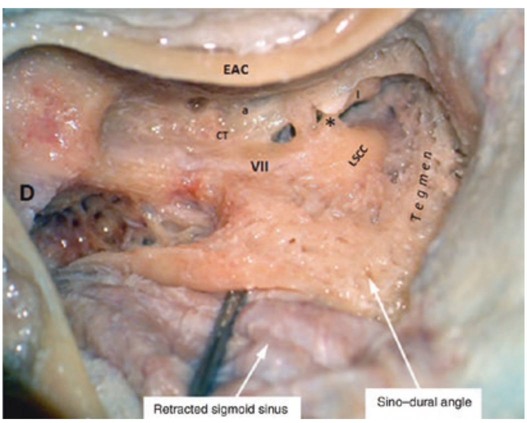

Fig. 6.28 Cadaveric left mastoidectomy showing the mastoid segment of the facial nerve (VII). Notice that the VII is anteromedial to the digastric ridge (D). The relationship between the tympanic annulus (a), chorda tympani (CT), and VII. The second genu of the facial nerve passes medial to the short process of the incus (I) and the lateral semicircular canal (LSCC); the VII drops down in the mastoid at the level of the midpoint of the LSCC in a direction parallel to that of the short process of the incus. * incudal buttress

The facial nerve exits the Fallopian canal via the stylomastoid foramen. The mean depth of the facial nerve from the mastoid cortex at the stylomastoid foramen is 13 mm. As the nerve exits the stylomastoid foramen at the anterior margin of the digastric groove, an adherent fibrous sheath of dense vascularized connective tissue surrounds it. The stylomastoid artery and veins are within this dense sheath. When it exits the stylomastoid foramen, the nerve travels between the digastric and stylohyoid muscles and enters the parotid gland.

Below the stylomastoid foramen, a sensory branch emerges from the facial nerve to innervate the posterior wall of the external auditory canal and a portion of the tympanic membrane.

The superior landmarks for the mastoid segment of the facial nerve are the lateral semicircular canal, to which the facial nerve runs anteroinferiorly, and the posterior semicircular canal, to which the nerve runs 2.5 mm anteriorly. The digastric ridge is the inferior landmark for the mastoid segment of the facial nerve.

Surgical Applications: **Mastoid Segment Identification During Mastoid Surgery**

Exposure of the mastoid segment of facial nerve is done through a cortical mastoidectomy. The most important landmarks for identifying the facial nerve in the mastoid cavity are the lateral semicircular canal, the short process of the incus, and the digastric ridge [35]. The axis of the VII corresponds to the axis of the short process of the incus.

The nerve is best identified by first imagining a line that begins just anterior to the inferior portion of the lateral semicircular canal and travels in an inferior direction toward the digastric ridge. The bone of the EAC is progressively thinned, in a direction parallel to the nerve, until the white sheath is identified through the yellow bone.

The drilling must be always done along the lateral aspect of the nerve.

6.2.3.6.3 The Nerve of Stapedial Muscle

The nerve fibers of the stapedial muscle arise centrally from some neurons emerging outside the nucleus of the facial nerve, situated below the IV ventricle, to join secondarily the motor neurons of the facial nerves [36, 37].

The nerve of the stapedial muscle is a small twig coming from the facial nerve as it descends in the posterior wall of the tympanic cavity behind the pyramidal eminence.

Clinical Notes
The distinct central origin of the stapedial nerve explains the normal finding of stapedial muscle reflex in congenital facial palsy (Mobius syndrome) and the isolated alteration of stapedial reflex without facial palsy in some brain stem lesions.

6.2.3.6.4 The Chorda Tympani Nerve

The chorda tympani is the terminal branch of the nervus intermedius. The chorda tympani leaves the mastoid segment of the facial nerve at a variable level, about 5–6 mm above the stylomastoid foramen. The facial nerve and the chorda tympani emergence form Plester's chordo-facial angle which varies between 26° and 35° (Figs. 6.29 and 6.30) [22].

The chorda tympani enters the middle ear through the chordal eminence. It passes between the incus and the handle of the malleus, above the tensor tympani tendon to exit through the canal of Huguier of the petrotympanic fissure. Then the chorda tympani passes on the medial surface of the mandibular fossa to finally join the lingual nerve in the infratemporal fossa (Fig. 6.31) [38].

The chorda tympani nerve carries:

- *Sensory afferent taste fibers*: these fibers of the chorda tympani nerve have their cell bodies in the geniculate ganglion and provide taste sensation from the anterior two-thirds of the tongue.
- *Preganglionic efferent secretory fibers* to the submaxillary and sublingual glands: these fibers have their cell bodies in the superior salivary nucleus; they synapse within the submaxillary ganglion, and then it provides secretory motor impulses to the submaxillary and sublingual glands.

Surgical Impact: **Chorda Tympani Nerve (CT) Injury During Middle Ear Surgery**
Iatrogenic chorda tympani nerve (CTN) injury during middle ear surgery is quite common. The most frequent type of chorda tympani injury is stretching, and cutting the nerve is less common. Canal wall down

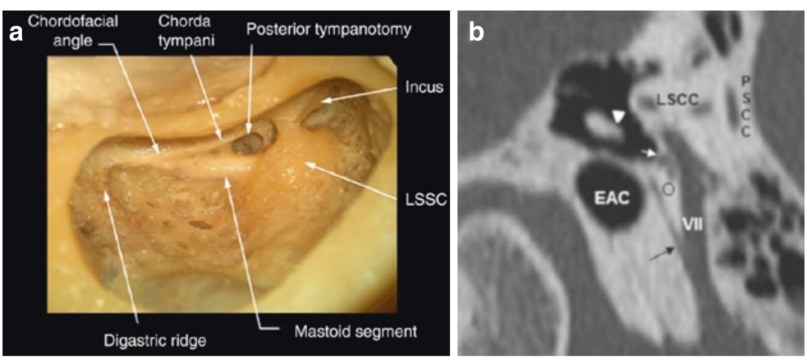

Fig. 6.29 (**a**) Left ear: cadaveric cut of a left ear showing the chordo-facial angle of Plester (Courtesy of Tardivet [20]). (**b**) Sagittal reconstruction of a CT showing the emergence of the chorda (*black arrow*) from the facial nerve (*VII*) and the bony wall (*circle*) between the chorda and the VII (facial recess approach). Facial recess (*white arrow*), short process of the incus (*white arrowhead*), *LSCC* lateral semicircular canal, *PSCC* posterior semicircular canal, *EAC* external auditory canal

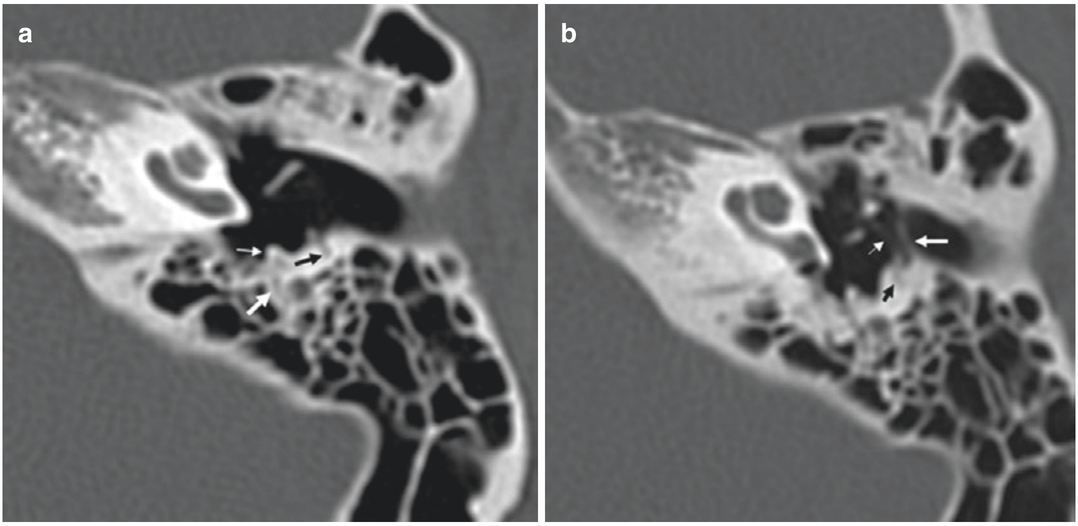

Fig. 6.30 Transverse CT images of a left ear from inferior to superior: (**a**) emergence of the chorda tympani (black arrow), lateral to the pyramidal eminence (thin white arrow). Facial nerve (thick white arrow). (**b**) Chorda tympani (small arrow) traversing the tympanic cavity, emergence of the chorda tympani (black arrow) behind the tympanic membrane (thick white arrow)

mastoidectomy and posterior tympanotomy have the highest risk of chorda tympani injury [39].

Only 25% of patients are aware of the symptoms after chorda tympani injury. Stretching or cutting the chorda tympani could give the same types of symptoms to the concerned patients.

Additional studies demonstrated that nerve stretching is associated with a greater degree of postoperative symptoms than nerve transsection, across a range of middle ear procedures [39, 40].

Nevertheless, these findings are in contrast to the results of testing the taste disturbance after stapedectomy, in which cutting of the nerve was found to cause significantly greater symptoms than manipulation alone [41]. The most common postoperative complaint is taste disturbance such a metallic taste. Although most patients experience gradual symptomatic recovery, about 90% of the symptomatic patients recover completely within 12 months. Persisting complaints may be troublesome [42]. The risk of taste disturbance should be addressed in the consent procedure. Postoperative chorda tympani symptoms are important to reveal in the history especially when indicating a contralateral stapes surgery.

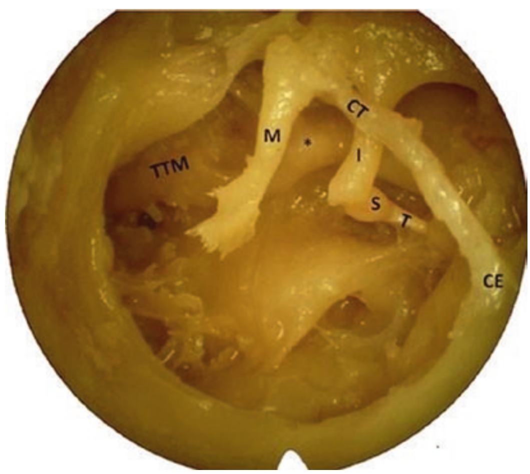

Fig. 6.31 Endoscopic view of a left middle ear showing the chorda tympani (*CT*) entering the middle ear through the chordal eminence (*C.E.*); it then passes between the incus (*I*) medially and the malleus (*M*) laterally, above the tensor tympani tendon (*) to exit the middle ear from the anterior wall. *T* stapedial tendon, *S* stapes, *TTM* tensor tympani muscle

6.2.4 Vascularization of the Facial Nerve (Fig. 6.32)

The segments of the facial nerve receive their blood supply from branches of the vertebrobasilar artery and the external carotid artery systems.

Within the pons, the facial nucleus receives its blood supply primarily from the anterior inferior cerebellar artery (AICA). The labyrinthine artery, a branch of the AICA, enters the internal auditory canal (IAC) with the facial nerve and provides blood supply to the meatal portion of the facial nerve.

The external carotid system gives to the tympanomastoid segments of the facial nerve two branches: the superficial petrosal artery and the stylomastoid artery.

6.2.4.1 Superficial Petrosal Artery

The superficial petrosal artery is an intracranial branch of the middle meningeal artery (MMA); it enters the middle ear through the facial hiatus with the greater superficial petrosal nerve. It supplies the geniculate ganglion and the tympanic segment of the facial nerve. It anastomoses with the stylomastoid artery at the level of the second genu.

6.2.4.2 Stylomastoid Artery

The stylomastoid artery arises from the external carotid artery system; it enters the middle ear and the facial canal through the stylomastoid foramen. It supplies the mastoid segment of the facial nerve. It anastomoses with the superficial petrosal artery of the MMA at the level of the second genu [43].

In 60% of patients, the stylomastoid artery arises from the occipital artery, and in 40% of patients, it arises from the postauricular artery [44]. The superficial petrosal artery and the stylomastoid artery contribute to an arterial arcade called the *facial arch* which supplies the tympanic and mastoid segments of the facial nerve. In most people, this arcade is supplied predominantly by the superficial petrosal artery [45] (Fig. 6.32). Furthermore, 10% of people lack a

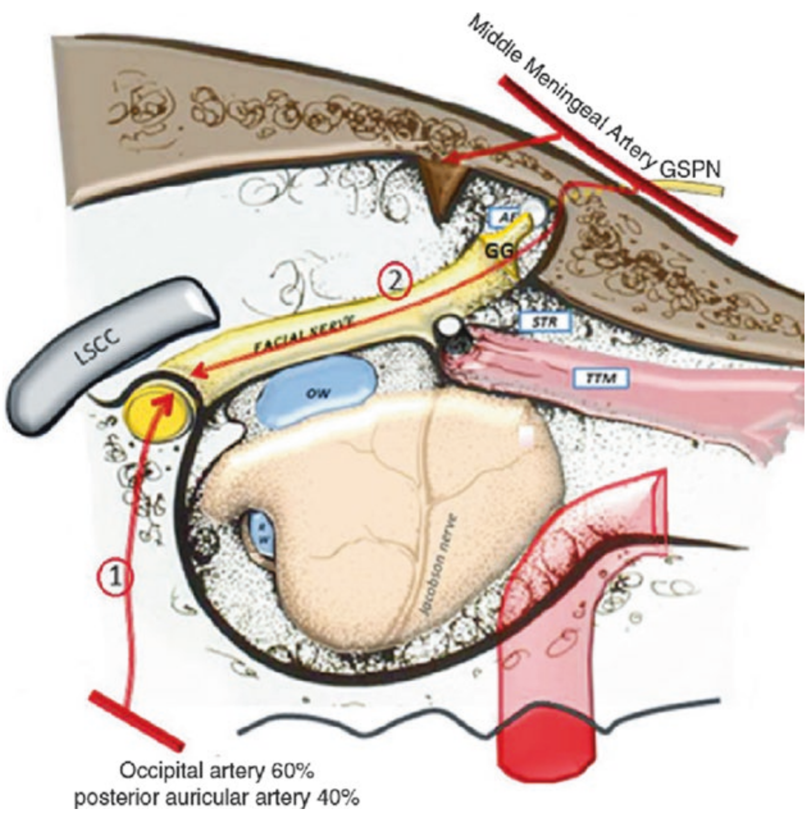

Fig. 6.32 Tympanomastoid segment vascularization. *1* stylomastoid artery, *2* superficial petrosal artery, *LSCC* lateral semicircular canal, *OW* oval window, *RW* round window, *TTM* tensor tympani muscle, *STR* supratubal recess, *AE* anterior epitympanum, *GG* geniculate ganglion, *GSPN* greater superficial petrosal nerve

blood supply from the MMA to the geniculate ganglion, meaning that the mastoid and tympanic segments receive their blood supply only from the stylomastoid artery [46].

Clinical Implications

In lateral skull base surgery, anterior and posterior *rerouting* of the facial nerve reduces drastically the blood supply of the facial nerve with a high risk of facial palsy. The blood supply of the mastoid segment of the facial nerve maintains this portion adherent to the canal, a point to take in consideration when dissecting the nerve from its canal [47].

Embolization in the territories of the external carotid artery is commonly indicated to treat vascular lesions including intractable epistaxis, hypervascular neoplasms, dural fistulae, and arteriovenous malformations. When a dual blood supply of the tympanomastoid segments of the facial nerve is present, a supraselective embolization (SSE), with occlusion of the stylomastoid artery, would not be at risk to induce paresis. However, in cases of an absent blood supply derivative from the MMA, embolization of the stylomastoid artery would likely result in a facial nerve deficit.

Since 6% of patients would be expected to derive their blood supply of the facial nerve tympanomastoid segments only from the stylomastoid artery originating from the occipital artery, patients undergoing supraselective embolization of the stylomastoid artery should be counseled on a theoretical 6% risk of having a vascular anatomic pattern that may place the facial nerve at increased risk during embolization [48]. The embolization agent, such as nonabsorbable polymers, also influences the risk of developing a cranial neuropathy [49].

Considering this risk, catheterizing the MMA is suggested to assess the length of the superficial petrosal artery [49]. If a dual blood supply to the facial nerve is confirmed, there is no risk of facial nerve paresis from embolization. But if the superficial petrosal artery branch is short, resorbable agents should be considered. Symptoms from ischemic facial nerve palsy during embolization of the external carotid artery branches occur immediately following the procedure and may be not fully recoverable [50].

Facial nerve *decompression* is one of several strategies for restoring nerve function in case of acute nerve palsy [51].

References

1. Louryan S. Développement du nerf facial. In: Martin-Duverneuil N, editor. A propos du nerf facial. Paris: Guerbet; 1994. p. 3–9.
2. Gavalas A, Ruhrberg C, Liver J, Henderson CE, Krumlauf R. Neuronal defects in the hindbrain of Hoxa 1, Hoxb1 and Hoxb2 mutants reflect regulatory interactions among these Hox genes. Development. 2003;130:5663–79.
3. Sataloff RT, Selber JC. Phylogeny and embryology of the facial nerve and related structures. Part II: embryology. Ear Nose Throat J. 2003;82:769–72.
4. Bast TH, Anson BJ, Richany SF. The development of the second branchial arch (Reichert's cartilage), facial canal and associated structures in man. Q Bull Northwest Univ Med Sch. 1956;30:235–49.
5. Declau F, Jacob W, Montoro S, Marquet J. Dehiscence of the facial canal: developmental aspects. Int J Pediatr Otorhinolaryngol. 1991;21:21–32.
6. Spector JG, Ge X. Ossification patterns of the tympanic facial canal in the human fetus and neonate. Laryngoscope. 1993;103:1052–65.
7. Gasser RF, Sigihara S, Shimada K. Three-dimensional development of the facial nerve path though the ear region in human embryos. Ann Otol Rhinol Laryngol. 1994;103:395–403.
8. Louryan SM. Imaging case study of the month: pure second arch syndrome. Ann Otol Rhinol Laryngol. 1993;102:904–5.
9. GulyaIn AJ. Developmental anatomy of the temporal bone and skull base. In: Glasscock-Shambaugh's surgery of the ear. 6th ed. Shelton: People's Medical Publishing House; 2010. p. 3–27.
10. Wetmore RF, Muntz HR, McGill TJ. Pediatric otolaryngology: principles and practice pathways. New York: Thieme Medical Publishers; 2000.
11. http://emedicine.medscape.com/article/835286-overview

12. Chandra S, Goyal M, Gandhi D, Gera S, Berry M. Anatomy of the facial nerve in the temporal bone: HRCT. Indian J Radiol Imaging. 1999;9(1):5–8.
13. Cornelia U, editor. Paralizii le nervu lui facial. Laşi: Ars Longa; 2001. p. 11–7.
14. Gantz Bruce J, Rubinstein Jay T. Intratemporal facial nerve surgery. In: CW Cummings, JM Fredrickson, LA Harker, CJ Krause, MA Richardson, DE Schuller, editors. Otolaryngology head and neck surgery. 3rd ed. St. Louis: Mosby—Year Book; 1998. 4(143). p. 2785–2799.
15. Magnan J, Chays A. [Functional surgery on the acoustic-facial pedicle]. Rev Laryngol Otol Rhinol (Bord) 1998;119(3):151–4. Review. French.
16. Magnan J, Caces F, Locatelli P, Chays A. Hemifacial spasm: endoscopic vascular decompression. Otolaryngol Head Neck Surg. 1997;117(4):308–14.
17. Badr-El-Dine M, El-Garem HF, Talaat AM, Magnan J. Endoscopically assisted minimally invasive microvascular decompression of hemifacial spasm. Otol Neurotol. 2002;23(2):122–8.
18. Magnan J, Chays A, Caces F, Lepetre-Gillot C, Cohen JM, Belus JF, et al. Role of endoscopy and vascular decompression in the treatment of hemifacial spasm. Ann Otolaryngol Chir Cervicofac. 1994;111(3):153–60. French.
19. Ge XX, Spector GJ. Labyrinthine segment and geniculate ganglion of the facial nerve in fetal and adult temporal bones. Ann Otol Rhinol Laryngol. 1981;90(suppl 85):1–12.
20. Tardivet L. Anatomie Chirurgicale du nerf facial intra-pétreux. Thèse Med. Aix Marseille University; 2003.
21. Proctor B. Surgical anatomy of the ear and temporal bone. New York: Thieme Medical Publishers; 1989.
22. Măru N, Cheiţă AC, Mogoantă CA, Prejoianu B. Intratemporal course of the facial nerve: morphological, topographic and morphometric features. Romanian J Morphol Embryol. 2010;51(2):243–8.
23. Levin SL. [Syndromes of combined damage to the greater and lesser superficial petrosal nerves (paradoxical phenomena of hyperemia of the face, salivation, lacrimation and mucus secretion)]. Zh Nevropatol Psikhiatr Im S S Korsakova. 1986;86(4):509–12.
24. Ozgirgin N, Cenjor C, Filipo R, Magnan J. Consensus on treatment algorithms for traumatic and iatrogenic facial paralysis. Mediterr J Otol. 2007;3:150–8.
25. Yadav S, Ranga A, Sirohiwal B. Surgical anatomy of tympano-mastoid segment of facial nerve. Indian J Otolaryngol Head Neck Surg. 2006;58(1):27–30.
26. Baxter A. Dehiscence of the fallopian canal. An anatomical study. J Laryngol Otol. 1971;85(6):587–94.
27. Kim CW, Rho YS, Ahn HY, Oh SJ. Facial canal dehiscence in the initial operation for chronic otitis media without cholesteatoma. Auris Nasus Larynx. 2008;35(3):353–6.
28. Miehlke A. Uber die Topographie des Faserverlaufes im Facialisstamm. Arch Ohren Nasen Kehlkopfheilkd. 1958;171:340.
29. Hofmann L. Der Faserverlauf im N. facialis. Z Hals Nas Ohrenheilk. 1924;10:86.
30. Kumar G, Castello M, Bucman CA. X-linked stapes gusher; CT findings in one patient. Am J Neuroradiol. 2003;24:1130–2.
31. Talbot JM, Wilson DF. Computed tomographic diagnosis of X-linked congenital mixed deafness, fixation of the stapedial footplate, and perilymphatic gusher. Am J Otol. 1994;15(2):177–82.
32. Jongkees LBW. Die chirurgische Behandlung der intratemporalen Facialislähmung. Dtsch Med Wochenschr. 1958;83:865.
33. Lindemann H. The fallopian canal. An anatomical study of its distal part. Acta Otolaryngol Suppl. 1960;158:204.
34. Adad B, Rasgon BM, Ackerson L. Relationship of the facial nerve to the tympanic annulus: a direct anatomic examination. Laryngoscope. 1999;109(8):1189–92.
35. Chi FL, Wang J, Yuan YS, Liu HJ, Gu J, Huang T, et al. Landmark of facial nerve in middle ear surgery. Zhonghua Er Bi Yan Hou Tou Jing Wai Ke Za Zhi. 2006;41(1):5–8.
36. Lyon MJ. The central location of the motor neurons to the stapedius muscle in the cat. Brain Res. 1978;143(3):437–44.
37. Joseph MP, Guinan JJ Jr, Fullerton BC, Norris BE, Kiang NY. Number and distribution of stapedius motoneurons in cats. J Comp Neurol. 1985;232:43–54.
38. Tóth M, Moser G, Patonay L, Oláh I. Development of the anterior chordal canal. Ann Anat. 2006;188(1):7–11.
39. Gopalan P, Kumar M, Gupta D, Phillips JJ. A study of chorda tympani nerve injury and related symptoms following middle-ear surgery. J Laryngol Otol. 2005;119(3):189–92.
40. Clark MP, O'Malley S. Chorda tympani nerve function at the middle ear surgery. Otol Neurotol. 2007;28(3):335–40.
41. Mahendran S, Hogg R, Robinson JM. To divide or manipulate the chorda tympani in stapedotomy. Eur Arch Otorhinolaryngol. 2005;262(6):482–7.
42. Kiverniti E, Watters G. Taste disturbance after mastoid surgery: immediate and long-term effects of chorda tympani nerve sacrifice. J Laryngol Otol. 2012;126(1):34–7.
43. Ozanne A, Pereira V, Krings T, et al. Arterial vascularization of the cranial nerves. Neuroimaging Clin N Am. 2008;18:431–9, xii.
44. Magnan J, Chays A, Gasquet R, Didier D, Garcia C, Bremond G. Anatomie chirurgicale de la tympanotomie postérieure. JF ORL. 1990;5:301–13.
45. Djindjian R, Merland JJ. Super-selective arteriography of the external carotid artery. Berlin: Springer; 1978. p. 14–123.
46. Marangos NM, Schumacher M. Facial palsy after glomus jugulare tumor embolization. J Laryngol Otol. 1999;113:268–70.
47. Sanna M, Khrais T, Mancini F, Russo A, Taibah A. The facial nerve in temporal bone and lateral skull base microsurgery. Stuttgart/New York: G Thieme Verlag; 2006.

48. Gartrell BC, Hansen MR, Gantz BJ, Gluth MB, Mowry SE, Aagaard-Kienitz BL, et al. Facial and lower cranial neuropathies after preoperative embolization of jugular foramen lesions with ethylene vinyl alcohol. Otol Neurotol. 2012;33(7):1270–5.
49. Valavanis A. Preoperative embolization of the head and neck: indications, patient selection, goals, and precautions. Am J Neuroradiol. 1986;7:943–52.
50. de Vries N, Versluis RJ, Valk J, et al. Facial nerve paralysis following embolization for severe epistaxis (case report and review of the literature). J Laryngol Otol. 1986;100:207–10.
51. Ramakrishnan Y, Alam S, Kotecha A, et al. Reanimation following facial palsy: present and future directions. J Laryngol Otol. 2010;124:1146–52.

The Eustachian Tube

7

Contents

S. Mansour et al., *Comprehensive and Clinical Anatomy of the Middle Ear*,
https://doi.org/10.1007/978-3-030-15363-2_7

The Eustachian tube (ET) or auditory tube is a slender tube that connects the middle ear cavity with the nasopharynx and serves to equalize air pressure on either side of the eardrum.

It is a hollow structure of bone and cartilage lined with a respiratory mucosa and equipped by a muscular opening mechanism.

It is part of a system of contiguous organs, including the nose, the middle ear, and the mastoid air cells that are devoted to middle ear ventilation, protection, and clearance. Although the physiology of the Eustachian tube is evident, its pathophysiologic involvement in middle ear inflammatory process remains debatable: would Eustachian tube dysfunction be the cause or a consequence of chronic otitis media?!

7.1 The Eustachian Tube Development

The Eustachian tube (ET) derives from the first pharyngeal (branchial) pouch, which extends laterally between the first and second pharyngeal arches to form the tubotympanic recess (TTR).

The distal part of the TTR becomes the primitive tympanic cavity, and the proximal part constricts to form the lumen of the fibrocartilaginous ET. These processes occur between 4 and 6 weeks of gestation [1].

Between the second and third week of gestation, during its lateral extension between the first and the second pharyngeal arches, the first pharyngeal pouch gets into contact with the first branchial groove which is the origin of the external auditory meatus (Fig. 7.1).

The structures associated with ET lumen develop from the mesenchyme surrounding the first pharyngeal pouch in a predictable sequence:

- Before the tenth week of gestation, only the epithelial lining of the lumen has differentiated.
- Between the tenth and 12th weeks, the levator veli palatini (LVP) and tensor veli palatini muscles (TVP) develop and become delineated from the surrounding mesenchyme [2, 3] (Fig. 7.2).

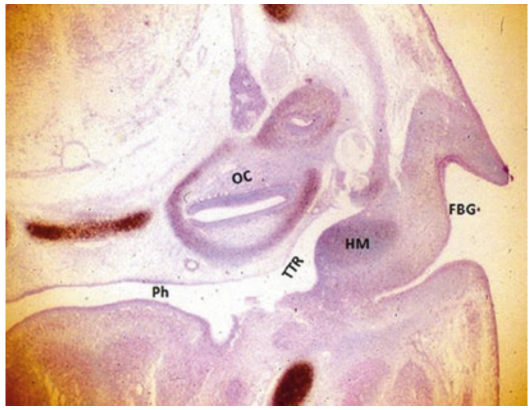

Fig. 7.1 The tubotympanic recess (TTR) in a mouse embryo of gestation day 12. *HM* handle of malleus; *Ph* pharynx; *OC* otic capsule; *FBG* first branchial ectodermal groove. This horizontal section demonstrates the continuity between the pouch and the pharynx. (Incorporation of radioactive sulfur with hematoxylin-eosin counterstaining)

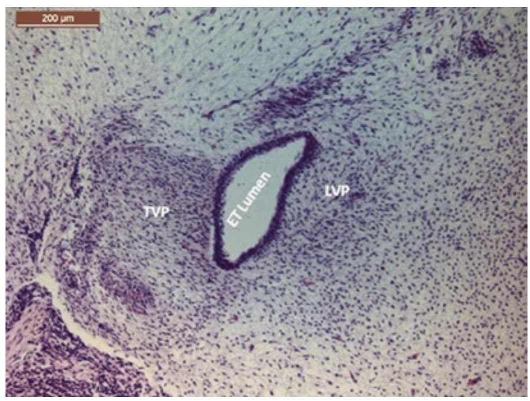

Fig. 7.2 Frontal section of the auditory tube rudiment in a 7-week 27 mm human embryo (end of the second month). *TVP* tensor veli palatini muscle anlage; *LVP* levator veli palatini muscle anlage. Hematoxylin-eosin staining

- The initial differentiation of the cartilage begins at the 14th week.
- By the 20th week, the initial center of chondrification has increased in size, and a perichondrium is clearly differentiated in the anteromedial portion of the tube [2, 3] (Fig. 7.3).

The main growth of the auditory tube concerns the length and lumen of the cartilaginous portion in the fetal period between weeks 16 and 28.

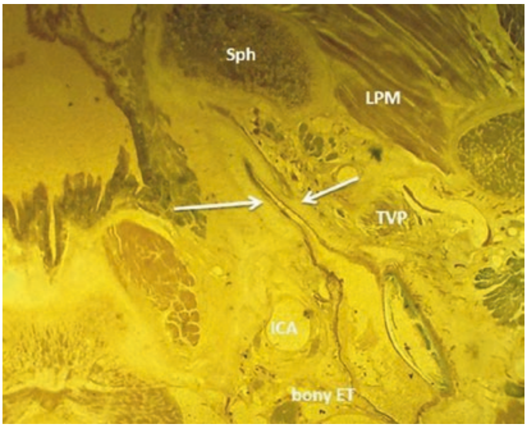

Fig. 7.3 A transverse cut of the base of skull in a 6-month, 250 mm fetus showing the Eustachian tube. Note the cartilaginous part is well developed (white arrows) and is in the same plane as the bony Eustachian tube (ET). *LPM* lateral pterygoid muscle; *Sph* sphenoid bone; *ICA* internal carotid artery; *TVP* tensor veli palatini muscle

These processes yield an ET structure very similar to that observed in the adult. During the rest of fetal life, morphometric changes occur in the ET structures. The most pronounced change is the increase in the length of the cartilaginous portion of the tube from 1 mm at the tenth week of gestation to 13 mm at birth.

While the fetus is growing, the tube deviates from the horizontal plane only about 10°, because the fetal cranial base is relatively flat; this situation persists until early childhood [2–5].

Clinical Application
Failure of constriction of the tubotympanic recess (TTR) due to a mesenchymal defect leads to widening of the presumed Eustachian tube and formation of a "persistent tubotympanic recess." This is illustrated in this case of an 18-year-old female patient, status post corrective repair of tetralogy of Fallot who presented with recurrent bilateral otorrhea with bilateral tympanic membrane perforations. Temporal bone CT scan showed bilateral persistent tubotympanic recess (Fig. 7.4).

This may be explained by the following:

1. The embryonic TTR, after initial evagination from the pharynx, could have been interrupted at the nasopharynx by misdevelopment of the surrounding defective mesenchyme.
2. Failure of the development of tubal cartilage and TTM leads to a persistently wide TTR. This malformation is attributed to a field defect arising from NCCs that affected at the same time the ET and the cardiac outflow tract, leading to tetralogy of Fallot.

Clinical Application
Patients with cardiac anomalies are considered prone to otitis media due to associated ET malformations and dysfunction. This association is explained by the fact that neural crest cells (NCC) are involved in the differentiation of branchial arches, including the precursor tissue of the cardiac outflow tract and Eustachian tube ([6]; thus defects arising from NCCs may lead to this association.

It has also been demonstrated that in Down syndrome (with associated congenital heart diseases in 43.3%) [7], the ET was extremely small and collapsed in several portions. Also in patients with Down syndrome, the density of cartilage cells was decreased at all ages, predisposing the canal to collapse. Also a generalized hypotonia of these patients can contribute to a decreased function of the TVP of the palate.

7.2 Postnatal Growth (Fig. 7.5)

The ET lengthens rapidly during early childhood: In infants, it is about 18 mm [8], half as long as in adults, and it reaches adult size by 7 years of age [9, 10]. During this process, the

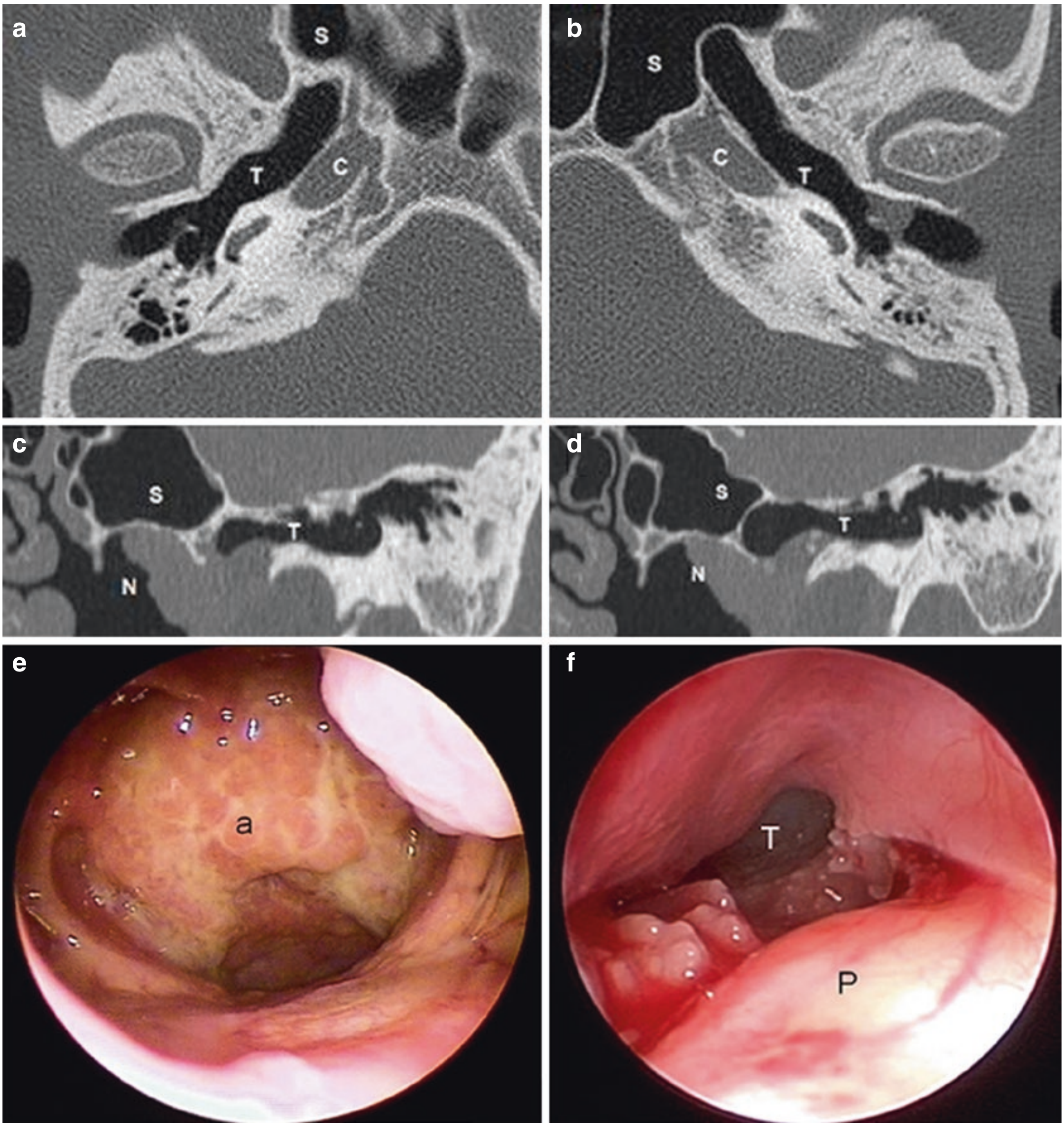

Fig. 7.4 (**a**, **b**, **c**, **d**) Temporal bone CT scan transverse cuts (A, right ear; B, left ear) and multiplanar reconstruction in the plane of the Eustachian tube (C, right ear; D, left ear) showing a bilateral persistent tubotympanic recess (T) ending as blind cul-de-sacs near the sphenoid sinus (S) with absence of an opening into the nasopharynx (N). The cartilaginous ET was absent on both sides. C: Horizontal canal of the petrous carotid artery. (**e**) Nasopharyngoscopy showing the presence of small adenoid (a) and absence of the torus tubarius. (**f**) Left ear intraoperative endoscopy using a 30° scope showing significant widening of the protympanum that continues as a persistent tubotympanic recess with a blind end (T). *P* promontory

bony portion growes relatively more than the cartilaginous one [11].

In infants, the cartilaginous and bony portions forms a linear connection between the pharynx and middle ear; but due to the craniofacial growth, the cartilaginous tube becomes displaced inferiorly to form in adults an angle of approximately 45° with the horizontal plane of the osseous portion [2, 12].

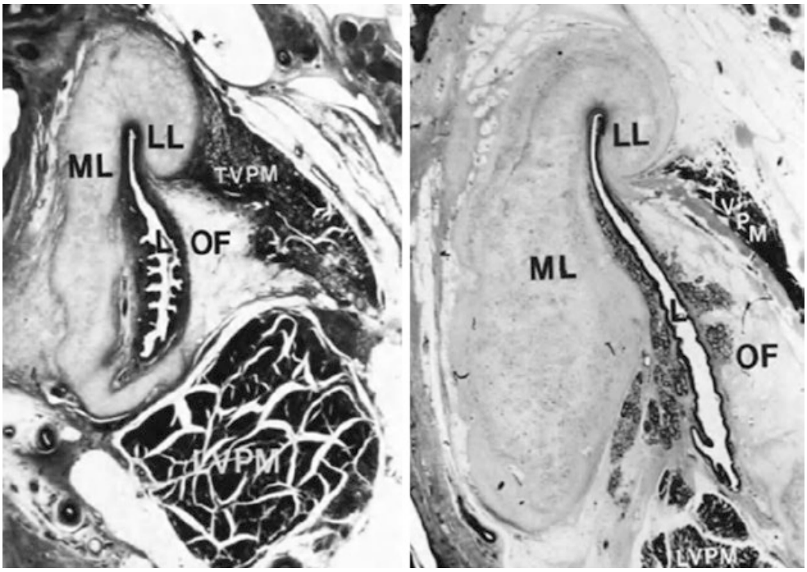

Fig. 7.5 Photomicrographs of cross sections through the mid-cartilaginous portion of the Eustachian tube (ET) of a 3-month-old female (left) and a 34-year-old male (right) showing the developmental difference of the Ostmann fat pad (OF) and the size of the ET. *L* lumen; *LL* lateral lamina of the Eustachian tube cartilage; *LVPM* levator veli palatini muscle; *ML* medial lamina of the Eustachian tube cartilage; *TVPM* tensor veli palatini muscle (Courtesy of I. Sando, MD) (Reproduced with permission from Eustachian tube: Structure, Function, Role in otitis media, by Charles D. Bluestone. pmph-usa.com)

The LVP muscle increases in cross-sectional area and in volume and reaches a more suitable vector for an efficient active tubal dilatation.

The ET of the infant is floppy and very distensible and lacks recoil phenomena of the hinge region. With time, the tubal cartilage stiffens, and the elastin component develops in the hinge region; this results in a reduced tubal compliance and increased recoil, which improves the protective mechanism of the ET [13].

The lumen of the ET increases almost five times from the newborn to a 20-year-old adult; the cross-sectional length of the lumen increases significantly with age, especially in the pharyngeal area of the tube. The lumen in most of the cartilaginous portion of the ET is significantly smaller in children than in adults [14]. Also the Ostmann fat pad increases in volume with age until adulthood, which contributes to a better protective function in adults [15].

7.3 Eustachian Tube Anatomy

The ET is a narrow osteocartilaginous channel connecting the tympanic cavity to the nasopharynx. Its lumen allows the passage of two different substances: one is gaseous for middle ear ventilation, and the second is fluid from the middle ear clearance. The ET begins at the tympanic orifice of the protympanum and ends at the pharyngeal orifice situated on the lateral wall of the nasopharynx (Fig. 7.6a). Its trajectory from posterolateral to anteromedial and from superior to inferior shows two slow curves as an inverted S.

The general shape of the ET resembles to an hourglass made of two unequal cones. The posterior cone is small and fixed and represents the bony ET; the anterior one is elongated and mobile and represents the fibrocartilaginous ET. Both cones are connected at a junctional zone, the *isthmus,* with an angle of 160° (Fig. 7.6b).

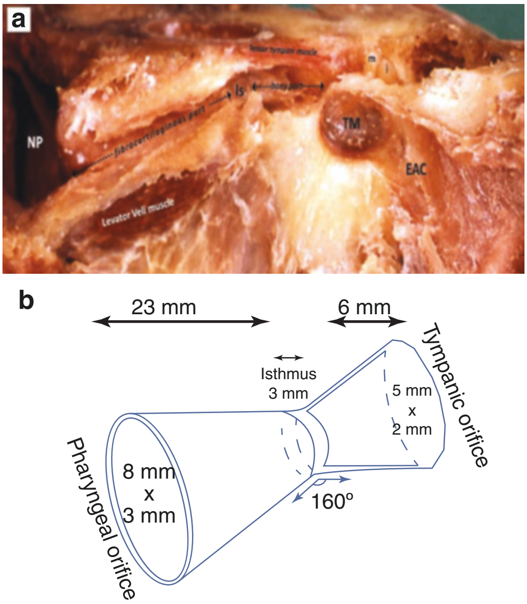

Fig. 7.6 (**a**) Cadaveric section of left temporal bone along the axis of the Eustachian tube showing the bony part and the associated tensor tympani muscle and the fibrocartilaginous part and associated levator veli palatini muscle as well as the isthmus (Is) between the two portions. *m* malleus head; *i* incus body; *NP* nasopharynx; *TM* tympanic membrane; *EAC* external auditory canal. (**b**) Corresponding schematic drawing of the Eustachian tube with its different dimensions (average)

In adults, the tubal axis forms with the plane of the hard palate an average angle of 36° (range 31–40°). The total length of the ET is 33 mm, divided as the following (Fig. 7.6):

- The bony part with 6.5 mm [16, 17]
- The junctional part with 3 mm
- The cartilaginous part with 23.5 mm

The bony portion is patent at all times, in contrary to the fibrocartilaginous portion that is closed at rest and opens during swallowing or when forced to open, such as during the Valsalva maneuver.

7.3.1 The Bony Portion of the Eustachian Tube

The bony part of ET lies completely within the petrous part of the temporal bone. It runs from the ostium in the middle ear cavity in an anteromedial direction, following the petrous apex, toward the petrosphenoid sulcus on the inferior surface of the skull base.

The tympanic orifice of the Eustachian tube, the ostium, lies in the middle third of the anterior wall of the middle ear cavity, 4 mm above the floor of the middle ear, close to the carotid canal (see Sect. 2.6.2). The ostium is of oval shape, and it measures about 5 mm horizontally and 2 mm vertically [12] (Fig. 7.6b).

The bony ET lumen is roughly triangular, measuring 2–3 mm vertically and 3–4 mm along the horizontal base [18].

The medial wall of the bony portion of the Eustachian tube consists of two parts: the cochlea posteriorly and the carotid anteriorly. The average thickness of the bony wall of the anteromedial portion is 1.5–3 mm. This bony wall is dehiscent in 2% of individuals, exposing the carotid artery [18] (Fig. 7.7).

The upper third of the endoluminal surface of the medial wall is covered by the bony canal of the tensor tympani muscle. The upper wall or roof of the bony tube corresponds to the tegmen tubari (Figs. 7.7 and 7.8). The lateral wall of the bony tube neighbors the canal of Hugier and the temporomandibular joint. At the ostium, the ET and the internal carotid share the same bony wall.

On the inferior surface of the base of skull, the anterior end of the bony tube is constricted and opens on the posterior part of the tubal sulcus.

Mucosal lining of the bony part is the same as middle ear: ciliated epithelium with few mucus-producing cells.

The petroux apex is pneumatized in almost half of examined temporal bones by CT images; of these, 92% featured a peritubal cell appearing to directly communicate with the tubal lumen [19]. These cells may open at any point along the ET, although this most frequently occurs posterolaterally. Peritubal cells linked to the ET lumen are potential points for CSF leakage after ear and skull base surgery such as the translabyrinthine approach for vestibular schwannoma resection [20].

Surgical Application

The majority of temporal bones with pneumatized petrous apex harbor peritubal air cells that may open directly into the ET lumen (Figs. 7.9 and 7.10). This explains the probability of cerebrospinal fluid rhinorrhea after translabyrinthine approach to the cerebellopontine angle, when ET obliteration is not performed sufficiently far into the lumen by the end of the procedure [21].

7.3.2 The Junctional Segment or Isthmus

The cartilaginous and bony portions of the ET join at a bottleneck area to form the junctional segment of the ET.

This segment is 3 mm long, 2 mm in height, and 1 mm wide. It lies between the carotid canal medially and the temporomandibular joint and the foramen spinosum with the middle meningeal artery laterally (Fig. 7.7). The junctional part of the ET may be a safe landmark to identify and protect the ICA during endoscopic endonasal surgery of the cranial base [22].

Due to its reduced caliber, this segment plays a protective role for the middle ear in preventing reflux of nasopharyngeal secretions and microorganisms to enter the middle ear cavity.

7.3.3 The Fibrocartilaginous Tube

The fibrocartilaginous portion of the ET is 20–24 mm long; it extends along the base of the skull from its junction with the bony portion of the tube until the medial pterygoid plate (Fig. 7.11). Posteriorly this part of the ET extends about 3 mm into the bony part and is firmly attached to the basal aspect of the skull by fibrous bands. It is angled 30°–40° to the transverse plane and 45° to the sagittal plane of the base of the skull [12]. At this level the fibrocartilaginous part

Fig. 7.8 Medial view of a sagittal cadaveric cut through a left middle ear (ME), showing the bony Eustachian tube (Pr) and the canal of tensor tympani muscle (asterisk), the isthmus (I), the cartilaginous Eustachian tube (ET), and its inferiorly related levator veli palatini muscle (LVP). The superior wall of the bony Eustachian tube is formed by the tegmen tubari

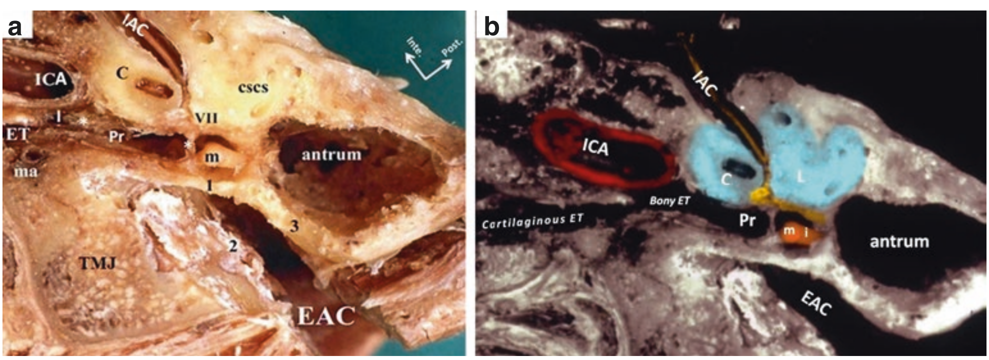

Fig. 7.7 (**a**) Transverse cut of a left ear showing in (**a**) the bony Eustachian tube (Pr: protympanum)) housing the tensor tympani muscle (*), the cartilaginous Eustachian tube (ET), and the isthmus (I). Notice the relation of the Eustachian tube and the cochlea (C) and the petrous internal carotid artery (ICA) medially and the temporomandibular joint (TMJ) and middle meningeal artery (ma) laterally. *EAC* external auditory canal; *1* attic outer wall; *2* anterior wall of EAC; *3* posterior wall of the EAC; *m* malleus; *VII* tympanic segment of facial nerve; *CSCS* superior semicircular canal. *IAC* internal auditory canal. (**b**) Same cut where the inner ear (L) and carotid artery (C) were highlighted with special colors. Notice the close relationship of the bony ET and isthmus with the carotid artery

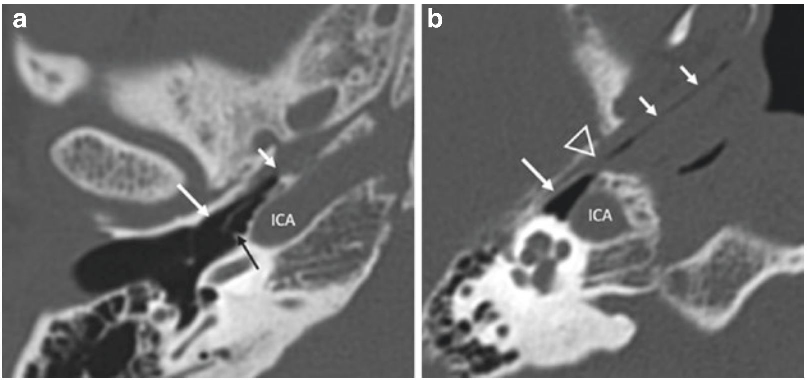

Fig. 7.9 CT images of the ET of a right ear and its relation to the intrapetrous carotid artery (ICA): (**a**) on the axial standard plan, only the bony part of the ET appears between the tympanic orifice (long white arrow) and the isthmus (short white arrow). Medially, the ET is separated from the intrapetrous carotid artery (ICA) by peritubal cells (black arrow). (**b**) An oblique reconstruction along the trajectory of the cartilaginous portion of the ET may allow to follow the visible thin lumen toward the pharyngeal orifice (short arrows). Isthmus (arrowhead), the osseous portion (long white arrow) until the tympanic orifice

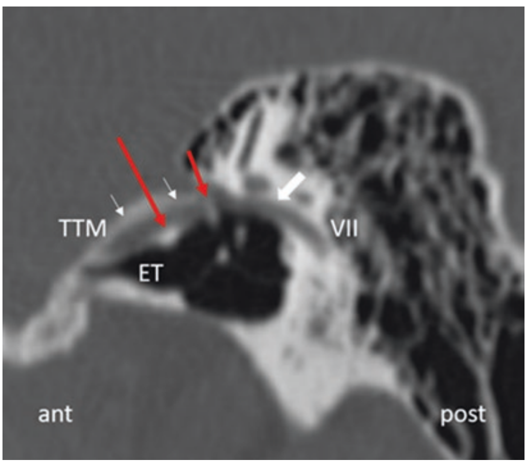

Fig. 7.10 A sagittal oblique CT reconstruction shows the end of the bony part of the ET (Eustachian tube, long red arrow) beneath the TTM (tensor tympani muscle, small white arrows) that continues till the cochleariform process (short red arrow). VII (thick white arrow, facial nerve)

is loosely attached in the sphenoid sulcus (*sulcus tubae*) between the greater wing of the sphenoid bone and the petrous portion of the temporal bone (Fig. 7.12). The nasopharyngeal end of the tubal cartilage crosses the superior border of the superior pharyngeal constrictor muscle to enter the nasopharynx; it is tightly fixed by a broad attachment to a tubercle on the posterior edge of the medial pterygoid plate [18].

The fibrocartilaginous tube is composed of two components: the cartilaginous part, the major component that is complete laterally, and the fibromembranous part inferiorly (Figs. 7.13 and 7.14).

7.3.3.1 The Cartilaginous Part (Fig. 7.14)

The cartilaginous portion of the ET is composed of one piece of cartilage that is shaped like a triangle at the top rear with a lower concavity. The apex or posterolateral end of this triangle joins the bony portion at the isthmus; the wider antero-medial end lies under the mucosa of the nasopharynx.

The tubal cartilage is an elastic cartilage, and this elasticity is crucial for the reset forces after the contraction of the TVP. The cartilage has an inverted J shape in cross section; it is like a dome with two arms of different length called laminae, described as a short *lateral lamina and* an elongated *medial lamina* with a *hinge* at the junction of the two laminae. The radial organization of elastic fibers around the dome of the cartilage suggests that motion of the lateral arm relative to the medial arm of the cartilage is possible.

- The medial lamina, much more voluminous than the lateral lamina, starts as a short structure of 9 mm of height at the isthmus to

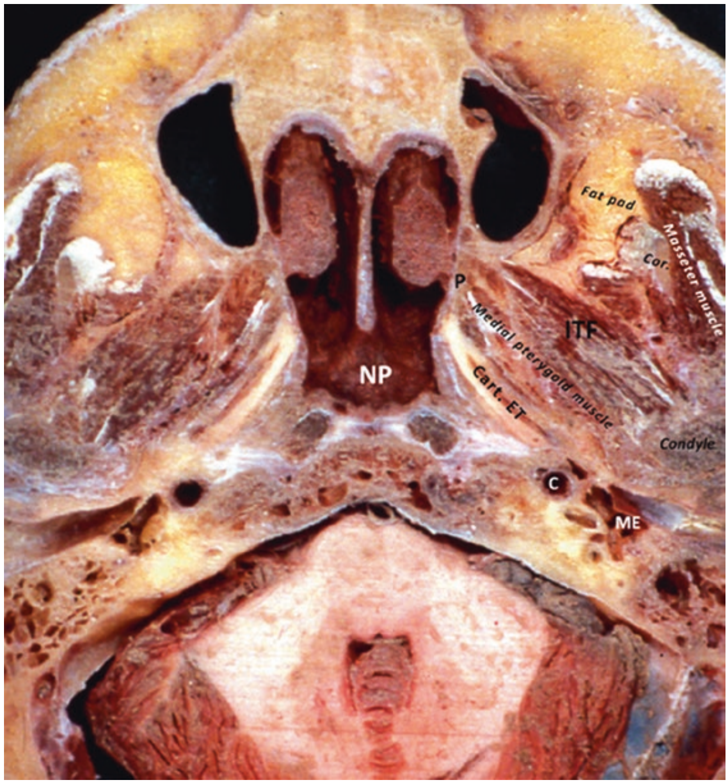

Fig. 7.11 Transverse section of a cadaveric head at the level of skull base just below the sphenoid greater wings showing the cartilaginous Eustachian tube (Cart. ET) extending along the base of the skull from its junction with the bony portion of the tube until the medial pterygoid plate. *ITF* infratemporal fossa; *P* medial pterygoid plate; *C* petrous portion of carotid artery; *cor* coronoid process of mandible; *NP* nasopharynx

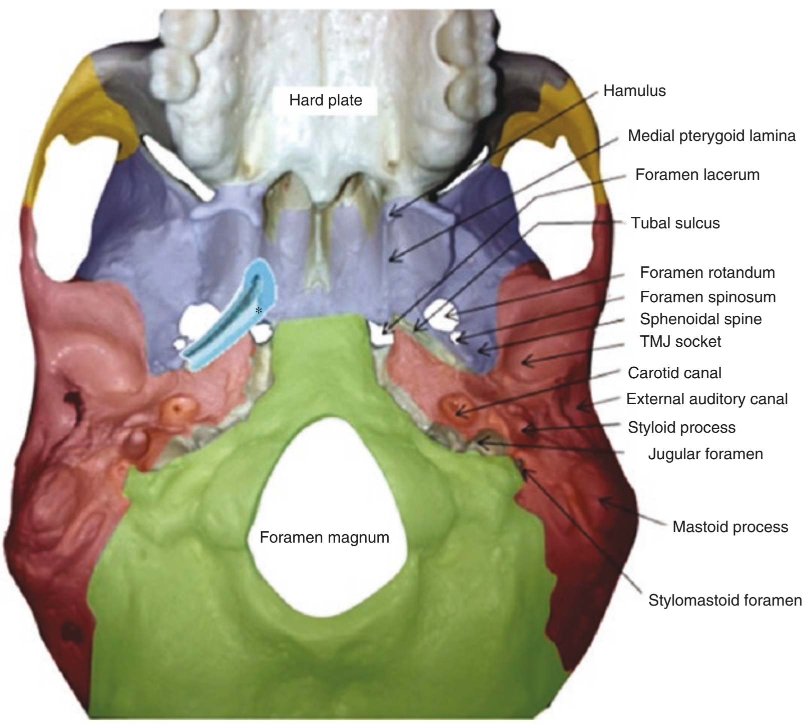

Fig. 7.12 Tubal cartilage (*) insertion in the sulcus tubae

increase rapidly to 13 mm just posterior to the attachment of the cartilage to the medial pterygoid plate [18]. The medial lamina extends more inferiorly than the lateral lamina to protrude into the nasopharynx and provides the skeleton for the *torus tubarius*. The medial lamina is quite mobile in its nasopharyngeal end and rotates medially during tubal dilatation principally by action of the levator veli palatini.

- The lateral lamina has a constant height of 2 mm over all its extension. Since the lateral lamina is shorter than the medial lamina, a fibrous membrane completes the remaining lateral wall of the Eustachian tube (Figs. 7.13 and 7.14).
- The hinge portion superiorly, rich in elastin, serves to return the lateral lamina to its original position after active opening of the tube by TVP muscle contraction.

The nasopharyngeal end of the Eustachian tube lies about 20 mm above the plane of the hard palate. The lateral lamina protrudes under the mucosa of the nasopharynx to form the *torus tubarius.*

The cartilaginous part of ET forms a valve that protects the middle ear from *pressure fluctuations* in the pharynx and decreases transmission of a *person's voice* to the middle ear cavity. The cartilage provides structural support to the Eustachian tube while still allowing mobility, and the function of the ET is intimately related to the structure, composition, and attachment of the cartilage.

7.3.3.2 The Fibrous Part

The fibrous part forms the lateral and the inferior wall of the fibrocartilaginous ET, called the *salpingopharyngeal fascia of von Tröltsch*. It is thick and resistant. Laterally, it serves as the site of insertion of the TVP muscle. The lateral part of the fascia of von Tröltsch is inserted to the base of skull at the petrosphenoid suture (*Proctor's ligament*), close to the foramen spinosum, the foramen ovale, and the base of the pterygoid process laterally (see Figs. 7.11 and 7.12).

> **Clinical Application**
> As ET cartilage is made up of elastic cartilage (rich in elastin), it does not calcify usually; however, ET cartilage calcifications were reported in the literature, evaluated with a rare prevalence of 0.6% of cases [23]. These calcifications concerned almost all the medial lamina cartilage and most frequently in the torus tubarius region [24]. Here the authors report a case of calcification of both laminae immediately anterior to the junctional zone (Fig. 7.15).

The medial part of the fascia of von Tröltsch is anchored superiorly to the inferior curvature of the lateral lamina of the tubal cartilage. The region between the fascia and the ET mucosa is occupied by a glandular tissue anteriorly and adipose tissue posteriorly.

7.3.3.3 Ostmann Fat Pad

Two different Ostmann fat pads have been anatomically described, the *lateral* and the *medial Ostmann fat pad:*

- **The lateral Ostmann fat pad (LOFP).** It is the most important fat pad and it has received the main attention and work regarding its functional anatomy. It is a lympho-adipose body, running the length of the cartilaginous ET located in the inferolateral aspect of the pharyngeal end of the Eustachian tube. It occupies the space between the ET membrane and the TVP muscle (Figs. 7.13 and 7.14).
  In the Würzburg material [25], the Ostmann fat pad has an average maximum thickness of 2.4 mm measured in transverse sections (this value is reached 20 mm posterolateral to the pharyngeal orifice). The fat pad becomes thinner toward the pharyngeal end of the tube.
  The Ostmann fat pad increases in volume during childhood, being most voluminous in adults, and regresses in the elderly. Schuknecht reported a relationship between important weight loss and a decrease in size of the fat pad

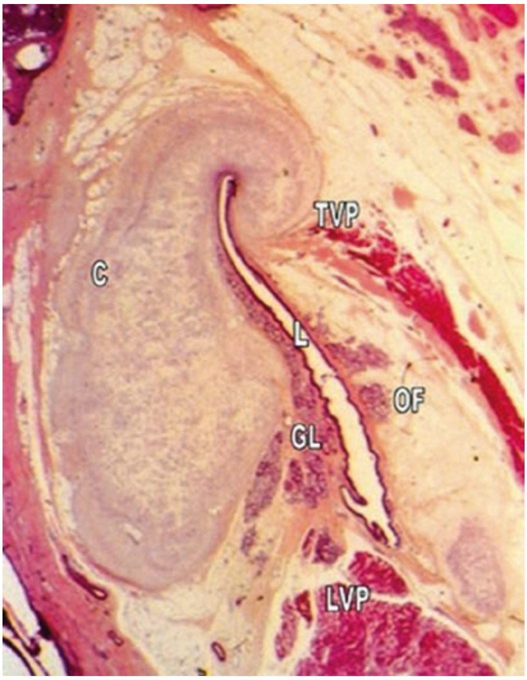

Fig. 7.13 Mid-cartilaginous portion of a normal left Eustachian tube of an adult temporal bone specimen. *C* cartilage; *L* lumen; *GL* submucosal glands; *LVP* levator veli palatini muscle; *TVP* tensor veli palatini muscle; *OF* Ostmann fat pad (Courtesy of I. Sando, MD) (Reproduced with permission from Eustachian tube: structure, Function, Role in otitis media, by Charles D. Bluestone. pmph-usa.com)

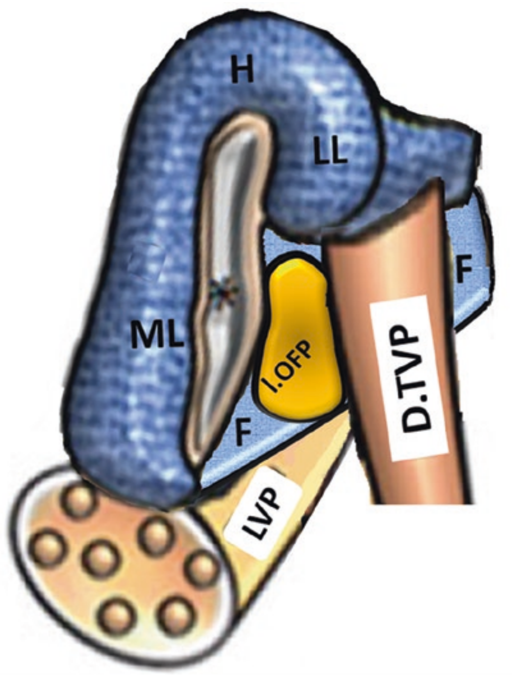

Fig. 7.14 Schematic drawing of the mid-cartilaginous portion of a normal left Eustachian tube showing the two laminae of the tubal cartilage, *ML* medial lamina; *LL* lateral lamina, connected by the hinge H. *: lumen, *LVP* levator veli palatini muscle; *D.TVP* deep part of tensor veli palatini muscle; *LOMF* lateral Ostmann fat pad; *F* fibrous membrane

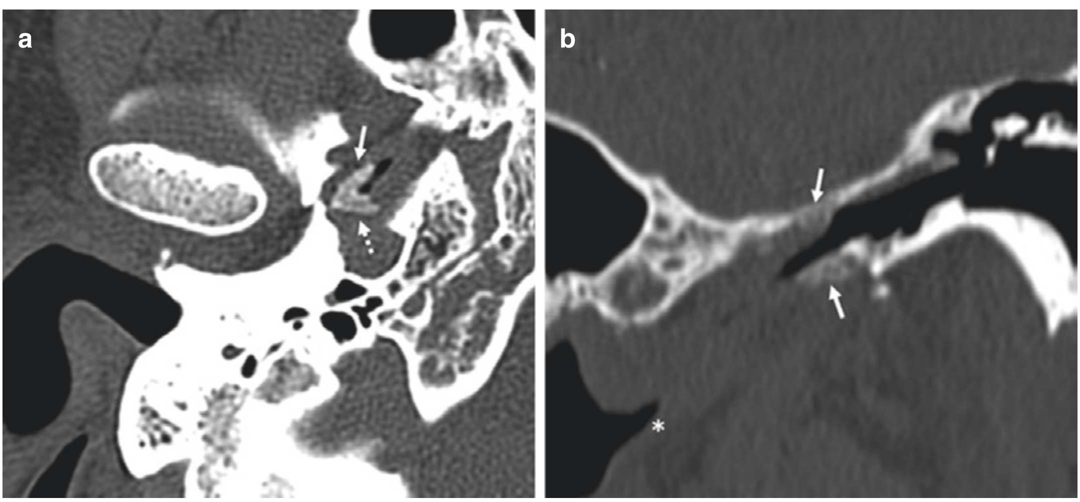

Fig. 7.15 (**a**) Axial CT image passing by the posterior part of the cartilaginous ET, showing a large calcification of the hinge, the lateral (white arrow) and medial lamina (dashed arrow). (**b**) Coronal CT reconstruction of the same calcifications in the plan along the ET-axis, the calcifications surround the lumen of the ET almost completely in this entirely cartilaginous part of the ET without intraluminal obstruction

and the appearance of a patulous ET [26]. In malnourished persons this pad of fat vanished causing patulous ET.

- ***Two different roles of the lateral Ostmann fat pad* have been described:**
  – The static pressure of the LOFP supports the passive closure of the ET after relaxation of the tensor veli palatini to protect the ME from ascending secretions and sound noises from the nasopharynx to the middle ear. It also helps in the evacuation of the ME due to sniffing.
  – It serves as a fulcrum for the deep layer of the TVP; it transfers the pressure of the contracting tensor muscle to the lower portion of the ET; hence the LOFP limits ET opening to its superior aspect (Rüdinger's safety canal) (Fig. 7.16) [27].
- **The medial Ostmann fat pad (MOFP)** (Fig. 7.16). It is situated between the lateral and medial suspensory ligaments, medial to the medial lamina, where it may be permeated by numerous fiber bundles from the basilar fibrocartilage and the medial suspensory ligament.
- ***Imaging of the Ostmann Fat Pads***
  CT and MR have both the ability to show the fat pads, when adapting the reconstruction plan three dimensionally. Once images obtained along the axis of ET, there is almost always a very thin lumen of the ET visible (Fig. 7.17b, c)*, facilitating the orientation.*
  On CT, the fatty aspect of the lateral fat pat is well recognized when focused on this region (the density measurement has typical negative values about − 20 to − 80 UH), and also the medial fat pad can be localized (Fig. 7.17).
  On MR, especially T1-weighted images demonstrate a good contrast between the hyperintense aspect of fat, surrounded by isointense muscles, and the hypointense air inside the almost collapsed ET lumen (Figs. 7.18 and 7.19).

7.3.3.4 The Pharyngeal End

The pharyngeal end of the ET passes above the superior constrictor muscle through the sinus of Morgagni to lay under the mucosa of the nasopharynx. The pharyngeal orifice lies approximately at the posterior level of the vomer, about 1.25 cm behind the posterior end of the inferior turbinate and approximately 2 cm above the plane of the hard palate (Fig. 7.20) [12].

The pharyngeal orifice is triangular in shape with an inferior base; it measures 8–10 mm in height and 3–5 mm in width (Figs. 7.6 and 7.21). The pharyngeal orifice is closed at rest and becomes elliptical or triangular with a superior apex during opening [28].

The anterolateral border is a vertical crease, called the salpingopalatine crease of Troeltsch. It corresponds to the lateral plate of the tubal cartilage and the TVP muscle.

The posteromedial border is prominent and corresponds to the medial lamella of the tubal car-

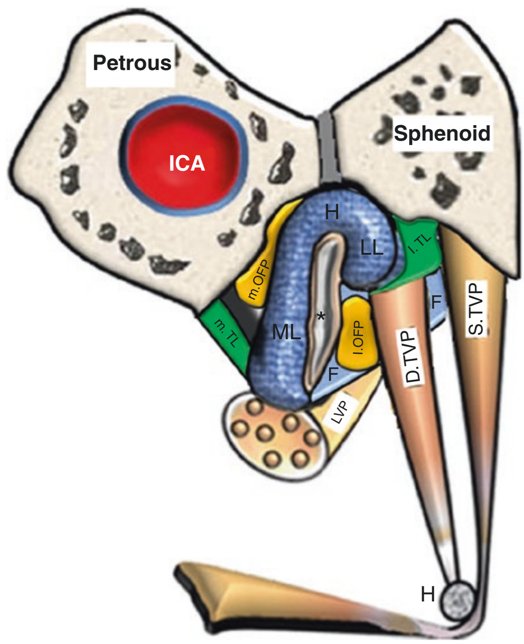

Fig. 7.16 Schematic drawing of mid-cartilaginous portion of a left Eustachian tube and its attachment to skull base. The ET is attached to skull base by medial tubal ligament m. TL and lateral tubal ligament L. TL. Around the ET, two fat pads exist, one medially (medial Ostmann fat pad m. OMF) between the medial lamina of the tubal cartilage and medial tubal cartilage ligament and one laterally (lateral Ostmann fat pad l. OMF) between the lateral lamina of the tubal cartilage and lateral tubal cartilage ligament. *: lumen, *LVP* levator veli palatini muscle; *D.TVP* deep part of tensor veli palatini muscle; *S.TVP* deep superficial part of tensor veli palatini muscle; *F* fibrous membrane

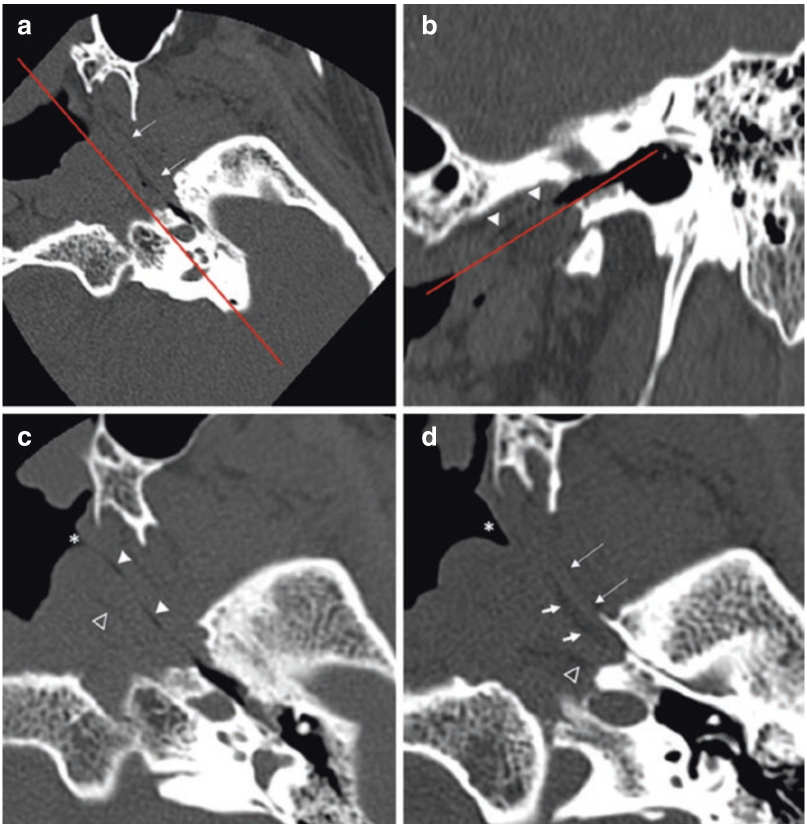

Fig. 7.17 (**a**) Standard axial plan, tensor veli palatini muscle (small arrows) well individualized. (**b**) Sagittal reconstruction along the red reference line of (**a**): demarcation of the ET lumen by a thin aeration line (plain arrowheads). (**c**) + (**d**) Reconstruction of consecutive axial oblique images along the red reference line of (**b**), pharyngeal orifice of the ET (*): in (**c**), a thin lumen of the ET (arrowheads), a thin hypodense line corresponding to the medial fat pad (empty arrowhead) is seen medially and at distance to the ET lumen. In (**d**), the image inferior to (**c**), the lateral Ostmann fat pad is seen as a long hypodense fusiform structure (short arrows) with typically fatty values on density measurements (between −20 and − 80 UH) and can be clearly individualized medial to the TVP muscle (long arrows)

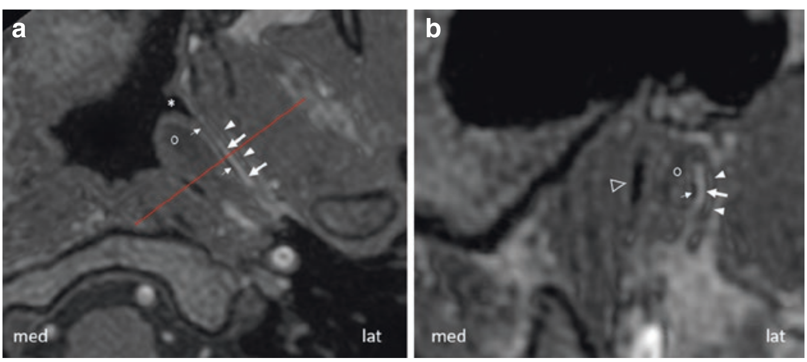

Fig. 7.18 MR image 3D T1 Dixon, proton density weighted: (**a**) reconstruction of an axial cut after inclining the volume along the oblique axis of the ET: (*) pharyngeal orifice of the ET; the lumen of the ET is virtual (thin arrows); the lateral Ostmann fat pad is seen as a hyperintense fusiform structure (two long arrows), medially to the tensor veli palatini muscle (arrowheads). (open circle) Medial lamina of the ET cartilage, (**b**) reconstruction perpendicular to the ET-axis, as indicated by the red line in the a image: the virtual lumen (small arrow) of the ET is laterally surrounded/bordered by the fat pad, a longitudinal rim of fatty tissue, that is in very close contact to the tensor veli palatini (arrowheads). (open circle) Medial lamina of the ET cartilage, (empty arrowhead) lumen of the Rosenmüller fossa

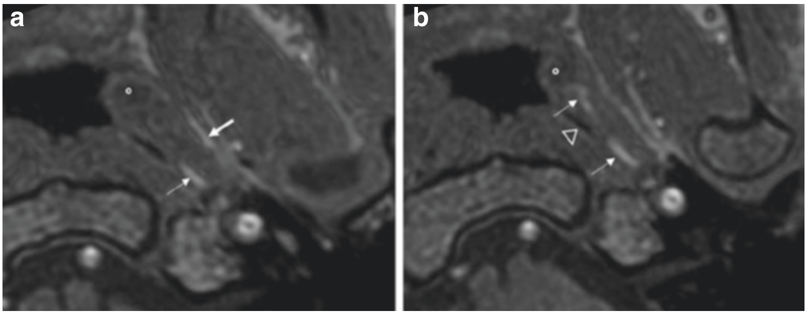

Fig. 7.19 Two axial views of proton density-weighted T1 MR images with 0.5 mm thickness reconstructed along the left ET-axis: (**a**) medial lamina of the ET cartilage (open circle), lateral Ostmann fat pad (thick arrow), medial Ostmann fat pad (thin arrow), (**b**) medial Ostmann fat pad (arrows), extended anteriorly until the posterior limit of the inferior part of the medial lamina (open circle)

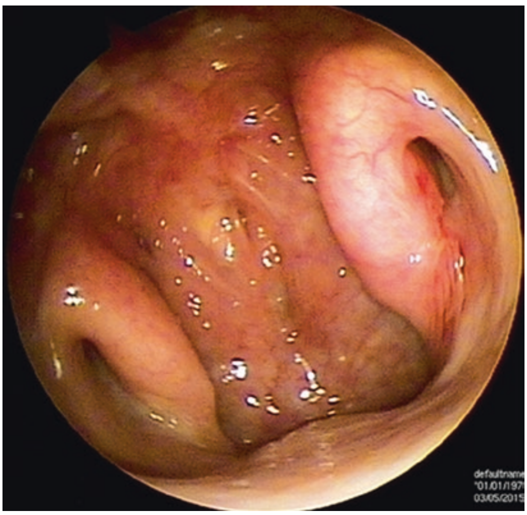

Fig. 7.20 Nasal endoscopy showing both ET pharyngeal openings and relation to palate

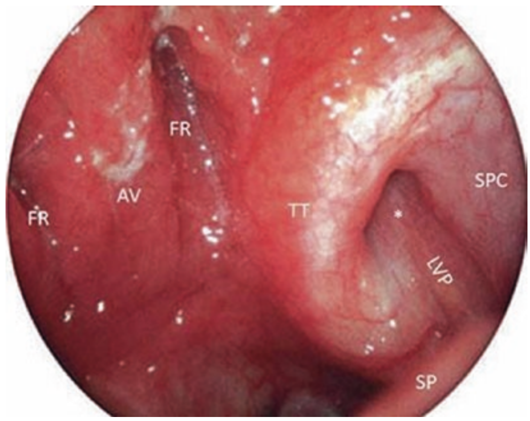

Fig. 7.21 Endoscopic view of left pharyngeal orifice. FR fossa of Rosenmüller, *AV* adenoid vegetation; *TT* torus tubarius; *SPC* salpingopalatine crease containing levator veli palatini muscle; *LVP* levator veli palatini muscle in the floor of the Eustachian tube; *SP* soft palate; * Eustachian tube lumen

tilage pressing against the nasopharyngeal mucosa; this prominent surelevation of the mucosa is called the torus tubarius (Fig. 7.21). The torus tubarius thickness is of 10–15 mm [18]. The mucosa of the torus tubarius is rich in glands and lymphoid tissue forming the *tonsil of Gerlach.*

The inferior border of the pharyngeal orifice is bounded by the levator veli palatini muscle.

Just medial and behind the torus tubarius, there is a recess called the *fossa of Rosenmüller,* which is a triangular recess of about 1.5 cm deep. Its apex is in close relationship with the carotid canal, and its base is closely related to the skull base with the foramen lacerum lying medially. Adenoid tissues usually extend into this recess giving soft tissue support to the ET (Fig. 7.21).

7.4 Topographic Anatomy of the ET and ICA

- In the plane of the sphenoid spine and foramen spinosum, the distance of the internal carotid artery (transverse petrous part) from the upper part of the tubal lumen averaged only 4.4 mm (1.4–8).

- In the petrous segment of the internal carotid artery only a thin, occasionally dehiscent, bony layer separates the artery from the tubal mucosa [29].
- The presence of the ICA is necessary for the development of the carotid bony canal. In the region of the tympanal ostium of the ET, a thin bony plate lies between the anterior wall of the tube and the ascending portion of the carotid artery. Marked bulging of the carotid artery into the protympanum was noticed in 13% of cases [30]. Cases of ectopic carotid with intrusion inside the ET lumen are reported [31].
- The ICA may relate closely to the pharyngeal part of the tube; positional variants near the pharyngeal orifice can be especially hazardous. Also Poe et al. have proposed that in diseases of the ET, the main focus should be in the functional valve area, located within the middle to upper portions of the cartilaginous ET over a length of about 10–15 mm [32]. Hence the potential for complications increases while progressing superiorly toward the cartilaginous and bony ET junctional point because the ICA gets increasingly closer to the ET [33].
- Therefore the surgical implications of positional variants of the internal carotid artery are self-evident and merit particular consideration when injections are administered for tissue augmentation along a patulous Eustachian tube.

7.5 Muscles of the Eustachian Tube

Four muscles are associated with the ET: the tensor veli palatini (TVP), the levator veli palatini (LVP), the salpingopharyngeus, and the tensor tympani muscle.

Eustachian tube is closed at rest and opens during swallowing or yawning. Active opening of the ET is induced by TVP muscle contraction [34–36]. *Closure of the tube is a passive phenomenon and is not the result of a muscular contraction*. It takes place secondarily to the passive reapproximation of the tubal walls by extrinsic forces exerted by the surrounding deformed tissues and also by the recoil of elastic fibers of the hinge portion [18].

7.5.1 The Tensor Veli Palatini (TVP) Muscle

The tensor veli palatini muscle originates from the bony wall of the scaphoid fossa and from the entire length of the short lateral lamina of the cartilage tube, to descend converging into a short tendon that turns medially around the pterygoid hamulus. It then fans out within the soft palate and mingles with the fibers from the opposite side in the midline raphe. The tensor veli palatini separates the Eustachian tube from the otic ganglion, the mandibular nerve and its branches, the chorda tympani, and the middle meningeal artery.

The TVP muscle is composed of two distinct bundles of muscle fibers: the lateral bundle (superficial) and the medial (deep) bundle that are separated by a fibroelastic layer (Fig. 7.22).

7.5.1.1 The Lateral Bundle

The lateral bundle is not related to the ET function. It has an inverted triangular shape with a superior base and an inferior apex. It starts superiorly at the scaphoid fossa of the sphenoid bone lateral to the ET cartilage and descends anteriorly, laterally, and inferiorly to converge in a tendon that rounds the hamular process of the medial pterygoid lamina. From the hamular process, it progresses to insert into the posterior border of the hard palate and into the palatine aponeurosis [18].

The lateral bundle of the TVP muscle ensures the tension of the soft palate.

7.5.1.2 The Medial Bundle

The medial bundle, also called the dilator tube muscle, has its superior origin in the posterior half of the lateral lamina of the ET cartilage. Its fibers descend sharply and converge in a tendon that inserts on the hamular process of the medial pterygoid plate.

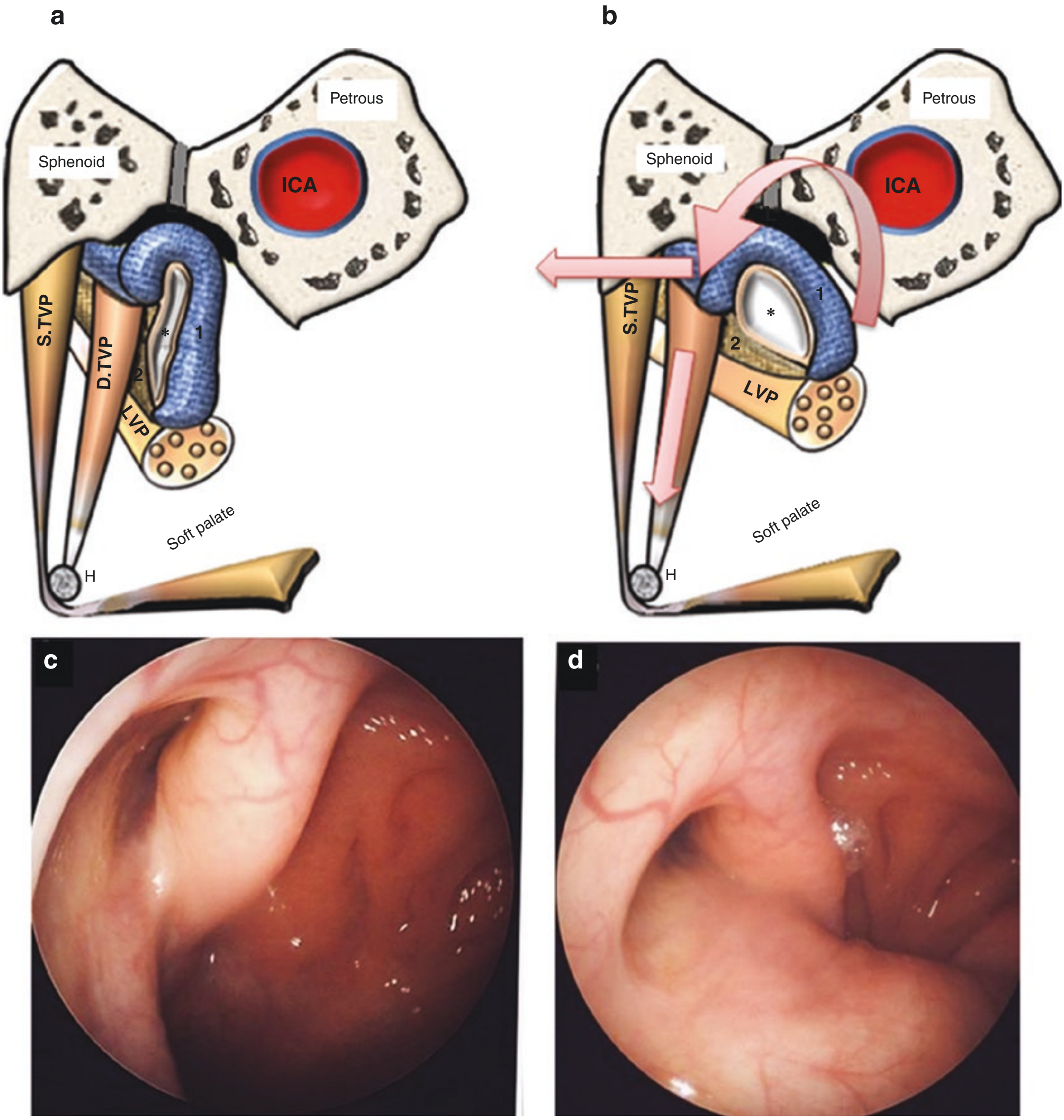

Fig. 7.22 Schematic representation (**a**, **b**) of paratubal muscles and the action of tensor veli palatini muscle and the corresponding opening of ET lumen (**c**, **d**). (**a**, **c**) During relaxation; (**b**, **d**) during contraction. *S.TVP* superficial bundle of tensor veli palatini muscle; medial bundle of DTVP deep bundle of tensor veli palatini muscle; *LVP* levator veli palatini muscle; *L* tubal ligament; *1* tubal cartilage; *2* tubal fibrous membrane; * tubal lumen; *H* hamulus; *ICA* internal carotid artery

The medial bundle is responsible for the active dilatation of the fibrocartilaginous tube by lateralization of the lateral lamina of the cartilage tube. The lateral layer compresses the lower part of the tube (membranous wall); thus the medial layer supports ventilation, and the lateral layer supports drainage and protection (Leuwer) [37–39].

Secondary attachments of the medial bundle are present sometimes at the maxillary tuberosity and the palatoglossal arch. These insertions suggest that even if the hamulus is infractured during cleft palate surgery, the TVP function could be maintained by preserving its maxillary insertion [40].

Both bundles are innervated by the mandibular nerve (V3).

There are three points of rotation for the TVP:

- The pterygoid hamulus
- The lateral Ostmann fat pad
- The medial pterygoid muscle

The medial pterygoid muscle is a chewing muscle which closes the mouth and helps in protruding the mandible. Its contraction causes a posteromedial movement of the TVP toward the cartilage increasing the tubal opening [41].

7.5.2 The Levator Veli Palatini (LVP) Muscle (Fig. 7.22)

The LVP muscle arises from the inferior aspect of the petrous apex of the temporal bone. Its rounded body passes inferomedially, paralleling and lying beneath the floor of the fibrocartilaginous tube lumen. The fibers of this muscle insert by fanning out and blending with the dorsal surface of the soft palate [12, 42]. The LVP muscle is related to the tube only by a loose connective tissue [34, 43].

It is essentially a muscle serving the soft palate, but it could also support the ET function by elevating the medial lamina of the cartilage at the pharyngeal orifice [44, 45]. In addition, being located inferolaterally to the ET and with its large cross-sectional area in this portion, the LVP may be related to the pumping clearance (drainage) function of the tube in such a way that the distal end of the tube closes first followed progressively toward the pharyngeal orifice, thus pumping out the middle ear secretions [46].

The levator veli palatini is innervated by the glossopharyngeal nerve (IX). Its main function is restricted to the competence of the soft palate.

7.5.3 The Salpingopharyngeal Muscle

The salpingopharyngeal muscle arises from the medial and inferior borders of the tubal cartilage via slips of muscular and tendinous fibers. Then the muscle courses inferoposteriorly to blend with the mass of the palatopharyngeal muscle. The salpingopharyngeal muscle is not involved in the function of the ET; it could keep in position the pharyngeal orifice of the ET.

It is innervated by the glossopharyngeal nerve IX [12, 43].

7.5.4 The Tensor Tympani Muscle

The tensor tympani muscle arises from the superior surface of the cartilaginous part of the auditory tube, the greater wing of the sphenoid, and the petrous part of the temporal bone. The muscle passes posterolaterally and always superiorly to the ET in its bony semicanal to the cochleariform process on the medial wall of the middle ear. Its tendon hooks around the cochleariform process to run laterally and insert into the medial aspect of the neck of the malleus. Contraction of the tensor tympani pulls the eardrum medially and restricts its mobility. Thus, sound transmission through the middle ear is attenuated when the tensor tympani is contracted.

The TTM is innervated by a branch of the mandibular nerve V3.

7.6 Eustachian Tube Blood Vessels

The arterial blood supply of the ET is derived from the ascending pharyngeal and middle meningeal arteries. The venous drainage is carried to the pharyngeal and pterygoid plexus of veins. The lymphatic chains drain into the retropharyngeal lymph nodes.

7.7 Eustachian Tube Nerves

The ostium and the cartilaginous portion of the ET are innervated by the pharyngeal branch of the sphenopalatine ganglion deriving from the maxillary nerve (V2). The bony portion of the ET is innervated by the tympanic plexus deriving from the glossopharyngeal nerve (IX).

7.8 *Addendum* : Physiology of Eustachian Tube Lumen and Mucosa

7.8.1 Eustachian Tube Lumen

At the tympanic orifice of the ET, the lumen is of 2 mm in height and 5 mm in width. The isthmus is the narrowest part as a vertical slot from 0.5 to 2 mm. Such variations have no influence on the middle ear ventilation. From the isthmus downward, the lumen expands continuously to become about 8–10 mm in height and 1–2 mm in width at its pharyngeal orifice.

7.8.2 Eustachian Tube Mucosa

The lumen of the ET is lined by a pseudostratified, columnar ciliated epithelium, which works to sweep material from the middle ear to the nasopharynx.

Goblet cells represent about 20% of the cell population of ET mucosa. The goblet cells are more prominent at the tympanic cavity end, contributing to the surfactant nature of the secretions (containing lecithin, lipid, and mucopolysaccharides) that decrease surface tension and keep the tube patent [47].

The density of cilia increases as the tube runs dorsolaterally to open into the nasopharynx, facilitating movement and drainage of mucus and other material.

The lumen mucosa presents different aspects in regard to its floor or its roof:

- The floor mucosa of the tube contains numerous goblet cells, copious ciliated cells, and glands.
- The roof mucosa of the tube has sparse goblet cells and cuboidal ciliated cells without seromucous glands.

Therefore, two different morpho-functional corridors are recognized in the ET lumen (Fig. 7.23):

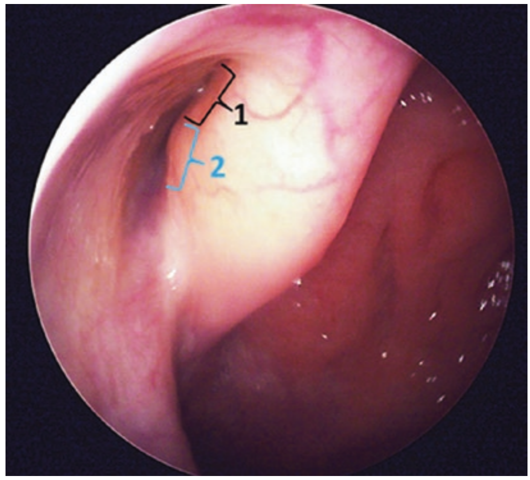

Fig. 7.23 Endoscopy of right ET showing the two corridors in the ET lumen: the superior corridor (1) or the roof is mainly for ventilation function, and inferior corridor (2) or the floor is mainly for mucociliary clearance

1. *Superior corridor (Rüdinger's safety canal)*: This is the upper compartment of the ET which is devoted to ventilation. The lumen of the ET measures 6.2 mm. Rudinger described in the upper part of the tube located in the cartilaginous groove a space 0.4–0.5 mm in diameter that is constantly patent and is occupied by air. This area is known as Rüdinger's safety canal [48]. It has an average diameter of 0.4 mm and commenced about 10 mm behind the pharyngeal orifice. It could not always be traced for the entire length of the cartilaginous part of the tube.
2. *Inferior corridor*: the floor, mainly surrounded by the muscular or membranous wall of the Eustachian tube and partly by the medial lamina of the cartilage. It shows frequently folds or micro-turbinates which seem to contribute to the mucociliary clearance and to the protection function of the Eustachian tube [49].

7.8.3 Eustachian Tube Dynamics

Active ventilatory function (active opening) of the ET depends heavily upon functional cooperation between the TVPM and the lateral lamina of the ET cartilage as well as the lateral membranous wall of the ET lumen. The ET lumen is considered to open actively by lateral shifting of the lateral luminal wall together with contraction of the TVPM, These findings indicate that poor development of the lateral lamina of the ET cartilage, and/or poor insertion of the TVPM into the lateral lamina, could lead to impaired active opening of the ET.

The opening of the ET is facilitated by the relaxation of the medial pterygoid due to an anterolateral movement of the TVPM while opening the mouth. Between the TVPM and the medial pterygoid muscle, there is the Weber-Liel fascia. On both sides of this fascia, Wenzel found fibromuscular interconnection [50]. Thus, both muscles at the medial third of the ET do not only passively shift against each other but represent a mechanical functional unit.

The functional unit composed of the TVPM, the lateral lamina of the tubal cartilage, the Ostmann fat pad, and the lateral suspensory ligament has the effect of dilating the upper portion of the tubal lumen while compressing the lower portions of the lumen. This creates a bidirectional mechanism that transports air toward the tympanic end of the tube and mucus toward the pharyngeal end. This mechanism is particularly active in the tubal segment where the Ostmann fat pad is most prominent, that is, the posterolateral portion of the cartilaginous tube just before the isthmus. This concept is supported by the absence of cilia in the roof area of the tube and the abundance of goblet cells in the lower portions [51].

In summary the action of ET opening is the result of an anterior pressure of the lateral part of the TVPM inducing a latero-caudal traction of the lateral lamina and medio-cranial rotation of the medial lamina.

The combination of mucosa, submucosa, Ostmann fat pad, and TVPM acts as a *valve* within the cartilaginous tubal lumen which performs a protective function by keeping the lateral mucosa opposed to the medial mucosa in the resting state.

Ostmann fat pad prevents air from entering the nasopharynx in the resting state when there is positive pressure in the tympanic cavity. Even at rest, the fat pad is believed to exert a certain amount of closing pressure on the tubal lumen.

7.8.4 Functions of the ET

The ET fulfills three main roles, which together facilitate middle ear homeostasis and the transmission of sound from the tympanic membrane to the cochlea.

- Equalization of middle ear pressure to the ambient atmospheric pressure: a need due to external pressure fluctuations and mucosal gas exchange.
- Mucociliary clearance of middle ear secretions.
- Prevention of the retrograde travel of speech sounds and pathogen-laden secretions up the ET from the nasopharynx (reflux).

Although the osseous portion of the ET remains patent and is not dynamic, the cartilaginous portion of the ET is normally closed and opens only for brief periods of time. This situation blocks the nasopharyngeal secretions or a gastric reflux from entering into the middle ear as well as it prevents autophony.

Brief intermittent periods of ET opening occur in normal individuals to insure middle ear ventilation. The ET opens 1.5 times every minute. Every opening lasts about 0.5 s, so ET openings last about 1 min a day [52]. These openings are the result of the contractions of TVPM.

In addition, the ET insures the function of the middle ear mucociliary clearance. The ciliated epithelial cells of the lumen floor provide a mucociliary “elevator” to push debris and secretions downward from the ET into the nasopharynx.

7.8.5 Neural Control of Eustachian Tube Function

A neural loop, between the baroreceptors of the ME cleft and the baroreceptors in the nasopharyngeal area connecting the solitary nucleus of the Pons, regulates the neural control of the ET opening and the ME gas exchanges [53–55]

For instance, a decrease in middle ear pressure as compared to nasopharyngeal pressure will be detected by the solitary nucleus of the Pons which

Clinical Application

Impairment of tubal functions can be divided into two main categories: *Eustachian tube dysfunction* when the tube does not open properly or *patulous Eustachian tube* when the tube remains inappropriately patent.

Eustachian Tube Dysfunction (ETD)

Classically ETD is the result of a mucosal inflammation with obstruction, or anatomical extrinsic obstruction, or failure of dilatation from muscular problems causing dilatory dynamic dysfunction.

Dilatatory dynamic dysfunction of the ET is a strong contributor for ETD in infants [55, 56].

Anatomical extrinsic obstruction must always be ruled out (adenoid hypertrophy, etc.).

In adults presenting unilateral ETD, nasopharyngeal or infratemporal fossa tumors must be ruled out (Fig. 7.24).

Intrinsic blockage of the ET is more common than anatomical extrinsic obstruction. It is often the result of mucosal inflammation (mucosal disease), possibly due to allergy or laryngopharyngeal reflux. Tobacco use results in a loss of the normal ciliary clearance of the mucosa and causes frequently ETD.

Patulous Eustachian Tube (PET) (Fig. 7.25)

PET occurs when the ET tube remains patent for long periods of time beyond the normal brief interval of opening. This condition could be related to Ostmann fat pad atrophy that may develop after substantial weight loss or post-pregnancy.

Patients with PET typically complain of autophony and aural fullness. When patients lie down, the symptoms usually abate due to venous engorgement of ET mucosa.

Infantile Eustachian Tube

The differences in the anatomy of the ET between infants and adults explain the functional differences that play an important role in the inflammatory pathology of the middle ear and their complications.

Dilatory dynamic dysfunction of the ET is a strong contributor for ET dysfunction in infants. In infants, the shallow tubal angle affects adversely the muscle vector of the TVP, which in addition to the highly compliant tubal cartilage leads to a failure of active opening of ET by TVP muscle contraction [56, 57].

Changes in the tubal angle and the cartilage strength until adulthood are responsible for more efficient active opening of the ET, improved protective role, and an improved clearance function (Fig. 7.5 and Table 7.1).

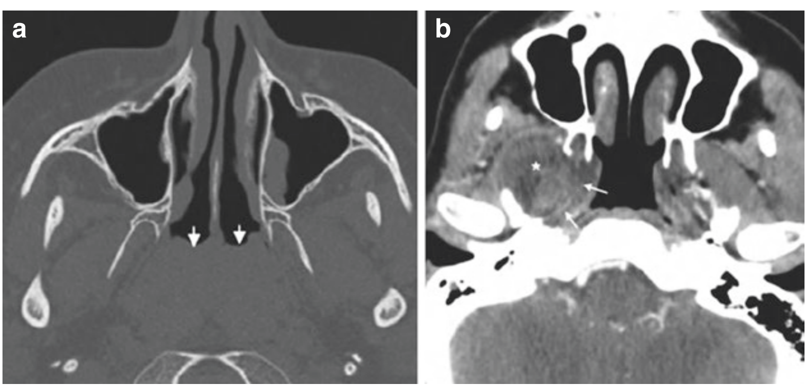

Fig. 7.24 (**a**) Transversal computed tomography of a 15-year-old boy with bilateral adhesive otitis media. Huge adenoid hypertrophy (white arrows) in the nasopharynx. (**b**) Transversal injected computed tomography of an adult showing a well-encapsulated globulous lesion (schwannoma) of the right infratemporal fossa (*), with a mass effect (white arrows) on the Eustachian tube

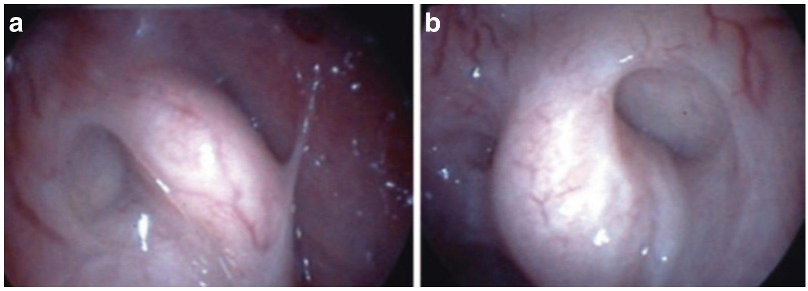

Fig. 7.25 Bilateral patulous Eustachian tube (**a**, right side; **b**, left side) in a patient who underwent bariatric surgery 6 months ago. Notice the incompetent pharyngeal opening of the ET on both sides

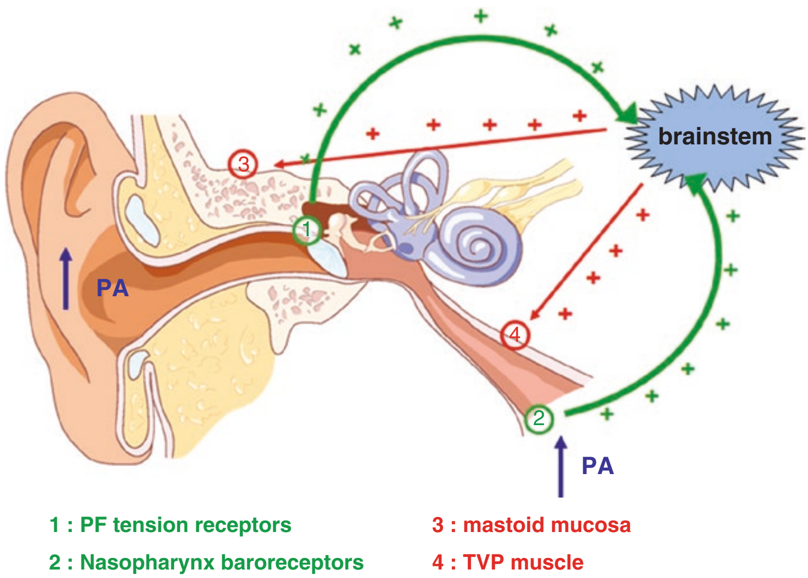

Fig. 7.26 A neural loop, between the baroreceptors of the ME cleft (1) and the baroreceptor in the nasopharyngeal pre-tubal area (2) connecting (green arrows) the solitary nucleus of the brain stem, regulates (red arrows) the neural control of the ET opening (4) and the mastoid mucosa gas exchanges (3)

Table 7.1 Table of anatomical differences of the Eustachian tube between infants and adults: (wider, shorter and more horizontal in infant)

	Infant	Adult
Length (mm)	Approximately 15–18 mm	Approximately 30–36 mm
Cartilaginous portion	Less than 2/3 of the tube	longer = 24 mm (2/3)
Bony portion	Longer (more than 1/3) and wider than in adult	shorter, narrower, = 12 mm (1/3)
Pharyngeal orifice	Height 4 mm, width 2 mm	Height 8 mm, width 2 mm
Angulation with respect to base of skull (°)	10 degrees	45 degrees
Tensor veli palatini muscle action	Less efficient	More efficient
Ostmann fat pad	Less prominent	Prominent

will initiate orders for tubal muscles to contract and open the ET (increase gaz ventilation) and for mastoid mucosal vessels to constrict (decrease mucosal gaz diffusion). Both mechanisms will increase middle ear pressure (Fig. 7.26).

7.9 Conclusion

The Eustachian tube is a complex anatomical structure which communicates the middle ear to the nasopharynx.

Imaging studies of the Eustachian tube encounter difficulties due to its oblique orientation to any standard imaging plan and an almost virtual lumen in the absence of a pathologic distension.

The ET is still not available for surgical exploration, due to its multiple organizational structures, its multidimensional orientation, and its delicate neighborhood.

Different interpretations of the function of the different anatomical constituents of the Eustachian tube are behind the lack of the full understanding of its dysfunction and secondary middle ear disorders.

References

1. Cummings CW, Frederickson JM, Harker LA, et al. Anatomy and physiology of the Eustachian tube. In: Otolaryngology: Head and Neck Surgery. St. Louis, MO: C.V. Mosby; 1986.
2. Proctor B. Embryology and anatomy of the Eustachian tube. Arch Otolaryngol. 1967;86:503–26.
3. Swarts JD, Rood SR, Doyle WJ. Fetal development of the auditory tube and paratubal musculature. Cleft Palate J. 1986;23:289–311.
4. Wolff D. The microscopic anatomy of the Eustachian tube. Ann Otol Rhinol Laryngol. 1934;43:483.
5. Tos M. Growth of the fetal Eustachian tube and its dimensions. Arch Klin Exp Ohren Nasen Kehlkopfheilkunde. 1971;198:177–86.
6. Todd JL, Todd NW. Conotruncal cardiac anomalies and otitis media. J Pediatr. 1997;131(2):215–9.
7. Dewangan M. Association of congenital heart diseases with extracardiac anomalies. Int J Contemp Pediatr. 2017;4(5).
8. Sadler-Kimes D, Siegel MI, Todhunter JS. Age-related morphologic differences in the components of the Eustachian tube/middle-ear system. Ann Otol Rhinol Laryngol. 1989;98:854–8.
9. Siegel MI, Cantekin EI, Todhunter JS, Sadler-Kimes D. Aspect ratio as a descriptor of Eustachian tube cartilage shape. Ann Otol Rhinol Laryngol. 1988;97(Suppl 133):16–7.
10. Siegel MI, Sadler-Kimes D, Todhunter JS. ET cartilage shape as a factor in the epidemiology of otitis media. In: Lim DJ, Bluestone CD, Klein JO, Nelson JD, editors. Recent advances in otitis media: proceedings of the Fourth International Symposium. Burlington: BC Decker; 1988. p. 114–7.
11. Ishijima K, Sando I, Balaban C, Suzuki C, Takasaki K. Length of the Eustachian tube and its postnatal development: computer-aided three dimensional reconstruction and measurement study. Ann Otol Rhinol Laryngol. 2000;109:542–8.
12. Graves GO, Edwards LF. The Eustachian tube: review of its descriptive, microscopic, topographic, and clinical anatomy. Arch Otolaryngol. 1944;39:359–97.
13. Matsune S, Sando I, Takahashi H. Comparative study of elastic at the hinge portion of eustachian tube cartilage in normal and cleft palate individuals. In: Lim DJ, Bluestone CD, Klein JO, et al., editors. Recent advances in otitis media: proceedings of the Fifth International Symposium. Burlington: BC Decker.
14. Suzuki C, Balaban CD, Sando I, et al. Postnatal development of Eustachian tube: a computer-aided 3-D reconstruction and measurement study. Acta Otolaryngol (Stockh). 1998;118:837–43.
15. Orita Y, Sando I, Hasebe S, Miura M. Postnatal change on the location of Ostmann's fatty tissue in the region lateral to Eustachian tube. Int J Pediatr Otorhinolaryngol. 2003;67:1105–12.
16. Prades JM, Dumollard JM, Calloc'h F, Merzougui N, Veyret C, Martin C. Descriptive anatomy of the human auditory tube. Surg Radiol Anat. 1998;20(5):335–40.
17. Sudo M, Sando I, Ikui A, Suzuki C. Narrowest (isthmus) portion of Eustachian tube: a computer-aided three-dimensional reconstruction and measurement study. Ann Otol Rhinol Laryngol. 1997;106:583–8.
18. Bluestone CD, Bluestone MB, Coulter J. Eustachian tube: structure, function, role in otitis media. Hamilton/Lewiston: BC Decker; 2005. p. 25–50.
19. Jen A, Sanelli PC, Banthia V, Victor JD, Selesnick SH. Relationship of petrous temporal bone pneumatization to the Eustachian tube lumen. Laryngoscope. 2004;114:656–60.
20. Jadhav AB, Fellows D, Hand AR, Tadinada A, Lurie AG. Classification and volumetric analysis of temporal bone pneumatization using cone beam computed tomography. Oral Surg Oral Med Oral Pathol Oral Radiol. 2014;117:376–3.
21. Jen A, Sanelli PC, Banthia V, et al. Relationship of petrous temporal bone pneumatization to the Eustachian tube lumen. Laryngoscope. 2004;114:656–60.
22. Ozturk K, Snyderman CH, Gardner PA, Fernandez-Miranda JC. The anatomical relationship between the eustachian tube and petrous internal carotid artery. Laryngoscope. 2012;122(12):2658–62. https://doi.org/10.1002/lary.23679. Epub 2012 Nov 14.
23. Buch K, Nadgir RN, Qureshi MM, Ozonoff A, Sakai O. Clinical significance of incidentally detected torus tubarius calcification. J Comput Assist Tomogr. 2017;41:828–32.
24. Morshedi MM, Mafee MF. Calcification of the cartilaginous Eustachian tube. Neuroradiology. 2012;54:525–7.
25. Pahnke J. Morphology, function, and clinical aspects of the eustachian tube. In: Jahnke K, editor. Middle ear surgery (current topics in otolaryngology—head and neck surgery). Stuttgart: Thieme. p. 1–22.
26. Schuknecht HF, Gulya AJ. Anatomy of the temporal bone with surgical implications. Philadelphia: Lea & Febiger; 1986.
27. Rodolph Lauwer. Endoscopic ear and eustachian tube surgery. An issue of Otolaryngologic Clinics of North America. October 2016.
28. Rood SR, Doyle WJ. The nasopharyngeal orifice of the auditory tube: implications for tubal dynamics anatomy. Cleft Palate J. 1982;19:119–28.
29. Pahnke J. Function, and clinical aspects of the Eustachian tube. Current topics in otolaryngology—head and neck surgery. Middle ear surgery: recent advances and future directions.
30. Savic D, Djeric D. Anatomical variations and relations in the medial wall of the bony portion of the eustachian tube. Acta Otolaryngol. 1985;99(5–6):551–6.

31. da Costa SS, et al. One case, two lessons: an aberrant internal carotid artery causing acquired cholesteatoma. Braz J Otorhinolaryngol. 2014;80(5):453–4.
32. Poe D, Pyykkö I, Valtonen H, Silvola J. Analysis of eustachian tube function by video endoscopy. Am J Otol. 2000;21:602–7.
33. Olander H, Järnstedt J, Poe D, Kivekäs I. Critical distance between the cartilaginous eustachian tube and the internal carotid artery (Syventävien opintojen kirjallinen työ Tampereen yliopisto Lääketieteen ja biotieteiden tiedekunta Syyskuu). Eur Arch Otorhinolaryngol. 2017;274(1):73–7.
34. Rich AR. A physiological study of the Eustachian tube and its related muscles. Bull Johns Hopkins Hosp. 1920;31:3005–10.
35. Cantekin EI, Doyle WJ, Reichert TJ, et al. Dilation of the Eustachian tube by electrical stimulation of the mandibular nerve. Ann Otol Rhinol Laryngol. 1979;88:40–51.
36. Honjo I, Okazaki N, Kumazawa T. Experimental study of the Eustachian tube function with regard to its related muscles. Acta Otolaryngol (Stockh). 1979;87:84–9.
37. Simkins C. Functional anatomy of the Eustachian tube. Arch Otolaryngol. 1943;38:476.
38. Goss C, editor. Gray's anatomy of the human body. Philadelphia: Lea & Febiger; 1967.
39. Canalis RF. Valsalva's contribution to otology. Am J Otolaryngol. 1990;11:420–7.
40. Abe M, Murakami G, Noguchi M, et al. Variations in the tensor veli palatini muscle with special reference to its origin and insertion. Cleft Palate Craniofac J. 2004;41:474–84.
41. Leuwer R. Otolaryngol Clin North Am. 2016;49:1097–106.
42. Bryant WS. The Eustachian tube: its anatomy and its movement: with a description of the cartilages, muscles, fasciae, and the fossa of Rosenmüller. Med Rec. 1907;71:931.
43. McMyn JK. The anatomy of the salpingopharyngeus muscle. J Laryngol Otol. 1940;55:1–22.
44. Swarts JD, Rood SR. The morphometry and three-dimensional structure of the adult Eustachian tube: implications for function. Cleft Palate J. 1990;27:374–81.
45. Sudo M, Sando I, Suzuki C. Three dimensional reconstruction and measurement of human Eustachian tube structures: a hypothesis of Eustachian tube function. Ann Otol Rhinol Laryngol. 1998;107:547–54.
46. Ishijima K, Sando I, Miura M, et al. Postnatal development of static volume of the Eustachian tube lumen. Ann Otol Rhinol Laryngol. 2002;111:832–5.
47. Tos M, Bak-Pedersen K. Goblet cell population in the normal middle ear and Eustachian tube of children and adults. Ann Otol Rhinol Laryngol. 1976;85(Suppl 25):44–50.
48. Rüdinger N. Ein Beitrag zur Anatomie und Histologie der Tuba Eustachii. Ärztl Intelligenz-Blatt. 1865;37:1–16.
49. Sando I, Takahashi H, Matsune S, et al. Localization of function in the Eustachian tube: a hypothesis. Ann Otol Rhinol Laryngol. 1994;103:311–4.
50. Wenzel S. Die Verschlussinsuffizienz der Tuba Auditiva—Neue Aspekte zur Pathogenese, Diagnostik und Therapie von Mittelohrprotektionssto rungen. Hamburg: Habilitationsschrift; 2004.
51. Jahnke K, editor. Middle ear surgery: recent advances and future directions. Current topics in otolaryngology—head and neck surgery. Stuttgart: Thieme.
52. Mondain M, Vidal D, Bouhanna S, Uziel A. Monitoring Eustachian tube opening: preliminary results in normal subjects. Laryngoscope. 1997;107:1414–9.
53. Eden AR. Neural control of middle ear aeration. New York: Mount Sinai School of Medicine; 1987.
54. Ceylan A, et al. Impact of Jacobson's (tympanic) nerve sectioning on middle ear functions. Otol Neurotol. 2007;28(3):341–4.
55. Eden AR, Gannon PJ. Neural control of middle ear aeration. Arch Otolaryngol Head Neck Surg. 1987;113(2):133–7.
56. Bylander A, Tjernstrom O, Ivarsson A. Pressure opening and closing functions of the Eustachian tube by inflation and deflation in children and adults with normal ears. Acta Otolaryngol (Stockh). 1983;96:255–68.
57. Bylander A, Tjernstrom O. Changes in Eustachian tube function with age in children with normal ears: a longitudinal study. Acta Otolaryngol (Stockh). 1983;96:467–77.

8 Human Middle Ear and Phylogenetic Impacts

Contents

The human auditory system is the result of the way various animal ancestors developed their auditory systems. Fish are the first vertebrate to develop hearing, perhaps 350 million years ago: primitive fish had an internal balance organ which eventually came to include an auditory receptor. As fish evolved, the labyrinth included curved canals and an utricle, as well as a saccule and a lagena. The lagena is an extension of the saccule and presumed to be the forerunner of the cochlea. Amphibia were the first vertebrate land dwellers. At first, their ears were poorly equipped for air-conduction hearing. To deal with terrestrial life, the development of the conductive apparatus was one of the great landmarks of vertebrate evolution. Amphibians took advantage of preexisting structures inherited from fish and elaborated them into a tympanic membrane and a single ossicle, the columella, to transmit vibratory energy from the air to the inner ear.

Reptiles appeared some 300 million years ago. The most common living reptiles nowadays are snakes, lizards, turtles, and crocodiles, but their most famous members, the dinosaurs, are extinct. The dinosaurs' main living heir, birds, arose perhaps 150 million years ago. The reptilian auditory system is more familiar to human one because it is the basic design that

S. Mansour et al., *Comprehensive and Clinical Anatomy of the Middle Ear*,
https://doi.org/10.1007/978-3-030-15363-2_8

was passed to all descendant animals, including humans. Mammals seem to have appeared around 200 million years ago from synapsid reptiles themselves appeared 300 million years ago. Reptiles have several jaw bones and one auditory ossicle: from the multiple jaw bones of the reptile, one became the mandible, and the others were modified into mammalian ossicles [1] (see below Sect. 8.1) [2]. In addition and in relation with these developmental steps, this chapter outlines the striking handicap of the middle ear due to its special immunity status and reports its particular defense mechanisms to aggression.

8.1 Comparative Anatomy and Phylogenetic Evolution of the Middle Ear Ossicles

The only ossicle in the middle ears of nonmammalian amniotes (including lizards, crocodilians, and their descendants, the birds) is the stapes.

In reptiles, the eardrum is connected to the inner ear via a single bone, the columella, while the upper and lower jaws contain several bones not found in mammals.

The earliest amniotes had a jaw joint composed of the articular (a small bone at the back of the lower jaw) and the quadrate (a small bone at the back of the upper jaw). Over the course of the evolution of mammals, one bone from the lower and one from the upper jaw (the articular and quadrate bones) lost their purpose in the jaw joint and became progressively integrated to the middle ear, connecting to the already existing stapes bone and forming a chain of three bones (the ossicles) which transmit sounds more efficiently and allow more accurate hearing. Having three ossicles in the middle ear is one of the defining features of mammals.

The classical Reichert-Gaupp theory considers as following (Table 8.1) the homologies between reptilian skull and jaw bones and mammalian middle ear ossicles [3–6].

These homologies are well established by numerous studies in the fields of comparative anatomy and embryology. It can explain, for instance, why the tensor tympani muscle is innervated by the trigeminal nerve, considering that this muscle was a masticatory one in reptiles. However, the separation between reptiles and mammals is not so clear. The new phylogenetic classification considers that mammalian reptiles (as cynodonts) and "true" mammals belong to the same group: the synapsids, which is characterized by a single temporal fossa.

Table 8.1 Enumeration of the homologies between the different skull and jaw bones of the reptiles corresponding to the ossicles of mammals

Reptile skull and jaw bones	Mammal ossicles
Articular	Malleus
Pre-articular	Anterior process of the malleus (gonial bone)
Angular	Tympanic bone
Quadrate	Incus
Columella	Stapes

In reptiles and birds, the suspension of the lower jaw corresponds to the articular-quadrate joint. The jaw is constituted by many bones (dentary with the teeth, angular, surangular, pre-articular, coronoid, articular, etc.) and articulated with a skull bone, the quadrate, which is itself a remnant of the pterygo-quadrate of the first vertebrates.

The transition between the "reptilian" suspension and the "mammalian" one (dento-squamosal joint) was not immediate during evolution; in cynodonts (cynodonts probably gave rise to mammals about 200 million years ago; however, they are not considered to be mammals themselves), the posterior bones of the jaw regress progressively, and the dentary takes a new contact with the squamosal. Several fossil species keep a "double joint" (articular-quadrate and dento-squamosal), and it is quite impossible to classify these species into reptiles or mammals—but this question is today obsolete at the light of the phylogenetic classification.

Some present mammals, considered as "primitive" (monotremata, marsupials), exhibit during their embryonic development some transient features evoking the reptilian pattern.

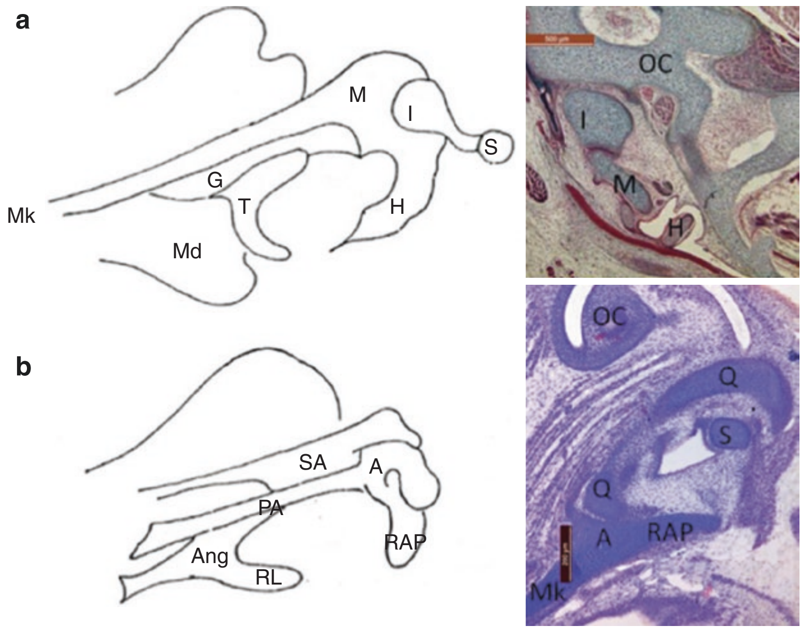

Fig. 8.1 (**a**, **b**) Comparison between schematic drawings of the middle ear ossicles of a marsupial embryo (*Didelphis*) (A) and of the mandibular-otic area in a cynodont (*Diademodon*) (B), redrawn from Hopson [7]. (**c**, **d**) Frontal section of the middle ear of a marsupial (*Didelphis*) (A) and sagittal section of the jaw joint of a diapsid reptile embryo (*Mabuia megalura*). The retroarticular process (RAP) of the articular bone (A) is classically considered as the homologous of the handle (H) of the malleus but several recent authors associate also this structure with the *processus brevis*. However, several recent works consider this process as the homologous of the *processus brevis*. *A* angular; *G* goniale; *M* malleus; *Md* mandible; *Mk* Meckel's cartilage; *OC* otic capsule; *PA* pre-articular; *Q* quadrate; *RAP* retroarticular process; *RL* reflected lamina of the angular bone (future tympanic ring); *S* stapes; *SA* surangular

Furthermore, the development of reptilian jaw bones seems to be very similar to mammalian middle ear ossicles embryogenesis [7–9] (Fig. 8.1). As a remnant of phylogenetic origin of the mammalian middle ear, the temporomandibular disk continues into the middle ear in humans and keeps the continuity of the anterior ligament of the malleus [10, 11]. Other connections between TMJ and the malleus are discussed in Sect. 3.1.1.4.

In cetaceans (whales, dolphins, etc.) and sirenians (aquatic, herbivorous mammals that inhabit swamps, rivers, estuaries, marine wetlands, and coastal marine waters), the tympanic bone is connected with the sound-conducting apparatus [11]. At the light of comparative anatomy, this fact could be easily explained. The tympanic bone corresponds to the angular reptilian bone and develops from an intramembranous anlage at the vicinity of the primordium of the anterior process of the malleus (the "gonial" bone, corresponding to the pre-articular).

The incorporation of the primary jaw joint into the mammalian middle ear was only possible due to the evolution of a new way to articulate the upper and lower jaws, with the formation of the dentary-squamosal joint or TMJ in humans. This important process gave rise to an increase of the bandwidth of hearing to high frequencies [12] and constitutes thus a Darwinian advantage selected by the evolution process.

The evolution of the three-ossicle ear in mammals is intricately connected with the evolution of a novel jaw joint, these two structures evolving together created the distinctive mammalian skull [13].

8.2 Middle Ear Functions Through Phylogenesis

8.2.1 Middle Ear Mechanics

8.2.1.1 The Benefit of the Triple Ossicles System

The mammalian middle ear is unique among tetrapods (mammals, amphibians, reptiles, and birds), in that it contains three distinct ossicles (the malleus, incus, and stapes) that form an indirect and flexible coupling path between the eardrum and cochlea, for which the majority of the ossicular mass is concentrated away from the cochlear entry axis. This differs markedly from the middle ears of non-mammalian tetrapods, in which eardrum motions are transmitted to the cochlea more or less in a straight line via a rod-like columella structure. (Fig. 8.2). Many theories have been presented as to the functional consequences and possible advantages of this peculiar arrangement:

- Most importantly, it renders mammals capable of hearing to much higher frequencies than non-mammals (>100 kHz vs. <12 kHz) [14–16].
- It allows the ossicles to adopt lower inertia vibrational modes at higher frequencies [17, 18].
- It provides flexibility to the ossicular system and thus protect the cochlea against high static pressures in the ear canal or impulsive stimuli [18–20].
- It allows leveraging the off-axis mass distribution and joint flexibility to reduce the amount of ossicular inertia transmitted the cochlea in response to skull vibrations from self-generated sounds due to vocalizations, breathing, pumping blood, etc., and thus allowing more attention to be focused on the external sounds critical for survival [18].

Due to evolution advances, the middle ear gained at the same time a complex and very efficient architecture but highly susceptible and vulnerable in front of aggressions of multiple forms.

8.2.1.2 Air as Isolator and Vehicle

Another phylogenetic innovation of the middle ear is to use air as an *isolator*: to isolate the ossicular chain from the bony walls of the temporal bone to be able to transmit effectively via the eardrum and the ossicular chain the sound waves of the external air environment to the cochlear fluid environment (no sound dissipation). This is the columellar effect of the ossicular chain suspended “in the air” by two annular ligaments (the eardrum and stapes annular ligament), where the air acts as sound *isolator*; for instance, an otosclerosis focus provokes the loss of the sound isolation property attributed to the annular ligament of the stapes.

Air does not have the same role at the external ear canal as in the ME: in the first compartment, the air vehicles a sound, and in the second, the

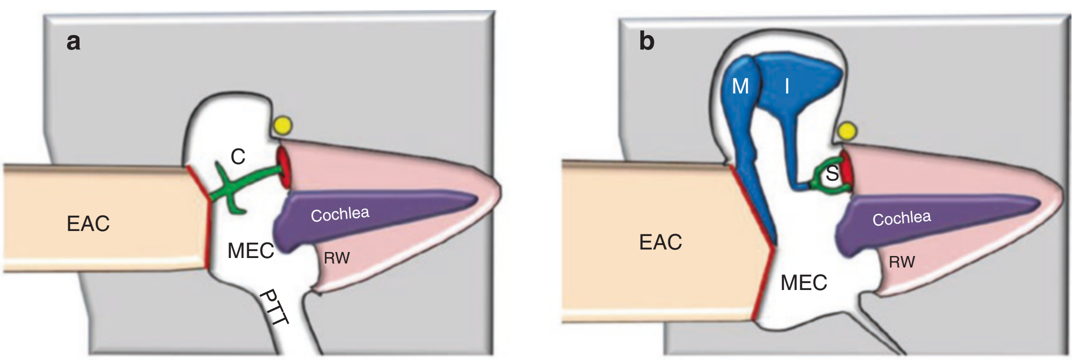

Fig. 8.2 Comparative anatomy between bird middle ear (**a**) and human middle ear (**b**). *c* columella; *S* stapes ; *I* incus ; *M* malleus; *RW* round window; *EAC* external auditory canal; *MEC* middle ear cavity; *PTT* pharyngotympanic tube

air isolates the sound wave from any dispersion into the skull bones.

Thus, the role of air in the middle ear is primarily to insure sound transmission (compliance), and the respiratory function of the middle ear is mostly to assist hearing and insure its homoeostasis (hearing loss in mucoid otitis media).

8.2.2 Gas Exchange

During phylogenesis, the exit of vertebrates out of water to live in air and on land required many innovations in the anatomical organization of the gill middle ear apparatus, thus finding itself in need to adapt and survive in the noxious environment that the air represents.

The middle ear became an *impedance mismatch transformer* for the advantage of an air-filled space to accomplish the role of a sound transmission system. Thus, the primary function of the middle ear was to provide and maintain a "gas pocket" at atmospheric pressure. Hence, mastoid pneumatization increases the mucosal area for gas exchange.

Embryogenesis shows that the lungs developed at the lower end of the branchial arches surrounding the heart, and the middle ear developed at the end of the superior extremity of these arches, under the base of the skull and in contact with the otic capsule. Also the middle ear developed from an expansion of the first endodermal pouch invading the mesenchyme of the temporal bone to be filled later on with air. This air colonization of the temporal bone will continue after birth with the development of the mastoid process (pneumatization) aiming to favor the objective of gas exchange.

The middle ear and the lung shared a neighborhood site of development with a similar task **to bring air to the body**. Middle ear and lung have comparative structures covered by a similar mucous membrane: to the trachea responds the Eustachian tube, to the bronchi and bronchioles respond the various tympanic isthmi and compartments of the middle ear, and finally the lung alveoli respond to the pneumatized mastoid. Each of these structures is lined by the same respiratory epithelium that gradually dedifferentiate to become at its most distal end only a thin single-cell layer to promote air-to-blood gas exchange.

However, the ventilation and drainage function of the Eustachian tube is suitable only for a healthy middle ear mucosa, but in the presence of an inflammatory process, the gas exchange through a hyperplastic thickened mucosa is not the same (but increased, leaving a gas deficit); hence the ET becomes unable to respond adequately to the need (ET dysfunction), followed by global dysventilation and clearance disorders with mucus retention. Actually the classic tubal dysfunction is thought to be more likely secondary to an intrinsic pathology of the middle ear rather than to a tube pathology per se.

The presence of air and its renewal in the respiratory system is an obvious vital need to allow gas exchange at the take off lung/blood level; also the presence of air in the middle ear and mastoid is needed for mucosa/blood gas exchange. The tubal ventilation is 1 cc per day of air renewal to ensure a gaseous equilibrium to the mucosa lining the tympanic cavities in healthy conditions. This rudimentary but sufficient respiratory function is done through a narrow tubal isthmus (0.5–2 mm) and allows the ET to remain closed most of the time (phenomenon needed to protect the ear from internal body sounds and reflux aggressions from the aerodigestive pathways). However, pulmonary ventilation ranges at a much higher scale: it must ensure renewal of 250 cc of air at each inhalation-expiration for an air/blood exchange surface of 75 m^2.

To illustrate this "respiratory request difference" between the two organs, one could compare the slim size of a transtympanic tube (TT) for the middle ear ventilation and the endotracheal tube size for assisted lung ventilation.

Middle ear and lung use both air as a medium for the *gas exchange*; in addition for a second purpose: the middle ear for its original objective, *the hearing* and the lower airways for a second objective*: the phonation.*

8.3 Middle Ear Immunity

Phylogenetically, the immune system is very ancient and appeared at very early stages during evolution. The adaptive immunity steps with their specific immune cells and antibodies evolved with the vertebrate lineage which is far earlier than the phylogenetic development of the middle ear, since the middle ear appeared at the time when animals transitioned from aquatic to terrestrial existence.

Therefore the late phylogenetic appearance of the middle ear rendered it an *immunodeficient organ*; the main defense mechanism against pathogens in the middle ear is primarily **innate**, relying on the *effective immune system,* that is deprived from the specific **adaptive** immunity. The normal mucosa of the middle ear possesses neither immunocompetent lymphocytes nor associated lymphoid tissues: this is why the mucosa of the tympanic cavity is *not an immune inductive site*.

Both the ineffective immune responses and an overzealous inflammatory response secondary to aggression are deleterious for the middle ear. For example, when the ME mucosa is exposed to injury or aggression, it may react by *hyperplasia* and then *metaplasia* with a transition into a mucus-secreting epithelium with numerous goblet cells and increased mucus secretion, which may result in a glue ear.

8.3.1 Middle Ear Innate Immunity

Innate immunity (also called natural or native immunity) provides the early line of defense against microbes. The mucosal immunological defense in the middle ear manifests by a number of mechanisms, including physicochemical barriers of mucus, the mucosal epithelial cells with their tight junction barrier, and the innate immune responses such as inflammation with a cascade of mediators, cellular infiltration, effusion, and antimicrobial protein secretions expressing the regulation of the middle ear mucosal response (Fig. 8.3).

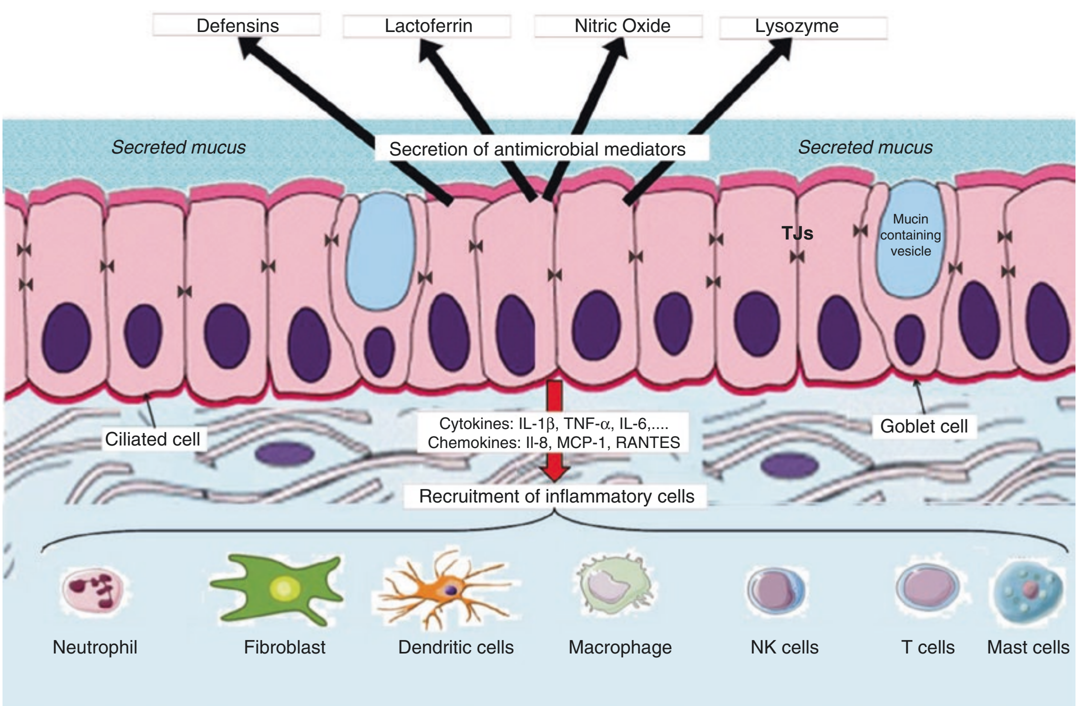

Fig. 8.3 Middle ear mucosal immunity

ME innate immunity includes the following principal components:

8.3.1.1 Physical and chemical barriers

The mucus layer covering the mucosal epithelium acts as a first physical and biochemical barrier. An additional layer of physical protection against microorganisms is provided by a tightly interlaced cell-to-cell network of epithelial cells which prevent microorganisms from violating the mucosa (Fig. 8.4).

Mucins of the mucociliary blanket lining the airways surface act by trapping germs and removing them through ciliary movements toward the Eustachian tube.

8.3.1.2 Antimicrobial components

Microorganisms that pass the mucin barrier get in contact with a range of soluble mediators present in the mucus, such *as lysozyme, lactoferrin, and defensin,* produced by epithelial cells. The production of these molecules can directly destroy the invading pathogen (Fig. 8.4).

8.3.1.3 Cellular components

An important mechanism of defense is the ingestion of microorganisms by phagocytic cells like macrophages, natural killer (NK) cells, and dendritic cells. Indeed, the phagocytic and microbicidal activities of these cells are essential for maintaining the middle ear in a clean and sterile state. During inflammation, these cells are recruited in higher number to infiltrate the lamina propria by cytokines and chemokines secreted by epithelial cells, dendritic cells, natural killer (NK) cells, and other innate lymphoid cells [3].

- ***Dendritic cells (DC) and Langerhans cells (LC)*** play an essential role in linking innate and adaptive immune responses as they have the ability to internalize a wide variety of pathogens and migrate, sensitize, and activate T cells in the nasopharynx. They are connectors between innate immune system and the adaptive system.
- ***Fibroblasts*** are the most common cells of the connective tissue; they are "sentinel cells" capable of producing various immune modulators.
- ***Mast cells***, strongly linked to histamine secretion, are predominantly found in the pars flaccida compared to the pars tensa. Mast cells are responsible of granulation tissue formation and recurrence or chronic course of inflammatory disease in chronic suppurative otitis media [4].

The innate immune system of the respiratory mucosa detects microbial infections and uses pattern recognition receptors (PRRs) to recognize the "molecular signature of pathogens," known as pathogen-associated molecular patterns (PAMPs). PRRs include toll-like receptors (TLRs) [5]. There are at least ten different TLRs found on the surface of epithelial cells of the human middle ear. TLR molecules provide protection against infection by recognizing intruding pathogens through their invariant PAMPS and then mobilizing the appropriate immune defense. The binding action to these receptors activates phagocytosis of bacteria by macrophages and neutrophils or the release of antiviral interferons. It is of interest to recall that toll-like receptors (TLRs) are PRRs that have been maintained or preserved during evolution from insects to humans and have a unique and important role in signaling the presence of infection; *the downregulation of TLR expression during otitis media can lead to inefficient host defense in the*

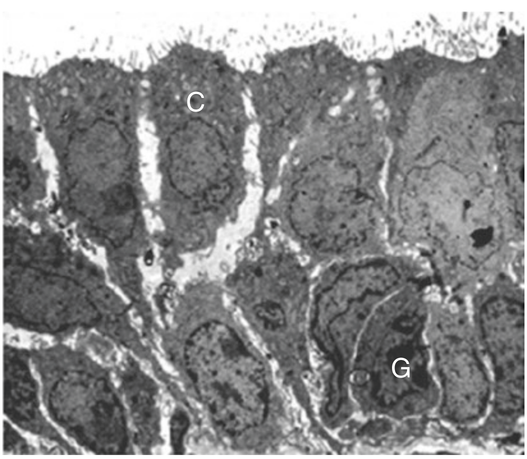

Fig. 8.4 Electronic microscopy slide of middle ear mucosa showing a clear view of different types of mucosa cells: ciliated cells (C), goblet cells with their mucus containing vacuoles (G)

middle ear [24]. Recent advances in oto-pathogens recognition via microbial pattern recognition receptors (PRR) and elucidation of complex signaling cascades have improved the understanding of the coordination and regulation of the middle ear mucosal response. *These advances support vaccine development aiming to reduce the risk of recurrent otitis media in children* [25].

8.3.2 Adaptive Immunity and Immune Memory

The **adaptive immunity** system (also called specific or acquired immunity) is characterized by *the ability to distinguish different substances*, called *specificity*, and *the ability to respond more vigorously to repeated exposures to the same microbe*, so known as ***Immune memory***. The unique components of adaptive immunity are lymphocytes (**T cells and B cells**). The adaptive immune system is only present in vertebrates and cartilaginous fish.

Adaptive immunity is found in the nasopharynx and decreases while approaching the Eustachian tube mucosa; middle ear mucosa is not phylogenetically well prepared to such activity. ME mucosa lacks the sufficient number of such immune cells or follicles needed for the adaptive immunity: antibodies detected in the middle ear during AOM derive predominantly from serum transudation and reflux of nasopharyngeal secretions through containing antibodies, with no evidence for independent, local antibody production.

For this reason the middle ear is not an inductive site.

8.3.3 Middle Ear Mucosal Response to Microorganisms

Following the transgression of microorganisms through the ME mucosa, there are two possible response stages, acute and chronic:

- <u>At the acute stage</u>, the middle ear reaction is usually effective through production of inflammatory mediators as cytokines IL8 via NF-KB signaling pathway, which stimulates infiltration of neutrophils into the inflammatory site [26]. Bacteria are rapidly killed, and infection is usually resolved within 7–10 days.
- <u>At the chronic stage</u>, ***lymphocytes*** become the major infiltrating inflammatory cells. Among them, natural killer (NK) cells secrete IFNγ (interferon), and macrophages secrete <u>*TNFα.*</u>
  - IFNγ is a **cytokine** that is critical for the innate immunity against bacteria and viruses. In chronic otitis media, IFNγ is highly upregulated in the middle ear mucosa and plays an important role in the immune response including the *activation of macrophages* (very high expression of IFNγ is associated with chronic otitis media and its sequelae.) [27].
  - *At the same time*, IFNγ and TNFα have negative effects on the mucociliary barrier of the middle ear mucosa, thus weakening again part of the innate immunity.
  - TGF-β is present with high level in the chronic stages of otitis media with effusion indicating that it participates in the suppression of the immune system and the proliferation of connective tissues in the middle ear cleft [28].
  - Also it has been found that middle ear pathogens induce the expression of Id1 and Id3 in rats. Id1, in turn, increases the expression of TNFα and IFNγ in the middle ear epithelial cells [29].

8.3.4 Middle Ear Immune Tolerance

Due to its solely innate immune status, with the lack of T and B cells in its mucosa, the middle ear presents the following phenomena:

- ***Tolerance to infection***: *<u>No middle ear immune memory</u> is build up against future attacks of infectious agents, resulting in recurrent otitis, chronic diseases, sequelae, etc*. The pathogens causing recurrent otitis media (rAOM) are the same as those causing acute otitis media (AOM).

- ***Tolerance to homograft without the need of immunodepression*** (success of homograft tympanoplasties by J. Marquet). In other organs of the body, homografts are subject to immune rejection, which it is not the case in the middle ear: *this is called* ***peripheric immunotolerance of the middle ear*** [30].

8.4 Addendum

Not to miss the latest major morphological phylogenetic innovation, the most recent event in the evolution process and specific to the mammalians, is the formation of the external ear canal. The first ectodermic groove forms the beginning of the EAC; it proceeds in the fetus by a cavitation phenomenon to be completed in the postnatal period. The increase in length of the bony external ear canal is governed by two dynamic phenomena:

- *Parietal expansion of the encephalic growth and the tension forces of the masticatory muscle on the tympanal bone along with*
- *Tension forces of the cervical musculature on the mastoid.*

At the bottom of the external ear canal, a dedifferentiation of the skin canal appears by a cavitation process from outside to inside associated to *<u>an immunological deficiency of the skin at this sit</u>e. The term skin is improper here, because skin is characterized by an epidermis and underneath dermis, but the bony external canal skin is nothing than a pluri-stratified keratinizing epithelium owing special properties (it is the same for the term mucosa in the middle ear which is mainly an unicellular epithelial layer, both ear canal and middle ear cavity have a rudimentary layer protection): in the fetal life, it permits the cavitation phenomenon, and after birth, it insures lateral cell migration as a self-cleaning process of the eardrum.*

When inflammation takes place, this keratinizing epithelium induces hyperplasia with enhanced capacity of opposite migration toward the inside space of the ME resulting in invagination of the epidermis similar to the cavitation process observed in the fetal life. Therefore, the hypothesis of cholesteatoma formation is held to be a reactivation of the fetal cavitation process under the condition of active inflammation!

8.5 Conclusion

This chapter has outlined how the middle ear, from its origin out of non-auditory structures, has been modified by adaptations into an important hearing organ. The evolution of the middle ear apparatus increased both the sensitivity to airborne sound and the frequency range of hearing. Phylogenesis and embryogenesis speak very well about the particular status and the behavior of the middle ear.

During species evolution from water to land living, phylogenesis implied the creation of a middle ear capable of important functions related to terrestrial life: *hearing and gas exchange*.

To enable the middle ear to accomplish such great performances, embryogenesis achieved a complex and highly articulated structure made out of multiple origins: the first two branchial arches, the ectoderm, the endoderm, and the mesoderm. Because of this complex original architecture, embryogenesis left the middle ear subject to organizational and structural difficulties or challenges to be faced with after birth.

Due to its delayed arrival, phylogenesis deprived the middle ear from a competent immunologic inductive potential, to become a fragile organ. Based only on its primitive innate immunity, the middle ear response to invading microorganisms results often in an increased production of mediator cascades, rendering itself victim of its own defense mechanism.

References

1. Allin EF, Hopson JA. Evolution of the auditory system in Synapsida ('mammal-like reptiles' and primitive mammals) as seen in the fossil record. In: Webster DB, Fay RR, Popper AN, editors. The evolutionary

biology of hearing. New York: Springer; 1992. p. 587–614.
2. Kardong KV. Vertebrates. Comparative anatomy, function, evolution. 6th ed. New York: McGraw Hill; 2012.
3. Westoll TS. New lights on the mammalian ear ossicles. Nature. 1944;154:770–1.
4. Goodrich ES. Studies on the structure and development of vertebrates, vol. 1. New York: Dover; 1958.
5. Allin EF. Evolution of the mammalian middle ear. J Morphol. 1975;147:403–38.
6. Louryan S. Morphogenèse et phylogenèse de l'oreille motenne des mammifères: quelques considérations. Rev Méd Bruxelles. 1987;8:141–4.
7. Hopson JA. The origin of the mammalian middle ear. Am Zool. 1966;6:437–50.
8. Louryan S. Développement des ébauches squelettiques du complexe mandibulo-otique chez *Mabuia Megalura* (*Lacertilia: Scincidae*). Ann Soc R Zool Belg. 1989;119:47–57.
9. Luo ZX. Developmental patterns in mesosoic evolution of mammal ears. Annu Rev Ecol Evol Syst. 2011;43:465–80.
10. Smeele LE. Ontogeny of relationship of human middle ear and temporomandibular (squamomandibular) joint. I. Morphology and ontogeny in man. Acta Anat. 1988;131:338–41.
11. Rodriguez-Vazquez JF, Merida-Velasco JR, Merida-Velasco JA, Jimenez-Collado J. Anatomical considerations on the discomalleolar ligament. J Anat. 1998;192:617–21.
12. Fleischner G. Evolutionary principles of the mammalian middle ear. Berlin: Springer; 1978.
13. Josbi L, Tucker AS. Evolution of the mammalian middle ear and jaw: adaptations and novel structures. J Anat. 2013;222:147–60.
14. Heffner RS, Heffner HE. Hearing. In: Greenberg G, Haraaway MM, editors. Comparitive psychology, a handbook. New York: Routledge; 1998. p. 290–3330.
15. Dooling RJ, Lohr B, Dent ML. Hearing in birds. In: Dooling RJ, Fay RR, Popper AN, editors. Comparative hearing: birds and reptiles. New York: Springer; 2000. p. 308–59.
16. Heffner HE, Heffner RS. High-frequency hearing. In: Dallos P, Oertel D, editors. Audition. San Diego: Elsevier; 2008. p. 55–60.
17. Willi UB, Ferrazzini MA, Huber AM. The incudo-malleolar joint and sound transmission losses. Hear Res. 2002;174(1–2):32–44.
18. Puria S, Steele C. Tympanic-membrane and malleus-incus-complex co-adaptations for high-frequency hearing in mammals. Hear Res. 2009;263(1–2):183–90. https://doi.org/10.1016/j.heares.2009.10.013.
19. Gottlieb PK, Vaisbuch Y, Puria S. Human ossicular-joint flexibility transforms the peak amplitude and width of impulsive acoustic stimuli. J Acoust Soc Am. 2018;143(6):3418.
20. Mason MJ. Of mice, moles and guinea pigs: functional morphology of the middle ear in living mammals. Hear Res. 2013;301:4–18. https://doi.org/10.1016/j.heares.2012.10.004.
21. Mittal R, et al. Role of innate immunity in the pathogenesis of otitis media. Int J Infect Dis. 2014;29:259–67.
22. Pajor A, Danilewicz M, Jankowski A, Durko T. Participation of mast cells in chronic otitis media. Folia Histochem Cytobiol. 2011;49:479–85.
23. Sasai M, Yamamoto M. Pathogen recognition receptors: ligands and signaling pathways by toll-like receptors. Int Rev Immunol. 2013;32:116–33.
24. Mittal R, Kodiyan J, Gerring R, Mathee K, Li J-D, Grati M'h, Liu XZ. Role of innate immunity in the pathogenesis of otitis media. Int J Infect Dis. 2014;29:259–67.
25. Mestecky J, Strober W, Russell MW, Cheroutre H, Lambrecht BN, Kelsall BL, editors. Mucosal immunology. 4th ed; 2015.
26. Juhn SK, et al. The role of inflammatory mediators in the pathogenesis of otitis media and sequelae. Clin Exp Otorhinolaryngol. 2008;1(3):117–38. https://doi.org/10.3342/ceo.2008.1.3.117. Epub 2008 Sep 30.
27. Zhou F. Molecular mechanisms of IFN-gamma to up-regulate MHC class I antigen processing and presentation. Int Rev Immunol. 2009;28:39–60.
28. Lee YW, Chung Y, Juhn SK, Kim Y, Lin J. Activation of the transforming growth factor beta pathway in bacterial otitis media. Ann Otol Rhinol Laryngol. 2011;120:204–13.
29. Avens Publishing Group. Inviting innovations. Int J Otorhinolaryngol. 2014; 1(1).
30. Lin J, Xu Y, Zhao Y. Adaptive immunity in the middle ear mucosa with chronic otitis media. Int J Otorhinolaryngol. 2014;1(1):5.

Index

S. Mansour et al., *Comprehensive and Clinical Anatomy of the Middle Ear*,
https://doi.org/10.1007/978-3-030-15363-2